THE PHARMACOKINETICS AND PHARMACODYNAMICS OF ANTIFUNGAL AGENTS FOR HIV-ASSOCIATED INVASIVE FUNGAL INFECTIONS

Thesis submitted in accordance with the requirements of the University of Liverpool for the degree of Doctor in Philosophy

by

Katharine Elizabeth Stott

Institute of Systems, Molecular and Integrative Biology
University of Liverpool, UK

&

Malawi Liverpool Wellcome Trust Clinical Research Programme
Blantyre, Malawi

January 2021

Declaration

The work presented herein is my own and has not been submitted for a degree or other award at any other institution.

Several components of this thesis result from collaborative work:
Chapters 2 and 3 partly represent analyses of data collected during a pharmacokinetic-pharmacodynamic substudy of a clinical trial, CryptoDex; International Standard Randomised Controlled Trial Number (ISRCTN)59144167. The substudy was designed and conducted by the study team an sites in Vietnam and Uganda, detailed in co-authorship list associated with each chapter.

The clinical pharmacokinetic and immunological data presented in chapters 4 and 6, respectively, were collected during a substudy of the AMBITION trial (ISRCTN10248064). The substudy was designed by myself and sample collection was achieved in collaboration with a team of clinicians at Malawi Liverpool Wellcome Trust Clinical Research Programme.

Chapter 5 describes an analysis of data collected during a pharmacokinetic-pharmacodynamic substudy of the IVAP trial (ISRCTN97524945). The substudy was designed and conducted by the study team on site in Vietnam, led by Dr Thuy Le of Duke University, North Carolina.

Immunological laboratory assays were led by Dumizulu Tembo, Dumisan Namakhwa and Cheusisime Kajanga at Malawi Liverpool Wellcome Trust Clinical Research Programme, under the supervision of Professor Henry Mwandumba. Bioanalysis for quantification of drug levels was performed by Dr Jennifer Unsworth, Dr Anahi Santoyo Castelazo and Sarah Whalley at the University of Liverpool.

Funding

This work was funded by a Wellcome Trust Clinical PhD Fellowship awarded to Katharine Stott (award number 203919/Z/16/Z).

Dedication

For Evan, and all of the adventures that you won't remember

Acknowledgements

The following people made this work possible:

The patients and their guardians in Malawi, Vietnam and Uganda, who consented to participate in research despite being critically unwell and in the knowledge that it would not help them directly, but that it may benefit others.

To my supervisors: Professors William Hope, Henry Mwandumba and David Lalloo. For your guidance, advice, practical support and faith in me, thank you.

The AMBITION clinical team in Blantyre, in particular: Dr Melanie Alufandika, Ebbie Gondwe, Wezzie Chimang'anga and Madalitso Chasweka, whose dedication to patient care and enthusiasm for the study were infectious. My lab colleagues from whom I learnt a great deal, Ajisa Ahmadu and Cheusisime Kajanga. Dr Reya Shah, who kept things ticking over while I was on maternity leave. The central AMBITION team and in particular Professors Joe Jarvis and Tom Harrison, Dr David Lawrence, Dr Nabila Youssouf and Philippa Griffin. A wonderful team to be welcomed into and to work alongside.

My collaborators outside of Malawi who trusted me with their precious data and welcomed me into their inspiring teams: Dr Thuy Le and Professor John Perfect at Duke University, North Carolina and Dr Justin Beardsley and Professor Jeremy Day at the Oxford University Clinical Research Unit in Ho Chi Minh City.

For their support and friendship in Malawi and beyond, Drs Stephen and Alice Ray, George Nampachira, Agnes Aaron, Dr Chris Jones, Brian Lewis, Maggie O'Toole and Professors Stephen and Melita Gordon to name just a few.

In Liverpool, Dr Jenny Unsworth, Jacky Crowley, Dr Shampa Das, Dr Ruwanthi Kolamunnage-Dona, Nikki Farrington, Adam Johnson, Laura McEntee, Dr Sara Boyd and Dr Chris Darlow. The wisdom and wit of this dream team kept the wheels rolling, particularly over the unpredictable and challenging past 12 months.

Finally, to Pete. For everything: thank you.

Scientific publications related to this thesis

Stott KE, Le T, Nguyen T, Whalley S, Unsworth J, Kolamunnage-Dona R, Hope W. *Population Pharmacodynamics of Itraconazole for Disseminated Infection Caused by* Talaromyces marneffei. Pending submission.

Stott KE, Loyse A, Jarvis J, Alufandika M, Harrison TS, Mwandumba HC, Day JN, Lalloo DG, Bicanic T, Perfect J, Hope W. *Cryptococcal meningoencephalitis: Time for Action*. The Lancet Infectious Diseases. Accepted for publication September 2020.

Cohen KA, **Stott KE**, Munsamy V, Manson AL, Earl AM, Pym AS. *Evidence for Expanding the Role of Streptomycin in the Management of Drug-Resistant Mycobacterium tuberculosis*. Antimicrob Agents Chemother. 2020 Aug 20;64(9):e00860-20. doi: 10.1128/AAC.00860-20. PMID: 32540971; PMCID: PMC7449167.

Lawrence DS, Youssouf N, Molloy SF, Alanio A, Alufandika M, Boulware DR, Boyer-Chammard T, Chen T, Dromer F, Hlupeni A, Hope W, Hosseinipour MC, Kanyama C, Lortholary O, Loyse A, Meya DB, Mosepele M, Muzoora C, Mwandumba HC, Ndhlovu CE, Niessen L, Schutz C, **Stott KE**, Wang D, Lalloo DG, Meintjes G, Jaffar S, Harrison TS, Jarvis JN. *AMBIsome Therapy Induction OptimisatioN (AMBITION): High Dose AmBisome for Cryptococcal Meningitis Induction Therapy in sub-Saharan Africa: Study Protocol for a Phase 3 Randomised Controlled Non-Inferiority Trial*. Trials. 2018 Nov 23;19(1):649. doi: 10.1186/s13063-018-3026-4. Erratum in: Trials. 2019 Jan 14;20(1):48. PMID: 30470259; PMCID: PMC6251219.

Stott KE, Pertinez H, Sturkenboom MGG, Boeree MJ, Aarnoutse R, Ramachandran G, Requena-Méndez A, Peloquin C, Koegelenberg CFN, Alffenaar JWC, Ruslami R, Tostmann A, Swaminathan S, McIlleron H, Davies G. *Pharmacokinetics of rifampicin in adult TB patients and healthy volunteers: a systematic review and meta-analysis*. J Antimicrob Chemother. 2018 Sep 1;73(9):2305-2313. doi: 10.1093/jac/dky152. PMID: 29701775; PMCID: PMC6105874.

Stott KE, Hope W. *Pharmacokinetics-pharmacodynamics of antifungal agents in the central nervous system.* Expert Opin Drug Metab Toxicol. 2018 Aug;14(8):803-815. doi: 10.1080/17425255.2018.1492551. Epub 2018 Jul 9. PMID: 29943650.

Stott KE, Beardsley J, Kolamunnage-Dona R, Castelazo AS, Kibengo FM, Mai NTH, Tùng NLN, Cuc NTK, Day J, Hope W. *Population Pharmacokinetics and Cerebrospinal Fluid Penetration of Fluconazole in Adults with Cryptococcal Meningitis*. Antimicrob Agents Chemother. 2018 Aug 27;62(9):e00885-18. doi: 10.1128/AAC.00885-18. Erratum in: Antimicrob Agents Chemother. 2018 Nov 26;62(12): PMID: 29914943; PMCID: PMC6125572.

Stott KE, Beardsley J, Whalley S, Kibengo FM, Mai NTH, Tùng NLN, Cuc NTK, Kolamunnage-Dona R, Hope W, Day J. *Population Pharmacokinetic Model and Meta-analysis of Outcomes of Amphotericin B Deoxycholate Use in Adults with Cryptococcal Meningitis*. Antimicrob Agents Chemother. 2018 Jun 26;62(7):e02526-17. doi: 10.1128/AAC.02526-17. Erratum in: Antimicrob Agents Chemother. 2018 Nov 26;62(12): PMID: 29735567; PMCID: PMC6021666.

Stott KE, Hope WW. *Therapeutic drug monitoring for invasive mould infections and disease: pharmacokinetic and pharmacodynamic considerations*. J Antimicrob Chemother. 2017 Mar 1;72(suppl_1):i12-i18. doi: 10.1093/jac/dkx029. PMID: 28355463.

Table of Contents

i. Table of figures

ii. Table of tables

iii. Table of boxes

iv. Abbreviations

AI	Activity index
AmB	Amphotericin B
AMBITION	High Dose AmBisome for Cryptococcal Meningitis Induction Therapy in sub-Saharan Africa
AMR	Antimicrobial Resistance
AUC	Area Under the concentration-time Curve
CCL	Chemokine (C-C motif) Ligand
CFU	Colony Forming Unit
Cmax	Maximum [drug] Concentration
CME	Cryptococcal Meningoencephalitis
Cmin	Minimum [drug] Concentration
CNS	Central Nervous System
CSF	Cerebrospinal Fluid
DAmB	Amphotericin B Deoxycholate
DMSO	Dimethyl sulfoxide
DNDi	Drugs for Neglected Diseases initiative
ECMO	Extra-Corporeal membrane oxygenation
ECV	Epidemiological Cutoff Value
eGFR	estimated Glomerular Filtration Rate
EFA	Early Fungicidal Activity
EMA	European Medicines Agency
FDA	Food and Drug Administration
FSC	Forward Scatter
G-CSF	Granulocyte Colony-Stimulating Factor
GM-CSF	Granulocyte Macrophage Colony-Stimulating Factor
HFIM	Hollow Fiber Infection Model
HIV	Human Immunodeficiency Virus
ICU	Intensive Care Unit
IFI	Invasive Fungal Infection
IFN	Interferon
IL	Interleukin
IV	Intravenous
LAmB	Liposomal Amphotericin B
LMIC	Low- and Middle-Income Countries
LP	Lumbar Puncture
MCP	Monocyte Chemoattractant Protein 1
MDRS	Modification of Diet in Renal Disease Study
MFI	Median fluorescence intensity
MIC	Minimum Inhibitory Concentration

MIP	Macrophage Inflammatory Protein
NPAG	Non-Parametric Adaptive Grid, a component of the Pmetrics software package (Neely 2012)
PAFE	Post Anti-Fungal Effect
PBS	Phosphate-buffered saline
PC	Principal Component
PCA	Principal component analysis
PD	Pharmacodynamic
PK	Pharmacokinetic
PLHIV	People Living with Human Immunodeficiency Virus
PTA	Probability of Target Attainment analysis
QCC	Quantitative Cryptococcal Cultures
RES	Reticuloendothelial System
RHICCA	Evaluating the reactivation of herpesviruses and inflammation as cardiovascular and cerebrovascular risk factors in antiretroviral therapy initiators in an African HIV-infected population
SSC	Side Scatter
TFA	Triflouroacetic Acid
TNF	Tumour Necrosis Factor
VEGF	Vascular Endothelial Growth Factor
VPC	Visual Predictive Check
WCC	White blood Cell Count

v. Abstract

The pharmacokinetics and pharmacodynamics of antifungal agents for HIV-associated invasive fungal infections.

Katharine Elizabeth Stott

Fungal infections cause an estimated 13 million life-threatening infections and 1.6 million deaths annually. The burden of invasive fungal infections (IFIs) reflects immunocompromise resulting from the rise in HIV/AIDS and iatrogenic immunosuppressive therapy. Cryptococcal meningoencephalitis and disseminated talaromycosis are archetypal conditions to illustrate the unmet medical need of IFIs. The optimum treatment regimens for cryptococcal meningoencephalitis and disseminated talaromycosis are unclear. As an alternative to serial clinical trials, PK-PD approaches offer enhanced efficiency, reduced cost and reduced risk to patients. Asides from PK parameters, additional factors that may influence treatment response include the host response to infection.

This thesis begins with an overview of the historical context of antifungal PK-PD, the wide-ranging factors that influence it and methods of measuring and modelling it. Following this, a population PK model of fluconazole in cryptococcal meningoencephalitis quantifies the variability of fluconazole penetration into cerebrospinal fluid (CSF) in 43 patients. Simulations predict a low probability of PK-PD target attainment at widely used dosages of fluconazole. A meta-analysis of studies reporting clinical outcomes from fluconazole monotherapy demonstrates only minor improvements in PD and clinical outcomes with escalating dosage. A second PK model describes the population PK of amphotericin B deoxycholate (DAmB) in 42 patients treated for cryptococcal meningoencephalitis. Inter-patient variability in DAmB PK is modest and unlikely to account for variability in clinical outcome. A meta-analysis of trials reporting clinical outcomes from DAmB monotherapy suggests that DAmB dosage explains most heterogeneity in CSF sterility, but not mortality outcomes. A third population model assesses the PK of liposomal amphotericin B (LAmB) administered as a single high dose to 32 patients with cryptococcal meningoencephalitis within an ongoing clinical trial. A bridging study is performed from murine data to predict PD outcome in humans following high dose LAmB regimens, using the posterior PK parameters derived from the population PK model. This analysis supports the dose of LAmB being used in the trial.

Using data from 76 clinical trial patients, a population PK-PD model of itraconazole in disseminated talaromycosis is constructed. While the model describes considerable variability in the PK of both itraconazole and its active metabolite, hydroxyitraconazole, a relationship between PK and PD cannot be demonstrated. This study suggests that the trial failed to demonstrate the non-inferiority of itraconazole versus DAmB due to a PK failure, the overwhelming majority of patients failing to mount adequate itraconazole exposure.

Finally, an immunophenotyping study is presented, describing networks of immune biomarkers in the CSF of patients with cryptococcal meningoencephalitis. Phagosomal function in whole blood is measured. Data are analysed from serial samples taken during the first 14 days of treatment. A proinflammatory immune signature is associated with increased phagosomal activity in monocyte populations and may contribute to favourable PD and clinical outcomes in cryptococcal meningoencephalitis.

In conclusion, pharmacometric analysis has been a neglected area of research, particularly in mycology. This work demonstrates that PK-PD tools can de-risk efforts to optimise antifungal treatment regimens, enhance the efficiency of those efforts and contribute to the preservation of the precious available antifungal armamentarium.

1 Introduction

1.1 Antimicrobial pharmacokinetic and pharmacodynamic analyses are essential for the future of modern medicine

1.1.1 A brief history of antimicrobial drug discovery

The discovery of arsphenamine in 1909 and penicillin in 1928 marked the beginning of the antibiotic revolution, which transformed modern medicine and indeed society as a whole by contributing to huge gains in average life expectancy and encouraging medical, surgical, oncological and obstetric advances that would previously not have been imaginable.[1,2] These discoveries heralded an era of intensive research into not only anti-bacterial compounds, but also those active against important viral and fungal pathogens – the so-called 'golden age' of antimicrobial discovery.[3] In 1943, streptomycin was discovered from actinomycetes in soil, inspiring several pharmaceutical companies to concentrate efforts on screening soil samples for further antimicrobial compounds from the 1940s to the 1960s. This was highly successful, ultimately producing many of the antimicrobial drugs still in use today.[3,4] When the yield of these phenotypic screening methods for natural products declined, medicinal chemistry and molecular genetics approaches were employed to enhance the utility of existing compounds.[5] Later, more sophisticated high throughput screening methods were aimed at the discovery of novel synthetic antimicrobial compounds.[3,5,6] Unfortunately, these were not nearly as productive as the early discovery approaches had been and widespread divestment in antimicrobial research followed.[7,8]

1.1.2 The critical importance of dose selection

Interest in antimicrobial PK-PD arose soon after the discovery of antimicrobial drugs, with early observations that the efficacy of some antibiotics (e.g. penicillin) is determined by the duration of drug exposure, while for others (e.g. streptomycin), the rate of bactericidal activity depends on peak drug concentration.[9,10] Summary PK measures such as the maximum drug concentration (Cmax), the area under the concentration-time curve (AUC) and the duration of drug exposure in a dosing interval can be expressed relative to the minimum inhibitory concentration (MIC) of the infecting organism. These PK-PD indices – Cmax/MIC, AUC/MIC and T/MIC - have been determined using dose-fractionation studies for virtually every antimicrobial class in use today and related to their efficacy *in-vitro* or in animal models. Moreover, the magnitude of PK-PD indices predictive of therapeutic efficacy in preclinical studies generally correlates well with the magnitude of PK-PD index required for efficacy in human therapy and thereby enables results to be bridged to humans.[11,12] Only in the past two decades, however, has the inclusion of PK-PD analysis in drug development been formally endorsed by the US FDA[13] and the EMA.[14] Prior to this, many antimicrobial agents were developed and brought to market without detailed preclinical pharmacometric analyses. For this reason, the recommended dosing regimen for many antimicrobial drugs is based on experience and habit rather than quantitative methods to optimise dosage or treatment schedule.[11,15,16] This raises the risk of

supratherapeutic levels and potential toxicity, and/or subtherapeutic levels leading to low efficacy and encouraging the selection of resistant microbial strains.

Indeed, simultaneous with the stalling of antimicrobial drug discovery has been the inexorable rise of antimicrobial resistance (AMR), which has reached critical levels worldwide.[17-19] AMR threatens to undo progress made towards many of the Sustainable Development Goals and is on course to cause 10 million annual deaths worldwide by 2050.[20] Low- and middle-income countries are forecast to be hardest hit and a reduction in annual global gross domestic product of 3.8% by 2050 is predicted.[21] A number of initiatives have been launched to search for and develop new antimicrobial agents[22] and innovative commercial incentive schemes have arisen.[23] While waiting for these strategies to bear fruit, it is clear that the current antimicrobial armamentarium must be preserved and utilised optimally. Post marketing PK-PD analyses present a method for scientifically designing or re-designing antimicrobial treatment regimens to select dosages that generate therapeutic drug levels and achieve optimal PD effect, whilst minimising the risk of toxicity and the selection of resistant organisms.[24] In addition, PK-PD analyses are increasingly employed to refine dosing regimens for special populations including children,[25,26] people with renal impairment[27] and obese patients,[28] and to assess the clinical relevance of patient characteristics and extrinsic factors that may influence PK.[24]

1.2 The optimised use of antifungal drugs is an area of urgent priority

1.2.1 The global burden of invasive fungal infections

Fungal infections cause enormous global morbidity and mortality, including an estimated 13 million life-threatening infections and 1.6 million deaths annually.[29] This is comparable to estimated annual deaths from tuberculosis[30] and four-fold the number caused by malaria.[31] Invasive fungal infections (IFIs) rarely occur in patients with intact immune systems, and the current burden of IFIs is largely reflective of immunocompromise resulting from the rise over recent decades in HIV/AIDS and iatrogenic immunosuppressive therapy. Despite the burden of suffering they inflict, fungal infections have historically been neglected by the research and funding community compared with bacterial or viral infectious diseases.[32,33] Between 2000 and 2017, funding from public and philanthropic actors in the G20 countries was US$ 1.7 billion for mycology – almost forty times less than funding for virology (US$ 62.9 billion), sixteen times less than funding for bacteriology (US$ 27.3 billion) and seven times less than funding for parasitology (US$ 11.5 billion).[34] The need for greater investment in the identification and management of IFIs is clear, and nowhere more so than in HIV-infected populations.[35] Despite great progress having been made with antiretroviral coverage globally, this has been insufficient to reduce mortality from IFIs.[36] While fewer patients are presenting to HIV services for the first time with advanced immunosuppression, this has been offset by increased numbers of individuals who present with low CD4+ counts having defaulted or failed ART.[36]

1.2.2 Cryptococcal meningoencephalitis and talaromycosis

Of the major HIV-associated mycoses, cryptococcal meningoencephalitis and disseminated talaromycosis are archetypal conditions to illustrate the unmet medical need of IFIs and they are the focus of this thesis. Cryptococcal meningoencephalitis is a preventable and treatable infection that is nevertheless associated with devastating morbidity and mortality. It is caused by the ubiquitous basidiomycete yeasts *Cryptococcus neoformans* and *Cryptococcus gattii.*[37] Among PLHIV there are estimated to be 223,000 incident cases of cryptococcal meningoencephalitis per year, and 181,000 deaths.[38] Cryptococcal meningoencephalitis is the most common fungal brain infection worldwide and the second most frequent cause of HIV-associated mortality after tuberculosis.[38,39] The vast burden of disease resides in low- and middle-income countries (LMICs),[38] where mortality even with the best available antifungal treatment regimen and even in a clinical trial setting is 24% at ten weeks.[40] In 2018 cryptococcal meningitis received just 0.2% (7.7 million USD) of available relevant research and development funding, compared with 17% (684.6 million USD) of funding directed towards R&D for tuberculosis and 16% (663.4 million USD) for malaria.[41]

Talaromycosis is caused by the dimorphic fungus *Talaromyces marneffei*. *T. marneffei* grows as a mould at 25 degrees Celcius and as a yeast at 37 degrees Celcius.[42] It is endemic to tropical Southeast Asia and in particular Vietnam, Thailand, Laos, Cambodia, Myanmar, Southern China, Hong Kong, Taiwan and Northwestern India.[43] In these regions, talaromycosis accounts for up to 15% of

AIDS-related hospital admissions.[44,45] Mortality from treated disseminated infection with *T. marneffei* is as high as 30 – 40%.[42,46,47]

Cryptococcal meningoencephalitis and talaromycosis share some sombre statistics; box 1.1.

Box 1-1: Epidemiological similarities between cryptococcal meningoencephalitis and talaromycosis

Both cryptococcal meningoencephalitis and disseminated talaromycosis are uniformly fatal without treatment.[46,48]

Both cryptococcal meningoencephalitis and disseminated talaromycosis disproportionately affect patients in LMICs.[38,42]

Incidence of both cryptococcal meningoencephalitis and disseminated talaromycosis has failed to decrease in PLHIV despite wider access to ART.[36,47]

Limited treatment options exist for both cryptococcal meningoencephalitis and disseminated talaromycosis, particularly in LMICs.[36,49]

The first line antifungal in both cases (amphotericin B deoxycholate) is associated with severe, life-threatening toxicity.[50-56]

1.2.3 The antifungal armamentarium is sorely limited

Clinical outcomes from IFIs are unacceptably poor and failure to achieve 50 percent treatment success is common.[35] Just four antifungal drug classes are currently licensed for the treatment of human mycoses. The polyenes (such as amphotericin B deoxycholate (DAmB) and liposomal amphotericin B (LAmB)) disrupt fungal cell membrane integrity. The pyrimidine analogue 5-flourocytosine (5-FC) was originally developed as an anti-cancer drug and acts by inhibiting DNA

synthesis. Azole drugs (for example fluconazole, itraconazole and voriconazole) inhibit lanosterol 14-α-demethylase, thereby blocking the synthesis of ergosterol, a key component of the fungal cell wall. Echinocandins inhibit (1-3)-β-D-glucan synthase, also interfering with cell wall formation. Of note, *Cryptococcus* spp. are intrinsically resistant to echinocandins[57-59] and *T. marneffei* displays limited sensitivity to this class of antifungals while in yeast form.[60] Echinocandins are not recommended for either infection, so just three antifungal drug classes are available for their treatment.

For cryptococcal meningoencephalitis, the reality in the majority of settings that bear the greatest burden of disease is that the only drug available for patients is fluconazole. The reason that neither polyenes or flucytosine are routinely administered in LMICs is multifactorial and includes lack of access to those drugs, challenges in administration and managing drug-induced toxicity, and concerns related to drug-drug interactions.[36,61] Fluconazole monotherapy is a wholly inadequate treatment strategy for cryptococcal meningoencephalitis, associated with between 40% and 70% mortality.[62-65] Since fluconazole is fungistatic rather than fungicidal, patients who survive an episode of cryptococcal meningoencephalitis must continue taking this drug for at least 12 months or until immune reconstitution.[52] Moreover, with current dosing strategies, fluconazole monotherapy promotes the expansion of azole-resistant subpopulations during treatment.[66,67] Primary resistance to amphotericin B has not been reported and cases of secondary resistance are vanishingly rare.[68-70] While primary resistance of

Cryptococcus spp. to flucytosine is uncommon,[71] the development of secondary resistance on treatment in up to 57% of cases precludes its use in monotherapy.[72]

Novel treatment options for IFIs are urgently required. The antifungal development pipeline has been characterised by slow progress for several decades. However, several novel agents are currently progressing through development (table 1.1). Of particular note are: APX001 and APX2096, of the novel Gwt1 inhibitor class of antifungals that demonstrate synergy with fluconazole; VT-1129 and VT1598 (Mycovia), tetrazole agents that demonstrate enhanced selectivity for fungal over mammalian cytochrome P450 enzymes compared with conventional azoles; T-2307 (Appili Therapeutics), an allylamine that inhibits mitochondrial membrane potential; and MAT2203 (Matinas), an encochleated formulation of amphotericin B that can be administered orally. A modified-release formulation of flucytosine is the subject of an ongoing project run by the Drugs for Neglected Diseases Initiative (DNDi).[73]

Table 1.1: Potential drugs in development for cryptococcal meningoencephalitis

Drug/ compound (Developer)	**Phase of development**	**Mechanism of action**	**Administration**	**Clinical PK profile**	**Potential utility for CME**	***In vitro* efficacy comparable to AmB?**	**Clinical tolerability**	**Refs**
APX001/ fosmanogepix (Amplyx)	Phase II.	Inhibits fungal wall transfer protein, Gwt1.	IV/ oral	NA	In combination with other antifungals; demonstrates PD synergy with fluconazole.	✓	Well tolerated in first-in-human studies.	130,131
SUBA-itraconazole (Mayne Pharma)	Phase II.	Inhibits ergosterol synthesis in cell membrane. (Itraconazole has shown inconsistent outcomes in CME and has highly variable PK.)	Oral	Rapid attainment of therapeutic plasma levels. Modest PK variability.	Potential for maintenance therapy in place of fluconazole.	..	Better tolerated than conventional itraconazole; mucositis and hepatotoxicity reported.	132
VL-2397 (ASP2397)	Early termination of phase II trial for aspergillosis – business decision.	Unknown intracellular target.	IV	Non-linear saturable binding kinetics.	In combination with other antifungals.	..	Well tolerated up to 1200 mg.	133
ATI-2307 (Appili Therapeutics)	Phase I complete; phase II planned for 2022.	Allylamine that inhibits mitochondrial membrane potential	Subcutaneous	NA	Greater potency than standard of care agents.	✓	Well tolerated at anticipated therapeutic dosages.	134,135
AR-12 (Arno Therapeutics)	Phase I.	Celecoxib derivative. Inhibits fungal acetyl-coA synthetase.	Oral	Highly variable PK.	In combination with other antifungals; demonstrates PD synergy with fluconazole.	..	Well tolerated at 800 mg BID.	136

Encochleated amphotericin B/ MAT2203 (Matinas)	Pre-clinical; FDA have granted QIDP and Fast Track designations.	Binds to ergosterol; fungicidal via pore formation in cell membrane.	Oral	NA	Potential oral alternative to current AmB preparations.	✓	Promises lower renal toxicity than IV formulations of AmB. Mitigates challenges associated with IV administration.	[137]
VT-1129 (Mycovia)	Pre-clinical; FDA have granted QIDP and Fast Track designations. Investigational New Product application filed with FDA.	Tetrazole: Inhibits ergosterol synthesis in cell membrane by selectively targeting CYP51.	Oral	NA	Potential low-cost agent for fluconazole-resistant strains of *Cryptococcus.*	..	NA	[138]
APX2096 (Amplyx)	Pre-clinical.	Gwt1 inhibitor prodrug; inhibits fungal wall transfer protein.	Oral/ intraperitoneal	NA	32-fold lower MIC against *C. neoformans* compared with APX001. Good CNS penetration. Demonstrates PD synergy with fluconazole.	✓	NA	[139]
Aureobasidin A (AureoGen Biosciences/ Merck & Co.)	Preclinical. Discovered 1989 – license patent granted in 2007 for further development.	Inhibits sphingolipid synthesis in cell membrane.	Oral/ subcutaneous	NA	Potent anticryptococcal activity *in vitro*.	..	NA	[133]

Table from [36]

CME: Cryptococcal meningoencephalitis; PK: pharmacokinetic; PD: pharmacodynamic; AmB: amphotericin B; BID: *bis in die* (twice per day); IV: intravenous; FDA: Food and Drug Administration. QIDP: Qualified Infectious Disease Product.

1.2.4 Antifungal pharmacokinetic-pharmacodynamic analysis is a neglected but vital field

The volume and scope of progress in antifungal drug development is both welcome and long overdue. It will likely be some years before this progress translates to expanded formularies available to treat IFIs in the clinical setting. In the meantime, it is paramount that the antifungal drugs currently available are used optimally. Despite over half a century of experience with both amphotericin B deoxycholate and flucytosine in the treatment of cryptococcal meningoencephalitis, the best regimen remains unclear. Numerous clinical trials have been conducted to investigate different dosages and treatment strategies using the limited drugs available for both cryptococcal meningoencephalitis and talaromycosis.[40,50,62,74-77] PK-PD analysis offers a more precise mechanism to understand the relationship between drug dosages, metabolism and antifungal effect. This understanding can then be harnessed, and dosage regimens manipulated in hypothetical scenarios to explore the impact of such manipulations on PD outcome. Compared with serial clinical trials, PK-PD approaches offer vastly enhanced efficiency, reduced cost and most importantly, reduced risk to patients.

In summary, there is a pressing need to optimise the use of antifungal drugs through improved understanding of their PK-PD, for several reasons:

1. Current treatment strategies for IFIs are inadequate, as evidenced by unacceptably poor clinical outcomes.

2. There is an exceptionally limited antifungal armamentarium available for the treatment of IFIs and those drugs that are available must be preserved through optimal use.
3. The practice of conducting serial clinical trials to answer questions of dosage without PK-PD support is inefficient in terms of time and cost, and potentially risky for trial participants.

1.3 Factors that influence antifungal pharmacokinetics

The key to successful antimicrobial pharmacotherapy is the attainment of effective drug concentrations at the target site, which in turn is influenced by the pharmacological properties of the drug, the pathology inflicted by the disease itself, and the physiology of the patient concerned. An understanding of these variables and their interrelatedness is central to designing treatment regimens that capitalise on the opportunity for therapeutic success.

1.3.1 Pharmacological characteristics that influence treatment success

Elucidation of the pharmacological properties of antifungal agents has historically been lacking, compromising the development of optimised antifungal treatment regimens.[78] Several antifungal drugs exhibit nonlinear or highly variable PK to the extent that therapeutic drug monitoring (TDM) is indicated to avoid under- or over-dosing.[79] In addition, PK profiles in the bloodstream may not reflect those at the site of infection. This discordance in the shape of

concentration-time profiles between physiological compartments is termed hysteresis (see [80]). In human cryptococcal meningitis, plasma concentrations of fluconazole may be lower than, equivalent to or higher than those in the central nervous system (CNS) and this relationship can fluctuate during the course of treatment.[81] In rodent models, liposomal amphotericin B,[82,83] amphotericin B deoxycholate[84] and caspofungin[85] persist in tissues longer than their plasma levels would indicate, which provides a potential explanation for the persistence of antifungal activity despite negligible plasma levels.

The physicochemical properties of a drug directly influence the attainment and maintenance of therapeutic concentrations at the site of infection. These properties include the molecular weight of the compound, its lipophilicity, protein binding and affinity for relevant efflux pumps. They are highly variable and are inconsistent between and within drug classes. The physicochemical properties of antifungals that influence PK-PD are summarised, with reference to CNS penetration, in table 1.2.

Table 1.2: Physicochemical properties of antifungal drugs

Drug	Molecular weight (g/mol)	Particle size (µm)	LogP	LogD at pH 7.4 (indicative of lipophilicity)	Plasma protein binding (%)[c]	Efflux pump affinity (P-gp substrate)	Correlation of measurable CNS concentration with biological activity	References
Fluconazole	309		2.17	0.5	10	No	Good	[80,86-90]
Itraconazole	705		6.99	4.9	98	Yes	Poor	[80,87-90]
Voriconazole	349		2.56	2.1	58	No	Good/ variable	[80,88-90]
Posaconazole	700		6.1	4.4	99	Yes	Poor	[80,88-90]
Isavuconazole	718		-3.33	3.6	99	No	Good	[80,88-92]
DAmB	924	<0.4	0.95	-2.8	>95	No	Poor	[80,88-90,93,94]
LAmB	924	0.05 - 0.08	0.95	-2.8	>95	Contentious	Poor	[80,88-90,94-96]
ABLC	924	1.6 – 11	0.95	-2.8	>95	No	Poor	[80,88-90,94]
ABCD	924	0.12 – 0.14	0.95	-2.8	>95	No	Poor	[80,88-90,94]
5FC	120		-0.89	-2.34	5	No	Good	[80,87-90]
Caspofungin	1093		-2.8	-3.88	98	No	Good	[80,88-90,97,98]
Micafungin	1140		-3.8	-1.62	98	No	Good	[80,88-90,97,98]
Anidulafungin	1291		0.21	-3.32	98	No	Good	[89,98,99]

Table adapted from [100]

1.3.2 Pathological determinants of drug concentrations at the site of infection

The pathological changes induced by IFIs exhibit huge inter- and intra-individual heterogeneity. Aspergillus has a predilection to angioinvasion and causes infarction and haemorrhage as it spreads haematogenously, usually from the primary site of the lungs to the brain and less commonly to other organs including the skin, kidneys, heart and liver.[101,102] The clinical manifestations of aspergillosis are related to underlying immune status and in particular neutropenia.[101] Invasive candidiasis may spread haematogenously to cause endophthalmitis, endocarditis, osteomyelitis or a range of other deep organ infections. Alternatively, *Candida* may be directly inoculated from a foreign device, for example to the peritoneum from a peritoneal dialysis catheter or following abdominal surgery.[103] Pathogenic species of *Cryptococcus* are strongly neurotropic and tend to disseminate to the CNS from the primary infection site of the lungs (where infection may be asymptomatic).[104-106] It is thought that talaromycosis is acquired through inhalation of environmental conidia, which then disseminate systemically through the reticuloendothelial system.[42] The partitioning of antifungal agents from the bloodstream to these organ sites is highly variable and this augments the PK variability presented by plasma profiles alone. Furthermore, at the sub-organ level, infected tissue compartments may be pharmacologically distinct. In the example of cryptococcal meningoencephalitis, there are multiple sub-compartments within the CNS such as the meninges, the cerebrospinal fluid (CSF), the brain parenchyma and the ventricles. Within the brain parenchyma itself, large cryptococcomas are common.[104,107] Concentrations

of antifungal agents in CNS compartments may therefore differ markedly from one compartment to another, as well as from levels measured in plasma. Pathophysiological considerations are key to understanding whether a drug is likely to reach therapeutic levels at the site of infection.

1.3.3 Attainment of target drug concentrations depends on the patient being treated

The impact of patient characteristics such as age, renal function, liver function, weight and body mass on PK has long been recognised. Through its impact on the function of multiple organ systems, critical illness can cause profound alterations in drug exposure. Since IFIs predominantly affect persons who are severely immunosuppressed, many of these patients are critically unwell - either with advanced HIV infection, following organ transplantation or as a consequence of immunosuppressive chemotherapy. In addition, these patients are frequently subject to significant polypharmacy, raising the risk of drug-drug interactions. The effect of critical illness on antifungal drug exposure has been described in multiple clinical studies encompassing all antifungal drug classes in clinical use.[108-113] However, since physicochemical properties of antifungal agents are inconsistent within drug classes, the impact of critical illness on PK cannot be generalised at the class level. Fluconazole AUC increases with deteriorating renal function in critical illness until renal replacement therapy is required, at which point the AUC is lower than that in patients with normal renal function.[114] Isavuconazole PK parameters, in contrast, are reported to be similar across

different patient populations regardless of disease or physiological status.[115] Micafungin AUC decreases by approximately 40% in patients admitted to intensive care facilities[116] and in patients with HIV infection,[117] compared with healthy volunteers.[27] Anidulafungin AUC is 22% lower in critically ill patients[118] than it is in healthy volunteers.[27] Model-simulated AUC values for amphotericin B deoxycholate are comparable between healthy volunteers and patients living with advanced HIV.[119,120] In general, PK variability increases in critically ill patients, whose physiology is hugely heterogeneous, adding further potential compromise to the efficacy of empiric dosing of antifungals in this patient group.[121] This variability results from altered drug clearance mechanisms – critically ill patients may have increased or decreased renal clearance; they may undergo renal replacement therapy or extracorporeal membrane oxygenation – as well as changes in volume of distribution caused by shifts in fluid balance including those caused by fluid resuscitation and oedema. In certain populations, food availability may be problematic, which can have a significant impact on antifungal bioavailability – for example in the case of voriconazole[122] and itraconazole.[123,124] Clearly, PK parameters cannot be assumed to be equivalent between healthy volunteers and the majority of patients suffering IFIs; population-specific analyses are key to optimising therapy.

1.4 Non-pharmacological factors that influence antifungal pharmacodynamics

The study of pharmacodynamics concerns the relationship between the concentration of a drug at its site of action, and its associated effect. While infection site PK is influenced by the physicochemical, pathophysiological and patient factors outlined above, the attainment of specific antifungal drug concentrations at the site of infection does not necessarily result in a predictable PD response. Asides from PK, PD is influenced by factors specific to both the host and the infecting pathogen itself.

1.4.1 The host response to invasive fungal infection

Many IFIs – for example cryptococcosis, talaromycosis, aspergillosis and histoplasmosis – are primarily acquired through inhalation of environmental conidia. In the setting of immune dysfunction and particularly defects in cell-mediated immunity, such as those induced by advanced HIV or immunosuppressive therapy, inhalation of fungal spores results in disseminated disease with multi-organ involvement.[104,125]

1.4.1.1 Macrophages can be instrumental in both clearance and propagation of infection

The host immune response to pathogenic fungi is complex and requires coordination between multiple innate and adaptive immune mechanisms.[126,127] In

the case of cryptococcal infection, inhaled cryptococcal spores are phagocytosed by alveolar macrophages, which present the first line of immune defence.[128] After phagocytosis, macrophages undergo rapid maturation with acidification and lysosomal fusion.[129-131] This triggers the release of proinflammatory cytokines and chemokines, regulates antigen presentation to T-cells, and promotes the recruitment of monocytes and neutrophils to the site of infection.[132,133] The aim of this process is sterilization or containment of infection within a granuloma.[126] However, cryptococcal cells can survive and replicate within host macrophages owing to a combination of the antioxidant properties of the cryptococcal capsule,[134] permeabilization of the phagolysosome,[135] and cryptococcal degradation of urea to CO2 and ammonia to limit phagolysosomal acidification.[136,137] Similarly, conidia of *T. marneffei* are phagocytosed by alveolar macrophages,[138] but are able to survive intracellularly thanks in part to Mp1p, a mannoprotein and virulence factor in the fungal cell wall.[139]

The effect of macrophage activity is therefore not straightforward, being involved in control of infection, as well as persistence and dissemination of disease.[126,140] Dominance of intracellular cryptococcal proliferation early in infection appears to protect host tissues from damage on one hand, while also hindering effective immune responses by reducing pro-inflammatory immune signalling.[141,142] Evidence for the apparently conflicting roles of macrophages in cryptococcal disease is summarised in table 1.3.

Table 1.3: The conflicting roles of macrophages in cryptococcal meningoencephalitis

Macrophage role	Evidence	Reference(s)
Macrophages benefit the immune response to cryptococcal disease		
Macrophages appear to be required to control fungal burden	Macrophage depletion leads to uncontrolled cryptococcal proliferation (models using zebrafish and rats)	141,143
	Alveolar macrophage activation is associated with intrapulmonary cryptococcal clearance	144,145
Macrophage depletion leads to host death	Mortality was universal and occurred within days in setting of macrophage depletion in an animal model of cryptococcal meningoencephalitis	146
Cryptococci have evolved to evade phagocytosis	The large cryptococcal cell capsule protects from phagocytosis and promotes virulence	147,148
Classical, pro-inflammatory macrophage activation is associated with better host outcomes	This is evident in experimental animal cryptococcosis models …as well as from clinical data	149-151 152-155
Macrophages contribute to the pathogenesis of cryptococcal disease		
Macrophages enable persistence and proliferation of cryptococcal cells	The majority of cryptococci become intracellular in the first hours of infection	141,156
	Cryptococcal cells can survive in the intracellular environment	135,157
	Early intracellular cryptococcal proliferation drives increases in fungal burden (models using zebrafish and mice)	129,141,143
Macrophages are involved in dissemination of cryptococcal cells	Macrophage depletion late in infection protects against dissemination of infection in experimental cryptococcosis in mice	158
	Cryptococcal cells can be transferred from one macrophage to another	159,160

1.4.1.2 T helper lymphocyte responses determine macrophage polarisation

Additional insight into the opposing roles of macrophages in cryptococcal disease can be found in studies of their activation pathways (figure 1.1). Classically activated, pro-inflammatory (M1) macrophages are associated with clearance of fungal burden, whereas alternative (M2) macrophage activation is associated with cryptococcal proliferation and dissemination.[161,162] Macrophage polarisation towards M1 or M2 phenotypes is itself stimulated by cytokines released by T helper lymphocytes, dendritic cells and natural killer cells and depends on a delicate balance between Th1- and Th2-type immune responses.[126,163] The burden of cryptococcal disease in people living with HIV (PLHIV) is plain evidence of the importance of a healthy $CD4^+$ T helper cell count in the immunological control of this infection.[38] The $CD4^+$ T-cell predominance observed in blood and CSF in healthy persons[164] is replaced by $CD8^+$ T-cells in PLHIV.[154,165] In *in-vitro* and animal experiments, effective immune responses are characterised by a predominance of Th1-type responses, with IFN-γ and TNF-α/β secretion, classical macrophage activation and associated inflammation.[149,166-169] Murine experiments using antibody neutralisation or genetic interference to decrease the levels of Th1-type cytokines such as IL-12,[170] IL-18[171] and IFN-γ[172] have demonstrated decreased survival from cryptococcal infection compared with wild-type animals. Intriguingly, lack of TNF-α does not appear to influence mouse survival, but administration of TNF-α confers a survival advantage.[173]

Clinical data also support the benefit of Th1-type responses. Decreased Th1-type responses in peripheral blood with reduced levels of IL-12 and IFN-γ

independently predict 14-day mortality from HIV-associated cryptococcal meningoencephalitis.[153] In CSF, decreased levels of proinflammatory cytokines such as IL-5, IL-6, granulocyte-colony stimulating factor and IFN-γ are associated with higher fungal burden and slower clearance of infection.[154,155,174] Low levels of CSF IFN-γ are also predictive of early mortality in HIV-associated cryptococcal meningoencephalitis.[154] Conversely, increased release of the Th1-type cytokines IL-4, IL-6, IL-8, IL-17, IFN-γ and TNF-α in CSF have been associated with mortality benefit.[152,155,175]

In contrast to Th1-type responses, Th2-type responses are characterised by IL-4, IL-10 and IL-13 cytokine predominance with alternative (M2) macrophage activation.[150,151,169] Immune responses with Th2 predominance are associated with poor clinical outcomes in murine studies of cryptococcal meningoencephalitis,[176] increased levels of IL-4[170] and IL-13[150] being inversely proportional to survival. The association between increased Th2-type responses and decreased survival has not been replicated in clinical samples from patients with HIV-associated cryptococcal meningoencephalitis.[154,175] Whether the difference in this observation between murine and clinical studies relates to intrinsic differences between murine and human immune systems, or is a function of the dynamism of CSF cytokine profiles over time during cryptococcal infection of the CNS (the temporal study of which is unmatched in murine and human investigations), is not clear.[175]

Figure 1.1: Model of the adaptive immune response to Cryptococcus neoformans

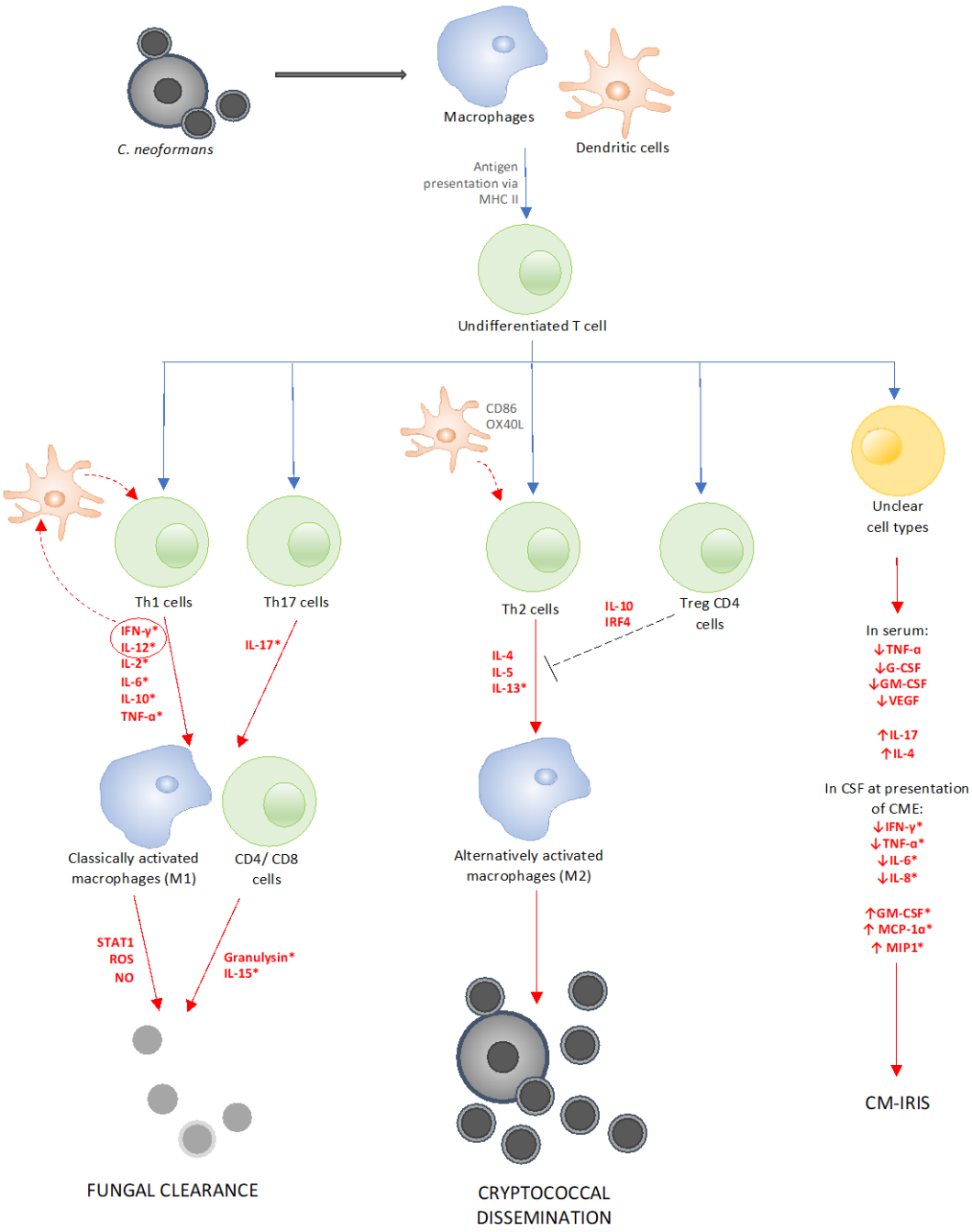

* indicates that the association of this cytokine/ chemokine with the indicated outcome has been demonstrated in clinical samples (as opposed to purely pre-clinical experiments).

Autopsy studies corroborate preclinical and clinical findings that a coordinated, pro-inflammatory, Th1-type response with classical macrophage activation is a beneficial immune reaction to cryptococcal meningoencephalitis. Post mortem, immunocompetent patients display typical inflammatory granuloma at the initial site of infection in the lungs, composed of dense aggregates of epithelioid macrophages and multinucleated giant cells containing numerous intracytoplasmic yeasts.[106,177] In the brain and spinal cord, there is prominent T-cell lymphocytic infiltration with granulomatous inflammation.[106] In contrast, autopsy studies of patients with HIV-associated cryptococcal meningoencephalitis demonstrate that in general, while inflammatory cells (predominantly macrophages) are present, they are few in number and are not epithelioid.[106] T-cells are scant and there is evidence of reduced antigen presentation.[177] In the lung, cryptococci are not contained within granulomas but are widely distributed both intra- and extracellularly.[177] In some cases there is massive proliferation of cryptococci in expanded alveoli, interstitial tissue and capillaries.[177] In the CNS too, a coordinated inflammatory response is lacking in patients with advanced HIV; T-cells are focally distributed and are not associated with either *C. neoformans* cells or macrophages.[106]

Taken together, these findings have generated interest in the potential role of IFN-γ, a key adaptive Th1-type cytokine, as an adjunct to antifungal therapy for HIV-associated cryptococcal meningoencephalitis. Inoculation of mice with an experimental strain of *C. neoformans* that produces IFN-γ resulted in the production of Th1-type cytokines in lungs, classical macrophage activation and

reduced pulmonary fungal burden.[178,179] Macrophages isolated from these mice were fungistatic against *C. neoformans ex vivo.*[179] Two clinical trials have demonstrated that administration of IFN-γ in combination with amphotericin-B therapy promotes an inflammatory response, increases fungal clearance from CSF and produces a trend towards improved survival.[174,180] Further work is needed to target and select those patients most likely to benefit from this immune adjuvant - likely those with minimal endogenous IFN-γ responses.[181] Another promising approach is the use of monoclonal antibodies directed against cryptococcal capsular polysaccharide. One such antibody, 18B7, has completed a phase I clinical trial.[182] In contrast, and in keeping with the beneficial role of inflammatory immune responses, a trial of the anti-inflammatory glucocorticoid dexamethasone as adjunctive therapy in HIV-associated cryptococcal meningitis was stopped early after showing no evidence of benefit and a trend towards increased mortality.[183] Patients in the adjunctive dexamethasone arm had more rapid declines in CSF-concentrations of the pro-inflammatory Th1-cytokine TNF-α over the first week of therapy.[184]

1.4.2 Characteristics of the infecting strain

1.4.2.1 Genotypic heterogeneity in fungal pathogens

IFIs do not result from infection with homogeneous strains of fungus. Rather, there is considerable pathogen variability both between and within patients. Molecular typing techniques have delineated five lineages of *C. neoformans*: VNI, VNII and VNB (which encompasses two distinct subdivisions

VNBI and VNBII)[185] are molecular types of *C. neoformans* var. *grubii*; VNIV corresponds to *C. neoformans* var. *neoformans*, and VNIII is the hybrid of var. *grubii* and var. *neoformans.*[186-188] Evidence suggests that an association between genotype, phenotype and virulence potential is likely.[189-192] Data from Botswana demonstrate significantly increased capsule thickness and cell diameter in VNBI isolates than either VNI or VNBII isolates, with worse mortality outcomes among patients infected with VNBI strains.[192] In Uganda, VNIII strains were found to be more strongly associated with mortality than other strains.[189] At the sub-lineage level, further clinical associations have been identified. Sequence type 5 strains of VNI isolated in Southeast Asia infect HIV seronegative patients significantly more frequently than they infect PLHIV.[190,191] In addition, better clinical outcomes from cryptococcal meningoencephalitis have been observed following infection with the VNIa-93 sub-clade which predominates in Uganda and Malawi, than with the VNIa-4 and VNIa-5 sub-clades which are common in Southeast Asia.[193]

Within an individual patient's infection there is also evidence of strain heterogeneity. Numerous clinical studies of infection with *C. neoformans* have shown that temporally distinct single-colony isolates from within the same episode of cryptococcosis or during relapse of infection represent different genotypes, suggesting that cases can be caused by infection with genetically distinct genotypes occurring in the environment.[67,194-197] With inadequate treatment such as that provided by fluconazole in monotherapy, genotypic heterogeneity in strains of *Cryptococcus* spp. expands during the course of infection.[67]

1.4.2.2 Phenotypic heterogeneity in invasive pathogenic fungi

Numerous pathogens are known to display phenotypic differences between individual cells of genetic clonality. Phenotypic heterogeneity enables adaptation to environmental stressors and the re-establishment of cell populations, and is essential to species survival.[198] It may also augment the virulence of a microbial population through enhanced pathogenicity or drug tolerance.[199] The clinical significance of microbial phenotypic heterogeneity has been extensively studied in mycobacteria[200-202] and other pathogenic bacteria.[203-205] The same concept applies to fungi, in which alterations in morphology can promote growth *in vivo*, mediate tissue damage, and enable evasion of host immune factors and recruitment of immune cells.[206-208]

Several *Cryptococcus* virulence factors have been characterised experimentally. These include induction of the cryptococcal polysaccharide capsule, production of melanin, production of extracellular vesicles, urease activity, thermotolerance and titan cell formation, and are summarized in table 1.4.

Table 1.4: Phenotypic virulence attributes of Cryptococcus neoformans

Virulence attribute	Mechanism of pathogenic action	References
Extracellular capsule production	Interferes with phagocytosis	209,210
	Promotes intracellular survival	129
	Disrupts antigen processing and presentation	133
	Protects against ROS	134
	Induces macrophage apoptosis	211
	Downregulates Th1 responses	212,213
	Induces soluble markers of Th2 responses	213-215
	Facilitates cryptococcal dissemination	216,217
Melanin deposition	Impedes phagocytosis of encapsulated cryptococcal cells	218,219
	Protects against ROS	220,221
	Increases antifungal tolerance	222,223
	Increases tolerance to fungicidal peptides	224
Extracellular vesicle production	Transport proteins associated with virulence	225
	Promote encapsulation of cryptococci	226 227 228
	Involved in melanin incorporation into cell wall	229
Urease activity	Promotes alternative macrophage polarization	230
	Increases phagolysosomal pH, possibly fostering dormancy and persistence	137,231
	Disruption of microvascular endothelium, enabling CNS invasion	232,233
Thermotolerance	Fundamental to establishing clinical infection	234
Titan cell formation	Evasion of phagocytosis	235,236
	Generation of genotypically heterogeneous daughter cells with varying propensity for immune evasion and drug resistance	237,238
	Association with Th2 immune responses	239

1.5 Assessing antifungal pharmacodynamics

Factors related to antifungal PK, host immunity and pathogen characteristics can be important sources of heterogeneity in PD response. Several established methods and models exist to assess and predict PD response.

1.5.1 Dynamic *in vitro* pharmacokinetic-pharmacodynamic models

1.5.1.1 Time-kill curves for in vitro pharmacodynamic experiments

Time-kill experiments are performed *in vitro* to record the response of a microbial population to drug exposure over time. This enables estimation of growth rate, death rate and the rate of emergence of resistance in a population. Antimicrobial drug concentrations in growth media can be altered over the course of an experiment or can remain static throughout. Various doses and drug combinations can be compared in terms of their PD effect. Time-kill experiments have been employed to investigate fungicidal activity for a range of antifungal compounds, including those pertinent to the treatment of cryptococcal meningoencephalitis and talaromycosis: amphotericin B,[240-243] flucytosine,[243,244] fluconazole,[242,245] itraconazole[245,246] and combinations of these agents.[243]

1.5.1.2 Hollow fibre infection models

The hollow fibre infection model (HFIM) is a dynamic *in vitro* model that enables simulation of PK profiles that mimic those observed in human studies. Two circuits are run in parallel, one of which represents the luminal PK

compartment, the other the extracapillary PD compartment, containing pathogens and/or cells. Drug-containing nutrient media is pumped through the luminal compartment, which includes porous hollow fibres. The flow rate in the luminal compartment is sufficient to result in equilibration of drug concentrations between the hollow fibres and the surrounding extracapillary space. Drug exposure of pathogens in the extracapillary compartment is controlled by altering the drug concentration in the nutrient media entering the capillary compartment. Drug-containing broth is removed from the circuit into a waste reservoir and replaced with fresh media at a rate proportional to the clearance rate observed for that drug/s in humans.

Using HFIMs it is possible to assess the impact of changes in drug exposure on microbial growth, microbial kill and the emergence of resistance. For example, a HFIM has been used demonstrate that when a wild-type laboratory strain of *C. neoformans* (H99) is exposed to low concentrations of fluconazole, any reduction in fungal burden is offset by the emergence of resistant subpopulations that are able to grow on agar containing 32 to 64 mg/litre of fluconazole.[66]

1.5.2 Animal models for the assessment of antifungal pharmacodynamics

Fungal disease models in animals differ in a number of fundamental ways to *in vitro* models. Central advantages and disadvantages of *in vitro* and *in vivo* infection models are outlined in table 1.5. Two animal models of cryptococcal meningoencephalitis have been developed. In the murine model, *C. neoformans* is inoculated either via inhalation to the respiratory tract,[247] or by intravenous

injection.[248,249] Predictable disseminated infection with encephalitis follows.[84] The volume of CSF in mice is too small to sample for quantitative cryptococcal cultures, however tissue homogenates can be used to generate PD read-outs following animal sacrifice. In the rabbit model of cryptococcal meningoencephalitis, both CSF and brain tissue samples can be used to quantify fungal burden. The former can be sampled serially to enable a PD profile to be examined in response to different dosing strategies and to mimic the seral CSF sampling possible in clinical trials of cryptococcal meningoencephalitis therapy.[250] By using animal models to demonstrate PD effect at the site of activity intended in human therapy (such as the CNS), drug penetration and efficacy at the infection site can be evaluated before progressing to clinical studies.

Table 1.5: Attributes of in vitro and animal pharmacodynamic studies

In vitro PD studies	**Animal PD studies**
Can precisely control pathogen drug exposure	Can study infection in specific body sites
In hollow fibre models, can closely mimic human PK profiles	Can evaluate host factors including immune response and protein binding
Can frequently resample PK and PD compartments	Can mimic human route of infection or dissemination of disease: inhalation, haematogenous, etc.
Can estimate 'pure' PK/PD target without interference of host factors	Refinement of models of particular diseases can yield robust and highly reproduceable experiments
Sophisticated models, for example of the BBB, can be used to study cellular mechanisms of pathogenesis as well as predict drug penetration into body compartments	PD readout can be the same as used in human patients – for example fungal burden in plasma or CSF
	Can account for heterogeneity in fungal virulence in response to host factors
	Cause of death can be uncertain, not reliable models for assessing IFI-associated mortality

PD: pharmacodynamic; PK: pharmacokinetic; CSF: cerebrospinal fluid; BBB: blood-brain barrier; IFI: invasive fungal infection

1.5.3 Clinical pharmacodynamic measurements

1.5.3.1 Minimum inhibitory concentrations, minimum inhibitory concentration breakpoints, and epidemiological cutoff values

While the study of genotypic and phenotypic heterogeneity between pathogenic strains of fungi provides valuable insights into pathogen-host interactions and the establishment of clinical infection, their relevance in the setting of antifungal therapy is not clear. In other words, if pathogenic fungi are subject to sufficient drug exposure, does this supersede the clinical impact of any virulence factors that may be present? Characterising strains according to their minimum inhibitory concentration (MIC) can function to capture microbial heterogeneity as it relates to the drugs available for treatment. The MIC of an antifungal agent to a particular organism is defined as the lowest concentration (in mg/L) of the drug that inhibits fungal growth.[251] MICs from clinical isolates assist in guiding therapy by indicating the susceptibility or resistance of an organism to an antimicrobial agent. In this way, the genotypic and phenotypic particularities of a strain are placed in context of whether they influence the strain's susceptibility to treatment. This analysis can be done on an individual patient level.

The classification of antimicrobials into time-dependent versus AUC- or Cmax-dependent PD effect conventionally uses the MIC of the infecting strain as the denominator in each PK-PD index (thus, time/MIC, AUC/MIC and Cmax/MIC). This approach has undoubtedly improved understanding of antimicrobial dosing. Over time, the interpretation of MICs has evolved to consider MIC breakpoints,

which are used to predict whether a microorganism is likely to respond *in vivo* to clinically relevant drug concentrations at the site of infection.[252] In the determination of MIC breakpoints, data such as known MIC distributions, resistance determinants, *in vivo* PK/PD indices and clinical outcomes are considered. By comparing the MIC of a particular strain to the consensus MIC breakpoint, drug-tolerant or resistant isolates can be identified. For antifungal agents, MIC breakpoints are exceptionally difficult to determine due to the paucity of clinical PK and outcome data.[252] An alternative MIC-based measure circumvents this lack of clinical information by aiming to estimate the *in vitro* efficacy of drugs: the epidemiological cutoff value (ECV). While they are unable to predict clinical success, ECVs can be used to predict drug-tolerant or resistant isolates in situations where a given agent has known activity against the fungal pathogen of interest, but sufficient data to establish MIC breakpoints do not exist. ECVs can be used for resistance surveillance at a population level.[253,254]

1.5.3.2 Drawbacks of using minimum inhibitory concentrations

Each of the assessments defined above place a high degree of confidence in MIC as a reliable and stable measurement. In reality, there are significant shortcomings to the use of MIC and MIC-derived measures to optimise therapeutic strategy. Firstly, MIC results have repeatedly been shown to vary between assays and laboratories.[255-257] Studies of inter-assay variability in yeast MIC have revealed considerable differences between visual methods, which are prone to observer bias, and spectrophotometric methods, which are more

objective by design.[258,259] For example, agreement between Etest and microdilution methods for testing itraconazole MICs against 9 strains of filamentous fungi vary from 0% to 100%.[260] Furthermore, agreement between antifungal MIC testing methods can depend on the fungal strain being examined and the growth medium used. Secondly, PK-PD indices that utilise MIC tend to assume a single static MIC value for the infecting organism of the patient being treated. This overlooks the fact that a patient may be infected with a number of microbial subpopulations simultaneously, the MICs of which may vary – or be 'heteroresistant'.[67] Thirdly, MICs for an individual patient's infection are often read a number of days following sample acquisition and treatment initiation, so that the result will not necessarily reflect the organisms currently causing pathology since these may have adapted in response to drug pressure.[67,261] Finally, the only pharmacodynamically active portion of drug is that which is not protein-bound. Protein binding varies considerably between anti-infective compounds and different patient populations may have different levels of plasma proteins available for binding, depending on their physiological state. Protein binding can be linear or non-linear, can alter according to the drug concentration in plasma and can have a significant impact on the exposure of pathogens to drug at the infection site. It is frequently only unbound drug that partitions to sites such as the CNS,[100] the skin and skeletal muscles.[261] Since PK-PD indices tend to use total, rather than unbound, drug concentration, this represents another limitation of the use of MICs in this context.

1.5.3.3 *Dynamic clinical biomarkers*

An alternative PD measure is to use a dynamic biomarker that is associated with clinical outcome. Examples in mycology include galactomannan for invasive aspergillosis and 1,3-β-D-glucan for disseminated candidiasis and invasive aspergillosis. For cryptococcal meningoencephalitis, early fungicidal activity (EFA) (i.e. a linear regression of $\log_{10}$ colony forming units (CFU)/mL of CSF vs. time) is routinely used as a primary endpoint for Phase II clinical studies and a secondary endpoint in Phase III trials.[40,74,262] This PD endpoint has been validated as a surrogate marker for mortality in multiple clinical studies, and EFA targets have been defined. Specifically, a pooled analysis of individual-level CSF data from 738 subjects suggests that an EFA of <0.20 Log_{10} CFU/mL/day versus >= 0.20 Log_{10} CFU/mL/day is associated with a hazard ratio for 18-week mortality of 1.60 (95% CI, 1.25 – 2.04, p=0.002).[263] A combined analysis of 501 ART-naïve patients demonstrated similarly that EFA values > 0.2 Log_{10}CFU/mL/day were associated with the greatest probability of survival.[264]

1.6 Pharmacokinetic-pharmacodynamic modelling

1.6.1 Introduction to pharmacokinetic-pharmacodynamic modelling

For the reasons outlined above, the prediction and evaluation of antifungal PK and PD is complex. Inter- and intra-individual variability in each contributing factor expands this complexity.[79,265] Nevertheless, the relationship between the concentration of a drug at its effect site and its PD effect is invariably better aligned than the relationship between the dose of a drug and its PD effect.

Antifungal PK-PD analyses provide supportive evidence that therapeutic effects are the result of drug exposure, are predictable and can be exploited for therapeutic benefit. Ideally, the information required to establish robust pharmacokinetic-pharmacodynamic (PK-PD) targets at the site of infection includes all of the points listed in box 1.2.

Box 1-2: Desirable information for the accurate setting of PK-PD targets for fungal infection

1. Principal PK parameter of interest, depending on whether drug activity is determined by maximum concentration (Cmax), area under the curve (AUC), or time above a given therapeutic threshold.
2. Drug susceptibility/ minimum inhibitory concentration (MIC) of the infecting fungus.
3. Magnitude of the PK-PD index required, in terms of the unbound concentration of drug that is sufficient to exert PD effect on the target organism.
4. Histopathology of site(s) of disease.
5. Rate constant describing the movement of drug from the circulation to the site of infection.
6. Rate constant(s) describing the movement of drug within anatomical sub-compartments of interest.
7. Rate constant(s) describing the elimination of drug from the target site.
8. Rate constant(s) describing the clearance of drug from the body.
9. Time-dependent differences in plasma and tissue drug concentrations (hysteresis).
10. PK parameters associated with toxicity in measurable physiological compartments (usually the systemic circulation).
11. Clinical and physiological covariates that influence the PK of the drug in question.
12. Population-level variability in each of these factors.

Adapted from [100]

Using this information, data can be modelled using a variety of approaches to predict clinical PK parameters and their association with PD outcomes. Classical population PK modelling (the 'top-down' approach) starts with the data and builds

a model comprised of theoretical, though not necessarily physiologically relevant, compartments. Physiologically based PK (PBPK) modelling (the 'bottom-up' approach) is a complementary technique that starts by considering the pharmacology of a drug at the organ or tissue level.[266] PK modelling provides a means of describing the statistical distribution of PK parameter estimates, so that sources of variability in those estimates can be explored through the examination of clinical covariates such as body size, weight and renal function. In addition, the effect of attributes of special populations can be explored – for example, ECMO in children[267] or renal replacement therapy in critically ill patients[268] - as can the influence of food[269] and genetic polymorphisms on the PK of a drug.[270] Population PK models derive mean parameter estimates, describe inter-individual variability and calculate residual variability as a sum of intra-individual variability, measurement error and model bias.[261]

1.6.2 Parametric versus non-parametric models

A number of established mathematical methods for population PK modelling exist. These can be broadly categorised into parametric and non-parametric modelling approaches. Parametric approaches assume that PK parameter values – for example volume, intercompartmental rate constants and clearance – have a Gaussian or log-normal distribution across the population.[261,271] Mean values are calculated for each PK parameter, as well as standard deviations to describe inter- and intra-individual variability, inter-occasion variability and residual variability. Overall parameter distributions are described in terms of

'fixed effects' (the mean parameter values) and 'random effects' (the standard deviations). Thus, parametric models are 'mixed effects' models and they enable a view of population PK that is constrained to assumptions made regarding the shape of PK parameter distributions prior to analysis of the PK data. The NONMEM programme (Icon plc) is the original example of software designed to perform parametric nonlinear mixed effects modelling.

In contrast, non-parametric PK modelling approaches apply no constraints to the parameter distributions whatsoever.[271] It is frequently the case that cohorts of patients comprise multiple subpopulations that handle drugs differently; for example, fast and slow metabolisers. Neither Gaussian nor log-normal distributions are able to describe such subpopulations, since in those cases the model PK parameter distributions are discrete rather than continuous.[271,272] Non-parametric approaches represent an attempt to estimate the precise, discrete PK parameter distributions for each patient under study. These models estimate the population distribution – which may contain multiple discrete spikes, rather than being a smooth continuous line – and reinforce it with up to as many support points as there are patients in the dataset. Each support point in a non-parametric model is a set of estimates for all discrete parameter values in the model, as well as a normalised estimate of the likelihood of that set of estimates in the population.[271,273] In principle, non-parametric methods more closely approximate the ideal (but impossible) scenario of having access to each patient's true PK parameter values in the population, than do parametric methods.[261] This

is because non-parametric models are built from the data rather than imposing any assumptions about the shape of the population distribution.

1.6.3 Pmetrics software for non-parametric pharmacokinetic-pharmacodynamic modelling

Non-parametric methods were initially described in the early 1980s[274,275] and were refined and improved over the following two decades.[276,277] The leading software for nonparametric unconstrained population modelling is Pmetrics,[273] an R package that encompasses Non-Parametric Adaptive Grid (NPAG) software. The NPAG software creates nonparametric population PK models consisting of discrete support points as described. NPAG models are mixed effects models, the (unconstrained) parameter values representing the random effects and the error model representing the fixed effects.[273] The error model comprises a polynomial equation to describe assay variance, plus one of either gamma, a multiplier of assay variance, or lambda, which is the additive term for assay variance.[273,278] Gamma and lambda are terms to account for extra process noise related to the parameter estimate, including errors in dosing and observation times.[278] NPAG is able to accurately identify PK outliers and subpopulations, as well as simulate populations in which dosing regimens have been manipulated to estimate PK in theoretical scenarios.[273] The simulator uses Monte-Carlo simulation to sample new sets of parameter values from the user-selected distributions described in the chosen PK-PD model.[278]

1.6.4 Pharmacokinetic-pharmacodynamic modelling of antifungal drugs

Many of the antifungal drugs in common use today - including amphotericin B, 5-FC, fluconazole and itraconazole - were developed before the routine use of modern PD approaches in drug development. Antifungal dosage guidelines are frequently based on experience rather than having a basis in PK-PD science. Pharmacometric tools offer an opportunity to evaluate established dosing practices and assess the likelihood, on a population level, that target PK parameters are being reached without undue risk of toxicity. Clinical attributes of the population under study can be interrogated for their influence on the attainment of target PK parameters. PD measures such as the MIC of the pathogen, the burden of infection (measured, for example, using quantitative cultures or described dynamically using EFA), and mortality outcomes, can be incorporated in PK-PD models. Hypothetical scenarios can be simulated to predict outcomes in response to changes in dosing strategy.

PK-PD modelling approaches have been applied to a range of clinical questions in antifungal therapeutics. Population PK models have been built from preclinical investigations of micafungin[279] and anidulafungin,[280] with Monte Carlo simulation used to bridge the results to neonatal populations at risk of *Candida* meningoencephalitis. Population PK modelling has been used to advocate for TDM of voriconazole[79,281] and against the necessity of TDM for isavuconazole.[282] A combination approach using PBPK modelling and incorporating published *in vivo* data has been used to predict drug-drug interactions with itraconazole.[283] Preclinical experiments using mouse and rabbit models of cryptococcal

meningoencephalitis demonstrated the non-inferior efficacy of abbreviated polyene regimens[83,84] and provided the basis for two large cryptococcal meningoencephalitis phase III clinical trials. The first was Antifungal Combinations for Treatment of Cryptococcal Meningitis in Africa (ACTA), which demonstrated the non-inferiority of one week of DAmB (1 mg/kg/day) plus flucytosine (100 mg/kg/day) followed by 7 days of fluconazole (1200 mg/day) versus regimens based on two weeks of DAmB, in terms of ten week mortality[14] and one year mortality.[57] The second trial is the ongoing AMBITION trial, which exploits the relative safety of LAmB and is designed to evaluate induction therapy with a single high dose of LAmB (10 mg/kg) plus 14 days of fluconazole (1200 mg/day) and flucytosine (100 mg/kg/day).[58]

1.7 Conclusion

The management of IFIs is an area of unmet medical need. Treatment options are profoundly limited, particularly in LMICs which bear the vast burden of HIV-associated IFIs. Cryptococcal meningoencephalitis and talaromycosis are model diseases to study in this regard, since mortality from both conditions is high, treatment regimens are suboptimal and PK-PD methodologies have not been extensively applied to attempt to address the issue of poor treatment outcomes in either disease. In addition, the role of host immune responses in clinical outcomes from HIV-associated IFIs requires further clarification, in particular phagocyte function.

1.8 Research objectives and overview of chapters

The overarching objective of this PhD is to describe the clinical PK-PD of currently available antifungal drugs for cryptococcal meningoencephalitis and talaromycosis. As described, this is both essential and challenging. Essential, because without a detailed understanding of the PK-PD of antifungal agents we use to treat these life-threatening infections, we cannot be certain that we are using those agents optimally and thereby maximising the likelihood of patient survival. Challenging, because PK-PD studies of drugs already in clinical use are limited by the inability to explore substantially different dosages and dosage regimens and confounded by pathophysiological alterations in the patients concerned. Nevertheless, these challenges also present opportunities because the activity of drugs can be assessed in the patient population in which they are most needed.

Chapters 2, 3 and 4 describe the population PK of antifungals in common use for cryptococcal meningoencephalitis. In chapter 2, the important question of the variability in CNS penetration of fluconazole is addressed. PK parameters derived from the population PK model are related to wild-type MIC distributions of fluconazole against *C. neoformans* and a meta-analysis of clinical trials reporting outcomes from the treatment of cryptococcal meningoencephalitis with fluconazole monotherapy is performed. Chapter 2 provides the pharmacological explanation for the long-recognised inadequacy of fluconazole monotherapy for cryptococcal meningoencephalitis. Chapter 3 describes a PK model of amphotericin B deoxycholate (DAmB), which is contextualised within a meta-

analysis of clinical trials that report outcomes from the treatment of cryptococcal meningoencephalitis with DAmB monotherapy. Chapter 3 demonstrates the limitations of relying on CSF sterility as a surrogate for mortality outcomes in cryptococcal meningoencephalitis and suggests additional contributors to death from cryptococcal meningoencephalitis. Chapter 4 describes the population PK of liposomal amphotericin B (LAmB) used in a novel regimen for cryptococcal meningoencephalitis, administered as a single high dose. A previously published PD model derived from murine data served as the basis for a bridging study that related PD outcomes in mice to those that would be expected in hypothetical human patients, using the posterior predictions from the clinical PK model and performing Monte Carlo simulations of various doses of LAmB. The necessity and limitations of this approach are discussed.

In chapter 5, the population PK and PD of itraconazole are described, based on data from a clinical trial that compared itraconazole to DAmB for talaromycosis. Itraconazole has an active metabolite, hydroxyitraconazole, so a model was constructed that accounted for the PK and PD of both agents. The analysis suggests that the failure of itraconazole to satisfy non-inferiority against DAmB in the clinical trial resulted from overwhelmingly low itraconazole PK parameters across the population. It provides a real-world example of the importance of a comprehensive consideration of PK-PD factors in a clinical drug trial before trial initiation, or at a minimum during the early stages of trial roll out.

Finally, chapter 6 considers the role of the host response in the outcome of cryptococcal meningoencephalitis. In keeping with the findings of chapter 3,

chapter 6 cautions against an overreliance on traditional PD biomarkers such as CSF sterility or fungicidal activity as indicators of mortality outcomes. A coordinated, proinflammatory immune response with associated increases in the phagosomal activity of neutrophils and monocytes is shown to correlate with favourable outcomes in terms of reduced CSF fungal burden at baseline, reduced lumbar puncture opening pressure and reduced mortality, in addition to increased EFA. More generally, chapter 6 demonstrates the importance of considering non-pharmacological factors in our attempts to understand patients' response to IFIs and their treatment.

2 Population pharmacokinetics and cerebrospinal fluid penetration of fluconazole in adults with cryptococcal meningitis.

2.1 Declaration regarding presentation of published work within postgraduate thesis

The work presented in this chapter has been published in a peer-reviewed journal, as follows: *Stott KE, Beardsley J, Kolamunnage-Dona R, Castelazo AS, Kibengo FM, Mai NT, Lê Nhu'Tùng N, Cuc NT, Day J, Hope W. Population pharmacokinetics and cerebrospinal fluid penetration of fluconazole in adults with cryptococcal meningitis. Antimicrobial Agents and Chemotherapy. 2018 Sep 1;62(9).*

As the first author of this publication, I curated the data for analysis, constructed and validated the PK model, simulated hypothetical dosing regimens, performed a probability of target attainment (PTA) analysis and performed meta-analyses of clinical outcomes. I wrote the first draft of the manuscript and all co-authors approved the final version for publication. All co-authors have granted their permission for this published manuscript to be re-formatted and included in this postgraduate thesis – see appendix A.

2.2 Abstract

Robust population pharmacokinetic (PK) data for fluconazole are scarce. The variability of fluconazole penetration into the central nervous system (CNS) is not known. A fluconazole PK study was conducted in 43 patients receiving oral fluconazole (usually 800 mg q24h) in combination with amphotericin B deoxycholate (1 mg/kg q24h) for cryptococcal meningoencephalitis. A 4-compartment PK model was developed, and Monte Carlo simulations performed for a range of fluconazole dosages. A meta-analysis of trials reporting outcomes of cryptococcal meningoencephalitis patients treated with fluconazole monotherapy was performed. Adjusted for bioavailability, the PK parameter means (standard deviation, SD) were: clearance, 0.72 (0.24) litres/hour; volume of the central compartment, 18.07 (6.31) litres; volume of CNS compartment, 32.07 (17.60) litres; first-order rate constant from central to peripheral compartment, 12.20 (11.17) $hours^{-1}$; from peripheral to central compartment, 18.10 (8.25) $hours^{-1}$; from central to CNS compartment 35.43 (13.74) $hours^{-1}$; from CNS to central compartment 28.63 (10.03) $hours^{-1}$. Simulations of area under concentration-time curve resulted in median (interquartile range) values 1143.2 (988.4 – 1378.0) mg.h/litre in plasma and 982.9 (781.0 – 1185.9) mg.h/litre in cerebrospinal fluid (CSF) after a dosage of 1200mg q24h. The mean simulated ratio of AUC_{CSF}:AUC_{plasma} was 0.89 (SD 0.44). The recommended dosage of fluconazole for cryptococcal meningoencephalitis induction therapy fails to attain the PD target in respect to the wild-type MIC distribution of *C. neoformans*. The meta-analysis

suggested modest improvements in both CSF sterility and mortality outcomes with escalating dosage. This study provides the pharmacodynamic rationale for the long-recognised fact that fluconazole monotherapy is an inadequate induction regimen for cryptococcal meningoencephalitis.

2.3 Introduction

Mortality from cryptococcal meningitis remains unacceptably high. More than 90% of the estimated 223,100 annual incident cases of cryptococcal meningitis occur in Sub-Saharan Africa and Asia-Pacific regions.[38] The most effective regimen for induction is amphotericin B deoxycholate and flucytosine.[40,74] However, access to these drugs is limited in many regions where the burden of cryptococcal meningitis is greatest.[36,284,285] In these settings, high-dose fluconazole is used for induction monotherapy, despite consistent evidence of reduced survival in comparison with other agents and combinations.[62,65,286]

Fluconazole was discovered by Pfizer Inc. (Sandwich, UK) in 1978.[287] The objective was to discover an orally bioavailable agent for the treatment of invasive mycoses with a lower propensity to develop resistance than flucytosine.[287] Fluconazole inhibits cytochrome P450-dependent demethylation of lanosterol in the ergosterol biosynthetic pathway.[288] The ratio of the area under the concentration-time curve (AUC) to the minimum inhibitory concentration (MIC) is the pharmacodynamic (PD) index that best links drug exposure of fluconazole with the observed antifungal effect.[248,289]

Successful antimicrobial therapy within the central nervous system depends on the achievement of effective drug concentrations within relevant sub-compartments that include the cerebrum, meninges and CSF.[290] Fluconazole has a low molecular weight (approximately 300g/mol), is weakly protein bound and is not known to be a substrate for central nervous system (CNS) efflux pumps.[88,89] Its ability to partition from the endovascular compartment into the CNS has been established in laboratory animal models[291,292] and clinical studies.[293,294] Brain:plasma penetration ratios up to 1.33 have been reported in humans.[294] However, there is a surprising paucity of population pharmacokinetic (PK) data for fluconazole in all clinical contexts. Furthermore, the extent and variability of penetration into the CNS is not known.

The primary aim of this study was to quantify the extent and variability of CNS penetration of fluconazole in adults with cryptococcal meningitis. We developed a population PK model that quantified the inter-individual variability in drug exposure in plasma and cerebrospinal fluid (CSF). We investigated the impact of a range of clinically relevant covariates on fluconazole PK. Monte Carlo simulation was used to assess the implications of PK variability in terms of achieving fluconazole PD targets. Finally, we conducted a meta-analysis of clinical trials of fluconazole monotherapy to estimate the contribution of dosage to clinical outcome.

2.4 Materials and Methods

2.4.1 Clinical pharmacokinetic studies

Patients from whom plasma and CSF samples were obtained for this PK study have been described previously.[262] Adult patients were initially recruited from a multi-centre randomised controlled trial of adjuvant dexamethasone in HIV-associated cryptococcal meningitis. The trial is reported elsewhere (n=3, International Standard Registered Clinical Number 59144167).[183] Following the early cessation of this trial, patients were recruited from a prospective descriptive study at the same sites (n=40). Study sites were The Hospital for Tropical Diseases in Ho Chi Minh City, Vietnam, and Masaka General Hospital, Uganda. The study protocols were approved by the relevant institutional review boards and regulatory authorities at each trial site and by the Oxford University Tropical Research Ethics Committee.

Fluconazole was administered orally. Where conscious level did not enable oral administration, fluconazole was administered via nasogastric tube. The majority of patients received 800mg fluconazole q24h. Two patients received one-off doses of 400mg q24h. Two received one-off doses of 600mg q24h. One patient's regimen of 800mg fluconazole q24h was escalated to 1200mg q24h for 6 days from day 8 of treatment. All patients received combination therapy with amphotericin B deoxycholate 1mg per kg per day, infused over 5-6 hours.

2.4.2 Measurement of fluconazole concentrations

Fluconazole concentrations were measured using a validated LC/MS/MS methodology (1260 Agilent UPLC coupled to an Agilent 6420 Triple Quad mass spectrometer, Agilent Technologies UK Ltd, Cheshire, UK). Fluconazole was extracted by protein precipitation; 300 µl of cold methanol containing the internal standard fluconazole-D4 at 0.625 mg/L (TRC, Canada) was added to 10 µl of sample (plasma or CSF). The solution was vortex mixed for 5 seconds and filtered through a Sirocco precipitation plate (Waters Ltd, Cheshire, UK). One hundred fifty µl of supernatant was transferred to a 96-well auto sampler plate, and 3 µL were injected on an Agilent ZORBAX C18 RRHD (2.1 X 50mm, 1.8 µm) (Agilent Technologies UK Ltd, Cheshire, UK).

Chromatographic separation was achieved using a gradient consisting of 70% A:30% B (0.1% formic acid in water as mobile phase A and 0.1% formic acid in methanol as mobile phase B). The organic phase was increased to 100% over 90 seconds, with additional 90 seconds of equilibration.

The mass spectrometer was operated in multiple reaction monitoring scan mode in positive polarity. The precursor ions were 307.11 *m/z* and 311.1 *m/z* for fluconazole and internal standard, respectively. The product ions for fluconazole were 220.1 *m/z* and 238.1 *m/z*; for the internal standard 223.2 m/z and 242.1 *m/z*. The source parameters were set as follows: capillary voltage 4000 V, gas temperature 300°C and nebulizer gas 15 lb/in^2. The standard curve for fluconazole encompassed the concentration range 1-120 mg/L and was constructed using blank matrix. The limit of quantitation was 1 mg/L. In plasma, the intra-day

coefficient of variation (CV) was <3.4% and the inter-day CV was <6.7%, over the concentration range 1-90 mg/L. In CSF, the intra-day CV was <5.2% and the inter-day CV was <5.3% over the same concentration range.

2.4.3 Population pharmacokinetic modelling

The concentration-time data for fluconazole in plasma and CSF were analysed using the non-parametric adaptive grid (NPAG) algorithm of the program Pmetrics[273] version 1.5.0 for R statistical package 3.1.1. The initial PK mathematical model fitted to the data contained four compartments and took the following form:

1. $\frac{dX(1)}{dt} = -Ka * X(1)$

2. $\frac{dX(2)}{dt} = Ka * X(1) - \left(Kcp + Kcs + \frac{SCL}{V}\right) * X(2) + Ksc * X(3) + Kpc * X(4)$

3. $\frac{dX(3)}{dt} = Kcs * X(2) - Ksc * X(3)$

4. $\frac{dX(4)}{dt} = Kcp * X(2) - Kpc * X(4)$

5. $Y(1) = X(2)/V$

6. $Y(2) = X(3)/Vcns$

Where equations (1), (2), (3) and (4) describe the rate of change in amount of drug in milligrams (mg) in the gut, central, CSF and peripheral compartment, respectively. *Ka* is the absorption rate constant from the gut to the central compartment. *X(1)*, *X(2), X(3)* and *X(4)* are the amount of fluconazole (mg) in the

gut, central (c), CSF (s) and peripheral compartments (p), respectively. *Kcp*, *Kpc*, *Kcs* and *Ksc* represent first-order transfer constants connecting the various compartments. *SCL* is the first-order clearance of drug (L/h) from the central compartment. *V* is the volume of the central compartment. The CSF compartment (*X(3)*) has an apparent CSF volume (*Vcns)*, given in litres.

Model error was attributed separately to process noise (including errors in sampling times or dosing) and assay variance. Process noise was modelled using lambda, an additive error term. The data were weighted by the inverse of the estimated assay variance.

The data for some patients indicated that they had taken fluconazole at an undocumented time prior to study enrolment, since there was detectable drug in the first PK sample. To accommodate this, non-zero initial conditions of all four compartments were estimated in the structural model. A switch was coded whereby the parameterised estimate of each initial condition was multiplied by a binary covariate equal to 1 where fluconazole was detected in the first PK sample, or 0 where no fluconazole was detected in the first PK sample.

2.4.4 Population pharmacokinetic covariate screening

The impact of patent weight, BMI, sex, ethnicity and baseline eGFR on the PK of fluconazole were investigated. Bidirectional stepwise multivariate linear regression was employed to assess the relationship between each covariate and the Bayesian estimates for volume of distribution and clearance from the central compartment from the standard population PK model. Covariates that were

retained with significant multivariate p-values (≤0.05) in the regression model were explored individually. The relationship between retained continuous covariates and Bayesian estimates of PK parameters was explored using univariate linear regression. The difference between Bayesian estimates of volume and clearance according to categorical covariates (sex and ethnicity) was compared using the Mann-Whitney test.

2.4.5 Population pharmacokinetic model diagnostics

The fit of the model to the data was assessed by visual inspection of diagnostic scatterplots displaying observed-versus-predicted values before and after the Bayesian step. Linear regression was performed and the coefficient of determination, intercept and regression slope noted for each model. In addition, the log-likelihood value, Akaike Information criterion (AIC), mean weighted error (a measure of bias) and bias-adjusted, mean weighted squared error (a measure of precision) were calculated and compared for each model.

2.4.6 Monte Carlo Simulation and calculation of probability of target attainment

Monte Carlo simulation (n = 5000) was performed in Pmetrics.[273] The support points from the final joint density were used. For the simulations, the initial conditions of all compartments were defaulted to zero. Fluconazole was administered at a range of dosages: 400mg q24h, 800mg q24h, 1200mg q24h and 2000mg q24h. The plasma and CSF AUC for fluconazole was calculated using

trapezoidal approximation after the sixth dose, from 144 to 168 hours after treatment initiation.

Wild type fluconazole MIC data were obtained from a previously published collection of 5,733 *C. neoformans* isolates estimated using Clinical and Laboratory Standards Institute (CLSI) methodology.[295] The modal MIC was 4mg/L (1,629 of 5,733 strains; 28%). Almost half of strains had MICs ≥ 4mg/L (2,834 of 5,733 strains; 49%). The epidemiological cut-off value for *C. neoformans* versus fluconazole was 8mg/L. This collection of strains included molecular types VNI to VNIV and the pattern of MIC distribution was comparable across all molecular types.[295] The proportion of simulated patients that would achieve a previously published plasma AUC/MIC target of 389.3 was determined. This target was defined as the magnitude of drug exposure required for fungal stasis (defined as prevention of progressive fungal growth) in a murine study that employed CLSI methodology.[248] To our knowledge, no CSF PK/PD target has been defined in preclinical or clinical studies of fluconazole for cryptococcal meningitis. In the present study, the probability of attaining this plasma PK/PD target was examined at each simulated fluconazole dose.

2.4.7 Meta-analysis of clinical outcome data

The AUC/MIC target used in the probability of target attainment analysis was derived from murine studies. To enhance clinical relevance, we sought PD data from humans. The PD data from patients in the present PK study are confounded by the co-administration of amphotericin B deoxycholate. For this

reason, a search for clinical trials of fluconazole monotherapy for cryptococcal meningitis was performed. The electronic databases Pubmed and Medline were searched on 31st January 2018 using the terms "fluconazole" and "cryptococcal meningitis". Preclinical studies and case reports were excluded. To reduce potential heterogeneity, only studies of HIV-positive participants were included in the meta-analysis. Baseline variables were chosen a priori for extraction from the studies if they had previously been determined to have a significant impact on clinical outcome. These were mental status, CSF fungal burden and patient age.[286,296] Where it was not reported, baseline CSF fungal burden was extrapolated from CSF cryptococcal antigen titre according to a correlation published by Jarvis et al.[286]

For consistency with the literature, we collected data on clinical outcomes commonly presented in cryptococcal meningitis trials: CSF sterility at 8-10 weeks, 2-week mortality and 10-week mortality. Mixed-effects meta-analysis adjusted for fluconazole dosage was performed. Fungal burden in CSF, CD4 count and proportion of patients with reduced Glasgow Coma Score (GCS) at baseline were explored to assess the degree to which these modifiers accounted for inter-study heterogeneity in clinical outcome. The mixed-effects model took the form:

$$\theta_i = \beta_0 + \beta_1 Z_{i1} + \cdots + \beta_1 Z_{ij} + u_i$$

where θ_i is the corresponding (unknown) true effect of the ith study, Z_{ij} is the value of the jth moderator variable for the ith study and u_i are study-specific random effects such that $u_i \sim N(0, \tau^2)$. Here, τ^2 denotes the amount of residual heterogeneity, estimated using the DerSimonian-Laird estimator.[297] Additional

model parameters were estimated via weighted least squares with weights relative to the estimated τ^2. The null hypothesis $H_0: \tau^2 = 0$ was tested using Cochran's Q-test, and model parameters were tested with the Wald-type test statistic.

2.5 Results

2.5.1 Patients

A total of 43 patients (23 from Vietnam and 20 from Uganda) were recruited over an 11-month period between January and November 2016. Twenty-two patients (52%) were female. The overall median (range) age was 33 years (20 – 73 years), weight 48 kg (32 – 68 kg), body mass index 18 kg/m^2 (12 – 25 kg/m^2), creatinine at enrolment 70 µmol/L (37 – 167 µmol/L) and estimated glomerular filtration rate using the Cockcroft Gault equation 84.8 mL/min/1.73m^2 (35.4 – 146.7 mL/min/1.73m^2). The baseline creatinine concentration was significantly lower in Vietnamese patients than in Ugandan patients (median 56 versus 79 µmol/L; p-value 0.02). However, this did not manifest as a significant difference in eGFR due to different age, sex and weight profiles between the two patient populations. There were no statistically significant differences between ethnic groups for other demographic variables. The demographic data are shown by ethnicity and for the study population as a whole in table 2.1.

Table 2.1: Patient demographics

Demographic or clinical characteristic	Vietnam	Uganda	Combined	p-value†
Sex [a] (Male:Female)	13:10	8:12	23:20	
Age (years) [b]				
Mean	38	33	35	
Median	33	33	33	
Range	20 - 73	24 - 50	20 - 73	0.75
Weight (kg) [c]				
Mean	46	49	48	
Median	45	49	48	
Range	32 - 68	35 - 60	32 – 68	0.23
BMI (kg/m^2) [d]				
Mean	18	18	18	
Median	18	18	18	
Range	12 - 25	15 - 22	12 - 25	0.73
Creatinine (µmol/L) [a]				
Mean	67	81	74	
Median	56	79	70	
Range	37 – 167	43 - 145	37 - 167	0.02
eGFR (ml/min/1.73m^2) [e]				
Mean	88.3	80.7	84.7	
Median	84.8	81.4	84.8	
Range	35.4 – 136.1	49.8 – 146.7	35.4 – 146.7	0.10

[a] *n* = 43; [b] *n* = 31; [c] *n* = 41; [d] *n* = 35; [e] *n* = 33

† p-value for difference between Vietnam and Uganda by Mann-Whitney test of significance.

BMI: Body Mass Index; eGFR: estimated Glomerular Filtration Rate, by Cockcroft-Gault equation.

2.5.2 Pharmacokinetic data

The final dataset included 312 plasma observations and 52 CSF observations from the Vietnamese cohort. From the Ugandan cohort, the dataset included 196 plasma observations and 115 CSF observations. A single CSF observation from 1 Ugandan patient was excluded because no fluconazole was detectable in an isolated sample after 13 days of therapy. This was inconsistent with results from other patients and could not be verified. The mean number of plasma samples and CSF samples per patient was 11.8 and 3.9, respectively. Figure 2.1 shows the raw plasma and CSF concentration-time profiles from study participants.

Figure 2.1: Fluconazole concentrations in 43 patients

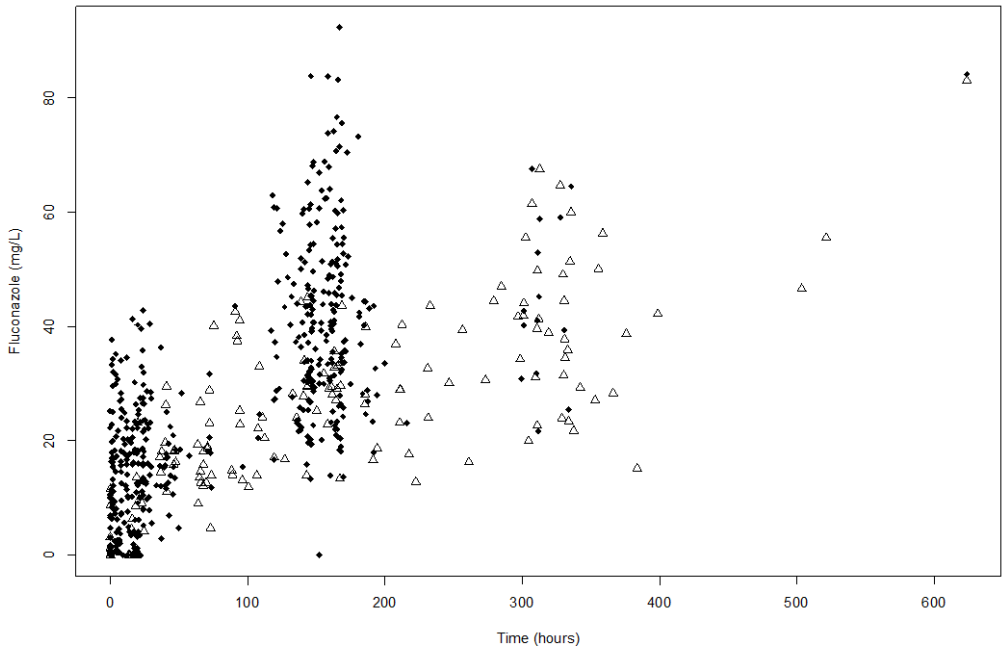

Black diamonds represent plasma concentrations. White triangles represent CSF concentrations.

2.5.3 Population pharmacokinetic analysis

The final mathematical model was a linear model comprised of an absorption compartment, central compartment, peripheral compartment and CSF compartment. The fit of the final model to the clinical data was acceptable. The mean parameter estimates better fitted the data than medians, and were used to calculate Bayesian estimates of drug exposure for each individual patient. A linear regression of the observed-versus-predicted fluconazole concentrations in plasma after the Bayesian step was given by: observed fluconazole concentration = 1.03*predicted fluconazole concentration + 0.27; r^2 = 0.80. For the observed-versus-predicted fluconazole concentrations in CSF, the linear regression was given by observed fluconazole concentration = 1.03*predicted fluconazole concentration - 0.07; r^2 = 0.81 (Figure 2.2 and table 2.2). The mean weighted population bias for fluconazole concentrations in plasma and CSF was 0.20 and -0.30, respectively. The bias-adjusted population imprecision in plasma and CSF was 2.21 and 1.55, respectively. The population PK parameter estimates for the final model are shown in table 2.3.

Figure 2.2: Scatter plots showing observed versus predicted values for the chosen population pharmacokinetic model after the Bayesian step

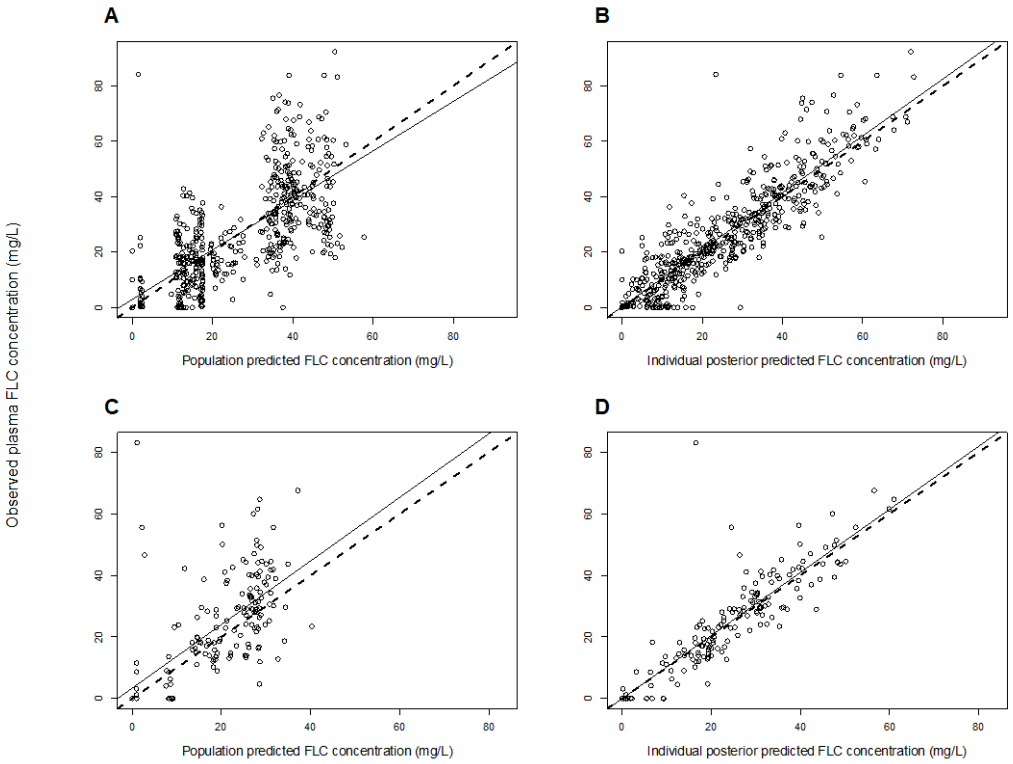

A: Population predicted concentration of fluconazole in plasma. R2 = 0.49; intercept = 2.89 (95% CI 0.51 – 5.27), slope = 0.89 (95% CI 0.82 – 0.97)

B: Individual posterior predicted concentration of fluconazole in plasma. R2 = 0.80; intercept = 0.27 (95% CI -1.08 – 1.62); slope = 1.03 (95% CI 0.98 – 1.07)

C: Population predicted concentration of fluconazole in CSF. R2 = 0.46; intercept = 3.39 (95% CI -0.09– 6.87), slope = 1.03 (95% CI 0.87 – 1.2)

D: Individual posterior predicted concentration of fluconazole in CSF. R2 = 0.81; intercept = -0.07 (95% CI -1.97 – 1.84); slope = 1.03 (95% CI 0.95 – 1.10)

Circles, dashed lines, and solid lines represent individual observed-predicted data points, line of identity, and the linear regression of observed-predicted values, respectively. All observed and predicted fluconazole concentrations in mg/L. FLC: fluconazole; CI: Confidence Interval.

Table 2.2: Evaluation of the predictive performance of the considered and final models

Model	Measured compartment	Log likelihood	AIC	Population bias	Population imprecision	Linear regression of observed-predicted values for each patient			
						$R^{2,a}$	Intercept	Slope	p-value†
Model 1	Plasma	-2451	4928	0.20	2.21	0.80	0.27	1.03	0.56
	CSF			-0.30	1.55	0.81	-0.07	1.03	
Model 2	Plasma	-2413	4854	0.36	2.38	0.80	0.01	1.03	
	CSF			-0.41	1.81	0.80	0.89	1.01	

Model 1 did not include any covariates. Model 2 incorporated a function to scale the volume of distribution in central compartment to patient weight.

AIC: Akaike Information criterion.

[a] Relative to the regression line fitted for the observed versus predicted values after the Bayesian step.

† Comparison of the joint distribution of population parameter values for each model.

Table 2.3: Population parameter estimates from the final 4-compartment pharmacokinetic model

Parameter	Mean	Median	Standard deviation
Ka (h^{-1})	8.78	1.73	11.98
SCL/F (L/h)	0.72	0.65	0.24
$Volume_c$ /F(L)	18.07	17.41	6.31
Kcp (h^{-1})	12.20	8.36	11.17
Kpc (h^{-1})	18.10	18.34	8.25
IC_{gut} (mg)	34.67	49.99	22.74
$IC_{central}$ (mg)	35.86	49.98	19.67
IC_{CNS} (mg)	31.06	49.96	23.47
$IC_{peripheral}$ (mg)	34.29	49.96	13.21
Kcs (h^{-1})	35.43	42.55	13.74
Ksc (h^{-1})	28.63	29.04	10.03
$Volume_{cns}$ /F(L)	32.07	30.49	17.60

SCL: clearance; $Volume_c$: volume of distribution in central compartment; F: bioavailability; Kcp: first-order rate constant from the central to peripheral compartment; Kpc, first-order rate constant from peripheral to central compartment; IC: initial conditions in respective compartments; Kcs: first-order rate constant from the central to CNS compartment; Ksc, first-order rate constant from CNS to central compartment; $Volume_{cns}$: volume of distribution in CNS compartment.

2.5.4 Covariate investigation

Multivariate linear regression of each subject's covariates versus the Bayesian posterior parameter values revealed a weak relationship between patient weight and estimated volume of distribution (slope 0.22, 95% confidence interval for the slope -0.06 to 0.51, p-value 0.05). Incorporation of weight into the PK model was therefore explored. However, values for log likelihood, Akaike information criterion (AIC) and population bias and imprecision were comparable between the two models. The simple base model was therefore used to describe the data and for the subsequent simulations. The model comparisons and the fit to data are summarized in table 2.2.

There was no relationship between the Bayesian estimates of clearance and volume, and ethnicity or sex in the base model. The mean (95% CI) clearance was 0.74 liters/hour (0.64 – 0.83) and 0.71 liters / hour (0.59 – 0.82) for Vietnamese and Ugandan patients, respectively; p= 0.51. The mean (95% CI) volume was 16.88 liters (14.33 – 19.44) and 19.44 liters (16.88 – 22.0) for Vietnamese and Ugandan patients, respectively; p= 0.16. In males, the mean (95% CI) clearance was 0.79 liters /hour (0.67 – 0.90). In females, clearance was 0.66 liters / hour (0.57 – 0.75); p= 0.09. In males, the mean (95% CI) volume was 18.07 liters (15.47 – 20.67). In females, volume was 18.07 liters / hour (15.41 – 20.73); p= 0.97.

2.5.5 Fluconazole penetration into the CSF

There was large variability in the AUCs generated from each patient's posterior estimates. The 38 patients who received 800mg fluconazole q24h had a median (IQR) $AUC_{144\text{-}168}$ of 945.4 (799.2 – 1139.8) mg.h/L in plasma and 784.2 mg.h/L (615.9 – 879.4) in CSF. From these posterior estimates, the mean ratio of AUC_{CSF}:AUC_{plasma} was 0.82 (standard deviation 0.22).

Monte Carlo simulation was used to estimate the distribution of drug exposure for dosages of 400mg, 800mg, 1200mg and 2000mg q24h of fluconazole (figure 2.3). PK variability was marked, both in plasma and CSF. After administration of a dosage of 1200mg fluconazole q24h, median (IQR) simulated plasma $AUC_{144\text{-}168}$ was 1143.2 mg.h/L (988.4 – 1378.0) and CSF $AUC_{144\text{-}168}$ was 982.9 mg.h/L (781.0 – 1185.9). The mean simulated ratio of AUC_{CSF}:AUC_{plasma} was 0.89 (SD 0.44).

Figure 2.3: AUC distributions in 5,000 simulated patients at escalating fluconazole dosages

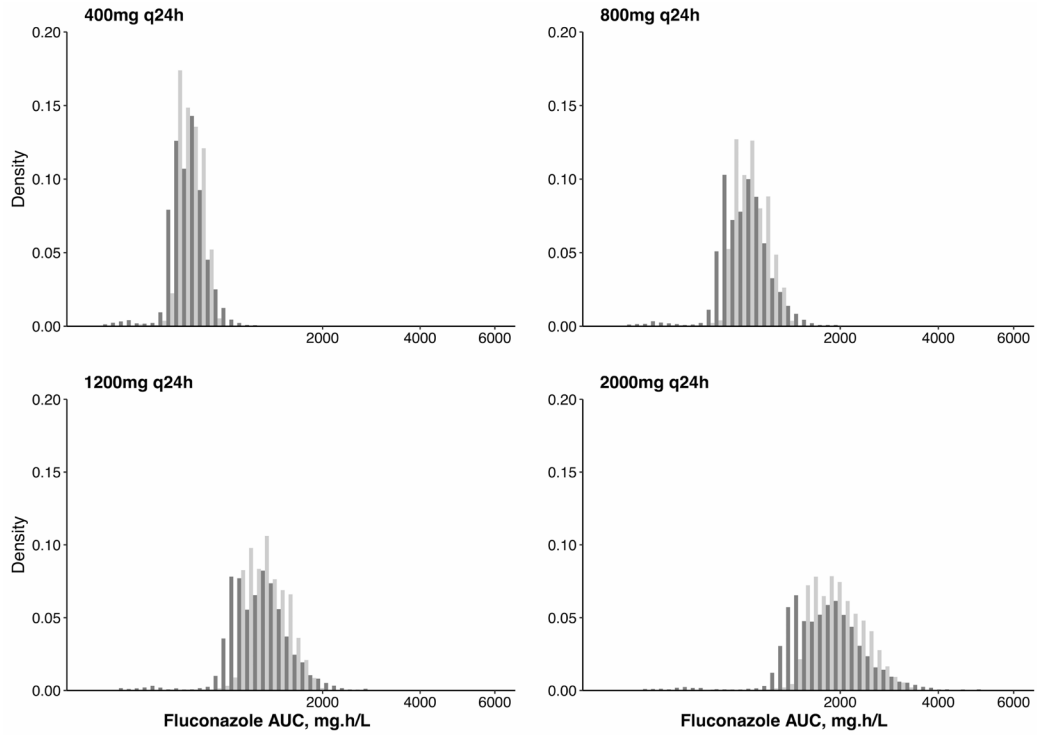

Light grey bars indicate simulated plasma $AUC_{144\text{-}168}$. Dark grey bars indicate simulated CSF $AUC_{144\text{-}168}$.

2.5.6 Probability of target attainment analysis

Monte Carlo simulation was used to predict the probability of achieving a total drug AUC:MIC ratio of ≥ 389.3 in plasma. This PD target was shown in a murine model of cryptococcal meningitis to be associated with a stasis endpoint (i.e. no net change in fungal density at the end of the experiment compared with that at treatment initiation).[248] Only 61% of simulated patients receiving 1200mg fluconazole q24h achieved this PD target when the MIC of the infecting strain was 2.0 mg/L. For MICs ≥ 4.0mg/L, < 1% of simulated patients administered 1200mg q24h achieved the PD target (figure 2.4).

Figure 2.4: Probability of pharmacodynamic target attainment in plasma as a function of isolate MIC and fluconazole dosage

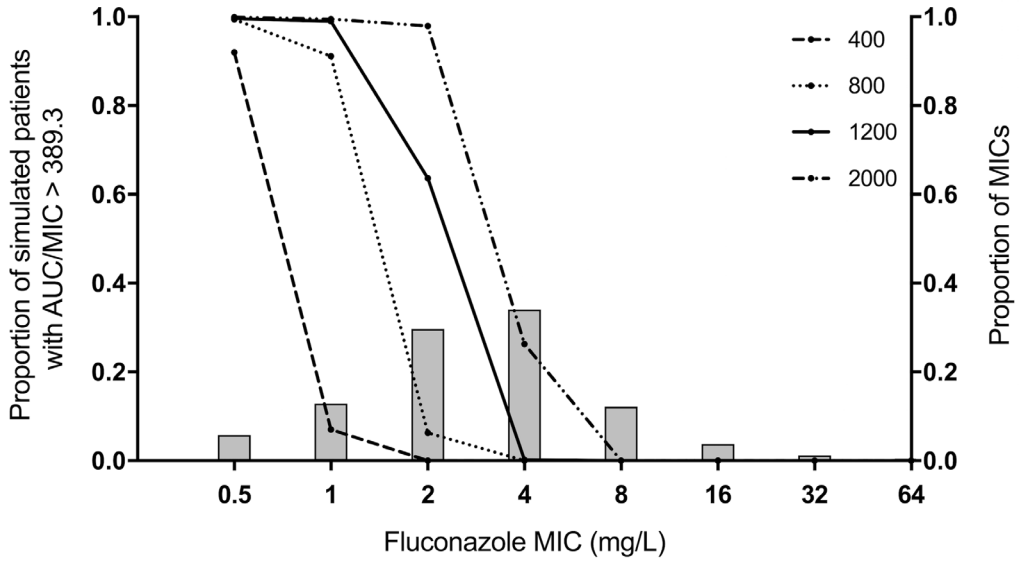

Each line represents the proportion of 5000 simulated patients that achieve the PD target at the respective dosage of fluconazole. The PD target was a plasma AUC/MIC ratio ≥ 389.3. Bars show the proportion of WT strains of *C.neoformans* at the indicated MIC.

2.5.7 Meta-analysis of clinical outcome data

A systematic review identified 163 relevant manuscripts, of which 11 were duplicates. After reviewing titles and abstracts, 28 studies were deemed potentially relevant for inclusion in the meta-analysis. Detailed examination of these studies resulted in the ultimate inclusion of 12 papers describing clinical outcomes from cryptococcal meningitis treated with fluconazole monotherapy. In total, 28 patients in 1 study received 200mg fluconazole q24h,[64] 19 patients in 2 studies received 400mg fluconazole q24h,[65,298] 97 patients in 3 studies 800mg q24h,[299-301] 113 patients in 4 studies 1200mg q24h,[62,300-302] and 1 study described outcomes of 16 patients on 1600mg[301] and 8 patients on 2g fluconazole q24h.[301]

All included patients were HIV positive. Baseline characteristics and reported clinical outcomes are presented in Table 2.4.

The final model suggests that the combination of dose and baseline fungal burden explains the total heterogeneity in the estimated proportion of patients with sterile CSF after 10 weeks of treatment (P-value for residual heterogeneity 0.64). However, there was not a significant relationship between dose and CSF sterility at 8-10 weeks (p-value 0.45). After adjustment for dose, the test for residual heterogeneity in both 2 and 10-week mortality was not significant (p-value 0.70 and 0.22, respectively), indicating that dose alone adequately explained total heterogeneity in mortality outcomes at both time points. For both 2 and 10-week mortality outcomes, there was a non-significant trend towards reduced mortality with escalating dosage (Figure 2.5).

Table 2.4: Baseline characteristics and clinical outcomes from trial data of fluconazole monotherapy, by dosing regimen

Fluconazole dosage (mg)	Country	Number of patients	Age*	GCS <15, %	CD4 cell count per mm^3 *	CSF burden, log10 CFU/mL	CSF sterility, fraction (%) of patients	Time CSF sterility charted	2 week mortality (%)	10 week mortality (%)	Reference
200	Uganda	28	33 (range 23-50)	43	Mean 73	.	4/8 (50)	2 months	10/25 (40)	16/25 (64)	Mayanja-Kizza 1998 [64]
400	USA	14	mean 38(SE 2)	0	Mean 44 (SE 13)	4§	6/14 (43)	10 weeks	NR	4/14 (29)	Larsen 1990 [298]
400	South Africa	5	39 (37-51)	60	41	5.53	NR	NR	NR	3/4 (75)	Bicanic 2007 [65]
800	Malawi	58	32 (29-39)	24	37 (11-58)	.	NR	NR	17/58 (29)	33/58 (57)	Rothe 2013 [299]
800	Uganda	30	35 (30-38)	33	7 (3-17)	5.7	NR	NR	11/30 (37)	18/30 (60)	Longley 2008 [300]
800	USA	9	35	100	8	4.8§	1/9 (11)	10 weeks	NR	8/9 (89)	Milefchik 2008 [301]
1200	Malawi	47	35 (32-40)	24	36 (17-62)	.	NR	NR	16/47 (34)	26/47 (55)	Gaskell 2014 [301]
1200	Uganda	30	33 (28-42)	60	14 (4-33)	5.9	NR	NR	6/27 (22)	13/27 (48)	Longley 2008 [300]
1200	USA	16	40	100	36	3.5§	6/16 (37.5)	10 weeks	NR	10/16 (62.5)	Milefchik 2008 [301]
1200	Malawi	20	36.5 (range 27-71)	40	25 (range 1-66)	5.30	1/20 (5)	2 weeks	7/19 (37)	11/19 (58)	Nussbaum 2010 [62]
1600	USA	16	35	100	33	3§	10/16 (62.5)	10 weeks	NR	6/16 (37.5)	Milefchik 2008 [301]
2000	USA	8	36	100	35	2.4§	5/8 (62.5)	10 weeks	NR	3/8 (37.5)	Milefchik 2008 [301]

*Median (interquartile rage) unless otherwise specified. §: Extrapolated from cryptococcal antigen titre. CSF: Cerebrospinal fluid. SE: Standard error. CFU: Colony-forming units.

Figure 2.5: Meta-analysis of clinical trials of fluconazole monotherapy showing dose-adjusted effects on A) 2-week mortality and B) 10-week mortality.

A

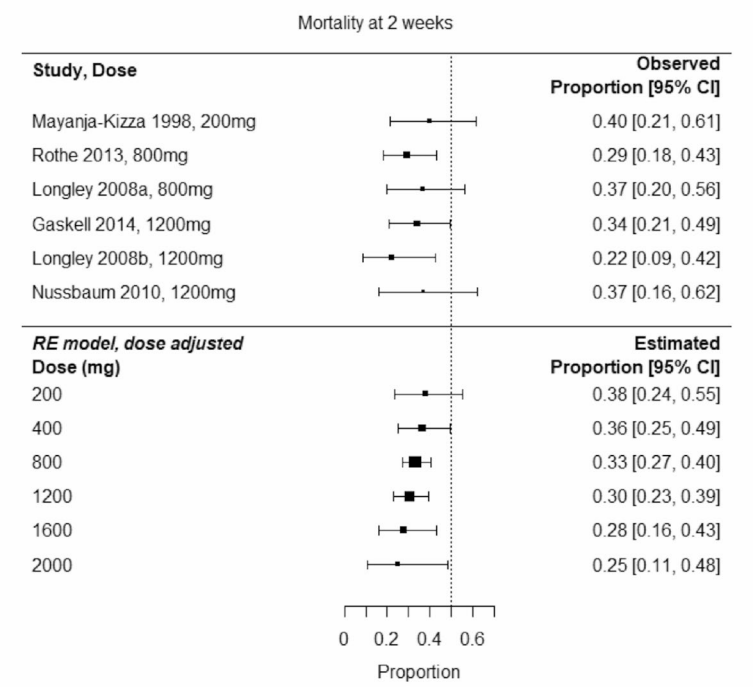

Right hand column provides observed and estimated proportions of patients dead at 2 weeks.

B

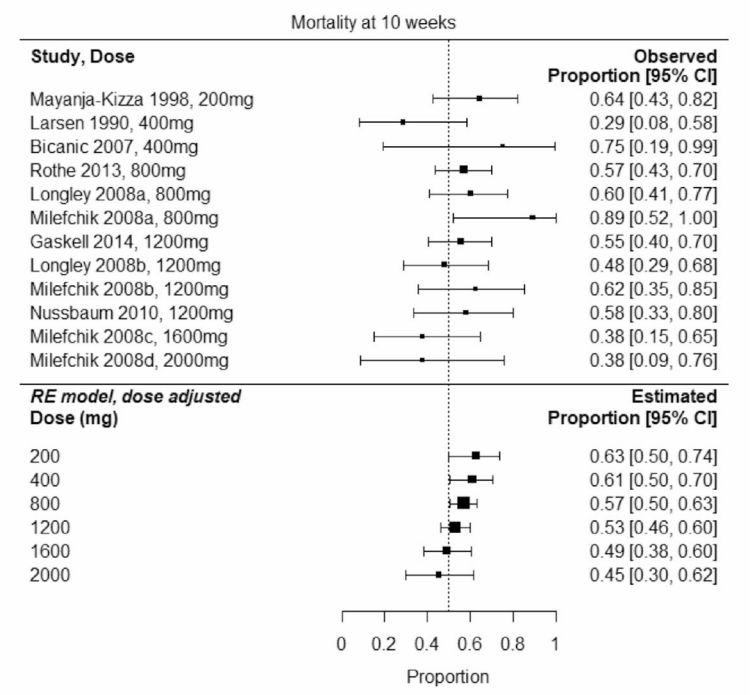

Right hand column provides observed and estimated proportions of patients dead at 10 weeks.

2.6 Discussion

Fluconazole is the only drug available for induction therapy for cryptococcal meningitis in many regions of the world where the incidence of disease is highest. An accumulating body of evidence suggests that fluconazole is a suboptimal agent for this indication.[303] While this has long been recognised, an explanation for the relatively poor efficacy of fluconazole is absent. This study presents a uniquely comprehensive clinical dataset describing the PK of fluconazole. It provides robust estimates of CNS penetration and the variability of those estimates. A high degree of CNS partitioning has been observed in previous clinical studies with fluconazole.[294,304] Distribution into the CNS is facilitated by low molecular weight, low protein binding and moderate lipophilicity.[86,88] Fluconazole has proven activity against *Cryptococcus neoformans*.[305,306] This study provides further understanding as to why, despite these attributes, fluconazole is an inferior agent for induction monotherapy for cryptococcal meningitis compared with amphotericin B deoxycholate.[62,65,286]

In contrast to previous studies of fluconazole PK,[28,307,308] our data do not suggest a significant relationship between fluconazole clearance and creatinine clearance, nor between patient weight and volume of distribution. The reason for this is not immediately clear but may relate to the relatively narrow range of creatinine clearance in our population, and the fact that the vast majority of patients in our cohort had low body weight, with the range of this covariate also being relatively narrow.

The PK model suggests that current regimens of fluconazole are inadequate for induction therapy for cryptococcal meningitis. This has routinely been ascribed to the overly simplistic notion that fluconazole is a fungistatic agent. Our analyses provide further insight into the limitations of this drug. Previous estimates of fluconazole CNS:plasma partition ratios have ranged from 0.52 to 1.33.[36,293,294,304,309] We have extended these estimates by rigorously quantifying the marked variability in the CSF PK. This variability has consequences at both microbiological and clinical levels. Suboptimal exposure of fluconazole promotes the expansion of intrinsically resistant cryptococcal subpopulations present at the initiation of therapy.[310] In addition, the evolution of *C. neoformans* during therapy to become increasingly triazole resistant has been demonstrated in clinical studies.[311,312] To be clinically effective, adequate concentrations of drug must be present at the site of infection for long enough to exert antimicrobial effect on both susceptible and resistant subpopulations. The present analysis demonstrates the challenges in achieving that aim.

At recommended fluconazole dosages of 1200mg q24h, the probability of PD target attainment (PTA) bisects the MIC distribution of WT *C. neoformans* isolates. This is consistent with the findings of Sudan *et al*.[248] Approximately half of patients will fail therapy because they are not able to generate the drug exposure required to prevent progressive fungal growth. Since clinical PK-PD targets are not available for fluconazole in cryptococcal meningitis, we have used a target derived from a murine study.[248] This assumes that CNS partitioning is the same in mice and humans. The cerebrum:plasma AUC ratio in the murine study

was 46.9%.[248] It is conceivable that this is in keeping with our CSF:plasma AUC ratio of 82%, though clearly it would be preferable to have clinical PK-PD targets defined. Furthermore, the PK-PD target we used was derived from plasma data and it would have been preferable to additionally aim for a PK-PD target in CSF. One additional challenge in achieving adequate drug exposure at the site of infection, which we were unable to account for, is the role of protein binding. Fluconazole is approximately 10% protein bound in plasma (Table 1.2). Our data reflect total fluconazole concentrations and it is possible that a portion of measured drug was protein bound and inactive, which raises the risk that PTA was slightly lower than our predictions suggest. Nevertheless, our PTA analysis is supported by the 53% 10-week mortality outcomes for patients receiving 1200mg fluconazole q24h, estimated in the meta-analysis. Importantly, such PTA analyses are based on an AUC/MIC of 389.3, which is more than an order of magnitude greater than the AUC/MIC ratio required for *Candida albicans.*[289]

Progressive escalation of the dosage of fluconazole is not likely to be an effective strategy for improving cryptococcal meningitis induction therapy. The drug exposure required to reliably treat isolates with MICs ≥ 4.0mg/L is difficult to achieve and potentially toxic. Our meta-analysis suggests that escalating dosages of fluconazole do not increase the proportion of patients with sterile CSF at 10 weeks. Dosages of 2000mg q24h do not appear to significantly improve 10-week mortality outcomes in comparison to 1200mg q24h. The ACTG study (https://clinicaltrials.gov/show/NCT00885703) is investigating the use of higher dosages of fluconazole (1600mg and 2000mg q24h) for the treatment of

cryptococcal meningitis in HIV-infected individuals and results are pending. The addition of flucytosine to high-dose fluconazole (≥ 1200mg q24h) for cryptococcal meningitis increases antifungal activity and improves mortality outcomes,[62,301] suggesting that combination therapy is required to optimise antifungal activity in fluconazole-containing regimens.

In summary, this study provides part of the pharmacodynamic rationale for the long-recognised fact that fluconazole monotherapy is an ineffective induction regimen for cryptococcal meningitis. We have developed a fluconazole population PK model that suggests that approximately half of patients with cryptococcal meningitis caused by WT strains of *C. neoformans* will be undertreated by currently recommended dosages of fluconazole for induction therapy. In doing so we have addressed a knowledge gap regarding the reason for the inferiority of this drug for cryptococcal meningitis. There is a pressing need for improved provision of affordable combination treatments and development of more effective drugs.

3 Amphotericin B Deoxycholate in adults with Cryptococcal meningoencephalitis; a Population Pharmacokinetic Model and Meta-Analysis of Outcomes

3.1 Declaration regarding presentation of published work within postgraduate thesis

The work presented in this chapter has been published in a peer-reviewed journal, as follows: *Stott KE, Beardsley J, Whalley S, Kibengo FM, Mai NT, Lê Nhu'Tùng N, Cuc NT, Kolamunnage-Dona R, Hope W, Day J. Population pharmacokinetic model and meta-analysis of outcomes of amphotericin B deoxycholate use in adults with cryptococcal meningoencephalitis. Antimicrobial agents and chemotherapy. 2018 Jul 1;62(7).*

As the first author of this publication, I curated the data for analysis, constructed and validated the PK model, simulated hypothetical dosing regimens, performed a probability of target attainment (PTA) analysis and performed meta-analyses of clinical outcomes. I wrote the first draft of the manuscript and all co-authors approved the final version for publication. All co-authors have granted their permission for this published manuscript to be re-formatted and included in this postgraduate thesis – see appendix A.

3.2 Abstract

There is a limited understanding of the population pharmacokinetics (PK) and pharmacodynamics (PD) of amphotericin B deoxycholate (DAmB) for cryptococcal meningoencephalitis (CME). A PK study was conducted in n=42 patients receiving DAmB 1 mg/kg q24h. A 2-compartment PK model was developed. Patient weight influenced clearance and volume in the final structural model. Monte Carlo simulations estimated drug exposure associated with various DAmB dosages. A search was conducted for trials reporting outcomes of CME patients treated with DAmB monotherapy and a meta-analysis was performed. The PK parameter means (standard deviation) were: clearance, 0.03 (0.01) x weight + 0.95 (0.02) litres/hour; volume, 0.89 (0.90) x weight + 1.54 (1.13) litres; first-order rate constant from central to peripheral compartment, 7.12 (6.50) $hours^{-1}$; from peripheral to central compartment, 12.13 (12.50) $hours^{-1}$. The meta-analysis suggested that DAmB dosage explained most of the heterogeneity in cerebrospinal fluid (CSF) sterility, but not in mortality outcomes. Simulations of area under concentration-time curve ($AUC_{144\text{-}168}$) resulted in median (interquartile range) values 5.83 mg.h/litre (4.66-8.55), 10.16 (8.07-14.55) and 14.51 (11.48-20.42), with dosages of 0.4, 0.7 and 1.0 mg/kg q24h respectively. DAmB PK is described adequately by a linear model that incorporates weight on clearance and volume. Inter-patient PK variability is modest and unlikely to be responsible for variability in clinical outcome. There is discordance between the impact that drug exposure has on CSF sterility and on mortality outcomes, which may be due to

cerebral pathology not reflected in CSF fungal burden, in addition to clinical variables.

3.3 Introduction

Cryptococcal meningoencephalitis is a leading infectious cause of morbidity and mortality worldwide, with approximately 223,100 incident cases and 181,100 deaths annually.[38] Ten week mortality for patients receiving the current standard-of-care is 24-31%.[74,75,174,286] There have been no new antifungal agents developed for use in LMICs in the last 3 decades. Given the paucity of new agents, one important strategy for improving clinical outcomes is a better understanding and use of currently available compounds.

Amphotericin B (AmB) is a polyene antifungal agent with broad spectrum activity against yeasts and moulds, as well as some parasites. AmB was initially isolated from a streptomycete and described in 1955.[313] AmB was the first therapeutic option for treatment of lethal invasive fungal diseases such as cryptococcal meningoencephalitis.[314,315] Amphotericin B deoxycholate (DAmB) is the most potent formulation of AmB on a mg-mg basis[316,317] and is a mainstay for the treatment of cryptococcal meningoencephalitis.

Clinical studies have progressively examined escalating dosages of 0.4mg/kg q24h[63,318], 0.7mg/kg q24h[77,319,320] and 1.0mg/kg q24h[74] of DAmB for cryptococcal meningoencephalitis. The primary motivation of these studies was identification of the dosage that induces maximal antifungal activity. A regimen of 1.0 mg/kg q24h in combination with flucytosine for seven days is currently

recommended for induction therapy.[52] DAmB dosages approaching 1.0 mg/kg q24h are associated with increased rates of cerebrospinal fluid (CSF) sterilisation[75] and improved mortality.[74,262,286] However, the broad clinical utility of DAmB is compromised by dose-limiting toxicities that include infusional reactions, phlebitis, nephrotoxicity and anaemia.[53,321] A detailed understanding of the therapeutic index for each DAmB dosage level is lacking.

Herein, we describe the development of a population pharmacokinetic model of DAmB. In addition, a meta-analysis of clinical trials of DAmB monotherapy was performed to estimate the contribution of various DAmB dosages to the observed heterogeneity in study outcomes. Finally, Monte Carlo simulations were performed to estimate the mean, median and dispersion of drug exposures that are associated with microbiological and clinical outcomes from DAmB monotherapy.

3.2 Materials and Methods

3.2.1 Clinical Pharmacokinetic Studies

Plasma samples were obtained from adults with HIV associated cryptococcal meningoencephalitis. Patients were initially recruited from a multicentre randomised controlled trial of adjuvant treatment with dexamethasone in HIV-associated cryptococcal meningoencephalitis reported elsewhere (n=3, International Standard Registered Clinical Number 59144167).[183] Following the early cessation of this trial, they were recruited from a prospective descriptive study at the same sites (n=39). Patients were recruited in 2 sites: The

Hospital for Tropical Diseases in Ho Chi Minh City Vietnam, and Masaka General Hospital, Uganda. The study protocols were approved by the relevant institutional review boards and regulatory authorities at each trial site and by the Oxford University Tropical Research Ethics Committee.

The protocol for the randomised controlled trial has been described previously.[322] Patients had HIV infection, a syndrome consistent with cryptococcal meningoencephalitis, and laboratory evidence of cryptococcal infection (positive India ink staining of CSF, culture of *Cryptococcus* spp. from CSF or blood, or cryptococcal antigen (CrAg) detected in CSF on CrAg lateral flow assay).[262] Patients who were pregnant, had renal failure, had gastrointestinal bleeding, had received more than 7 days of anti-cryptococcal antifungal therapy, were already taking corticosteroids, or required corticosteroid therapy for co-existing conditions were excluded. The inclusion and exclusion criteria for the prospective descriptive study were identical to those of the clinical trial. Patients received 1 mg/kg DAmB once daily by intravenous infusion over 5-6 hours, as well as 800mg fluconazole per day. Two patients recruited during the clinical trial received dexamethasone according to the following regimen: 0.3mg/kg/day intravenously (IV) for week 1, 0.2mg/kg/day IV for week 2, then orally 0.1mg/kg/day for week 3, 3mg/day week 4, 2mg/day week 5, 1mg/day week 6, then stop. For the first five patients enrolled, blood samples were obtained immediately prior to intravenous DAmB infusion, and then at 1, 2, 4, 8, 12, 16, 20 and 24. The results for these patients informed a subsequent sampling strategy defined using optimal design theory such that patients were sampled pre-dose, then at 1, 2, 4, 8, 12 and 24 hours after the

initiation of infusion. PK sampling occurred on treatment days 1 or 2, and 7. Whenever patients had lumbar punctures performed for other clinical indications such as raised intracranial pressure, paired plasma samples were collected for subsequent PK analysis. Therefore, additional sparse samples were taken up to 17 days after initial dosing. Quantitative fungal counts were determined for each lumbar puncture, as described previously.[320]

3.2.2 Measurement of Amphotericin B Concentrations

Amphotericin B concentrations in plasma were measured using high-performance liquid chromatography (HPLC) with a Shimadzu Prominence HPLC system (Shimadzu, Milton Keynes, UK). Amphotericin B was extracted by protein precipitation. A total of 300 µL of methanol that contained piroxicam 2 mg/L (Sigma Aldrich, Dorset, UK) as internal standard was added to 100 µL of matrix. Samples were vortexed for 5 seconds and then centrifuged at 13,000 x g for 3 minutes.

One hundred-fifty µL of supernatant was removed and placed in a 96-well plate, to which 50 µL of water was added. A 50µL aliquot was injected onto a Kinetex 5µ XB-C18 liquid chromatography column (Phenomenex, Macclesfield, UK). Chromatographic separation was achieved using a gradient with the starting conditions of 75% A:25% B (0.1% formic acid in water as mobile phase A and 0.1% formic acid in acetonitrile as mobile phase B). Mobile phase B was increased to 80% over five minutes and then reduced to starting conditions for two minutes of

equilibration. Amphotericin B and internal standard were detected using UV detection at wavelengths of 406nm and 385nm; they eluted after 4.1 and 4.6 minutes, respectively.

The standard curve for amphotericin B encompassed the concentration range 0.05- 8.0 mg/L and was constructed using blank matrix. The limit of quantitation was 0.05 mg/L. The coefficient of variation was <9.3% over the concentration range 0.05-8 mg/L. The intra- and inter-day variation was <7.9%.

3.2.3 Population Pharmacokinetic Modelling

A PK model was fitted to the data using the non-parametric adaptive grid (NPAG) algorithm of the program Pmetrics[273] version 1.5.0 for R statistical package 3.1.1. The data were weighted by the inverse of the estimated assay variance. Both two- and three-compartment models were tested, with zero-order intravenous input and first-order elimination from the central compartment. The two-compartment model took the following form:

a) $\frac{dX(1)}{dt} = R(1) - \left[\frac{SCL}{V} + K12\right] * X(1) + K21 * X(2)$

b) $\frac{dX(2)}{dt} = K12 * X(1) - K21 * X(2)$

c) $Y(1) = \frac{X(1)}{V}$

Where equations (a) and (b) describe the rate of change of the amount of drug (mg) in the central and the peripheral compartments, respectively. *X(1)* and *X(2)* are the amount of AmB in milligrams (mg) in the central (c) and peripheral (p) compartments respectively. *R(1)* is the intravenous infusion of DAmB into the

central compartment. *SCL* is the first-order clearance of drug (L/h) from the central compartment. *V* is the volume of the central compartment. *K12* and *K21* are the first-order inter-compartmental rate constants. Equation (c) is the model output, with *Y(1)* representing the concentration of amphotericin B in the central compartment. The three-compartment model contained an additional equation to connect the third compartment to the second compartment in series:

d) $\frac{dX(3)}{dt} = K23 * X(2) - K32 * X(3)$

An initial condition was estimated to accommodate detectable drug in the first PK sample from those patients who received a dose of DAmB at an undocumented time before study enrolment. The non-zero initial conditions of *X(1)* and *X(2)* were estimated by assigning the respective parameters in the structural model (not shown in the equations above). A switch was coded whereby a parameterised estimate of the initial condition was multiplied by a binary covariate equal to 1 where the first PK sample was drawn after a dose of DAmB, or 0 where this represented a pre-dose sample.

Once the standard model was fitted (Model 1), the effects of patient weight, baseline eGFR and patient ethnicity on the PK of DAmB were investigated. Bidirectional stepwise multivariate linear regression of each subject's covariates versus the Bayesian posterior parameter values revealed a significant ($P < 0.05$) relationship between both weight and eGFR with estimated PK parameters. Univariate linear regression was employed, firstly to assess the relationship between patient weight and the Bayesian estimates for both clearance and volume. Since a positive relationship was observed between weight and both PK

parameters, the population PK model was re-fitted to the data (Model 2) with incorporation of the following equations to describe (e) clearance *(SCL)*, and (f) volume *(V)*, as functions of patient weight (*Wt*):

e) $SCL = Int\_c + (Wt * Sl\_c)$

f) $V = Int\_v + (Wt * Sl\_v)$

Where *Int* is the intercept and *Sl* the slope of the linear regression describing the relationship between weight and clearance or volume, and the intercept and slope for each of these PK parameters is parameterised separately. Thus, equation (a) of the structural model was replaced with:

a.2) $\frac{dX(1)}{dt} = R(1) - \left[\frac{Int_c + (Wt * Sl_c)}{Int_v + (Wt * Sl_v)} + K12\right] * X(1) + K21 * X(2).$

In addition, a power function was explored to describe the relationship between weight and clearance. In this model (Model 3), clearance was parameterised and scaled with weight to the exponent 0.75. This exponent has previously been demonstrated to usefully scale for size.[323,324] A linear relationship was maintained between volume and weight. Thus, in Model 3, equation (a) was replaced with:

a.3) $\frac{dX(1)}{dt} = R(1) - \left[\frac{SCL * Wt\text{^}0.75}{V * Wt} + K12\right] * X(1) + K21 * X(2).$

Univariate linear regression was similarly employed to assess the relationship between eGFR and the Bayesian estimates for clearance and volume. A weaker but nevertheless positive association was demonstrated. Consequently, a further structural model was fitted to the data (Model 4), with the following equation (g) explored to describe clearance (*SCL*):

g) $SCL = Int\_c + (Wt * Sl\_c) * (\frac{eGFR}{med_{eGFR}})$

Where *eGFR* is the estimated glomerular filtration rate calculated for each patient by the Cockcroft-Gault equation and *med_eGFR* is the population median estimated glomerular filtration rate. In Model 4, equation (a) was replaced with:

$$\text{a.4)}\ \frac{dX(1)}{dt} = R(1) - \left[\frac{Int_c + (Wt * Sl_c) * \left(\frac{eGFR}{med_{eGFR}}\right)}{Int_v + (Wt * Sl_v)} + K12\right] * X(1) + K21 * X(2).$$

To explore whether there were significant differences between the model predicted PK parameters in Vietnamese and Ugandan patients, Bayesian estimates of volume of distribution and clearance from the central compartment were compared using a Mann-Whitney test and a Student's t-test respectively. Since no significant relationship between ethnicity and DAmB PK was apparent, this variable was not incorporated in the final model.

The fit of the model to the data was assessed using a linear regression of observed-versus-predicted values before and after the Bayesian step. The coefficient of determination of the linear regression was noted in combination with the intercept and slope of the regression for each model. Model comparison was achieved through calculation of the log-likelihood value, the Akaike Information criterion (AIC), the mean weighted error (a measure of bias), and the bias-adjusted, mean weighted squared error (a measure of precision). To verify the ability of the final model to predict observed concentrations with acceptable accuracy, a visual predictive check (VPC) of the data was performed. For the VPC, the covariance matrix in Pmetrics was utilised to simulate 1000 patients administered DAmB on a mg per kg basis. Simulated weight was limited to the range observed in our clinical cohort.

3.2.4 Meta-analysis of clinical outcome data

The pharmacodynamic data from patients enrolled in the present clinical trial are confounded by the co-administration of fluconazole.[262] Therefore, a search was performed for clinical trials of treatment for cryptococcal meningoencephalitis with at least one arm comprised of adult patients receiving DAmB monotherapy. For consistency, included trials were limited to those that recruited HIV-positive patients. Baseline clinical variables with demonstrated ability to predict patient mortality were selected a-priori and extracted from the studies; namely altered mental status, patient age and baseline CSF fungal burden.[286,296] To aid meaningful trial comparison, baseline fungal burden and baseline CSF cryptococcal antigen titre were extrapolated from one another where they were not explicitly reported in the study, applying a correlation presented by Jarvis et al.[286]

We collated a variety of clinical trial outcomes based on those that were commonly reported across trials of DAmB monotherapy: documented CSF sterility during trial follow-up, mortality at 2 weeks and, where possible, mortality at 10 weeks. Meta-analysis was performed on each outcome using a dose-adjusted random effects model to account for the baseline heterogeneity in the included studies. We included dose as a moderator variable in the model to assess the degree to which it explained heterogeneity in clinical outcome.[325] The resulting mixed-effects model took the form:

$$\theta_i = \beta_0 + \beta_1 dose_i + u_i$$

Where β_0 and β_1 are the model parameters intercept and dose respectively; $dose_i$ is the dose given in the ith study, assuming study-specific random effects; and $u_i \sim N(0, \tau^2)$, where τ^2 is the amount of residual heterogeneity among the true effects θ_i that is not accounted for by dose. We calculated to what extent dose as a moderator influenced the true average effect, and estimated the corresponding proportions of each outcome measure.

3.2.5 Monte Carlo Simulations

Monte Carlo simulations were performed in Pmetrics.[273] Model 2 was used. Amphotericin B deoxycholate was administered on a mg/kg basis and infused over 5.5 hours. The initial condition of the central and peripheral compartment was defaulted to zero. The weight-based dosage of DAmB was converted to an absolute dosage by multiplying by the simulated patient's weight. This process served to mimic the bedside drug administration in the original clinical trial, in which dosing was planned on a mg/kg basis but the absolute dose that was ultimately administered was determined by the patient's weight.

Drug exposure was quantified using the DAmB AUC.[316,317,326] The simulated AUC for each patient was estimated 144 to 168 hours post therapy initiation. Simulations were performed to estimate the AUC that resulted from dosages administered in clinical trials of DAmB monotherapy for which PD measures were available – specifically, 0.4, 0.7 and 1.0mg/kg q24h.[63,74,77,319,320]

3.3 Results

3.3.1 Demographics

A total of 42 patients (22 from Vietnam and 20 from Uganda) were recruited over an 11-month period between January and November 2016. Twenty two patients (52 %) were female. The overall median (range) age was 33 years (20 – 73 years), weight 48 kg (32 – 68 kg) and body mass index 18 kg/m^2 (12 – 25 kg/m^2), creatinine at enrolment 69 µmol/L (37 – 167 µmol/L) and estimated glomerular filtration rate using the Cockcroft Gault equation 76.7 mL/min/1.73m^2 (35.4 – 146.7 mL/min/1.73m^2). The demographic data are shown by ethnicity and overall in table 3.1. There were no statistically significant differences between ethnic groups in any demographic variable.

Table 3.1: Patient demographics

Demographic or clinical characteristic	Vietnam	Uganda	Combined	p-value for difference between Vietnam and Uganda
Sex [a] (Male:Female)	12:10	8:12	20:22	
Age (years) [b]				
Mean	38	33	36	0.75†
Median	33	33	33	
Range	20 - 73	24 - 50	20 - 73	
Weight (kg) [c]				
Mean	47	49	48	0.21†
Median	46	49	48	
Range	32 - 68	35 - 60	32 – 68	
BMI (kg/m^2) [d]				
Mean	18	18	18	0.73$^{\Delta}$
Median	18	19	18	
Range	12 - 25	15 - 22	12 - 25	
Creatinine (µmol/L) [a]				
Mean	71	81	75	0.06†
Median	62	79	69	
Range	37 – 167	43 - 145	37 - 167	
eGFR (ml/min/1.73m^2) [e]				
Mean	90.6	79.3	84.7	0.19†
Median	89.8	73.5	76.7	
Range	35.4 – 136.1	49.8 – 146.7	35.4 – 146.7	

[a] *n* = 42

[b] *n* = 28

[c] *n* = 39

[d] *n* = 33

[e] *n* = 26

† Mann-Whitney test of significance

$^{\Delta}$ Unpaired t test of significance

BMI: Body Mass Index; eGFR: estimated Glomerular Filtration Rate, by Cockcroft-Gault equation

3.3.2 Pharmacokinetic data

The final dataset included 282 of 312 total observations from the Vietnamese cohort and 197 of 241 total observations from the Ugandan cohort (mean 11.4 samples per patient, range 6-18). In total, 74 plasma samples were excluded because of absent information on the time PK samples were drawn. Figure 3.1 shows the raw plasma concentration-time profiles from study participants.

Figure 3.1: Amphotericin B serum concentrations in 42 patients

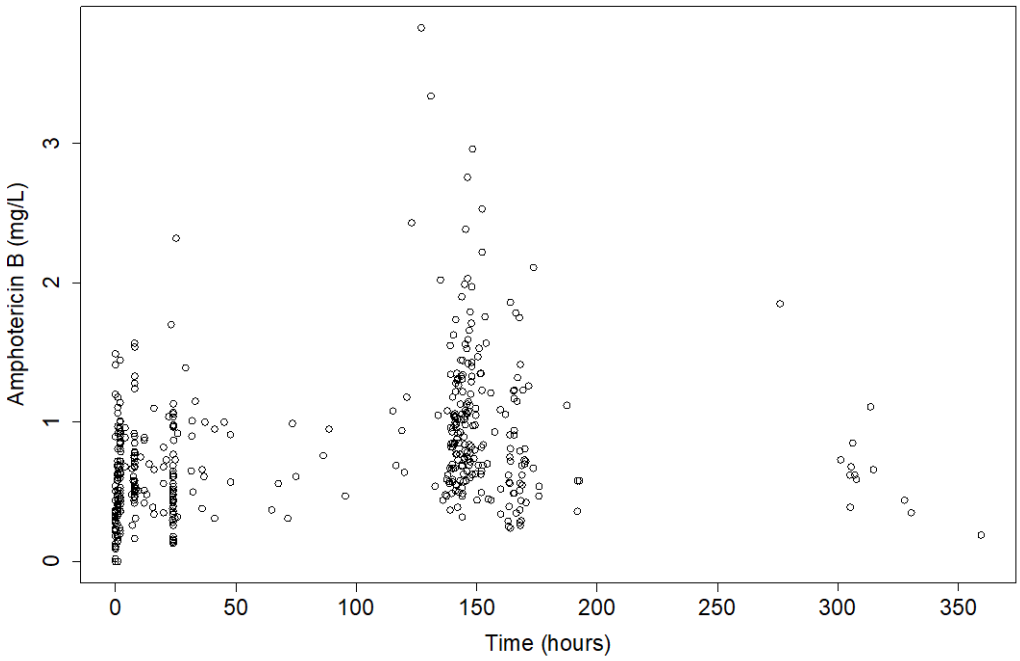

Patients received 1.0 mg/kg of amphotericin B deoxycholate (DAmB), infused over 5-6 hours.

3.3.3 Population pharmacokinetic models

Initial exploration of structural models revealed that a two-compartment model fitted the data better than a three-compartment model. Specifically, the three-compartment structural model resulted in a more negative log likelihood value (-55.5 versus -42.8) and higher AIC (127.3 versus 101.9). Accordingly, subsequent model development was based on a two-compartment base model.

Model 1 was a standard two-compartment model without inclusion of covariates. Linear regressions of the Bayesian estimates of clearance and volume (derived from the mean population PK parameter values from Model 1) with weight and estimated glomerular filtration rate (eGFR) as covariates are presented

in Figures 2a and 2b, respectively. A relationship was apparent between patient weight and both estimated clearance (slope 1.2, 95% confidence interval for estimate of slope 0.51 to 1.88, p=0.002) and estimated volume of the central compartment, (slope 1.08, 95% CI 0.05 to 2.11; p<0.001). Similarly, linear regression described a positive relationship between eGFR and estimated clearance (slope of linear regression 0.01, 95% CI for the slope 0 to 0.02, p<0.001) and volume (slope 0.67, 95% CI 0.36 to 0.98, p<0.001). These covariates were incorporated into the structural model as follows: Model 2 incorporated weight as a covariate with a linear term for clearance; Model 3 incorporated weight as a covariate with a non-linear term for clearance and Model 4 incorporated both weight and baseline renal function as covariates in the equations, with linear clearance. Population PK parameter estimates for all 4 models are shown in table 3.2. There were no statistically significant differences in estimated clearance and volume from the standard model (Model 1) according to ethnicity. The mean (95% CI) clearance was 2.03 litres/h (1.69 – 2.38) and 2.24 litres/h (1.91 – 2.56) for Vietnamese and Ugandan patients, respectively; p-value 0.37. The mean (95% CI) volume was 33.55 litres (17.96 – 49.13) and 63.93 litres (40.98 – 86.88) for Vietnamese and Ugandan patients, respectively; p-value 0.09.

Figure 3.2: Linear regression of the relationship between (A) patient weight and (B) estimated glomerular filtration rate and Bayesian posterior estimates for clearance and volume of distribution

A

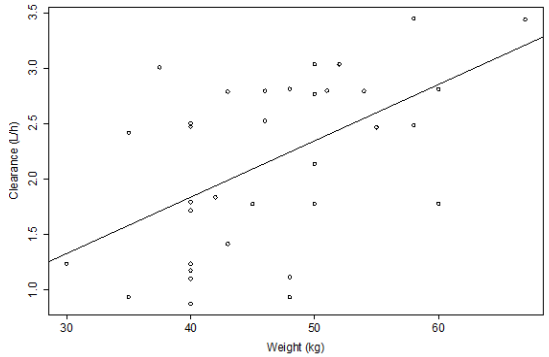

R2=0.32. Clearance = 0.05*weight – 0.2

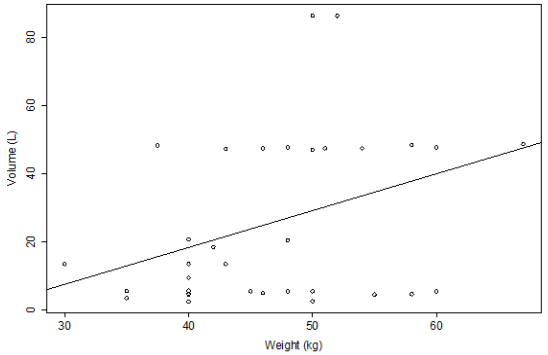

R2=0.12. Volume = 1.08*weight – 24.8

B

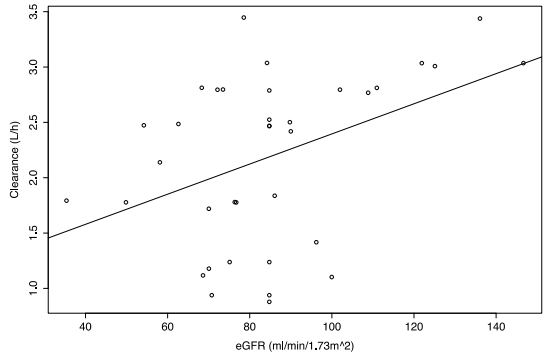

R2=0.17. Clearance = 0.01*weight + 1.03

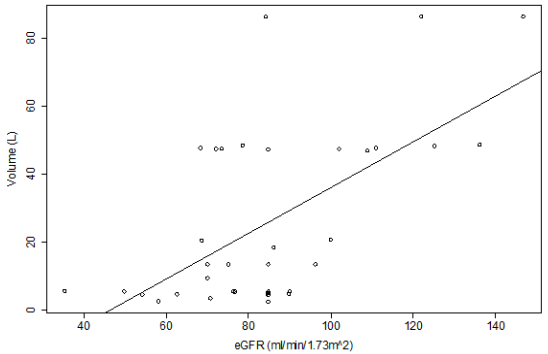

R2=0.36. Volume = 0.67*weight – 31.13

Circles are Bayesian estimates from each patient. Solid line: linear regression.

Table 3.2: Parameter estimates for the initial and modified two-compartment pharmacokinetic models

Parameter and model	Mean	Median	Standard deviation
Model 1			
SCL (L/h)	2.19	2.46	0.77
Vc (L)	27.77	13.88	28.06
K12 (h^{-1})	3.84	2.16	6.57
K21 (h^{-1})	1.14	0.32	3.06
IC (mg)	10.16	2.55	9.00
Model 2			
SCL_{slope} (L/h/kg)	0.03	0.03	0.01
$SCL_{intercept}$ (L/h)	0.67	0.57	0.01
Vc_{slope} (L/kg)	0.82	0.36	0.80
$Vc_{intercept}$ (L)	1.76	1.99	1.29
K12 (h^{-1})	5.36	3.83	6.76
K21 (h^{-1})	9.92	0.46	12.27
IC (mg)	20.29	6.03	27.75
Model 3			
SCL (L/h/kg)	0.12	0.12	0.04
Vc (L/kg)	1.40	0.51	1.75
K12 (h^{-1})	1.69	0.50	4.09
K21 (h^{-1})	8.31	0.27	12.32
IC (mg)	30.10	7.87	40.56
Model 4			
SCL_{slope} (L/h)	0.01	0.01	0.01
$SCL_{intercept}$ (L/h)	1.50	1.31	0.74
Vc_{slope} (L)	1.26	0.52	1.39
$Vc_{intercept}$ (L)	1.64	0.01	2.96
K12 (h^{-1})	3.86	0.73	7.74
K21 (h^{-1})	11.24	0.40	13.44
IC (mg)	26.15	6.17	26.76

SCL: Clearance; Vc: Volume of distribution in central compartment; K12: first-order rate constant from the central to peripheral compartment; K21, first-order rate constant from peripheral to central compartment; IC: initial condition.

For all 4 two-compartment models the fit of the model to the data was acceptable. The model diagnostics are presented in table 3.3. The coefficient of determination of a linear regression of observed-versus-predicted plots after the Bayesian step was 0.72, 0.74, 0.69 and 0.73 for Models 1, 2, 3 and 4, respectively. The intercept and slope approximated 0 and 1 respectively for each regression (table 3.3). The mean parameter values predicted the observed values better than the medians. The measures of population bias and imprecision were comparable between the models, with bias -0.85, -0.34, -0.23 and -0.43 and imprecision 3.13, 2.97, 2.16 and 3.29 for Models 1, 2, 3 and 4 respectively. The more positive log likelihood value and lower Akaike information criterion (AIC) for Model 2 implied that the inclusion of weight as a covariate explained a portion of the observed variance.

Table 3.3: Evaluation of the predictive performance of the initial and final model

						Linear regression of observed-predicted values for each patient		
Model	**Log likelihood**	**Number of cycles to convergence**	**AIC**	**Population bias**	**Population imprecision**	**$R^{2,a}$**	**Intercept**	**Slope**
Model 1	-56.3	1137	124.8	-0.85	3.13	0.72	0.08	0.97
Model 2	-42.8	1251	101.9	-0.34	2.97	0.74	0.01	1.01
Model 3	-102.7	577	221.7	-0.23	2.16	0.69	0.00	1.04
Model 4	-43.1	1704	102.7	-0.43	3.29	0.73	0.01	1.02

Model 2 included a linear function to scale DAmB clearance to patient weight.
Model 3 included a non-linear function to scale DAmB clearance to patient weight.
Model 4 included a function to scale DAmB clearance to patient weight and eGFR.
[a] Relative to the regression line fitted for the observed versus predicted values after the Bayesian step.

The model that incorporated an exponential term for clearance (Model 3) decreased the log likelihood value and increased the AIC (table 3.3). The inclusion of eGFR in Model 4 failed to increase the log likelihood value or reduce the AIC further. In addition, there was no statistically significant difference between Model 1 and either Model 3 or Model 4; the latter models were therefore rejected. Model 2 was chosen as the final model. Observed-versus-predicted plots for the population and Bayesian posterior values in the final model are shown in figure 3.3. Figure 3.4 shows a visual predictive check (VPC) of the final model.

Figure 3.3: Scatter plots showing observed versus predicted values for the chosen population pharmacokinetic model after the Bayesian step (model 2)

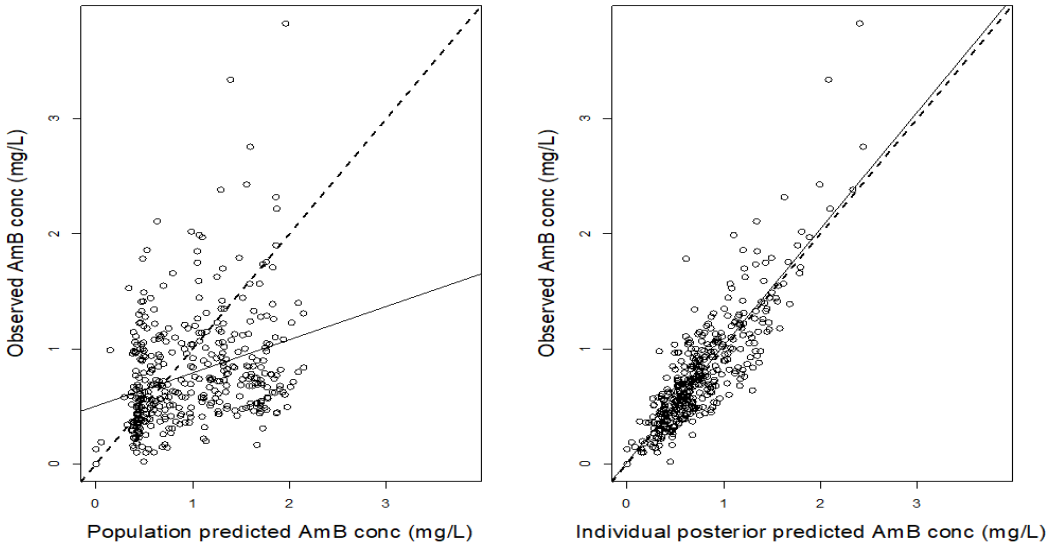

R2=0.17
Intercept = 0.18 (95% CI 0.03 – 0.32)
Slope = 0.89 (95% CI 0.70 – 1.09)

R2=0.74
Intercept = 0.01 (95% CI -0.04 – 0.07)
Slope = 1.01 (95% CI 0.95 – 1.07)

Circles, dashed lines, and solid lines represent individual observed-predicted data points, line of identity, and the linear regression of observed-predicted values, respectively. All observed and predicted amphotericin B concentrations in mg/L. AmB: Amphotericin B; CI: Confidence Interval.

Figure 3.4: Visual predictive check of the final model

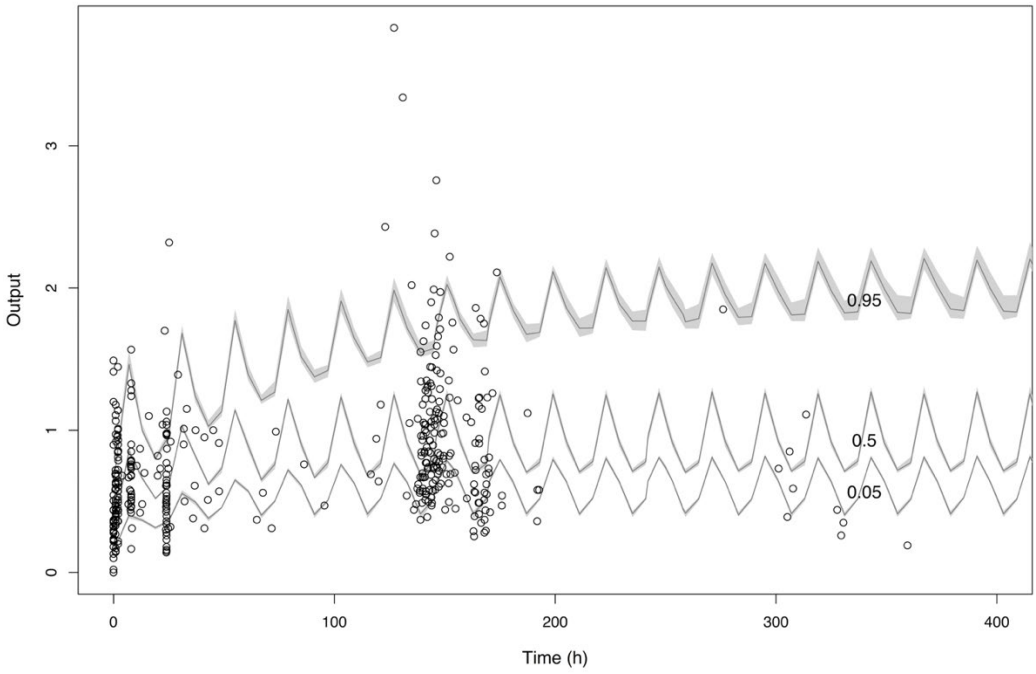

Black circles indicate observed DAmB concentrations. The continuous lines represent the 5th, 50th and 95th percentiles of DAmB concentrations in 1000 simulated patients. In total, 83.4% of observed DAmB concentrations fall within the 5th and 95th percentiles estimated by the final model, indicating adequate model fit.

3.3.4 Meta-analysis of clinical outcome data

Five clinical trials that included a DAmB monotherapy arm were identified. There was one trial in which 63 patients received 0.4 mg/kg q24h[63], 3 in which a combined 208 patients received 0.7 mg/kg q24h[77,319,320] and 1 in which 99 patients received 1.0 mg/kg q24h.[74] An additional study that reported clinical outcomes in untreated cryptococcal meningoencephalitis patients was also included. The baseline variables and clinical outcomes of these study arms are summarised in table 3.4. Due to the small number of studies, we were unable to adjust for baseline variables that may have had an impact on outcome measures (age, CD4 cell count, baseline level of consciousness, baseline fungal burden and baseline cryptococcal antigenaemia). The forest plots of the dose-adjusted random effects model are shown in figure 3.5. The model suggests that dose adjustment accounts for 77% of the heterogeneity in CSF sterility (p=0.007) but did not have a significant impact on the heterogeneity in either 2- or 10-week mortality outcomes (33%, p= 0.139 and 39%, p=0.092 respectively).

Table 3.4: Clinical outcomes from trial data of DAmB monotherapy, by dosing regimen

DAmB regimen	Location	Number of patients	Median age	Median CD4 cell count per mm^3	Reduced LOC at baseline, no./total no (%)	Median baseline fungal burden, log_{10} CFU/ml	Baseline CSF CrAg titre, median	Documented CSF sterility, no./total no (%)	Mortality at 2 weeks, no./total no (%)	Mortality at 10 weeks, no./total no (%)	Percentage decrease haemoglobin, median (range)	Hypokalaemia	Reference
No treatment	Zambia	100	32	NR	NR	NR	NR	*0/100 (presumed)*	65/100 (65)	100/100 (100)	NR	NR	Mwaba et al, Postgrad Med J. 2001[48]
0.4 mg/kg q24h	USA	63	37	NR	16/63 (25)	NR *≈ 4.2*	1:512*	25/63 (40)	5/63 (8)	NR; 9/63 at 12 weeks (14%)	NR	NR	Saag et al, NEJM 1992[63]
0.7 mg/kg q24h	Thailand	16	34	9	1/16 (6)	5.63 (5.19 – 5.97)	1:512	NR	2/16 (13)	3/16 (19)	NR	NR	Brouwer et al, Lancet 2004[320]
0.7 mg/kg q24h	Australia/ The Nether-lands	13	41	35	2/13 (15)	NR *≈ 3.9*	1:256	3/8 (37)	0/13 (0)	2/13 (15)	20 (45-5) at 10 weeks Fall in Hb >2g/dL: 2/13 (15%)	4/13 (31) <3mEg/L	Leenders et al, AIDS 1997[319]
0.7 mg/kg q24h	USA	179	37	18	18/179 (10)	NR *≈ 4.8*	1:1024	91/179 (51)	11/202 (5)	NR	NR in consistent way	NR in consistent way	Van der Horst et al, NEJM 1997[77]
1.0 mg/kg q24h	Vietnam	99	28	18	31/97 (32)	5.91 (5.49 – 6.48)	NR *≈1:4096*	52/99 (53)	25/99 (25)	44/99 (44)	All anaemia 62/99 (63). Grade 3-4[±]: 46/99 (46)	All 54/99 (55). Gr 3-4: 20/99 (20)	Day et al, NEJM 2013[74]

LOC: level of consciousness; no.: number; CFU: Colony Forming Units; NR: not reported; CSF: cerebrospinal fluid; CrAg: cryptococcal antigen. NEJM : New England Journal Of Medicine. * Reported in.[77] Italic text indicates value extrapolated from available data. ± Grade 3-4 anaemia defined as haemoglobin <8 g/dL. ^ Grade 3-4 hypokalaemia defined as <2.5 mmol/L.

Figure 3.5: Meta-analysis of clinical trials of DAmB monotherapy showing dose adjusted effects on A) CSF sterility, B) Mortality at 2 weeks and C) Mortality at 10 weeks

A)

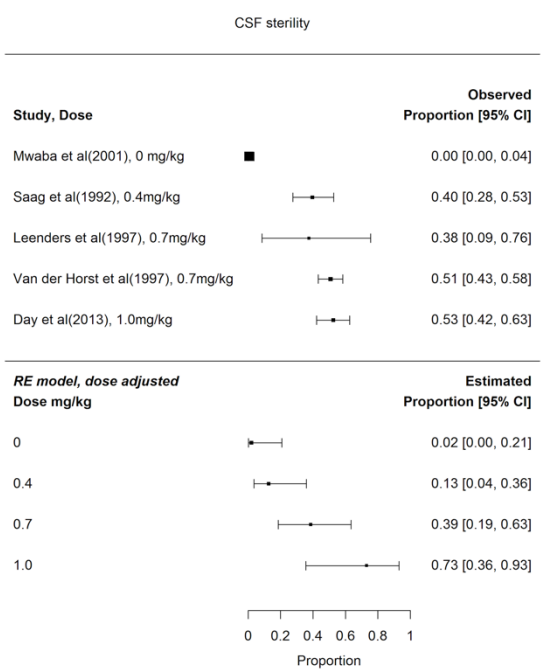

Tau value for unadjusted model: 4.22. Tau value for dose-adjusted model: 0.98. Dose adjustment accounts for (4.22 – 0.98)/4.22 = 77% of heterogeneity in clinical outcome. P-value for dose adjustment 0.007.

B)

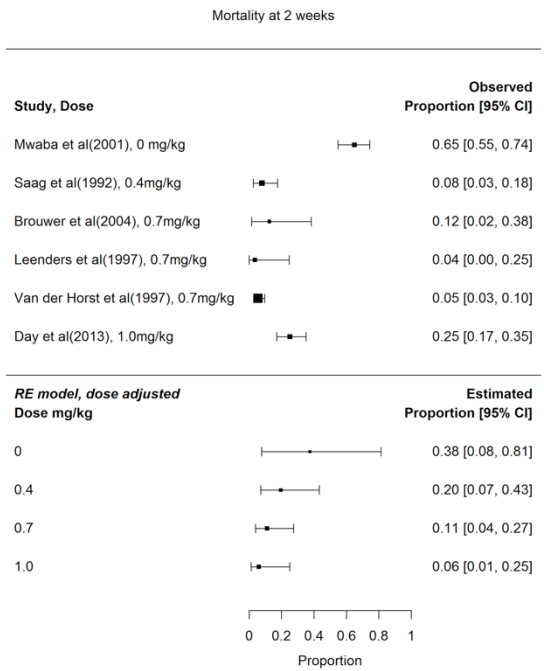

Tau value for unadjusted model: 1.90. Tau value for dose-adjusted model: 1.28. Dose adjustment accounts for (1.90 – 1.28)/1.90 = 33% of heterogeneity in clinical outcome. P-value for dose adjustment 0.14.

C)

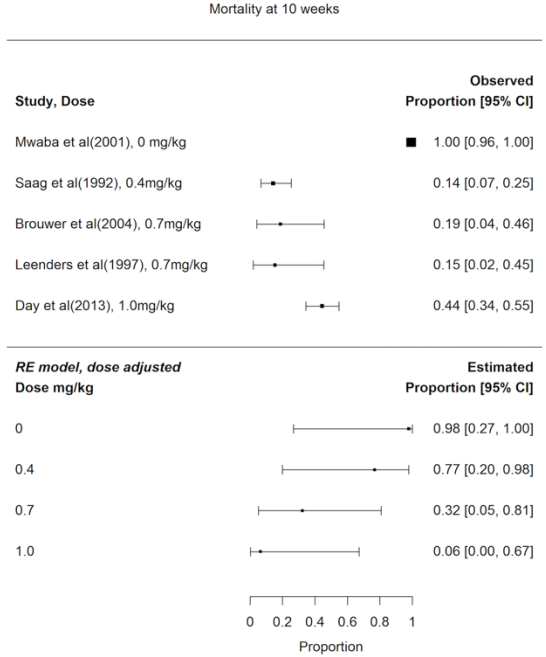

Tau value for unadjusted model: 9.0. Tau value for dose-adjusted model: 4.93. Dose adjustment accounts for (9.00 – 4.93)/9.00 = 45% of heterogeneity in clinical outcome. P-value for dose adjustment 0.07.

3.3.5 Monte Carlo simulations

Monte Carlo simulations (n = 5,000) were performed from the final population PK model. This enabled exploration of the consequences of the population PK variability, quantified in the final model, on plasma DAmB concentrations in a simulated population receiving the dosage regimens for which clinical trial outcome data were available. The median (interquartile range) $AUC_{144-168}$ was 5.91 mg/L*h (4.96 – 9.33 mg/L*h) for patients receiving DAmB 0.4 mg/kg q24h, 10.21 mg/L*h (8.51 – 15.72 mg/L*h) for 0.7 mg/kg q24h and 14.61 mg/L*h (12.14 – 22.03 mg/L*h) for 1.0mg/kg q24h. The $AUC_{144-168}$ distributions from the simulations are shown in figure 3.6.

Figure 3.6: AUC distributions based on Monte Carlo simulations

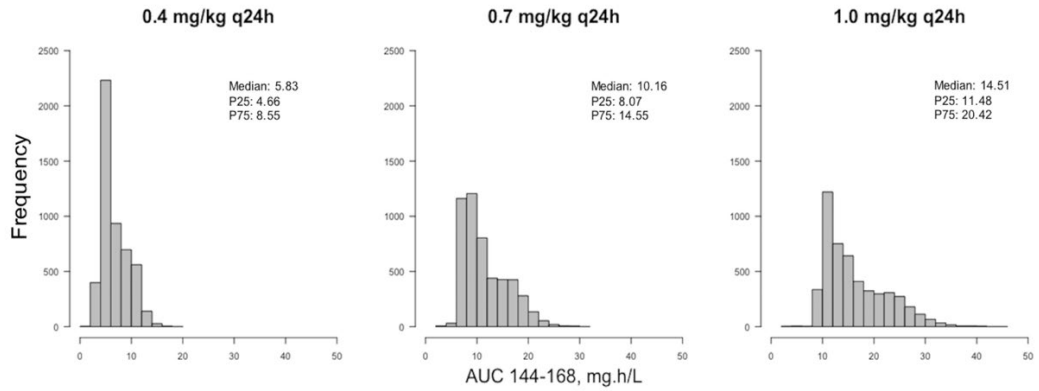

Simulated dosing regimens are 0.4, 0.7 and 1.0 mg/kg q24h. Medians, 25th and 75th percentiles displayed on each histogram (P25 and P75).

3.4 Discussion

We conducted a PK study in HIV positive adults with cryptococcal meningoencephalitis in regions of high disease burden, and developed a population PK model that enabled the extent of interpatient variability to be quantified. We described the PK of DAmB using a 2-compartment PK model with intravenous (IV) infusion and first-order clearance of drug from the central compartment. Simulated AUCs reveal relatively modest PK variability, suggesting that the frequently poor clinical outcomes are not the result of significant PK variability. The relationship between weight and drug clearance suggests that weight accounts for a portion of the observed variance. Dosage adjustment on the basis of weight is necessary to ensure lighter patients are not over-dosed and heavier patients are not under-dosed. However, the lack of impact of either eGFR or ethnicity on the PK suggests that dosage adjustment for these variables is not necessary to achieve comparable drug exposure across patient populations.

The model-simulated median AUC of 10.17 mg.h/L following a regimen of 0.7 mg/kg q24h is consistent with AUCs estimated using non-compartmental techniques. For example, Bekersky et al calculated an $AUC_{0\text{-}24}$ of 13.9 +/- 2 mg.h/L after 0.6 mg/kg IV in healthy volunteers.[327] However, the simulations following 1mg/kg resulted in a median AUC of 14.52 mg.h/L, which is considerably lower than that derived from a non-compartmental analysis (NCA) conducted by Ayestarán *et al* for the same dose administered to neutropenic patients (28.98 +/- 15.46 mg.h/L).[328] The reason for this is not immediately clear but may relate to physiological differences between these two critically unwell patient cohorts.[329]

Our meta-analysis of clinical outcomes from studies of DAmB monotherapy is limited by the fact that the included studies recorded CSF sterility at diverse time points ranging from 2 weeks[77] to 10 weeks.[63] Nevertheless, the meta-analysis suggests that the dosage of DAmB has a significant impact on the proportion of patients with sterile CSF and that achieving CSF sterility is dose-dependent up to 1mg/kg q24h. However, DAmB does not have a dose-dependent relationship with mortality at either 2 or 10 weeks.

The potential reasons that DAmB dosage has a positive impact on CSF sterilisation, but not mortality are as follows: first, AmB toxicity may contribute to mortality.[53,321] Nephrotoxicity is dose-dependent and likely multifactorial. It is associated with 4.5 times increase in the odds of mortality from cryptococcal meningoencephalitis at 10 weeks.[53] Free drug interacts with the distal tubules of the nephron causing increased monovalent ion delivery, with consequent afferent arteriolar constriction.[54] Direct tubular toxicity results in hypokalaemia and hypomagnesaemia leading to cardiotoxicity.[54,55] Conversely, rapid infusion of AmB can result in extracellular shift of potassium, causing hyperkalaemia and cardiac dysrhythmias.[56] Anaemia occurs in up to 75% of patients treated with DAmB as a result of direct suppression of erythropoiesis.[54] Severe anaemia more than doubles the odds of 10-week mortality from cryptococcal meningoencephalitis.[53] Secondly, mortality may be driven by factors not directly resulting from either disease or treatment. For example, nosocomial bacteraemia may occur in up to 15-18% of patients hospitalised for cryptococcal meningoencephalitis.[330] Third, fungal burden – and therefore conceivably, time

to CSF sterility - is just one of multiple clinical variables associated with mortality in cryptococcal meningoencephalitis. Older age, altered mental status, low body weight, high peripheral white blood cell count and anaemia are independently associated with mortality at either 2 or 10 weeks.[286] Immune reconstitution inflammatory syndrome (IRIS) remains a significant cause of mortality, occurring in 3 - 49% of cryptococcal meningoencephalitis patients surviving to initiation of antiretroviral treatment and carrying a mortality rate of up to 36%.[262,331] Raised intracranial pressure is an additional factor associated with mortality and at least 1 therapeutic lumbar puncture imparts a relative survival advantage of 69% in the first 10 days of treatment.[332] Finally, the trial cohorts included in the meta-analysis were from diverse sites in Africa, Asia, Europe and the USA. Factors such as health seeking behaviour and nutritional status may have influenced mortality outcomes. Our meta-analysis did not include any baseline factors besides DAmB dosage and we are therefore unable to identify whether they account for the heterogeneity in mortality that is not explained by DAmB dosage.

The discordance between the influence that drug dosage has on CSF sterilisation and mortality is reflective of a growing consensus that CSF sterility is just one of many determinants of mortality in cryptococcal meningoencephalitis. A systematic review of 27 clinical trials determined that there was no correlation between CSF sterility at 2 weeks and all-cause mortality at either 2 or 10 weeks.[296] The most biologically plausible explanation for this is that fungal burden in the CSF may not reflect the extensive encephalitis that is characteristic of cryptococcal meningitis (which is more accurately termed meningoencephalitis).

Histopathological defects are more marked in patients co-infected with HIV; fungi accumulate in perivascular spaces, are deposited [predominantly extracellularly] in brain parenchyma, and form granulomatous cryptococcomas in brain tissue.[104,106] It is conceivable that brain parenchymal damage is a dominant determinant of mortality and that clearance of fungi in CSF is not mirrored by clearance in the cerebrum and other CNS sub-compartments. CSF sterility is an imperfect surrogate for the extent to which drug has penetrated to and sterilised the central nervous system.

The meta-analysis suggests a strong dose-exposure-response relationship. Higher dosages are likely to be required to achieve efficacious drug exposure at the site of infection. DAmB has a large molecular weight (924 g/mol) and complex binding properties.[89] It is greater than 95% protein bound in plasma (Table 1) and does not readily penetrate the intact blood-brain barrier. Its concentration in meninges and cryptococcomas has been technically difficult to quantify in any finer detail than brain homogenates in preclinical models.[84,333] We were therefore required to extrapolate the CNS PK-PD relationships of DAmB based solely on plasma PK data, without certainty about how this relates to CNS PK. Furthermore, there is a lack of clarity regarding the DAmB concentration required for therapeutic efficacy at the site of infection. Animal studies estimate that the cerebral concentration of DAmB at which the suppression of growth is half-maximal is 0.02 mg/litre in mice and 0.154 mg/litre in rabbits.[84] AmB exposure above the level required to optimise antifungal activity appears only to contribute to toxicity.[83,84] Our simulations suggest that the optimal plasma AUC value in

humans lies somewhere between 10-15 mg.h/L, though the information required to extrapolate this to cerebral DAmB concentrations is not currently available. The application of non-invasive, high-resolution technologies including Matrix-Assisted Lazer Desorption and Ionisation- Mass Spectroscopy Imaging (MALDI-MSI) is now possible, and offers the exciting potential to elucidate the PK/PD index associated with efficacy at the site of infection by enabling quantification of drug in specific cerebral sites, as has been demonstrated in murine models with gatifloxacin,[334] doxycycline,[335] pretomanid[336] and rifampicin.[337]

It may be the case that the maximal antifungal effect of DAmB is achieved with a dose of approximately 0.7 mg/kg, or slightly higher, and that gains made above this dose in terms of CSF sterility are offset by losses in terms of excessive toxicity. This may explain why significant increases in the proportion of patients achieving CSF sterility are not mirrored by reductions in mortality. The present analysis is not sufficient to more precisely define the optimal dosage of DAmB. This is partly due to the lack of consensus regarding DAmB exposure targets. We are unable to propose exposure targets based on our dataset, which does not include site-specific PK or detailed toxicodynamic data. In addition, the pharmacodynamic and clinical outcome data presented herein are derived from patient cohorts that are distinct from the patients that provided samples for the PK analysis. DAmB monotherapy at dosages of 0.7 mg/kg q24h and 1.0 mg/kg q24h has not been directly compared in a randomised controlled trial. However, comparison of these dosages in combination with 5FC has been performed. Bicanic *et al* demonstrated increased early fungicidal activity with 1mg/kg q24h

DAmB versus 0.7mg/kg q24h DAmB, both in combination with 5FC 100mg/kg/day in four divided dosages, but this was not reflected in reductions in mortality. A higher percentage of deaths was seen in the higher dose DAmB arm at both 2 weeks (9% versus 3%) and 10 weeks (26% versus 21%) but this was not statistically significant (p= 0.62 and 0.77 at 2 and 10 weeks, respectively).[75]

In summary, these analyses suggest that the optimal dosage of DAmB for the treatment of cryptococcal meningoencephalitis lies between 0.7-1.0 mg/kg q24h. The precise drug exposure target that optimises clinical outcomes without producing significant toxicity remains to be defined. The extent of inter-individual PK variability in DAmB is modest and unlikely to account for the consistently poor clinical outcomes from cryptococcal meningoencephalitis.

4 Population pharmacokinetics of liposomal amphotericin B in adults with HIV-associated cryptococcal meningoencephalitis.

4.1 Introduction

Over recent years, considerable interest has arisen in the use of abbreviated amphotericin B-based induction regimens for cryptococcal meningoencephalitis. Shortening the duration of amphotericin B therapy offers the potential benefits of reduced hospital admission times, lower requirement for laboratory monitoring for toxicity, less burden on nursing staff to set up and administer intravenous infusions and lower financial costs associated with each of these factors. The Antifungal Combinations for Treatment of Cryptococcal Meningitis in Africa (ACTA) trial drove huge progress in this regard, demonstrating that 7 days of DAmB (1 mg/kg/day) plus flucytosine (100 mg/kg/day) followed by 7 days of fluconazole (1200 mg/day) is non-inferior to regimens based on two weeks of DAmB, in terms of mortality at ten weeks[14] and one year.[57]

Liposomal amphotericin B (LAmB) is a formulation of amphotericin B that delivers drug in unilamellar liposomes consisting of a spherical phospholipid bilayer into which amphotericin B compound is incorporated. Each liposome is less than 100 nm in diameter and has a particle size of 0.05-0.08 μm (table 1.2). LAmB is particularly suited to abbreviated therapy for cryptococcal meningoencephalitis because it has a relatively good safety profile that permits higher dosages,[338] a long terminal elimination phase in tissues[83,339] and it achieves 4- to 10-fold greater concentrations in brain tissue than other polyene

formulations at equivalent dosages.[333] Despite over 25 years of clinical experience with LAmB for treatment of a range of IFIs in adults and children, there are limited data describing the pharmacological properties of the drug and in particular its population pharmacokinetics.[26,340-342] There are no population PK models describing LAmB at high doses in abbreviated regimens in adult patients.

In rabbits and mice, abbreviated LAmB regimens produce sustained antifungal activity.[83] The AMBIsome Therapy Induction OptimisatioN (AMBITION) trial seeks to determine whether the same is true in humans.[343] The current PK study was conducted as a substudy of phase III of the AMBITION trial. By describing the population PK of LAmB administered at a high dose and in an abbreviated regimen to trial participants, we provide a basis for understanding the action of this drug in a clinically relevant population. An improved understanding of the PK of LAmB is essential to optimise abbreviated dosing of this drug.

4.2 Materials and methods

4.2.1 Clinical study

In phase III of AMBITION, patients with HIV-associated cryptococcal meningoencephalitis were randomised to either a single high dose of LAmB (10 mg/kg/day) followed by 14 days of flucytosine (100 mg/kg/day) plus fluconazole (1200 mg/day) – the intervention arm - or 7 days of DAmB (1 mg/kg/day) plus flucytosine (100 mg/kg/day), followed by 7 days of fluconazole (1200 mg/day) – the control arm.[343] The primary endpoint was all-cause mortality.[343] The present PK study recruited patients allocated to the intervention arm. Due to the

combination regimen received by participants in the AMBITION trial and the fact that the oral component of induction therapy differed between study arms, we were unable to assess the PD of LAmB using data from this cohort.

The PK substudy was conducted at Queen Elizabeth Central Hospital in Blantyre, Malawi. Ethical approval was granted by the Malawi National Health Sciences Research Committee as well as the Research Ethics Committee of the London School of Hygiene and Tropical Medicine. All patients who had capacity to do so provided written, informed consent for participation in the trial and then separately for inclusion in the PK substudy. Where patients were incapacitated, consent was obtained from a next of kin with legal responsibility and then re-attempted with the patient if it became possible according to their clinical status.

4.2.2 Pharmacokinetic sampling

LAmB was administered over a 2-hour period following pre-hydration with 1 litre of 0.9% sodium chloride containing 20 mmol potassium chloride. Blood samples were collected on day 1 at 0, 2, 4, 7, 12 and 23 hours after the LAmB infusion was started, and then on day 7 at 2, 4, 7, 12 and 23 hours. A volume of 2 mL of blood was collected into heparinised collection tubes and placed on ice at the bedside. Within 30 minutes of collection, samples were centrifuged at 1500g for 10 minutes at 4°C. Plasma was stored at -80°C until shipment to the University of Liverpool.

4.2.3 Bioanalysis of pharmacokinetic samples

Amphotericin B concentrations in plasma were quantified by reverse phase ultra-performance liquid chromatography (UPLC) interfaced with a triple quadrupole mass spectrometer using the ACQUITY UPLC system (Waters, Manchester, UK). Amphotericin B was extracted by protein precipitation, using natamycin as internal standard in methanol (2.5 µg/mL) and with 200 µL natamycin/ methanol solution to 50 µL patient sample. Positive pressure was applied to filter out the protein precipitate and collect the supernatant. A volume of 200 µL was added to each well containing supernatant before samples were analysed by UPLC – tandem mass spectrometry. A 5 µL aliquot was injected onto the reverse phase ACQUITY UPLC HSS T3 column (Waters, Manchester, UK) to separate compounds based on their hydrophobicity. Gradient starting conditions were 95% A : 5% B, with 0.1% formic acid in water as mobile phase A and 0.1% formic acid in acetonitrile as mobile phase B. Mobile phase B was increased to 99% over 2 minutes and then reduced to starting conditions for 1 minute of equilibration. Flow rate was 0.4 mL/minute.

The calibration line for amphotericin B encompassed the concentration range 0.25- 50.0 mg/L and was constructed using blank matrix. The lower limit of quantitation was 0.25 mg/L. The coefficient of variation was <9.0% over the concentration range 0.25- 50.0 mg/L. The intra- and inter-day variation was <15%.

4.2.4 Minimum inhibitory concentration testing

MICs to amphotericin B were determined in triplicate by Etest according to the manufacturer's instructions (Biomerieux, France). Briefly, cryptococcal colonies grown from CSF on days 1, 7 and 14 of treatment were inoculated into distilled water and the solution adjusted to 1.0 McFarland standard. The solution was streaked three times, with 60-degree rotation between each application, onto RPMI agar (with L glutamine, without sodium bicarbonate). This streaking procedure was performed twice per plate. Once the agar was dry, sterile forceps were used to apply the Etest strip to the surface. Results were read after 48 hours incubation at 30°C and 100% growth inhibition. *Candida albicans* ATCC 90028 was the quality control strain. Etests were performed in real time during the clinical study, rather than on stored isolates.

4.2.5 Population pharmacokinetic modelling

The PK data were analysed using the non-parametric adaptive grid (NPAG) algorithm of the program Pmetrics version 1.5.2 for R version 3.6.1.[273] Both two- and three-compartment structural models were explored to fit patient data, with zero-order input into the central compartment and options of both first order and non-linear (Michaelis Menten) elimination kinetics from the central compartment. Both mean and median parameter values were examined. The fit of the various models to the data was assessed and compared on the basis of observed-versus-predicted values before and after the Bayesian step, the coefficient of

determination of the linear regression of these data, the Akaike Information criterion (AIC), the log-likelihood value, the mean weighted error (a measure of bias) and the bias-adjusted, mean weighted squared error (a measure of precision). The chosen base model took the following form:

1. $\frac{dX(1)}{dt} = R(1) - \left(\frac{SCL}{V} + K12\right) * X(1) + K21 * X(2)$
2. $\frac{dX(2)}{dt} = K12 * X(1) - K21 * X(2)$
3. $Y(1) = \frac{X(1)}{V}$

Equations 1 and 2 describe the rate of change of the amount of drug (mg) in the central compartment and the peripheral compartment, respectively. R(1) is the intravenous infusion of LAmB into the central compartment. SCL is the first-order clearance of drug from the central compartment in L/h. The volume of the central compartment is represented by V. K12 and K21 are the first order intercompartmental rate constants. The model output (concentration of amphotericin B in the central compartment) is described by equation 3. The three-compartment model that was tested included an additional equation to describe movement of drug from the general peripheral compartment (2) to a separate compartment (3), designed to represent the CNS; equation 4.

4. $\frac{dX(3)}{dt} = K23 * X(2) - K32 * X(3)$

To determine whether non-linear clearance kinetics better described the movement of amphotericin B out of the central compartment than first order clearance kinetics, models that replaced equation 1 with equation 5 were run:

5. $\frac{dX(1)}{dt} = R(1) - \left(\frac{Vmax}{Km*V+X(1)} + K12\right) * X(1) + K21 * X(2)$

In equation 5, Vmax represents the maximal rate of enzymatic metabolism of amphotericin B in mg/hr and Km represents the concentration of amphotericin B in the central compartment when enzyme activity is half maximal.

Bidirectional stepwise multivariate linear regression was employed to identify any significant associations between clinical covariates and LAmB PK. Patient age, weight, CD4+ cell count, baseline serum creatinine and baseline creatinine clearance (derived from Cockroft-Gault equation) were investigated as independent predictors of the Bayesian posterior estimates of PK parameters from the baseline model. No such associations were found to be statistically significant and consequently no clinical covariates were incorporated into the population model.

4.2.6 Toxicity

Potential relationships between drug exposure and toxicity were explored. Exposure was measured in the first 24 hours and over the first week of therapy by calculating $AUC_{0\text{-}24}$ and $AUC_{0\text{-}168}$ through trapezoidal approximation in Pmetrics using the Bayesian posterior PK predictions from the population model.[273] Toxicity was defined as changes from baseline values prior to commencement of therapy, with the following parameters: a drop in haemoglobin of $\geq$ 2 g/dl or to $\leq$ 8 g/dl; a rise in creatinine of 35 μmol/L or $\geq$ double baseline value; a fall in potassium to <3.0 mmol/L or a rise in alanine transferase to $\geq$ 3 times baseline value. Toxic levels were recorded at any time during the first week of treatment.

4.2.7 Monte Carlo simulations

The Pmetrics-integrated Monte Carlo engine was used to simulate 9999 patients administered single doses of LAmB ranging from 1 mg/kg to 15 mg/kg. To mimic the clinical trial, all LAmB doses administered to simulated patients were delivered by IV infusion over 2 hours. The simulations served dual purposes. Firstly, simulation of the 10 mg/kg single dose regimen was used for internal model validation by means of a visual predictive check (VPC). This was performed to verify the accuracy with which the model predicted observed amphotericin B concentrations. The VPC was constructed by plotting simulated concentration-time profiles (5^{th}, 50^{th} and 95^{th} percentile) over observed concentrations. The proportion of observed concentrations that fell within the 5^{th} and 95^{th} percentiles was measured. Secondly, simulations of AUC resulting from a range of single LAmB doses provided insight into the expected parameters of drug exposure and the extent of PK variability resulting from those regimens.

4.2.8 Bridging studies

Since patients in phase III of AMBITION received flucytosine (100 mg/kg/day) and fluconazole (1200 mg/day) alongside LAmB, it was not possible to relate clinical PD outputs from the trial to LAmB PK specifically. A PD model defined in a preclinical murine model of cryptococcal meningoencephalitis[83] was therefore used, with the AUC determined by trapezoidal approximation for each

simulated human patient substituted into the inhibitory E_{max} model generated from murine data:

6. $$Effect\ (log_{10}\ CFU/g) = C_{dens} - \left(\frac{E_{max} * AUC}{EC_{50} + AUC}\right)$$

where C_{dens} is the cerebral density of cryptococcus at baseline, E_{max} is the maximum antifungal effect produced by LAmB, EC_{50} the exposure of LAmB that produces 50% of the maximal antifungal effect, and AUC the area under the concentration-time curve for each simulated patient. This E_{max} model was previously used to predict residual fungal burden at 10 days.[83] A linear regression was performed to predict the intercept and slope for each simulated patient's fungal burden over time, and from the linear regression values a predicted day 10 residual fungal burden was calculated.

4.3 Results

4.3.1 Patient cohort

In total, 32 patients allocated to the intervention arm of AMBITION phase III were recruited to the PK study between November 2018 and October 2019. Demographic and baseline clinical data are displayed in table 4.1.

Table 4.1: Baseline patient data

Demographic or clinical characteristic			
Sex (Male:Female)	21:11		
	Mean	**Median**	**Range**
Age (years)	36.7	35.5	20 - 67
Weight (kg)	51.9	50.0	40.0 – 83.0
Haemoglobin (g/dL)	10.9	11.0	7.0 – 17.0
Creatinine (mmol/L)	69.1	64.5	21.0 – 155.0
Creatinine clearance (mL/minute)	106.5	105.2	36.5 – 369.0
Urea (mmol/L)	4.4	4.0	2.0 - 369.0
Potassium (mmol/L)	3.8	3.8	2.5 - 5.5
Alanine transferase (IU/L)	26.8	19.0	3.0 – 95.0
CD4+ T-cell count (cells/mm^3)	11.1	11.5	0.0 – 24.0
HIV viral load (Log_{10} copies/mL)	5.54	4.84	0 – 6.22

4.3.2 Pharmacokinetic data

The PK dataset contained 282 plasma observations from 32 patients, a mean of 8.8 samples per patient. Figure 4.1 displays the plasma concentrations of amphotericin B across the entire cohort.

Figure 4.1: Amphotericin B concentrations in plasma in 32 patients

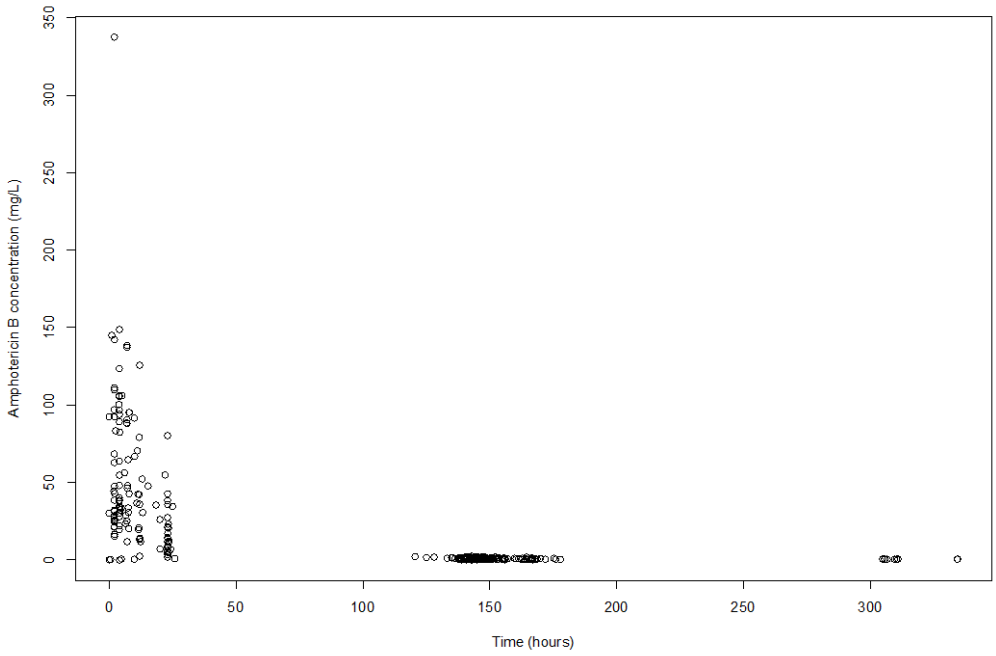

4.3.3 Minimum inhibitory concentrations

A total of 57 clinical strains isolated from CSF were available for MIC testing. The modal MIC was 0.19 mcg/mL (19 strains), with median MIC 0.19 mg/L and range 0.01 – 0.64 mg/L (figure 4.2).

Figure 4.2: Distribution of MICs from 57 clinical CSF samples in the study population

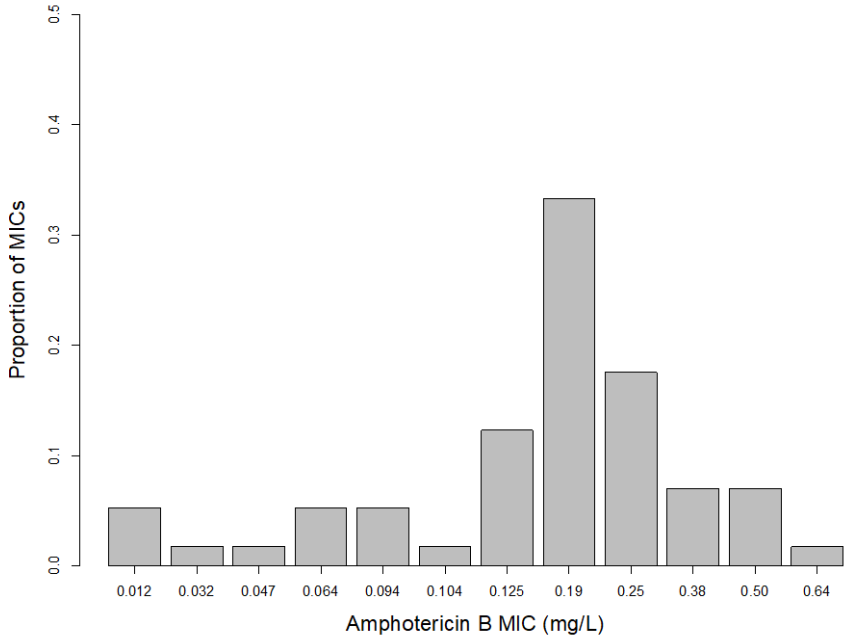

4.3.4 Population pharmacokinetic model

Compared with the two-compartment model, the three-compartment model did not result in improved AIC, log likelihood or measures of imprecision or bias. Similarly, no substantial improvement in these measures of fit was achieved when the first-order clearance model was replaced with a non-linear clearance mechanism. Using the two-compartment model as reference, there was no significant difference in the fit of the three-compartment model or the non-linear clearance model (p-value for the comparison of the joint distribution of population parameter values between each model > 0.05, table 4.2). The third compartment and the non-linear clearance model were both therefore discarded.

Table 4.2: Model comparison

Model structure	-2 * log likelihood	AIC	Population bias	Population imprecision	Posterior bias	Posterior imprecision	p-value
Two compartments	2470	2480	-0.347	2.588	-0.088	0.861	NA
Three compartments	2493	2508	-0.247	2.874	-0.0651	0.850	0.439
Non-linear clearance, two compartments	2488	2503	-0.203	3.065	-0.017	0.928	0.572

AIC: Akaike Information Criterion

Multivariate linear regression of clinical covariates did not reveal any significant associations between the Bayesian posterior estimates of clearance and volume versus age, sex, weight, renal function (baseline creatinine and creatinine clearance), or CD4+ cell count. The baseline two-compartment PK model was therefore not modified. The final chosen model was the simplest option, comprising two compartments, linear clearance and no scaling by clinical variables. The observed-versus-predicted values for amphotericin B after a single dose of 10 mg/kg are shown in figure 4.3. Population PK parameter estimates from the final model are displayed in table 4.3.

Figure 4.3: Scatter plots of observed versus predicted values for the chosen population pharmacokinetic model after the Bayesian step

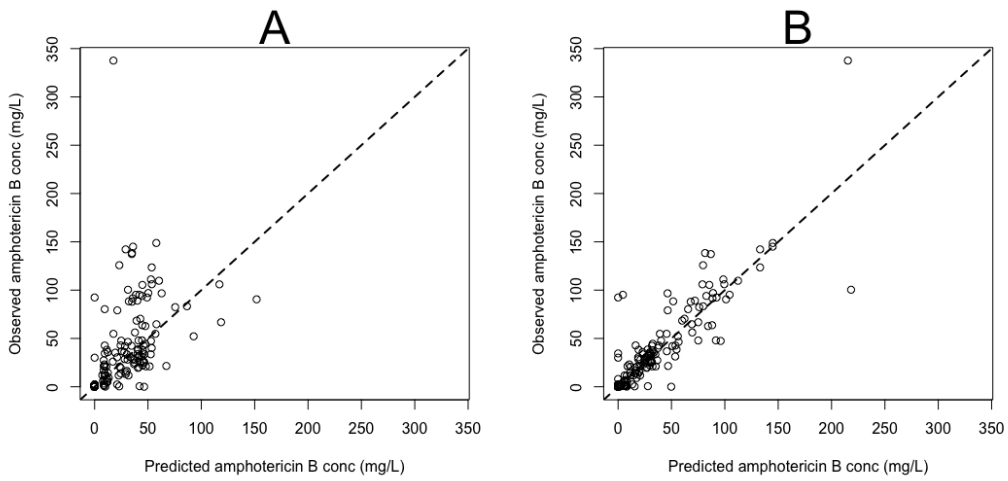

(A) Fit of the final model to the plasma data from the population. Predicted concentration = 6.08 + (1.02 * observed concentration); r^2 = 0.39.

(B) Fit of the Bayesian posterior PK estimates for individual patients from the final model to the observed data. Predicted concentration = 1.75 + (1.0 * observed concentration); r^2 = 0.81.

Table 4.3: Population parameter estimates from the final 4-compartment pharmacokinetic model

Parameter	Mean	Median	Standard deviation
Clearance (L/h)	0.72	0.56	0.43
Volume (L)	5.67	6.34	2.88
K_{12}	12.39	8.34	10.18
K_{21}	22.52	22.30	5.73

4.3.5 Internal model validation

Taking the median weight in the cohort of 50 kg, a VPC was performed by simulating 9999 patients who were administered a single dose of LAmB (10 mg/kg) and using the final PK model. In total, 90.1% of observations from the original

datafile fell within the 5th and 95th simulated percentiles, indicating adequate model fit (figure 4.4).

Figure 4.4: Visual predictive check of the final model

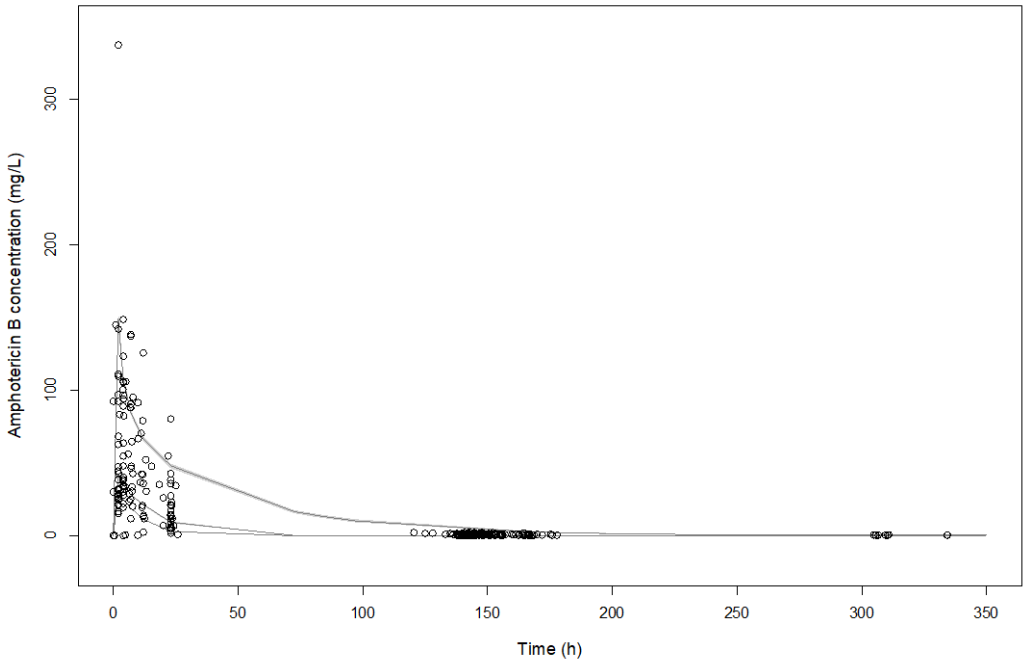

Black circles indicate observed amphotericin B concentrations. The continuous lines represent the 5th, 50th and 95th percentiles of DAmB concentrations in 1000 simulated patients. In total, 90.1% of observed amphotericin B concentrations fall within the 5th and 95th percentiles estimated by the final model.

4.3.6 Pharmacodynamic relationship

A relationship between exposure and response was apparent from the murine data, which revealed a fungistatic effect with adequate exposure to LAmB.[83] In the inhibitory E_{max} model derived from the murine data, C_{dens}, E_{max} and EC_{50} were 7.503 $\log_{10}$ CFU/g, 3.894 and 19.15 mg/L, respectively. According to this model, maximum antifungal effect in mice is attained with an $AUC_{0\text{-}24}$ of approximately 580 mg.h/L, which followed a single dose of 20 mg/kg LAmB.

Beyond this, progressively increasing $AUC_{0\text{-}24}$ values achieve negligible gains in PD effect (figure 4.5).

Figure 4.5: Inhibitory E_{max} model describing the relationship between LAmB AUC and antifungal effect

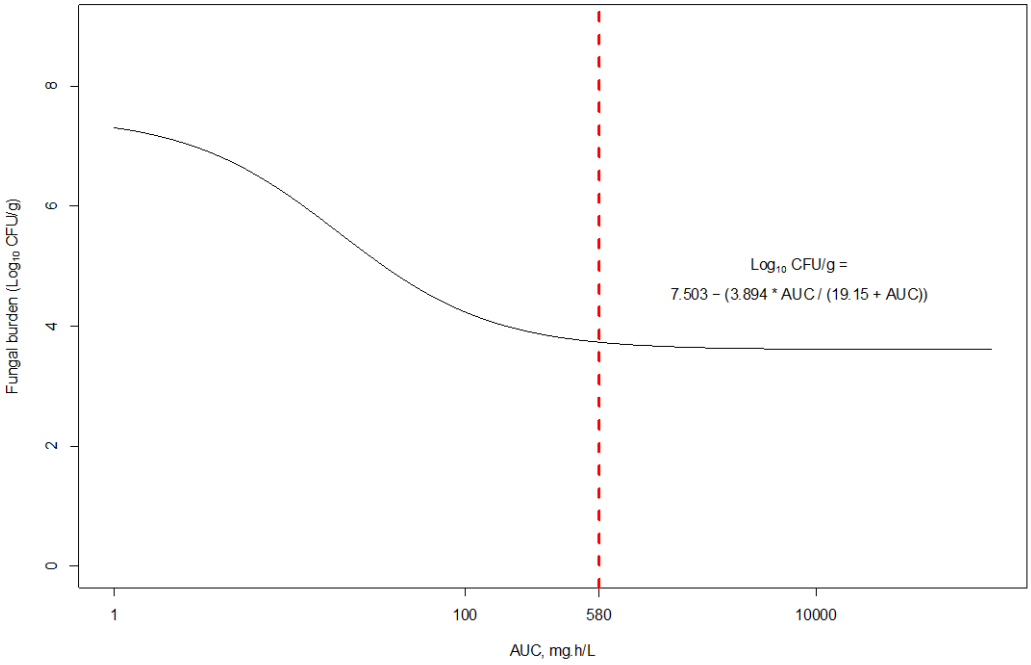

4.3.7 Monte Carlo simulation and bridging studies

Monte Carlo simulations were performed in Pmetrics using the final two-compartmental model.[273] Dosages of LAmB from 1 mg/kg to 15 mg/kg were simulated. In each simulated regimen, LAmB was infused over 2 hours as a single dose on day 1. The predicted values for $AUC_{0\text{-}24}$ and associated antifungal effect according to the E_{max} model derived from murine data are displayed in figure 4.6.

Figure 4.6: Simulated area under the concentration-time curve and residual fungal burden in 9999 patients receiving abbreviated LAmB regimens

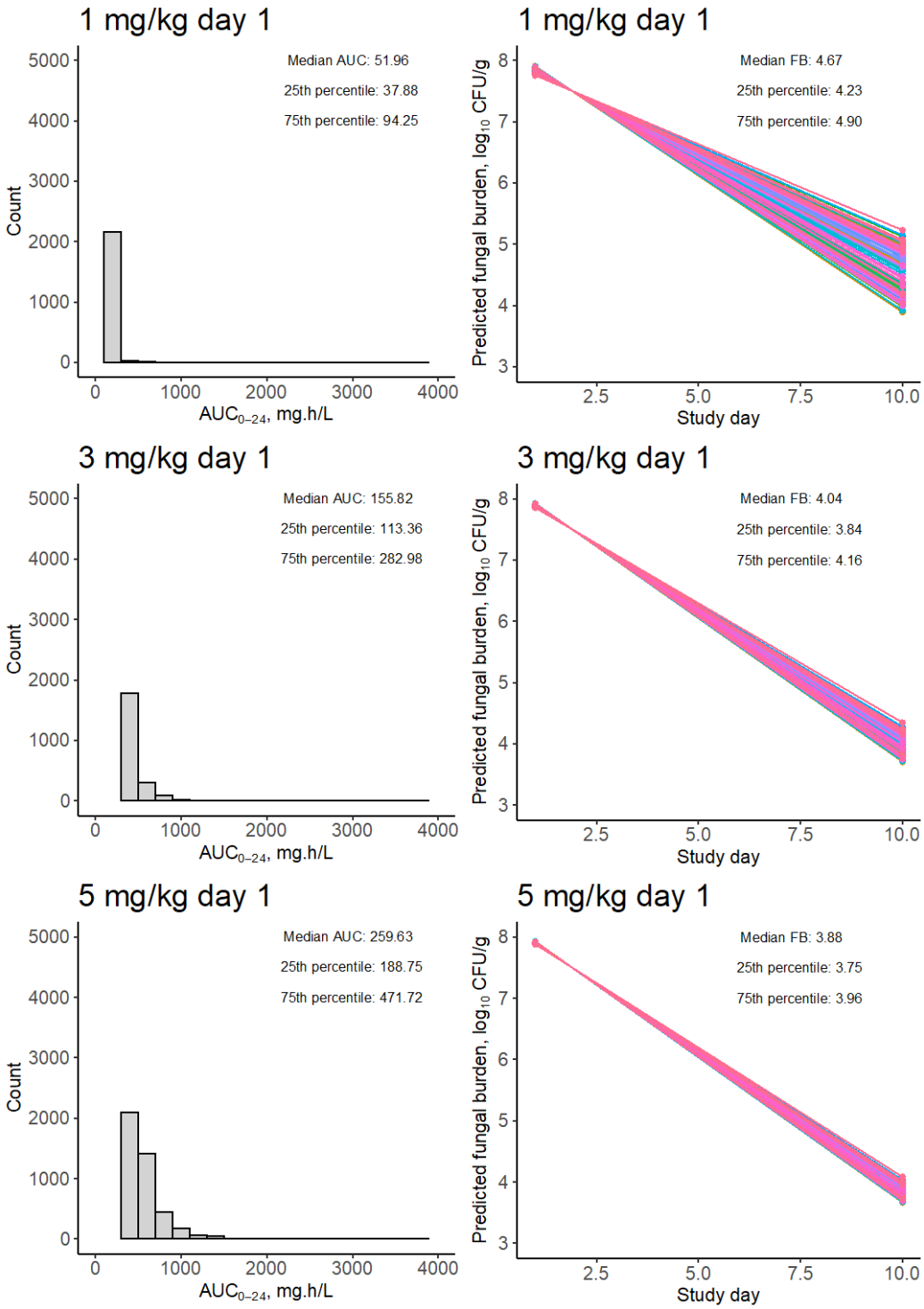

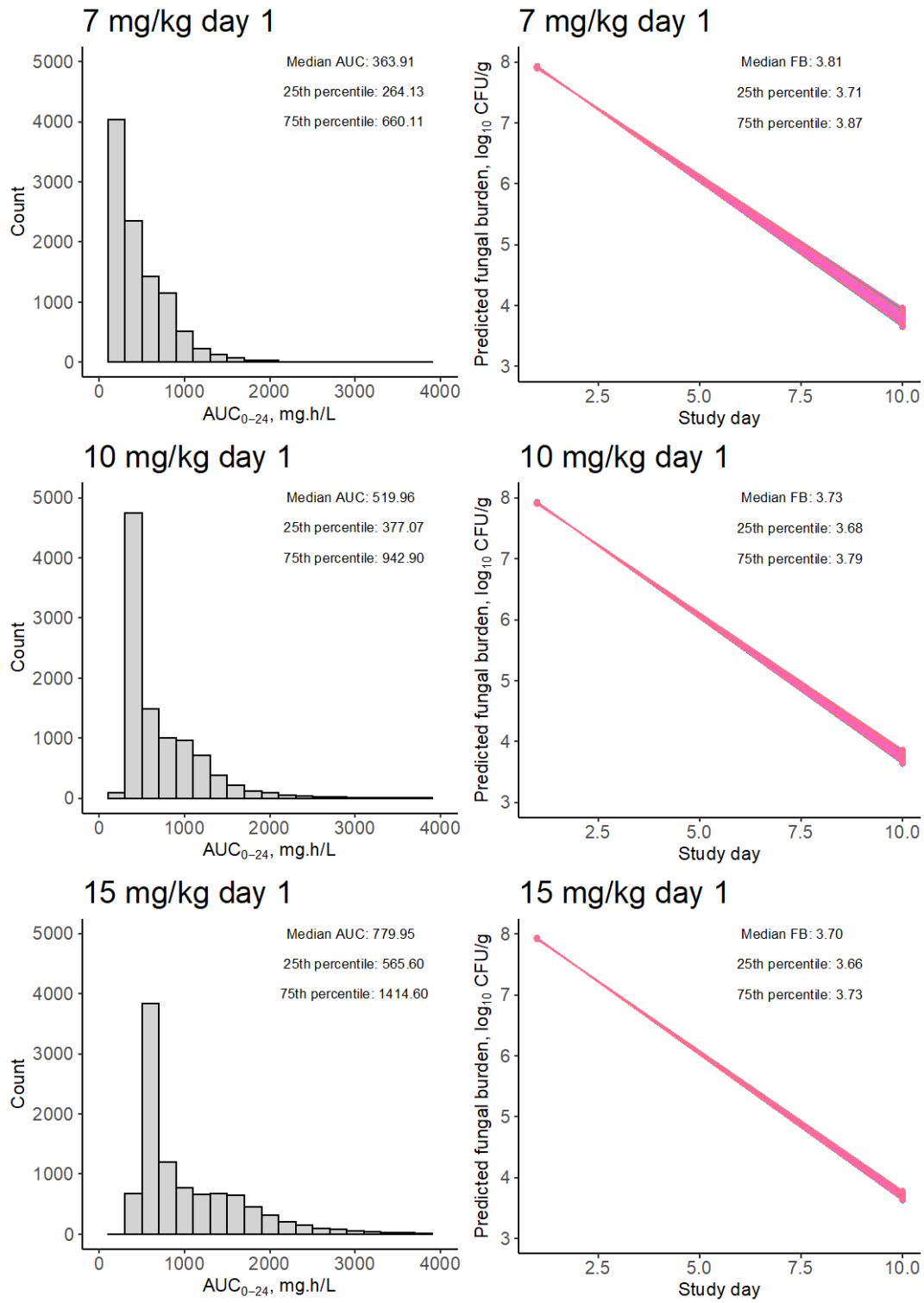

Histograms on the left display simulated $AUC_{0\text{-}24}$ following a single dose of LAmB on day 1. Line plots on the right show predicted fungal burden in cerebral tissue on day 10. With greater doses of LAmB, the variability in residual fungal burden at 10 days declines. The benefit in terms of overall reduction in fungal burden begins to plateau after doses are increased above 10 mg/kg. FB: fungal burden.

4.3.8 Measures of toxicity

Anaemia was common in the clinical cohort, with baseline haemoglobin ≤ 8 g/dL in 16% of patients (n=5). Anaemia developed on treatment in 56% of patients (n=18). Renal injury with a rise in creatinine was evident in 47% of patients during the course of treatment (n=15). Before treatment, hypokalaemia (potassium ≤ 3.0 mmol/L) was present in 6% of patients (n=2), however 25% of patients became hypokalaemic during the course of treatment (n=8). Finally, 22% of patients (n=7) developed a rise in ALT by ≥ 3 times baseline value. There were no significant correlations between LAmB exposure (in terms of either $AUC_{0\text{-}24}$ or $AUC_{0\text{-}168}$) and any of these measures of toxicity.

4.4 Discussion

This study is the first to assess and model the population PK of LAmB administered as a single high dose to adult patients with cryptococcal meningoencephalitis. A simple 2-compartment model with first order clearance of drug from the central compartment fit the data well and enabled the extent of inter-individual variability in PK to be quantified at the population level. PK models describing concentration-dependent clearance mechanisms did not provide any improvement in model fit over models describing first order clearance of amphotericin B. This finding contrasts with other reports, which suggest that nonlinear clearance mechanisms may be activated with high doses of LAmB (7.5 – 15 mg/kg/day).[344] However, both the present analysis and another[341] that modelled data derived from adult patients administered a dose of 10 mg/kg found

no evidence of nonlinear PK at this dose and it may be that these alternative clearance mechanisms are only activated at doses higher than 10 mg/kg. In addition, since patients in the present study received a uniform weight-based dosage of LAmB and there was modest variation in bodyweight among the cohort, we had limited ability to detect PK nonlinearity.

Simulated AUCs produced from high dose LAmB regimens exhibited considerable variability. Exploration of clinical covariates (i.e. age, sex, measures of renal function and CD4+ cell count) did not reveal the source of this variability. It is possible that the complex logistical nature of this study, which was conducted in a relatively chaotic clinical setting of limited resources, accounted for some variation in drug administration and PK sampling times, though all reasonable efforts were made to mitigate this. A degree of variability may be accounted for by process noise inherent to the laboratory drug assay. However, a substantial portion of the PK variability observed in this study likely represents true PK variability that is characteristic of LAmB itself, as has been reported by others.[26,341] Indeed, we are not the first to report the absence of a relationship between weight and LAmB PK[342] and it has been suggested that any such signal may be obscured by the inherent PK variability of the drug.[341]

We found no relationship between LAmB exposure and the frequency of adverse events. The fact that LAmB was well tolerated in our cohort is unsurprising, since 10 mg/kg of LAmB is routinely administered for visceral leishmaniasis and dosages as high as 15 mg/kg/day are well tolerated in adult patients.[344,345] The low propensity of LAmB to cause nephrotoxicity, compared

with DAmB, may be related to the lipoprotein binding affinities of each formulation; LAmB preferentially binds high density lipoproteins (HDL), which are taken up by the reticuloendothelial system (RES).[346,347] Levels of amphotericin B in the kidney are therefore lower than those in the RES after LAmB administration.[347] In contrast, DAmB has an affinity for low density lipoproteins (LDL), receptors for which are highly expressed on glomerular endothelium.[348,349] Furthermore, the liposome vehicle of amphotericin B in LAmB may enhance the drug's selectivity for fungal cell membranes over mammalian cell membranes, through the interaction of the liposome with fungal phospholipases.[344,350,351]

Resistance to amphotericin B is rare, likely due to the extreme fitness costs to yeasts imposed by the evolution of such resistance.[70,352] Clinical strains isolated from our cohort exhibited universally low MICs. The biological relevance of this is difficult to interpret, however, since the factors that determine amphotericin B susceptibility at the site of infection in the CNS (for example, drug penetration, local pathophysiology and immune response) are not replicated in the laboratory conditions under which MICs are measured, and in any case vary between mice and humans. We therefore quantified drug exposure in terms of PK in isolation ($AUC_{0\text{-}24}$), rather than qualifying it with a PD measure such as AUC/MIC.

Since the clinical PD data were confounded by the coadministration of additional antifungal agents in our cohort, we used a previously published PD model from murine data[83] and bridged those findings to hypothetical human patients using the posterior predictions from our PK model and Monte Carlo simulations. The population PK variability captured in our PK model and explored

further in the simulations enabled predictions of PD variability. The central assumption to performing a bridge in this manner is that drug partitioning from plasma to the site of infection is comparable in mice and humans, and that the PD relationship is consistent between these species.[279] These assumptions permit the characterisation of drug exposure in terms of the pathogen itself, rather than the host, so that this exposure can be translated between different hosts. In mice, the concentration of LAmB in the cerebrum scales in proportion to plasma concentrations and there appears to be minimal delay in drug partitioning between the central and CNS compartments;[83] plasma levels are therefore likely to provide a reasonable surrogate for CNS levels. Of note, we were unable to verify the relationship between plasma and CNS LAmB PK in the present study, since we had access to plasma PK data only. LAmB is greater than 95% bound to plasma proteins (Table 1) and is consistently detectible at only negligible levels in CSF.[119] We were therefore obliged to extrapolate PK-PD relationships between plasma PK and CNS PD, without certainty regarding LAmB penetration into the CNS. Nevertheless, our simulations predict a dose-response relationship between single dose LAmB and reduction in CNS fungal burden. The magnitude of this dose-response relationship declined with doses in excess of approximately 7 to 10 mg/kg, above which reductions in fungal burden were less pronounced with each dose escalation. The benefit of increasing dosage above 10 mg/kg is to reduce the population variability around achieving maximal antifungal response, rather than increasing the magnitude of that response. This adds support to the choice of 10

mg/kg as the dosage for single dose LAmB regimens for cryptococcal meningoencephalitis.

While the murine model that we reference has provided a relevant basis for this bridging study, preclinical PD data from short-course LAmB regimens are scarce and it would be preferable to have additional corroborative information to support our findings. In particular, data from rabbits rather than mice may provide additional insights into the PK of LAmB in abbreviated regimens. The rabbit model of cryptococcal meningoencephalitis has several advantages over the murine model in terms of its applicability to clinical infection and PD. Firstly, infection in rabbits can be traced with serial aspiration of CSF to quantify fungal burden, mimicking investigations of clinical infection.[250] Secondly, immunocompetent rabbits (like humans but unlike mice) are naturally resistant to disseminated cryptococcal infection and require immunosuppression prior to inoculation of yeast.[250,353] Third, a chronic basilar meningitis develops in rabbits and humans that is associated with mononuclear cell infiltration in the CSF.[165,250] Fourth, many adverse prognostic features for cryptococcal meningoencephalitis are shared between rabbits and humans, including high cryptococcal antigen titres in CSF, high baseline fungal burden in CSF, paucity of CSF leukocytes and systemic dissemination of infection.[250,286,303,354] Finally, LAmB clearance in rabbits is reportedly non-linear and so this model may offer a more clinically relevant PK-PD model for human doses of LAmB that are greater than 10 mg/kg/day, where non-linear clearance is reported.[344,348] Lestner et al found that while maximal anti-cryptococcal activity was achieved in mice with an $AUC_{0\text{-}24}$ of 580 ± 30 mg.h/L after

a single dose, experiments in rabbits demonstrated that a sustained CNS response required three consecutive daily doses of 5 mg/kg, a cumulative AUC_{0-72} of 2,499 mg.h/L.[83] To achieve this AUC in humans would require huge dosages with unacceptable risks of toxicity. Moreover, the relevance of an AUC measured over 72 hours to human cryptococcal PD is unclear. Is it necessary to achieve therapeutic concentrations over a prolonged period of 72 hours rather than 24 hours? Single-dose data from humans would suggest that a higher AUC of shorter duration is sufficient for sustained antifungal effect, and this maximises the practical benefits of the abbreviated IV regimen - particularly in resource-constrained settings. This highlights an important limitation of measuring drug exposure using AUC - measures of concentration and time are amalgamated such that there is some loss of precision in terms of the target shape of that AUC. Detailed PK/PD studies in rabbits that test single ascending dosages as well as various short-course daily regimens may provide valuable insight into this dilemma.

The pharmacological mechanisms that explain why LAmB should be effective in single-dose or abbreviated regimens remain somewhat elusive. Despite the simplicity with which our population model was able to capture the plasma PK of LAmB, the drug exhibits complex molecular pharmacology which is not fully understood. It is clear from our model that plasma concentrations fall to negligible levels 48 – 72 hours after a single dose of 10 mg/kg of LAmB. From preclinical models and from the phase II trial of AMBITION, we know that despite the fall in plasma levels the drug appears to exert ongoing anti-cryptococcal

activity that is noninferior to prolonged regimens of DAmB.[83,343,355] This would imply that there is ongoing drug exposure at the site of infection – that is, in the meninges and/or cerebral tissue. Certainly LAmB has a long terminal half-life in both plasma and cerebrum – approximately 152 hours in one study[327] - however one would nevertheless expect that if concentration-time profiles in the CNS and in plasma were synchronised, drug exposure in the CNS would fall to subtherapeutic levels over too short a time for antifungal effect to be adequate. It has been suggested that there is an exhaustive number of CNS binding sites for amphotericin B, from which the drug does not readily disengage. Once saturated, these sites form a reservoir of drug that has ongoing antifungal activity.[83] This theory is supported by our PD simulations, which predict that while single dosages of LAmB above 10 mg/kg result in progressively increased AUC_{0-24}, they impart limited additional PD effect beyond reducing the variability around achieving maximal antifungal activity. Similarly, studies comparing daily administration of different dosages of LAmB for cryptococcal meningoencephalitis[338] and other disease states[356-358] found no additional antifungal activity at higher dosages. Alternatively, or perhaps in addition to persistence of drug in the CNS, it is possible that concentrations of amphotericin B achieved in meninges and/or cerebral tissue are considerably higher than those in plasma, though murine data does not support this possibility.[83]

There are a number of limitations of this study, many of which apply to PK-PD bridging studies in general.[78] We used a murine PK-PD model of single dose LAmB to simulate PD response in humans. Several differences between the

experimental murine model and our own clinical population PK study have the potential to limit the reliability of the bridge. The murine experiment used a laboratory strain of *C. neoformans*, which may have altered virulence compared to the clinical strains causing cryptococcal meningoencephalitis in the clinical cohort. The impact of this possibility on our bridging study would have been minimised by our AUC rather than AUC/MIC-based analysis. Experimental models of cryptococcal meningoencephalitis study an acute infection, the pathology of which may be markedly different from the chronic, indolent pathology that characterises clinical cryptococcal meningoencephalitis. Pathophysiological differences potentially impact drug partitioning into CNS sub-compartments, as we have reviewed elsewhere.[100] In all bridging studies of this nature, there is an inherent assumption that the PD endpoint of interest in animals is predictive of clinical outcome in humans. In the largest simulated PD response following a single dose of 15 mg/kg, the median fungal burden remaining in cerebrum was 3.70 $\log_{10}$ CFU/g. Whether this is sufficient antifungal activity in immunocompromised humans is debateable. Indeed, the differences in immune status between experimental mice, which are inherently susceptible to disseminated cryptococcal infection without requiring iatrogenic immunocompromise and humans who are overwhelmingly profoundly immunocompromised when they develop cryptococcal meningoencephalitis, render comparisons between the groups fraught with uncertainty. In addition, the murine PD model assumed a mono-exponential decline in PD, which may not reflect the heterogeneity in PD response among fungal subpopulations that

appear to be present in clinical disease.[67,262] The assumption of mono-exponential fungal decline risks the prediction of CNS sterility when residual infection may exist, with implications for the risk of ongoing disease or relapse. The only way to validate the targets derived from animal data as clinically applicable PD endpoints is to corroborate those targets with extensive clinical outcome data, which at present do not exist for the treatment of cryptococcal meningoencephalitis with LAmB.

In summary, this study provides the first population PK model of high single dose LAmB in patients with HIV-associated cryptococcal meningoencephalitis. The bridging study represents an initial attempt to contextualise the drug exposure produced by this regimen in terms of its predicted PD impact, and was a necessary strategy to adopt in the absence of non-confounded PD data from humans. The bridging approach was also mindful of the fact that opportunities to conduct a PK-PD study in humans with HIV-associated cryptococcal meningoencephalitis administered a single dose of LAmB in monotherapy are unlikely to be forthcoming in the foreseeable future, since regimens with a backbone of fluconazole and flucytosine have been shown to be safe and relatively efficacious.[40] As stated, more detailed studies of LAmB monotherapy at high doses in rabbits may help to elucidate the PK-PD relationships of single dose regimens. Finally, this study underscores the importance of thorough and detailed PK-PD analysis in the development of novel antifungals, by demonstrating the challenges associated with post-hoc PK-PD analysis.

5 Population Pharmacodynamics of Itraconazole for Disseminated Infection Caused by Talaromyces marneffei

5.1 Abstract

First-line treatment of talaromycosis with amphotericin B deoxycholate (DAmB) is labour intensive and toxic. Itraconazole is an appealing alternative antifungal agent. Pharmacokinetic (PK) and pharmacodynamic (PD) analyses of itraconazole in talaromycosis are lacking. Pharmacokinetic data were obtained from 76 patients and serial CFU counts in blood were available for 66 of these. Both itraconazole and its active metabolite, hydroxyitraconazole, were measured and modelled alongside the PD data in a population model. Itraconazole PK variability was considerable, with area under the concentration-time curve over 24 hours (AUC_{24}) mean ± standard deviation 3.34 ± 4.31 mg*h/liter. Hydroxyitraconazole pharmacokinetics were similarly variable: AUC_{24} 3.57 ± 4.46 mg*h/liter. Levels of both analytes were overwhelmingly low; itraconazole minimum concentration (Cmin) 0.11 ± 0.16 mg/liter; hydroxyitraconazole Cmin 0.13 ± 0.17 mg/liter. The mean maximal rates of drug-induced killing for itraconazole and hydroxyitraconazole were 0.206 and 0.208 log_{10} CFU/mL/h, respectively. The concentrations of itraconazole and hydroxyitraconazole that induced half-maximal rates of kill were 13.449 and 8.640 mg/liter, respectively. Forty-eight percent of patients who were fungaemic at presentation remained fungaemic after 14 days of itraconazole therapy. There was no relationship between itraconazole Cmin:MIC and time to sterilisation of the bloodstream (HR 1.01, 95% CI 0.99 to 1.03, p=0.43), time to death (HR 0.99, 95% CI 0.96 to 1.02,

p=0.77) or early fungicidal activity (EFA) (predicted $\log_{10}$ EFA/ml/day = -0.64 - 0.004 * (Cmin:MIC), p = 0.18). Similarly, there was no relationship between AUC:MIC and time to sterilisation of the bloodstream (HR 1.00, 95% CI 0.99 to 1.00, p=0.50), time to death (HR 1.00, 95% CI 0.99 to 1.00, p=0.91) or EFA (predicted $\log_{10}$ EFA/ml/day = -0.64 - 0.0001 * (AUC:MIC), p = 0.19). This study illustrates why, despite encouraging preclinical data, itraconazole failed to satisfy non-inferiority criteria against DAmB for talaromycosis. This was a PK failure and the case for itraconazole in talaromycosis remains open.

5.2 Introduction

Talaromyces marneffei is a thermally dimorphic fungus with endemicity limited to Southeast Asia (northern Thailand, Vietnam and Myanmar), South Asia (northeastern India) and East Asia (southern China, Hong Kong and Taiwan)[359]. In these regions, talaromycosis is the third most common opportunistic infection after tuberculosis and cryptococcal meningoencephalitis and a leading cause of morbidity and mortality among people living with HIV/AIDS.[44,360] Mortality rates are as high as 30% at 6 months, despite modern antifungal chemotherapy and supportive care.[44,361,362] Talaromycosis is also increasingly reported in patients with underlying immunosuppressive conditions other than HIV.[363] Disseminated infection manifests as fever, bone marrow involvement (anemia, leukopenia, thrombocytopenia), skin lesions, weight loss, lymphadenopathy, hepatosplenomegaly, respiratory failure and circulatory collapse.[44,364]

Itraconazole is an orally bioavailable broad-spectrum antifungal agent with a relatively favorable safety profile in comparison to other systemic antifungal agents.[50] It is used for the prevention and treatment of a wide range of fungal diseases including aspergillosis, candidiasis and those caused by dimorphic fungi such as histoplasmosis, blastomycosis and talaromycosis.[365-369] Itraconazole is lipophilic, poorly soluble at physiological pH and highly protein bound.[100] It partitions into lipid-rich tissues and drug exposure increases at the effect site in the setting of tissue infection and inflammation.[365,370] Higher exposures are associated with greater clinical response but also increased likelihood of toxicity.[371-378] Itraconazole has recently been shown in a randomized clinical trial to be inferior to amphotericin B deoxycholate (DAmB) for the induction phase of treatment for talaromycosis, with risk of death at week 24 11.3% in the DAmB group and 21.0% in the itraconazole group ($p < 0.001$).[50]

This study describes the population pharmacokinetics (PK) and pharmacodynamics (PD) of itraconazole for patients with talaromycosis. The PK-PD study was performed as a substudy of the aforementioned clinical trial that compared itraconazole to DAmB for the initial 14 day induction phase of treatment of talaromycosis.[50] The pharmacodynamics of itraconazole were estimated using serial quantification of fungal density in the bloodstream of patients that were fungaemic.

5.3 Materials and methods

5.3.1 Clinical study

The PK and PD data were collected during a substudy of a multicentre prospective randomised clinical trial (Itraconazole versus Amphotericin B for Talaromycosis (IVAP) trial, ISRCTN59144167[50]), which compared clinical response and mortality following treatment with itraconazole (300mg q12h for 3 days followed by 200mg q12h for 11 days) to DAmB (0.7 mg/kg/day) for induction therapy for HIV-associated talaromycosis.[50] Patients were recruited between October 2012 and December 2015 from the Hospital for Tropical Diseases in Ho Chi Minh City, Vietnam. Patients in the itraconazole arm were encouraged to take a small meal or to drink cola prior to drug administration, which was directly observed during the 14-day induction period of treatment. Patients over 18 years of age with culture-confirmed talaromycosis and HIV infection were eligible for the trial. Exclusion criteria included infection of the central nervous system, pregnancy, liver transaminase level > 400 U/litre, absolute neutrophil count < 500 cells/mm^3, creatinine clearance < 30 ml/min, or existing prescription of any antifungal therapy for more than 48 hours. IVAP trial participants at the Hospital for Tropical Diseases in Ho Chi Minh City were invited to participate in the PK-PD substudy. Ethical approval was granted by the Hospital for Tropical Diseases, the Oxford University Tropical Research Ethics Committee, and the Vietnam Ministry of Health.

5.3.2 Pharmacokinetic and pharmacodynamic sampling

A total of 76 patients randomised to receive itraconazole agreed to participate in the PK-PD substudy. For the PK, 2 mL of blood was collected in heparinised collection tubes and placed immediately on ice. Within 30 minutes of collection, samples were centrifuged at 2000 rpm for 15 minutes and the plasma stored at -80 °C until analysis. Itraconazole and hydroxyitraconazole were extracted on site in Ho Chi Minh City (extraction procedure described below). Samples containing acetonitrile as internal standard were plated onto Sabouraud dextrose agar in three independent experiments to confirm sterility. Samples containing extracted drug were stored at -80°C until shipment to the University of Liverpool for analysis.

For the PD analysis, blood was collected for daily quantitative culture for the first 4 days of treatment and then on alternate days for the remainder of the first 14 days of treatment, until there was no microbial growth. Quantitative culture was performed by serially diluting 100 μL of blood 10-fold and plating onto Sabouraud dextrose agar. Plates were incubated at 37°C for quantification of fungal burden.

5.3.3 Bioanalysis of pharmacokinetic samples

Itraconazole and hydroxyitraconazole concentrations in plasma were measured using LC-MS/MS methodology (1260 Agilent UPLC coupled to an Agilent 6420 Triple Quad mass spectrometer, Agilent Technologies UK Ltd, Cheshire, UK). Itraconazole was extracted in Vietnam by protein precipitation. In total, 300 μL of

acetonitrile containing 6,7-Dimethyl-2,3-Di-(2-Pyridyl)-Quinoxaline 10 ng/mL was added to 100 µL of matrix. Samples were vortexed thoroughly and then centrifuged at 13600 rpm for 3 minutes. Three hundred µl of supernatant was removed and placed in a 500 µL Eppendorf tube for storage at -80 degrees Celsius prior to shipping to the University of Liverpool. Samples were thawed and vortexed before 150 µL supernatant was transferred to a 96-well autosampler plate. Thirty µL was injected on an Agilent ZORBAX C18 RRHD (2.1 X 50mm, 1.8 µm) (Agilent Technologies UK Ltd, Cheshire, UK).

Chromatographic separation was achieved using a gradient consisting of 60% A:40% B (0.1% aqueous Trifluoroacetic Acid (TFA) as mobile phase A and 0.1% TFA in acetonitrile as mobile phase B). The mass spectrometer was operated in positive ion mode and a multiple reaction monitoring (MRM) method used for optimum sensitivity and selectivity. The limit of quantitation of both itraconazole and hydroxyitraconazole was 0.005 µg/mL. The intra-day coefficient of variation (CV) for itraconazole was < 13.5% and the inter-day CV < 10.5%, over the concentration range 0.005 – 8.0 µg/mL. For hydroxyitraconazole, the intra-day CV was < 9.0 % and the inter-day CV was < 8.7% over the same concentration range.

5.3.4 Minimum inhibitory concentration testing

The MICs of itraconazole against *Talaromyces marneffei* were determined in duplicate using standardised CLSI microdilution methodology for yeasts, as previously described.[379,380]

5.3.5 Population pharmacokinetic modelling

Concentration-time data for itraconazole in plasma were modelled using the population PK program Pmetrics (version 1.5.0).[273] The population PK of itraconazole were solved as a first step, before constructing and fitting a population PD model.

The base PK model was itself constructed in a 2-step process, since itraconazole has an active metabolite, hydroxyitraconazole. Firstly, a model was developed to describe the PK of the parent drug. Three clearance models were tested: linear clearance only, Michaelis-Menten clearance (concentration-dependent, saturable clearance) and a combination of both of these mechanisms. The final base model for the PK of the parent drug took the form:

1. $\frac{dX(1)}{dt} = -Ka * X(1)$
2. $\frac{dX(2)}{dt} = Ka * X(1) - \left(K23 + \frac{Vmax}{Km*Vp+X(2)}\right) * X(2) + K23 * X(3)$
3. $\frac{dX(3)}{dt} = K23 * X(2) - K32 * X(3)$

Where equations 1, 2 and 3 describe the rate of change in amount of itraconazole in milligrams in the gut, central and peripheral compartments, respectively. *Ka* is the absorption rate constant from the gut to the central compartment. X(1), X(2) and X(3) are the amounts of itraconazole in the gut, central and peripheral compartments respectively, in milligrams. K23 and K32 represent first-order transfer constants connecting the central and peripheral compartments. Vmax is the maximal rate of enzymatic metabolism of itraconazole (mg/hr) and Km (mg/L) is the concentration of itraconazole in the central compartment at which enzyme activity is half maximal. Vp is the volume of the central compartment in litres.

The same variations of clearance mechanism were investigated to incorporate the hydroxyitraconazole (metabolite) data in the PK model. In this case, solely linear clearance, without a saturable clearance component, provided the best fit to the data. The following differential equations were added to the PK model:

4. $\frac{dX(4)}{dt} = \left(\frac{Vmax}{Km*Vp+X(2)}\right) * X(2) - \mathrm{K45} * \mathrm{X}(4) + \mathrm{K54} * \mathrm{X}(5) - \left(\frac{\mathrm{SclM}}{\mathrm{Vm}}\right) * \mathrm{X}(4)$

5. $\frac{dX(5)}{dt} = K45 * X(4) - K54 * X(5)$

Where equations 4 and 5 describe the rate of change in amount of hydroxyitraconazole in milligrams in the central and peripheral compartments, respectively. Accordingly, X(4) and X(5) are the amounts of hydroxyitraconazole in those compartments in milligrams, with K45 and K54 the first-order intercompartmental rate constants. SclM is the first-order clearance of hydroxyitraconazole from the central compartment (litres/hour), and Vm the volume of the central compartment of hydroxyitraconazole in litres. Vm was fixed as a ratio of Vp, taken from the median ratio of parent to metabolite concentrations at each time point in the data.

Multivariate bidirectional linear regression of each subject's covariates against the posterior parameter values was performed to determine whether any clinical variables impacted PK parameters. The fit of the model to the data was assessed using a visual inspection and linear regression of the observed-predicted scatter plots both before and after the Bayesian step. Measures of precision and bias were assessed. Models were compared by assessing 2 x difference in log-

likelihood values evaluated against a chi-square distribution with the appropriate number of degrees of freedom (difference in number of parameters between candidate models). Information loss was estimated using the Akaike information criterion. Predictive performance was evaluated in terms of bias and precision through calculation of the mean weighted error and the mean weighted squared error, respectively.

Since the data were collected in a real-world clinical environment, precise drug administration and blood sampling times varied between individuals. Estimates of drug exposure in uniform time intervals across different individuals were therefore not possible. The Cmin for each patient was calculated as the mean of the lowest model-estimated PK output per day, over the time frame for which there were data (and therefore model estimates) for that patient. The AUC was calculated as the total average AUC for the treatment course divided by the number of 24-hour intervals for which data were available per patient. This was done in Pmetrics from each patient's posterior mean parameter estimates using the trapezoidal rule.

5.3.6 Pharmacodynamic modelling

The population PK model described above was used to obtain the mean Bayesian estimates for each patient's PK parameters. These were fixed for each patient and input to ADAPT 5[381] in order to estimate the weighting functions for the PD. The weighting functions were estimated using the variance model: variance = [intercept + slope*fb]^2, where fb is the fungal burden measured from

the quantitative cultures. Each patient's PD data were fitted to the PD model one individual at a time, employing the following structural model:

$$6.\quad \frac{dN}{dt} = -\left[\left(Kkill_{max}p * \left(\frac{\frac{X(2)^{Hp}}{Vp}}{\frac{X(2)^{Hp}}{Vp}+EC50p^{Hp}}\right)\right) + \left(Kkill_{max}m * \left(\frac{\frac{X(4)^{Hm}}{Vm}}{\frac{X(4)^{Hm}}{Vm}+EC50m^{Hm}}\right)\right)\right] * N$$

In this model, *N* is the number of CFUs in the bloodstream, *t* is time and *dN/dt* is the rate of change of fungal burden in the bloodstream. $Kkill_{max}$, EC50 and H are the maximal rate of fungal kill, the concentration of drug that induces half maximal rate of killing, and the Hill (slope) function, respectively. The model enabled itraconazole and hydroxyitraconazole to affect the PD simultaneously and independently: parameters suffixed with 'p' refer to the parent drug, itraconazole; those suffixed with 'm' to the metabolite, hydroxyitraconazole. As previously, X(2) and X(4) are the amounts of itraconazole and hydroxyitraconazole in the central compartment respectively, in milligrams. The initial condition, *IC*, represents an estimate of the pre-treatment fungal density in the bloodstream. These PD parameters were estimated for each patient alongside the weighting functions (intercept and slope) from the variance model. These weighting functions were then transcribed into the PD datafile for Pmetrics and the model was run in Pmetrics to arrive at a solution for the population PD. Population PD model fit was determined according to the same criteria as were used for the population PK model. Bayesian posterior estimates of the population PD parameters were then obtained from the final PD model.

In building the PD model, several methods for handling data below the lower limit of quantification (LLQ) were investigated. This was necessary because the quantitative cultures were performed by serially diluting 100 μL of blood and

the lowest fungal count recorded was 0.699 log_{10} CFU/mL; that is, 5 CFU/mL. It is possible that there were samples with CFU counts below 5 CFU/mL but that these colonies were not picked up in the 100µl of blood plated and were therefore recorded as zero. Thus, there is a degree of uncertainty inherent in measurements towards the lower values of the measurement, as is true for many laboratory assays. The PD model was run with these 'zero' CFU counts supplied to Pmetrics as 1 (i.e. unchanged; 0 log_{10} CFU/mL), as LLQ/2 (0.350 log_{10} CFU/mL), and by discarding these datapoints altogether, to determine which of these 3 methods provided the best model fit. Early fungicidal activity (EFA) was calculated by performing a linear regression on Log_{10} CFU/mL versus day of CSF culture, taking the slope of the regression line as the EFA for each patient.

5.3.7 Statistical modelling

For patients who had both PK and PD data available, Cox proportional hazard models were fitted to examine the effect of AUC/MIC and Cmin/MIC for itraconazole on the time to sterilization of fungal cultures and the time to death. The Cox models took the form: $h(t) = h_0(t)exp\ (\beta_1 * PDI + \beta_2 * BFB)$ where *t* is time to event, *h(t)* is the hazard function and $h_0(t)$ is the baseline hazard. β_1 and β_2 are the coefficients for regression. The hazard ratio is estimated by $exp(\beta_i)$. *PDI* and *BFB* are the pharmacodynamic index (either AUC/MIC or Cmin/MIC) and the baseline fungal burden, respectively. The relationship between each pharmacodynamic index and EFA was assessed using a linear regression model,

which took the form: $EFA = \beta_0 + \beta_1 * PDI + \beta_2 * BFB + \varepsilon$, where β_0 is the intercept, β_1 and β_2 are the coefficients for the regression and ε is the model error term.

5.4 Results

5.4.1 Study participants

Pharmacokinetic data were available from 76 patients and pharmacodynamic data were available for 65 of these. All 76 patients had culture-positive disseminated talaromycosis, with *T. marneffei* isolated from blood, skin lesions, lymph nodes and/or serous fluid. The 66 patients included in the pharmacodynamic study were all fungaemic.

Forty-three percent of patients were female. The median age was 33 years (interquartile range, 29 – 36), weight 45 kg (IQR 45 – 50), body mass index 17.1 kg/m^2 (IQR, 15.6 – 19.0) and estimated glomerular filtration rate (eGFR) using the abbreviated Modification of Diet in Renal Disease Study (MDRS) calculation 113.9 $ml/min/1.73m^2$ (IQR, 86.7 – 139.1). All patients had advanced HIV disease, with median CD4 cell count 9 cells per microlitre (IQR, 4 to 20).

5.4.2 Pharmacokinetic data

The dataset included 1316 itraconazole observations and 1314 hydroxyitraconazole (OH-itraconazole) observations, 17.32 and 17.29 observations of itraconazole and OH-itraconazole, respectively per patient. The median ratio of OH-itraconazole concentration/itraconazole concentration per

time point was 0.905. Figure 5.1 shows the raw concentration data for both analytes.

Figure 5.1: Itraconazole and hydroxyitraconazole concentrations in 76 patients

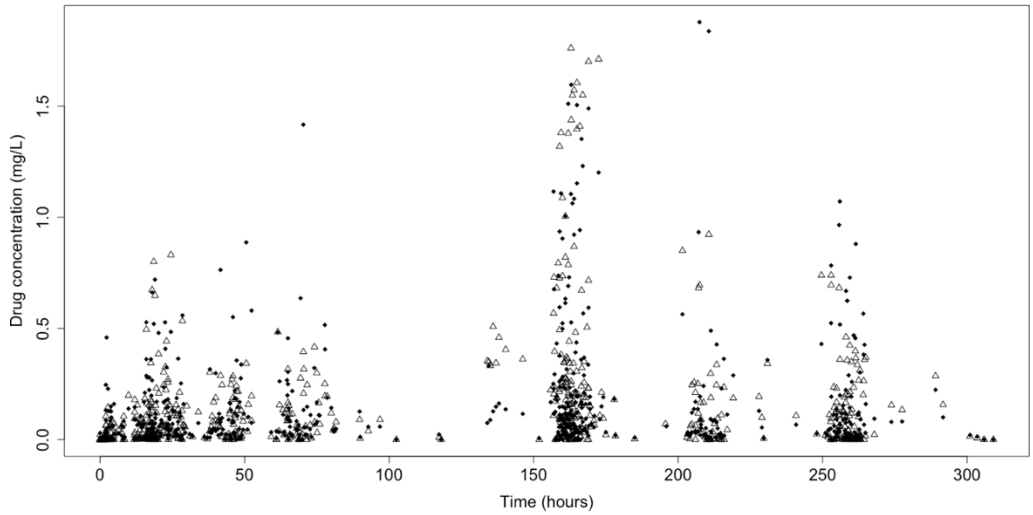

Black diamonds represent itraconazole concentrations. White triangles represent hydroxyitraconazole concentrations. The median concentration of hydroxyitraconazole to itraconazole per time point is 0.905.

5.4.3 Population pharmacokinetic analysis

The PK model was built in two stages. First, the parent drug (itraconazole) was modelled in isolation with a saturable term for drug clearance. The second stage of model building involved adding metabolite (i.e. OH-itraconazole) data into the model. The saturable clearance mechanism of the parent drug fed into the central compartment of the metabolite. An acceptable fit of the base model to the data was achieved with first-order clearance of the metabolite from the central compartment.

The potential impact of covariates on the PK was assessed. Multivariate linear regression of covariates did not reveal any significant relationships between the Bayesian posterior PK estimates (i.e. clearance, volume) versus age, sex, weight, BMI, renal function (creatinine level and eGFR) or CD4 cell count. Hence, further model building was not performed. The final PK model comprised five compartments, representing the gastrointestinal tract, the parent drug in the central compartment (circulation), the metabolite in the central compartment, the parent drug in the peripheral compartment and the metabolite in the peripheral compartment (figure 5.2).

Figure 5.2: Structure of the pharmacokinetic-pharmacodynamic model for itraconazole in talaromycosis

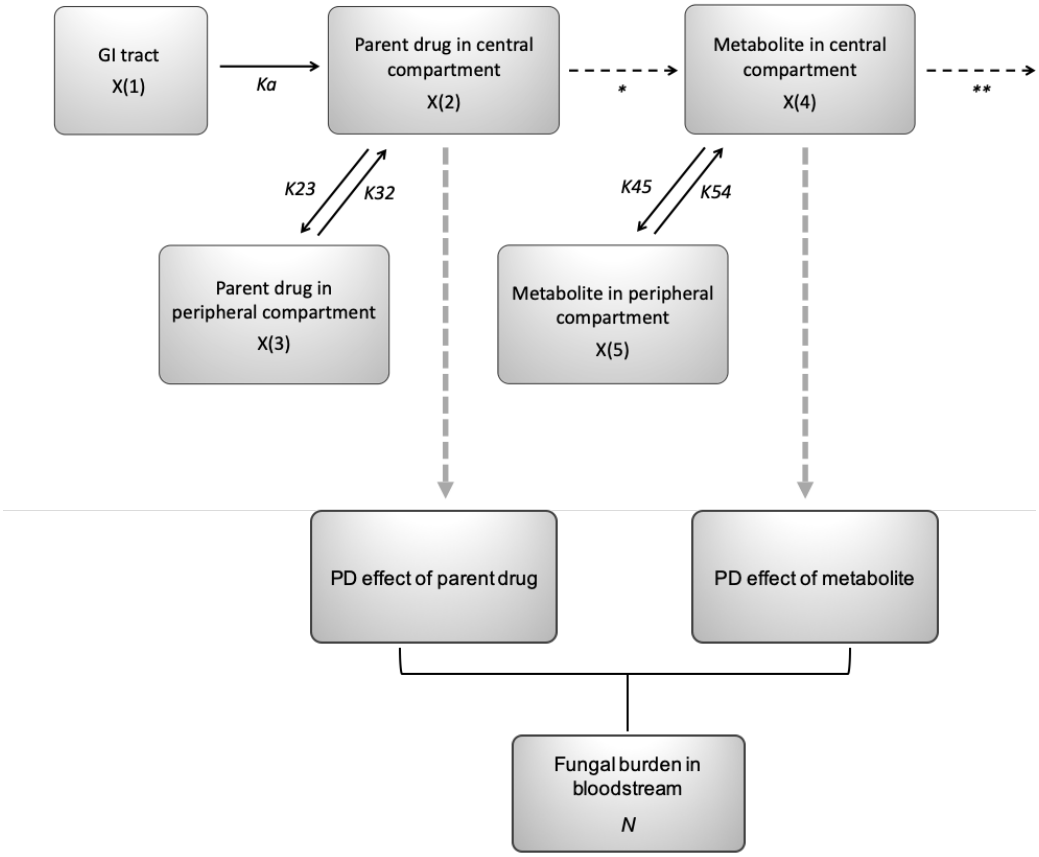

After ingestion, itraconazole is absorbed from the gastrointestinal tract into the bloodstream according to the absorption rate constant, *Ka*. Saturable hepatic metabolism of itraconazole results in the presence of hydroxyitraconazole in the bloodstream. Both itraconazole and hydroxyitraconazole undergo bidirectional transfer between the central and peripheral compartments. Hydroxyitraconazole is partially removed from the central compartment through first-order clearance. The PD effect on the burden of talaromycosis in the bloodstream is produced by the additive effect of itraconazole and hydroxyitraconazole in the bloodstream. Black dashed arrows indicate clearance mechanisms. Grey dashed arrows indicate the PK compartments that produce PD effects. Solid black arrows indicate rate constants.

* Saturable clearance of parent drug by hepatic metabolism. ** First order clearance of metabolite. GI: gastrointestinal. PD: pharmacodynamic. X(1): amount of itraconazole in the gut. X(2): amount of itraconazole in the bloodstream. X(3): amount of itraconazole in the peripheral compartment. X(4): amount of hydroxyitraconazole in the bloodstream. X(5): amount of hydroxyitraconazole in the peripheral compartment. K23, K32, K45, K54: first-order transfer constants between central and peripheral compartments. *N*: number of colony-forming units in the bloodstream.

The observed-versus-predicted values for the plasma concentrations of itraconazole and hydroxyitraconazole are shown in figure 5.3. Parameter values for the final model are summarised in table 5.1. Mean predicted parameter values described the observed values better than medians and were used in subsequent modelling and analyses.

Figure 5.3: Scatter plots of observed versus predicted values for the chosen population pharmacokinetic model after the Bayesian step

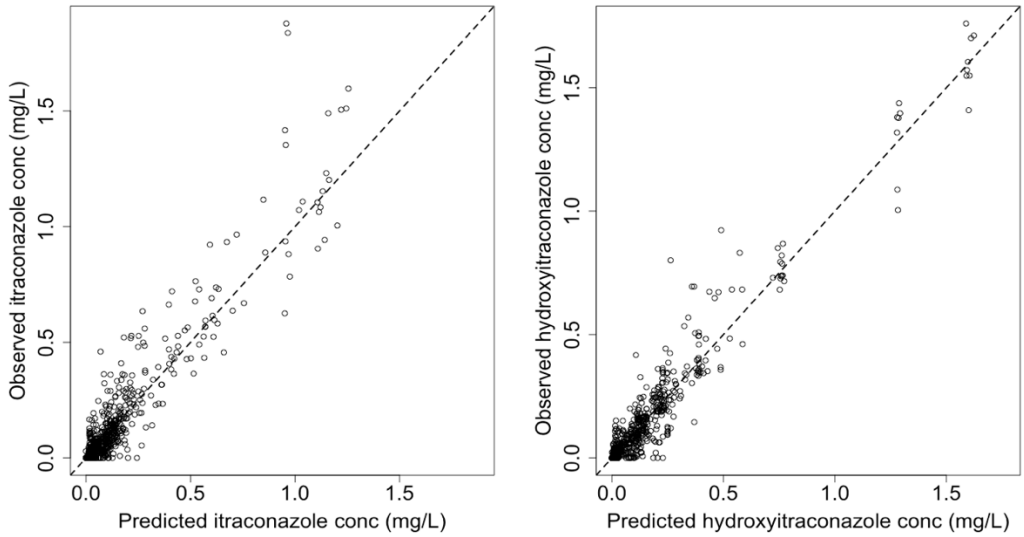

Left panel: itraconazole concentrations. r^2 0.88; intercept -0.005 (95% confidence interval -0.01 to 0.004); regression slope 1.10 (95% CI 1.07 to 1.13). Right panel: hydroxyitraconazole concentrations. r^2 0.93; intercept -0.001 (95% CI -0.01 to 0.005); regression slope 1.02 (95% CI 0.996 to 1.04).

Table 5.1: Parameter estimates for the final pharmacokinetic model

Parameter (Units)	Mean	Median	Standard deviation
Ka (h^{-1})	1.781	0.238	4.275
Vp (liters)	783.762	668.104	287.724
K23 (h^{-1})	16.200	20.831	12.804
K32 (h^{-1})	6.449	1.152	9.554
Vmax (mg/hour)	55.836	37.767	36.512
Km (mg/liter)	0.426	0.223	0.473
K45 (h^{-1})	1.562	0.005	5.501
K54 (h^{-1})	25.713	29.986	9.191
SclM (liters/hour)	133.351	135.899	70.765
Vm (liters)	866.057*	738.255*	287.724

Ka, absorption rate constant from the gut to the central compartment; Vp, volume of the central compartment for itraconazole; K23, first-order transfer constant of itraconazole from the central to the peripheral compartment; K32, first-order transfer constant of itraconazole from the peripheral to the central compartment; Vmax, maximal rate of enzymatic metabolism of itraconazole; Km, concentration of itraconazole in the central compartment at which clearance is half maximal; K45, first-order transfer constant of hydroxyitraconazole from the central to the peripheral compartment; K54, first-order transfer constant of hydroxyitraconazole from the peripheral to the central compartment; SclM; first-order clearance of hydroxyitraconazole from the central compartment; Vm, volume of the central compartment for hydroxyitraconazole. *fixed as 1.105*Vp

The distribution of mean values for the area under the concentration-time curve per 24-hour period (AUC_{24}) and minimum concentration per dosing interval (Cmin) are shown in Figure 5.4. The mean AUC_{24} of itraconazole was 3.34 mg*h/liter (standard deviation 4.31 mg*h/liter; coefficient of variation 129%), median AUC_{24} 1.91 mg*h/liter. For hydroxyitraconazole, the mean AUC_{24} was 3.57 mg*h/litre (standard deviation 4.46 mg*h/litre; CV 125%), median AUC_{24} 2.27 mg*h/litre. The mean Cmin of itraconazole was 0.11 mg/litre (standard deviation 0.16

mg/litre, CV 147%), median Cmin 0.06 mg/litre. For hydroxyitraconazole, the mean Cmin was 0.13 mg/litre (standard deviation 0.17 mg/litre, CV 132%), median Cmin 0.08 mg/litre.

5.4.4 *In vitro* susceptibility tests

Minimum inhibitory concentrations (MICs) against itraconazole were determined by broth microdilution using CLSI methodology (M38)[382] for isolates from 69 patients. Of these, 70% had an MIC of 0.008 mg/litre, 27% 0.016 mg/litre and 3% 0.03 mg/litre.

Figure 5.4: Histograms of the distribution of average AUC values (A) and mean C_{min} values (B) for the 76 patients in the pharmacokinetic study

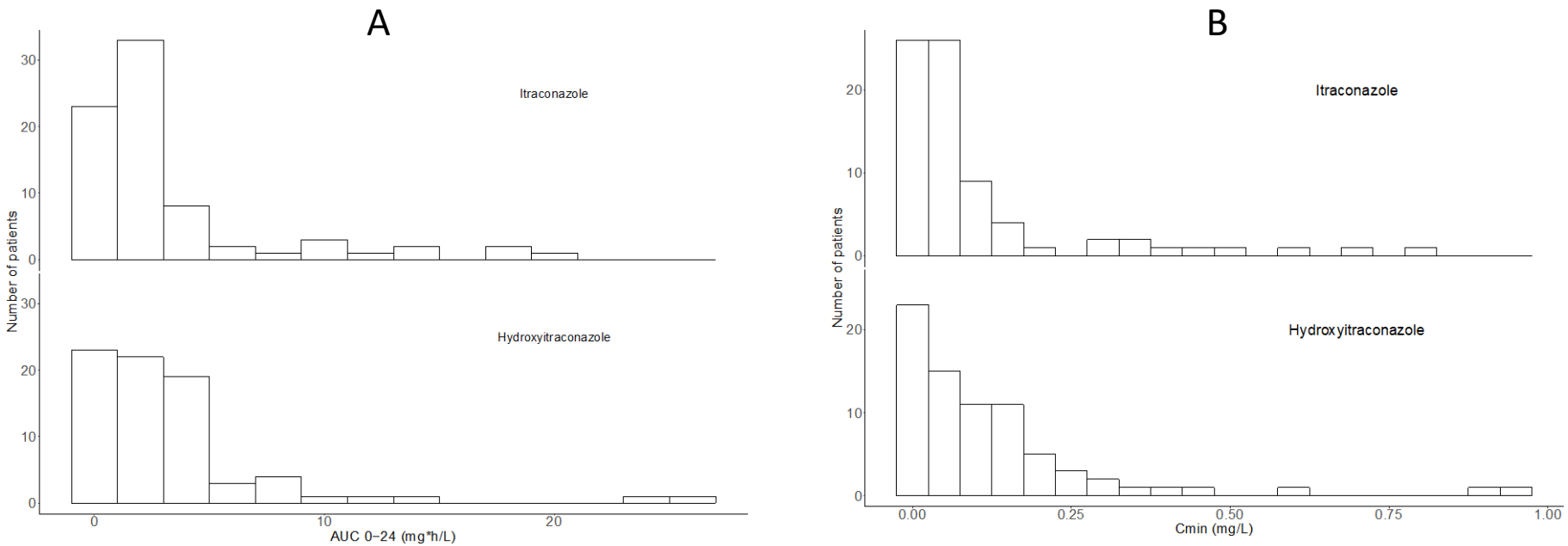

Average AUC values were calculated as the AUC over the entire duration of treatment for each patient, divided by the number of days of treatment. Cmin values were calculated as the mean of each daily Cmin per patient. The mean AUC_{24} of itraconazole was 3.34 mg*h/liter (standard deviation 4.31 mg*h/liter; coefficient of variation 129%), median AUC_{24} 1.91 mg*h/liter. For hydroxyitraconazole, the mean AUC_{24} was 3.57 mg*h/litre (standard deviation 4.46 mg*h/litre; CV 125%), median AUC_{24} 2.27 mg*h/litre. The mean Cmin of itraconazole was 0.11 mg/litre (standard deviation 0.16 mg/litre, CV 147%), median Cmin 0.06 mg/litre. For hydroxyitraconazole, the mean Cmin was 0.13 mg/litre (standard deviation 0.17 mg/litre, CV 132%), median Cmin 0.08 mg/litre.

5.4.5 Population pharmacodynamic modelling

Pharmacodynamic data were available from 65 patients who received itraconazole. In total, 342 quantitative cultures were obtained with a mean of 5.26 observations per patient. There was a large degree of variation in the time-to-sterilisation of blood cultures with a mean 330 hours and a range of 13 – 3306 hours. The median EFA was -0.3 Log_{10} CFU/mL/day, with range -1.6 to 0.1.

The PD model was fitted to the data in two steps. First, the PK was solved as described above. The mean Bayesian estimates for each individual's PK were fixed and taken forwards for the pharmacodynamic modelling. The pharmacodynamics were then solved by supplying each patient's PK as a covariate alongside the dosing history and individual pharmacodynamic data. The problem of clean plates was assessed in a number of different ways as described, but ultimately 'zero' values supplied as LLQ/2 provided the best model fit to the data, with acceptable levels of bias and imprecision (Figure 5.5). The parameter estimates for the population PD model are summarised in table 5.2. Mean parameter values predicted the observed values better than medians. After completion of the 14-day induction phase of treatment, 25 of the 52 patients in the itraconazole arm who were fungaemic at baseline remained fungaemic (48%; Figure 5.6(a)). The time-course of the reduction in fungal burden over the first 14 days of itraconazole treatment in all 65 patients for whom PD data were available is displayed in Figure 5.6(b).

Figure 5.5: Scatter plots of observed versus predicted values for the chosen population pharmacodynamic model after the Bayesian step

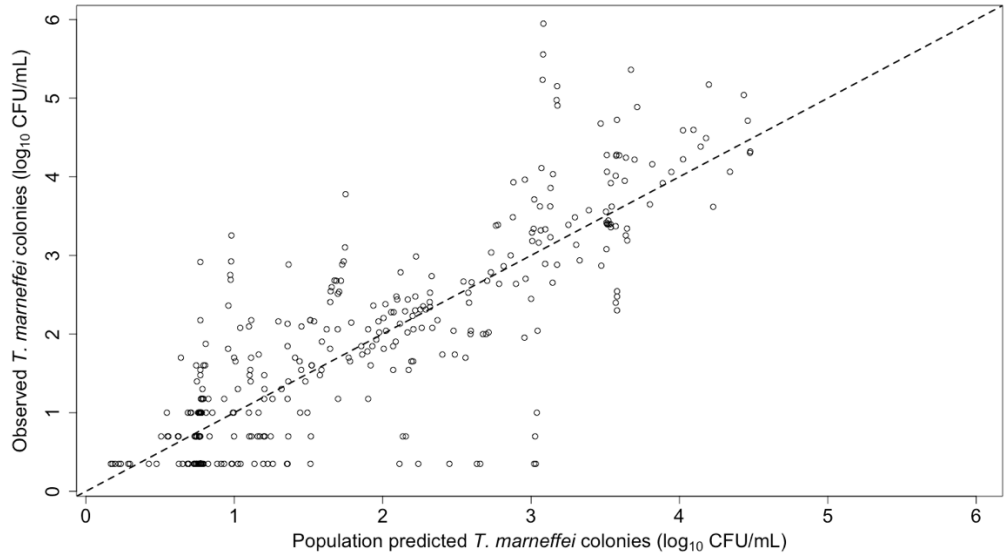

For the linear regression, r^2 0.68; intercept -0.07 (95% confidence interval -0.09 to 0.22); slope 0.99 (95% CI 0.92 to 1.07).

Table 5.2: Parameter estimates for the final pharmacodynamic model

Parameter	Mean	Median	Standard deviation
$Kkill_{max}p$ ($log_{10}CFU/mL/h$)	0.206	0.010	0.436
Hp	2.194	2.999	1.176
EC50p (mg/liter)	13.449	14.976	3.222
$Kkill_{max}m$ ($log_{10}CFU/mL/h$)	0.208	0.055	0.422
Hm	1.325	0.671	0.957
EC50m (mg/liter)	8.640	6.697	3.515
IC (CFU/mL)	1442.141	5.909	4412.916

$Kkill_{max}$, maximum rate of drug-induced killing of *T. marneffei*; H, Hill/ slope function; EC50, plasma concentration of drug that induces half-maximal kill rate; IC, estimated fungal density just prior to initiation of itraconazole. Parameters suffixed with 'p' describe the parent drug, itraconazole. Parameters suffixed with 'm' refer to the metabolite, hydroxyitraconazole.

Figure 5.6: Pharmacodynamics of itraconazole

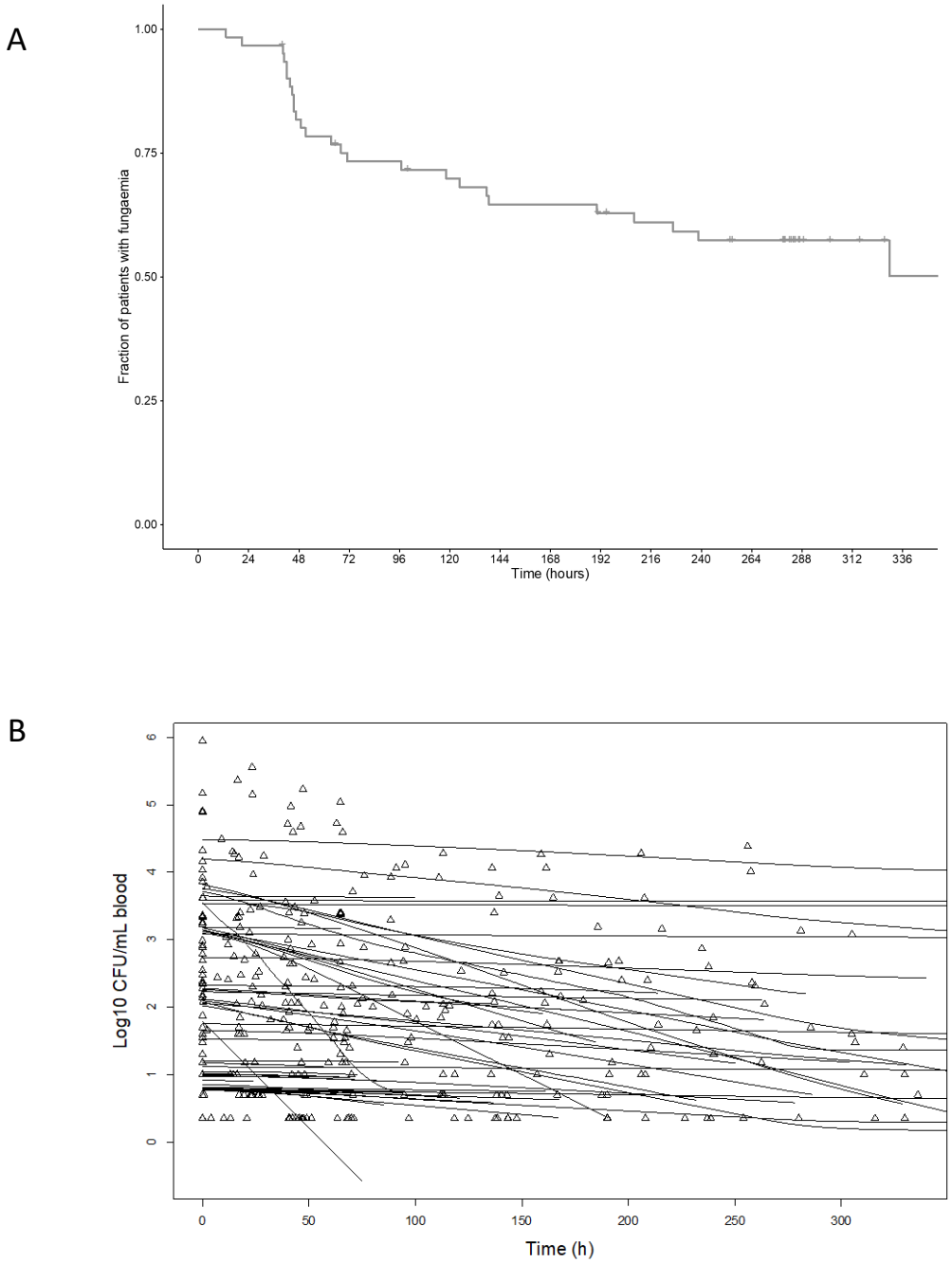

(a) Kaplan-Meier plot of the time to sterilisation (limited to the 14-day induction phase of treatment).

(b) Time course of reduction in fungal burden for the 65 patients who provided PD data. Open triangles are observed data points from individual patients; solid lines are model estimates of each patient's PD profile.

5.4.6 Pharmacodynamics

We explored both AUC/MIC and Cmin/MIC as measures of drug exposure. Potential relationships were sought between drug exposure and various pharmacodynamic endpoints that included time-to-sterilisation, time-to-death and EFA in the first 14 days. Higher initial fungal burden was significantly associated with a longer time-to-sterilisation (HR 0.25; 95% confidence interval 0.17 to 0.37; p<0.001). There was a trend towards an association between baseline fungal burden and time-to-death (HR 1.47, 95% CI 0.97 to 2.19, p < 0.1). All subsequent analyses were adjusted for baseline fungal burden.

Cox proportional hazard models revealed that there was no relationship between Cmin:MIC and time-to-sterilization (HR 1.01, 95% CI 0.99 to 1.03, p=0.43) or time-to-death (HR 0.99, 95% CI 0.96 to 1.02, p=0.77). Similarly, there was no relationship between AUC:MIC and time to sterilisation of the bloodstream (HR 1.00, 95% CI 0.99 to 1.00, p=0.50) or time to death (HR 1.00, 95% CI 0.99 to 1.00, p=0.91) (figure 5.7). Linear regression following adjustment for baseline fungal burden revealed that Cmin:MIC had no significant impact on EFA (EFA (log_{10} CFU/ml/day) = -0.64 - 0.004 * (Cmin:MIC), p = 0.18). There was also no significant relationship between AUC:MIC and EFA (EFA (log_{10} CFU/ml/day) = -0.64 – 0.0001* (AUC:MIC), p = 0.19). These relationships are displayed in Figure 5.8. In case these negative findings were a function of the fact that a small number of patients achieved rapid sterilisation of the bloodstream, data from individual patients with the greatest EFA values and fastest time to sterilization were examined closely for

higher AUC and Cmin values, and for higher AUC:MIC and Cmin:MIC values. No such correlation was found.

Figure 5.7: Cox model predictions of hazard ratios depending on PD index

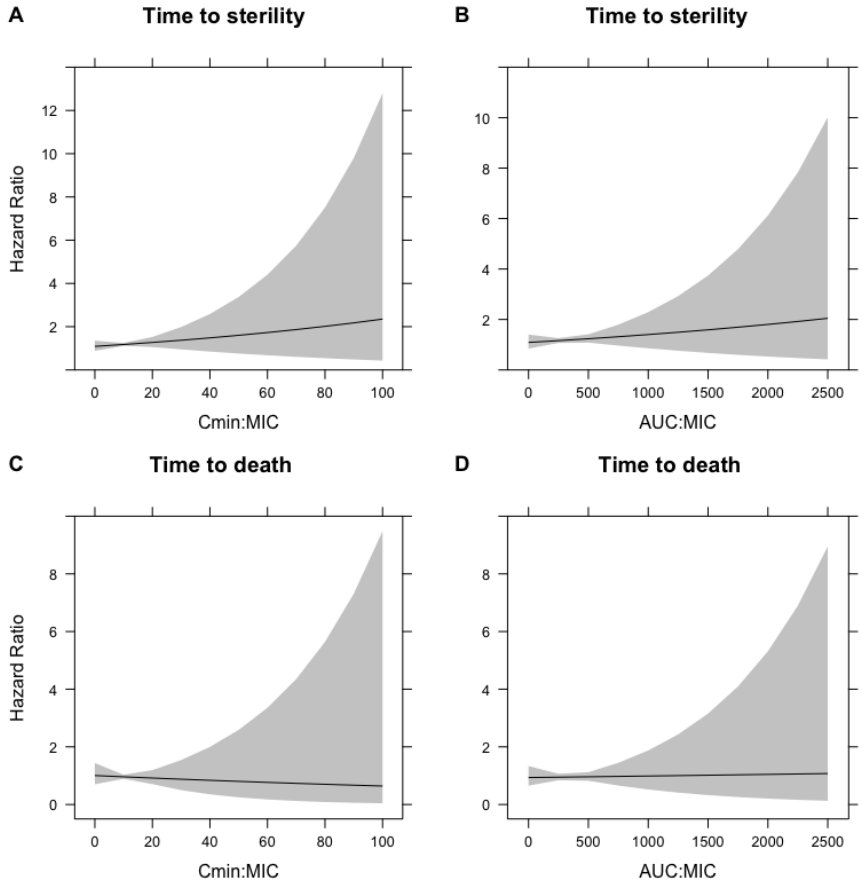

All models are adjusted for the median baseline fungal burden of 2.2 log10 CFU/ml. A: The hazard ratio for time to sterility with increasing Cmin:MIC is 1.01 (95% confidence interval 0.99 to 1.03), p=0.43. B: The hazard ratio for time to sterility with increasing AUC:MIC is 1.00 (95% confidence interval 0.99 to 1.00), p=0.50. C: The hazard ratio for time to death with increasing Cmin:MIC is 0.99 (95% confidence interval 0.96 to 1.02), p=0.77. D: The hazard ratio for time to death with increasing AUC:MIC, adjusted for the fungal burden, is 1.00 (95% confidence interval 0.99 to 1.00), p=0.91.

Figure 5.8: Relationship between pharmacodynamic indices and early fungicidal activity

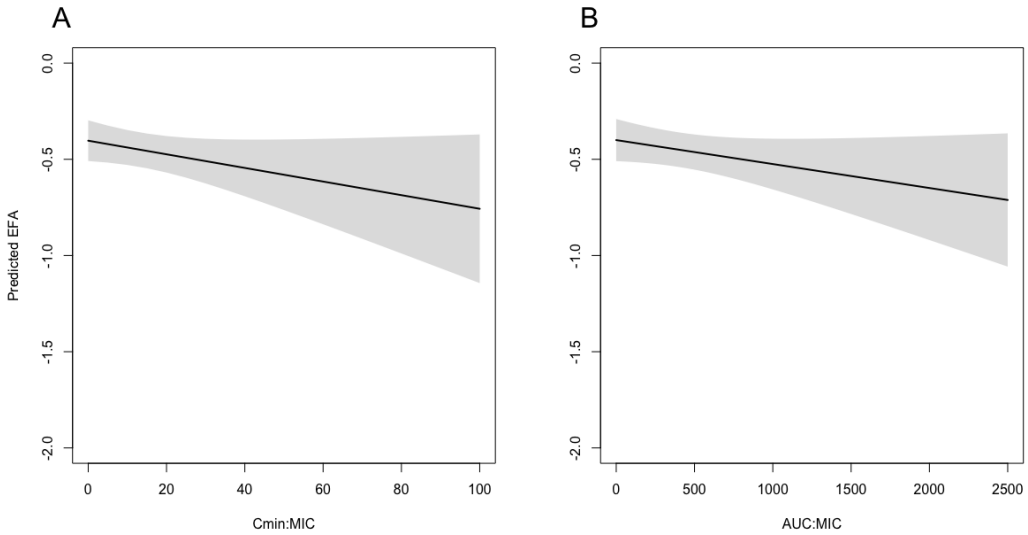

(A) Predicted $\log_{10}$ EFA = -0.64 - 0.004 * (Cmin:MIC), p = 0.18. A one-unit increase in Cmin:MIC decreases the $\log_{10}$ EFA by -0.004 CFU/mL/day (95% confidence interval -0.010 to 0.002. (B) Predicted $\log_{10}$ EFA = -0.64 - 0.0001 * (AUC:MIC), p = 0.19. A one-unit increase in AUC:MIC decreases the $\log_{10}$ EFA by -0.0001 CFU/mL/day (95% confidence interval -0.0003 to 0.0001). Both linear regression models were adjusted for a median baseline fungal burgen of 2.2 $\log_{10}$ CFU/ml.

5.5 Discussion

Itraconazole is attractive as a potential agent for the treatment for talaromycosis because of its potent *in vitro* activity against *T. marneffei,*[383,384] its improved tolerability profile compared with DAmB and its oral bioavailability. Multiple large case series have demonstrated outcomes from talaromycosis treated with itraconazole that are comparable to those after treatment with DAmB.[44,385,386] However, itraconazole induction therapy was shown in the IVAP trial to be associated with excessive mortality from talaromycosis at 6 months and significantly reduced fungicidal activity when compared with DAmB.[50] Our study suggests that the poor PD clinical outcomes from itraconazole are related to concentration-dependent therapeutic failure.

Our PK parameter estimates for itraconazole are in keeping with those described in previous population PK models.[269] Itraconazole is extensively metabolised in the liver with negligible renal clearance. Renal function did not account for any portion of PK variability in the present analysis. In addition, there was very modest variability in weight among study participants who all had advanced HIV disease, which was insufficient to fully explore the potential impact of weight on PK. The rates of kill induced by itraconazole and hydroxyitraconazole were similar. This finding is consistent with *in vitro* potencies of itraconazole and hydroxyitraconazole, which are comparable against a large range of fungal pathogens.[387] There are scarce data available on the relative potencies of itraconazole and hydroxyitraconazole against *T. marneffei* in particular, hence our

approach of enabling distinct PD influence of each of the parent drug and its metabolite in the structural PKPD model.

Drug exposure targets for itraconazole have been established for oropharyngeal candidiasis, invasive aspergillosis, cryptococcosis and histoplasmosis based on observations that patients tend to have better clinical outcomes with trough concentrations of at least 0.5-1 mg/litre.[367,369,375,388,389] The appropriate PK-PD target for patients with talaromycosis is not known. Our study did not provide further insight into this issue because a relationship between drug exposure and microbiological and/or clinical response was not evident, despite exploration of multiple different PK and PD measures and indices. There were too few patients with drug exposures high enough to elicit maximal antifungal activity and thereby separate the population into groups with a high and low probability of therapeutic success. We were also unable to explore models of multi-exponential decline in fungal burden, despite this rich dataset, because there were so few patients with an appreciable PD response. At the end of the 14-day induction period, approximately 50% of patients were still fungaemic. There was extensive variability in the PK, such that one would expect a relationship between the PK and the PD to be apparent if it exists. MICs were low and cannot be implicated in the poor PD response observed. What is remarkable about our data is the almost universally low levels of itraconazole detected in the plasma of the patient population. Only 3 of 76 patients (4%) achieved a Cmin of 0.5 mg/litre. Therefore, almost all patients were at the lower end of the exposure-response curve as defined for other fungal pathogens, and simply did not mount sufficient

drug exposure to generate a PD response. Our data is subject to a potential limitation - due to biosafety regulations, drug was extracted from samples in Vietnam prior to shipment to the UK. Extraction of calibration curves and quality control assays were then performed at the University of Liverpool. The potential for data discrepancies induced by these methodologies was limited by freezing the calibration curve and quality control samples following extraction, so that they were subject to the same conditions as patient samples. it is nevertheless reassuring that our estimates for the population PK are consistent with those described elsewhere.[269]

The concept of concentration-dependent therapeutic failure is well understood for the triazoles and results from a number of issues common to this class of antifungals. Firstly, oral bioavailability is frequently suboptimal. In the case of itraconazole, dissolution and absorption depend on an acidic environment (pK_a value 3.7). In healthy volunteers, itraconazole absorption from capsule formulations has been improved by 80% by co-administration of cola (pH 2.5)[390] and Cmax increased by approximately 70% after a meal.[124] Patients in the IVAP trial were encouraged to eat a meal or drink cola prior to drug administration. However, since the basis for these recommendations were data collected from studies of healthy volunteers, it is possible that these are insufficient or ineffective approaches to gastric acidification in the presence of HIV-associated achlorhydria or gastrointestinal disease.[391] The second contributor to concentration-dependent therapeutic failure in triazoles is significant PK variability, principally related to variation in oxidative metabolism.[392] Itraconazole is extensively

metabolised by cytochrome (CY)P450 3A4 isoenzymes, the phenotype of which varies significantly between individuals. In our model, estimates of AUC_{0-24} were highly variable, with coefficient of variation (CV%) values of 129% and 125% for the parent drug and the metabolite, respectively. Similarly, CV values for estimates of Cmin were 147% and 132% for the parent and the metabolite, respectively. Thirdly, drug-drug interactions are common among the triazoles and we were unable to account for these in this analysis. First-line antiretroviral treatment in Vietnam at the time of the trial consisted of tenofovir, lamivudine and efavirenz, the latter replaced with nevirapine when clinically indicated. Efavirenz in an inducer of numerous hepatic enzymes, including CYP3A4. Coadministration of itraconazole (200 mg bid) and efavirenz (600 mg od) decreases itraconazole Cmax, AUC and Cmin by 37%, 39% and 44%, respectively and decreases hydroxyitraconazole Cmax, AUC and Cmin by 37%, 35% and 43%, respectively.[393] Nevirapine induces both CYP3A4 and CYP2B6, and has been proposed as an inducer of P-glycoprotein.[394] Nevirapine reduces itraconazole Cmax, AUC and Cmin by 62%, 39% and 13% respectively.[395] Finally, the formulation of itraconazole is known to have significant impact on serum drug concentrations, the oral bioavailability of capsule formulations being approximately 30% that of oral solutions.[124,374] Patients in the described cohort were administered a capsule formulation of itraconazole from Stada (now Stellapharm), Vietnam. To the best of our knowledge, there are no published data on the bioequivalence of this formulation versus other formulations of itraconazole.

Whether the low EFA observed in this study differs significantly from placebo is not known and ethically impossible to establish. Ultimately, however, the reduced fungicidal activity may have directly resulted in adverse clinical outcomes including increased mortality. Evidence for this would require further study including a dataset with enough variability in PD effect to establish whether a link between EFA and mortality exists. More generally, this PK-PD sub-study illustrates that in clinical trial settings, as in practice, it is imperative that antimicrobial dosing is specifically tailored to the target population rather than inferred from healthy volunteers, or populations that are in other ways potentially distinct in a physiological sense. This is not straightforward in the case of itraconazole, which was developed in an era before the quantitative pharmacometric approaches adopted during modern drug development were commonplace. Neither is it straightforward in a population of patients with advanced HIV, whose physiology may be markedly heterogeneous. Faced with these challenges, a number of measures may be appropriate to de-risk clinical trials by strengthening the PK-PD studies associated with those trials (box 5.1).

The large PK variability of itraconazole, and capacity for drug interactions, mean that TDM is widely advocated in clinical practice to achieve therapeutic levels. This study represents an opportunity to define target levels for TDM, yet it is unable to do so due to the universally low levels of drug exposure achieved and consequent lack of PD effect produced in the study population. Moreover, treatment guidelines for talaromycosis were recently updated as a result of the IVAP trial, to state that all patients with talaromycosis should receive amphotericin

B induction therapy regardless of disease severity.[396] The evidence for this has been graded as the highest possible (AI), since data demonstrating the inferiority of itraconazole were obtained from a large randomised controlled trial. This could deprioritise the future question of the role of itraconazole in talaromycosis.

A different formulation, dosage and/or or mode of administration may have provided higher systemic drug exposure and led to better mycological and clinical outcomes. This PK-PD substudy illustrates the importance of antimicrobial dosing and administration that is specifically tailored to the target population rather than inferred from healthy volunteers, as well as the pivotal role of PK-PD analyses in clinical trials of therapeutics. Without exposure-response information, it is impossible to optimise dose selection or interpret the significance of altered drug exposure. As a consequence, patients may receive medication that offers suboptimal safety or efficacy, or be deprived of therapeutic options altogether.

Box 5-1: Strategies to strengthen PK aspects of clinical trials of antimicrobial therapy

1. Establish a target for drug exposure

   Identify a PK target that controls the biomarker (for example, fungal burden). If necessary, an approximation of this can be determined through the translation of data obtained from animal models or *in vitro* work such as a hollow fibre model.

2. Model PK in special populations and in response to administration conditions

   Can clinically relevant alterations in drug exposure be predicted in response to age, weight, renal impairment or hepatic impairment? Does food affect bioavailability? Does the timing of drug administration have a significant impact on safety and/or efficacy?

3. Assess bioequivalence

   Careful assessment of generic drug formulations to ascertain bioequivalence with reference formulations is essential for reliability and generalisability of trial findings.

4. Perform an interim PK analysis

   After 10 or 20 patients have been recruited, an interim analysis could assess whether drug exposure is in line with putative PK targets. This could serve as an early checkpoint to mitigate against significant under- or over-dosing. The ideal scenario would be TDM for trial participants as part of study procedures, though this of course requires a validated PK target.

5. Consider drug-drug interactions

   Data on co-administered medications must be collected, including dosage and frequency of administration, to explore sources of PK variability in trial drug and inform decisions around dosage adjustment.

6 Immune signatures in CSF and functional analysis of phagocytes in whole blood from patients with HIV-associated cryptococcal meningoencephalitis

6.1 Introduction

Pharmacodynamic and clinical outcomes from cryptococcal meningoencephalitis are not influenced by the attainment of PK targets alone. The host response is central to the pathogenesis of cryptococcal infection, determining whether infection is contained within pulmonary granulomas or is able to disseminate throughout the body and to the central nervous system.[104,126] The ability of cryptococcal cells to survive and replicate within host macrophages not only promotes persistence and spread of infection, but is thought to enable cryptococcal evasion of immune surveillance, interfering with inflammatory signalling that forms part of an effective host response.[134-136,397] Defects in both humoral and cellular immune pathways have been identified that are associated with severity of infection and response to treatment. For example, in murine cryptococcal infection, survival is decreased in the setting of decreased concentrations of proinflammatory Th1-type cytokines such as interleukin (IL)-12, IL-18 and interferon-gamma (IFN-γ).[170-172] Similarly, in human cerebrospinal fluid (CSF), low concentrations of IFN-γ, IL-6 and granulocyte colony stimulating factor (G-CSF) are associated with high fungal burden, slower clearance of infection and increased mortality.[152,154] Conversely, a robust early proinflammatory response and classical (M1) macrophage activation increases early fungicidal activity (EFA)

and imparts a mortality benefit.[90-93] In addition, a Th17-type response with increased circulating IL-17A, IL-21, IL-6 and transforming growth factor (TGF)-β contributes to anti-cryptococcal responses.[398-400]

In terms of cellular immunity, murine experiments have demonstrated that depletion of host macrophages and dendritic cells results in dramatically reduced survival from cryptococcal infection.[146,401] The burden of cryptococcal meningoencephalitis in HIV-infected persons is testament to the importance of CD4+ T cells in control of infection and there is a negative correlation between CSF CD4+ T cell count and CSF fungal burden in clinical cryptococcal meningoencephalitis.[154] CD4+ T cells produce IFN-γ, contributing to beneficial inflammation with classical macrophage activation.[149] However, there is evidence from HIV-seronegative patients with cryptococcal meningoencephalitis that even in the setting of a relatively strong cellular immune response with ample proinflammatory Th1-type cytokines, monocyte/macrophages may undergo alternative (M2) activation and display signs of defective phagocytic activity.[402] Moreover, while Th2-type responses and alternative macrophage activation have detrimental effects on outcome in murine models of cryptococcal meningoencephalitis,[150,170,176] this has not been observed in human infection.[152,154]

The relationship between T-cell responses, macrophage activation pathways and clinical manifestations and outcomes from cryptococcal infection are therefore not straightforward or dichotomous. In this study we aimed to provide further insight into the host response to cryptococcal infection in the CNS

by examining both soluble biomarkers in CSF and phagocyte functional activity in peripheral whole blood. Phagocyte function was quantified through measurement of phagocytosis and phagosomal superoxide burst, which - alongside nitric oxide synthase pathways – is essential for phagocyte microbicidal activity. Superoxide burst occurs when nicotinamide adenine dinucleotide phosphate (NADPH) oxidase on the phagolysosome membrane pumps electrons into the phagolysosome, triggering the production of superoxide (O_2^-) radicals, known as reactive oxygen species (ROS).[403] ROS interact with numerous essential microbial cellular targets and inflict direct damage on microbial DNA.[403,404] We employed a flow cytometry-based assay that measures the phagocytic activity and superoxide burst of both neutrophils and monocytes, with the aim of assessing the degree to which these specific phagocyte lineages contribute to fungicidal activity during clinical cryptococcal meningoencephalitis. This functional phagocyte assay was performed on samples of whole blood in real time rather than on isolated or cultured cells, so that the activity of the phagocytes under study was examined in the context of potentially important chemokines, cytokines and antibodies – thereby maintaining some of the physiological conditions that exist *in vivo*.[405]

This study was performed as a substudy of the AMBITION trial, recruiting patients with HIV-associated cryptococcal meningoencephalitis (HIV/CM) from both study arms.[343] In this chapter, we initially quantify concentrations of biomarkers measured in samples of CSF collected at three serial time points over the first 14 days of therapy. We examine the interrelatedness of these cytokines

and chemokines, and their association with indicators of disease severity and clinical outcome. We next report on the functional activity of neutrophils and monocytes at serial time points over the first 14 days of therapy, in patients with HIV/CM and in both HIV-positive and HIV-negative control patients, and the association of that activity with clinical outcomes. Finally, associations between immune signatures derived from the soluble biomarkers and phagocyte function are sought.

6.2 Materials and methods

6.2.1 Study participants and clinical procedures

Participants were recruited from Queen Elizabeth Central Hospital in Blantyre, Malawi. HIV-positive patients with a confirmed first episode of cryptococcal meningoencephalitis (diagnosed by positive CSF cryptococcal antigen test or India Ink stain) were recruited from the phase III AMBITION trial.[343] Ethical approval for AMBITION was obtained from the Malawi National Health Sciences Research Committee as well as the Research Ethics Committee of the London School of Hygiene and Tropical Medicine. All patients who had capacity to do so provided written, informed consent for participation in the trial. Where patients were incapacitated, consent was obtained from a next of kin with legal responsibility and then re-attempted with the patient if it became possible according to their clinical status. Patients were enrolled within 48 hours of presentation. The maximum antifungal therapy received by any patient prior to recruitment as part of routine clinical care was 2 consecutive daily doses of

fluconazole (1200 mg). No patient received amphotericin B or flucytosine prior to recruitment. CSF was obtained by lumbar puncture (LP) prior to initiation of study drugs (day 1) and then on day 7 and 14 per study protocol, with opening pressure recorded at each time point. Additional LPs were performed as required for management of raised intracranial pressure throughout the patient's hospital admission. Blood samples were collected into sodium-heparin tubes for the phagocyte functional assay on day 1 (prior to initiation of study drugs), day 7 and day 14. Patients in the AMBITION trial were randomised 1:1 to receive cryptococcal meningoencephalitis induction therapy with either a single high dose of LAmB (10 mg/kg/day) followed by 14 days of flucytosine (100 mg/kg/day) plus fluconazole (1200 mg/day) – the intervention arm - or 7 days of DAmB (1 mg/kg/day) plus flucytosine (100 mg/kg/day), followed by 7 days of fluconazole (1200 mg/day) – the control arm. As part of the AMBITION trial, quantitative cryptococcal culture (QCC) was performed on days 1, 7 and 14 using serial dilutions of 100 μl CSF with colony counting after 48 hours growth at 30°C. In addition, CSF cell count, white cell differential, protein and glucose were performed as part of routine clinical care. For this sub-study, patients were followed up for 10 weeks with respect to mortality outcomes.

For the phagocyte functional assay, blood samples were obtained from control participants at a single time point. HIV-positive control participants (no clinical evidence of cryptococcal meningoencephalitis) were recruited from the 'Evaluating the reactivation of herpesviruses and inflammation as cardiovascular and cerebrovascular risk factors in antiretroviral therapy initiators in an African

HIV-infected population' (RHICCA) study, described elsewhere.[406] HIV-negative controls were recruited from either the RHICCA study, and from the 'Characterisation of the breakdown in immune competence of the lung that favours development of tuberculosis in HIV-infected adults' (CLIC) study. Both RHICCA and CLIC studies received ethical approval from the research ethics committees of the University of Malawi, College of Medicine and the Liverpool School of Tropical Medicine. All control participants provided written informed consent.

6.2.2 Measurement of soluble biomarkers in CSF

All CSF samples were processed within 1 hour of collection. Samples were centrifuged at 3000 rpm (1500 g) for 10 minutes at 4°C prior to freezing at -80°C until analysis on site in Malawi (Malawi Liverpool Wellcome Trust Clinical Research Programme). We used the Luminex multianalyte platform (Luminex, Merck Millipore, Herts UK) to measure CSF concentrations of IFN-γ, tumour necrosis factor-alpha (TNF-α), granulocyte-macrophage colony-stimulating factor (GM-CSF), granulocyte colony-stimulating factor (G-CSF), IL-2, IL-4, IL-5, IL-6, IL-7, IL-8 (CXCL8), IL-10, IL-17A, IL-12p70, IL-1 receptor antagonist (IL-1ra), IL-12p40, IL-15, IFN-γ inducible protein 10 (IP-10/ CXCL10), vascular endothelial growth factor (VEGF)-A, monocyte chemoattractant protein 1/ chemokine (C-C motif) ligand 2 (MCP-1/ CCL2), macrophage inflammatory protein (MIP)-1a/ CCL3, MIP-1b/CCL4 and RANTES/ CCL5, according to the manufacturer's instructions.

6.2.3 Phagocyte functional activity in whole blood

Zymosan reporter particles were prepared as described previously.[405] Briefly, 6 mg zymosan (Sigma-Aldrich) was washed three times in 1x phosphate-buffered saline (PBS) by centrifugation at 10,000 rpm for 1 minute. Washed zymosan particles were doubly coupled to a calibration fluorochrome (Alexa Fluor 405-SE, Invitrogen) and a fluorescent reporter (OxyBURST® Green H_2DCFDA-SE, Invitrogen) that is sensitive to oxidation. To achieve zymosan coupling, washed particles were suspended in 950 μl coupling buffer (0.1 M boric acid adjusted to pH 8.0 with NaOH) containing 10 μl of 25 mg/ml OxyBURST/ DMSO solution and 5 μl of 5 mg/ml Alexa Fluor 405-SE/DMSO solution. After mixing, this zymosan/ coupling buffer suspension was incubated in the dark at room temperature for 1 hour, before being washed in 1 ml coupling buffer. Zymosan particles were resuspended in coupling buffer and incubated in the dark at room temperature twice more, with a coupling buffer wash between each incubation. After a total of three 1-hour incubation periods in coupling buffer, zymosan particles were washed 3 times in PBS before storage in PBS containing 0.01% sodium azide in the dark at 4°C. The final stock concentration of zymosan reporter particles was approximately 5 x 10^6 particles/ml.

To assess whole blood phagocyte function, 50 μl zymosan stock particle suspension was washed three times in 1 ml of RPMI-1640 to remove sodium azide. Particles were resuspended in 250 μl RPMI-1640 to a final dilution of 1:6, with an approximate concentration of 8 x 10^6 zymosan particles/ml. Within 2 hours of

blood draw, whole blood was diluted 1:1 with warmed RPMI-1640 and incubated with 20 μl washed zymosan particle suspension at 37°C with rocking. In parallel, 1:1 diluted blood in RPMI-1640 was processed as a control.

Phagocytosis and superoxide burst were measured at 10, 30, 60 and 90 minutes after the addition of reporter particles. At each time point, 100 μl diluted blood was removed from the incubating solution and stained with anti-CD45 PerCP, anti-CD66b APC and anti-CD14 PE-Cy7 antibodies at concentrations of 1:33, 1:50 and 1:100, respectively. After 10 minutes of staining, 3 ml of BD FACS lysing solution (containing formaldehyde and diethylene glycol; BD Biosciences) was added to the zymosan-containing tube and the control tube to arrest biological activity, fix leukocytes and lyse red blood cells. Each tube was incubated at room temperature for 10 minutes after addition of the lysing solution, before cells were washed in 1x PBS by centrifugation at 500 g for 10 minutes. Cells were resuspended in 500 μl PBS and counting beads (Countbright, Life Technologies) were added per manufacturer's instruction. Cells were analysed on a BD LSR Fortessa flow cytometer (Becton Dickinson, USA) with forward scatter threshold (FSC) set at 5000. Total antibody compensation beads (AbC^{TM}, Invitrogen, BD Biosciences) were used and data analysed using FlowJo software version 10.0 (Tree Star, San Carlos, CA).

6.2.4 Flow cytometry analysis of whole blood phagocytes

The gating strategy used to identify monocytes and neutrophils is outlined in Figure 6.1A. Absolute cell numbers were counted using counting beads. The

proportion of cells that had phagocytosed zymosan reporter particles was calculated by quantifying the expression of the calibration fluorochrome. The median fluorescence intensity (MFI) of zymosan positive and zymosan negative cells was recorded at 10, 30, 60 and 90 minutes (Figure 6.1B).

Figure 6.1: Gating strategy for identification of neutrophils and monocytes in whole blood and quantification of phagocyte phagosomal superoxide burst

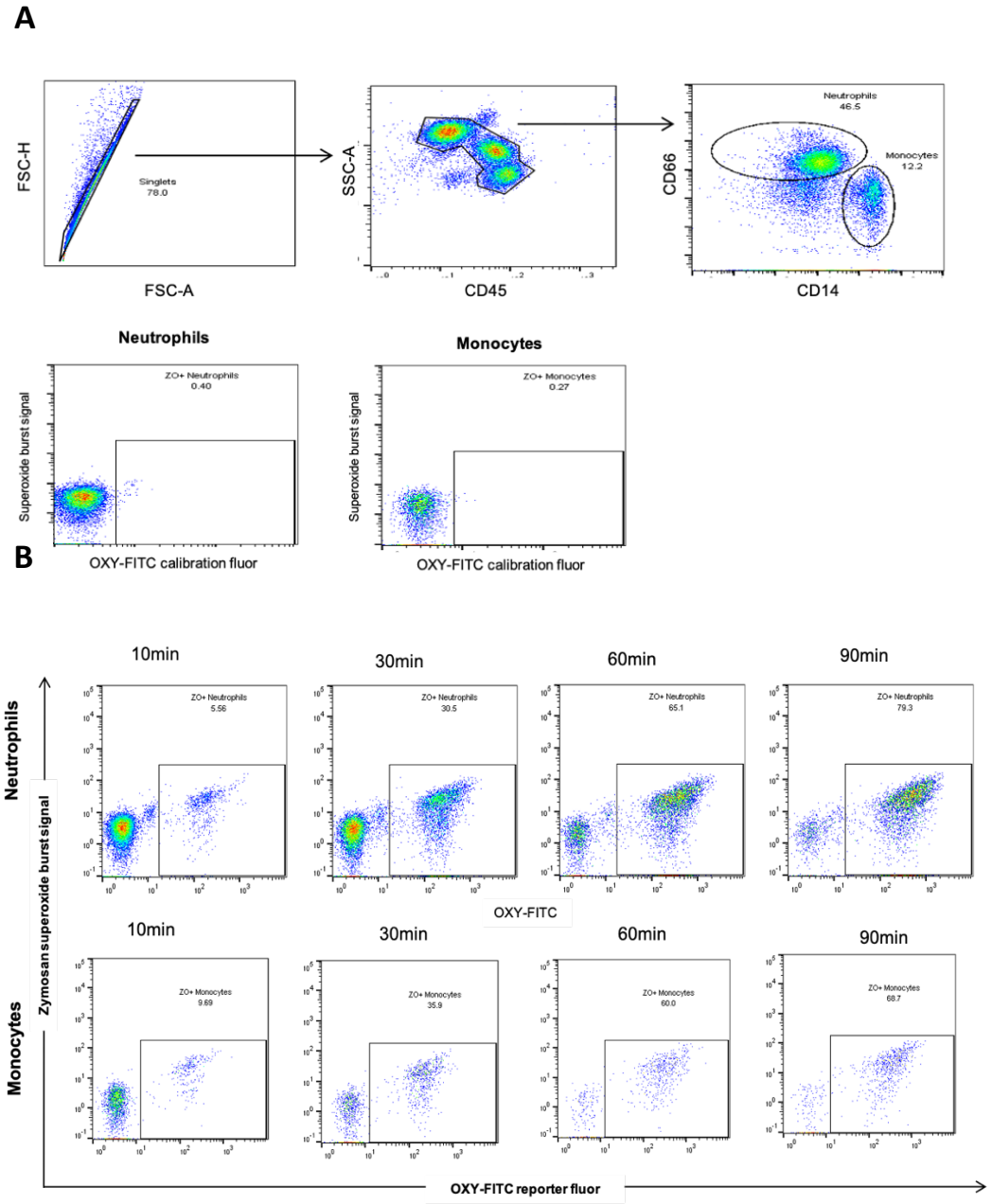

Figure 6.1 **A**) Gating strategy: neutrophils and monocytes were identified using forward scatter height (FSC-H) and FSC-area (FSC-A) to exclude singlets, aggregates, cryptococcal cells and cellular debris. The CD45 versus side scatter area (SCC-A) plot identified phagocytes of interest and these were subclassified based on staining for CD14 versus CD66. Control (no cryptococcal meningoencephalitis) samples were examined without addition of zymosan reporter particles to define the gate for identification of phagocytes undergoing superoxide burst. **B**) Phagosomal superoxide burst activity in neutrophils and monocytes over time. Zymosan-induced superoxide burst is detected by the oxidation-sensitive reporter fluorochrome and increases over time and compared with control samples.

6.2.5 Data analysis

Statistical analysis was performed in R version 1.1.383 (© 2009 – 2017 RStudio, Inc.). The final data set for this study, including soluble biomarker concentrations, phagocyte functional activity, CSF cell counts and differential, CSF biochemistry and clinical variables comprised 38 variables. Two statistical techniques were employed to reduce the dimensionality of the large set of soluble biomarkers: principal component analysis (PCA) and network analysis. PCA reduces the number of dimensions in a dataset by describing linear functions (principal components, PCs) that capture the variance in a dataset and which are unrelated to one another, thereby increasing the interpretability of the data while minimising information loss.[407] Multiple comparisons are avoided because the dataset is then examined in terms of a series of PCs that account for a decreasing proportion of the overall variance of the dataset, rather than in terms of individual variables. Network analysis, in contrast, is a technique with its basis in network theory, which enables the visualisation of relationships between variables by mapping them according to the symmetry or otherwise of their proximity to one another. A threshold of acceptable correlation values is chosen and used to construct an adjacency matrix. The adjacency matrix is used to create a network of 'nodes' (the variables) and 'edges' (the connection between each variable). Network analysis places significance on the associations between variables, creating a web of variables and highlighting clusters of variables that are more closely related to one another than to other variables. The cytokine network analyses presented here were performed after filtering associations to include

only those that showed strong correlations (Pearson's correlation coefficient, r, $\geq$ 0.70; p-value < 0.05).

Prior to PCA and network analysis, analyte concentrations were log transformed and normalised to the mean. A 'slope' value was calculated for each biomarker for each patient as a linear regression of the concentration of that biomarker over time (between study days 1 and 14). PCA and network analyses were performed on both the log-transformed, normalised biomarker values from day 1 of the study, and on the slope of the change in value of each biomarker over the duration of the study. To assess phagocyte function, an Activity Index (AI) of phagosomal superoxide burst was calculated for both neutrophils and monocytes at each time point (10, 30, 60 and 90 minutes), on each sampling day (1, 7 and 14), by subtracting the MFI of the zymosan-negative cells from the MFI of the zymosan-positive cells and dividing this by twice the robust standard deviation of the zymosan-negative cells. This standardised the data with respect to inter-individual variability in cellular auto fluorescence. AI results were summarised for further analyses (described below) as a peak AI value for both neutrophils and monocytes for each study day, and a slope value for each cell type per patient, calculated as a linear regression of peak AI value per day versus time. The clinical study and initial analytical strategy are outlined in Figure 6.2.

Figure 6.2: Clinical study and initial analytical strategy

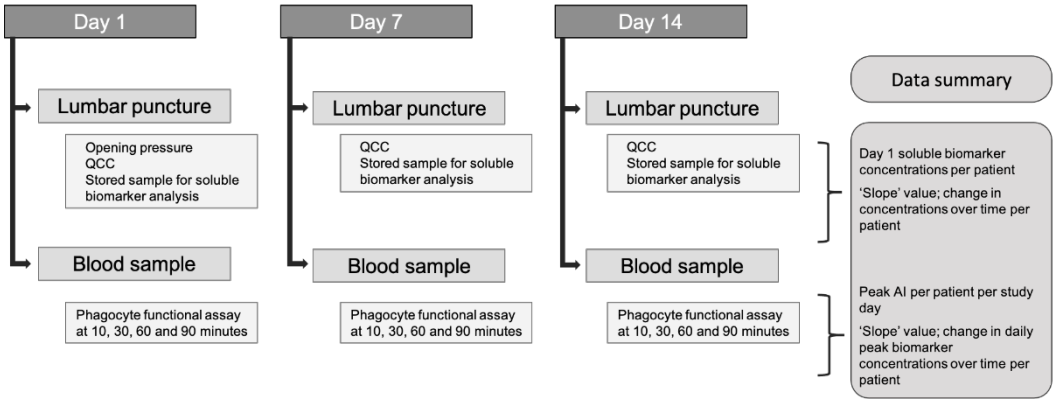

Figure 6.2. Samples of CSF and blood were collected on days 1, 7 and 14 for the laboratory assays indicated. Data were summarised for further analysis as described in the box on the right of the diagram. QCC: quantitative cryptococcal culture.

A number of clinical outcome variables were examined with respect to the measured soluble biomarkers and measures of phagocyte function: fungal burden (log_{10} colony-forming units (CFU)/ml CSF) on day 1 prior to study drug administration, day 7 and day 14; opening intracranial pressure (cm H2O) at baseline; early fungicidal activity (EFA) - calculated for each patient as a linear regression of log_{10} CFU/mL of CSF versus time - and date of death (followed up to 10 weeks). Opening pressure was explored as both a continuous and a categorical variable, the latter defined as low opening pressure if it was recorded as $\leq$ 30 cm H_2O, high if $\geq$ 30 cm H_2O. Early fungicidal activity (EFA) was also explored as both a continuous and a categorical variable, defined as low EFA if the rate was $\leq$ 0.2 log_{10}CFU/mL/day and high EFA if > 0.2 Log_{10}CFU/mL/day. This EFA cut-off value was chosen because EFA > 0.2 Log_{10}CFU/mL/day is associated with survival.[263,264] Associations between the PCs, the described measures of phagocyte AI, CSF cell counts and biochemistry and clinical outcome variables, were examined using

Pearson's correlation coefficient. Linear regression was used to examine the relationship between PCs and continuous clinical outcome variables and logistic regression for categorical outcome variables. The relationship between PCs and time to death was described using Cox proportional hazards models. Models that examined associations with mortality were adjusted for baseline fungal burden, since this is consistently associated with mortality from HIV/CM.[286] Associations with opening pressure were adjusted for baseline fungal burden in CSF, since these variables are correlated.[408] Associations with EFA were adjusted for baseline fungal burden and study arm. Data were non-normally distributed; as such, unpaired groups were compared using the Mann-Whitney U test. Paired groups were compared using the Wilcoxon test. Statistical significance was defined as a p-value < 0.05.

6.3 Results

6.3.1 Participants

CSF was available from 65 patients with confirmed HIV-associated cryptococcal meningoencephalitis. In total, whole blood was collected from 19 patients with HIV/CM, 15 HIV-positive control patients and 15 HIV-negative controls. The number of HIV/CM patients for whom both CSF was analysed for soluble immune mediators, and blood for phagocytic function, was 11 (8 HIV/CM patients provided samples for the phagocytosis assay only). The median age was 37 years (interquartile range (IQR) 34 – 42), median weight 50 kg (IQR 47 – 56) and median CD4+ T cell count 37 cells/mm^3 (IQR 15 – 94). Of 65 patients for whom

CSF data were available, 24 (37%) were female. The cumulative case fatality rate was 9% at 2 weeks (6/65) and 28% at 10 weeks (18/65).

6.3.2 CSF soluble biomarkers: study day 1

Baseline CSF biomarker concentrations are shown in Figure 6.3. Values for IL-4 were below the limit of detection in 61 of 65 cases, so IL-4 measurements were excluded from further analysis. The distribution of biomarker concentration values was consistent for the majority of cytokines/ chemokines across different study days, with modest variation in log-transformed, normalised concentrations (Figure 6.4).

Figure 6.3: Baseline CSF soluble biomarker concentrations in 65 patients with HIV-associated cryptococcal meningoencephalitis

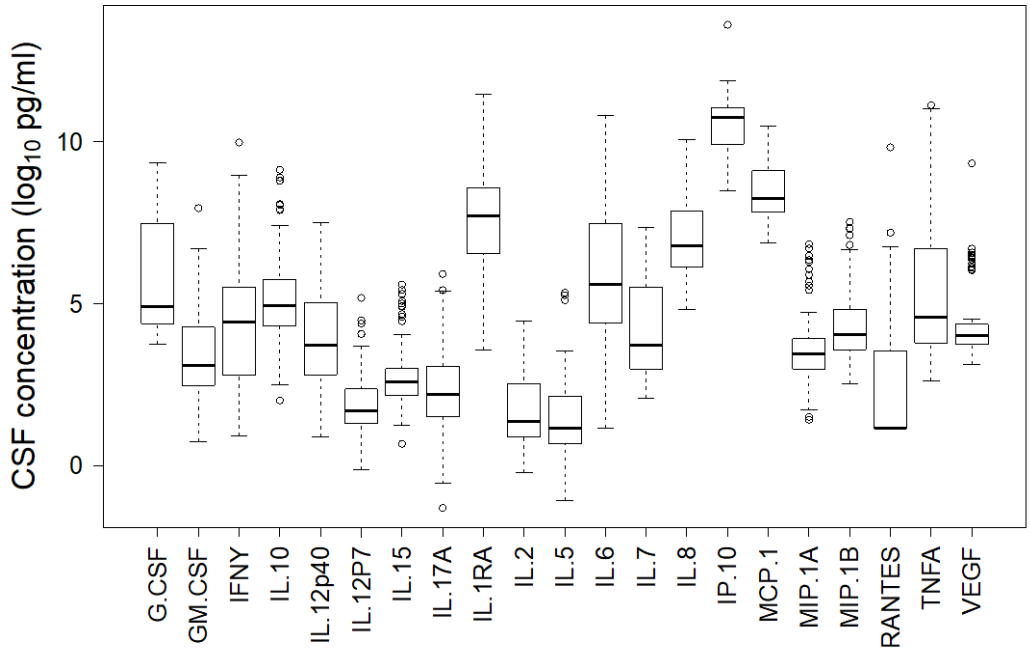

Figure 6.3. Boxes indicate interquartile range, with median marked inside box. Whiskers represent 10th and 90th percentiles.

Figure 6.4: Density plots showing log-transformed concentrations of soluble biomarkers on different study days, normalised to the mean value of each cytokine

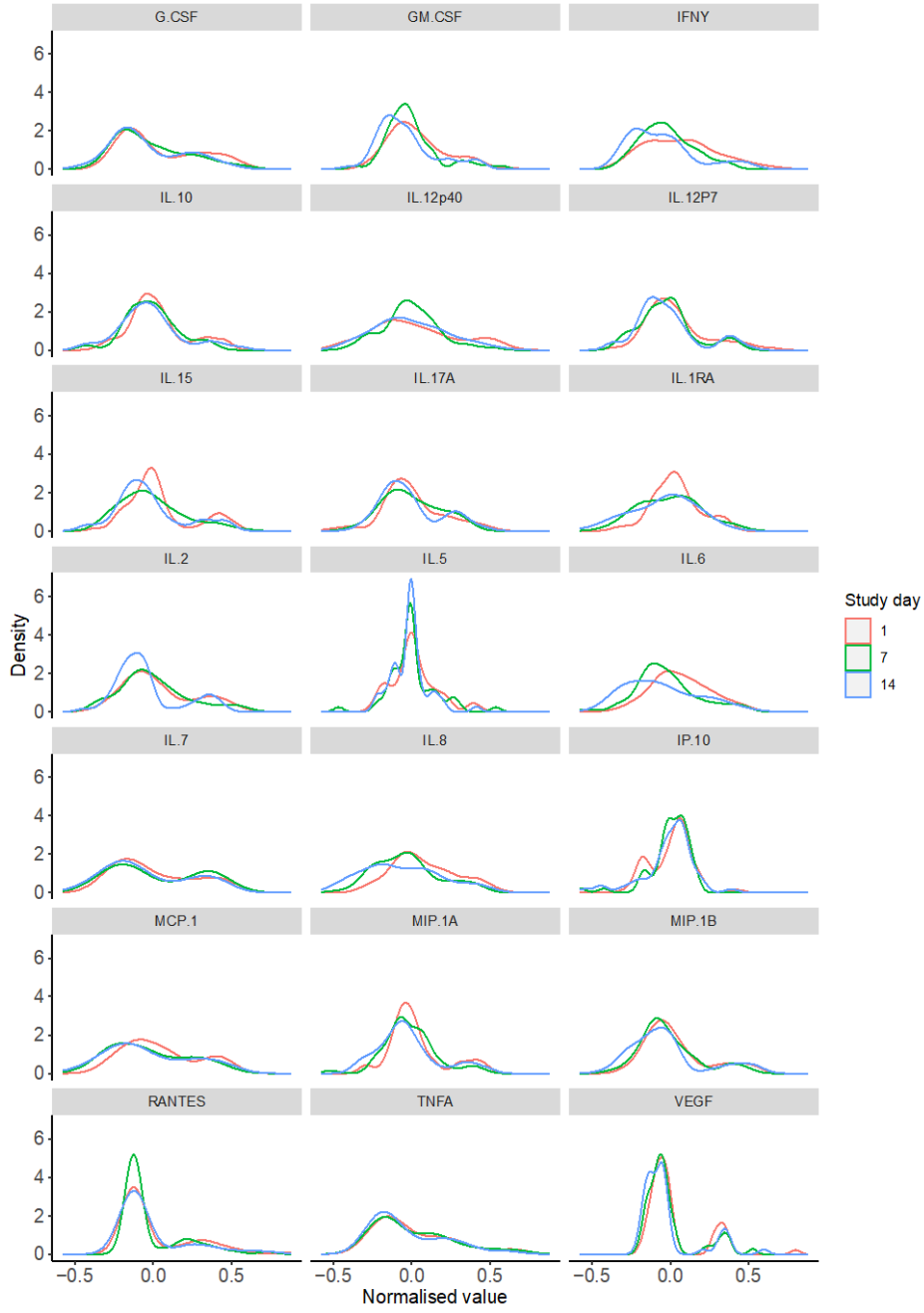

PCA was used to search for soluble biomarkers contributing to PCs that accounted for a substantial proportion of the variance in the dataset. From the PCA of day 1 biomarker concentrations, PC1 and PC2 accounted for 61.5% and

10.5% of the variance respectively (Figure 6.5A). The PC loadings for each cytokine demonstrated a that a large group of biomarkers of Th1-, Th2- and Th17-type responses drove the variance in PC1 and that the contribution of each of those biomarkers to PC1 was approximately equal (Figures 6.5B and 6.5C). Thus, PC1 scores were moderately positive across almost all biomarkers, with a large number of predominantly pro-inflammatory and adaptive cytokines and chemokines that are involved in monocyte/ macrophage chemoattraction or stimulation. The variance in PC2, in contrast, was primarily accounted for by positive loading scores in a group of just three biomarkers: TNF-α (associated with inflammatory, Th-1 type immune responses), G-CSF and IL-7 (associated with stimulation and development of granulocytes and T-lymphocytes, respectively), with neutral or negative loadings in all other markers besides IL-15, which contributed a low-positive loading score to PC2. The chemokines RANTES and IP-10, and the anti-inflammatory cytokines IL-10 and IL-1RA, were inversely correlated with PC2 scores (Figures 6.5 B and 6.5 C).

Figure 6.5: Principal component analysis of soluble biomarker concentrations on study day 1

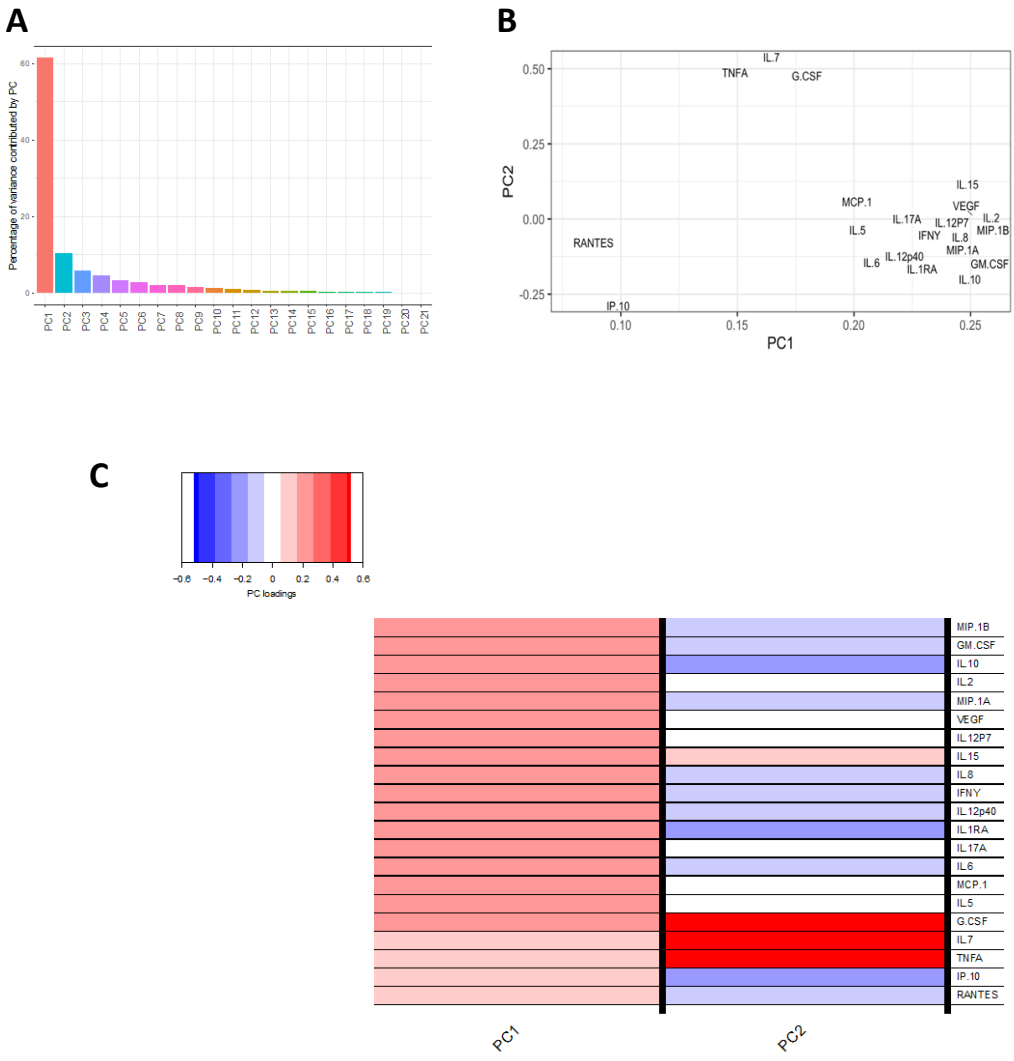

A) PC1 and PC2 accounted for 61.5% and 10.5% of the variance respectively. **B)** The majority of soluble biomarkers in the dataset form a group to account for the variance in PC1. PC2 is overwhelmingly characterised by positive loadings in TNF-α, G-CSF and IL-7. **C)** The loading scores for PC1 are homogeneous and modestly positive across 17 of 21 contributing biomarkers. PC2 is overwhelmingly characterised by positive loadings in TNF-α, G-CSF and IL-7, with neutral or negative loadings in all other markers besides IL-15.

6.3.3 Relationships between CSF soluble biomarkers on study day 1 and clinical outcomes

Having defined correlated variables that contribute to PC1 and PC2, which cumulatively explain 72% of the variance in the dataset of cytokines measured on

day 1, associations between those PCs and immunological and clinical variables were sought. PC1 and PC2 were applied as independent variables in models to assess their relationship with peripheral CD4+ T cell count, CSF leucocyte count, CSF lymphocyte percentage, baseline fungal burden in CSF, EFA in CSF, lumbar puncture opening pressure and mortality at 10 weeks (Table 6.1 and Table 6.2, Figure 6.6). For a unit increase in PC1, CSF white cell count was predicted to increase by 0.26 cells per mm^3 and opening pressure by 0.31 cm H_2O. In addition, there was a trend towards increased risk of death in patients with higher PC1 scores (Cox proportional hazard ratio 1.11 for PC1, adjusted for baseline fungal burden; p value 0.09). Logistic regression corroborated the association between PC1 and opening pressure, predicting that for a unit increase in PC1, the odds of having high opening pressure (defined as ≥ 30 cm H_2O) increase by a factor of 1.35. PC2 was not significantly associated with mortality in the Cox proportional hazards model (Table 6.1). There was no significant association between PC1 or PC2 and either EFA or mortality when these clinical outcomes were examined as categorical variables in logistic regression models (Table 6.2).

Table 6.1: Correlations between PC scores and laboratory and clinical variables

	PC1		PC2	
Variable	Pearson's r	p value	Pearson's r	p value
Peripheral CD4+ cell count (per mm^3)	-0.12	0.64	0.11	0.67
CSF WCC (per mm^3)	**0.26**	**0.04**	-0.04	0.75
CSF lymphocytes (% of CSF WCC)	0.10	0.73	-0.62	0.56
Opening pressure (cm H_2O)*	**0.31**	**0.01**	-0.08	0.49
Baseline fungal burden (log_{10} CFU/ml)	-0.11	0.38	-0.01	0.92
EFA (log_{10} CFU/ml/day)	-0.03	0.8	0.01	0.94
Mortality at 10 weeks	Cox PH estimate	0.09	Cox PH estimate	0.29
	1.11		0.78	

*Association between PC1 and opening pressure remained significant after adjusting for baseline fungal burden; p-value 0.01. CSF WCC: cerebrospinal fluid white cell count; CFU: colony-forming units. PH: proportional hazards. Significant associations highlighted in red.

Table 6.2: Odds ratios for categorical outcomes given increases in PC scores

	PC1		**PC2**	
Variable	Odds ratio (CI)	p value	Odds ratio (CI)	p value
Early fungicidal activity (high)	1.02 (0.86 – 1.25)	0.77	0.91 (0.61 – 1.43)	0.66
Opening pressure (high)	**1.35 (1.14 – 1.65)**	**0.001**	0.74 (0.38 – 1.20)	0.28
Mortality at 10 weeks (death)	1.15 (0.97 – 1.37)	0.11	0.78 (0.43 – 1.25)	0.35

CI: Confidence interval from 2.5% - 97.5%. Models evaluating odds ratios for opening pressure and mortality were adjusted for baseline fungal burden. Significant associations highlighted in red.

Figure 6.6: Associations between PCs 1 and 2 and clinical outcome variables

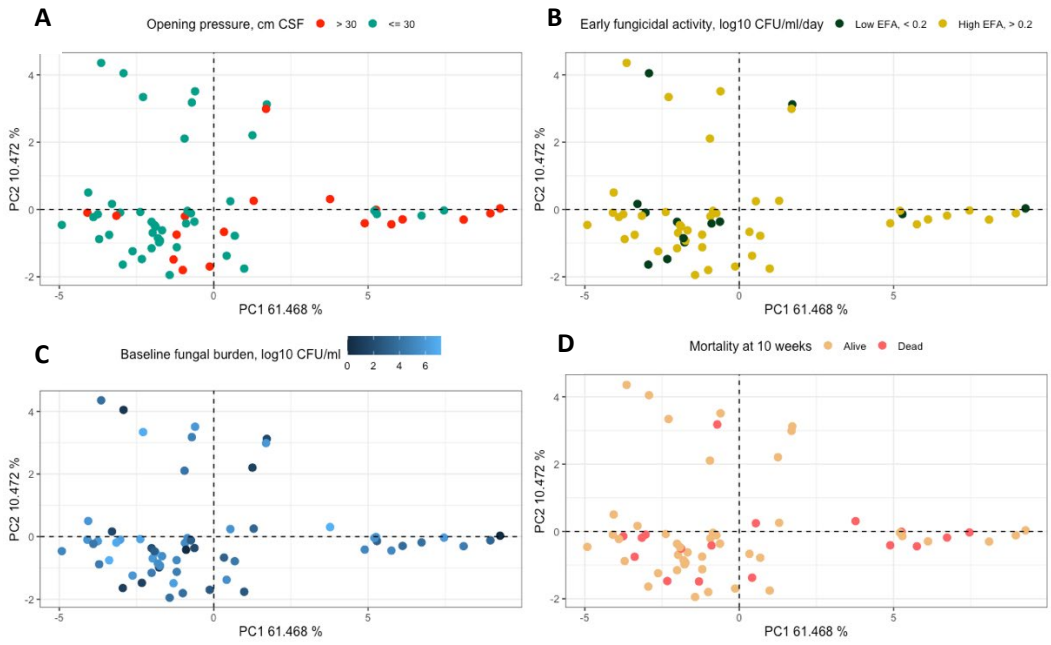

Figure 6.6 **A**) Linear regression predicted that for a unit increase in PC1, opening pressure was predicted to increase by 0.31 cm H_2O. In a logistic regression model, the odds of having high opening pressure increase by a factor of 1.35 for each unit increase in PC1. **B – D**) There was no significant association between PC scores and early fungicidal activity, baseline fungal burden or mortality at 10 weeks.

6.3.4 Network analysis: study day 1

Relationships between day 1 concentrations of soluble biomarkers were further analysed using network analysis. Applying network analysis to variables from study day 1, a recurring pattern emerged whereby the same biomarkers that contributed strongly to PC2 (TNF-α, G-CSF and IL-7) correlated more closely with one another than they did with any other soluble biomarkers in patients with favourable clinical outcomes of low opening pressure and survival at 10 weeks (figure 6.7A - D). The pattern was less clear when patients were categorised according to fast or slow EFA, where the dissociation of TNF-α, G-CSF and IL-7 from

the rest of the network was approximately equal between groups (Figure 6.7E and 6.7F).

Figure 6.7: Network plots of the associations among 21 soluble biomarkers in CSF of patients with HIV-associated cryptococcal meningoencephalitis

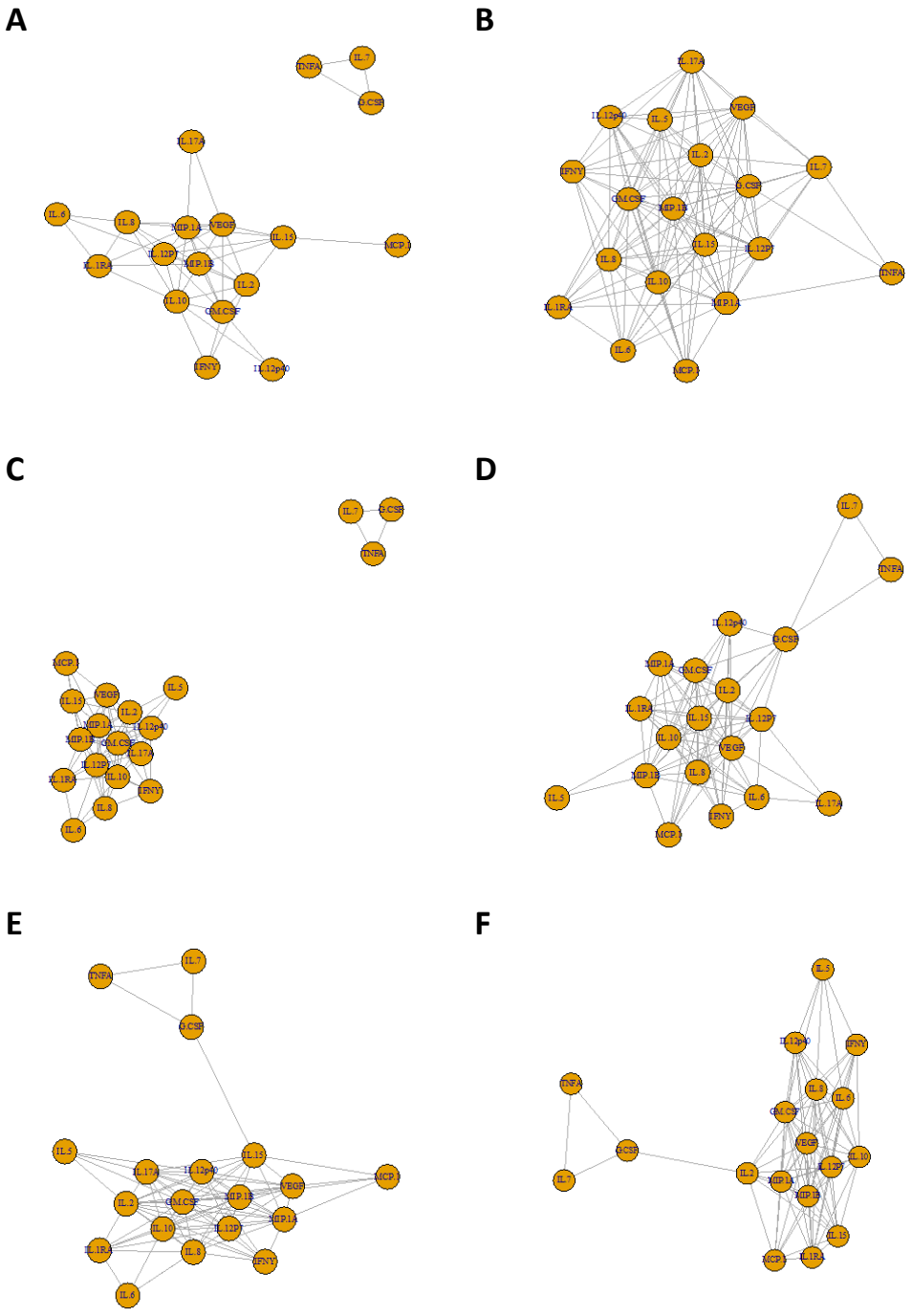

Figure 6.7: Network plots of the associations among 21 soluble biomarkers in CSF for **A**) patients with opening pressure ≤ 30 cm H_2O, **B**) patients with opening pressure > 30 cm H_2O, **C**) patients who survived to 10 weeks, **D**) patients who were dead by 10 weeks, **E**) patients with high EFA and **F**) patients with low EFA.

6.3.5 CSF soluble biomarkers: change in concentration over time

Concentrations of soluble biomarkers in CSF were available from 61 patients on day 1, 55 patients on day 7 and 53 patients on day 14. A linear regression of the log-transformed, normalised concentration of each biomarker for each patient over time on treatment provided a 'slope' value for each cytokine per patient. There was modest inter-cytokine variation in the mean slope value over the study period, though the variability in slope values for each cytokine was more heterogeneous (figure 6.8).

Figure 6.8: Change in CSF biomarker concentrations over time in patients with HIV-associated cryptococcal meningoencephalitis

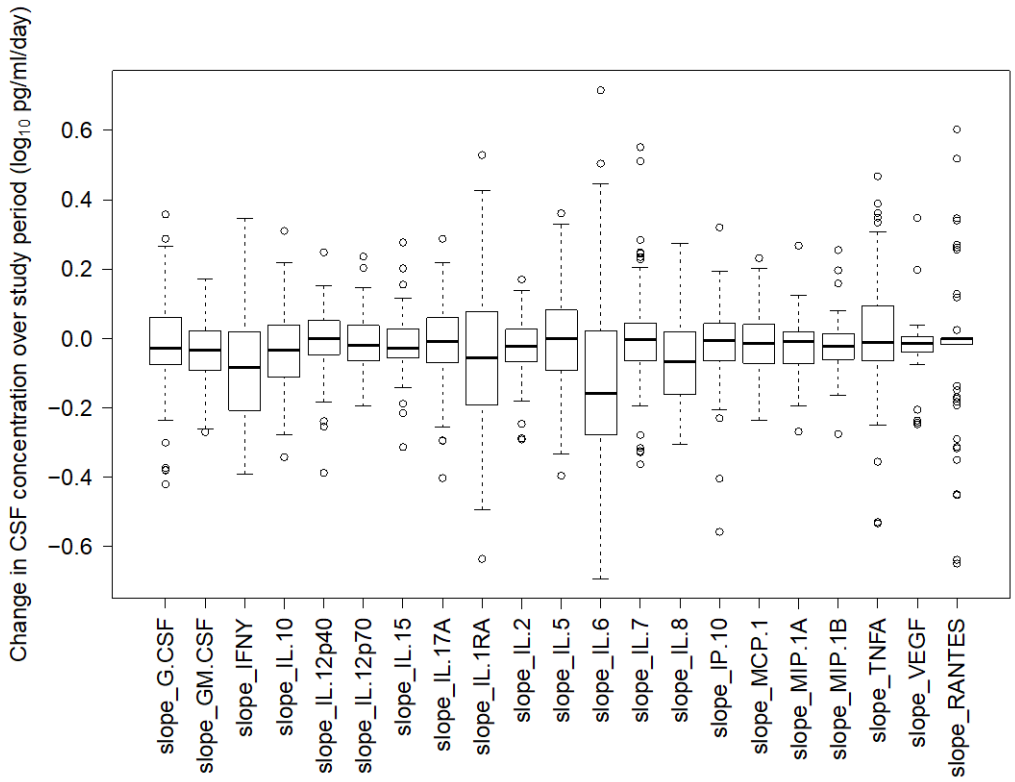

Figure 6.8: Boxes indicate interquartile range, with median marked inside box. Whiskers represent 10th and 90th percentiles.

PCA of the slope values for each biomarker in each patient revealed that the first two PCs of correlated cytokines and chemokines accounted for the majority of variance in the dataset. PC1 accounted for 52.3% of the variance, and PC2 10.0% (Figure 6.9A). As with the PCA of day 1 results, a large group of co-correlated variables drove the variance in PC1 and the contribution of the majority of those variables to PC1 was proximately equal (figures 6.9B and 6.9C). The variance in PC2, in contrast, was primarily accounted for by negative loading scores in the slopes of the same biomarkers that provided positive contributions to PC2 in the PCA of day 1 results: TNF-α, G-CSF and IL-7 (figures 6.9B and 6.9C). There was no statistically significant difference in PC1 or PC2 values between study arms (p value < 0.05).

Figure 6.9: Principal component analysis of the slope of soluble biomarker concentrations over time on treatment

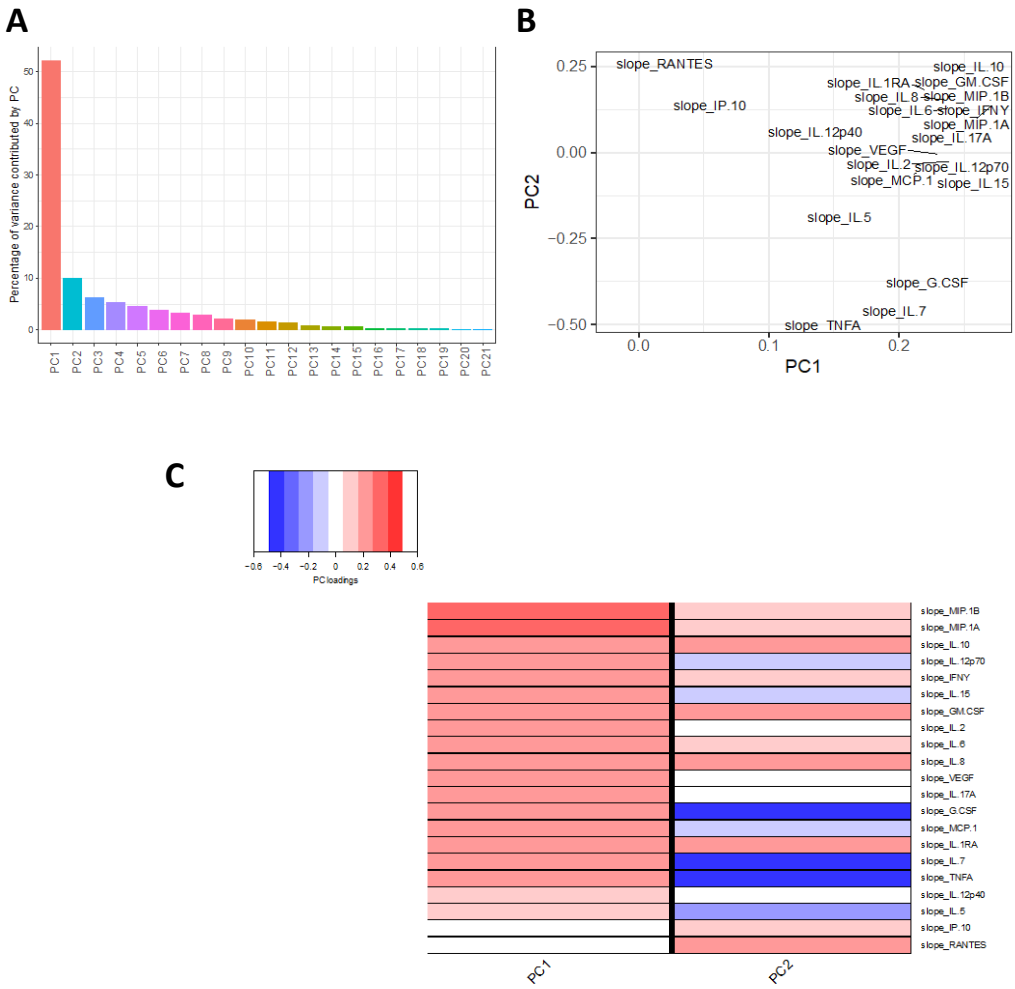

Figure 6.9: **A)** PC1 and PC2 accounted for 52.3% and 10.0% of the variance respectively. **B)** The majority of slope values form a group to account for the variance in PC1. PC2 is characterised by negative loadings in G-CSF, IL-7 and TNF-α, and to a lesser degree IL-5. **C)** As with the PCA for day 1 values, the loading scores for PC1 in the PCA of slope values are relatively homogeneous and modestly positive across 15 of 21 contributing biomarkers, with the slope values of MIP-1A and MIP-1B contributing slightly more positive loading scores. PC2 is overwhelmingly characterised by negative loadings in the slopes of G-CSF, IL-7 and TNF-α.

6.3.6 Relationships between change in soluble biomarker concentrations over time and clinical outcomes

PC1 and PC2 of the slopes of each soluble biomarker were applied as independent variables to assess their relationship with mortality and EFA (Figure 6.10). There was no association between EFA and PC1, either in univariate regression analysis or when adjusting for baseline fungal burden and study arm (p value 0.57 unadjusted; 0.53 adjusted). PC2 was significantly associated with EFA when adjusted for baseline fungal burden and study arm, however the predicted unit change was negligible - for every unit increase in PC2, EFA increased by 0.03 $\log_{10}$ CFU/ml/day (p value 0.01). Logistic regression revealed that there was no significant association between the PCA of the slope of cytokine concentrations over time and mortality at 10 weeks when adjusted for baseline fungal burden (p value for association between PC1 and mortality at 10 weeks, 0.77; between PC2 and mortality at 10 weeks, 0.18). A Cox proportional hazard model revealed no association between PC1 or PC2 of slope values and time to death. Similarly, there was no association between PC1 or PC2 and EFA when the latter was expressed as a categorical variable, either unadjusted or adjusted for baseline fungal burden and study arm (p value for association between PC1 and EFA category, 0.49; between PC2 and EFA category, 0.29).

Figure 6.10: Associations between PCs 1 and 2 and clinical outcome variables

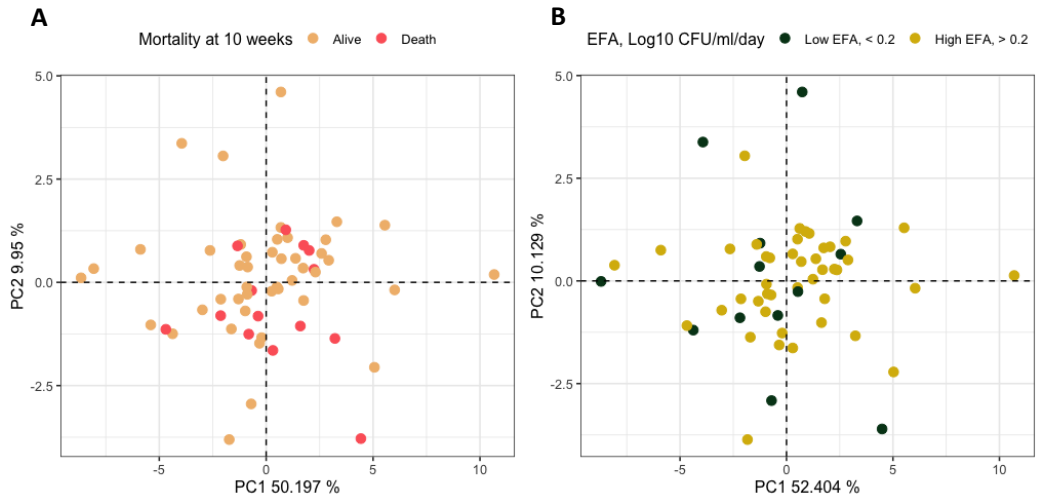

Figure 6.10: There was no significant association between PCs 1 and 2 from the PCA of slope values, and either **A**) mortality at 10 weeks, or **B**) early fungicidal activity.

6.3.7 Network analysis: change in soluble biomarker concentrations over time

Network analysis was applied to the slope values for each soluble biomarker over time. The slopes of the same three biomarkers that contributed strongly positive loading scores to PC2 in the PCA of day 1 concentrations, and negative loading scores to the PCA of the slope values for biomarkers (TNF-α, G-CSF and IL-7), were seen to correlate more closely with one another than they did with any other soluble biomarkers in patients with favourable clinical outcomes of high EFA and survival at 10 weeks (Figure 6.11A to D).

Taking both day 1 PCA results and slope value PCA results together, there is a suggestion that a coordinated immune response in TNF-α, G-CSF and IL-7 may be beneficial, with higher values prior to treatment initiation and stable or decreasing values during treatment. With the exception of the relationship between TNF-α and opening pressure, these cytokines were not themselves associated with clinical outcomes in isolation (Figure 6.12). However, their

significant association with cytokines that are characteristic of Th1- and Th17-type immune responses (Figure 6.13) implies that they form an integral part of pro-inflammatory pathways that promote classical macrophage activation.

Figure 6.11: Network plots of the associations among 21 soluble biomarkers in CSF of patients with HIV-associated cryptococcal meningoencephalitis

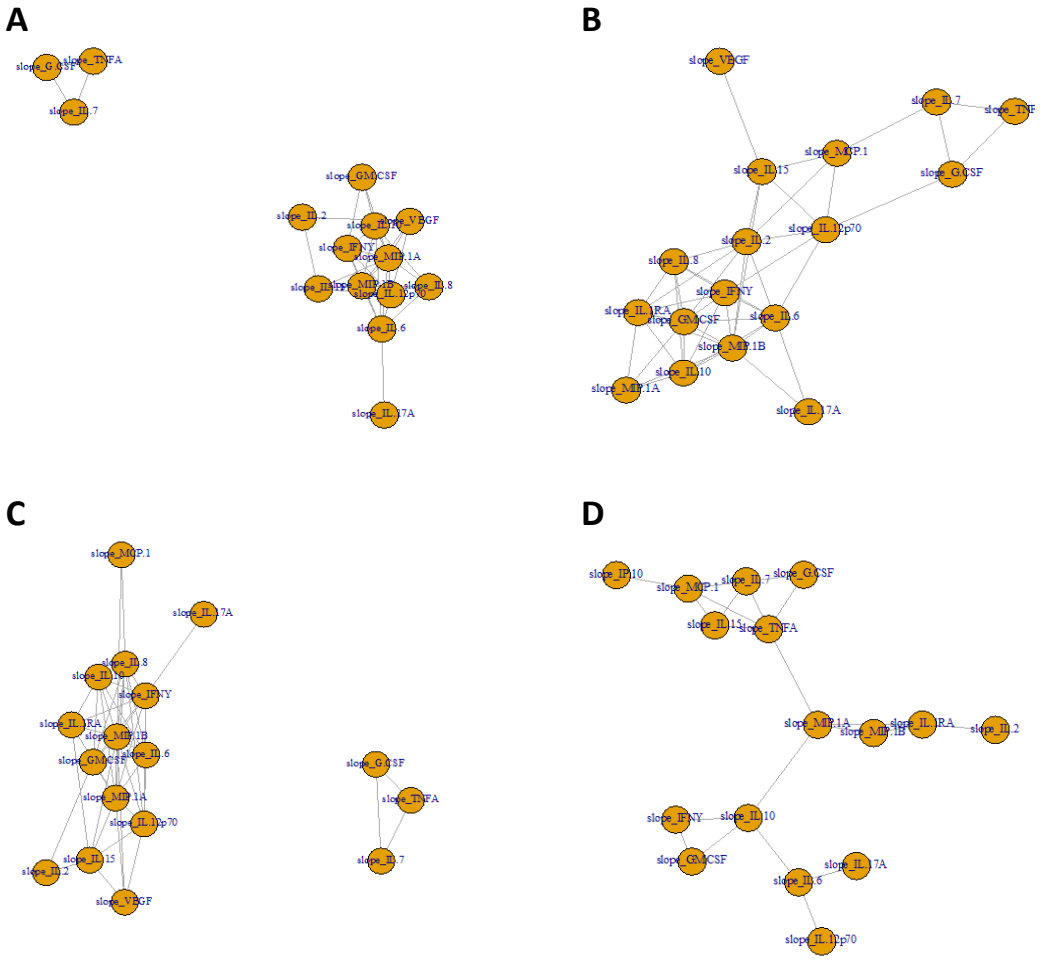

Figure 6.11: Network plots of the associations among the slopes of 21 soluble biomarkers in CSF for **A**) patients with EFA ≤ 0.2 $\log_{10}$ CFU/ml/day, **B**) patients with EFA > 0.2 $\log_{10}$ CFU/ml/day, **C**) patients who survived to 10 weeks and **D**) patients who were dead by 10 weeks.

Figure 6.12: Associations between TNF-□/G-CSF and IL-7 and clinical outcomes or markers of disease severity

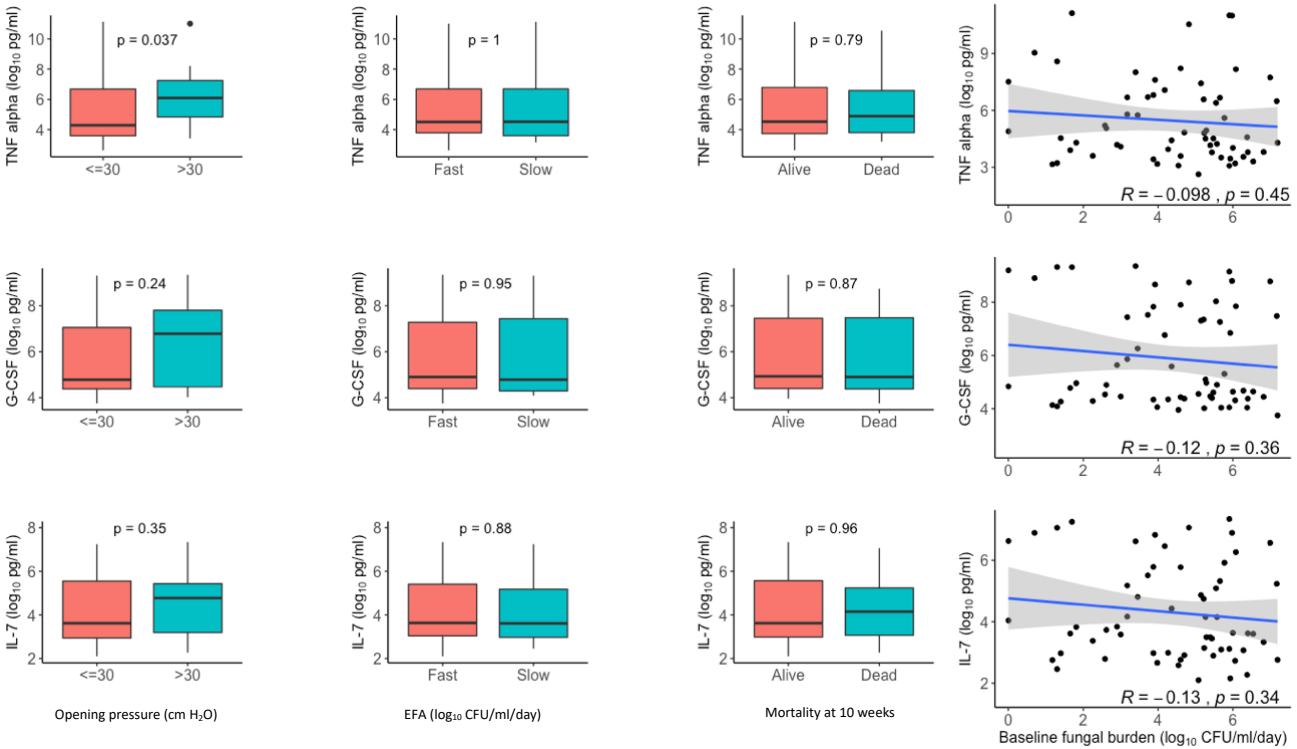

Figure 6.12: Associations between TNF-α (top row), G-CSF (middle row) and IL-7 (bottom row) and clinical outcomes of opening pressure (column 1), early fungicidal activity (column 2), 10-week mortality (column 3) and baseline fungal burden (column 4). Fast EFA defined as > 0.2 $\log_{10}$ CFU/ml/day, slow EFA ≤ 0.2 $\log_{10}$ CFU/ml/day. Box plots show median and inter-quartile range, with whiskers indicating range. Categorical variables compared using Mann-Whitney test. Dot plots show best-fit regression line and 95% confidence intervals, with Pearson's regression coefficient ('R').

Figure 6.13: Associations between TNF-α, G-CSF and IL-7 and clinical outcomes or markers of disease severity

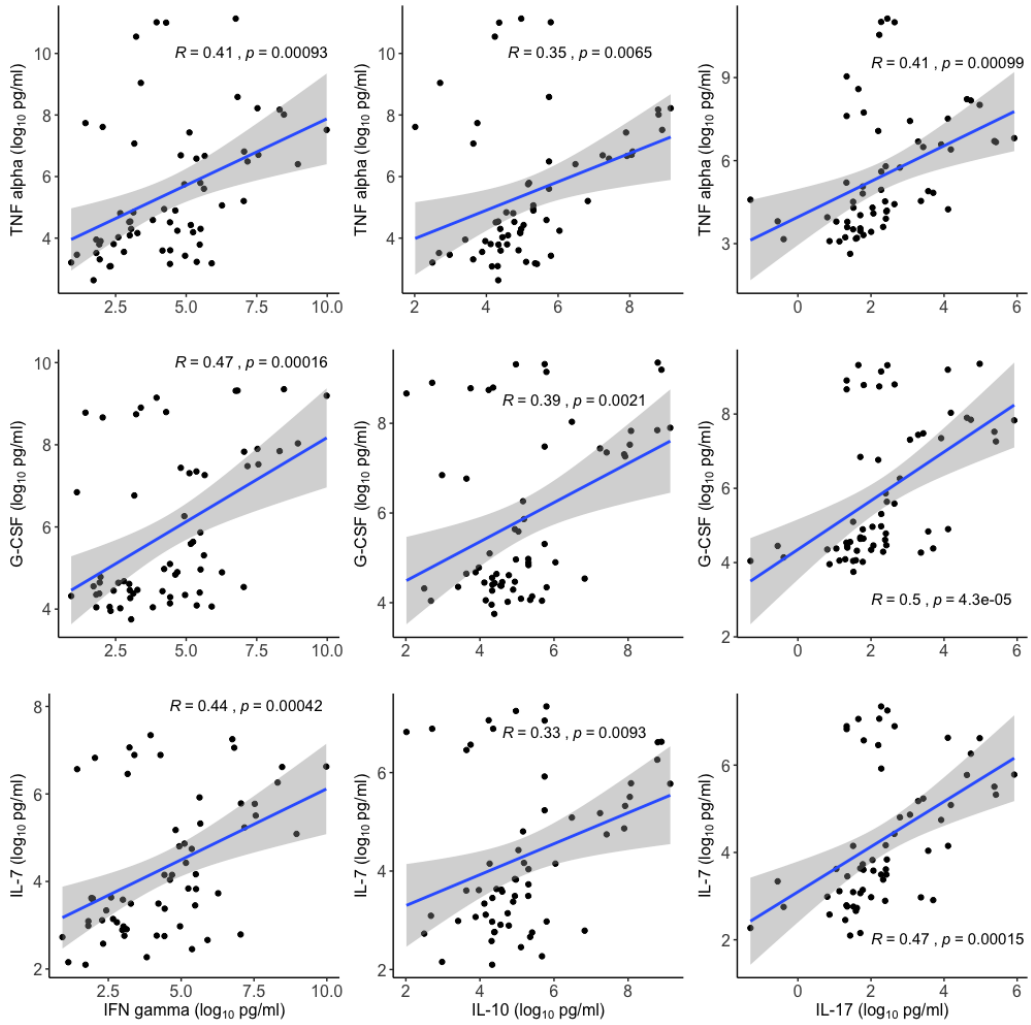

Figure 6.13: Correlations between TNF-α (top row), G-CSF (middle row) and IL-7 (bottom row) and biomarkers that are characteristic of Th1-type responses (IFN-γ, column 1), regulatory responses (IL-10, column 2) and Th17-type immune responses (IL-17, column 3). Dot plots showing best-fit regression line, 95% confidence interval and Pearson's correlation coefficient ('R').

6.3.8 Phagocyte functional activity

Phagosomal superoxide burst activity in neutrophils and monocytes was measured at 10, 30, 60 and 90 minutes. The fluorescence of cells that had internalised zymosan reporter particles was compared with the cells that had not internalised zymosan reporter particles. Both the proportion of zymosan positive

cells and the intensity of superoxide reporter fluorescence increased over the course of the assay in both neutrophils and monocytes (Figure 6.14A and 6.14B). Oxidation of both neutrophils and monocytes occurred rapidly and within 60 minutes for both cell types across HIV-negative controls, HIV-positive controls and in HIV/CM patients (Figure 6.14A and 6.14B). In HIV/CM patients, but not control patients, AI generally reached a plateau after 60 minutes. At all assay time points, neutrophil and monocyte AI was reduced in patients with HIV/CM compared with both HIV-positive and HIV-negative controls. Neutrophil AI was reduced in HIV-positive controls compared with HIV-negative controls (Figure 6.14 A and C). In HIV/CM patients, oxidative activity in neutrophils was unchanged between study days 1, 7 and 14 (Figure 6.14A), whereas in monocytes there was a trend towards recovery of oxidative activity throughout the study period to day 14 (Figure 6.14B and 6.14D). There was no significant difference in phagocytic activity between AMBITION study arms in either neutrophils or monocytes (p value < 0.05 for comparisons between study arms at all AI time points).

Figure 6.14: Activity index of superoxide burst over time in control subjects and patients with HIV-associated cryptococcal meningoencephalitis

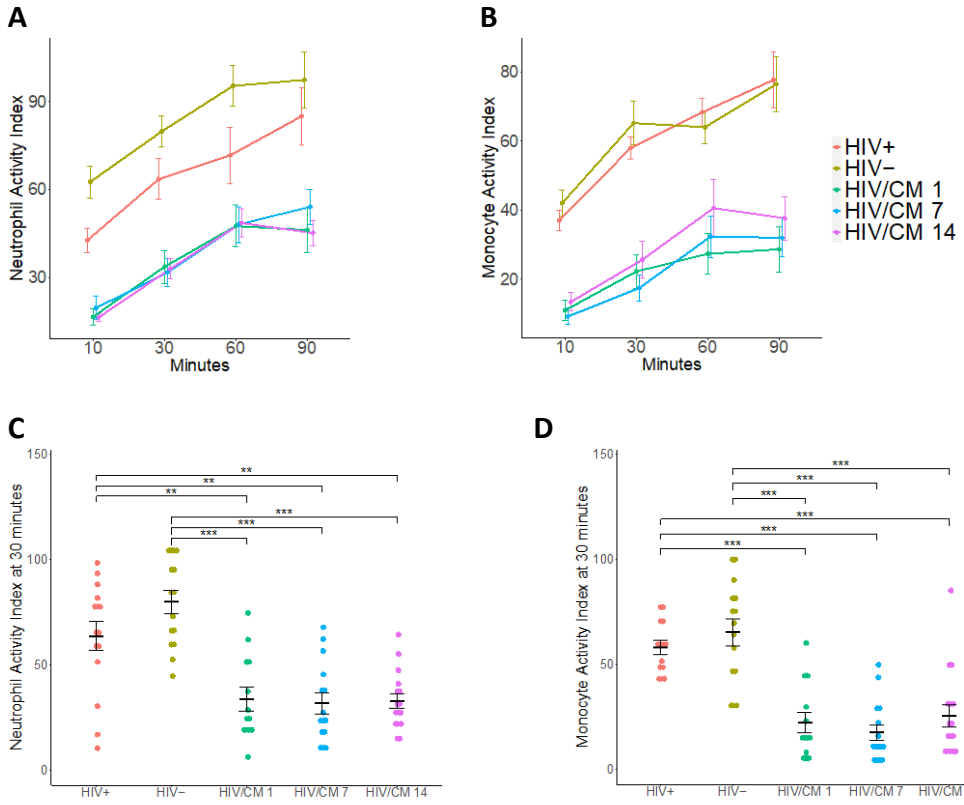

Figure 6.14: Activity index in **A**) neutrophils and **B**) monocytes over the duration of the assay. AI was significantly different between both HIV positive (HIV +) and HIV negative (HIV -) controls and HIV/CM patients on all study days, in both **C**) neutrophils and **D**) monocytes. All p values for comparisons < 0.001 (t test for pairwise comparisons).

6.3.9 Relationships between phagocyte function and clinical outcomes

The slope of AI values over the study period was calculated through a linear regression of peak AI values per patient per day and was assessed to give an indication of phagocyte recovery during antifungal therapy. Both the peak AI value per patient on study day 1 and the slope of peak AI values over the duration of the study (from days 1 to 14) were examined as independent variables for their impact on baseline fungal burden, opening pressure and EFA (Table 6.3). Peak

neutrophil AI was negatively associated with opening pressure (Pearson's r -0.33, p 0.04) and baseline fungal burden (r -0.50, p 0.001), and positively associated with EFA (r 0.33, p 0.04). The slope of neutrophil AI was positively associated with CSF white cell count (r 0.41, p 0.01). Peak and slope AI in monocytes was positively associated with opening pressure (r 0.36, p 0.02 and r 0.45, p 0.004 for peak and slope monocyte AI values, respectively). There was insufficient data to examine the relationships between measures of AI and mortality at 10 weeks.

Table 6.3: Relationship between phagocyte function and laboratory and clinical variables

	Peak AI - neutrophils		**AI slope - neutrophils**		**Peak AI - monocytes**		**AI slope - monocytes**	
Variable	Pearson's r	p value	Pearson's r	p value	Pearson's r	p value	Pearson's r	p value
CSF WCC (per mm^3)	-0.16	0.31	**0.41**	**0.01**	-0.26	0.11	0.01	0.93
Opening pressure (cm H_2O)*	**-0.33**	**0.04**	0.29	0.08	**0.36**	**0.02**	**0.45**	**0.004**
Baseline fungal burden (Log_{10} CFU/ml)	**-0.50**	**0.001**	-0.03	0.86	0.17	0.28	0.11	0.53
EFA (Log_{10} CFU/ml/day)	**0.33**	**0.04**	0.03	0.88	-0.27	0.11	-0.18	0.27

*Association between peak AI in neutrophils, peak AI in monocytes and AI slope in monocytes and opening pressure remained significant after adjusting for baseline fungal burden ($p<0.05$ for each correlation). Significant associations highlighted in red.

Since there was a suggestion that some measures of phagosome function were significantly associated with clinical outcomes, we constructed a correlation plot to explore the relationships between these AI measures and the PCs derived

from the PCA of soluble biomarkers on day 1 (Figure 6.15). There were positive correlations between the AI slope value in monocytes and both PC1 (Pearson's r 0.58, p value 0.0001) and PC2 (r 0.71, p value < 0.0001), however it is notable that the subset of patients for whom there were data for both biomarker quantification and functional phagocytosis was just n=11.

Figure 155: Correlation plot to explore relationships between measures of phagocytic activity index and soluble biomarker PCs

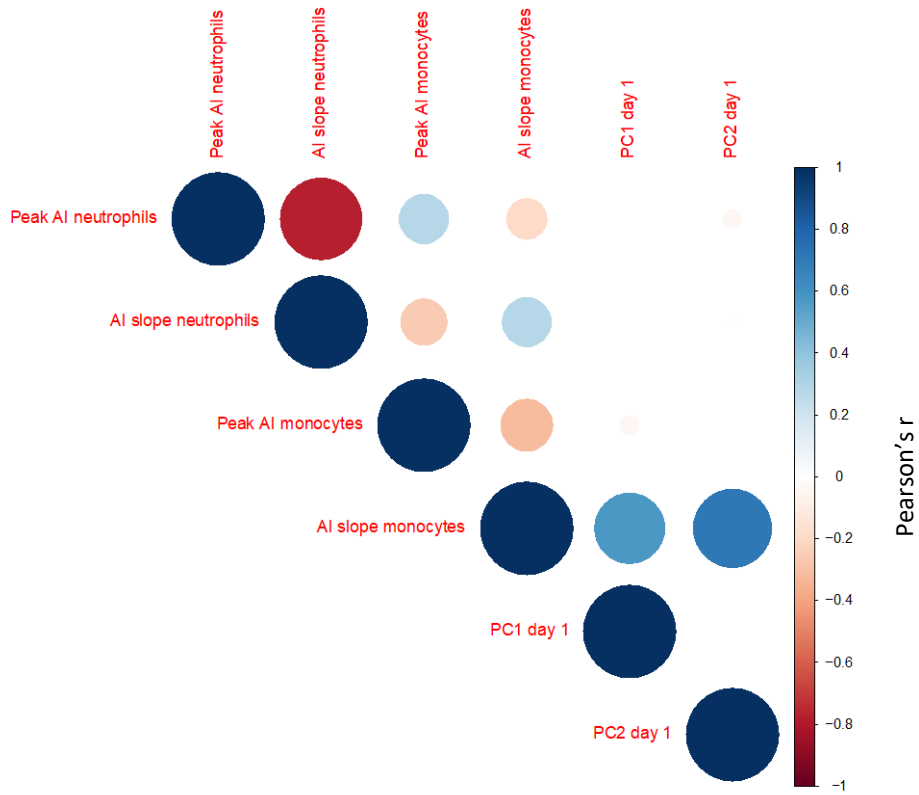

Figure 6.15: Larger circles indicate stronger correlations. Deeper blue shades indicate more positive correlations; deeper red shades more negative correlations. Blank regions indicate that the association between the relevant two variables was not statistically significant (p value >0.05).

6.4 Discussion

In this study we present a comprehensive analysis of the phenotype of the immune response at the site of clinical HIV-associated cryptococcal meningoencephalitis. This includes serial measurements of soluble biomarkers over time as well as examining whole blood functional phagocyte activity – to our knowledge the first time these measures have been applied in conjunction to HIV/CM patients. Our analysis of CSF soluble biomarkers on study day 1 suggests that a coordinated proinflammatory response is associated with favourable clinical outcomes – in particular, the coordination of TNF-α, G-CSF and IL-7 concentrations was associated with lower intracranial pressure and survival at 10 weeks. The analysis of the trend, or slope, in CSF cytokine concentrations over time revealed additional associations with EFA and corroborated the finding that a coordinated profile among these three cytokines has a positive impact on survival.

TNF-α is released from cells of monocyte/ macrophage lineage and functions as a core inflammatory mediator, involved in protection against a wide range of pathogens including *Listeria monocytogenes*, *Salmonella typhimurium*, *Mycobacterium tuberculosis* and *Candida albicans*.[409-412] TNF-α activates macrophages and polymorphonuclear leukocytes (PMNs), including neutrophils, triggering superoxide burst and nitric oxide-dependent cell killing.[413] In addition, TNF-α stimulates IFN-γ production, the beneficial role of which is well documented in patients with HIV/CM.[174,180] There is some evidence that

cryptococcal cells themselves inhibit the production of TNF-α,[173] which may partly explain its inverse correlation with fungal burden and EFA.

G-CSF promotes the differentiation of stem cells into neutrophils and monocytes, increasing their numbers as well as their phagocytic and microbicidal activity.[414,415] *In vitro* experiments have suggested that G-CSF may also have direct immunomodulatory properties, since the addition of G-CSF to neutrophils, monocytes or monocyte-derived macrophages led to enhanced cryptococcal killing both in the presence and absence of azole antifungal treatment.[416] There are reports from HIV-negative patients with cryptococcal meningoencephalitis of the identification of autoantibodies to another colony-stimulating factor, GM-CSF, suggesting the importance of colony-stimulating factors in immunity to cryptococcal meningoencephalitis.[417]

IL-7 is an essential cytokine for lymphopoiesis, evidenced by the absence of B- and T-cells in animals deficient in IL-7[418-420] and of T-cells in humans lacking IL-7.[421] IL-7 appears to play a key role in T-cell homeostasis – its release from stromal cells is thought to be triggered by low levels of circulating CD4+ T-cells, resulting in expansion of both CD4+ and CD8+ T-cells, regardless of baseline levels of CD8+ T-cells.[422,423] This is in keeping with the observation that the $CD4^+$ T-cell predominance observed in blood and CSF in healthy persons is replaced by $CD8^+$ T-cells in PLHIV.[154,165]

These cytokines do not operate in isolation and our finding that their concentrations are closely correlated with biomarkers characteristically associated with Th1-type immune responses (IFN-γ), regulatory cytokines (IL-10)

and Th17-type responses (IL-17) support the conclusion that they form part of a larger proinflammatory network that promotes beneficial clinical responses to HIV/CM. This is in keeping with other clinical studies of the host response to cryptococcal meningoencephalitis in CSF, which demonstrate that reduced concentrations of Th1-type biomarkers in CSF such as IL-6, G-CSF and IFN-γ are associated with higher fungal burden, slower clearance of infection and early mortality.[152,154,155,174] The use of dexamethasone as an adjunct to antifungal therapy for HIV/CM is associated with rapid early declines in TNF-α in CSF, slower fungal clearance and a trend towards excess mortality.[183,184] Conversely, increased concentrations of the Th1-type cytokines IL-6, IL-8, IL-17, IFN-γ and TNF-α in CSF are associated with survival benefit.[152,155,175]

The phagocyte functional assay suggested that phagocytosis and phagosomal superoxide burst were significantly reduced in HIV/CM patients compared with control participants in both neutrophils and monocytes, and in HIV-positive controls compared with HIV-negative controls in neutrophils. Peak AI in neutrophils on day 1 was associated with markers of clinical benefit – reduced opening pressure and fungal burden, and increased EFA. However, the same was not true of monocytes, in which increased AI was associated with increased opening pressure. This is consistent with phagocyte biology – neutrophils do not proliferate and have a short half-life *in vivo* of approximately 6-12 hours.[424] Following phagocytosis and the production of ROS, neutrophils undergo apoptosis – a process that is essential to limit the release of inflammatory mediators and constrain tissue damage.[425,426] This may explain why despite the significant

associations between peak AI in neutrophils and clinical outcomes, the slope in neutrophil AI over time was not significantly associated with these indices. Once neutrophils have phagocytosed invading cryptococci in the acute setting, their populations diminish, and other immune factors take over antifungal action. Monocyte populations, in contrast, have an *in vivo* half-life of approximately 22 hours and monocyte apoptosis can be blocked by proinflammatory cytokines including TNF-a and G-CSF.[427,428] The significant association between monocyte AI slope and opening pressure, that was not seen between neutrophil AI slope and opening pressure, may therefore reflect ongoing monocyte activity over the study period, enabled by inhibition of monocyte apoptosis by the presence of inflammatory cytokines (themselves also associated with opening pressure, as demonstrated in the PCA and network analyses).

Notably, peak neutrophil AI was negatively correlated with opening pressure, whereas peak and slope monocyte AI values were positively correlated with opening pressure. An explanation for this may be that the short half-life of neutrophils results in their predominant action being that of phagocytosis prior to apoptosis, whereas the ongoing action of monocytes - which includes not only phagocytosis but also antigen presentation and production of proinflammatory cytokines[429] - contributes to more widespread inflammation in the CNS, which is overall beneficial but amplifies the risk of increased intracranial pressure. The hypothesis that the overriding feature of monocyte activity in this setting is the contribution to generalised inflammatory activity rather than reduction in fungal burden through phagocytosis is supported by the positive correlation of monocyte

AI slope with PC1 and PC2 from the PCA of day 1 soluble biomarker concentrations.

Despite its prospective nature and the fact that it presents a detailed overview of immune biomarkers and phagocyte function from serial samples collected over time, this study is subject to a number of limitations. Firstly, our cohort was relatively small and heterogeneous. In particular, samples for the phagocyte functional assay were collected from a limited number of patients and a substantial proportion of these were distinct from the patients who provided CSF samples for multiplex biomarker analysis. It would have been preferable to have data from all assays from all patients and we recommend that correlations between biomarker concentrations and phagocytic activity index are sought in larger cohorts. Secondly, we do not have samples of CSF from control patients without cryptococcal meningoencephalitis, due to ethical considerations that restrict the collection of CSF without clinical indication. Thirdly, prospective clinical findings (EFA and mortality) were likely influenced by the PK of the drugs received by patients. While we controlled for study arm in the analysis of prospective clinical findings, we did not have access to individual PK parameters for all study drugs, which may have exhibited significant inter-individual variability. Finally, the principal clinical indicator for which we found consistent findings throughout or data and which tied our results together was opening pressure. It is likely that non-immune factors played a role in increasing intracranial pressure, for which we were unable to account in this study. For example, while we adjusted our analyses for fungal burden, we did not measure *Cryptococcus* cell or capsule

size, both of which are associated with increased intracranial pressure via obstruction of CSF drainage.[154,430]

In summary, we have added to an emerging body of literature that suggests the importance of proinflammatory Th1-type activity in the host response to cryptococcal meningoencephalitis. The association of phagocyte function with soluble immune biomarker signatures provides further insight into the mechanism of host anticryptococcal activity. In keeping with previous clinical studies, we have not seen a dichotomous Th1/Th2 response in CSF.[152] Instead, a complex network of closely correlated biomarkers that may be categorised as Th1, Th2 and/or Th17 appears to result in generalised inflammation that is associated with phagocyte function in monocytes and is beneficial in terms of clinical response in HIV/CM.

7 Conclusion

7.1 Principal finding: the neglect of PK-PD analyses stalls progress in antifungal therapeutics and is potentially harmful to patients.

Pharmacokinetic and pharmacodynamic analyses have been underutilised in the field of therapeutics for invasive fungal infections (IFIs), where they present an opportunity for improved understanding of treatment outcomes. In turn, PK-PD analyses have the potential to enhance the accuracy and efficiency of efforts to optimise the treatment of these deadly diseases. This is the central conclusion of this thesis, drawing on evidence from each of chapters 2 – 6.

Several clinical observations formed the basis of the investigations presented in this thesis. Decades of experience with treating HIV-associated cryptococcal meningoencephalitis have concluded that fluconazole monotherapy, even at high doses, fails to achieve satisfactory clinical outcomes at a population level, while treatment with amphotericin B deoxycholate (DAmB) produces greater rates of treatment success as well as greater rates of toxicity. A novel liposomal amphotericin B (LAmB)-based regimen offers hope for a less toxic and logistically more straightforward strategy. Despite promising pharmacological attributes, itraconazole was inferior to DAmB for the treatment of disseminated talaromycosis in a recent clinical trial. Until now, however, the PK-PD rationale for these observations has remained elusive or has been inferred from preclinical observations. This thesis examines the PK-PD principles underlying these observations based on clinical data derived from relevant patient populations.

In chapter 2, the inferiority of fluconazole monotherapy compared with polyene-based therapy is explained in PK-PD terms. Despite proven anticryptococcal activity and excellent CNS partitioning, fluconazole fails to attain PD targets even in wild type strains of *C. neoformans*. Extensive variability in systemic fluconazole PK and its CNS penetration increases the risk of suboptimal exposure. Similarly, chapter 3 demonstrates the PK-PD basis for the clinical outcomes observed following DAmB administration for cryptococcal meningoencephalitis. This drug sterilises CSF in a dose-dependent manner, but at doses approaching 1.0 mg/kg the benefit of CSF sterilisation is offset by increased mortality, which may be related to excessive toxicity or pathophysiological changes that we were unable to account for. The PK model and bridging study presented in chapter 4 suggests that the novel high dose LAmB-based regimen currently being trialled for cryptococcal meningoencephalitis is dosed optimally in terms of achieving maximal PD effect. These analyses, therefore, have provided at least part of the pharmacological explanation for clinical observations in these drug-disease combinations. The fact that all PK samples were taken from patients currently undergoing treatment for HIV-associated cryptococcal meningoencephalitis rather than from healthy volunteers increases the confidence with which these findings can be applied to relevant patient populations.

PK-PD studies are essential components of some larger scientific endeavours, though their inclusion in those endeavours is frequently neglected. Chapters 4 and 5 highlight the importance of PK-PD studies in drug development

and clinical trial design, respectively. In chapter 4, it was not possible to link the population model built to describe LAmB PK to clinical PD data, since incomparable combination treatment regimens were administered in the two trial arms of AMBITION. That is to say that the non-polyene component of each trial arm differed, so the PD effect of the polyene could not be isolated. A murine bridging study was performed to generate data to simulate the PD effect of high dose LAmB, with associated limitations as described in chapter 4. Had thorough clinical PK-PD studies been incorporated into the development of LAmB, this approximation of PD effect through the murine bridging study would not have been necessary. Chapter 5 describes a missed opportunity within the clinical trial investigating the non-inferiority of itraconazole versus DAmB for talaromycosis to generate data to explain the trial outcome pharmacologically, or to set a target for therapeutic drug monitoring of itraconazole in this disease, since very few of the patients mounted sufficient drug exposure to generate PD effect. This limitation may have been avoided had PK-PD studies been incorporated into trial design at an earlier stage.

PK-PD factors are not the sole determinants of clinical outcome from IFIs. This is demonstrated in chapters 3 and 6. The analysis presented in chapter 3 indicates the dosage at which PD benefits begin to be outweighed by mortality that may be unrelated to CSF fungal burden. Chapter 6 presents a detailed examination of the host response to cryptococcal meningoencephalitis and suggests that immunological factors are important in determining clinical outcome. In addition, this chapter provides novel insights into the role of

phagosomal activity as part of a coordinated inflammatory response against disseminated cryptococcal infection. This adds to a growing body of literature that indicates that there is a potential role for immunomodulatory therapy in cryptococcal meningoencephalitis, which may be in addition to traditional antifungal therapy.

The analyses presented in this thesis are subject to a number of general limitations. In chapter 2, our conclusions regarding the probability of PD target attainment are based on the assumed relevance of a PK-PD target derived from murine data. Similarly in chapter 4, LAmB PD is modelled based on an inhibitory E_{max} model generated from murine data. In chapter 3, the DAmB PD data from patients in the PK study population were confounded by the co-administration of fluconazole, so PD outcomes were modelled based on a meta-analysis of clinical studies in comparable, but necessarily different, patient populations. In all of these analyses, then, PD data originated from patients or subjects that were unmatched to the patients that the PK data originated from. Nevertheless, the PD data used were the most applicable data available, and overall findings were biologically and clinically plausible in each case.

For PK datapoints where the level was below the bioanalytical limit of quantitation (LLQ), we investigated various methods for handling these values: datapoints below the LLQ were set either to half the LLQ, to zero, or were treated as missing values. There are limitations to each of these approaches since they have the effect of artifactually prolonging the half-life of the drug, curtailing the half-life or withholding information, respectively. In each of the PK models, we

selected the option that enabled the best fit. In chapters 2, 3 and 4, the impact of these approaches on simulated PD outcomes would be minimal, since PD was linked to AUC, which is mainly determined by measurable drug levels. In chapter 5, itraconazole exposure was so low in the population that the consequences of each approach would again have been minimal. However, the uncertainty surrounding these datapoints undoubtedly reduces the degree to which the PK models can reflect reality.

7.2 Future directions

In IFIs, as in other infectious diseases, there exists large heterogeneity in PD outcomes. Despite receiving the same dose and regimen of the same drug or combination of drugs, treatment response varies markedly from patient to patient.[74,322] PK analyses such as those presented here can quantify variability in drug exposure, including that at the site of infection, and suggest the degree to which this is responsible for variability in PD and clinical response. However, as illustrated in chapter 6, non-pharmacological aspects of infection can also impact upon clinical outcomes. The reliance on PD trends such as EFA as surrogate indicators of mortality in clinical studies[263,264] raises the importance of an appreciation of the broad determinants of those trends. A clear next step for this research is to investigate non-pharmacological determinants of PD response in more detail. In the example of cryptococcal meningoencephalitis, a search for immune signatures in CSF in a larger patient population with matched control samples would be valuable, particularly focussing on pre-treatment levels of

soluble biomarkers since these were the most informative in our analysis. A similar analysis in peripheral blood samples may offer additional insight. Verification of the signal emerging from our functional phagocytosis assay, that suggests that phagosomal activity forms part of a widespread beneficial pro-inflammatory response to cryptococcal meningoencephalitis, should similarly be sought in greater patient numbers.

An additional source of heterogeneity in PD response may arise from the microbiological characteristics of the infecting organism itself. Again, to take the example of cryptococcal meningoencephalitis, there is evidence that isolates of particular genomic lineages of *Cryptococcus spp.* exhibit distinctive phenotypes and are associated with higher rates of mortality than other lineages.[192] There are further clinical associations with genomic strain characteristics at the sub-lineage level.[189-191,193] Moreover, there is increasing evidence of strain heterogeneity within an individual patient's infection, and the expansion of heterogeneity in terms of drug tolerance or resistance during suboptimal drug treatment.[67,194,431-433] Phenotypic virulence attributes may conceivably also vary within an individual patient's infection. The impact of genotypic and phenotypic attributes on markers of PD response, such as EFA, has not been clarified.

An especially valuable future line of research would be to acquire matched individual-level data on the PK parameters, immunological networks and microbiological characteristics of clinical infection with *Cryptococcus spp.* – or other invasive fungal pathogens. In this scenario, the relative contribution of each of those features to PD response and ultimately to clinical outcome could be

calculated. For example, if a host has a weak inflammatory response to cryptococcal infection in the CNS, and/ or is infected with a particularly virulent strain of *Cryptococcus spp.*, can adequate drug exposure compensate for that and produce a favourable PD outcome? And secondarily, would such an outcome guarantee a favourable clinical outcome or are there nuances to this relationship that could be established clinically?

7.3 Conclusion

Pharmacometric analysis has historically been a neglected area of research in the antimicrobial arena and particularly in mycology. Each chapter in this thesis illuminates to some degree the scientific explanation for a clinical observation and thereby highlights the utility of clinical PK-PD research in relevant patient populations. More generally, this work demonstrates that PK-PD tools can de-risk efforts to optimise antifungal treatment regimens, enhance the efficiency of those efforts and contribute to the preservation of the precious antifungal armamentarium that is currently available.

8 References

1. US Centers for Disease Control and Prevention. National Center for Health Statistics. cdc.gov (accessed 3rd August 2020).
2. Mohr KI. History of Antibiotics Research. *Curr Top Microbiol Immunol* 2016; **398**: 237-72.
3. Hutchings MI, Truman AW, Wilkinson B. Antibiotics: past, present and future. *Current Opinion in Microbiology* 2019; **51**: 72-80.
4. Newman DJ, Cragg GM. Natural products as sources of new drugs from 1981 to 2014. *Journal of natural products* 2016; **79**(3): 629-61.
5. Katz L, Baltz RH. Natural product discovery: past, present, and future. *Journal of industrial microbiology & biotechnology* 2016; **43**(2-3): 155-76.
6. Lewis K. The Science of Antibiotic Discovery. *Cell* 2020; **181**(1): 29-45.
7. Drusano GL, Louie A, MacGowan A, Hope W. Suppression of Emergence of Resistance in Pathogenic Bacteria: Keeping Our Powder Dry, Part 1. *Antimicrobial Agents and Chemotherapy* 2016; **60**(3): 1183-93.
8. Payne DJ, Gwynn MN, Holmes DJ, Pompliano DL. Drugs for bad bugs: confronting the challenges of antibacterial discovery. *Nature Reviews Drug Discovery* 2007; **6**(1): 29-40.
9. Eagle H, Fleischman R, Musselman AD. Effect of schedule of administration on the therapeutic efficacy of penicillin; importance of the aggregate time penicillin remains at effectively bactericidal levels. *Am J Med* 1950; **9**(3): 280-99.
10. Garrod LP. Bactericidal action of streptomycin. *British Medical Journal* 1948; **1**(4547): 382.
11. Ambrose PG, Bhavnani SM, Rubino CM, et al. Pharmacokinetics-pharmacodynamics of antimicrobial therapy: it's not just for mice anymore. *Clin Infect Dis* 2007; **44**(1): 79-86.
12. Craig WA. In vitro and animal PK/PD models. Fundamentals of Antimicrobial Pharmacokinetics and Pharmacodynamics: Springer; 2014: 23-44.
13. Administration FaD. Challenge and opportunity on the critical path to new medical products: U.S. Department of Health and Human Services, 2004.
14. Agency EM. Points to consider on pharmacokinetics and pharmacodynamics in the development of antibacterial medicinal products. European Agency for the Evaluation of Medicinal Products London, United Kingdom; 2000.
15. Echols RM. The selection of appropriate dosages for intravenous ciprofloxacin. *Journal of Antimicrobial Chemotherapy* 1993; **31**(5): 783-7.
16. Stott KE, Pertinez H, Sturkenboom MGG, et al. Pharmacokinetics of rifampicin in adult TB patients and healthy volunteers: a systematic review and meta-analysis. *Journal of Antimicrobial Chemotherapy* 2018: dky152-dky.
17. Spellberg B, Guidos R, Gilbert D, et al. The Epidemic of Antibiotic-Resistant Infections: A Call to Action for the Medical Community from the Infectious Diseases Society of America. *Clinical Infectious Diseases* 2008; **46**(2): 155-64.

18. Boucher HW, Talbot GH, Bradley JS, et al. Bad Bugs, No Drugs: No ESKAPE! An Update from the Infectious Diseases Society of America. *Clinical Infectious Diseases* 2009; **48**(1): 1-12.
19. O'Neill J. Tackling Drug-resistant Infections Globally: Final Report and Recommendations. The Review on Antimicrobial Resistance. London: HM Government and the Wellcome Trust. 2016. *Google Scholar There is no corresponding record for this reference* 2018.
20. O'Neill J. Review on antimicrobial resistance: tackling a crisis for the health and wealth of nations. *London: HM Government* 2014.
21. Adeyi O, Baris E, Jonas O, et al. Drug-resistant infections: a threat to our economic future. *World Bank Group, Washington, DC* 2017.
22. Kostyanev T, Bonten MJM, O'Brien S, et al. The Innovative Medicines Initiative's New Drugs for Bad Bugs programme: European public–private partnerships for the development of new strategies to tackle antibiotic resistance. *Journal of Antimicrobial Chemotherapy* 2015; **71**(2): 290-5.
23. Department of Health and Social Care. World-first scheme underway to tackle AMR and protect UK patients. gov.uk; 2020.
24. Agency EM. Guideline on the use of pharmacokinetics and pharmacodynamics in the development of antimicrobial medicinal products. European Medicines Agency London, United Kingdom; 2016.
25. Huurneman LJ, Neely M, Veringa A, et al. Pharmacodynamics of Voriconazole in Children: Further Steps along the Path to True Individualized Therapy. *Antimicrobial Agents and Chemotherapy* 2016; **60**(4): 2336-42.
26. Lestner JM, Groll AH, Aljayyoussi G, et al. Population Pharmacokinetics of Liposomal Amphotericin B in Immunocompromised Children. *Antimicrob Agents Chemother* 2016; **60**(12): 7340-6.
27. Hebert MF, Smith HE, Marbury TC, et al. Pharmacokinetics of micafungin in healthy volunteers, volunteers with moderate liver disease, and volunteers with renal dysfunction. *The Journal of Clinical Pharmacology* 2005; **45**(10): 1145-52.
28. Alobaid AS, Wallis SC, Jarrett P, et al. Effect of Obesity on the Population Pharmacokinetics of Fluconazole in Critically Ill Patients. *Antimicrob Agents Chemother* 2016; **60**(11): 6550-7.
29. Global Action Fund for Fungal Infections. Fungal disease frequency. https://www.gaffi.org/why/fungal-disease-frequency/ (accessed 17 August 2020).
30. World Health Organization. Gobal Tuberculosis Report 2019. 2019. https://www.who.int/tb/global-report-2019 (accessed 17 August 2020).
31. World Health Organization. Global Health Observatory (GHO) data: Number of malaria deaths. 2017. https://www.who.int/gho/malaria/epidemic/deaths/en/ (accessed 17 August 2020).
32. Loyse A, Burry J, Cohn J, et al. Leave no one behind: response to new evidence and guidelines for the management of cryptococcal meningitis in low-income and middle-income countries. *Lancet Infect Dis* 2019; **19**(4): e143-e7.

33. Molloy SF, Chiller T, Greene GS, et al. Cryptococcal meningitis: A neglected NTD? *PLOS Neglected Tropical Diseases* 2017; **11**(6): e0005575.
34. Head MG, Brown RJ, Newell M-L, Scott JAG, Batchelor J, Atun R. The allocation of US$105 billion in global funding from G20 countries for infectious disease research between 2000 and 2017: a content analysis of investments. *The Lancet Global Health* 2020; **8**(10): e1295-e304.
35. Brown GD, Denning DW, Gow NAR, Levitz SM, Netea MG, White TC. Hidden Killers: Human Fungal Infections. *Science Translational Medicine* 2012; **4**(165): 165rv13-rv13.
36. Stott KE, Loyse A, Jarvis JN, et al. Cryptococcal Meningoencephalitis: Time For Action. *Lancet Infect Dis* 2020; **In press**.
37. May RC, Stone NRH, Wiesner DL, Bicanic T, Nielsen K. Cryptococcus: from environmental saprophyte to global pathogen. *Nature Reviews Microbiology* 2016; **14**(2): 106-17.
38. Rajasingham R, Smith RM, Park BJ, et al. Global burden of disease of HIV-associated cryptococcal meningitis: an updated analysis. *Lancet Infect Dis* 2017.
39. Gottfredsson M, Perfect JR. Fungal meningitis. *Semin Neurol* 2000; **20**(3): 307-22.
40. Molloy SF, Kanyama C, Heyderman RS, et al. Antifungal Combinations for Treatment of Cryptococcal Meningitis in Africa. *N Engl J Med* 2018; **378**(11): 1004-17.
41. Chapman N, Boubell A, Barnsley P, et al. Neglected disease research and development: Uneven progress: G-FINDER, 2019.
42. Le T, Thanh NT, Thwaites GE. 90 - Talaromycosis (Penicilliosis). In: Ryan ET, Hill DR, Solomon T, Aronson NE, Endy TP, eds. Hunter's Tropical Medicine and Emerging Infectious Diseases (Tenth Edition). London: Content Repository Only!; 2020: 682-5.
43. Vanittanakom N, Cooper CR, Fisher MC, Sirisanthana T. Penicillium marneffei Infection and Recent Advances in the Epidemiology and Molecular Biology Aspects. *Clinical Microbiology Reviews* 2006; **19**(1): 95.
44. Le T, Wolbers M, Chi NH, et al. Epidemiology, Seasonality, and Predictors of Outcome of AIDS-Associated Penicillium marneffei Infection in Ho Chi Minh City, Viet Nam. *Clinical Infectious Diseases* 2011; **52**(7): 945-52.
45. Hu Y, Zhang J, Li X, et al. Penicillium marneffei infection: an emerging disease in mainland China. *Mycopathologia* 2013; **175**(1-2): 57-67.
46. Qiu Y, Liao H, Zhang J, Zhong X, Tan C, Lu D. Differences in clinical characteristics and prognosis of Penicilliosis among HIV-negative patients with or without underlying disease in Southern China: a retrospective study. *BMC infectious diseases* 2015; **15**(1): 525.
47. Qin Y, Huang X, Chen H, et al. Burden of Talaromyces marneffei infection in people living with HIV/AIDS in Asia during ART era: a systematic review and meta-analysis. *BMC infectious diseases* 2020; **20**(1): 551-.
48. Mwaba P, Mwansa J, Chintu C, et al. Clinical presentation, natural history, and cumulative death rates of 230 adults with primary cryptococcal meningitis in Zambian AIDS patients treated under local conditions. *Postgraduate Medical Journal* 2001; **77**(914): 769-73.

49. Limper AH, Adenis A, Le T, Harrison TS. Fungal infections in HIV/AIDS. *Lancet Infect Dis* 2017; **17**(11): e334-e43.
50. Le T, Kinh NV, Cuc NTK, et al. A Trial of Itraconazole or Amphotericin B for HIV-Associated Talaromycosis. *New England Journal of Medicine* 2017; **376**(24): 2329-40.
51. Department of Health and Human Services USA. Panel on Opportunistic Infections in Adults and Adolescents with HIV. Guidelines for the prevention and treatment of opportunistic infections in adults and adolescents with HIV: recommendations from the Centers for Disease Control and Prevention, the National Institutes of Health, and the HIV Medicine Association of the Infectious Diseases Society of America.; 2019.
52. World Health Organization. Guidelines for the diagnosis, prevention, and management of cryptococcal disease in HIV-infected adults, adolescents and children. Geneva: World Health Organization, 2018.
53. Bicanic T, Bottomley C, Loyse A, et al. Toxicity of amphotericin B deoxycholate-based induction therapy in patients with HIV-associated cryptococcal meningitis. *Antimicrobial agents and chemotherapy* 2015; **59**(12): 7224-31.
54. Laniado-Laborin R, Cabrales-Vargas MN. Amphotericin B: side effects and toxicity. *Rev Iberoam Micol* 2009; **26**(4): 223-7.
55. Deray G. Amphotericin B nephrotoxicity. *J Antimicrob Chemother* 2002; **49 Suppl 1**: 37-41.
56. Barcia JP. Hyperkalemia associated with rapid infusion of conventional and lipid complex formulations of amphotericin B. *Pharmacotherapy* 1998; **18**(4): 874-6.
57. Krishnarao TV, Galgiani JN. Comparison of the in vitro activities of the echinocandin LY303366, the pneumocandin MK-0991, and fluconazole against Candida species and Cryptococcus neoformans. *Antimicrobial Agents and Chemotherapy* 1997; **41**(9): 1957-60.
58. Abruzzo GK, Flattery AM, Gill CJ, et al. Evaluation of the echinocandin antifungal MK-0991 (L-743,872): efficacies in mouse models of disseminated aspergillosis, candidiasis, and cryptococcosis. *Antimicrobial Agents and Chemotherapy* 1997; **41**(11): 2333-8.
59. Bartizal K, Gill CJ, Abruzzo GK, et al. In vitro preclinical evaluation studies with the echinocandin antifungal MK-0991 (L-743,872). *Antimicrobial Agents and Chemotherapy* 1997; **41**(11): 2326-32.
60. Lei HL, Li LH, Chen WS, et al. Susceptibility profile of echinocandins, azoles and amphotericin B against yeast phase of Talaromyces marneffei isolated from HIV-infected patients in Guangdong, China. *European Journal of Clinical Microbiology & Infectious Diseases* 2018; **37**(6): 1099-102.
61. Kneale M, Bartholomew JS, Davies E, Denning DW. Global access to antifungal therapy and its variable cost. *Journal of Antimicrobial Chemotherapy* 2016; **71**(12): 3599-606.
62. Nussbaum JC, Jackson A, Namarika D, et al. Combination flucytosine and high-dose fluconazole compared with fluconazole monotherapy for the

treatment of cryptococcal meningitis: a randomized trial in Malawi. *Clin Infect Dis* 2010; **50**(3): 338-44.
63. Saag MS, Powderly WG, Cloud GA, et al. Comparison of amphotericin B with fluconazole in the treatment of acute AIDS-associated cryptococcal meningitis. The NIAID Mycoses Study Group and the AIDS Clinical Trials Group. *N Engl J Med* 1992; **326**(2): 83-9.
64. Mayanja-Kizza H, Oishi K, Mitarai S, et al. Combination therapy with fluconazole and flucytosine for cryptococcal meningitis in Ugandan patients with AIDS. *Clin Infect Dis* 1998; **26**(6): 1362-6.
65. Bicanic T, Meintjes G, Wood R, et al. Fungal Burden, Early Fungicidal Activity, and Outcome in Cryptococcal Meningitis in Antiretroviral-Naive or Antiretroviral-Experienced Patients Treated with Amphotericin B or Fluconazole. *Clinical Infectious Diseases* 2007; **45**(1): 76-80.
66. Hope W, Stone NRH, Johnson A, et al. Fluconazole Monotherapy Is a Suboptimal Option for Initial Treatment of Cryptococcal Meningitis Because of Emergence of Resistance. *mBio* 2019; **10**(6): e02575-19.
67. Stone NR, Rhodes J, Fisher MC, et al. Dynamic ploidy changes drive fluconazole resistance in human cryptococcal meningitis. *The Journal of clinical investigation* 2019; **129**(3).
68. Witt MD, Lewis RJ, Larsen RA, et al. Identification of patients with acute AIDS-associated cryptococcal meningitis who can be effectively treated with fluconazole: the role of antifungal susceptibility testing. *Clin Infect Dis* 1996; **22**(2): 322-8.
69. Aller A, Martin-Mazuelos E, Lozano F, et al. Correlation of fluconazole MICs with clinical outcome in cryptococcal infection. *Antimicrobial agents and chemotherapy* 2000; **44**(6): 1544-8.
70. Eliopoulos GM, Perea S, Patterson TF. Antifungal Resistance in Pathogenic Fungi. *Clinical Infectious Diseases* 2002; **35**(9): 1073-80.
71. Brandt ME, Pfaller MA, Hajjeh RA, et al. Trends in antifungal drug susceptibility of Cryptococcus neoformans isolates in the United States: 1992 to 1994 and 1996 to 1998. *Antimicrobial agents and chemotherapy* 2001; **45**(11): 3065-9.
72. Whelan WL. The genetic basis of resistance to 5-fluorocytosine in Candida species and Cryptococcus neoformans. *CRC Critical Reviews in Microbiology* 1987; **15**(1): 45-56.
73. European and Developing Countries Clinical Trials Partnership. Advances in product development for effective prevention, treatment and management of co-infections and co-morbidities – 2018. http://www.edctp.org/projects-2/edctp2-projects/advances-in-product-development-for-effective-prevention-treatment-and-management-of-co-infections-and-co-morbidities-2018/ (accessed 26 May 2020).
74. Day JN, Chau TT, Wolbers M, et al. Combination antifungal therapy for cryptococcal meningitis. *N Engl J Med* 2013; **368**(14): 1291-302.
75. Bicanic T, Wood R, Meintjes G, et al. High-dose amphotericin B with flucytosine for the treatment of cryptococcal meningitis in HIV-infected patients: a randomized trial. *Clin Infect Dis* 2008; **47**(1): 123-30.

76. Jackson AT, Nussbaum JC, Phulusa J, et al. A phase II randomized controlled trial adding oral flucytosine to high-dose fluconazole, with short-course amphotericin B, for cryptococcal meningitis. *AIDS* 2012; **26**(11): 1363-70.
77. van der Horst CM, Saag MS, Cloud GA, et al. Treatment of Cryptococcal Meningitis Associated with the Acquired Immunodeficiency Syndrome. *New England Journal of Medicine* 1997; **337**(1): 15-21.
78. Hope WW, Drusano GL. Antifungal pharmacokinetics and pharmacodynamics: bridging from the bench to bedside. *Clin Microbiol Infect* 2009; **15**(7): 602-12.
79. Stott KE, Hope WW. Therapeutic drug monitoring for invasive mould infections and disease: pharmacokinetic and pharmacodynamic considerations. *J Antimicrob Chemother* 2017; **72**(suppl_1): i12-i8.
80. Felton T, Troke PF, Hope WW. Tissue penetration of antifungal agents. *Clin Microbiol Rev* 2014; **27**(1): 68-88.
81. Stott KE, Beardsley J, Kolamunnage-Dona R, et al. Population Pharmacokinetics and Cerebrospinal Fluid Penetration of Fluconazole in Adults with Cryptococcal Meningitis. *Antimicrob Agents Chemother* 2018; **62**(9).
82. Bekersky I, Boswell GW, Hiles R, Fielding RM, Buell D, Walsh TJ. Safety, toxicokinetics and tissue distribution of long-term intravenous liposomal Amphotericin B (AmBisome®): a 91-day study in rats. *Pharmaceutical research* 2000; **17**(12): 1494-502.
83. Lestner J, McEntee L, Johnson A, et al. Experimental Models of Short Courses of Liposomal Amphotericin B for Induction Therapy for Cryptococcal Meningitis. *Antimicrob Agents Chemother* 2017.
84. Livermore J, Howard SJ, Sharp AD, et al. Efficacy of an abbreviated induction regimen of amphotericin B deoxycholate for cryptococcal meningoencephalitis: 3 days of therapy is equivalent to 14 days. *MBio* 2014; **5**(1): e00725-13.
85. Louie A, Deziel M, Liu W, Drusano MF, Gumbo T, Drusano GL. Pharmacodynamics of caspofungin in a murine model of systemic candidiasis: importance of persistence of caspofungin in tissues to understanding drug activity. *Antimicrobial Agents and Chemotherapy* 2005; **49**(12): 5058-68.
86. Pasko MT, Piscitelli SC, Van Slooten AD. Fluconazole: a new triazole antifungal agent. *Dicp* 1990; **24**(9): 860-7.
87. Troke PF, Andrews RJ, Pye GW, Richardson K. Fluconazole and Other Azoles: Translation of in Vitro Activity to in Vivo and Clinical Efficacy. *Reviews of Infectious Diseases* 1990; **12**(Supplement_3): S276-S80.
88. Gubbins PA, EJ. Antifungal therapy. In: Anaissie EM, MR; Pfaller, MA, ed. Clinical Mycology. 2nd ed: Churchill Livingstone, Elsevier; 2009: 161 - 96.
89. Kethireddy S, Andes D. CNS pharmacokinetics of antifungal agents. *Expert opinion on drug metabolism & toxicology* 2007; **3**(4): 573-81.
90. P L, U W, A S-H. Isavuconazole and Other Azoles with Respect to Physicochemical and Pharmacokinetic Properties Affecting Tissue Penetration. ECCMID. Vienna; 2017.
91. Girmenia C. New generation azole antifungals in clinical investigation. *Expert Opin Investig Drugs* 2009; **18**(9): 1279-95.

92. NationalCenterforBiotechnologyInformation. Isavuconazonium. PubChem Compound Database; CID=6918606. https://pubchem.ncbi.nlm.nih.gov/compound/6918606
93. Bekersky I, Fielding RM, Dressler DE, Lee JW, Buell DN, Walsh TJ. Plasma protein binding of amphotericin B and pharmacokinetics of bound versus unbound amphotericin B after administration of intravenous liposomal amphotericin B (AmBisome) and amphotericin B deoxycholate. *Antimicrobial Agents & Chemotherapy* 2002; **46**(3): 834-40.
94. Hartsel S, Bolard J. Amphotericin B: new life for an old drug. *Trends in Pharmacological Sciences* 1996; **17**(12): 445-9.
95. Wu JQ, Shao K, Wang X, et al. In vitro and in vivo evidence for amphotericin B as a P-glycoprotein substrate on the blood-brain barrier. *Antimicrob Agents Chemother* 2014; **58**(8): 4464-9.
96. Stevens DA, Clemons KV, Martinez M, Chen V. The Brain, Amphotericin B, and P-Glycoprotein. *Antimicrobial Agents and Chemotherapy* 2015; **59**(2): 1386.
97. Clemons KV, Espiritu M, Parmar R, Stevens DA. Comparative efficacies of conventional amphotericin b, liposomal amphotericin B (AmBisome), caspofungin, micafungin, and voriconazole alone and in combination against experimental murine central nervous system aspergillosis. *Antimicrob Agents Chemother* 2005; **49**(12): 4867-75.
98. Hospenthal DR, Rinaldi MG. Diagnosis and Treatment of Fungal Infections: Springer International Publishing; 2015.
99. Groll AH, Mickiene D, Petraitiene R, et al. Pharmacokinetic and pharmacodynamic modeling of anidulafungin (LY303366): reappraisal of its efficacy in neutropenic animal models of opportunistic mycoses using optimal plasma sampling. *Antimicrob Agents Chemother* 2001; **45**(10): 2845-55.
100. Stott KE, Hope W. Pharmacokinetics–pharmacodynamics of antifungal agents in the central nervous system. *Expert Opinion on Drug Metabolism & Toxicology* 2018; **14**(8): 803-15.
101. Hope W, Walsh T, Denning D. The invasive and saprophytic syndromes due to Aspergillus spp. *Medical mycology* 2005; **43**(Supplement_1): S207-S38.
102. Kosmidis C, Denning DW. The clinical spectrum of pulmonary aspergillosis. *Thorax* 2015; **70**(3): 270.
103. Lagunes L, Rello J. Invasive candidiasis: from mycobiome to infection, therapy, and prevention. *European Journal of Clinical Microbiology & Infectious Diseases* 2016; **35**(8): 1221-6.
104. Klock C, Cerski M, Goldani LZ. Histopathological aspects of neurocryptococcosis in HIV-infected patients: autopsy report of 45 patients. *Int J Surg Pathol* 2009; **17**(6): 444-8.
105. Lanjewar DN, Jain PP, Shetty CR. Profile of central nervous system pathology in patients with AIDS: an autopsy study from India. *AIDS* 1998; **12**(3): 309-13.
106. Lee SC, Dickson DW, Casadevall A. Pathology of cryptococcal meningoencephalitis: analysis of 27 patients with pathogenetic implications. *Hum Pathol* 1996; **27**(8): 839-47.

107. McMullan BJ, Sorrell TC, Chen SC-A. Cryptococcus gattii infections: contemporary aspects of epidemiology, clinical manifestations and management of infection. *Future microbiology* 2013; **8**(12): 1613-31.
108. Hahn J, Choi J, Chang M. Pharmacokinetic changes of antibiotic, antiviral, antituberculosis and antifungal agents during extracorporeal membrane oxygenation in critically ill adult patients. *Journal of Clinical Pharmacy and Therapeutics* 2017; **42**(6): 661-71.
109. Kuti EL, Kuti JL. Pharmacokinetics, antifungal activity and clinical efficacy of anidulafungin in the treatment of fungal infections. *Expert opinion on drug metabolism & toxicology* 2010; **6**(10): 1287-300.
110. Sime FB, Stuart J, Butler J, et al. Pharmacokinetics of intravenous posaconazole in critically ill patients. *Antimicrobial agents and chemotherapy* 2018; **62**(6).
111. Sinnollareddy M, Peake SL, Roberts MS, Lipman J, Roberts JA. Using pharmacokinetics and pharmacodynamics to optimise dosing of antifungal agents in critically ill patients: a systematic review. *International journal of antimicrobial agents* 2012; **39**(1): 1-10.
112. Spriet I, Annaert P, Meersseman P, et al. Pharmacokinetics of caspofungin and voriconazole in critically ill patients during extracorporeal membrane oxygenation. *Journal of antimicrobial chemotherapy* 2009; **63**(4): 767-70.
113. Yagasaki K, Gando S, Matsuda N, et al. Pharmacokinetics and the most suitable dosing regimen of fluconazole in critically ill patients receiving continuous hemodiafiltration. *Intensive care medicine* 2003; **29**(10): 1844-8.
114. Muilwijk EW, de Lange DW, Schouten JA, et al. Suboptimal dosing of fluconazole in critically ill patients – time to rethink dosing. *Antimicrobial Agents and Chemotherapy* 2020: AAC.00984-20.
115. Kovanda LL, Desai AV, Lu Q, et al. Isavuconazole Population Pharmacokinetic Analysis Using Nonparametric Estimation in Patients with Invasive Fungal Disease (Results from the VITAL Study). *Antimicrobial Agents and Chemotherapy* 2016; **60**(8): 4568.
116. Mainas E, Apostolopoulou O, Siopi M, et al. Comparative pharmacokinetics of the three echinocandins in ICU patients. *Journal of Antimicrobial Chemotherapy* 2020.
117. Undre N, Stevenson P, Baraldi E. Pharmacokinetics of micafungin in HIV positive patients with confirmed esophageal candidiasis. *European journal of drug metabolism and pharmacokinetics* 2012; **37**(1): 31-8.
118. Liu P, Ruhnke M, Meersseman W, Paiva JA, Kantecki M, Damle B. Pharmacokinetics of anidulafungin in critically ill patients with candidemia/invasive candidiasis. *Antimicrobial agents and chemotherapy* 2013; **57**(4): 1672-6.
119. Bekersky I, Fielding RM, Dressler DE, Lee JW, Buell DN, Walsh TJ. Pharmacokinetics, Excretion, and Mass Balance of Liposomal Amphotericin B (AmBisome) and Amphotericin B Deoxycholate in Humans. *Antimicrobial Agents and Chemotherapy* 2002; **46**(3): 828-33.

120. Stott KE, Beardsley J, Whalley S, et al. Amphotericin B Deoxycholate in adults with Cryptococcal Meningitis; a Population Pharmacokinetic Model and Meta-Analysis of Outcomes. *Antimicrob Agents Chemother* 2018.
121. Roberts JA, Taccone FS, Lipman J. Understanding PK/PD. *Intensive Care Med* 2016; **42**(11): 1797-800.
122. Purkins L, Wood N, Kleinermans D, Greenhalgh K, Nichols D. Effect of food on the pharmacokinetics of multiple-dose oral voriconazole. *British journal of clinical pharmacology* 2003; **56**: 17-23.
123. Van de Velde VJ, Van Peer AP, Heykants JJ, et al. Effect of food on the pharmacokinetics of a new hydroxypropyl-beta-cyclodextrin formulation of itraconazole. *Pharmacotherapy* 1996; **16**(3): 424-8.
124. Barone JA, Koh JG, Bierman RH, et al. Food interaction and steady-state pharmacokinetics of itraconazole capsules in healthy male volunteers. *Antimicrob Agents Chemother* 1993; **37**(4): 778-84.
125. Antinori S, Galimberti L, Magni C, et al. Cryptococcus neoformans infection in a cohort of Italian AIDS patients: natural history, early prognostic parameters, and autopsy findings. *European Journal of Clinical Microbiology & Infectious Diseases* 2001; **20**(10): 711-7.
126. Coelho C, Bocca AL, Casadevall A. The intracellular life of Cryptococcus neoformans. *Annu Rev Pathol* 2014; **9**: 219-38.
127. Esher SK, Zaragoza O, Alspaugh JA. Cryptococcal pathogenic mechanisms: a dangerous trip from the environment to the brain. *Mem Inst Oswaldo Cruz* 2018; **113**(7): e180057.
128. Giles SS, Dagenais TR, Botts MR, Keller NP, Hull CM. Elucidating the pathogenesis of spores from the human fungal pathogen Cryptococcus neoformans. *Infect Immun* 2009; **77**(8): 3491-500.
129. Feldmesser M, Kress Y, Novikoff P, Casadevall A. Cryptococcus neoformans is a facultative intracellular pathogen in murine pulmonary infection. *Infect Immun* 2000; **68**.
130. Levitz SM, Nong SH, Seetoo KF, Harrison TS, Speizer RA, Simons ER. Cryptococcus neoformans resides in an acidic phagolysosome of human macrophages. *Infect Immun* 1999; **67**.
131. Artavanis-Tsakonas K, Love JC, Ploegh HL, Vyas JM. Recruitment of CD63 to Cryptococcus neoformans phagosomes requires acidification. *Proc Natl Acad Sci U S A* 2006; **103**(43): 15945-50.
132. Garelnabi M, May RC. Variability in innate host immune responses to cryptococcosis. *Mem Inst Oswaldo Cruz* 2018; **113**(7): e180060.
133. Vecchiarelli A, Dottorini M, Pietrella D, et al. Role of human alveolar macrophages as antigen-presenting cells in Cryptococcus neoformans infection. *Am J Respir Cell Mol Biol* 1994; **11**(2): 130-7.
134. Zaragoza O, Chrisman CJ, Castelli MV, et al. Capsule enlargement in Cryptococcus neoformans confers resistance to oxidative stress suggesting a mechanism for intracellular survival. *Cell Microbiol* 2008; **10**(10): 2043-57.
135. Tucker SC, Casadevall A. Replication of Cryptococcus neoformans in macrophages is accompanied by phagosomal permeabilization and accumulation

of vesicles containing polysaccharide in the cytoplasm. *Proc Natl Acad Sci USA* 2002; **99**.
136. Smith LM, Dixon EF, May RC. The fungal pathogen Cryptococcus neoformans manipulates macrophage phagosome maturation. *Cell Microbiol* 2015; **17**(5): 702-13.
137. Fu MS, Coelho C, De Leon-Rodriguez CM, et al. Cryptococcus neoformans urease affects the outcome of intracellular pathogenesis by modulating phagolysosomal pH. *PLoS Pathogens* 2018; **14**(6): e1007144.
138. Kudeken N, Kawakami K, Saito A. Role of superoxide anion in the fungicidal activity of murine peritoneal exudate macrophages against Penicillium marneffei. *Microbiology and immunology* 1999; **43**(4): 323-30.
139. Woo PC, Lau SK, Lau CC, et al. Mp1p is a virulence factor in Talaromyces (Penicillium) marneffei. *PLoS neglected tropical diseases* 2016; **10**(8): e0004907.
140. Rudman J, Evans RJ, Andrew Johnston S. Are Macrophages the Heroes or Villains During Cryptococcosis? *Fungal Genetics and Biology* 2019: 103261.
141. Bojarczuk A, Miller KA, Hotham R, et al. Cryptococcus neoformans Intracellular Proliferation and Capsule Size Determines Early Macrophage Control of Infection. *Sci Rep* 2016; **6**: 21489.
142. Zaragoza O. Basic principles of the virulence of Cryptococcus. *Virulence* 2019; **10**(1): 490-501.
143. Shao X, Mednick A, Alvarez M, van Rooijen N, Casadevall A, Goldman DL. An innate immune system cell is a major determinant of species-related susceptibility differences to fungal pneumonia. *J Immunol* 2005; **175**.
144. Chen GH, Olszewski MA, McDonald RA, et al. Role of granulocyte macrophage colony-stimulating factor in host defense against pulmonary Cryptococcus neoformans infection during murine allergic bronchopulmonary mycosis. *Am J Pathol* 2007; **170**(3): 1028-40.
145. Osterholzer JJ, Chen G-H, Olszewski MA, et al. Chemokine Receptor 2-Mediated Accumulation of Fungicidal Exudate Macrophages in Mice That Clear Cryptococcal Lung Infection. *The American Journal of Pathology* 2011; **178**(1): 198-211.
146. Osterholzer JJ, Milam JE, Chen GH, Toews GB, Huffnagle GB, Olszewski MA. Role of dendritic cells and alveolar macrophages in regulating early host defense against pulmonary infection with Cryptococcus neoformans. *Infect Immun* 2009; **77**(9): 3749-58.
147. McClelland EE, Bernhardt P, Casadevall A. Estimating the relative contributions of virulence factors for pathogenic microbes. *Infect Immun* 2006; **74**(3): 1500-4.
148. Chang YC, Kwon-Chung KJ. Complementation of a capsule-deficient mutation of Cryptococcus neoformans restores its virulence. *Mol Cell Biol* 1994; **14**(7): 4912-9.
149. Kawakami K, Kohno S, Kadota J, et al. T cell-dependent activation of macrophages and enhancement of their phagocytic activity in the lungs of mice inoculated with heat-killed Cryptococcus neoformans: involvement of IFN-gamma and its protective effect against cryptococcal infection. *Microbiol Immunol* 1995; **39**(2): 135-43.

150. Muller U, Stenzel W, Kohler G, et al. IL-13 induces disease-promoting type 2 cytokines, alternatively activated macrophages and allergic inflammation during pulmonary infection of mice with Cryptococcus neoformans. *J Immunol* 2007; **179**(8): 5367-77.
151. Stenzel W, Muller U, Kohler G, et al. IL-4/IL-13-dependent alternative activation of macrophages but not microglial cells is associated with uncontrolled cerebral cryptococcosis. *Am J Pathol* 2009; **174**(2): 486-96.
152. Jarvis JN, Meintjes G, Bicanic T, et al. Cerebrospinal fluid cytokine profiles predict risk of early mortality and immune reconstitution inflammatory syndrome in HIV-associated cryptococcal meningitis. *PLoS Pathogens* 2015; **11**(4): e1004754.
153. Scriven JE, Graham LM, Schutz C, et al. A Glucuronoxylomannan-Associated Immune Signature, Characterized by Monocyte Deactivation and an Increased Interleukin 10 Level, Is a Predictor of Death in Cryptococcal Meningitis. *J Infect Dis* 2016; **213**(11): 1725-34.
154. Scriven JE, Graham LM, Schutz C, et al. The CSF Immune Response in HIV-1-Associated Cryptococcal Meningitis: Macrophage Activation, Correlates of Disease Severity, and Effect of Antiretroviral Therapy. *J Acquir Immune Defic Syndr* 2017; **75**(3): 299-307.
155. Siddiqui AA, Brouwer AE, Wuthiekanun V, et al. IFN-gamma at the site of infection determines rate of clearance of infection in cryptococcal meningitis. *J Immunol* 2005; **174**(3): 1746-50.
156. Casadevall A. Amoeba provide insight into the origin of virulence in pathogenic fungi. *Adv Exp Med Biol* 2012; **710**: 1-10.
157. Diamond RD, Bennett JE. Growth of Cryptococcus neoformans within human macrophages in vitro. *Infect Immun* 1973; **7**.
158. Charlier C, Nielsen K, Daou S, Brigitte M, Chretien F, Dromer F. Evidence of a role for monocytes in dissemination and brain invasion by Cryptococcus neoformans. *Infect Immun* 2009; **77**(1): 120-7.
159. Ma H, Croudace JE, Lammas DA, May RC. Direct cell-to-cell spread of a pathogenic yeast. *BMC Immunol* 2007; **8**.
160. Alvarez M, Casadevall A. Cell-to-cell spread and massive vacuole formation after Cryptococcus neoformans infection of murine macrophages. *BMC Immunol* 2007; **8**.
161. Leopold Wager CM, Wormley FL, Jr. Is Development of a Vaccine against Cryptococcus neoformans Feasible? *PLOS Pathogens* 2015; **11**(6): e1004843.
162. Mukaremera L, Nielsen K. Adaptive Immunity to Cryptococcus neoformans Infections. *J Fungi (Basel)* 2017; **3**(4).
163. Lindell DM, Ballinger MN, McDonald RA, Toews GB, Huffnagle GB. Diversity of the T-cell response to pulmonary Cryptococcus neoformans infection. *Infect Immun* 2006; **74**(8): 4538-48.
164. Ho EL, Ronquillo R, Altmeppen H, Spudich SS, Price RW, Sinclair E. Cellular Composition of Cerebrospinal Fluid in HIV-1 Infected and Uninfected Subjects. *PLoS One* 2013; **8**(6): e66188.

165. Meya DB, Okurut S, Zziwa G, et al. Cellular immune activation in cerebrospinal fluid from ugandans with cryptococcal meningitis and immune reconstitution inflammatory syndrome. *J Infect Dis* 2015; **211**(10): 1597-606.
166. Uicker WC, McCracken JP, Buchanan KL. Role of CD4+ T cells in a protective immune response against Cryptococcus neoformans in the central nervous system. *Med Mycol* 2006; **44**(1): 1-11.
167. Buchanan KL, Doyle HA. Requirement for CD4(+) T lymphocytes in host resistance against Cryptococcus neoformans in the central nervous system of immunized mice. *Infection & Immunity* 2000; **68**(2): 456-62.
168. Wormley FL, Jr., Perfect JR, Steele C, Cox GM. Protection against cryptococcosis by using a murine gamma interferon-producing Cryptococcus neoformans strain. *Infect Immun* 2007; **75**(3): 1453-62.
169. Ballou ER, Johnston SA. The cause and effect of Cryptococcus interactions with the host. *Curr Opin Microbiol* 2017; **40**: 88-94.
170. Decken K, Kohler G, Palmer-Lehmann K, et al. Interleukin-12 is essential for a protective Th1 response in mice infected with Cryptococcus neoformans. *Infect Immun* 1998; **66**(10): 4994-5000.
171. Kawakami K, Koguchi Y, Qureshi MH, et al. Reduced host resistance and Th1 response to Cryptococcus neoformans in interleukin-18 deficient mice. *FEMS Microbiol Lett* 2000; **186**(1): 121-6.
172. Hoag KA, Lipscomb MF, Izzo AA, Street NE. IL-12 and IFN-gamma are required for initiating the protective Th1 response to pulmonary cryptococcosis in resistant C.B-17 mice. *Am J Respir Cell Mol Biol* 1997; **17**(6): 733-9.
173. Kawakami K, Qifeng X, Tohyama M, Qureshi MH, Saito A. Contribution of tumour necrosis factor-alpha (TNF-alpha) in host defence mechanism against Cryptococcus neoformans. *Clin Exp Immunol* 1996; **106**(3): 468-74.
174. Jarvis JN, Meintjes G, Rebe K, et al. Adjunctive interferon-gamma immunotherapy for the treatment of HIV-associated cryptococcal meningitis: a randomized controlled trial. *Aids* 2012; **26**(9): 1105-13.
175. Jarvis JN, Meintjes G, Bicanic T, et al. Cerebrospinal fluid cytokine profiles predict risk of early mortality and immune reconstitution inflammatory syndrome in HIV-associated cryptococcal meningitis. *PLoS Pathog* 2015; **11**(4): e1004754.
176. Koguchi Y, Kawakami K. Cryptococcal infection and Th1-Th2 cytokine balance. *Int Rev Immunol* 2002; **21**(4-5): 423-38.
177. Shibuya K, Hirata A, Omuta J, et al. Granuloma and cryptococcosis. *Journal of Infection and Chemotherapy* 2005; **11**(3): 115-22.
178. Hardison SE, Ravi S, Wozniak KL, Young ML, Olszewski MA, Wormley FL. Pulmonary Infection with an Interferon-γ-Producing Cryptococcus neoformans Strain Results in Classical Macrophage Activation and Protection. *The American Journal of Pathology* 2010; **176**(2): 774-85.
179. Hardison SE, Herrera G, Young ML, Hole CR, Wozniak KL, Wormley FL. Protective Immunity against Pulmonary Cryptococcosis Is Associated with STAT1-Mediated Classical Macrophage Activation. *The Journal of Immunology Author Choice* 2012; **189**(8): 4060-8.

180. Pappas PG, Bustamante B, Ticona E, et al. Recombinant interferon-gamma 1b as adjunctive therapy for AIDS-related acute cryptococcal meningitis. *J Infect Dis* 2004; **189**(12): 2185-91.
181. Jarvis JN, Casazza JP, Stone HH, et al. The phenotype of the Cryptococcus-specific CD4+ memory T-cell response is associated with disease severity and outcome in HIV-associated cryptococcal meningitis. *J Infect Dis* 2013; **207**(12): 1817-28.
182. Larsen RA, Pappas PG, Perfect J, et al. Phase I evaluation of the safety and pharmacokinetics of murine-derived anticryptococcal antibody 18B7 in subjects with treated cryptococcal meningitis. *Antimicrob Agents Chemother* 2005; **49**(3): 952-8.
183. Beardsley J, Wolbers M, Kibengo FM, et al. Adjunctive Dexamethasone in HIV-Associated Cryptococcal Meningitis. *N Engl J Med* 2016; **374**(6): 542-54.
184. Beardsley J, Hoang NLT, Kibengo FM, et al. Do intra-cerebral cytokine responses explain the harmful effects of dexamethasone in HIV-associated cryptococcal meningitis? *Clinical Infectious Diseases* 2018: ciy725-ciy.
185. Desjardins CA, Giamberardino C, Sykes SM, et al. Population genomics and the evolution of virulence in the fungal pathogen Cryptococcus neoformans. *Genome Research* 2017; **27**(7): 1207-19.
186. Boekhout T, Theelen B, Diaz M, et al. Hybrid genotypes in the pathogenic yeast Cryptococcus neoformans. *Microbiology* 2001; **147**(Pt 4): 891-907.
187. Meyer W, Castañeda A, Jackson S, et al. Molecular typing of IberoAmerican Cryptococcus neoformans isolates. *Emerging Infectious Diseases* 2003; **9**(2): 189-95.
188. Latouche GN, Huynh M, Sorrell TC, Meyer W. PCR-restriction fragment length polymorphism analysis of the phospholipase B (PLB1) gene for subtyping of Cryptococcus neoformans isolates. *Appl Environ Microbiol* 2003; **69**(4): 2080-6.
189. Wiesner DL, Moskalenko O, Corcoran JM, et al. Cryptococcal genotype influences immunologic response and human clinical outcome after meningitis. *MBio* 2012; **3**(5).
190. Day JN, Qihui S, Thanh LT, et al. Comparative genomics of Cryptococcus neoformans var. grubii associated with meningitis in HIV infected and uninfected patients in Vietnam. *PLoS Negl Trop Dis* 2017; **11**(6): e0005628.
191. Day JN, Hoang TN, Duong AV, et al. Most cases of cryptococcal meningitis in HIV-uninfected patients in Vietnam are due to a distinct amplified fragment length polymorphism-defined cluster of Cryptococcus neoformans var. grubii VN1. *J Clin Microbiol* 2011; **49**(2): 658-64.
192. Carter DA, Fernandes KE, Brockway A, et al. Phenotypic variability correlates with clinical outcome in Cryptococcus isolates obtained from Botswanan HIV/AIDS patients. *bioRxiv* 2018.
193. Ashton PM, Thanh LT, Trieu PH, et al. Three phylogenetic groups have driven the recent population expansion of Cryptococcus neoformans. *Nat Commun* 2019; **10**(1): 2035.
194. Haynes KA, Sullivan DJ, Coleman DC, et al. Involvement of multiple Cryptococcus neoformans strains in a single episode of cryptococcosis and

reinfection with novel strains in recurrent infection demonstrated by random amplification of polymorphic DNA and DNA fingerprinting. *J Clin Microbiol* 1995; **33**(1): 99-102.
195. Igreja RP, Lazéra MoS, Wanke B, Galhardo MC, Kidd SE, Meyer W. Molecular epidemiology of Cryptococcus neoformans isolates from AIDS patients of the Brazilian city, Rio de Janeiro. *Med Mycol* 2004; **42**(3): 229-38.
196. Jain N, Wickes BL, Keller SM, et al. Molecular epidemiology of clinical Cryptococcus neoformans strains from India. *J Clin Microbiol* 2005; **43**(11): 5733-42.
197. Litvintseva AP, Kestenbaum L, Vilgalys R, Mitchell TG. Comparative analysis of environmental and clinical populations of Cryptococcus neoformans. *J Clin Microbiol* 2005; **43**(2): 556-64.
198. Avery SV. Microbial cell individuality and the underlying sources of heterogeneity. *Nature Reviews Microbiology* 2006; **4**: 577.
199. Halliwell SC, Smith MCA, Muston P, Holland SL, Avery SV. Heterogeneous Expression of the Virulence-Related Adhesin Epa1 between Individual Cells and Strains of the Pathogen Candida glabrata. *Eukaryotic Cell* 2012; **11**(2): 141.
200. Aldridge BB, Fernandez-Suarez M, Heller D, et al. Asymmetry and aging of mycobacterial cells lead to variable growth and antibiotic susceptibility. *Science* 2012; **335**(6064): 100-4.
201. Zhang Y, Yew WW, Barer MR. Targeting persisters for tuberculosis control. *Antimicrob Agents Chemother* 2012; **56**(5): 2223-30.
202. Keren I, Minami S, Rubin E, Lewis K. Characterization and transcriptome analysis of Mycobacterium tuberculosis persisters. *MBio* 2011; **2**(3): e00100-11.
203. Helaine S, Cheverton AM, Watson KG, Faure LM, Matthews SA, Holden DW. Internalization of Salmonella by macrophages induces formation of nonreplicating persisters. *Science* 2014; **343**(6167): 204-8.
204. Correia FF, D'Onofrio A, Rejtar T, et al. Kinase activity of overexpressed HipA is required for growth arrest and multidrug tolerance in Escherichia coli. *J Bacteriol* 2006; **188**(24): 8360-7.
205. Keren I, Kaldalu N, Spoering A, Wang Y, Lewis K. Persister cells and tolerance to antimicrobials. *FEMS Microbiol Lett* 2004; **230**(1): 13-8.
206. Li Z, Nielsen K. Morphology Changes in Human Fungal Pathogens upon Interaction with the Host. *Journal of Fungi* 2017; **3**(4): 66.
207. Boyce KJ, Andrianopoulos A. Fungal dimorphism: the switch from hyphae to yeast is a specialized morphogenetic adaptation allowing colonization of a host. *FEMS Microbiol Rev* 2015; **39**(6): 797-811.
208. Noble SM, Gianetti BA, Witchley JN. Candida albicans cell-type switching and functional plasticity in the mammalian host. *Nat Rev Microbiol* 2017; **15**(2): 96-108.
209. Bose I, Reese AJ, Ory JJ, Janbon G, Doering TL. A Yeast under Cover: the Capsule of Cryptococcus neoformans. *Eukaryotic Cell* 2003; **2**(4): 655-63.
210. Steenbergen JN, Shuman HA, Casadevall A. Cryptococcus neoformans interactions with amoebae suggest an explanation for its virulence and intracellular pathogenic strategy in macrophages. *Proc Natl Acad Sci U S A* 2001; **98**(26): 15245-50.

211. Villena SN, Pinheiro RO, Pinheiro CS, et al. Capsular polysaccharides galactoxylomannan and glucuronoxylomannan from Cryptococcus neoformans induce macrophage apoptosis mediated by Fas ligand. *Cell Microbiol* 2008; **10**(6): 1274-85.
212. Vecchiarelli A, Retini C, Pietrella D, et al. Downregulation by cryptococcal polysaccharide of tumor necrosis factor alpha and interleukin-1 beta secretion from human monocytes. *Infect Immun* 1995; **63**(8): 2919-23.
213. Walenkamp AM, Chaka WS, Verheul AF, et al. Cryptococcus neoformans and its cell wall components induce similar cytokine profiles in human peripheral blood mononuclear cells despite differences in structure. *FEMS Immunol Med Microbiol* 1999; **26**(3-4): 309-18.
214. Vecchiarelli A, Retini C, Monari C, Tascini C, Bistoni F, Kozel TR. Purified capsular polysaccharide of Cryptococcus neoformans induces interleukin-10 secretion by human monocytes. *Infect Immun* 1996; **64**.
215. Almeida GM, Andrade RM, Bento CA. The capsular polysaccharides of Cryptococcus neoformans activate normal CD4(+) T cells in a dominant Th2 pattern. *J Immunol* 2001; **167**(10): 5845-51.
216. Barbosa FM, Fonseca FL, Holandino C, Alviano CS, Nimrichter L, Rodrigues ML. Glucuronoxylomannan-mediated interaction of Cryptococcus neoformans with human alveolar cells results in fungal internalization and host cell damage. *Microbes Infect* 2006; **8**(2): 493-502.
217. Vecchiarelli A, Monari C. Capsular Material of Cryptococcus neoformans: Virulence and Much More. *Mycopathologia* 2012; **173**(5): 375-86.
218. Wang Y, Aisen P, Casadevall A. Cryptococcus neoformans melanin and virulence: mechanism of action. *Infect Immun* 1995; **63**(8): 3131-6.
219. Mednick AJ, Nosanchuk JD, Casadevall A. Melanization of Cryptococcus neoformans affects lung inflammatory responses during cryptococcal infection. *Infect Immun* 2005; **73**(4): 2012-9.
220. Jacobson ES, Tinnell SB. Antioxidant function of fungal melanin. *Journal of Bacteriology* 1993; **175**(21): 7102-4.
221. Wang Y, Casadevall A. Susceptibility of melanized and nonmelanized Cryptococcus neoformans to nitrogen- and oxygen-derived oxidants. *Infection and Immunity* 1994; **62**(7): 3004-7.
222. Wang Y, Casadevall A. Growth of Cryptococcus neoformans in presence of L-dopa decreases its susceptibility to amphotericin B. *Antimicrob Agents Chemother* 1994; **38**(11): 2648-50.
223. van Duin D, Casadevall A, Nosanchuk JD. Melanization of Cryptococcus neoformans and Histoplasma capsulatum reduces their susceptibilities to amphotericin B and caspofungin. *Antimicrob Agents Chemother* 2002; **46**(11): 3394-400.
224. Doering TL, Nosanchuk JD, Roberts WK, Casadevall A. Melanin as a potential cryptococcal defence against microbicidal proteins. *Med Mycol* 1999; **37**(3): 175-81.
225. Rodrigues ML, Nakayasu ES, Oliveira DL, et al. Extracellular vesicles produced by Cryptococcus neoformans contain protein components associated with virulence. *Eukaryotic cell* 2008; **7**(1): 58-67.

226. Oliveira DL, Nimrichter L, Miranda K, et al. Cryptococcus neoformans cryoultramicrotomy and vesicle fractionation reveals an intimate association between membrane lipids and glucuronoxylomannan. *Fungal Genetics and Biology* 2009; **46**(12): 956-63.
227. De Jesus M, Nicola AM, Rodrigues ML, Janbon G, Casadevall A. Capsular localization of the Cryptococcus neoformans polysaccharide component galactoxylomannan. *Eukaryotic cell* 2009; **8**(1): 96-103.
228. Rodrigues ML, Nimrichter L, Oliveira DL, et al. Vesicular polysaccharide export in Cryptococcus neoformans is a eukaryotic solution to the problem of fungal trans-cell wall transport. *Eukaryot Cell* 2007; **6**(1): 48-59.
229. Eisenman HC, Frases S, Nicola AM, Rodrigues ML, Casadevall A. Vesicle-associated melanization in Cryptococcus neoformans. *Microbiology* 2009; **155**(12): 3860-7.
230. Osterholzer JJ, Surana R, Milam JE, et al. Cryptococcal urease promotes the accumulation of immature dendritic cells and a non-protective T2 immune response within the lung. *Am J Pathol* 2009; **174**(3): 932-43.
231. Alanio A, Vernel-Pauillac F, Sturny-Leclere A, Dromer F. Cryptococcus neoformans host adaptation: toward biological evidence of dormancy. *MBio* 2015; **6**(2).
232. Olszewski MA, Noverr MC, Chen G-H, et al. Urease expression by Cryptococcus neoformans promotes microvascular sequestration, thereby enhancing central nervous system invasion. *The American journal of pathology* 2004; **164**(5): 1761-71.
233. Shi M, Li SS, Zheng C, et al. Real-time imaging of trapping and urease-dependent transmigration of Cryptococcus neoformans in mouse brain. *J Clin Invest* 2010; **120**(5): 1683-93.
234. Perfect JR. Cryptococcus neoformans: the yeast that likes it hot. *FEMS Yeast Res* 2006; **6**(4): 463-8.
235. Zaragoza O, Nielsen K. Titan cells in Cryptococcus neoformans: Cells with a giant impact. *Current opinion in microbiology* 2013; **16**(4): 409-13.
236. Okagaki LH, Strain AK, Nielsen JN, et al. Cryptococcal Cell Morphology Affects Host Cell Interactions and Pathogenicity. *PLoS Pathogens* 2010; **6**(6): e1000953.
237. Dambuza IM, Drake T, Chapuis A, et al. The Cryptococcus neoformans Titan cell is an inducible and regulated morphotype underlying pathogenesis. *PLoS Pathog* 2018; **14**(5): e1006978.
238. Gerstein AC, Fu MS, Mukaremera L, et al. Polyploid titan cells produce haploid and aneuploid progeny to promote stress adaptation. *MBio* 2015; **6**(5): e01340-15.
239. Crabtree JN, Okagaki LH, Wiesner DL, Strain AK, Nielsen JN, Nielsen K. Titan cell production enhances the virulence of Cryptococcus neoformans. *Infect Immun* 2012; **80**(11): 3776-85.
240. Cantón E, Pemán J, Gobernado M, Viudes A, Espinel-Ingroff A. Patterns of amphotericin B killing kinetics against seven Candida species. *Antimicrobial agents and chemotherapy* 2004; **48**(7): 2477-82.

241. Ralph ED, Khazindar AM, Barber KR, Grant CW. Comparative in vitro effects of liposomal amphotericin B, amphotericin B-deoxycholate, and free amphotericin B against fungal strains determined by using MIC and minimal lethal concentration susceptibility studies and time-kill curves. *Antimicrobial Agents and Chemotherapy* 1991; **35**(1): 188.
242. Klepser ME, Ernst EJ, Lewis RE, Ernst ME, Pfaller MA. Influence of test conditions on antifungal time-kill curve results: proposal for standardized methods. *Antimicrobial agents and chemotherapy* 1998; **42**(5): 1207-12.
243. Keele DJ, DeLallo VC, Lewis RE, Ernst EJ, Klepser ME. Evaluation of amphotericin B and flucytosine in combination against Candida albicans and Cryptococcus neoformans using time-kill methodology. *Diagnostic Microbiology and Infectious Disease* 2001; **41**(3): 121-6.
244. Lewis RE, Klepser ME, Pfaller MA. In vitro pharmacodynamic characteristics of flucytosine determined by time-kill methods. *Diagn Microbiol Infect Dis* 2000; **36**(2): 101-5.
245. Burgess DS, Hastings RW. A comparison of dynamic characteristics of fluconazole, itraconazole, and amphotericin B against Cryptococcus neoformans using time-kill methodology. *Diagn Microbiol Infect Dis* 2000; **38**(2): 87-93.
246. Öz Y, Özdemir HG, Gökbolat E, Kiraz N, Ilkit M, Seyedmousavi S. Time-Kill Kinetics and In Vitro Antifungal Susceptibility of Non-fumigatus Aspergillus Species Isolated from Patients with Ocular Mycoses. *Mycopathologia* 2016; **181**(3-4): 225-33.
247. Mukaremera L, McDonald TR, Nielsen JN, et al. The Mouse Inhalation Model of Cryptococcus neoformans Infection Recapitulates Strain Virulence in Humans and Shows that Closely Related Strains Can Possess Differential Virulence. *Infection and Immunity* 2019; **87**(5): e00046-19.
248. Sudan A, Livermore J, Howard SJ, et al. Pharmacokinetics and pharmacodynamics of fluconazole for cryptococcal meningoencephalitis: implications for antifungal therapy and in vitro susceptibility breakpoints. *Antimicrob Agents Chemother* 2013; **57**(6): 2793-800.
249. O'Connor L, Livermore J, Sharp AD, et al. Pharmacodynamics of liposomal amphotericin B and flucytosine for cryptococcal meningoencephalitis: safe and effective regimens for immunocompromised patients. *J Infect Dis* 2013; **208**(2): 351-61.
250. Perfect JR, Lang S, Durack DT. Chronic cryptococcal meningitis: a new experimental model in rabbits. *The American journal of pathology* 1980; **101**(1): 177.
251. Rodriguez-Tudela J, Arendrup M, Barchiesi F, et al. EUCAST Definitive Document EDef 7.1: method for the determination of broth dilution MICs of antifungal agents for fermentative yeasts: Subcommittee on Antifungal Susceptibility Testing (AFST) of the ESCMID European Committee for Antimicrobial Susceptibility Testing (EUCAST)∗. *Clinical Microbiology and Infection* 2008; **14**(4): 398-405.
252. Lockhart SR, Ghannoum MA, Alexander BD. Establishment and Use of Epidemiological Cutoff Values for Molds and Yeasts by Use of the Clinical and

Laboratory Standards Institute M57 Standard. *Journal of Clinical Microbiology* 2017; **55**(5): 1262.
253. Pfaller MA, Diekema DJ, Ghannoum MA, et al. Wild-Type MIC Distribution and Epidemiological Cutoff Values for Aspergillus fumigatus and Three Triazoles as Determined by the Clinical and Laboratory Standards Institute Broth Microdilution Methods. *Journal of Clinical Microbiology* 2009; **47**(10): 3142.
254. Pfaller MA, Espinel-Ingroff A, Canton E, et al. Wild-type MIC distributions and epidemiological cutoff values for amphotericin B, flucytosine, and itraconazole and Candida spp. as determined by CLSI broth microdilution. *J Clin Microbiol* 2012; **50**(6): 2040-6.
255. Mouton JW, Meletiadis J, Voss A, Turnidge J. Variation of MIC measurements: the contribution of strain and laboratory variability to measurement precision. *Journal of Antimicrobial Chemotherapy* 2018; **73**(9): 2374-9.
256. Espinel-Ingroff A, Pfaller M, Erwin ME, Jones RN. Interlaboratory evaluation of Etest method for testing antifungal susceptibilities of pathogenic yeasts to five antifungal agents by using Casitone agar and solidified RPMI 1640 medium with 2% glucose. *Journal of Clinical Microbiology* 1996; **34**(4): 848.
257. Espinel-Ingroff A, Arendrup MC, Pfaller MA, et al. Interlaboratory variability of caspofungin MICs for Candida spp. using CLSI and EUCAST methods: should the clinical laboratory be testing this agent? *Antimicrobial Agents and Chemotherapy* 2013; **57**(12): 5836.
258. Blanco M, Pérez-Giraldo C, Blanco J, Morán F, Hurtado C, Gómez-García A. In vitro studies of activities of some antifungal agents against Candida albicans ATCC 10231 by the turbidimetric method. *Antimicrobial agents and chemotherapy* 1992; **36**(4): 898-901.
259. Del Poeta M, Barchiesi F, Arzeni D, Marinucci G, Scalise G. Turbidimetric and visual criteria for in vitro susceptibility testing of Cryptococcus neoformans clinical isolates: Turbidimetrische und visuelle Kriterien für einen In vitro-Empfindlichkeitstest für klinische Isolate von Cryptococcus neoformans. *Mycoses* 1994; **37**(11-12): 411-6.
260. Pfaller MA, Messer SA, Mills K, Bolmström A. In vitro susceptibility testing of filamentous fungi: comparison of Etest and reference microdilution methods for determining itraconazole MICs. *Journal of clinical microbiology* 2000; **38**(9): 3359-61.
261. Vinks AA, Derendorf H, Mouton JW. Fundamentals of antimicrobial pharmacokinetics and pharmacodynamics: Springer; 2014.
262. Beardsley J, Wolbers M, Kibengo FM, et al. Adjunctive Dexamethasone in HIV-Associated Cryptococcal Meningitis. *New England Journal of Medicine* 2016; **374**(6): 542-54.
263. Pullen MF, Hullsiek KH, Rhein J, et al. CSF early fungicidal activity as a surrogate endpoint for cryptococcal meningitis survival in clinical trials. *Clin Infect Dis* 2020.
264. Molefi M, Chofle AA, Molloy SF, et al. AMBITION-cm: intermittent high dose AmBisome on a high dose fluconazole backbone for cryptococcal meningitis

induction therapy in sub-Saharan Africa: study protocol for a randomized controlled trial. *Trials* 2015; **16**: 276.
265. de Lange ECM. The mastermind approach to CNS drug therapy: translational prediction of human brain distribution, target site kinetics, and therapeutic effects. *Fluids and Barriers of the CNS* 2013; **10**(1): 12.
266. Srinivas N, Maffuid K, Kashuba ADM. Clinical Pharmacokinetics and Pharmacodynamics of Drugs in the Central Nervous System. *Clinical Pharmacokinetics* 2018.
267. Watt KM, Benjamin DK, Jr., Cheifetz IM, et al. Pharmacokinetics and safety of fluconazole in young infants supported with extracorporeal membrane oxygenation. *The Pediatric infectious disease journal* 2012; **31**(10): 1042-7.
268. Patel K, Roberts JA, Lipman J, Tett SE, Deldot ME, Kirkpatrick CM. Population Pharmacokinetics of Fluconazole in Critically Ill Patients Receiving Continuous Venovenous Hemodiafiltration: Using Monte Carlo Simulations To Predict Doses for Specified Pharmacodynamic Targets. *Antimicrobial Agents and Chemotherapy* 2011; **55**(12): 5868.
269. Abuhelwa AY, Mudge S, Hayes D, Upton RN, Foster DJ. Population In Vitro-In Vivo Correlation Model Linking Gastrointestinal Transit Time, pH, and Pharmacokinetics: Itraconazole as a Model Drug. *Pharm Res* 2016.
270. Li X, Frechen S, Moj D, et al. A Physiologically Based Pharmacokinetic Model of Voriconazole Integrating Time-Dependent Inhibition of CYP3A4, Genetic Polymorphisms of CYP2C19 and Predictions of Drug–Drug Interactions. *Clinical Pharmacokinetics* 2020; **59**(6): 781-808.
271. Jelliffe RW, Neely M. Individualized drug therapy for patients: basic foundations, relevant software and clinical applications: Academic Press; 2016.
272. Jelliffe RW, Schumitzky A, Bayard D, et al. Model-Based, Goal-Oriented, Individualised Drug Therapy. *Clinical Pharmacokinetics* 1998; **34**(1): 57-77.
273. Neely MN, van Guilder MG, Yamada WM, Schumitzky A, Jelliffe RW. Accurate detection of outliers and subpopulations with Pmetrics, a nonparametric and parametric pharmacometric modeling and simulation package for R. *Ther Drug Monit* 2012; **34**(4): 467-76.
274. Mallet A. A maximum likelihood estimation method for random coefficient regression models. *Biometrika* 1986; **73**(3): 645-56.
275. Lindsay BG. The geometry of mixture likelihoods: a general theory. *The annals of statistics* 1983: 86-94.
276. Schumitzky A. Nonparametric EM Algorithms for estimating prior distributions. *Applied Mathematics and Computation* 1991; **45**(2): 143-57.
277. Leary R, Jelliffe R, Schumitzky A, Van Guilder M. A unified parametric/nonparametric approach to population PK/PD modeling. Annual Meeting of the Population Approach Group in Europe, Paris, France; 2002; 2002.
278. Neely MN. Pmetrics User's Manual: University of Southern California Laboratory of Applied Pharmacokinetics.
279. Hope WW, Mickiene D, Petraitis V, et al. The Pharmacokinetics and Pharmacodynamics of Micafungin in Experimental Hematogenous Candida Meningoencephalitis: Implications for Echinocandin Therapy in Neonates. *The Journal of Infectious Diseases* 2008; **197**(1): 163-71.

280. Warn PA, Livermore J, Howard S, et al. Anidulafungin for neonatal hematogenous Candida meningoencephalitis: identification of candidate regimens for humans using a translational pharmacological approach. *Antimicrob Agents Chemother* 2012; **56**(2): 708-14.
281. Hope WW. Population pharmacokinetics of voriconazole in adults. *Antimicrob Agents Chemother* 2012; **56**(1): 526-31.
282. Kaindl T, Andes D, Engelhardt M, Saulay M, Larger P, Groll AH. Variability and exposure–response relationships of isavuconazole plasma concentrations in the Phase 3 SECURE trial of patients with invasive mould diseases. *Journal of Antimicrobial Chemotherapy* 2018; **74**(3): 761-7.
283. Chen Y, Ma F, Lu T, et al. Development of a Physiologically Based Pharmacokinetic Model for Itraconazole Pharmacokinetics and Drug–Drug Interaction Prediction. *Clinical Pharmacokinetics* 2016; **55**(6): 735-49.
284. Bicanic T, Wood R, Bekker LG, Darder M, Meintjes G, Harrison TS. Antiretroviral roll-out, antifungal roll-back: access to treatment for cryptococcal meningitis. *The Lancet Infectious Diseases* 2005; **5**(9): 530-1.
285. Loyse A, Thangaraj H, Easterbrook P, et al. Cryptococcal meningitis: improving access to essential antifungal medicines in resource-poor countries. *Lancet Infect Dis* 2013; **13**(7): 629-37.
286. Jarvis JN, Bicanic T, Loyse A, et al. Determinants of mortality in a combined cohort of 501 patients with HIV-associated Cryptococcal meningitis: implications for improving outcomes. *Clin Infect Dis* 2014; **58**(5): 736-45.
287. Richardson K, Cooper K, Marriott MS, Tarbit MH, Troke PF, Whittle PJ. Discovery of Fluconazole, a Novel Antifungal Agent. *Reviews of Infectious Diseases* 1990; **12**: S267-S71.
288. Vanden Bossche H, Koymans L, Moereels H. P450 inhibitors of use in medical treatment: focus on mechanisms of action. *Pharmacol Ther* 1995; **67**(1): 79-100.
289. Andes D, van Ogtrop M. Characterization and quantitation of the pharmacodynamics of fluconazole in a neutropenic murine disseminated candidiasis infection model. *Antimicrob Agents Chemother* 1999; **43**(9): 2116-20.
290. Felton TW, McCalman K, Malagon I, et al. Pulmonary penetration of piperacillin and tazobactam in critically ill patients. *Clin Pharmacol Ther* 2014; **96**(4): 438-48.
291. Arndt CA, Walsh TJ, McCully CL, Balis FM, Pizzo PA, Poplack DG. Fluconazole penetration into cerebrospinal fluid: implications for treating fungal infections of the central nervous system. *Journal of Infectious Diseases* 1988; **157**(1): 178-80.
292. Madu A, Cioffe C, Mian U, et al. Pharmacokinetics of fluconazole in cerebrospinal fluid and serum of rabbits: validation of an animal model used to measure drug concentrations in cerebrospinal fluid. *Antimicrob Agents Chemother* 1994; **38**(9): 2111-5.
293. Tucker RM, Williams PL, Arathoon EG, et al. Pharmacokinetics of fluconazole in cerebrospinal fluid and serum in human coccidioidal meningitis. *Antimicrobial Agents and Chemotherapy* 1988; **32**(3): 369-73.

294. Thaler F, Bernard B, Tod M, et al. Fluconazole penetration in cerebral parenchyma in humans at steady state. *Antimicrobial Agents and Chemotherapy* 1995; **39**(5): 1154-6.
295. Espinel-Ingroff A, Aller AI, Canton E, et al. Cryptococcus neoformans-Cryptococcus gattii Species Complex: an International Study of Wild-Type Susceptibility Endpoint Distributions and Epidemiological Cutoff Values for Fluconazole, Itraconazole, Posaconazole, and Voriconazole. *Antimicrobial Agents and Chemotherapy* 2012; **56**(11): 5898-906.
296. Montezuma-Rusca JM, Powers JH, Follmann D, Wang J, Sullivan B, Williamson PR. Early Fungicidal Activity as a Candidate Surrogate Endpoint for All-Cause Mortality in Cryptococcal Meningitis: A Systematic Review of the Evidence. *PLOS ONE* 2016; **11**(8): e0159727.
297. DerSimonian R, Laird N. Meta-analysis in clinical trials. *Control Clin Trials* 1986; **7**(3): 177-88.
298. Larsen RA, Leal MA, Chan LS. Fluconazole compared with amphotericin B plus flucytosine for cryptococcal meningitis in AIDS. A randomized trial. *Ann Intern Med* 1990; **113**(3): 183-7.
299. Rothe C, Sloan DJ, Goodson P, et al. A prospective longitudinal study of the clinical outcomes from cryptococcal meningitis following treatment induction with 800 mg oral fluconazole in Blantyre, Malawi. *PLoS One* 2013; **8**(6): e67311.
300. Longley N, Muzoora C, Taseera K, et al. Dose response effect of high-dose fluconazole for HIV-associated cryptococcal meningitis in southwestern Uganda. *Clin Infect Dis* 2008; **47**(12): 1556-61.
301. Milefchik E, Leal MA, Haubrich R, et al. Fluconazole alone or combined with flucytosine for the treatment of AIDS-associated cryptococcal meningitis. *Medical Mycology* 2008; **46**(4): 393-5.
302. Gaskell KM, Rothe C, Gnanadurai R, et al. A prospective study of mortality from cryptococcal meningitis following treatment induction with 1200 mg oral fluconazole in Blantyre, Malawi. *PLoS One* 2014; **9**(11): e110285.
303. Beyene T, Zewde AG, Balcha A, et al. Inadequacy of High-Dose Fluconazole Monotherapy Among Cerebrospinal Fluid Cryptococcal Antigen (CrAg)-Positive Human Immunodeficiency Virus-Infected Persons in an Ethiopian CrAg Screening Program. *Clin Infect Dis* 2017; **65**(12): 2126-9.
304. Fischman AJ, Alpert NM, Livni E, et al. Pharmacokinetics of 18F-labeled fluconazole in healthy human subjects by positron emission tomography. *Antimicrob Agents Chemother* 1993; **37**(6): 1270-7.
305. Palou de Fernandez E, Patino MM, Graybill JR, Tarbit MH. Treatment of cryptococcal meningitis in mice with fluconazole. *J Antimicrob Chemother* 1986; **18**(2): 261-70.
306. Kartalija M, Kaye K, Tureen JH, et al. Treatment of experimental cryptococcal meningitis with fluconazole: impact of dose and addition of flucytosine on mycologic and pathophysiologic outcome. *Journal of Infectious Diseases* 1996; **173**(5): 1216-21.
307. Aoyama T, Hirata K, Hirata R, et al. Population pharmacokinetics of fluconazole after administration of fosfluconazole and fluconazole in critically ill patients. *J Clin Pharm Ther* 2012; **37**(3): 356-63.

308. McLachlan AJ, Tett SE. Pharmacokinetics of fluconazole in people with HIV infection: a population analysis. *Br J Clin Pharmacol* 1996; **41**(4): 291-8.
309. Brammer KW, Farrow PR, Faulkner JK. Pharmacokinetics and tissue penetration of fluconazole in humans. *Rev Infect Dis* 1990; **12 Suppl 3**: S318-26.
310. Sanglard D. Resistance of human fungal pathogens to antifungal drugs. *Current Opinion in Microbiology* 2002; **5**(4): 379-85.
311. Chen Y, Farrer RA, Giamberardino C, et al. Microevolution of Serial Clinical Isolates of Cryptococcus neoformans var. grubii and C. gattii. *MBio* 2017; **8**(2).
312. Bicanic T, Harrison T, Niepieklo A, Dyakopu N, Meintjes G. Symptomatic relapse of HIV-associated cryptococcal meningitis after initial fluconazole monotherapy: the role of fluconazole resistance and immune reconstitution. *Clin Infect Dis* 2006; **43**(8): 1069-73.
313. Donovick R, Gold W, Pagano JF, Stout HA. Amphotericins A and B, antifungal antibiotics produced by a streptomycete. I. In vitro studies. *Antibiot Annu* 1955; **3**: 579-86.
314. Carton CA. Treatment of central nervous system cryptococcosis: a review and report of four cases treated with actidione. *Ann Intern Med* 1952; **37**(1): 123-54.
315. Mosberg WH, Jr., Arnold JG, Jr. Torulosis of the central nervous system; review of literature and report of 5 cases. *Ann Intern Med* 1950; **32**(6): 1153-83.
316. Andes D, Safdar N, Marchillo K, Conklin R. Pharmacokinetic-Pharmacodynamic Comparison of Amphotericin B (AMB) and Two Lipid-Associated AMB Preparations, Liposomal AMB and AMB Lipid Complex, in Murine Candidiasis Models. *Antimicrobial Agents and Chemotherapy* 2006; **50**(2): 674-84.
317. Lestner JM, Howard SJ, Goodwin J, et al. Pharmacokinetics and pharmacodynamics of amphotericin B deoxycholate, liposomal amphotericin B, and amphotericin B lipid complex in an in vitro model of invasive pulmonary aspergillosis. *Antimicrobial Agents & Chemotherapy* 2010; **54**(8): 3432-41.
318. Bennett JE, Dismukes WE, Duma RJ, et al. A Comparison of Amphotericin B Alone and Combined with Flucytosine in the Treatment of Cryptoccal Meningitis. *New England Journal of Medicine* 1979; **301**(3): 126-31.
319. Leenders AC, Reiss P, Portegies P, et al. Liposomal amphotericin B (AmBisome) compared with amphotericin B both followed by oral fluconazole in the treatment of AIDS-associated cryptococcal meningitis. *AIDS* 1997; **11**(12): 1463-71.
320. Brouwer AE, Rajanuwong A, Chierakul W, et al. Combination antifungal therapies for HIV-associated cryptococcal meningitis: a randomised trial. *Lancet* 2004; **363**(9423): 1764-7.
321. Wingard JR, Kubilis P, Lee L, et al. Clinical significance of nephrotoxicity in patients treated with amphotericin B for suspected or proven aspergillosis. *Clin Infect Dis* 1999; **29**(6): 1402-7.
322. Day J, Imran D, Ganiem AR, et al. CryptoDex: a randomised, double-blind, placebo-controlled phase III trial of adjunctive dexamethasone in HIV-infected

adults with cryptococcal meningitis: study protocol for a randomised control trial. *Trials [Electronic Resource]* 2014; **15**: 441.
323. Hope WW, Seibel NL, Schwartz CL, et al. Population pharmacokinetics of micafungin in pediatric patients and implications for antifungal dosing. *Antimicrob Agents Chemother* 2007; **51**(10): 3714-9.
324. Brown JH, West GB. Scaling in biology: Oxford University Press on Demand; 2000.
325. Viechtbauer W. Conducting meta-analyses in R with the metafor package. *Journal of Statistical Software* 2010; **36**(3): 1-48.
326. Andes D, Stamsted T, Conklin R. Pharmacodynamics of Amphotericin B in a Neutropenic-Mouse Disseminated-Candidiasis Model. *Antimicrobial Agents and Chemotherapy* 2001; **45**(3): 922-6.
327. Bekersky I, Fielding RM, Dressler DE, Lee JW, Buell DN, Walsh TJ. Pharmacokinetics, excretion, and mass balance of liposomal amphotericin B (AmBisome) and amphotericin B deoxycholate in humans. *Antimicrob Agents Chemother* 2002; **46**(3): 828-33.
328. Ayestarán A, López RM, Montoro JB, et al. Pharmacokinetics of conventional formulation versus fat emulsion formulation of amphotericin B in a group of patients with neutropenia. *Antimicrobial Agents and Chemotherapy* 1996; **40**(3): 609-12.
329. Roberts JA, Abdul-Aziz MH, Lipman J, et al. Individualised antibiotic dosing for patients who are critically ill: challenges and potential solutions. *The Lancet Infectious Diseases* 2014; **14**(6): 498-509.
330. Rajasingham R, Williams D, Meya DB, Meintjes G, Boulware DR, Scriven J. Nosocomial drug-resistant bacteremia in 2 cohorts with cryptococcal meningitis, Africa. *Emerg Infect Dis* 2014; **20**(4): 722-4.
331. Longley N, Harrison TS, Jarvis JN. Cryptococcal immune reconstitution inflammatory syndrome. *Curr Opin Infect Dis* 2013; **26**(1): 26-34.
332. Rolfes MA, Hullsiek KH, Rhein J, et al. The effect of therapeutic lumbar punctures on acute mortality from cryptococcal meningitis. *Clin Infect Dis* 2014; **59**(11): 1607-14.
333. Groll AH, Giri N, Petraitis V, et al. Comparative efficacy and distribution of lipid formulations of amphotericin B in experimental Candida albicans infection of the central nervous system. *J Infect Dis* 2000; **182**(1): 274-82.
334. Shobo A, Baijnath S, Bratkowska D, et al. MALDI MSI and LC-MS/MS: Towards preclinical determination of the neurotoxic potential of fluoroquinolones. *Drug Test Anal* 2016; **8**(8): 832-8.
335. Munyeza CF, Shobo A, Baijnath S, et al. Rapid and widespread distribution of doxycycline in rat brain: a mass spectrometric imaging study. *Xenobiotica* 2016; **46**(5): 385-92.
336. Shobo A, Bratkowska D, Baijnath S, et al. Tissue distribution of pretomanid in rat brain via mass spectrometry imaging. *Xenobiotica* 2016; **46**(3): 247-52.
337. Shobo A, Bratkowska D, Baijnath S, et al. Visualization of Time-Dependent Distribution of Rifampicin in Rat Brain Using MALDI MSI and Quantitative LCMS/MS. *Assay Drug Dev Technol* 2015; **13**(5): 277-84.

338. Hamill RJ, Sobel JD, El-Sadr W, et al. Comparison of 2 doses of liposomal amphotericin B and conventional amphotericin B deoxycholate for treatment of AIDS-associated acute cryptococcal meningitis: a randomized, double-blind clinical trial of efficacy and safety. *Clin Infect Dis* 2010; **51**(2): 225-32.
339. Gubbins PO, Amsden JR, McConnell SA, Anaissie EJ. Pharmacokinetics and buccal mucosal concentrations of a 15 milligram per kilogram of body weight total dose of liposomal amphotericin B administered as a single dose (15 mg/kg), weekly dose (7.5 mg/kg), or daily dose (1 mg/kg) in peripheral stem cell transplant patients. *Antimicrobial Agents & Chemotherapy* 2009; **53**(9): 3664-74.
340. Hong Y, Shaw PJ, Nath CE, et al. Population pharmacokinetics of liposomal amphotericin B in pediatric patients with malignant diseases. *Antimicrobial Agents & Chemotherapy* 2006; **50**(3): 935-42.
341. Hope WW, Goodwin J, Felton TW, Ellis M, Stevens DA. Population pharmacokinetics of conventional and intermittent dosing of liposomal amphotericin B in adults: a first critical step for rational design of innovative regimens. *Antimicrobial Agents & Chemotherapy* 2012; **56**(10): 5303-8.
342. Wurthwein G, Young C, Lanvers-Kaminsky C, et al. Population pharmacokinetics of liposomal amphotericin B and caspofungin in allogeneic hematopoietic stem cell recipients. *Antimicrob Agents Chemother* 2012; **56**(1): 536-43.
343. Lawrence DS, Youssouf N, Molloy SLF, et al. AMBIsome Therapy Induction OptimisatioN (AMBITION): High Dose AmBisome for Cryptococcal Meningitis Induction Therapy in sub-Saharan Africa: Study Protocol for a Phase 3 Randomised Controlled Non-Inferiority Trial. *Trials* 2018; **19**(1): 649.
344. Walsh TJ, Goodman JL, Pappas P, et al. Safety, tolerance, and pharmacokinetics of high-dose liposomal amphotericin B (AmBisome) in patients infected with Aspergillus species and other filamentous fungi: maximum tolerated dose study. *Antimicrobial Agents & Chemotherapy* 2001; **45**(12): 3487-96.
345. Sundar S, Chakravarty J, Agarwal D, Rai M, Murray HW. Single-dose liposomal amphotericin B for visceral leishmaniasis in India. *New England Journal of Medicine* 2010; **362**(6): 504-12.
346. Wasan KM, Kennedy AL, Cassidy SM, et al. Pharmacokinetics, distribution in serum lipoproteins and tissues, and renal toxicities of amphotericin B and amphotericin B lipid complex in a hypercholesterolemic rabbit model: single-dose studies. *Antimicrobial agents and chemotherapy* 1998; **42**(12): 3146-52.
347. Wasan KM, Morton RE, Rosenblum MG, Lopez-Berestein G. Decreased Toxicity of Liposomal Amphotericin B Due to Association of Amphotericin B with High-Density Lipoproteins. *Journal of pharmaceutical sciences* 1994; **83**(7): 1006-10.
348. Lee JW, Amantea MA, Francis PA, et al. Pharmacokinetics and safety of a unilamellar liposomal formulation of amphotericin B (AmBisome) in rabbits. *Antimicrob Agents Chemother* 1994; **38**(4): 713-8.
349. van Etten EW, Otte-Lambillion M, van Vianen W, Kate MTt, Bakker-Woudenberg IA. Biodistribution of liposomal amphotericin B (AmBisome) and amphotericin B-desoxycholate (Fungizone) in uninfected immunocompetent

mice and leucopenic mice infected with Candida albicans. *Journal of Antimicrobial Chemotherapy* 1995; **35**(4): 509-19.
350. Mehta R, Lopez-Berestein G, Hopfer R, Mills K, Juliano R. Liposomal amphotericin B is toxic to fungal cells but not to mammalian cells. *Biochimica et Biophysica Acta (BBA)-Biomembranes* 1984; **770**(2): 230-4.
351. Adler-Moore JP, Proffitt RT. Development, characterization, efficacy and mode of action of AmBisome, a unilamellar liposomal formulation of amphotericin B. *Journal of Liposome Research* 1993; **3**(3): 429-50.
352. Vincent BM, Lancaster AK, Scherz-Shouval R, Whitesell L, Lindquist S. Fitness Trade-offs Restrict the Evolution of Resistance to Amphotericin B. *PLOS Biology* 2013; **11**(10): e1001692.
353. Atkinson Jr AJ, Bennett JE. Experience with a new skin test antigen prepared from Cryptococcus neoformans. *American Review of Respiratory Disease* 1968; **97**(4): 637-43.
354. Boulware DR, Meya DB, Bergemann TL, et al. Clinical features and serum biomarkers in HIV immune reconstitution inflammatory syndrome after cryptococcal meningitis: a prospective cohort study. *PLoS Med* 2010; **7**(12): e1000384.
355. Jarvis J, Leeme T, Chofle A, et al. Ambition-CM: High-dose liposomal amphotericin for HIV-related cryptococcal meningitis. CROI. Seattle, Washington; 2017.
356. Ellis M, Spence D, Pauw Bd, et al. An EORTC International Multicenter Randomized Trial (EORTC Number 19923) Comparing Two Dosages of Liposomal Amphotericin B for Treatment of Invasive Aspergillosis. *Clinical Infectious Diseases* 1998; **27**(6): 1406-12.
357. Wingard JR, White MH, Anaissie E, Raffalli J, Goodman J, Arrieta A. A randomized, double-blind comparative trial evaluating the safety of liposomal amphotericin B versus amphotericin B lipid complex in the empirical treatment of febrile neutropenia. L Amph/ABLC Collaborative Study Group. *Clin Infect Dis* 2000; **31**(5): 1155-63.
358. Cornely OA, Maertens J, Bresnik M, et al. Liposomal amphotericin b as initial therapy for invasive mold infection: a randomized trial comparing a high–loading dose regimen with standard dosing (AmBiLoad Trial). *Clinical infectious diseases* 2007; **44**(10): 1289-97.
359. HIV. PoGftPaToOliAaAw. Guidelines for the Prevention and Treatment of Opportunistic Infections in HIV-infected Adults and Adolescents: Recommendations from the Centers for Disease Control and Prevention, the National Institutes of Health, and the HIV Medicine Association of the Infectious Diseases Society of America. http://aidsinfo.nih.gov/contentfiles/lvguidelines/adult_oi.pdf (accessed 10 Feb 2020).
360. Duong TA. Infection Due to Penicillium marneffei, an Emerging Pathogen: Review of 155 Reported Cases. *Clinical Infectious Diseases* 1996; **23**(1): 125-30.
361. Son VT, Khue PM, Strobel M. Penicilliosis and AIDS in Haiphong, Vietnam: evolution and predictive factors of death. *Med Mal Infect* 2014; **44**(11-12): 495-501.

362. Kawila R, Chaiwarith R, Supparatpinyo K. Clinical and laboratory characteristics of penicilliosis marneffei among patients with and without HIV infection in Northern Thailand: a retrospective study. *BMC Infectious Diseases* 2013; **13**(1): 464.
363. Chan JFW, Lau SKP, Yuen K-Y, Woo PCY. Talaromyces (Penicillium) marneffei infection in non-HIV-infected patients. *Emerging Microbes & Infections* 2016; **5**(1): 1-9.
364. Supparatpinyo K, Khamwan C, Baosoung V, Sirisanthana T, Nelson KE. Disseminated Penicillium marneffei infection in southeast Asia. *The Lancet* 1994; **344**(8915): 110-3.
365. Lestner J, Hope WW. Itraconazole: an update on pharmacology and clinical use for treatment of invasive and allergic fungal infections. *Expert Opin Drug Metab Toxicol* 2013; **9**(7): 911-26.
366. Dismukes WE, Bradsher RW, Cloud GC, et al. Itraconazole therapy for blastomycosis and histoplasmosis. *The American Journal of Medicine* 1992; **93**(5): 489-97.
367. Wheat J, Hafner R, Korzun AH, et al. Itraconazole treatment of disseminated histoplasmosis in patients with the acquired immunodeficiency syndrome. *The American Journal of Medicine* 1995; **98**(4): 336-42.
368. Wilcox CM, Darouiche RO, Laine L, Moskovitz BL, Mallegol I, Wu J. A Randomized, Double-Blind Comparison of Itraconazole Oral Solution and Fluconazole Tablets in the Treatment of Esophageal Candidiasis. *The Journal of Infectious Diseases* 1997; **176**(1): 227-32.
369. Denning DW, Tucker RM, Hansen LH, Stevens DA. Treatment of invasive aspergillosis with itraconazole. *The American Journal of Medicine* 1989; **86**(6): 791-800.
370. Imbert F, Jardin M, Fernandez C, et al. Effect of efflux inhibition on brain uptake of itraconazole in mice infected with Cryptococcus neoformans. *Drug Metab Dispos* 2003; **31**(3): 319-25.
371. Boogaerts MA, Verhoef GE, Zachee P, Demuynck H, Verbist L, De Beule K. Antifungal prophylaxis with itraconazole in prolonged neutropenia: correlation with plasma levels. *Mycoses* 1989; **32 Suppl 1**: 103-8.
372. Tricot G, Joosten E, Boogaerts MA, Vande Pitte J, Cauwenbergh G. Ketoconazole vs. itraconazole for antifungal prophylaxis in patients with severe granulocytopenia: preliminary results of two nonrandomized studies. *Rev Infect Dis* 1987; **9 Suppl 1**: S94-9.
373. Glasmacher A, Hahn C, Leutner C, et al. Breakthrough invasive fungal infections in neutropenic patients after prophylaxis with itraconazole. *Mycoses* 1999; **42**(7-8): 443-51.
374. Cartledge JD, Midgely J, Gazzard BG. Itraconazole solution: higher serum drug concentrations and better clinical response rates than the capsule formulation in acquired immunodeficiency syndrome patients with candidosis. *J Clin Pathol* 1997; **50**(6): 477-80.
375. Sharkey PK, Rinaldi MG, Dunn JF, Hardin TC, Fetchick RJ, Graybill JR. High-dose itraconazole in the treatment of severe mycoses. *Antimicrob Agents Chemother* 1991; **35**(4): 707-13.

376. Denning DW, Tucker RM, Hanson LH, Stevens DA. Itraconazole in opportunistic mycoses: cryptococcosis and aspergillosis. *J Am Acad Dermatol* 1990; **23**(3 Pt 2): 602-7.
377. Wheat J, Hafner R, Korzun AH, et al. Itraconazole treatment of disseminated histoplasmosis in patients with the acquired immunodeficiency syndrome. AIDS Clinical Trial Group. *Am J Med* 1995; **98**(4): 336-42.
378. Lestner JM, Roberts SA, Moore CB, Howard SJ, Denning DW, Hope WW. Toxicodynamics of Itraconazole: Implications for Therapeutic Drug Monitoring. *Clinical Infectious Diseases* 2009; **49**(6): 928-30.
379. CLSI. Reference method for broth dilution antifungal susceptibility testing of filamentous fungi, approved standard. 2 ed. Wayne, PA: Clinical and Laboratory Standards Institute; 2009.
380. Le T, Ly VT, Thu NTM, et al. Population Pharmacodynamics of Amphotericin B Deoxycholate for Disseminated Infection Caused by Talaromyces marneffei. *Antimicrob Agents Chemother* 2019; **63**(2).
381. D'Argenio D, Schumitzky A, Wang X. ADAPT 5 user's guide: pharmacokinetic/pharmacodynamic systems analysis software . Los Angeles, CA: Biomedical Simulations Resource; 2009.
382. Clinical and Laboratory Standards Institute. Reference method for broth dilution antifungal susceptibility testing of filamentous fungi. Approved standard. 2nd ed. M38 –A2. Wayne, PA: Clinical and Laboratory Standards Institute,; 2008.
383. Sekhon AS, Padhye AA, Garg AK. In vitro sensitivity of Penicillium marneffei and Pythium insidiosum to various antifungal agents. *European Journal of Epidemiology* 1992; **8**(3): 427-32.
384. Liu D, Liang L, Chen J. In vitro antifungal drug susceptibilities of Penicillium marneffei from China. *Journal of Infection and Chemotherapy* 2013; **19**(4): 776-8.
385. Larsson M, Nguyen LHT, Wertheim HFL, et al. Clinical characteristics and outcome of Penicillium marneffei infection among HIV-infected patients in northern Vietnam. *AIDS Research and Therapy* 2012; **9**(1): 24.
386. Vu VH, Ngo A, Ngo V, et al. Penicilliosis in Vietnam: a series of 94 patients. *La Revue de medecine interne* 2010; **31**(12): 812-8.
387. Odds FC, Bossche HV. Antifungal activity of itraconazole compared with hydroxy-itraconazole in vitro. *J Antimicrob Chemother* 2000; **45**(3): 371-3.
388. Ashbee HR, Barnes RA, Johnson EM, Richardson MD, Gorton R, Hope WW. Therapeutic drug monitoring (TDM) of antifungal agents: guidelines from the British Society for Medical Mycology. *J Antimicrob Chemother* 2014; **69**(5): 1162-76.
389. Denning DW, Tucker RM, Hanson LH, Hamilton JR, Stevens DA. Itraconazole therapy for cryptococcal meningitis and cryptococcosis. *Archives of Internal Medicine* 1989; **149**(10): 2301-8.
390. Jaruratanasirikul S, Kleepkaew A. Influence of an acidic beverage (Coca-Cola) on the absorption of itraconazole. *Eur J Clin Pharmacol* 1997; **52**(3): 235-7.
391. Bhaijee F, Subramony C, Tang S-J, Pepper DJ. Human immunodeficiency virus-associated gastrointestinal disease: common endoscopic biopsy diagnoses. *Pathology research international* 2011; **2011**.

392. Lewis RE. Antifungal therapeutic drug monitoring. *Current Fungal Infection Reports* 2010; **4**(3): 158-67.
393. limited B-MSP. Sustiva 600 mg Film-Coated Tablets Summary of Product Characteristics. Uxbridge, Middlesex; 2015.
394. Jaruratanasirikul S, Sriwiriyajan S. Pharmacokinetic study of the interaction between itraconazole and nevirapine. *Eur J Clin Pharmacol* 2007; **63**(5): 451-6.
395. European Medicines Agency. Viramune Summary of Product Characteristics, 2020.
396. USA DoHaHS. Panel on Opportunistic Infections in Adults and Adolescents with HIV. Guidelines for the prevention and treatment of opportunistic infections in adults and adolescents with HIV: recommendations from the Centers for Disease Control and Prevention, the National Institutes of Health, and the HIV Medicine Association of the Infectious Diseases Society of America.; 2019.
397. Fu MS, Coelho C, De Leon-Rodriguez CM, et al. Cryptococcus neoformans urease affects the outcome of intracellular pathogenesis by modulating phagolysosomal pH. *PLoS Pathog* 2018; **14**(6): e1007144.
398. Korn T, Oukka M, Kuchroo V, Bettelli E. Th17 cells: effector T cells with inflammatory properties. *Semin Immunol* 2007; **19**(6): 362-71.
399. Onishi RM, Gaffen SL. Interleukin-17 and its target genes: mechanisms of interleukin-17 function in disease. *Immunology* 2010; **129**(3): 311-21.
400. Murdock BJ, Teitz-Tennenbaum S, Chen GH, et al. Early or late IL-10 blockade enhances Th1 and Th17 effector responses and promotes fungal clearance in mice with cryptococcal lung infection. *J Immunol* 2014; **193**(8): 4107-16.
401. Monga DP. Role of macrophages in resistance of mice to experimental cryptococcosis. *Infection and immunity* 1981; **32**(3): 975-8.
402. Panackal AA, Wuest SC, Lin YC, et al. Paradoxical Immune Responses in Non-HIV Cryptococcal Meningitis. *PLoS Pathog* 2015; **11**(5): e1004884.
403. Fang FC. Antimicrobial reactive oxygen and nitrogen species: concepts and controversies. *Nature Reviews Microbiology* 2004; **2**(10): 820-32.
404. Imlay JA, Linn S. DNA damage and oxygen radical toxicity. *Science* 1988; **240**(4857): 1302-9.
405. Gupta-Wright A, Tembo D, Jambo KC, et al. Functional Analysis of Phagocyte Activity in Whole Blood from HIV/Tuberculosis-Infected Individuals Using a Novel Flow Cytometry-Based Assay. *Frontiers in Immunology* 2017; **8**: 1222.
406. Peterson I, Ntusi N, Jambo K, et al. Evaluating the reactivation of herpesviruses and inflammation as cardiovascular and cerebrovascular risk factors in antiretroviral therapy initiators in an African HIV-infected population (RHICCA): a protocol for a longitudinal cohort study. *BMJ Open* 2019; **9**(9): e025576.
407. Jolliffe IT, Cadima J. Principal component analysis: a review and recent developments. *Philosophical Transactions of the Royal Society A: Mathematical, Physical and Engineering Sciences* 2016; **374**(2065): 20150202.

408. Bicanic T, Brouwer AE, Meintjes G, et al. Relationship of cerebrospinal fluid pressure, fungal burden and outcome in patients with cryptococcal meningitis undergoing serial lumbar punctures. *AIDS* 2009; **23**(6): 701-6.
409. Havell EA. Production of tumor necrosis factor during murine listeriosis. *J Immunol* 1987; **139**(12): 4225-31.
410. Nakano Y, Onozuka K, Terada Y, Shinomiya H, Nakano M. Protective effect of recombinant tumor necrosis factor-alpha in murine salmonellosis. *J Immunol* 1990; **144**(5): 1935-41.
411. Denis M. Involvement of cytokines in determining resistance and acquired immunity in murine tuberculosis. *J Leukoc Biol* 1991; **50**(5): 495-501.
412. Steinshamn S, Waage A. Tumor necrosis factor and interleukin-6 in Candida albicans infection in normal and granulocytopenic mice. *Infect Immun* 1992; **60**(10): 4003-8.
413. Laudanna C, Miron S, Berton G, Rossi F. Tumor necrosis factor-alpha/cachectin activates the O2(-)-generating system of human neutrophils independently of the hydrolysis of phosphoinositides and the release of arachidonic acid. *Biochem Biophys Res Commun* 1990; **166**(1): 308-15.
414. Graybill JR, Bocanegra R, Lambros C, Luther MF. Granulocyte colony stimulating factor therapy of experimental cryptococcal meningitis. *Journal of Medical and Veterinary Mycology* 1997; **35**(4): 243-7.
415. Roilides E, Walsh TJ, Pizzo PA, Rubin M. Granulocyte colony-stimulating factor enhances the phagocytic and bactericidal activity of normal and defective human neutrophils. *J Infect Dis* 1991; **163**(3): 579-83.
416. Chiller T, Farrokhshad K, Brummer E, Stevens DA. Effect of granulocyte colony-stimulating factor and granulocyte-macrophage colony-stimulating factor on polymorphonuclear neutrophils, monocytes or monocyte-derived macrophages combined with voriconazole against Cryptococcus neoformans. *Med Mycol* 2002; **40**(1): 21-6.
417. Rosen LB, Freeman AF, Yang LM, et al. Anti-GM-CSF autoantibodies in patients with cryptococcal meningitis. *J Immunol* 2013; **190**(8): 3959-66.
418. von Freeden-Jeffry U, Vieira P, Lucian LA, McNeil T, Burdach SE, Murray R. Lymphopenia in interleukin (IL)-7 gene-deleted mice identifies IL-7 as a nonredundant cytokine. *J Exp Med* 1995; **181**(4): 1519-26.
419. Peschon JJ, Morrissey PJ, Grabstein KH, et al. Early lymphocyte expansion is severely impaired in interleukin 7 receptor-deficient mice. *J Exp Med* 1994; **180**(5): 1955-60.
420. Bhatia SK, Tygrett LT, Grabstein KH, Waldschmidt TJ. The effect of in vivo IL-7 deprivation on T cell maturation. *J Exp Med* 1995; **181**(4): 1399-409.
421. Puel A, Ziegler SF, Buckley RH, Leonard WJ. Defective IL7R expression in T(-)B(+)NK(+) severe combined immunodeficiency. *Nat Genet* 1998; **20**(4): 394-7.
422. Fry TJ, Mackall CL. Interleukin-7: master regulator of peripheral T-cell homeostasis? *Trends Immunol* 2001; **22**(10): 564-71.
423. Komschlies KL, Gregorio TA, Gruys ME, Back TC, Faltynek CR, Wiltrout RH. Administration of recombinant human IL-7 to mice alters the composition of B-lineage cells and T cell subsets, enhances T cell function, and induces regression of established metastases. *J Immunol* 1994; **152**(12): 5776-84.

424. Summers C, Rankin SM, Condliffe AM, Singh N, Peters AM, Chilvers ER. Neutrophil kinetics in health and disease. *Trends Immunol* 2010; **31**(8): 318-24.
425. DeLeo F. Modulation of phagocyte apoptosis by bacterial pathogens. *Apoptosis* 2004; **9**(4): 399-413.
426. Alemán M. Neutrophil apoptosis in the context of tuberculosis infection. *Tuberculosis* 2015; **95**(4): 359-63.
427. Mangan DF, Wahl SM. Differential regulation of human monocyte programmed cell death (apoptosis) by chemotactic factors and pro-inflammatory cytokines. *J Immunol* 1991; **147**(10): 3408-12.
428. van Furth R, Cohn ZA. The origin and kinetics of mononuclear phagocytes. *J Exp Med* 1968; **128**(3): 415-35.
429. Mildner A, Yona S, Jung S. A close encounter of the third kind: monocyte-derived cells. *Adv Immunol* 2013; **120**: 69-103.
430. Robertson EJ, Najjuka G, Rolfes MA, et al. Cryptococcus neoformans ex vivo capsule size is associated with intracranial pressure and host immune response in HIV-associated cryptococcal meningitis. *J Infect Dis* 2014; **209**(1): 74-82.
431. Igreja RP, Lazera Mdos S, Wanke B, Galhardo MC, Kidd SE, Meyer W. Molecular epidemiology of Cryptococcus neoformans isolates from AIDS patients of the Brazilian city, Rio de Janeiro. *Med Mycol* 2004; **42**(3): 229-38.
432. Jain N, Wickes BL, Keller SM, et al. Molecular epidemiology of clinical Cryptococcus neoformans strains from India. *Journal of Clinical Microbiology* 2005; **43**(11): 5733-42.
433. Litvintseva AP, Kestenbaum L, Vilgalys R, Mitchell TG. Comparative analysis of environmental and clinical populations of Cryptococcus neoformans. *Journal of Clinical Microbiology* 2005; **43**(2): 556-64.

Appendices

Appendix A: Co-author agreements for inclusion of published manuscripts in PhD thesis

19th November 2020

Dear co-author,

RE: *Stott KE, Beardsley J, Kolamunnage-Dona R, Castelazo AS, Kibengo FM, Mai NT, Lê Nhu'Tùng N, Cuc NT, Day J, Hope W.* ***Population pharmacokinetics and cerebrospinal fluid penetration of fluconazole in adults with cryptococcal meningitis.*** *Antimicrobial Agents and Chemotherapy. 2018 Sep 1;62(9).*

I plan to include the Author Accepted Manuscript of our paper as a chapter in my PhD thesis. This will be prepared for submission to the University of Liverpool and will be available on an open access basis from the University of Liverpool repository. As you know, the paper is already published on an open access basis in Antimicrobial Agents and Chemotherapy.

I would be grateful if you would sign below to indicate that you are happy for me to proceed to include the paper in my PhD thesis.

Many thanks and kind regards,

Katharine Stott

Dr Katharine Stott MRCP MSc MRes DTM&H
Wellcome Trust Clinical PhD Fellow
Malawi Liverpool Wellcome Trust Clinical Research Programme &
Department of Molecular and Clinical Pharmacology, University of Liverpool

Co-author signature:

Print name:

19th November 2020

Dear co-author,

RE: *Stott KE, Beardsley J, Kolamunnage-Dona R, Castelazo AS, Kibengo FM, Mai NT, Lê Nhu'Tùng N, Cuc NT, Day J, Hope W.* ***Population pharmacokinetics and cerebrospinal fluid penetration of fluconazole in adults with cryptococcal meningitis.*** *Antimicrobial Agents and Chemotherapy. 2018 Sep 1;62(9).*

I plan to include the Author Accepted Manuscript of our paper as a chapter in my PhD thesis. This will be prepared for submission to the University of Liverpool and will be available on an open access basis from the University of Liverpool repository. As you know, the paper is already published on an open access basis in Antimicrobial Agents and Chemotherapy.

I would be grateful if you would sign below to indicate that you are happy for me to proceed to include the paper in my PhD thesis.

Many thanks and kind regards,

Katharine Stott

Dr Katharine Stott MRCP MSc MRes DTM&H
Wellcome Trust Clinical PhD Fellow
Malawi Liverpool Wellcome Trust Clinical Research Programme &
Department of Molecular and Clinical Pharmacology, University of Liverpool

Co-author signature:

Print name: Ruwanthi Kolamunnage-Dona

19th November 2020

Dear co-author,

RE: *Stott KE, Beardsley J, Kolamunnage-Dona R, Castelazo AS, Kibengo FM, Mai NT, Lê Nhu'Tùng N, Cuc NT, Day J, Hope W.* ***Population pharmacokinetics and cerebrospinal fluid penetration of fluconazole in adults with cryptococcal meningitis.*** *Antimicrobial Agents and Chemotherapy. 2018 Sep 1;62(9).*

I plan to include the Author Accepted Manuscript of our paper as a chapter in my PhD thesis. This will be prepared for submission to the University of Liverpool and will be available on an open access basis from the University of Liverpool repository. As you know, the paper is already published on an open access basis in Antimicrobial Agents and Chemotherapy.

I would be grateful if you would sign below to indicate that you are happy for me to proceed to include the paper in my PhD thesis.

Many thanks and kind regards,

Katharine Stott

Dr Katharine Stott MRCP MSc MRes DTM&H
Wellcome Trust Clinical PhD Fellow
Malawi Liverpool Wellcome Trust Clinical Research Programme &
Department of Molecular and Clinical Pharmacology, University of Liverpool

Co-author signature:

Print name: Jeremy Day

19th November 2020

Dear co-author,

RE: *Stott KE, Beardsley J, Kolamunnage-Dona R, Castelazo AS, Kibengo FM, Mai NT, Lê Nhu'Tùng N, Cuc NT, Day J, Hope W.* ***Population pharmacokinetics and cerebrospinal fluid penetration of fluconazole in adults with cryptococcal meningitis.*** *Antimicrobial Agents and Chemotherapy. 2018 Sep 1;62(9).*

I plan to include the Author Accepted Manuscript of our paper as a chapter in my PhD thesis. This will be prepared for submission to the University of Liverpool and will be available on an open access basis from the University of Liverpool repository. As you know, the paper is already published on an open access basis in Antimicrobial Agents and Chemotherapy.

I would be grateful if you would sign below to indicate that you are happy for me to proceed to include the paper in my PhD thesis.

Many thanks and kind regards,

Katharine Stott

Dr Katharine Stott MRCP MSc MRes DTM&H
Wellcome Trust Clinical PhD Fellow
Malawi Liverpool Wellcome Trust Clinical Research Programme &
Department of Molecular and Clinical Pharmacology, University of Liverpool

Co-author signature:

Print name:

William Hope

UNIVERSITY OF LIVERPOOL

19th November 2020

Dear co-author,

RE: *Stott KE, Beardsley J, Kolamunnage-Dona R, Castelazo AS, Kibengo FM, Mai NT, Lê Nhu'Tùng N, Cuc NT, Day J, Hope W.* ***Population pharmacokinetics and cerebrospinal fluid penetration of fluconazole in adults with cryptococcal meningitis.*** *Antimicrobial Agents and Chemotherapy. 2018 Sep 1;62(9).*

I plan to include the Author Accepted Manuscript of our paper as a chapter in my PhD thesis. This will be prepared for submission to the University of Liverpool and will be available on an open access basis from the University of Liverpool repository. As you know, the paper is already published on an open access basis in Antimicrobial Agents and Chemotherapy.

I would be grateful if you would sign below to indicate that you are happy for me to proceed to include the paper in my PhD thesis.

Many thanks and kind regards,

Katharine Stott

Dr Katharine Stott MRCP MSc MRes DTM&H
Wellcome Trust Clinical PhD Fellow
Malawi-Liverpool Wellcome Trust Clinical Research Programme &
Department of Molecular and Clinical Pharmacology, University of Liverpool

Co-author signature:

Print name:

NGUYEN THI HOANG MAI

UNIVERSITY OF LIVERPOOL

19th November 2020

Dear co-author,

RE: *Stott KE, Beardsley J, Kolamunnage-Dona R, Castelazo AS, Kibengo FM, Mai NT, Lê Nhu'Tùng N, Cuc NT, Day J, Hope W.* ***Population pharmacokinetics and cerebrospinal fluid penetration of fluconazole in adults with cryptococcal meningitis.*** *Antimicrobial Agents and Chemotherapy. 2018 Sep 1;62(9).*

I plan to include the Author Accepted Manuscript of our paper as a chapter in my PhD thesis. This will be prepared for submission to the University of Liverpool and will be available on an open access basis from the University of Liverpool repository. As you know, the paper is already published on an open access basis in Antimicrobial Agents and Chemotherapy.

I would be grateful if you would sign below to indicate that you are happy for me to proceed to include the paper in my PhD thesis.

Many thanks and kind regards,

Katharine Stott

Dr Katharine Stott MRCP MSc MRes DTM&H
Wellcome Trust Clinical PhD Fellow
Malawi Liverpool Wellcome Trust Clinical Research Programme &
Department of Molecular and Clinical Pharmacology, University of Liverpool

Co-author signature:

Print name: Nguyễn Lê Nhu' Tùng

UNIVERSITY OF LIVERPOOL

19th November 2020

Dear co-author,

RE: *Stott KE, Beardsley J, Kolamunnage-Dona R, Castelazo AS, Kibengo FM, Mai NT, Lê Nhu'Tùng N, Cuc NT, Day J, Hope W.* ***Population pharmacokinetics and cerebrospinal fluid penetration of fluconazole in adults with cryptococcal meningitis.*** *Antimicrobial Agents and Chemotherapy. 2018 Sep 1;62(9).*

I plan to include the Author Accepted Manuscript of our paper as a chapter in my PhD thesis. This will be prepared for submission to the University of Liverpool and will be available on an open access basis from the University of Liverpool repository. As you know, the paper is already published on an open access basis in Antimicrobial Agents and Chemotherapy.

I would be grateful if you would sign below to indicate that you are happy for me to proceed to include the paper in my PhD thesis.

Many thanks and kind regards,

Katharine Stott

Dr Katharine Stott MRCP MSc MRes DTM&H
Wellcome Trust Clinical PhD Fellow
Malawi Liverpool Wellcome Trust Clinical Research Programme &
Department of Molecular and Clinical Pharmacology, University of Liverpool

Co-author signature:

Print name: Ngo Thi Kim Cuc

UNIVERSITY OF LIVERPOOL

19th November 2020

Dear co-author,

RE: *Stott KE, Beardsley J, Kolamunnage-Dona R, Castelazo AS, Kibengo FM, Mai NT, Lê Nhu'Tùng N, Cuc NT, Day J, Hope W.* ***Population pharmacokinetics and cerebrospinal fluid penetration of fluconazole in adults with cryptococcal meningitis.*** *Antimicrobial Agents and Chemotherapy. 2018 Sep 1;62(9).*

I plan to include the Author Accepted Manuscript of our paper as a chapter in my PhD thesis. This will be prepared for submission to the University of Liverpool and will be available on an open access basis from the University of Liverpool repository. As you know, the paper is already published on an open access basis in Antimicrobial Agents and Chemotherapy.

I would be grateful if you would sign below to indicate that you are happy for me to proceed to include the paper in my PhD thesis.

Many thanks and kind regards,

Katharine Stott

Dr Katharine Stott MRCP MSc MRes DTM&H
Wellcome Trust Clinical PhD Fellow
Malawi Liverpool Wellcome Trust Clinical Research Programme &
Department of Molecular and Clinical Pharmacology, University of Liverpool

Co-author signature:

Print name: FREDDIE MUKASA KIBENGO

UNIVERSITY OF LIVERPOOL

19th November 2020

Dear co-author,

RE: *Stott KE, Beardsley J, Whalley S, Kibengo FM, Mai NT, Lê Nhu'Tùng N, Cuc NT, Kolamunnage-Dona R, Hope W, Day J.* ***Population pharmacokinetic model and meta-analysis of outcomes of amphotericin B deoxycholate use in adults with cryptococcal meningoencephalitis.*** *Antimicrobial Agents and Chemotherapy. 2018 Jul 1;62(7).*

I plan to include the Author Accepted Manuscript of our paper as a chapter in my PhD thesis. This will be prepared for submission to the University of Liverpool and will be available on an open access basis from the University of Liverpool repository. As you know, the paper is already published on an open access basis in Antimicrobial Agents and Chemotherapy.

I would be grateful if you would sign below to indicate that you are happy for me to proceed to include the paper in my PhD thesis.

Many thanks and kind regards,

Katharine Stott

Dr Katharine Stott MRCP MSc MRes DTM&H
Wellcome Trust Clinical PhD Fellow
Malawi Liverpool Wellcome Trust Clinical Research Programme &
Department of Molecular and Clinical Pharmacology, University of Liverpool

Co-author signature:

Print name: FREDDIE MUKASA KIBENGO

19th November 2020

Dear co-author,

RE: *Stott KE, Beardsley J, Whalley S, Kibengo FM, Mai NT, Lê Nhu'Tùng N, Cuc NT, Kolamunnage-Dona R, Hope W, Day J.* ***Population pharmacokinetic model and meta-analysis of outcomes of amphotericin B deoxycholate use in adults with cryptococcal meningoencephalitis.*** *Antimicrobial Agents and Chemotherapy. 2018 Jul 1;62(7).*

I plan to include the Author Accepted Manuscript of our paper as a chapter in my PhD thesis. This will be prepared for submission to the University of Liverpool and will be available on an open access basis from the University of Liverpool repository. As you know, the paper is already published on an open access basis in Antimicrobial Agents and Chemotherapy.

I would be grateful if you would sign below to indicate that you are happy for me to proceed to include the paper in my PhD thesis.

Many thanks and kind regards,

Katharine Stott

Dr Katharine Stott MRCP MSc MRes DTM&H
Wellcome Trust Clinical PhD Fellow
Malawi Liverpool Wellcome Trust Clinical Research Programme &
Department of Molecular and Clinical Pharmacology, University of Liverpool

Co-author signature:

Print name:

19th November 2020

Dear co-author,

RE: *Stott KE, Beardsley J, Whalley S, Kibengo FM, Mai NT, Lê Nhu'Tùng N, Cuc NT, Kolamunnage-Dona R, Hope W, Day J.* ***Population pharmacokinetic model and meta-analysis of outcomes of amphotericin B deoxycholate use in adults with cryptococcal meningoencephalitis.*** *Antimicrobial Agents and Chemotherapy. 2018 Jul 1;62(7).*

I plan to include the Author Accepted Manuscript of our paper as a chapter in my PhD thesis. This will be prepared for submission to the University of Liverpool and will be available on an open access basis from the University of Liverpool repository. As you know, the paper is already published on an open access basis in Antimicrobial Agents and Chemotherapy.

I would be grateful if you would sign below to indicate that you are happy for me to proceed to include the paper in my PhD thesis.

Many thanks and kind regards,

Katharine Stott

Dr Katharine Stott MRCP MSc MRes DTM&H
Wellcome Trust Clinical PhD Fellow
Malawi Liverpool Wellcome Trust Clinical Research Programme &
Department of Molecular and Clinical Pharmacology, University of Liverpool

Co-author signature:

Print name: Jeremy Day

19th November 2020

Dear co-author,

RE: *Stott KE, Beardsley J, Whalley S, Kibengo FM, Mai NT, Lê Nhu'Tùng N, Cuc NT, Kolamunnage-Dona R, Hope W, Day J.* ***Population pharmacokinetic model and meta-analysis of outcomes of amphotericin B deoxycholate use in adults with cryptococcal meningoencephalitis.*** *Antimicrobial Agents and Chemotherapy. 2018 Jul 1;62(7).*

I plan to include the Author Accepted Manuscript of our paper as a chapter in my PhD thesis. This will be prepared for submission to the University of Liverpool and will be available on an open access basis from the University of Liverpool repository. As you know, the paper is already published on an open access basis in Antimicrobial Agents and Chemotherapy.

I would be grateful if you would sign below to indicate that you are happy for me to proceed to include the paper in my PhD thesis.

Many thanks and kind regards,

Katharine Stott

Dr Katharine Stott MRCP MSc MRes DTM&H
Wellcome Trust Clinical PhD Fellow
Malawi Liverpool Wellcome Trust Clinical Research Programme &
Department of Molecular and Clinical Pharmacology, University of Liverpool

Co-author signature: 

Print name: Ruwanthi Kolamunnage-Dona

19th November 2020

Dear co-author,

RE: *Stott KE, Beardsley J, Whalley S, Kibengo FM, Mai NT, Lê Nhu'Tùng N, Cuc NT, Kolamunnage-Dona R, Hope W, Day J.* ***Population pharmacokinetic model and meta-analysis of outcomes of amphotericin B deoxycholate use in adults with cryptococcal meningoencephalitis.*** *Antimicrobial Agents and Chemotherapy. 2018 Jul 1;62(7).*

I plan to include the Author Accepted Manuscript of our paper as a chapter in my PhD thesis. This will be prepared for submission to the University of Liverpool and will be available on an open access basis from the University of Liverpool repository. As you know, the paper is already published on an open access basis in Antimicrobial Agents and Chemotherapy.

I would be grateful if you would sign below to indicate that you are happy for me to proceed to include the paper in my PhD thesis.

Many thanks and kind regards,

Katharine Stott

Dr Katharine Stott MRCP MSc MRes DTM&H
Wellcome Trust Clinical PhD Fellow
Malawi Liverpool Wellcome Trust Clinical Research Programme &
Department of Molecular and Clinical Pharmacology, University of Liverpool

Co-author signature:

Print name:
William Hope

LIVERPOOL

19th November 2020

Dear co-author,

RE: *Stott KE, Beardsley J, Whalley S, Kibengo FM, Mai NT, Lê Nhu'Tùng N, Cuc NT, Kolamunnage-Dona R, Hope W, Day J.* ***Population pharmacokinetic model and meta-analysis of outcomes of amphotericin B deoxycholate use in adults with cryptococcal meningoencephalitis.*** *Antimicrobial Agents and Chemotherapy. 2018 Jul 1;62(7).*

I plan to include the Author Accepted Manuscript of our paper as a chapter in my PhD thesis. This will be prepared for submission to the University of Liverpool and will be available on an open access basis from the University of Liverpool repository. As you know, the paper is already published on an open access basis in Antimicrobial Agents and Chemotherapy.

I would be grateful if you would sign below to indicate that you are happy for me to proceed to include the paper in my PhD thesis.

Many thanks and kind regards,

Katharine Stott

Dr Katharine Stott MRCP MSc MRes DTM&H
Wellcome Trust Clinical PhD Fellow
Malawi Liverpool Wellcome Trust Clinical Research Programme &
Department of Molecular and Clinical Pharmacology, University of Liverpool

Co-author signature:

Print name:

NGUYEN THI HOANG MAI

UNIVERSITY OF LIVERPOOL

19th November 2020

Dear co-author,

RE: *Stott KE, Beardsley J, Whalley S, Kibengo FM, Mai NT, Lê Nhu'Tùng N, Cuc NT, Kolamunnage-Dona R, Hope W, Day J.* ***Population pharmacokinetic model and meta-analysis of outcomes of amphotericin B deoxycholate use in adults with cryptococcal meningoencephalitis.*** *Antimicrobial Agents and Chemotherapy. 2018 Jul 1;62(7).*

I plan to include the Author Accepted Manuscript of our paper as a chapter in my PhD thesis. This will be prepared for submission to the University of Liverpool and will be available on an open access basis from the University of Liverpool repository. As you know, the paper is already published on an open access basis in Antimicrobial Agents and Chemotherapy.

I would be grateful if you would sign below to indicate that you are happy for me to proceed to include the paper in my PhD thesis.

Many thanks and kind regards,

Katharine Stott

Dr Katharine Stott MRCP MSc MRes DTM&H
Wellcome Trust Clinical PhD Fellow
Malawi Liverpool Wellcome Trust Clinical Research Programme &
Department of Molecular and Clinical Pharmacology, University of Liverpool

Co-author signature:

Print name: Ngo Thi Kim Cuc

UNIVERSITY OF LIVERPOOL

19th November 2020

Dear co-author,

RE: *Stott KE, Beardsley J, Whalley S, Kibengo FM, Mai NT, Lê Nhu'Tùng N, Cuc NT, Kolamunnage-Dona R, Hope W, Day J.* ***Population pharmacokinetic model and meta-analysis of outcomes of amphotericin B deoxycholate use in adults with cryptococcal meningoencephalitis.*** *Antimicrobial Agents and Chemotherapy. 2018 Jul 1;62(7).*

I plan to include the Author Accepted Manuscript of our paper as a chapter in my PhD thesis. This will be prepared for submission to the University of Liverpool and will be available on an open access basis from the University of Liverpool repository. As you know, the paper is already published on an open access basis in Antimicrobial Agents and Chemotherapy.

I would be grateful if you would sign below to indicate that you are happy for me to proceed to include the paper in my PhD thesis.

Many thanks and kind regards,

Katharine Stott

Dr Katharine Stott MRCP MSc MRes DTM&H
Wellcome Trust Clinical PhD Fellow
Malawi Liverpool Wellcome Trust Clinical Research Programme &
Department of Molecular and Clinical Pharmacology, University of Liverpool

Co-author signature:

Print name: Nguyễn Lê Nhu' Tùng

19th November 2020

Dear co-author,

RE: *Stott KE, Beardsley J, Whalley S, Kibengo FM, Mai NT, Lê Nhu'Tùng N, Cuc NT, Kolamunnage-Dona R, Hope W, Day J.* ***Population pharmacokinetic model and meta-analysis of outcomes of amphotericin B deoxycholate use in adults with cryptococcal meningoencephalitis.*** *Antimicrobial Agents and Chemotherapy. 2018 Jul 1;62(7).*

I plan to include the Author Accepted Manuscript of our paper as a chapter in my PhD thesis. This will be prepared for submission to the University of Liverpool and will be available on an open access basis from the University of Liverpool repository. As you know, the paper is already published on an open access basis in Antimicrobial Agents and Chemotherapy.

I would be grateful if you would sign below to indicate that you are happy for me to proceed to include the paper in my PhD thesis.

Many thanks and kind regards,

Katharine Stott

Dr Katharine Stott MRCP MSc MRes DTM&H
Wellcome Trust Clinical PhD Fellow
Malawi Liverpool Wellcome Trust Clinical Research Programme &
Department of Molecular and Clinical Pharmacology, University of Liverpool

Co-author signature:

Print name: Sarah Whalley

Appendix B: Published manuscripts related to PhD thesis

AMERICAN SOCIETY FOR MICROBIOLOGY | Antimicrobial Agents and Chemotherapy®

MECHANISMS OF RESISTANCE

Evidence for Expanding the Role of Streptomycin in the Management of Drug-Resistant *Mycobacterium tuberculosis*

Keira A. Cohen,[a] Katharine E. Stott,[b,c] Vanisha Munsamy,[d] Abigail L. Manson,[e] Ashlee M. Earl,[e] Alexander S. Pym[d]

[a]Division of Pulmonary and Critical Care Medicine, Johns Hopkins University School of Medicine, Baltimore, Maryland, USA
[b]Antimicrobial Pharmacodynamics and Therapeutics, Institute of Translational Medicine, University of Liverpool, Liverpool, United Kingdom
[c]Malawi-Liverpool-Wellcome Trust Clinical Research Programme, Blantyre, Malawi
[d]Africa Health Research Institute (AHRI), Durban, South Africa
[e]Broad Institute of Harvard and M.I.T., Cambridge, Massachusetts, USA

ABSTRACT In 2019, the WHO tuberculosis (TB) treatment guidelines were updated to recommend only limited use of streptomycin, in favor of newer agents or amikacin as the preferred aminoglycoside for drug-resistant *Mycobacterium tuberculosis*. However, the emergence of resistance to newer drugs, such as bedaquiline, has prompted a reanalysis of antitubercular drugs in search of untapped potential. Using 211 clinical isolates of *M. tuberculosis* from South Africa, we performed phenotypic drug susceptibility testing (DST) to aminoglycosides by both critical concentration and MIC determination in parallel with whole-genome sequencing to identify known genotypic resistance elements. Isolates with low-level streptomycin resistance mediated by *gidB* were frequently misclassified with respect to streptomycin resistance when using the WHO-recommended critical concentration of 2 μg/ml. We identified 29 *M. tuberculosis* isolates from South Africa with low-level streptomycin resistance concomitant with high-level amikacin resistance, conferred by *gidB* and *rrs* 1400, respectively. Using a large global data set of *M. tuberculosis* genomes, we observed 95 examples of this corresponding resistance genotype (*gidB-rrs* 1400), including identification in 81/257 (31.5%) of extensively drug resistant (XDR) isolates. In a phylogenetic analysis, we observed repeated evolution of low-level streptomycin and high-level amikacin resistance in multiple countries. Our findings suggest that current critical concentration methods and the design of molecular diagnostics need to be revisited to provide more accurate assessments of streptomycin resistance for *gidB*-containing isolates. For patients harboring isolates of *M. tuberculosis* with high-level amikacin resistance conferred by *rrs* 1400, and for whom newer agents are not available, treatment with streptomycin may still prove useful, even in the face of low-level resistance conferred by *gidB*.

KEYWORDS *Mycobacterium tuberculosis*, aminoglycosides, drug resistance mechanisms, multidrug resistance, tuberculosis, whole-genome sequencing

Despite recent advances, tuberculosis (TB) remains the number one infectious killer worldwide (1). The ongoing global epidemic of drug-resistant TB and limited effective treatment regimens for drug-resistant *Mycobacterium tuberculosis* have resulted in significant morbidity and mortality (1). Recognition of the inadequacy of the current antitubercular drug development pipeline, and the emergence of resistance to new drugs—including bedaquiline (2–9), delaminid (3, 4), clofazimine (5, 7), and linezolid (6)—has prompted a reanalysis of the existing arsenal of antitubercular drugs in search of untapped potential. Streptomycin may be one such underutilized drug.

Discovered in 1944, streptomycin, an injectable streptidine aminoglycoside antibiotic, was the first antimicrobial agent with proven activity against *M. tuberculosis*. In

Citation Cohen KA, Stott KE, Munsamy V, Manson AL, Earl AM, Pym AS. 2020. Evidence for expanding the role of streptomycin in the management of drug-resistant *Mycobacterium tuberculosis*. Antimicrob Agents Chemother 64:e00860-20. https://doi.org/10.1128/AAC.00860-20.

Address correspondence to Keira A. Cohen, kcohen8@jhmi.edu.

Received 5 May 2020
Returned for modification 1 June 2020
Accepted 6 June 2020
Accepted manuscript posted online 15 June 2020
Published 20 August 2020

TABLE 1 Distribution of resistance-associated mutations in a South African data set[a]

Drug	Gene	Polymorphism[b]	Number of isolates
Streptomycin	*rpsL*	K43R	31
		K88R	8
	rrs (non-1400)	513	7
		516	6
		907	1
	gidB	nt 62, del 1 bp	1
		nt 103, del 1 bp	1
		nt 108, del 1 bp	3
		nt 116, del 1 bp	3
		nt 282, del 130 bp	78
		nt 368, del 2 bp	1
		A134E	3
		A138V	2
		A141E	2
Kanamycin/amikacin	*rrs*	1400	50
Kanamycin	*eis*	promoter −14	2

[a]Of the 211 South African isolates, 140 were found to have genotypic streptomycin resistance with mutations in *rpsL*, *rrs* (non-1400), and *gidB*, as detailed in the table. Fifty strains were found to have genotypic amikacin/kanamycin resistance with mutations in *rrs* 1400, and two isolates had kanamycin resistance with an *eis* promoter mutation.
[b]nt, nucleotide; del, deletion; bp, base pairs.

conjunction with isoniazid and para-aminosalicylic acid (PAS), streptomycin formed part of the first multidrug combination chemotherapy for TB, introduced in 1952. Its initial widespread use led to the early emergence of streptomycin resistance, which subsequently limited its clinical utility. Streptomycin remained an integral component of first-line TB therapy until the 1980s, and its empirical use in retreatment TB regimens was recommended until recently (10).

While the majority of the molecular determinants of aminoglycoside resistance are known, commercial diagnostic tests that assay for genotypic streptomycin resistance are lacking. Resistance to streptomycin does not contribute to the definition of extensively drug resistant (XDR) TB, which is defined as multidrug-resistant (MDR) isolates with additional resistance to quinolones and other injectable agents (amikacin, kanamycin) (11). Streptomycin is currently classified as a group C second-line agent for use in longer MDR-TB regimens (10), which are recommended in limited circumstances only. While XDR isolates are frequently cross-resistant to second-line injectable agents, there may be untapped potential for continued use of streptomycin for low-level resistance.

In our large collection of *M. tuberculosis* isolates from South Africa, we characterized aminoglycoside-resistance phenotypes in conjunction with whole-genome sequencing to identify patterns of aminoglycoside resistance. Subsequently, we used a global data set of over 5,000 *M. tuberculosis* genomes to assess the occurrence of genotypic low-level streptomycin resistance concomitant with high-level amikacin resistance worldwide.

RESULTS

Using 211 sequenced clinical isolates of *M. tuberculosis* from South Africa (Table S2 in the supplemental material), we performed critical concentration testing for streptomycin and kanamycin, and observed incomplete cross-resistance between these two aminoglycosides (Table S3). Amikacin critical concentration was not performed due to anticipated near complete cross-resistance with kanamycin (12), which was confirmed by our MIC testing (Fig. S1). Using genomic sequences for these 211 isolates, we sought known drug resistance markers for these aminoglycoside drugs. A total of 140 isolates were found to have genotypic markers of streptomycin resistance, with mutations in *rpsL*, *rrs* (non-1400), and *gidB*, whereas 50 isolates had mutations in *rrs* 1400, which confers high-level resistance to both amikacin and kanamycin (Table 1). Two isolates

TABLE 2 Distribution of co-occurring genotypic resistances to streptomycin and amikacin/kanamycin in a South African data set[a]

	Amikacin/kanamycin genotype			
Streptomycin genotype	**WT**	***rrs* 1400**	***eis* promoter**	**Total**
WT	67	2	2	71
rpsL	33	2	0	35
rrs (non-1400)	8	5	0	13
gidB	44	**41**[b]	0	85
Total	152	50	2	204

[a]Of note, 7 isolates were identified to contain more than one streptomycin resistance mutation, as described in Table S4 in the supplemental material.
[b]The boldface type indicates the number of isolates with co-occurrence of *gidB* and *rrs* 1400 mutations that confer low-level streptomycin and high-level amikacin resistance.

contained mutations in the promoter region of *eis*, which confers resistance to kanamycin, but not to streptomycin or amikacin. Co-occurrence of streptomycin and amikacin/kanamycin resistance genotypes was determined (Table 2), including identification of seven isolates with more than one streptomycin-resistance-determining mutation (Table S4).

In comparing MIC data from Sensititre testing with known aminoglycoside resistance genotypes, we evaluated the relationship between genotypic and phenotypic resistance to streptomycin (Fig. 1A), amikacin (Fig. 1B), and kanamycin (Fig. S1). There was a bell-shaped distribution (Fig. 1A) of isolates containing *gidB* mutations with low-level streptomycin resistance (median MIC 4 μg/ml; interquartile range [IQR], 2 to 4 μg/ml) (Table 3). By critical concentration testing per the WHO-recommended guidelines, the majority of isolates with *gidB* mutations (76%, 70/92) were classified as resistant to streptomycin. In contrast, high-level streptomycin resistance was observed in isolates with either *rrs* (non-1400) or *rpsL* mutations, with median MIC 32 μg/ml (IQR, 16 to 32 μg/ml) and 32 μg/ml (IQR, 16 to 32 μg/ml), respectively. Three isolates with no identifiable streptomycin mutations were noted to have high MICs to streptomycin (MIC 16 to 32 μg/ml), suggesting that additional streptomycin resistance mutations remain to be discovered, but this could also be due to errors in phenotyping. Nearly every isolate with high-level amikacin and kanamycin resistance contained an *rrs* 1400 mutation (Fig. 1B, Fig. S2).

When comparing the MIC of each isolate to streptomycin and amikacin, numerous isolates had mismatched phenotypes, indicating that resistance to amikacin did not confer resistance to streptomycin, and vice versa (Fig. 2). In particular, 29 isolates from South Africa exhibited low-level streptomycin resistance (MIC 4 μg/ml or 8 μg/ml) and concomitant high-level amikacin resistance (MIC $\geq$16 μg/ml) (circled area, Fig. 2). These findings suggest that use of streptomycin instead of amikacin would be the preferred aminoglycoside for treatment of these isolates. The vast majority of isolates with this phenotype (93%, 27/29) contained a *gidB* resistance genotype, and 100% (29/29) contained an *rrs* 1400 mutation.

From the genomic data, we constructed a phylogeny to determine the interrelatedness of isolates with (i) low-level streptomycin resistance and (ii) concomitant low-level streptomycin and high-level amikacin resistance in phenotypic testing (Fig. 3). The 57 isolates with low-level streptomycin resistance were distributed throughout the phylogeny. The majority (25/29, 86%) of South African isolates with low-level streptomycin and high-level amikacin resistance belonged to the Tugela Ferry XDR clone, which was responsible for epidemic XDR in the region in the early 2000s (13). However, there were four isolates outside this cluster, indicating that this phenomenon was not unique to this clone.

To determine whether the phenomenon of low-level streptomycin and high-level amikacin resistance occurred outside South Africa, we analyzed our large data set of 5,310 *M. tuberculosis* isolates from 43 countries (14). Within this data set, 257 isolates contained mutations for resistance to all four drugs that define XDR (rifampin, isoniazid,

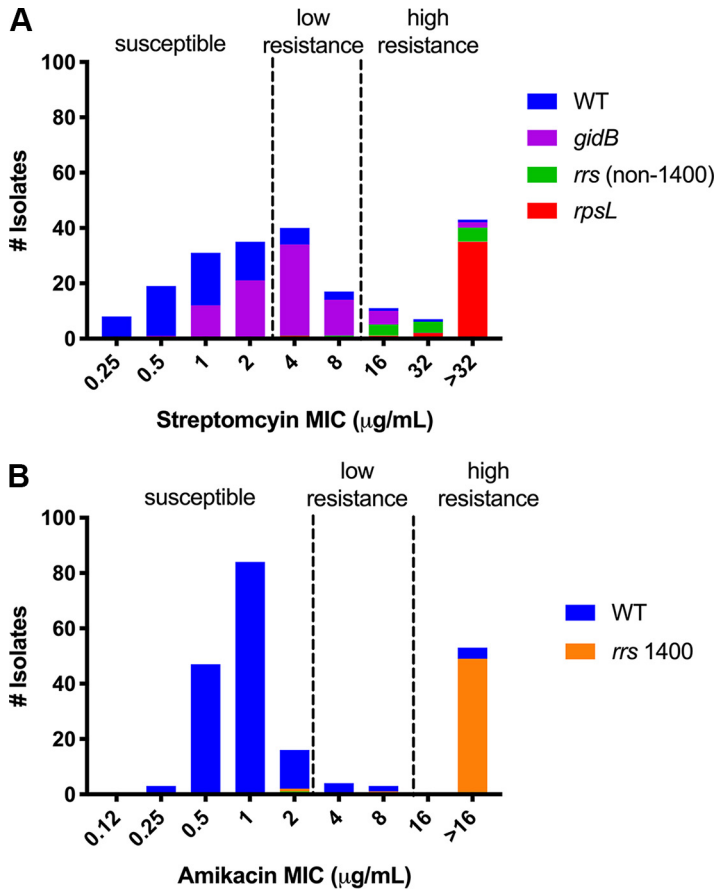

FIG 1 Clinical strains of *M. tuberculosis* were observed to have a range of susceptibility to aminoglycosides, mediated by resistance genotype. A total of 211 isolates of *M. tuberculosis* from South Africa underwent MIC determination and aminoglycoside resistance genotyping to identify mutations that confer resistance to streptomycin or amikacin, respectively. (A) Streptomycin MIC testing revealed a bell-shaped curve distribution of *gidB* strains with low-level streptomycin resistance, whereas strains containing *rrs* (non-1400) or *rpsL* mutations had higher resistance. Of note, three isolates containing resistance elements in both *gidB* and *rpsL* were included among the *rpsL* isolates. (B) Amikacin MIC testing revealed high-level resistance among strains containing the *rrs* 1400 mutation. Kanamycin MIC results mirrored that of amikacin (Fig. S1 in the supplemental material).

ofloxacin, and amikacin). As phenotypic data were not available for this data set, we used co-occurrence of a *gidB* resistance mutation and *rrs* 1400 mutation as a genotypic predictor of this combination of low-level streptomycin resistance and high-level amikacin resistance (Fig. 4). We identified 378 unique isolates with *gidB* mutations, including 95 isolates with co-occurrence of *gidB* mutations and *rrs* 1400 mutation (Table S5). All 95 isolates contained resistance-conferring mutations to both isoniazid and rifampin (MDR genotype) in addition to resistance to either ofloxacin or kanamycin (pre-XDR), and 81/95 of these isolates were XDR. Of the 257 XDR isolates in the 5,310-isolate data set, 81 (31.5%) of the XDR isolates contained this *gidB-rrs* 1400

TABLE 3 *gidB* mutations confer low-level streptomycin resistance, whereas *rrs* and *rpsL* mutations confer high-level resistance

Streptomycin genotype	Median MIC to streptomycin in μg/ml (IQR)[a]
WT	1 (0.5–2)
gidB	4 (2–4)
rrs (non-1400)	32 (16–32)
rpsL	32 (32–32)

[a]For each streptomycin resistance genotype, median MIC to streptomycin and interquartile range (IQR) is listed.

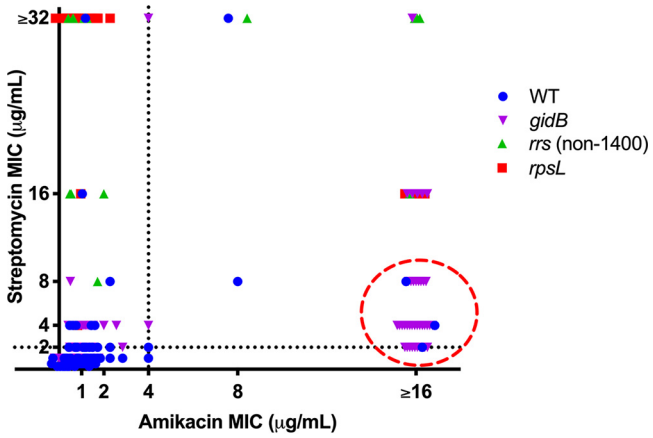

FIG 2 Significant numbers of *M. tuberculosis* isolates exhibit concomitant low-level streptomycin resistance and high-level amikacin resistance. Isolates are represented by streptomycin genotype (see key) and plotted as a function of the relative phenotypic resistance to both amikacin and streptomycin. The red dotted circle indicates the 29 isolates with concomitant low-level streptomycin resistance and high-level amikacin resistance.

combination, indicating frequent occurrence in global XDR-TB. The majority of isolates with the *gidB-rrs* 1400 pattern were LAM4 and likely members of the Tugela Ferry XDR clade. However, there were nine other spoligotypes with isolates containing this pattern, indicating multiple independent evolutionary events. Beyond South Africa, isolates with this resistance pattern were also identified in Belarus, China, Iran, Portugal, Romania, South Korea, and Sweden, indicating that this phenomenon of streptomycin-low and amikacin-high resistance is of global importance for management of drug-resistant TB.

DISCUSSION

In both a South African and a global data set, significant numbers of *M. tuberculosis* isolates contained mutations associated with concomitant low-level streptomycin resistance and high-level amikacin resistance. Current guidelines that recommend only limited use of streptomycin (10) may be unwittingly withholding a potentially lifesaving, inexpensive, and available drug from certain patients with drug-resistant TB. Similarly, current WHO-endorsed laboratory procedures for performing phenotypic DST to streptomycin by critical concentration may obscure the potential utility of streptomycin by not distinguishing between high and low-level resistance.

Given additional newer agents with excellent activity against drug-resistant TB, such as bedaquiline, the updated 2019 WHO guidelines limit use of aminoglycosides (10). Kanamycin is no longer recommended in the treatment of drug-resistant TB patients on longer regimens. Amikacin is now the preferred aminoglycoside, and its use is limited to adults on longer regimens in situations in which DST results confirm susceptibility and for whom high-quality audiometry testing for hearing loss can be performed. Streptomycin use is recommended only when amikacin is not available, and again in situations when DST results confirm susceptibility and in whom safety monitoring can be ensured.

While treatment-related ototoxicity and nephrotoxicity are well established, streptomycin could still hold therapeutic potential for individuals with drug-resistant TB harboring isolates with low-level streptomycin resistance. If an aminoglycoside is being considered for inclusion in a drug-resistant TB regimen, if the *rrs* 1400 mutation is present, which confers high-level resistance to amikacin, than we recommend selection of streptomycin, even in the face of low-level resistance, such as that conferred by *gidB*. To our knowledge, clinical outcomes for individuals harboring isolates with low-level streptomycin resistance mediated by *gidB* and treated with a streptomycin-containing regimen have not been assessed. An expanded role for streptomycin in drug-resistant

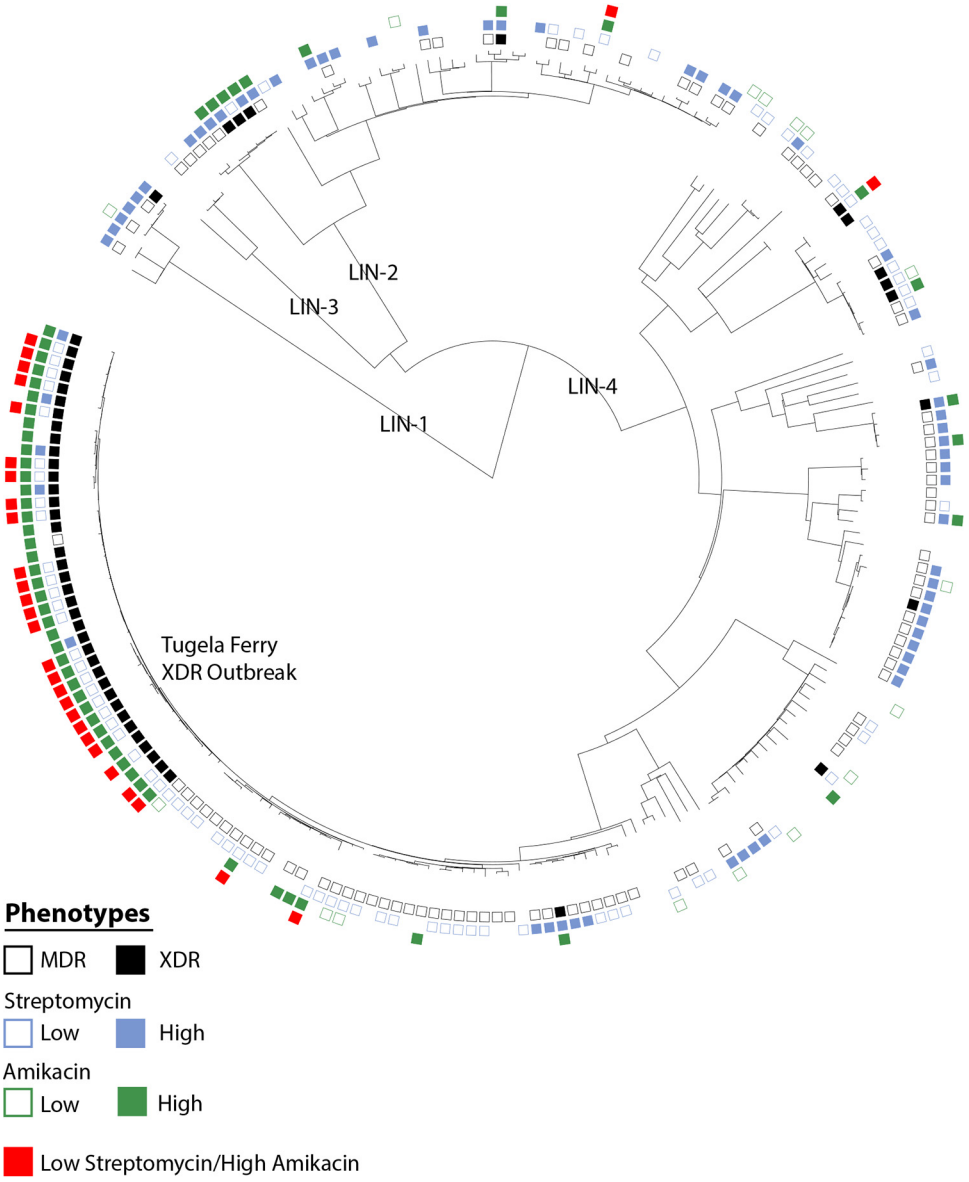

FIG 3 Concomitant low-level streptomycin and high-level amikacin phenotypic resistance in South African *M. tuberculosis* isolates across the phylogeny. Midpoint rooted maximum-likelihood phylogeny of 211 *M. tuberculosis* isolates, containing representatives of four of the seven known *M. tuberculosis* lineages. Phenotypic MDR and XDR are indicated by black and white boxes at the tip of each leaf node. The levels of phenotypic resistance to streptomycin (low, MIC 4 to 8 μg/ml; high, MIC $\geq$16 μg/ml) and amikacin (low, MIC 4 to 8 μg/ml; high, MIC $\geq$16 μg/ml) are indicated by box color, per the key. Strains with concomitant low-level streptomycin resistance and high-level amikacin resistance are indicated in red. While the majority of isolates with low-level streptomycin resistance and high-level amikacin resistance pertained to the Tugela Ferry XDR outbreak clone, four examples were observed outside the outbreak clone, indicating that this was not an isolated evolutionary event.

TB may also increase risk of adverse events related to drug toxicity. Ensuring safety of a streptomycin-based regimen would necessitate implementation of monitoring procedures, including audiometry and measurements of renal function, which constitute an additional burden—especially for resource-limited settings.

In South Africa, due to a clonal outbreak of XDR-TB in Tugela Ferry, a large fraction of circulating XDR-TB isolates contain an 130-bp deletion in *gidB* that confers low-level streptomycin resistance and an *rrs* 1400 mutation that confers high-level cross-resistance to amikacin, kanamycin, and capreomycin (15, 16). In a recent long-term cohort study of XDR-TB treatment outcomes in South Africa, only 1% of patients were treated with streptomycin, whereas 98% received capreomycin (17). As treatment

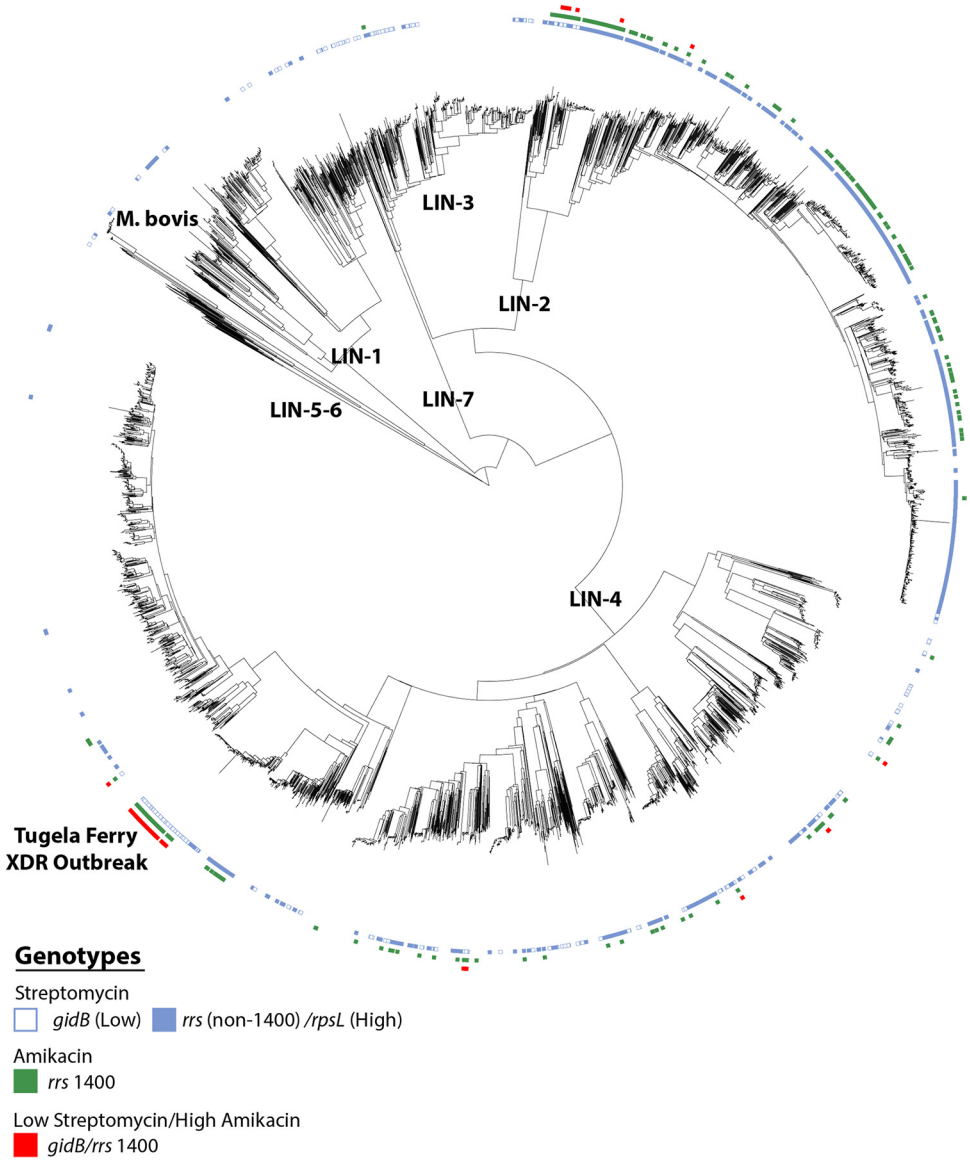

FIG 4 Concomitant low-level streptomycin and high-level amikacin genotypic resistance evolved repeatedly in a global data set of *M. tuberculosis*. Midpoint rooted maximum-likelihood phylogeny of 5,310 *M. tuberculosis* strains from a global data set containing representatives of all seven known *M. tuberculosis* lineages. The presence and levels of genotypic resistance to streptomycin (low, *gidB*; high, *rrs* [non-1400] and *rpsL*) and amikacin (high, *rrs* 1400) are indicated by box color near the leaf nodes. Ninety-five isolates with genotypic mutations predicted to confer both low-level streptomycin resistance and high-level amikacin resistance (*gidB-rrs* 1400) are indicated in red. Concomitant low-level streptomycin resistance and high-level amikacin resistance occurred across the phylogeny, indicating that this phenomenon is of global relevance for TB control.

outcomes for XDR-TB in South Africa were notoriously abysmal (17), including streptomycin may prove useful for patients in whom new drugs are not available because of resistance or contraindications.

Current WHO-endorsed laboratory procedures for performing phenotypic DST to streptomycin by critical concentration fail to provide key information relevant to streptomycin inclusion in a regimen for drug-resistant TB. The MIC distribution for isolates containing *gidB* mutations straddles the WHO-recommended critical concentration of 2 μg/ml (Fig. 1A). This modest increase in MIC among isolates containing *gidB* mutations in comparison to wild-type isolates likely contributes to inconsistencies in testing. Isolates containing *gidB* mutations are frequently misclassified in terms of their susceptibility to streptomycin on critical concentration testing (as occurred in 24% of

isolates in this study). As critical concentration testing is typically performed only at a single concentration, isolates with low-level streptomycin resistance—which may potentially be treated successfully with streptomycin—cannot be distinguished from those with high-level resistance. Similarly, wild-type strains that do not contain genotypes predicted to confer resistance to streptomycin can exhibit low-level streptomycin resistance that is above the critical concentration threshold (as seen in four South African isolates in this study), which may result in withholding a potentially useful drug.

The WHO-recommended critical concentration for streptomycin in *M. tuberculosis* is based on weak scientific evidence (12). The upper limit of wild-type MIC distribution, termed the epidemiological cutoff value (ECOFF), for streptomycin is 2 μg/ml (18). That this is the same value as the critical concentration in DST reflects the lack of clinical and pharmacokinetic/pharmacodynamic data to inform a more practical selection of a critical concentration. Potential strategies to address this issue include: (i) raising the streptomycin critical concentration; (ii) adding a second streptomycin drug concentration to traditional critical concentration testing (e.g., test at both 2 μg/ml and 8 μg/ml to disambiguate between low-level and high-level streptomycin resistance); (iii) performing additional reflex testing when an isolate is identified by traditional critical concentration DST to be resistant to both streptomycin and kanamycin (e.g., more detailed phenotypic analysis or streptomycin resistance genotype determination); or (iv) forgoing critical concentration testing in all forms and instead expanding genotypic aminoglycoside resistance testing.

Recent efforts to expand the complement of drug resistance mutation panels included on rapid molecular TB diagnostics have not included streptomycin (19). Whole-genome sequencing (WGS) studies of clinical isolates of *M. tuberculosis* have demonstrated that the majority (92% to 95%) of streptomycin-resistant isolates can be explained by known mutations (20, 21). Thus, omitting streptomycin resistance determinants from rapid drug resistance panels is a missed opportunity to both identify and grade streptomycin resistance relative to amikacin resistance. One potential reason for this exclusion is mutations in *gidB* can occur anywhere in the gene, where they cause frameshift, nonsense, or deletion mutations. Thus, they are difficult to identify with current SNP-based diagnostics and instead require whole-gene-based strategies, such as high-resolution melt analysis (22) or rapid WGS.

It is important to address several limitations of this study. MIC determination was performed with Sensititre, which is not the gold standard for *M. tuberculosis* DST. However, prior investigation comparing Sensititre with traditional methods have shown excellent concordance for aminoglycoside testing (23, 24). In addition, phenotyped isolates derived only from South Africa, and the population structure contained clonal XDR isolates from the Tugela Ferry epidemic. However, the phenomenon of genotypic resistance conferring low-level streptomycin and high-level amikacin resistance was also seen outside this clone. Thus, this observation carries implications for *M. tuberculosis* treatment in other settings.

Our findings suggest that current critical concentration methods for streptomycin resistance determination and the design of molecular diagnostics for resistance may need to be revisited for improved categorization of isolates harboring *gidB* mutations, which confer low-level streptomycin resistance. In the context of limited therapeutic options for drug-resistant *M. tuberculosis*, our results show the potential utility of streptomycin, even for isolates observed to have low-level resistance from *gidB* mutations.

MATERIALS AND METHODS

Clinical isolates. We selected for inclusion a random subset of 211 clinical isolates of susceptible and drug-resistant *M. tuberculosis* from South Africa from our larger sequenced strain set (15).

Drug susceptibility testing by critical concentration. As previously described (15), DST was performed prospectively by critical concentration on Middlebrook 7H11 using the WHO-recommended drug concentrations for streptomycin (2.0 μg/ml) and kanamycin (6.0 μg/ml). Amikacin critical concentration was not performed, as isolates with acquired resistance to amikacin essentially always have resistance to kanamycin (12).

MIC determination. MIC determination for three aminoglycosides (amikacin, kanamycin, and streptomycin) was performed using MycoTB Sensititre plates (TREK Diagnostic Systems), per the manufacturer's instructions. The lowest concentration of drug that did not show visible growth was recorded as the MIC to the respective drug.

Whole-genome sequencing and analysis. Whole-genome sequencing (WGS) and analysis were performed as previously described (15). Genotypic resistance to streptomycin, amikacin, and kanamycin was defined as identification of polymorphisms that are known to be associated with drug resistance, per the refined genotypic resistance definition in Desjardins and Cohen et al. (20) (Table S1). Isolates belonging to the Tugela Ferry XDR clone were identified by phylogenetic clustering with the reference isolates KZN605, collected during the epidemic, as well as the presence of canonical drug-resistance mutations (15). SNP calls from Cohen et al. were used (15). RAxML version 7.3.0 (25) was used to construct a phylogenetic tree from concatenated SNPs, with 1,000 bootstrap replicates.

Data availability. All sequencing data can be found in the Sequence Read Archive NCBI umbrella project identifier PRJNA183624.

SUPPLEMENTAL MATERIAL

Supplemental material is available online only.

SUPPLEMENTAL FILE 1, PDF file, 0.2 MB.

SUPPLEMENTAL FILE 2, XLSX file, 0.04 MB.

ACKNOWLEDGMENTS

We acknowledge the support of the Africa Health Research Institute (AHRI) to conduct the research. We thank Nonkqubela Bantubani of the Medical Research Council (MRC) in Durban, in addition to Max O'Donnell and Nesri Padayatchi for contributing clinical isolates of *M. tuberculosis*, which were used in this study. We thank Koleka P. Mlisana and Nomonde R. Mvelase of the KwaZulu-Natal National Health Laboratory Service.

This work was supported by funding from the National Heart Lung and Blood Institute, National Institutes of Health (K08 HL139994), and a Burroughs Wellcome Fund Career Award for Medical Scientists to K.A.C. K.E.S. is a Wellcome Trust Clinical Ph.D Fellow (203919/Z/16/Z). This project has been supported in part with federal funds from the National Institute of Allergy and Infectious Diseases, National Institutes of Health, Department of Health and Human Services, under contract number HHSN272200900018C and grant number U19AI110818 to the Broad Institute.

None of the authors have a commercial or other association that may pose a conflict of interest.

K.A.C., K.E.S., and A.S.P. conceived of the study and designed the experiments. K.A.C. and V.M. performed the wet-lab experiments. K.A.C., K.E.S., and A.L.M. analyzed the data. K.A.C. and K.E.S. wrote the manuscript. A.M.E. and A.S.P. supervised and coordinated the project. All authors have read the manuscript and confirm that they meet ICMJE criteria for authorship.

REFERENCES

1. World Health Organization. 2019. Global tuberculosis report 2019. World Health Organization, Geneva, Switzerland.
2. Andries K, Villellas C, Coeck N, Thys K, Gevers T, Vranckx L, Lounis N, de Jong BC, Koul A. 2014. Acquired resistance of Mycobacterium tuberculosis to bedaquiline. PLoS One 9:e102135. https://doi.org/10.1371/journal.pone.0102135.
3. Bloemberg GV, Keller PM, Stucki D, Trauner A, Borrell S, Latshang T, Coscolla M, Rothe T, Hömke R, Ritter C, Feldmann J, Schulthess B, Gagneux S, Böttger EC. 2015. Acquired resistance to bedaquiline and delamanid in therapy for tuberculosis. N Engl J Med 373:1986–1988. https://doi.org/10.1056/NEJMc1505196.
4. Hoffmann H, Kohl TA, Hofmann-Thiel S, Merker M, Beckert P, Jaton K, Nedialkova L, Sahalchyk E, Rothe T, Keller PM, Niemann S. 2016. Delamanid and bedaquiline resistance in Mycobacterium tuberculosis ancestral Beijing genotype causing extensively drug-resistant tuberculosis in a Tibetan Refugee. Am J Respir Crit Care Med 193:337–340. https://doi.org/10.1164/rccm.201502-0372LE.
5. Xu J, Wang B, Hu M, Huo F, Guo S, Jing W, Nuermberger E, Lu Y. 2017. Primary clofazimine and bedaquiline resistance among isolates from patients with multidrug-resistant tuberculosis. Antimicrob Agents Chemother 61:e00239-17. https://doi.org/10.1128/AAC.00239-17.
6. Zimenkov DV, Nosova EY, Kulagina EV, Antonova OV, Arslanbaeva LR, Isakova AI, Krylova LY, Peretokina IV, Makarova MV, Safonova SG, Borisov SE, Gryadunov DA. 2017. Examination of bedaquiline- and linezolid-resistant Mycobacterium tuberculosis isolates from the Moscow region. J Antimicrob Chemother 72:1901–1906. https://doi.org/10.1093/jac/dkx094.
7. Villellas C, Coeck N, Meehan CJ, Lounis N, de Jong B, Rigouts L, Andries K. 2016. Unexpected high prevalence of resistance-associated Rv0678 variants in MDR-TB patients without documented prior use of clofazimine or bedaquiline. J Antimicrob Chemother 72:684–690. https://doi.org/10.1093/jac/dkw502.
8. Veziris N, Bernard C, Guglielmetti L, Le Du D, Marigot-Outtandy D, Jaspard M, Caumes E, Lerat I, Rioux C, Yazdanpanah Y, Tiotiu A, Lemaitre N, Brossier F, Jarlier V, Robert J, Sougakoff W, Aubry A. 2017. Rapid emergence of Mycobacterium tuberculosis bedaquiline resistance: lessons to avoid repeating past errors. Eur Respir J 49:1601719. https://doi.org/10.1183/13993003.01719-2016.
9. Martinez E, Hennessy D, Jelfs P, Crighton T, Chen S-A, Sintchenko V. 2018. Mutations associated with in vitro resistance to bedaquiline in Mycobacterium tuberculosis isolates in Australia. Tuberculosis (Edinb) 111:31–34. https://doi.org/10.1016/j.tube.2018.04.007.

10. World Health Organization. 2019. WHO consolidated guidelines on drug-resistant tuberculosis. World Health Organization, Geneva, Switzerland.
11. Jassal M, Bishai WR. 2009. Extensively drug-resistant tuberculosis. Lancet Infect Dis 9:19–30. https://doi.org/10.1016/S1473-3099(08)70260-3.
12. World Health Organization. 2008. Policy guidance on drug-susceptibility testing (DST) of second-line antituberculosis drugs. World Health Organization, Geneva, Switzerland.
13. Gandhi NR, Moll A, Sturm AW, Pawinski R, Govender T, Lalloo U, Zeller K, Andrews J, Friedland G. 2006. Extensively drug-resistant tuberculosis as a cause of death in patients co-infected with tuberculosis and HIV in a rural area of South Africa. Lancet 368:1575–1580. https://doi.org/10.1016/S0140-6736(06)69573-1.
14. Manson AL, Cohen KA, Abeel T, Desjardins CA, Armstrong DT, Barry CE, Brand J, Chapman SB, Cho S-N, Gabrielian A, Gomez J, Jodals AM, Joloba M, Jureen P, Lee JS, Malinga L, Maiga M, Nordenberg D, Noroc E, Romancenco E, Salazar A, Ssengooba W, Velayati AA, Winglee K, Zalutskaya A, Via LE, Cassell GH, Dorman SE, Ellner J, Farnia P, Galagan JE, Rosenthal A, Crudu V, Homorodean D, Hsueh P-R, Narayanan S, Pym AS, Skrahina A, Swaminathan S, Van der Walt M, Alland D, Bishai WR, Cohen T, Hoffner S, Birren BW, Earl AM, TBResist Global Genome Consortium. 2017. Genomic analysis of globally diverse Mycobacterium tuberculosis strains provides insights into the emergence and spread of multidrug resistance. Nat Genet 49:395–402. https://doi.org/10.1038/ng.3767.
15. Cohen KA, Abeel T, Manson McGuire A, Desjardins CA, Munsamy V, Shea TP, Walker BJ, Bantubani N, Almeida DV, Alvarado L, Chapman SB, Mvelase NR, Duffy EY, Fitzgerald MG, Govender P, Gujja S, Hamilton S, Howarth C, Larimer JD, Maharaj K, Pearson MD, Priest ME, Zeng Q, Padayatchi N, Grosset J, Young SK, Wortman J, Mlisana KP, O'Donnell MR, Birren BW, Bishai WR, Pym AS, Earl AM. 2015. Evolution of extensively drug-resistant tuberculosis over four decades: whole genome sequencing and dating analysis of Mycobacterium tuberculosis isolates from KwaZulu-Natal. PLoS Med 12:e1001880. https://doi.org/10.1371/journal.pmed.1001880.
16. Shah NS, Auld SC, Brust JCM, Mathema B, Ismail N, Moodley P, Mlisana K, Allana S, Campbell A, Mthiyane T, Morris N, Mpangase P, van der Meulen H, Omar SV, Brown TS, Narechania A, Shaskina E, Kapwata T, Kreiswirth B, Gandhi NR. 2017. Transmission of extensively drug-resistant tuberculosis in South Africa. N Engl J Med 376:243–253. https://doi.org/10.1056/NEJMoa1604544.
17. Pietersen E, Ignatius E, Streicher EM, Mastrapa B, Padanilam X, Pooran A, Badri M, Lesosky M, van Helden P, Sirgel F, Warren R, Dheda K. 2014. Long-term outcomes of patients with extensively drug-resistant tuberculosis in South Africa: a cohort study. Lancet 383:1230–1239. https://doi.org/10.1016/S0140-6736(13)62675-6.
18. Juréen P, Ängeby K, Sturegård E, Chryssanthou E, Giske CG, Werngren J, Nordvall M, Johansson A, Kahlmeter G, Hoffner S, Schön T. 2010. Wild-type MIC distributions for aminoglycoside and cyclic polypeptide antibiotics used for treatment of Mycobacterium tuberculosis infections. J Clin Microbiol 48:1853–1858. https://doi.org/10.1128/JCM.00240-10.
19. Xie YL, Chakravorty S, Armstrong DT, Hall SL, Via LE, Song T, Yuan X, Mo X, Zhu H, Xu P, Gao Q, Lee M, Lee J, Smith LE, Chen RY, Joh JS, Cho Y, Liu X, Ruan X, Liang L, Dharan N, Cho S-N, Barry CE, Ellner JJ, Dorman SE, Alland D. 2017. Evaluation of a rapid molecular drug-susceptibility test for tuberculosis. N Engl J Med 377:1043–1054. https://doi.org/10.1056/NEJMoa1614915.
20. Desjardins CA, Cohen KA, Munsamy V, Abeel T, Maharaj K, Walker BJ, Shea TP, Almeida DV, Manson AL, Salazar A, Padayatchi N, O'Donnell MR, Mlisana KP, Wortman J, Birren BW, Grosset J, Earl AM, Pym AS. 2016. Genomic and functional analyses of Mycobacterium tuberculosis strains implicate ald in D-cycloserine resistance. Nat Genet 48:544–551. https://doi.org/10.1038/ng.3548.
21. Walker TM, Kohl TA, Omar SV, Hedge J, Del Ojo Elias C, Bradley P, Iqbal Z, Feuerriegel S, Niehaus KE, Wilson DJ, Clifton DA, Kapatai G, Ip CLC, Bowden R, Drobniewski FA, Allix-Béguec C, Gaudin C, Parkhill J, Diel R, Supply P, Crook DW, Smith EG, Walker AS, Ismail N, Niemann S, Peto T. a. 2015. Whole-genome sequencing for prediction of Mycobacterium tuberculosis drug susceptibility and resistance: a retrospective cohort study. Lancet Infect Dis 15:1193–1202. https://doi.org/10.1016/S1473-3099(15)00062-6.
22. Pholwat S, Liu J, Stroup S, Gratz J, Banu S, Rahman SMM, Ferdous SS, Foongladda S, Boonlert D, Ogarkov O, Zhdanova S, Kibiki G, Heysell S, Houpt E. 2015. Integrated microfluidic card with TaqMan probes and high-resolution melt analysis to detect tuberculosis drug resistance mutations across 10 genes. mBio 6:e02273-14. https://doi.org/10.1128/mBio.02273-14.
23. Hall L, Jude KP, Clark SL, Dionne K, Merson R, Boyer A, Parrish NM, Wengenack NL. 2012. Evaluation of the Sensititre MycoTB plate for susceptibility testing of the Mycobacterium tuberculosis complex against first- and second-line agents. J Clin Microbiol 50:3732–3734. https://doi.org/10.1128/JCM.02048-12.
24. Lee JS, Armstrong DT, Ssengooba W, Park J-A, Yu Y, Mumbowa F, Namaganda C, Mboowa G, Nakayita G, Armakovitch S, Chien G, Cho S, Via LE, Barry CE, Ellner JJ, Alland D, Dorman SE, Joloba ML. 2013. The Sensititre MYCOTB MIC plate for testing Mycobacterium tuberculosis susceptibility to first- and second-line drugs. Antimicrob Agents Chemother 58:11-8. https://doi.org/10.1128/AAC.01209-13.
25. Stamatakis A. 2006. RAxML-VI-HPC: maximum likelihood-based phylogenetic analyses with thousands of taxa and mixed models. Bioinformatics 22:2688–2690. https://doi.org/10.1093/bioinformatics/btl446.

Lawrence et al. Trials (2018) 19:649
https://doi.org/10.1186/s13063-018-3026-4

Trials

STUDY PROTOCOL Open Access

AMBIsome Therapy Induction OptimisatioN (AMBITION): High Dose AmBisome for Cryptococcal Meningitis Induction Therapy in sub-Saharan Africa: Study Protocol for a Phase 3 Randomised Controlled Non-Inferiority Trial

David S. Lawrence[1,2*], Nabila Youssouf[1,2], Síle F. Molloy[3], Alexandre Alanio[4], Melanie Alufandika[5], David R. Boulware[6,7], Timothée Boyer-Chammard[4], Tao Chen[8], Francoise Dromer[4], Admire Hlupeni[9], William Hope[10], Mina C. Hosseinipour[11], Cecilia Kanyama[11], Oliver Lortholary[4], Angela Loyse[3], David B. Meya[6], Mosepele Mosepele[2,12], Conrad Muzoora[6], Henry C. Mwandumba[5,8], Chiratidzo E. Ndhlovu[9], Louis Niessen[8], Charlotte Schutz[13], Katharine E. Stott[5,10], Duolao Wang[8], David G. Lalloo[8], Graeme Meintjes[13], Shabbar Jaffar[8], Thomas S. Harrison[3] and Joseph N. Jarvis[1,2]

Abstract

Background: Cryptococcal meningitis (CM) is a major cause of mortality in HIV programmes in Africa despite increasing access to antiretroviral therapy (ART). Mortality is driven in part by limited availability of amphotericin-based treatment, drug-induced toxicities of amphotericin B deoxycholate and prolonged hospital admissions. A single, high-dose of liposomal amphotericin (L-AmB, Ambisome) on a fluconazole backbone has been reported as non-inferior to 14 days of standard dose L-AmB in reducing fungal burden. This trial examines whether single, high-dose L-AmB given with high-dose fluconazole and flucytosine is non-inferior to a seven-day course of amphotericin B deoxycholate plus flucytosine (the current World Health Organization [WHO] recommended treatment regimen).

(Continued on next page)

* Correspondence: david.s.lawrence@lshtm.ac.uk
[1]Department of Clinical Research, Faculty of Infectious and Tropical Diseases, London School of Hygiene and Tropical Medicine, London, UK
[2]Botswana-Harvard AIDS Institute Partnership, Gaborone, Botswana
Full list of author information is available at the end of the article

(Continued from previous page)

Methods: An open-label phase III randomised controlled non-inferiority trial conducted in five countries in sub-Saharan Africa: Botswana, Malawi, South Africa, Uganda and Zimbabwe. The trial will compare CM induction therapy with (1) a single dose (10 mg/kg) of L-AmB given with 14 days of fluconazole (1200 mg/day) and flucytosine (100 mg/kg/day) to (2) seven days amphotericin B deoxycholate (1 mg/kg/day) given alongside seven days of flucytosine (100 mg/kg/day) followed by seven days of fluconazole (1200 mg/day). The primary endpoint is all-cause mortality at ten weeks with a non-inferiority margin of 10% and 90% power. Secondary endpoints are early fungicidal activity, proportion of grade III/IV adverse events, pharmacokinetic parameters and pharmacokinetic/pharmacodynamic associations, health service costs, all-cause mortality within the first two and four weeks, all-cause mortality within the first ten weeks (superiority analysis) and rates of CM relapse, immune reconstitution inflammatory syndrome and disability at ten weeks. A total of 850 patients aged ≥ 18 years with a first episode of HIV-associated CM will be enrolled (425 randomised to each arm). All patients will be followed for 16 weeks. All patients will receive consolidation therapy with fluconazole 800 mg/day to complete ten weeks of treatment, followed by fluconazole maintenance and ART as per local guidance.

Discussion: A safe, sustainable and easy to administer regimen of L-AmB that is non-inferior to seven days of daily amphotericin B deoxycholate therapy may reduce the number of adverse events seen in patients treated with amphotericin B deoxycholate and shorten hospital admissions, providing a highly favourable and implementable alternative to the current WHO recommended first-line treatment.

Trial registration: ISRCTN, ISRCTN72509687. Registered on 13 July 2017.

Keywords: Cryptococcal meningitis, HIV, AmBisome, Amphotericin B, Fluconazole, Flucytosine, Clinical trial

Background

Early mortality among people initiating HIV treatment in Africa is considerably higher than in high-income countries [1–4]. Despite antiretroviral therapy (ART) roll-out, approximately half of HIV-infected individuals in sub-Saharan Africa are not on ART and about one-third still present for care with very low CD4 counts. The incidence of opportunistic co-infections such as CM in this group is high [5] and CM remains the most common cause of adult meningitis in much of Africa [6]. As a result, cryptococcal meningitis (CM) is a major cause of mortality in HIV-infected patients in Africa and is associated with 10–20% of all HIV-related deaths [7]. Furthermore, the number of CM cases remains high despite increased ART access; they now include both ART-naïve and ART-experienced patients, with half of patients diagnosed with CM having had prior exposure to ART but with persisting low CD4 counts due to non-adherence and/or ART failure [8–10]. The poor outcomes reported using currently available antifungal therapy in African centres are a critical driver of this high mortality. Mortality using amphotericin B deoxycholate-based therapy in Africa, even in clinical trial settings, remains in the region of 35–45% [10–13]. Amphotericin B deoxycholate therapy requires hospitalisation for at least seven days and its toxicity profile requires costly laboratory monitoring. The average hospitalisation cost for CM treated with amphotericin B deoxycholate is USD 800–1000 in Zimbabwe where the annual per capita gross domestic product is < USD 1000. Many clinical centres in sub-Saharan Africa lack access to reliable laboratory monitoring and have limited nursing capacity making safe administration of conventional amphotericin B deoxycholate difficult or impossible. Consequently, amphotericin B deoxycholate therapy is often not available in Africa. Fluconazole, the oral alternative widely used in Africa, is much less rapidly fungicidal than amphotericin-B, even at a dosage of up to 1200 mg/day, and mortality at ten weeks is 50–60% [14, 15]. Given the HIV prevalence and incidence in Southern and East Africa, inadequate ART coverage, suboptimal monitoring of individuals on ART leading to treatment failure and limited access to screening and pre-emptive treatment for CM, CM will remain a major cause of morbidity and mortality in the region for the foreseeable future. New treatment strategies are urgently needed.

Until recently, World Health Organization (WHO) treatment guidelines recommended a 14-day course of amphotericin B deoxycholate-based treatment for CM induction therapy. The recently completed phase III ACTA trial showed that patients receiving a short, seven-day course of amphotericin B deoxycholate plus flucytosine had lower mortality at ten weeks (24%, 95% confidence interval [CI]: 16–32) compared to patients receiving 14-day course of amphotericin B plus flucytosine (38%, 95% CI: 29–47, unadjusted hazard ratio [HR] 0.56, 95% CI: 0.35–0.91) [10]. The trial also confirmed that flucytosine (5FC) is a significantly superior partner drug for amphotericin B-based treatments compared with fluconazole, leading to a substantial mortality reduction of 38% (95% CI: 16–55, $p = 0.002$). As a consequence, the WHO guidelines were revised and now recommend first-line treatment with seven days of amphotericin B deoxycholate and flucytosine 100 mg/kg/day followed by seven days of fluconazole 1200 mg/

day. In settings where flucytosine is unavailable, which reflects most settings in Africa, the guidelines continue to recommend 14 days of amphotericin B deoxycholate with fluconazole [16].

A newer lipid-based formulation of amphotericin B deoxycholate (L-AmB or AmBisome©) is particularly suited for use in short-course yet highly effective induction treatment for HIV-associated CM, due to: (1) the potential for high dosing made possible by the lower rates of drug-induced toxicity; and (2) the long tissue half-life. In the context of HIV-associated CM, 14-day courses of conventional amphotericin B deoxycholate are associated with an average drop in haemoglobin of 2.3 g/dL and a mean increase in creatinine of 73% [17]. Even at high doses, L-AmB is associated with significantly less nephrotoxicity and anaemia as well as lower rates of infusion reactions than conventional amphotericin B deoxycholate [18]. The long tissue half-life of L-AmB following high-dose administration in patients is well-established [19–22], as is its effective penetration into brain tissue [23]. The concept of single or intermittent dosing with very high doses is also established in both prophylaxis in haematology patients and treatment of visceral leishmaniasis in lower- and middle-income countries [24]. Single doses of up to 15 mg/kg have been safely given; doses of 10 mg/kg are routinely given with demonstration of efficacy for treatment of visceral leishmaniasis and invasive fungal infections [24, 25]. Pharmacokinetic data from animal models [20] and humans [19] suggest that increasing L-AmB dosing from the currently recommended 3–4 mg/kg may lead to improved outcomes and, as with standard amphotericin B, that intermittent dosing regimens may be as effective as daily therapy [20]. Although L-AmB is recommended as treatment for HIV-associated CM in several national guidelines, optimal dosing is unknown and the strategy of short-course high dosing of L-AmB has not yet been tested in a phase III clinical trial [18].

A randomised controlled trial comparing L-AmB 3 mg/kg/day, L-AmB 6 mg/kg/day and amphotericin B deoxycholate 0.7 mg/kg/day, all given for 14 days, showed no difference in mortality outcome between any of these regimens [18]; 3 mg/kg/day is widely used as the standard dose. However, murine models suggest dosing of 3 mg/kg/day may be sub-optimal [20]. Further evidence to support this comes from the recently completed phase II AMBITION trial which was performed with the primary objective of determining the rate of cryptococcal clearance from cerebrospinal fluid (CSF), presented as Early Fungicidal Activity (EFA), of three alternative schedules of intermittent high-dose L-AmB in comparison with 14 days of standard daily L-AmB for induction therapy for HIV-associated CM [26]. Eighty participants were recruited at sites in Botswana and Tanzania and randomised to one of four treatment arms: (1) L-AmB 10 mg/kg day 1 (single dose); (2) L-AmB 10 mg/kg day 1, L-AmB 5 mg/kg day 3 (two doses); (3) L-AmB 10 mg/kg day 1, L-AmB 5 mg/kg days 3 and 7 (three doses); or (4) the control arm, being standard 14-day L-AmB (3 mg/kg/day). All treatment arms received high-dose fluconazole (1200 mg/day) for 14 days. This phase II trial was stopped by the Data Monitoring Committee (DMC) at the pre-planned interim analysis stage of 80 patients as the primary endpoint had been reached with the recommendation that the trial proceed onto the current clinical endpoint phase III trial using single dose L-AmB. The primary analysis showed that the EFA in all three short-course high-dose arms was comparable to, or greater than, the control arm, with statistical non-inferiority between all short-course arms and control at the pre-defined non-inferiority (NI) of 0.2 $\log_{10}$ colony forming units (CFU)/mL/day difference (Fig. 1). There was no evidence for any dose response effect with additional L-AmB doses, suggesting maximal fungicidal activity was achieved with a single 10 mg/kg dose. All three high-dose short-course L-AmB regimens were well tolerated, with only one Division of AIDS (DAIDS) grade IV laboratory toxicity event occurring during induction therapy, and a total of seven grade III and no grade IV clinical adverse events (AEs) associated with high-dose L-AmB. This toxicity profile compared to 33% of patients reporting grade III or IV anaemia in a combined cohort of 368 patients treated in Africa with conventional amphotericin B for 14 days [27]. There were no safety concerns with short-course treatment and no patients receiving short-course L-AmB required additional 'rescue' L-AmB therapy. Overall mortality in the trial was 29% at ten weeks, comparing very favourably with recent trials of amphotericin B deoxycholate-based treatments, with no significant difference between arms [17].

However, although EFA is an extremely valuable tool to rapidly screen novel antifungal treatment regimens and is associated with mortality [28], it has not been validated as a true 'surrogate' marker of outcome. Large phase III trials with a mortality endpoint are critical to define the optimal treatment regimens for HIV-associated CM and are essential to influence policy.

Method/design

Study design

The AMBITION trial is an open label, phase III, randomised controlled non-inferiority, multi-centre trial to compare single, high-dose L-AmB treatment to seven-day amphotericin B deoxycholate-based treatment for HIV-associated CM (Additional files 1 and 2).

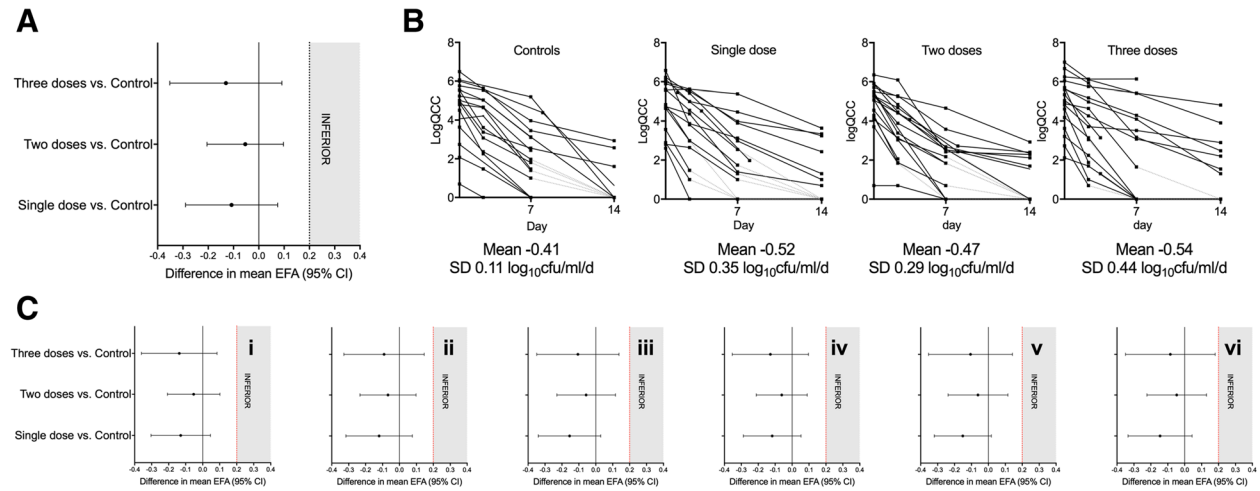

Fig. 1 Primary and key secondary outcomes of the AMBITION Step I phase-II randomised controlled trial. The figure shows: (**a**) all three short-course treatment arms were non-inferior to control; (**b**) EFA and the individual patient slopes over the initial 14 days of treatment; and (**c**) all three short-course treatment arms remained non-inferior to control when controlling for baseline fungal burden (QCC), baseline CD4 count, baseline mental status, QCC and CD4 count, QCC count, CD4 count, mental status and QCC, CD4 count, mental status, sex, age and ART status [26]

Hypothesis

Short-course, high-dose L-AmB given with 14 days of high-dose fluconazole and flucytosine will be non-inferior to seven days of daily-dosed amphotericin B deoxycholate given with seven days of flucytosine, followed by seven days of high-dose fluconazole, for the treatment of HIV-associated CM with all-cause mortality as the primary efficacy endpoint.

Objectives

The primary objective is to determine whether single, high-dose L-AmB given with 14 days of high-dose fluconazole and flucytosine is non-inferior to seven days of daily-dosed amphotericin B deoxycholate given with seven days of flucytosine, followed by seven days of high-dose fluconazole in terms of all-cause mortality in HIV-associated CM patients.

Setting

The trial will be conducted in six large referral hospitals across five countries in sub-Saharan Africa. The sites include: Princess Marina Hospital, Gaborone, Botswana; Mitchells Plain District Hospital, Cape Town, South Africa; Parirenyatwa Central Hospital, Harare, Zimbabwe; Queen Elizabeth Central Hospital, Blantyre, Malawi; Kamuzu Central Hospital, Lilongwe, Malawi; and the Infectious Diseases Institute, Kampala and Mbarara, Uganda.

Outcome measures

The primary outcome measure is all-cause mortality within the first ten weeks after randomisation (non-inferiority). Secondary outcome measures include: EFA derived from serial lumbar punctures (LPs) on days 1, 7 and 14; proportions of patients in each arm developing clinical and DAIDS laboratory-defined grade III/IV AEs; median % change from baseline in laboratory defined parameters; PK parameters and PK/PD associations of single high-dose L-AmB; health service costs; all-cause mortality within the first two and four weeks; all-cause mortality within the first ten weeks (superiority analysis); rates of cryptococcal relapse / IRIS within the first ten weeks; and disability at ten weeks.

Sample size

The WHO now recommends seven days amphotericin B deoxycholate-based regimens for the treatment of CM if flucytosine is available as an adjunctive antifungal. A non-inferiority design has been chosen as the primary aim of this trial is to identify an alternative safe and easy to administer short-course L-AmB treatment regimen that can be implemented in settings where giving amphotericin B deoxycholate-based treatment is difficult or impossible. An efficacious single dose L-AmB treatment would also markedly facilitate CM therapy in settings currently using amphotericin B deoxycholate-based treatment, reducing the duration of hospitalisation and the associated risks (e.g. nosocomial sepsis) and costs. Ten-week mortality in our previous trials using amphotericin B deoxycholate-based regimens at the study sites has been in the range of 28–41% [13, 29]; it was 30% with short-course high-dose L-AmB treatments in the recent phase II study. Assuming 35% ten-week mortality in both the control and test groups and using a 10% non-inferiority margin (i.e. the upper margin of the one-sided 95% CI of the difference in ten-week

mortality between the two arms does not exceed 10%) and one-sided 5% type one error, 390 participants would be required per arm to achieve 90% power. This sample size will also have 83.25% power at a one-sided $\alpha = 0.025$ or two-sided $\alpha = 0.05$. The 10% non-inferiority margin has been chosen to ensure that only clinically unimportant differences are deemed non-inferior and is in keeping with conventional practice. If the ten-week mortality is increased to 40% the equivalent sample size is 412 per arm. Making a conservative allowance for withdrawals and losses to follow-up of up to 8% (losses are in the range of 2–4% in similar trials [10]), or a higher than anticipated mortality rate, we plan to enrol 425 participants per arm. Thus, we will randomise a total of 850 participants. This will be the largest CM treatment trial conducted in Africa.

Inclusion and exclusion criteria

Consecutive patients aged ≥ 18 years with a first episode of CM (confirmed by either India ink or cryptococcal antigen [CrAg] test in the CSF) will be enrolled. Participants must be HIV-infected or willing to undertake an HIV test if their status is unknown. Participants must provide written informed consent or, if unable to consent, have a next of kin who agrees to the patient participating in the study, providing written consent. Pregnant (confirmed by urinary or serum pregnancy test) or lactating women, patients with a previous serious reaction to study drugs, or patients on antifungal treatment at CM treatment doses (amphotericin B deoxycholate ≥ 0.7 mg/kg or fluconazole ≥ 800 mg/day) for > 48 h or concomitant medication that is contraindicated with the study drugs at the time of assessment will be excluded.

Consent

Written informed consent to enter the trial and be randomised will be obtained from participants or, in the case of those lacking capacity to consent, from next of kin with legal responsibility (if appropriate and in keeping with national guidance and regulations). Consent will be obtained after explanation of the aims, methods, benefits and potential hazards of the trial, and before any trial-specific procedures are performed or any blood is taken for the trial. Once the patient's mental status improves and they regain the capacity to consent, persons enrolled via surrogate consent will be re-consented, with care taken to ensure they understand that they are: (1) free to withdraw from the research study; and (2) if they do withdraw, this will not jeopardise their future care. Patients who withdraw will revert to the standard of care at the treatment site (usually amphotericin B deoxycholate and fluconazole daily for two weeks or fluconazole monotherapy for two weeks). It will be made unambiguously clear that the participant (or guardian) is free to refuse to participate in all or any aspect of the research trial, at any time and for any reason, without incurring any penalty or affecting their access to the standard treatment available at the recruiting site (or that of their relative). Separate consent forms will be completed for the storage and/or genetic analysis of samples as determined by local guidelines. Original signed consent forms will be kept by the investigator and documented in the electronic case report form (eCRF), a copy given to the participant or family and a copy placed in the participant's medical notes.

Allocation

Patients will be randomised individually using a computer-generated programme. Randomisation codes will be generated via a permuted-block randomisation method and stratified by site. Block sizes will vary at four and six. Randomisation lists will be created for each site by an independent statistician and each list will be housed on the electronic data capture system (EDC) for that particular site. The full lists will be inaccessible to trial staff. Randomised allocation for each trial participant will be provided to trial staff from the randomisation list for that site. Internally, the EDC selects against the electronic randomisation and guarantees to make the selection in the natural order of the list. Once a selection is made, the randomisation record is tagged with the participant study allocated identifier, date and time of randomisation, and other EDC system audit values (username, machine name, etc).

Interventions

Participants will be randomised to receive either intravenous L-AmB 10 mg/kg on day 1 given with 14 days of oral fluconazole 1200 mg/day and oral flucytosine 100 mg/kg/day (intervention) or intravenous amphotericin B deoxycholate 1 mg/kg/d for seven days given with seven days of oral flucytosine 100 mg/kg/day followed by seven days of oral fluconazole 1200 mg/day (control) (Fig. 2). After the two-week induction phase, all participants will then receive oral fluconazole 800 mg/day to complete ten weeks therapy and 200 mg/day thereafter. ART will be commenced four to six weeks after initiation of antifungal therapy, in line with national guidelines. Given the combination of oral and intravenous therapies, the differing duration in days of intravenous therapy and the known drug-induced toxicities that require monitoring and managing, blinding of treatment allocation was deemed to be impractical. To counter this, an objective endpoint of all-cause mortality has been chosen. In addition, all staff performing quantitative cell cultures are blind to treatment, as are coordinating investigators, including the Trial Management Group (TMG) members.

Rescue medication

Although the results from our phase II trial demonstrate that it is unlikely that CSF fungal burden will increase

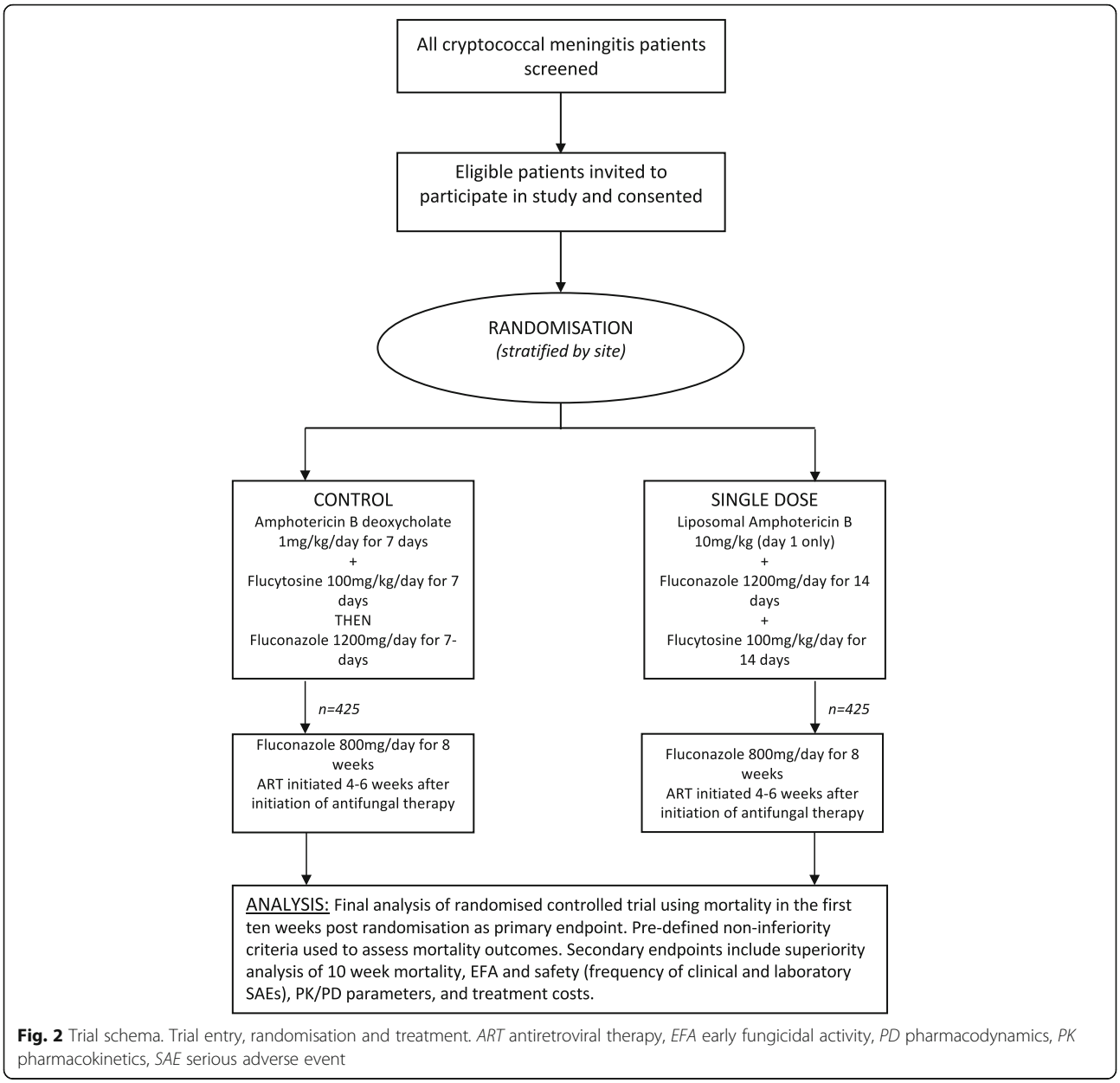

Fig. 2 Trial schema. Trial entry, randomisation and treatment. *ART* antiretroviral therapy, *EFA* early fungicidal activity, *PD* pharmacodynamics, *PK* pharmacokinetics, *SAE* serious adverse event

after initiation of treatment, if the day 7 LP identifies an increase in CFU from baseline this will be reported as a serious adverse event (SAE) and experienced, senior clinicians at the coordinating centre will be responsible for managing this situation on a case-by-case basis to ensure all participants receive effective induction therapy.

Schedule

All participants will be admitted to hospital for a minimum of one week. As the induction phase occurs over two weeks if participants are well enough to be discharged after day 7 and before day 14, treatment will be given under close outpatient supervision during the second week, ensuring compliance to the trial intervention and facilitating close clinical and laboratory monitoring. After the intensive phase, participants will be seen in clinic at four, six, eight and ten weeks and a single telephone follow-up to ascertain vital status and level of disability will be made at week 16. Every effort will be made (e.g. with mobile telephone calls, home visits and financial help with travelling expenses) to obtain accurate and complete follow-up data for ten weeks after the start of treatment. Particular attention will be paid to the possibility, in ART-naïve participants, of developing IRIS after starting ART [30].

Participants will have a full history and examination at baseline (Table 1). Blood will be drawn for full blood count (FBC), urea, creatinine, electrolytes and alanine transaminase (ALT). If unknown, HIV serology will be

Table 1 Schedule of enrolment, interventions and assessments adapted from the Standard Protocol Items: Recommendations for Interventional Trials (SPIRIT) figure

	Screening	Week 1							Week 2							Week 4	Week 6	Week 8	Week 10	Week 16
Study day	≤D0	D1	D2	D3	D4	D5	D6	D7	D8	D9	D10	D11	D12	D13	D14					
Consent and randomisation																				
Eligibility criteria	X	X																		
PIS and signed consent	X	X																		
Randomisation	X	X																		
Treatment																				
Intervention: Ambisome 10 mg/kg		X																		
Intervention: Fluconazole 1200 mg/day		X	X	X	X	X	X	X	X	X	X	X	X	X	X					
Intervention: Flucytosine 100 mg/kg/day		X	X	X	X	X	X	X	X	X	X	X	X	X	X					
Control: Amphotericin B deoxycholate 1 mg/kg		X	X	X	X	X	X	X												
Control: Flucytosine 100 mg/kg/day		X	X	X	X	X	X	X												
Control: Fluconazole 1200 mg/day									X	X	X	X	X	X	X					
All participants: Fluconazole 800 mg/day															X	X	X	X	X	
All participants: 200 mg/day																			X	X
Clinical, safety and compliance assessment																				
Inpatient clinical review		X	X	X	X	X	X	X	X	X	X	X	X	X	X					
Outpatient follow-up																X	X	X	X	
Week 16 telephone																				X
Clinical labs																				
HIV testing		X																		
Pregnancy test (urine/serum)[a]		X																		
Full blood count		X						X							X	X				
CD4 count		X																		
ALT		X						X							X	X				
Urea, creatinine and electrolytes		X		X		X		X			X		X		X	X				
Drug levels		X						X												
Quantitative PCR sub-study		X		X				X							X					
Semi-quantitative cryptococcal antigen		X																		
CSF																				
Opening pressure		X						X							X					
Cell count and differential[b]		X																		
Protein, glucose[b]		X																		

Table 1 Schedule of enrolment, interventions and assessments adapted from the Standard Protocol Items: Recommendations for Interventional Trials (SPIRIT) figure *(Continued)*

	Screening	Week 1							Week 2							Week 4	Week 6	Week 8	Week 10	Week 16
Study day	≤D0	D1	D2	D3	D4	D5	D6	D7	D8	D9	D10	D11	D12	D13	D14					
Routine culture[b]		X																		
India ink examination[b,c]		X																		
Cryptococcal antigen[b,c]		X																		
Quantitative fungal culture		X						X							X					
CSF drug levels		X						X							X					
Immune parameters		X						X							X					
Semi-quantitative cryptococcal antigen		X																		

[a]For women of childbearing age; [b]Part of routine care; [c]India ink or cryptococcal antigen required for inclusion

performed in addition to CD4 and viral load samples, as clinically indicated. Women of reproductive age will have a pregnancy test (urine or serum). All participants will have an LP for opening pressure, total and differential white cell count, protein, glucose, India ink, CrAg, routine culture, quantitative fungal culture and immune parameters. Further blood samples will be collected on days 3, 5, 7, 10, 12, 14 and 28 for urea and creatinine. FBC and ALT will be repeated on days 7, 14 and 28. Additional samples will be taken alongside monitoring blood tests for sub-studies, including PK/PD studies. LPs will be repeated on days 7 and 14 for opening pressure, quantitative fungal culture, CSF drug levels and immune parameters. Raised intracranial pressure will be managed with LPs as per a standard operating procedure. Cryptococcal clearance rates will be calculated using summary statistics for each patient: the rate of decrease in $\log_{10}$ CFU per mL CSF per day derived from the slope of the linear regression of $\log_{10}$ CFU against time for each patient. A linear regression model will be used to compare mean rates of decline EFA for each arm, giving summary differences with 95% CI and significance levels [31, 32]. We will adjust analyses for potential confounding factors, including baseline fungal burden. Disability at ten weeks will be assessed using two simple questions and a modified Rankin scale.

Statistical methods

The primary endpoint (all-cause mortality at ten weeks) will be analysed using a generalised linear model (GLM). The model will have treatment group as the sole predictor, a binomial distribution and an identity-link function, from which the (unadjusted) risk difference between the treatment groups and its one-sided 95% CI will be estimated. If the upper limit of the one-sided 95% CI falls below the non-inferiority margin of 10%, non-inferiority will be declared. Sensitivity analyses of the primary endpoint making different assumptions for the losses to follow-up will be conducted. Covariate-adjusted analyses for the primary endpoint will be conducted by adding pre-specified covariates into the GLM model to derive the adjusted risk difference and the upper limit of one-sided 95% CI. Imputation for baseline missing covariates will be made for the covariate-adjusted analysis. Subgroup analysis of the primary endpoint will also be performed on prespecified covariates.

The analyses of the secondary endpoints will be based on superiority test using a 5% two-sided significance level. Analyses of survival data will be conducted using unadjusted Cox regression analysis to calculate the HR and 95% CI between the treatment groups. Kaplan–Meier survival curves by treatment group will be calculated and displayed. A log-rank test will be conducted to compare the survival curves between the treatment groups. Analyses of binary secondary outcomes will be performed in a similar way as the primary endpoint analysis using GLMs with treatment group as the sole predictor. The point estimate of the treatment effect with two-sided 95% CI will be derived. The safety analysis will be descriptive and the frequency and proportions of participants suffering clinical and laboratory-defined side effects will be generated by treatment arms. Other statistical analyses may be performed if deemed necessary.

Data will be analysed using SAS 9.4 and Stata 13. Findings will be reported according to the Consolidated Standards of Reporting Trials (CONSORT) guidelines for randomised controlled trials. Primary analyses will be based on the intention-to-treat population and secondary analyses will be based on the per-protocol population. All analyses will be described in detail in the finalised and signed statistical analysis plan before data are locked and unblinding occurs.

Dissemination of results

The results of the trial will be analysed, presented and published as soon as possible. The TMG will form the basis of the Writing Committee and will advise on the nature of the publication. The names of all investigators will be included in the authorship of any publication. An authorship policy will be agreed by all investigators before the commencement of the trial. The independent members of the Trial Steering Committee (TSC) and DMC will be listed with their affiliations in the acknowledgements or appendix sections of the main publication. The funders will have no role in the decision to publish or the content of the publication.

Ethical approval

The Research Ethics Committee of the London School of Hygiene and Tropical Medicine have approved the protocol v2.1 07.11.17 (ref. 14,355). Approval has also been granted by the following: University of Botswana Office of Research and Development (UBR/RES/IRB/BIO/042); Botswana Ministry of Health and Wellness Health Research and Development Division (HPDME:13/18/1); Princess Marina Hospital Research and Ethics Committee (PMH 5/79(407-1-2017); University of Cape Town Human Research Ethics Committee (642/2017); Malawi National Health Sciences Research Committee (1907); Mulago Hospital Research and Ethics Committee (MHREC 1297); and the Medical Research Council of Zimbabwe (MRCZ/A/2263). Any amendments will be submitted and approved by each ethics committee.

Timeline

In total, 850 participants will be recruited over a three-year period with a planned trial completion date of

31 December 2020. This is feasible based upon previous experience and rates of CM at the hospital sites.

Ancillary studies

PK/PD

The PK/PD of L-AmB, fluconazole and flucytosine and the impact of PK variability on outcome will be described. Plasma samples will be collected at the end of the L-AmB infusion and then at 2, 4, 8, 12 and 24 h in a sub-study of participants at the Blantyre study site. A portion (0.5 mL) of the CSF sample obtained for quantitative counts will be reserved to measure fluconazole and flucytosine concentrations and thereby estimate the extent of penetration of these drugs into the CSF. Amphotericin levels will not be measured in CSF since they are known to be negligible. A PK-PD model will be constructed to explore the persistence of amphotericin B within the central nervous system and the resultant antifungal effect. Amphotericin penetration into the CNS will be estimated using compartmental modelling techniques. Monte Carlo simulation will enable further insights into the regimen(s) that may be associated with maximal antifungal activity.

Economic analysis

An economic analysis will be conducted to provide evidence for the cost-effectiveness of short-course L-AmB treatment. The objective of the economic analysis is to estimate the cost consequences and the cost-effectiveness of short-course L-AmB treatment compared to current care. Both societal and healthcare perspectives are chosen and health service patient costs including household costs, treatment cost and hospitalisations in both arms will be compared over the trial period in a probabilistic approach, using Monte Carlo bootstrapping methods in STATA, @Risk software and TreeAge. In the country-specific cost-consequence analyses, the societal and health service costs will be compared and used along with the trial-wide primary endpoint data to perform cost-effectiveness modelling using a decision-tree model for each country with historical data as comparison.

Semi-quantitative CrAg testing and diagnostic quantitative polymerase chain reaction (PCR)

A newly developed point of care, lateral flow, semi-quantitative CrAg test is now available from Institut Pasteur and Biosynex. We will use this semi-quantitative test in real time to determine antigen titre at baseline, in blood and CSF, and compare results to the currently established point of care test. Secondary trial analyses will include the association of baseline titre with outcome and exploration of the possibility of a differential treatment response between arms according to baseline titre. If such a differential response was observed, this sub-study could provide the rationale for and demonstrate the means for individualised treatment, based on a rapid assessment of antigen load. A novel diagnostic quantitative PCR (DNA and RNA) tool will be also be used in each treatment arm and correlated with quantitative culture counts. We aim to estimate the fungal load and fungal viability in blood and CSF at baseline using the PCR in addition to fungal load kinetics on treatment. The objective will be to develop a practical alternative to time-consuming quantitative cultures in order to improve detection of fungaemia and measurement of fungal burden and develop a novel biomarker for assessing the best fungicidal treatments in this and subsequent research studies.

Quality control and assurance

Trial oversight will be provided by the TMG, TSC and Independent DMC. The study sponsor is the London School of Hygiene and Tropical Medicine. The sites will be monitored at regular intervals with visits by the trial manager/monitor in order to monitor the conduct of the trial and ensure that the principles of International Conference of Harmonisation (ICH) Good Clinical Practice (GCP) are being adhered to. Sites will be visited by an internal monitor for initiation visits before starting recruitment, after the first 10–15 participants, at 40% and 70% of recruitment targets and at trial closure, with additional visits made if required. Visits will ensure that all training has been completed, that drug supply and equipment are in place and that all staff are up to date on the protocol and procedures. A monitor from the Sponsor will visit at least three of the six sites. Central monitoring will be performed in addition to the on-site monitoring procedures. Bimonthly reports on the progress of the trial as well as the frequency of DAIDS laboratory-defined grade III/IV AEs/SAEs/suspected unexpected serious adverse events (SUSARs) will be compiled by the trial manager/statistician and reviewed by the Sponsor. All Grade IV AEs, all SAEs and all SUSARs will be reported to the TMG within 24 h [27].

Data collection and data management

eCRF data collected and validated using the EDC will be stored in an electronic database that is protected using a scheme of authentication and encryption. Paper documents, such as clinical notes and administrative documentation, will be kept in a secure location and held for at least five years after the end of the trial. During this period, all data should be accessible to the competent or equivalent authorities, the sponsor and other relevant parties with suitable notice. Security of electronic records and data is a significant concern. All components of the distributed data systems will use authentication and encryption to render subject identity and personal health information unusable, unreadable or indecipherable to

unauthorised individuals. Full drive encryption will be implemented at the hardware layer of all devices storing protected health information. A three-factor scheme will be used to authenticate users through the hardware layer to the application layer where personal health information is available. The applications will have user profiles to control access to certain data and reports. The application and database layers will use a combination of hashing and encryption for sensitive and personal data. Mobile devices and the staff operating them will not be equipped with the encryption keys to decrypt selected sensitive data fields.

Confidentiality

We will follow the principles of the UK Data Protection Act (DPA) regardless of the countries where the trial is being conducted. Consent forms will be stored under the supervision of each local primary investigator (PI) in a secured office and accessible to trial staff only. Participants' personal details are stored in an encrypted, separate server to the main database and participants are identified by their study number throughout the trial.

Termination of the study

The trial will be considered closed when the last patient has completed ten weeks of active follow-up in the study, the 16-week telephonic follow-up call, and all follow-up and laboratory reports, including repeat plasma HIV viral load testing in ART failure cases, have been received. Early termination could occur if the DMC decides there is an unacceptable level of AEs in either test arm or if the intervention arm is shown to be inferior with stringent p value testing.

Indemnity

The sponsor of the trial is the London School of Hygiene and Tropical Medicine and as such provides indemnity for the trial. All personnel involved in the trial will be expected to be indemnified by their employing authority. Local insurance will be taken out where local regulations require this.

Discussion

The potential impact of a safe, sustainable regimen of high-dose L-AmB with non-inferior efficacy when compared to one week of daily-dosed amphotericin B deoxycholate would be to reduce the number of AEs seen in patients treated with amphotericin and shorten the length of hospital admissions. It is hoped that our economic analysis will demonstrate the cost-effectiveness of this intervention across all our sites in southern Africa and provide a highly favourable alternative to the current WHO-recommended first-line treatment.

Trial status

The study is jointly funded through the European and Developing Countries Clinical Trials Partnership (EDCTP), Swedish International Development Cooperation Agency (SIDA) and Wellcome Trust / Medical Research Council (UK) / UKAID Joint Global Health Trials. Recruitment commenced in Botswana in January 2018 and in South Africa in July 2018; recruitment will commence at the other sites pending the requisite ethical and regulatory approvals.

Additional files

Additional file 1: AMBITION Study Protocol v2.1 date: 7th November 2017. (PDF 1954 kb)

Additional file 2: AMBITION Study SPIRIT Checklist. (DOC 121 kb)

Abbreviations

5FC: Flucytosine; ACTA: Advancing Cryptococcal Meningitis Treatment for Africa; AE: Adverse event; ALT: Alanine transaminase; AMBIsome Therapy Induction OptimisatioN; ART: Antiretroviral therapy; CFU: Colony-forming units; CI: Confidence interval; CM: Cryptococcal meningitis; CrAg: Cryptococcal antigen; CSF: Cerebrospinal fluid; DAIDS: Division of AIDS; DMC: Data Monitoring Committee; DPA: Data Protection Act; eCRF: Electronic case record form; EDC: Electronic data capture; EDCTP: European and Developing Countries Clinical Trials Partnership; EFA: Early fungicidal activity; FBC: Full blood count; GCP: Good Clinical Practice; GLM: Generalised linear model; HR: Hazard ratio; ICH: International Conference of Harmonisation; IRIS: Immune reconstitution inflammatory syndrome; L-AmB: Liposomal amphotericin B deoxycholate; LP: Lumbar puncture; LSHTM: London School of Hygiene and Tropical Medicine; NI: Non-inferiority; PD: Pharmacodynamics; PI: Primary investigator; PK: Pharmacokinetics; SAE: Serious adverse event; SAR: Serious adverse reaction; SUSAR: Suspected unexpected serious adverse reaction; TMG: Trial Management Group; TSC: Trial Steering Committee; USD: United States Dollar; WHO: World Health Organization

Acknowledgements

We acknowledge the support offered by the individual sites and staff: Princess Marina Hospital, Gaborone, Botswana; Queen Elizabeth Central Hospital, Blantyre and Kamuzu Central Hospital, Lilongwe, Malawi; Mitchell's Plain Hospital, Cape Town, South Africa; Parirenyatwa Hospital, Harare, Zimbabwe; Mulago Hospital, Kampala and Mbarara Regional Referral Hospital, Mbarara, Uganda; the Trial Steering Committee and the Independent Data Monitoring Committee for monitoring the trial.

Funding

The study is jointly funded through the European and Developing Countries Clinical Trials Partnership (EDCTP), Swedish International Development Cooperation Agency (SIDA) and Wellcome Trust / Medical Research Council (UK) / UKAID Joint Global Health Trials. The AmBisome for the trial has been donated by Gilead. The funders had no role in the design of the trial, nor will they be involved in the collection, analysis and interpretation of data or the preparation of manuscripts. Katharine Stott is a Wellcome Trust Clinical PhD Fellow (203919/Z/16/Z).

Availability of data and materials

Not applicable.

Authors' contributions

DSL wrote the initial manuscript and is the International Lead Clinician for the AMBITION study. NY and SFM helped write the manuscript and are the International Trial Manager and Trial Epidemiologist, respectively. DRB, AH, MH, CK, DBM, MM, CM, HCM, CEN and CS are site investigators. TC and DW are statisticians for the study. LN leads the Health Economics sub-study. KES and WH oversee the PK/PD sub-study. AA, OL, FD and TBC coordinate the

semi-quantitative CrAg and qPCR sub-studies. TBC is international clinical adviser to the study. AL is an expert adviser within the TMG. SJ, DGL and GM provided expert input into the conceptualisation and design of the study. TSH conceived and designed the trial and is the co-principal investigator. JNJ conceived and designed the trial and is the co-principal investigator. All authors read and approved the final manuscript.

Ethics approval and consent to participate

The Research Ethics Committee of the London School of Hygiene and Tropical Medicine (ref. 14,355) have approved the protocol. We will not begin recruitment at any of the African sites until local ethical approval has been obtained. Any further amendments will be submitted and approved by each ethics committee.

Written informed consent to enter the trial and be randomised will be obtained from participants or, in the case of those lacking capacity to consent, from family/guardians/persons with legal responsibility (if appropriate and in keeping with national guidance and regulations). Consent will be obtained after explanation of the aims, methods, benefits and potential hazards of the trial, and before any trial-specific procedures are performed or any blood is taken for the trial. Patients with altered mental status who are unable to consent will be enrolled into the study if their next of kin gives informed consent or assent (in keeping with appropriate national guidance and regulations) on their behalf. As soon as the patient's mental status improves consent will be obtained as above, with care taken to ensure they understand that they are free to withdraw from the study and if they do so this will not jeopardise their future care. Participants who withdraw will revert to the standard of care at the treatment site (usually amphotericin B deoxycholate and fluconazole daily for two weeks or fluconazole monotherapy for two weeks). It must be made completely and unambiguously clear that the participant (or guardian) is free to refuse to participate in all or any aspect of the trial, at any time and for any reason, without incurring any penalty or affecting their access to the standard treatment available at the recruiting site (or that of their relative). Separate consent forms will be completed for the storage and/or genetic analysis of samples as determined by local guidelines. Original signed consent forms will be kept by the investigator and documented in the eCRF, a copy given to the participant or family and a copy placed in the participant's medical notes.

Consent for publication

Not applicable.

Competing interests

JNJ and TSH were the recipients of a Gilead Investigator Initiated Award (completed). TSH has received speaker fees from Gilead Sciences and Pfizer.

Publisher's Note

Author details

[1]Department of Clinical Research, Faculty of Infectious and Tropical Diseases, London School of Hygiene and Tropical Medicine, London, UK. [2]Botswana-Harvard AIDS Institute Partnership, Gaborone, Botswana. [3]Research Centre for Infection and Immunity, St George's University of London, London, UK. [4]Molecular Mycology Unit and National Reference Centre for Invasive Mycoses, Institut Pasteur, Paris, France. [5]Malawi-Liverpool-Wellcome Trust Clinical Research Programme, University of Malawi College of Medicine, Blantyre, Malawi. [6]Infectious Diseases Institute, College of Health Sciences, Makerere University, Kampala, Uganda. [7]Department of Medicine, University of Minnesota, Minneapolis, MN, USA. [8]Department of Clinical Sciences and International Public Health, Liverpool School of Tropical Medicine, Liverpool, UK. [9]Department of Medicine, University of Zimbabwe College of Health Sciences, Parirenyatwa Hospital, Harare, Zimbabwe. [10]Department of Molecular and Clinical Pharmacology, University of Liverpool, Liverpool, UK. [11]Lilongwe Medical Relief Trust (UNC Project), Lilongwe, Malawi. [12]Department of Internal Medicine, University of Botswana, Gaborone, Botswana. [13]Wellcome Centre for Infectious Diseases Research in Africa (CIDRI-Africa), Institute of Infectious Disease and Molecular Medicine, and Department of Medicine, University of Cape Town, Cape Town, South Africa.

Received: 16 August 2018 Accepted: 29 October 2018
Published online: 23 November 2018

References

1. Braitstein P, Brinkhof MW, Dabis F, Schechter M, Boulle A, Miotti P, et al. Mortality of HIV-1-infected patients in the first year of antiretroviral therapy: comparison between low-income and high-income countries. Lancet. 2006; 367(9513):817–24.
2. Lawn SD, Harries AD, Anglaret X, Myer L, Wood R. Early mortality among adults accessing antiretroviral treatment programmes in sub-Saharan Africa. AIDS. 2008;22(15):1897–908.
3. Amuron B, Namara G, Birungi J, Nabiryo C, Levin J, Grosskurth H, et al. Mortality and loss-to-follow-up during the pre-treatment period in an antiretroviral therapy programme under normal health service conditions in Uganda. BMC Public Health. 2009;9:290.
4. Gupta A, Nadkarni G, Yang WT, Chandrasekhar A, Gupte N, Bisson GP, et al. Early mortality in adults initiating antiretroviral therapy (ART) in low- and middle-income countries (LMIC): a systematic review and meta-analysis. PLoS One. 2011;6(12):e28691.
5. Jarvis JN, Boulle A, Loyse A, Bicanic T, Rebe K, Williams A, et al. High ongoing burden of cryptococcal disease in Africa despite antiretroviral roll out. AIDS. 2009;23(9):1182–3.
6. Jarvis JN, Meintjes G, Williams A, Brown Y, Crede T, Harrison TS. Adult meningitis in a setting of high HIV and TB prevalence: findings from 4961 suspected cases. BMC Infect Dis. 2010;10:67.
7. Rajasingham R, Smith RM, Park BJ, Jarvis JN, Govender NP, Chiller TM, et al. Global burden of disease of HIV-associated cryptococcal meningitis: an updated analysis. Lancet Infect Dis. 2017;17(8):873–81.
8. Wall EC, Everett DB, Mukaka M, Bar-Zeev N, Feasey N, Jahn A, et al. Bacterial meningitis in Malawian adults, adolescents, and children during the era of antiretroviral scale-up and Haemophilus influenzae type b vaccination, 2000-2012. Clin Infect Dis. 2014;58(10):e137–45.
9. Jarvis JN, Harrison TS. Forgotten but not gone: HIV-associated cryptococcal meningitis. Lancet Infect Dis. 2016;16(7):756–8.
10. Molloy SF, Kanyama C, Heyderman RS, Loyse A, Kouanfack C, Chanda D, et al. Antifungal combinations for treatment of cryptococcal meningitis in Africa. N Engl J Med. 2018;378(11):1004–17.
11. Jarvis JN, Bicanic T, Loyse A, Namarika D, Jackson A, Nussbaum JC, et al. Determinants of mortality in a combined cohort of 501 patients with HIV-associated Cryptococcal meningitis: implications for improving outcomes. Clin Infect Dis. 2014;58(5):736–45.
12. Bicanic T, Wood R, Meintjes G, Rebe K, Brouwer A, Loyse A, et al. High-dose amphotericin B with flucytosine for the treatment of cryptococcal meningitis in HIV-infected patients: a randomized trial. Clin Infect Dis. 2008;47(1):123–30.
13. Jarvis JN, Meintjes G, Rebe K, Williams GN, Bicanic T, Williams A, et al. Adjunctive interferon-gamma immunotherapy for the treatment of HIV-associated cryptococcal meningitis: a randomized controlled trial. AIDS. 2012;26(9):1105–13.
14. Longley N, Muzoora C, Taseera K, Mwesigye J, Rwebembera J, Chakera A, et al. Dose response effect of high-dose fluconazole for HIV-associated cryptococcal meningitis in southwestern Uganda. Clin Infect Dis. 2008; 47(12):1556–61.
15. Jackson AT, Nussbaum JC, Phulusa J, Namarika D, Chikasema M, Kanyemba C, et al. A phase II randomized controlled trial adding oral flucytosine to high-dose fluconazole, with short-course amphotericin B, for cryptococcal meningitis. AIDS. 2012;26(11):1363–70.
16. WHO. Guidelines for the diagnosis, prevention, and management of cryptococcal disease in HIV-infected adults, adolescents and children. Geneva: World Health Organization; 2018.
17. Bicanic T, Bottomley C, Loyse A, Brouwer AE, Muzoora C, Taseera K, et al. Toxicity of amphotericin B deoxycholate-based induction therapy in patients with HIV-associated cryptococcal meningitis. Antimicrob Agents Chemother. 2015;59(12):7224–31.
18. Hamill RJ, Sobel JD, El-Sadr W, Johnson PC, Graybill JR, Javaly K, et al. Comparison of 2 doses of liposomal amphotericin B and conventional amphotericin B deoxycholate for treatment of AIDS-associated acute cryptococcal meningitis: a randomized, double-blind clinical trial of efficacy and safety. Clin Infect Dis. 2010;51(2):225–32.
19. Hope WW, Goodwin J, Felton TW, Ellis M, Stevens DA. Population pharmacokinetics of conventional and intermittent dosing of liposomal

amphotericin B in adults: a first critical step for rational design of innovative regimens. Antimicrob Agents Chemother. 2012;56(10):5303–8.
20. O'Connor L, Livermore J, Sharp AD, Goodwin J, Gregson L, Howard SJ, et al. Pharmacodynamics of liposomal amphotericin B and flucytosine for cryptococcal meningoencephalitis: safe and effective regimens for immunocompromised patients. J Infect Dis. 2013;208(2):351–61.
21. Gubbins PO, Amsden JR, McConnell SA, Anaissie EJ. Pharmacokinetics and buccal mucosal concentrations of a 15 milligram per kilogram of body weight total dose of liposomal amphotericin B administered as a single dose (15 mg/kg), weekly dose (7.5 mg/kg), or daily dose (1 mg/kg) in peripheral stem cell transplant patients. Antimicrob Agents Chemother. 2009;53(9):3664–74.
22. Mehta P, Vinks A, Filipovich A, Vaughn G, Fearing D, Sper C, et al. High-dose weekly AmBisome antifungal prophylaxis in pediatric patients undergoing hematopoietic stem cell transplantation: a pharmacokinetic study. Biol Blood Marrow Transplant. 2006;12(2):235–40.
23. Vogelsinger H, Weiler S, Djanani A, Kountchev J, Bellmann-Weiler R, Wiedermann CJ, et al. Amphotericin B tissue distribution in autopsy material after treatment with liposomal amphotericin B and amphotericin B colloidal dispersion. J Antimicrob Chemother. 2006;57(6):1153–60.
24. Sundar S, Chakravarty J, Agarwal D, Rai M, Murray HW. Single-dose liposomal amphotericin B for visceral leishmaniasis in India. N Engl J Med. 2010;362(6):504–12.
25. Cornely OA, Maertens J, Bresnik M, Ebrahimi R, Ullmann AJ, Bouza E, et al. Liposomal amphotericin B as initial therapy for invasive mold infection: a randomized trial comparing a high-loading dose regimen with standard dosing (AmBiLoad trial). Clin Infect Dis. 2007;44(10):1289–97.
26. Jarvis J, Leeme T, Molefi M, Chofle AA, Bidwell G, Tsholo K, et al. Short course high-dose liposomal amphotericin B for HIV-associated cryptococcal meningitis: A phase-II randomized controlled trial. CID. 2018; https://doi.org/10.1093/cid/ciy515.
27. U.S. Department of Health and Human Services, National Institutes of Health, National Institute of Allergy and Infectious Diseases. Division of AIDS (DAIDS) Table for Grading the Severity of Adult and Pediatric Adverse Events. Maryland: Division of AIDS, National Institute of Allergy and Infectious Diseases, National Institutes of Health, US Department of Health and Human Services; 2017.
28. Day JN, Chau TT, Lalloo DG. Combination antifungal therapy for cryptococcal meningitis. N Engl J Med. 2013;368(26):2522–3.
29. Beardsley J, Wolbers M, Day JN. Dexamethasone in cryptococcal meningitis. N Engl J Med. 2016;375(2):189–90.
30. Haddow LJ, Colebunders R, Meintjes G, Lawn SD, Elliott JH, Manabe YC, et al. Cryptococcal immune reconstitution inflammatory syndrome in HIV-1-infected individuals: proposed clinical case definitions. Lancet Infect Dis. 2010;10(11):791–802.
31. Bicanic T, Muzoora C, Brouwer AE, Meintjes G, Longley N, Taseera K, et al. Independent association between rate of clearance of infection and clinical outcome of HIV-associated cryptococcal meningitis: analysis of a combined cohort of 262 patients. Clin Infect Dis. 2009;49(5):702–9.
32. Brouwer AE, Rajanuwong A, Chierakul W, Griffin GE, Larsen RA, White NJ, et al. Combination antifungal therapies for HIV-associated cryptococcal meningitis: a randomised trial. Lancet. 2004;363(9423):1764–7.

J Antimicrob Chemother
doi:10.1093/jac/dky152

Journal of Antimicrobial Chemotherapy

Pharmacokinetics of rifampicin in adult TB patients and healthy volunteers: a systematic review and meta-analysis

K. E. Stott [1]*, H. Pertinez[1], M. G. G. Sturkenboom[2], M. J. Boeree[3], R. Aarnoutse[3], G. Ramachandran[4], A. Requena-Méndez[5], C. Peloquin[6], C. F. N. Koegelenberg[7], J. W. C. Alffenaar[2], R. Ruslami[8], A. Tostmann[9], S. Swaminathan[10], H. McIlleron[11] and G. Davies[1,12]

[1]Department of Molecular and Clinical Pharmacology, Institute of Translational Medicine, University of Liverpool, Liverpool, UK; [2]Department of Clinical Pharmacy and Pharmacology, University Medical Center Groningen, University of Groningen, Groningen, The Netherlands; [3]Radboud University Medical Center, Nijmegen, The Netherlands; [4]Department of Biochemistry and Clinical Pharmacology, National Institute for Research in Tuberculosis, Chennai, India; [5]CRESIB, Barcelona Institute for Global Health, University of Barcelona, Barcelona, Spain; [6]College of Pharmacy and Emerging Pathogens Institute, University of Florida, Gainesville, FL, USA; [7]Department of Pulmonology, Stellenbosch University & Tygerberg Academic Hospital, Cape Town, South Africa; [8]Department of Pharmacology and Therapy, Universitas Padjadjaran, Bandung, Indonesia; [9]Department of Primary and Community Care, Radboud University Medical Centre, Nijmegen, The Netherlands; [10]Indian Council of Medical Research, New Delhi, India; [11]Division of Clinical Pharmacology, University of Cape Town, Cape Town, South Africa; [12]Institute of Global Health, University of Liverpool, Liverpool, UK

*Corresponding author. E-mail: katstott@liverpool.ac.uk orcid.org/0000-0001-7079-7957

Received 19 January 2018; returned 12 February 2018; revised 20 March 2018; accepted 31 March 2018

Objectives: The objectives of this study were to explore inter-study heterogeneity in the pharmacokinetics (PK) of orally administered rifampicin, to derive summary estimates of rifampicin PK parameters at standard dosages and to compare these with summary estimates for higher dosages.

Methods: A systematic search was performed for studies of rifampicin PK published in the English language up to May 2017. Data describing the C_{max} and AUC were extracted. Meta-analysis provided summary estimates for PK parameter estimates at standard rifampicin dosages. Heterogeneity was assessed by estimation of the I^2 statistic and visual inspection of forest plots. Summary AUC estimates at standard and higher dosages were compared graphically and contextualized using preclinical pharmacodynamic (PD) data.

Results: Substantial heterogeneity in PK parameters was evident and upheld in meta-regression. Treatment duration had a significant impact on the summary estimates for rifampicin PK parameters, with C_{max} 8.98 mg/L (SEM 2.19) after a single dose and 5.79 mg/L (SEM 2.14) at steady-state dosing, and AUC 72.56 mg·h/L (SEM 2.60) and 38.73 mg·h/L (SEM 4.33) after single and steady-state dosing, respectively. Rifampicin dosages of at least 25 mg/kg are required to achieve plasma PK/PD targets defined in preclinical studies.

Conclusions: Vast inter-study heterogeneity exists in rifampicin PK parameter estimates. This is not explained by the available modifying variables. The recommended dosage of rifampicin should be increased to improve efficacy. This study provides an important point of reference for understanding rifampicin PK at standard dosages as efforts to explore higher dosing strategies continue in this field.

Introduction

When it was introduced as part of combination therapy for TB in the 1960s, rifampicin revolutionized treatment and shortened the duration of therapy from 18 to 9 months. This would subsequently be shortened further to 6 months with the addition of pyrazinamide.[1] Despite experience gained over the past five decades, the optimal dosage of rifampicin has not been established definitively. The current recommendation of 10 mg/kg in guidelines from the WHO has not changed since the introduction of rifampicin, at which time it was based on toxicological and financial concerns, with limited pharmacokinetic (PK) data available.[2,3]

For therapeutic drug monitoring (TDM) of rifampicin in TB treatment, a C_{max} of 8–24 mg/L (free plus bound drug) was suggested in the 1990s. This recommendation was based on a review of observed PK parameters and on expert opinion. Data from patients infected with HIV were not included.[4,5] There was no pharmacodynamic (PD) component to the target, as MIC data were lacking in

patient samples at that time. In the ensuing 20 year period, this original reference range was accepted as the target for rifampicin C_{max} in numerous studies addressing the utility of TDM for rifampicin.[6–11] Treatment response is slow if rifampicin concentrations fall below this range.[12,13]

More sophisticated PK/PD analyses have since been performed on data from murine and human studies and there is a growing consensus that current dosages of rifampicin are inadequate; drug exposure appears scarcely to reach the upstroke of the dose–response curve.[14] Accordingly, the target range of C_{max} for rifampicin TDM has been revised to emphasize the need to exceed 8 mg/L, rather than focus on an upper limit.[15] At steady-state, drug exposure is thought to increase more than proportionally in response to modest dose increases.[16] Increased dosages of rifampicin correlate with day 2 early bactericidal activity in a near-linear fashion in TB patients.[17] There is an accumulating body of evidence demonstrating the safety and efficacy of higher-than-standard rifampicin doses in *in vitro*, animal and human studies and the adoption of this approach holds great appeal as a strategy to shorten TB treatment.[18–23]

Dose fractionation experiments have demonstrated that the PK/PD index most closely linked to rifampicin microbial kill is AUC/MIC, a finding corroborated by hollow-fibre models, which have additionally shown that C_{max}/MIC is more closely linked to the suppression of resistance and the post-antibiotic effect.[20,21] In TB patients, the 0–24 h AUC has a greater value than C_{max} or clinical features in predicting long-term clinical outcome.[24]

Scientific comparison of the findings of clinical trials investigating high rifampicin dosages requires an understanding of the PK parameters achieved with currently used dosages, so that the impact of dose escalation can be appreciated. For this reason, we conducted a systematic review and meta-analysis of published data describing rifampicin PK. As C_{max}/MIC and AUC/MIC are the PK/PD indices best characterized, we focused on these PK parameters. The objectives of this study were: (i) to explore the inter-study heterogeneity in rifampicin PK; (ii) to derive summary estimates of rifampicin PK parameters at standard dosages; (iii) to compare these with summary estimates for higher-than-standard rifampicin dosages; and (iv) to contextualize these PK estimates using the available PD data.

Methods

Search strategy and selection criteria

Studies were identified in accordance with the Preferred Reporting Items for Systematic Reviews and Meta-Analyses (PRISMA) guidelines.[25] PubMed, Scopus and MEDLINE electronic databases were searched. In PubMed and Scopus, titles and abstracts were searched using the terms 'rifampicin' OR 'rifampin' OR 'antituberculous' OR 'antimycobacterial' AND 'pharmacokinetics', to identify studies reported in the English language up to May 2017. The MEDLINE database was searched using the keywords 'pharmacokinetic*' OR 'bioequivalence' AND title words 'rifampicin' OR tubercul*'. Two reviewers (K. E. S. and G. D.) screened titles and abstracts for relevance and appraised full texts for inclusion in the meta-analysis using pre-specified selection criteria. Key articles were identified by consensus between K. E. S. and G. D. Prospective clinical studies were included if they collected PK data from adult patients with *Mycobacterium tuberculosis* infection and/or healthy adult volunteers receiving orally administered rifampicin.

Patients who received rifampicin for indications other than TB were excluded, because physiological fluctuations associated with different disease states are known to interfere with PK.[26] Studies that collected data relating to paediatric populations were excluded, as were non-human studies, abstracts, reviews and correspondence. Papers reporting PK parameters derived from modelling analyses were excluded for several reasons: variability in modelling methods has the potential to introduce additional heterogeneity; over-parameterization of models can lead to statistical shrinkage and loss of data variability; and datasets are often reported in both modelling and non-compartmental analyses (NCAs), which would risk reporting some data in duplicate. Finally, studies assessing the impact of rifampicin on the PK of another drug, rather than reporting the PK of rifampicin itself, were excluded.

Assessment of quality of studies

No validated tool exists to assess methodological rigour in PK studies. The priority is that samples are collected from subjects representative of target populations receiving dosage regimens of interest and relevance, rather than subjects who are randomized to one or other intervention. We considered this in our selection of studies, as well as ensuring that authors clearly described the pharmaceutical product, bioanalytical methods and statistical tools used.

Data extraction

A data extraction form was designed and one reviewer (K. E. S.) extracted data from the included studies on the following items in addition to rifampicin PK parameters: study design; study population; sex; age; body weight; HIV status; treatment regimen; duration of treatment; rifampicin dose; whether rifampicin was administered as a separate drug or in a fixed-dose combination; whether dosing was daily or intermittent; PK sampling times; assay method; and data analysis method. These variables were selected *a priori* as it was felt that they were the factors most likely to impact rifampicin PK. Rifampicin was considered to be at steady-state if it had been administered for $\geq$7 days to allow for saturation of first-pass metabolism and the establishment of metabolic autoinduction.

Data synthesis

In many of the studies, more than one group of participants was compared, e.g. HIV-positive and HIV-negative participants.[27] In others, more than one treatment was compared, e.g. in a crossover trial comparing separate drug formulations with fixed-dose combinations.[28] These groups were analysed in the same way that data were presented in the papers; that is, separate study arms were analysed separately rather than mean values being calculated for each study. This meant that some studies contributed two or more sets of PK parameters to the meta-analysis. To enable comparison of PK parameters across all studies, data were collected as means and standard deviations. Where summary statistics were not published in this format, authors were contacted to request that they share either raw data or results of an NCA of their data. If data were summarized as median and range or IQR and raw data or NCA results were unobtainable from the authors, we estimated the mean and standard deviation from the summary statistics provided using previously described methods.[29]

As the C_{max} of rifampicin occurs around 2 h after ingestion and half-life is of the order of 2.5–4 h,[30] concentrations remaining in plasma after 24 h from ingestion will be negligible. This was supported by the lack of a statistically significant difference between the estimates of AUC produced from the 0–24 h time interval and the 0–48 h time interval and those calculated from the 0–infinity (∞) interval. The AUC_{0-24}, AUC_{0-48} and $AUC_{0-\infty}$ results were therefore combined into a single measure of AUC and only these estimates were included in the final analysis to minimize design-related heterogeneity. Hereafter, any reference to AUC refers to the combined AUC_{0-24}, AUC_{0-48} and $AUC_{0-\infty}$ estimates. Although rifampicin is 80%–90%

protein bound and the active portion is believed to be unbound drug, studies reported total drug PK parameters; this analysis used the same.[15,30]

Summary measures

Data were analysed in Microsoft Excel version 15.28 (Microsoft 2016) and using the metafor package in R version 3.3.1.[31] The main objective of the analysis was to collate and summarize available data on the PK parameters of rifampicin derived from subjects taking WHO-recommended dosages. The focus of the meta-analysis was therefore on the 8–12 mg/kg dosing bracket. A linear model was used to incorporate the following variables: HIV status (positive or negative); TB status (positive or negative); combination therapy [limited to patients taking rifampicin monotherapy versus those taking combination therapy with isoniazid, pyrazinamide and ethambutol (RHZE)]; intermittent dosing; diabetes status; and treatment duration. A restricted maximum likelihood mixed-effects model was used to perform a meta-analysis of C_{max} and AUC estimates, with application of the DerSimonian–Laird estimator of residual heterogeneity. This approach fits a random-effects model. Standard errors of the study-specific estimates are adjusted to incorporate a measure of the heterogeneity among the effects of independent variables observed in different studies.[32] The degree to which demographic and clinical variables accounted for inter-study heterogeneity was assessed using meta-regression. Heterogeneity of PK estimates overall and within subgroups was assessed by estimation of the I^2 statistic and visual inspection of forest plots.

A second objective was to explore the effect of higher-than-recommended doses of rifampicin on drug exposure. The >12 mg/kg group of studies was split into more specific dosing subgroups and the mean and standard error derived from meta-analysis in standard weight-based dosing categories was compared with the summary statistics extracted from studies of higher rifampicin dosages. As the number of studies at higher dosages was small, we were unable to incorporate dose escalation as a variable in the meta-regression, so graphical comparison of summary statistics from studies at standard and higher dosages was performed instead.

Results

The search retrieved 3075 titles, of which 70 studies were deemed eligible, containing 179 distinct study arms (Figure S1, available as Supplementary data at *JAC* Online). The characteristics of the studies are summarized in Table S1. The cohorts contained a total of 3477 study participants. HPLC was used to measure rifampicin levels in 66 of the 70 studies. The remaining studies used spectrophotometry[33–35] or a plate diffusion assay.[36] These three studies were retained in the meta-analysis because their exclusion did not significantly impact overall PK parameter estimates.

By far the most common weight-based dosing category in the included studies was 8–12 mg/kg (118 of 163 study arms for which dosing information was extracted, 72%), in line with WHO rifampicin dosing guidelines. Unless explicitly stated, results presented hereafter pertain to those studies in which patients received this recommended dose.

C_{max} data were highly heterogeneous and influenced by treatment duration

C_{max} was highly heterogeneous between studies, with an I^2 statistic of 95.36% (95% CI 95.13%–97.15%). Meta-regression of C_{max} estimates with a multivariate model including all variables found two modifiers to have a statistically significant impact on C_{max}: duration of treatment and TB status. The effect on inter-study variability was minor, however: $I^2 = 91.36\%$ (95% CI 90.50%–94.77%) after meta-regression. The population summary estimates for C_{max} after univariate analysis were 11.51 mg/L (SEM 0.38) after single dosing and 7.04 mg/L (SEM 0.58) after steady-state dosing ($P = 0.001$) (Figure S2). In multivariate analysis, the difference in C_{max} estimate according to dosing duration was upheld. Single dosing ($n = 1139$ in 66 study arms) resulted in an adjusted mean C_{max} of 8.98 mg/L (SEM 1.34) and steady-state dosing ($n = 904$ in 42 study arms) resulted in an adjusted C_{max} of 5.79 mg/L (SEM 0.90) ($P = 0.001$). The adjusted summary estimate of C_{max} for healthy volunteers ($n = 946$ in 60 study arms) as compared with TB patients ($n = 1075$ in 46 study arms) was 8.98 mg/L (SEM 1.34) in healthy volunteers and 6.39 mg/L (SEM 0.85) in TB patients ($P = 0.01$). Notably, the majority of healthy volunteer cohorts were studied after a single dose of rifampicin (109/120 healthy volunteer cohorts, 91%) and most TB patients were studied after steady-state dosing (53/63 TB patient cohorts, 84%). When multivariate analysis was limited to subjects dosed at steady-state, TB status had a negligible and non-significant modifying effect on C_{max}: healthy volunteers 7.08 mg/L (SEM 1.21); TB patients 7.04 mg/L (SEM 1.28) ($P = 0.98$). No other modifying variables had a significant impact on the adjusted C_{max} estimate (Table S2).

Only treatment duration had a consistently significant impact on AUC in univariate analysis

In keeping with the findings in relation to the C_{max} estimate, inter-study variability in the AUC estimate was extreme, with an I^2 statistic of 99.53% (95% CI 99.28%–99.60%) in the meta-analysis before inclusion of modifying variables. In univariate analysis, the effect of steady-state dosing was to approximately halve the mean AUC estimate, from 72.56 (SEM 2.60) to 38.73 mg·h/L (SEM 4.33) ($P < 0.0001$) (Table 1 and Figure 1). Univariate analysis indicated significant associations between the AUC estimate and three additional covariates: HIV status, TB status and whether rifampicin was dosed in monotherapy or in combination (Table 1). However, steady-state dosing was disproportionately represented compared with single dosing in both HIV-positive patients and TB patients (100% and 82% of HIV-positive and TB patients, respectively, were studied at steady-state). Once these analyses were repeated with data limited to steady-state dosing, neither HIV status nor TB status had a significant impact on the AUC estimate (Figure 2a and b). Similarly, when the analysis was limited to those who underwent steady-state dosing, combination therapy made no significant difference to the AUC estimate: AUC 39.54 (SEM 3.83) versus 36.73 mg·h/L (SEM 4.88) for rifampicin monotherapy versus RHZE combination therapy ($P = 0.57$).

Significance of effect of treatment duration on AUC was upheld in meta-regression, but vast heterogeneity remained

When all modifying variables were incorporated into a mixed-effects meta-regression model, the impact on inter-study heterogeneity was negligible ($I^2 = 98.69\%$, 95% CI 98.38%–99.14%). Only treatment duration had a significant impact on AUC: adjusted AUC 56.26 mg·h/L (SEM 13.90) after a single dose and 20.94 mg·h/L (SEM 6.49) after steady-state dosing (Table 2). After multivariate meta-regression analysis, combination therapy with RHZE no longer had a significant impact on AUC. A diagnosis of diabetes

Table 1. Univariate analysis of variables influencing estimated rifampicin AUC

Variable and category	Number of study arms	Number of patients	AUC estimate (mg·h/L)	95% CI	SEM	*P*
Duration of therapy						
single dose	58	1053	72.56	66.39–78.74	2.60	<0.0001
steady-state dosing (>1 week)	34	846	38.73	33.82–42.67	4.33	
HIV status						
HIV negative	14	236	56.66	47.37–65.96	4.08	
HIV positive	9	126	37.16	27.08–47.23	6.56	0.003[a]
mixed HIV population	14	569	41.36	34.82–47.90	5.77	0.005[a]
TB status						
TB patients	36	947	46.14	39.39–52.89	5.29	<0.0001
healthy volunteers	56	952	69.41	62.17–76.66	3.31	
Drug combination						
rifampicin monotherapy	11	122	63.21	54.53–71.89	4.43	0.0478
RHZE	39	842	51.70	40.29–63.11	5.82	
Diabetes status						
no diabetes	12	227	84.56	73.70–95.42	5.54	0.44
diabetes	2	42	73.17	44.46–101.88	14.65	
Dosing frequency						
daily dosing	87	1617	61.52	55.62–67.42	3.01	0.35
intermittent dosing	3	189	46.01	13.69–78.33	16.49	

Univariate analysis indicated significant differences in estimated AUC depending on treatment duration, HIV status, TB status and combination therapy.
Steady-state refers to dosing for ≥7 days to allow for saturation of first-pass metabolism and the establishment of metabolic autoinduction.
P values indicate significance of difference between pooled AUC estimates within each study variable.
[a]*P* value for difference from HIV-negative population.

had a negligible, although statistically significant, modifying effect on the AUC estimate (Table 2).

Current rifampicin dosages for TB are unlikely to be sufficient for PK/PD target attainment

There appeared to be a slightly greater than proportional increase in AUC with increasing dosage (Table 3 and Figure 3a), although additional data from ongoing trials will help to clarify this. In seeking to relate these reported drug exposures to measures of clinical outcome, we used published PK/PD indices associated with efficacy in murine studies[21] and MIC data from human clinical WT *M. tuberculosis* isolates.[37] These murine studies report that an AUC/MIC of 271 is required for a 1 log cfu reduction *in vivo*.[21] The rifampicin WT MIC distribution ranges from 0.03 to 0.5 mg/L, with a median of 0.25 mg/L and proposed epidemiological cut-off value (ECOFF) of 0.5 mg/L.[37] Taking the median WT MIC of 0.25 mg/L, doses of 13 mg/kg appear sufficient to achieve the AUC/MIC target of 271. Taking the ECOFF MIC of 0.5 mg/L, however, available data indicate that a rifampicin dose of ≥25 mg/kg is required to attain this PK/PD target associated with a 1 log cfu reduction (Figure 3b).

Discussion

This meta-analysis, to our knowledge the most comprehensive to have been conducted on rifampicin PK, has demonstrated vast inter-study heterogeneity in PK parameter estimates. Having collated data collected globally, spanning 35 years and with the inclusion of HIV status, TB status, combination therapy, intermittent dosing, diabetes status and treatment duration as modifying variables, we have been unable to explain this heterogeneity. The vast heterogeneity within and between studies has made it impossible to assess the degree to which physiological differences between individual patients impacts upon rifampicin PK or PK variability, as has been reported with other antimicrobials.[38,39]

The summary estimates of C_{max} and AUC will serve as useful reference points for clinicians and academics concerned with the dosing of rifampicin for TB. At standard, WHO-recommended doses, mean rifampicin C_{max} and AUC are both significantly reduced in patients dosed at steady-state: C_{max} 8.98 versus 5.79 mg/L and AUC 72.56 versus 38.73 mg·h/L after a single dose and steady-state dosing, respectively. These decreases in PK parameters are expected due to extensive, saturable first-pass metabolism and well-characterized autoinduction of metabolism, resulting in enhanced clearance after repeated doses.[30,40,41] Whilst there was a trend towards HIV positivity being associated with lower rifampicin AUC, this did not hold up in meta-regression analysis, which may explain the conflicting results of previous investigations into the effect of HIV positivity on rifampicin exposure.[5,27,42–44] The case of AUC in TB patients versus healthy volunteers was similar in that the significance of the association was lost in meta-regression analysis.

With increasing dose, there is a greater than proportional increase in AUC. This is encouraging for the community that is seeking to increase rifampicin exposure. Taking 38.73 mg·h/L as the mean rifampicin AUC at steady-state dosing of 8–12 mg/kg and the ECOFF MIC of 0.5 mg/L[37] gives an AUC/MIC ratio of 77, far

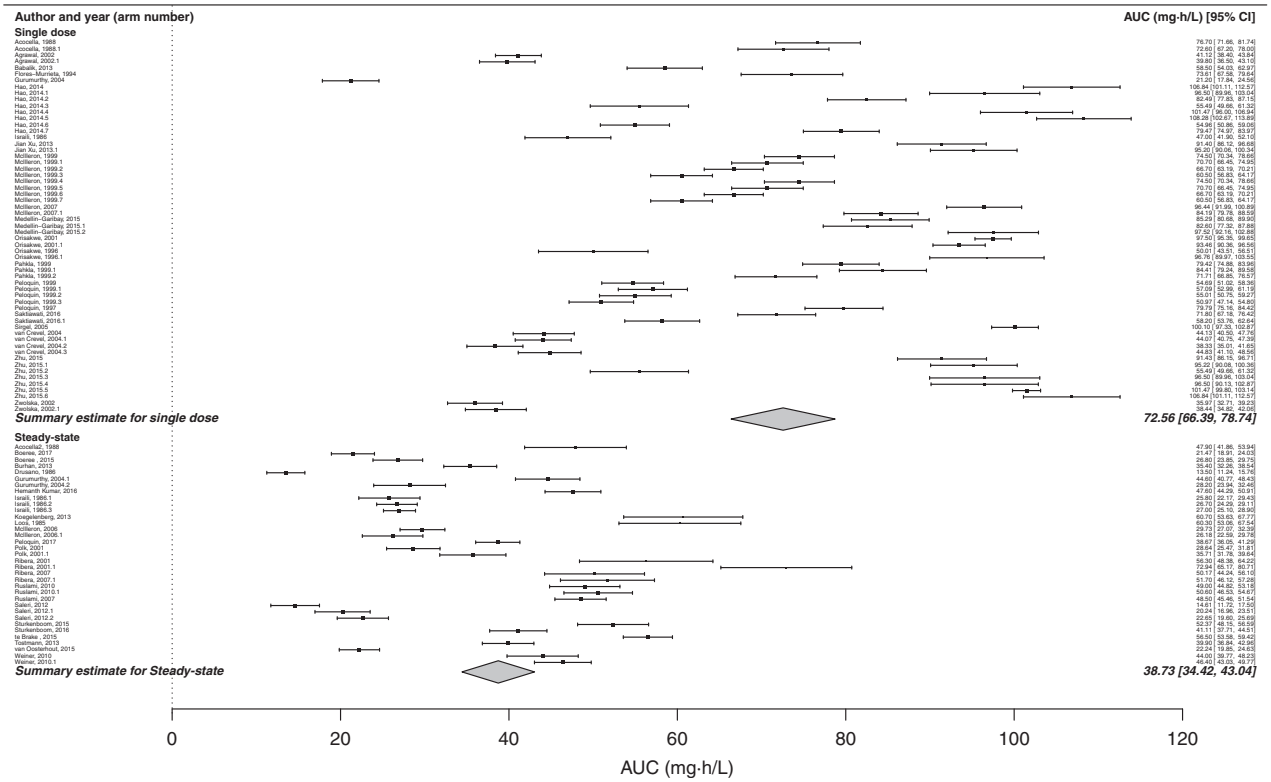

Figure 1. Forest plot displaying estimated rifampicin AUC after univariate analysis according to dosing duration. In univariate analysis, the effect of steady-state dosing was to approximately halve the estimated rifampicin AUC ($P < 0.0001$).

below the optimal PK/PD index suggested by Jayaram *et al.*[21] from murine data (prior to reference). Taking the MIC value from the very lower end of the WT range (0.03 mg/L) gives a ratio of 1291. The discrepancy between these ratios may explain in part why some patients develop rifampicin resistance on currently recommended doses while others are successfully treated with the same dose. The PK variability demonstrated herein is likely also to contribute to this phenomenon. Of note, this PK/PD index indicates the potency of a single drug used in isolation and does not reflect the efficacy of rifampicin used in clinical settings and in combination with other agents. There are also likely to be microbiological and host immune factors that influence treatment success. Our calculations nevertheless highlight the inadequacy of current rifampicin doses and the need for these to increase.

This analysis is limited by the fact that many studies summarized their results as median and range or IQR and, as stated, where raw data could not be obtained from authors of those studies means and standard errors were estimated using a previously described method.[29] This may have introduced inaccuracies. Our categorization of studies according to weight-based dosing was necessarily crude and in some cases based on the average weight of the study population in question. In addition, we were not able to consider the impact of covariates that were not consistently measured on heterogeneity in PK estimates. These included co-medications and associated drug–drug interactions, specific formulations of rifampicin that have been demonstrated to exhibit altered PK,[33,45,46] and patient ethnicity.

We acknowledge that the heterogeneity amongst the included studies, likely caused in part by these and other design and reporting factors, is extreme. Nevertheless, we believe that our largely descriptive analysis has value in highlighting the importance of these factors, in addition to the widely recognized role of inter-individual variability, in terms of their impact on the PK of rifampicin.[47,48] The extreme residual inter-study variability not accounted for by our meta-regression analysis may thus represent significant true biological variability between study populations, which should be further explored. In addition, the degree of PK variability that is attributable to protein-bound versus unbound rifampicin is not known. Future studies that directly assess these factors would be valuable, as would studies that employ mathematical PK models to quantify rifampicin PK variability. Monte Carlo simulation of rifampicin exposure based upon the AUC distributions presented in this meta-analysis would enable exploration of various dosing regimens. If these simulations could incorporate predictions of toxicity and drug resistance, they would support risk reduction of novel regimens before they enter clinical use.

This meta-analysis has collated and quantitatively summarized the existing literature on the PK of rifampicin, which is believed to be the key driver of PD and ultimately treatment outcome. It provides an important point of reference for understanding rifampicin

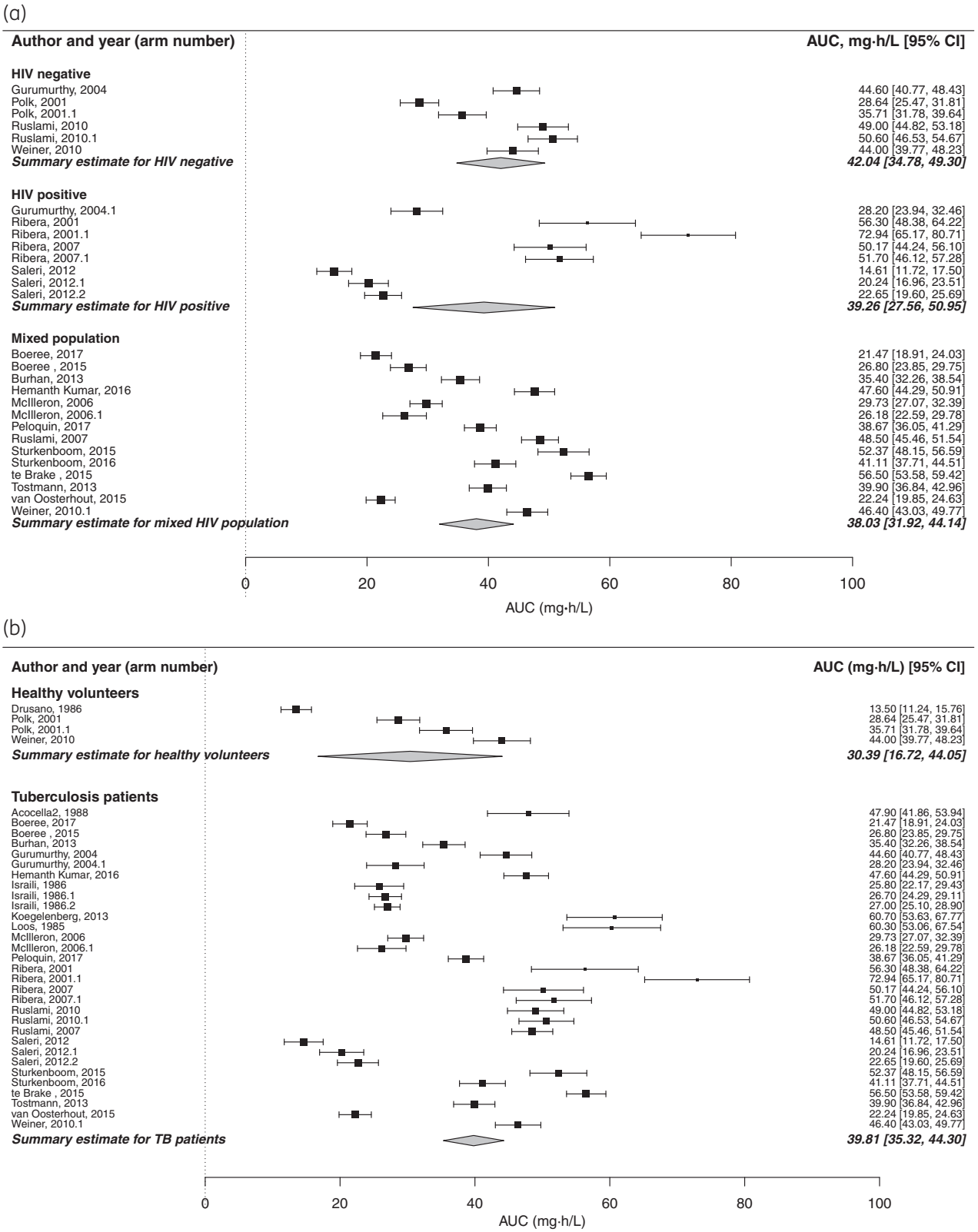

Figure 2. (a) Forest plot displaying estimated rifampicin AUC after univariate analysis according to HIV status; data are limited to steady-state dosing. Once data were limited to steady-state dosing, HIV status no longer had a significant impact on rifampicin AUC estimate. *P* values for comparison were >0.05. (b) Forest plot displaying estimated rifampicin AUC after univariate analysis according to TB status; data are limited to steady-state dosing. Once data were limited to steady-state dosing, TB status no longer had a significant impact on the rifampicin AUC estimate. *P* value for comparison was >0.05.

Table 2. Meta-regression of variables influencing estimated rifampicin AUC

Variable and category	Adjusted AUC estimate (mg·h/L)	95% CI	SEM	*P*
Duration of therapy				
single dose	56.26	29.01–83.50	13.90	<0.0001
steady-state dosing (>1 week)	20.94	8.28–33.60	6.49	<0.0001
HIV status				
HIV negative	53.16	41.63–64.68	5.85	0.60
HIV positive	48.13	33.26–63.61	7.74	0.31
mixed HIV population	54.53	37.08–71.98	8.90	0.85
TB status				
TB patients	56.26	43.22–69.29	6.65	0.10
healthy volunteers	67.09	54.11–80.07	6.62	0.10
Drug combination				
rifampicin monotherapy	87.71	59.48–113.93	13.89	0.72
RHZE	72.19	50.91–101.47	12.90	0.67
Diabetes status				
no diabetes	109.97	61.03–158.91	24.97	0.03
diabetes	113.30	59.03–167.55	27.68	0.04
Dosing frequency				
daily dosing	54.94	24.42–85.46	15.57	0.93
intermittent dosing	39.02	17.01–60.95	11.18	0.12

Meta-regression of all available variables found that treatment duration alone had a substantial and significant impact on estimated rifampicin AUC. Steady-state refers to dosing for ≥7 days to allow for saturation of first-pass metabolism and the establishment of metabolic autoinduction.
P values indicate significance of difference between pooled AUC estimates and overall population estimate.

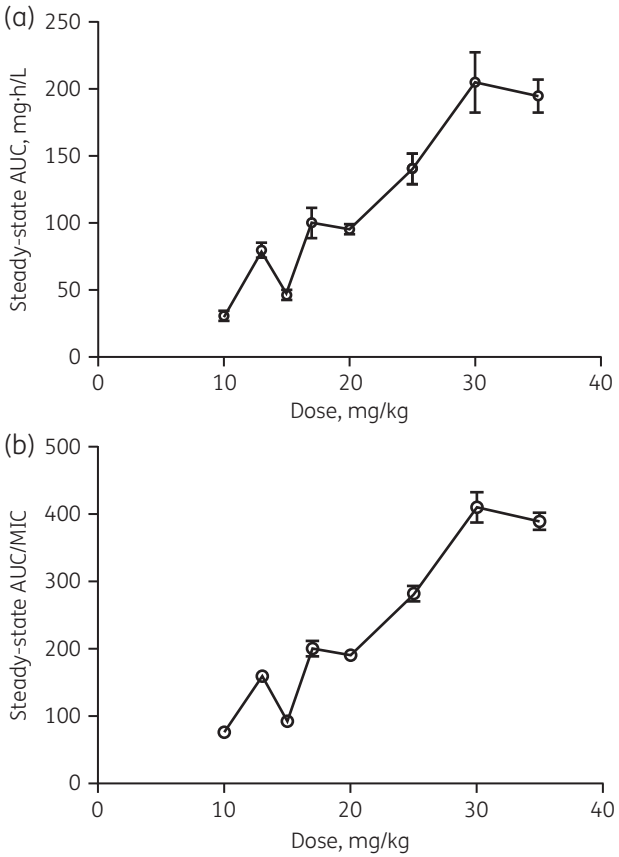

Figure 3. (a) Impact of increasing dose on rifampicin AUC. With increasing dose, there appears to be a greater than proportional increase in AUC. Error bars show SEM. Data are displayed in Table 3. (b) Impact of increasing dose on rifampicin AUC/MIC. Taking the ECOFF MIC of 0.5 mg/L, available data indicate that a rifampicin dose of ≥25 mg/kg is required to attain the PK/PD target associated with a 1 log cfu reduction (an AUC/MIC of 271).

Table 3. Rifampicin AUC at steady-state: meta-analysed standard dose compared with higher dosages

Rifampicin dose (mg/kg)	Number of subjects	Mean AUC (mg·h/L)	SEM	References
8–12	846	38.2	4.3	[a]
13	23	79.7	5.4	16
15	55	46.4	3.4	49
17	11	100.1	11.0	50
20	113	95.2	3.8	23,49–51
25	15	140.5	11.2	23
30	15	204.8	22.6	23
35	35	194.6	12.3	23,51

With increasing dose, there is a greater than proportional increase in AUC. Data are displayed in Figure 3(a).
Steady-state refers to dosing for ≥7 days to allow for saturation of first-pass metabolism and the establishment of metabolic autoinduction.
[a]All references in meta-analysis (see Table S1).

efficacy at current dosages as exploration of higher dosages continues.

Acknowledgements

Preliminary results from this work were presented at the European Conference of Clinical Microbiology and Infectious Diseases, Vienna, Austria, 2017 (Abstract no. 0S0842).

We would like to thank Elin Svensson, Ronald E. Polk, Kelly Dooley and Lindsey te Brake for their contribution of data and feedback on the manuscript.

Funding

This work was supported by the Wellcome Trust (grant number 203919/Z/16/Z to K. E. S. and grant number 206379/Z/17/Z to H. M.) and the South African National Research Foundation (grant number 90729 to H. M).

Transparency declarations

None to declare.

Author contributions

K. E. S. and G. D. devised and designed the study. K. E. S. and G. D. conducted the literature search. K. E. S. performed data extraction and analysis. K. E. S., H. P. and G. D. interpreted the data. K. E. S. prepared the manuscript. All authors reviewed, amended and approved the submitted manuscript.

Supplementary data

Figures S1 and S2 and Tables S1 and S2 are available as Supplementary data at *JAC* Online.

References

1 Zumla A, Nahid P, Cole ST. Advances in the development of new tuberculosis drugs and treatment regimens. *Nat Rev Drug Discov* 2013; **12**: 388–404.

2 WHO, 'StopTB' Initiative. *Guidelines for Treatment of Tuberculosis, Fourth Edition*. http://www.who.int/tb/publications/2010/9789241547833/en/.

3 van Ingen J, Aarnoutse RE, Donald PR *et al*. Why do we use 600 mg of rifampicin in tuberculosis treatment? *Clin Infect Dis* 2011; **52**: e194–9.

4 Peloquin C. Therapeutic drug monitoring: principles and applications in mycobacterial infections. *Drug Therapy* 1992; **22**: 31–6.

5 Peloquin CA, Nitta AT, Burman WJ *et al*. Low antituberculosis drug concentrations in patients with AIDS. *Ann Pharmacother* 1996; **30**: 919–25.

6 Magis-Escurra C, van den Boogaard J, Ijdema D *et al*. Therapeutic drug monitoring in the treatment of tuberculosis patients. *Pulm Pharmacol Ther* 2012; **25**: 83–6.

7 Babalik A, Mannix S, Francis D *et al*. Therapeutic drug monitoring in the treatment of active tuberculosis. *Can Respir J* 2011; **18**: 225–9.

8 Holland DP, Hamilton CD, Weintrob AC *et al*. Therapeutic drug monitoring of antimycobacterial drugs in patients with both tuberculosis and advanced human immunodeficiency virus infection. *Pharmacotherapy* 2009; **29**: 503–10.

9 Tappero JW, Bradford WZ, Agerton TB *et al*. Serum concentrations of antimycobacterial drugs in patients with pulmonary tuberculosis in Botswana. *Clin Infect Dis* 2005; **41**: 461–9.

10 Chideya S, Winston CA, Peloquin CA *et al*. Isoniazid, rifampin, ethambutol, and pyrazinamide pharmacokinetics and treatment outcomes among a predominantly HIV-infected cohort of adults with tuberculosis from Botswana. *Clin Infect Dis* 2009; **48**: 1685–94.

11 Hemanth Kumar AK, Kannan T, Chandrasekaran V *et al*. Pharmacokinetics of thrice-weekly rifampicin, isoniazid and pyrazinamide in adult tuberculosis patients in India. *Int J Tuberc Lung Dis* 2016; **20**: 1236–41.

12 Heysell SK, Moore JL, Keller SJ *et al*. Therapeutic drug monitoring for slow response to tuberculosis treatment in a state control program, Virginia, USA. *Emerg Infect Dis* 2010; **16**: 1546–53.

13 Chigutsa E, Pasipanodya JG, Visser ME *et al*. Impact of nonlinear interactions of pharmacokinetics and MICs on sputum bacillary kill rates as a marker of sterilizing effect in tuberculosis. *Antimicrob Agents Chemother* 2015; **59**: 38–45.

14 Ji B, Truffot-Pernot C, Lacroix C *et al*. Effectiveness of rifampin, rifabutin, and rifapentine for preventive therapy of tuberculosis in mice. *Am Rev Respir Dis* 1993; **148**: 1541–6.

15 Alsultan A, Peloquin CA. Therapeutic drug monitoring in the treatment of tuberculosis: an update. *Drugs* 2014; **74**: 839–54.

16 Ruslami R, Nijland HM, Alisjahbana B *et al*. Pharmacokinetics and tolerability of a higher rifampin dose versus the standard dose in pulmonary tuberculosis patients. *Antimicrob Agents Chemother* 2007; **51**: 2546–51.

17 Diacon AH, Patientia RF, Venter A *et al*. Early bactericidal activity of high-dose rifampin in patients with pulmonary tuberculosis evidenced by positive sputum smears. *Antimicrob Agents Chemother* 2007; **51**: 2994–6.

18 Davies GR, Nuermberger EL. Pharmacokinetics and pharmacodynamics in the development of anti-tuberculosis drugs. *Tuberculosis (Edinb)* 2008; **88** Suppl 1: S65–74.

19 Mitnick CD, McGee B, Peloquin CA. Tuberculosis pharmacotherapy: strategies to optimize patient care. *Expert Opin Pharmacother* 2009; **10**: 381–401.

20 Gumbo T, Louie A, Deziel MR *et al*. Concentration-dependent *Mycobacterium tuberculosis* killing and prevention of resistance by rifampin. *Antimicrob Agents Chemother* 2007; **51**: 3781–8.

21 Jayaram R, Gaonkar S, Kaur P *et al*. Pharmacokinetics-pharmacodynamics of rifampin in an aerosol infection model of tuberculosis. *Antimicrob Agents Chemother* 2003; **47**: 2118–24.

22 de Steenwinkel JE, Aarnoutse RE, de Knegt GJ *et al*. Optimization of the rifampin dosage to improve the therapeutic efficacy in tuberculosis treatment using a murine model. *Am J Respir Crit Care Med* 2013; **187**: 1127–34.

23 Boeree MJ, Diacon AH, Dawson R *et al*. A dose-ranging trial to optimize the dose of rifampin in the treatment of tuberculosis. *Am J Respir Crit Care Med* 2015; **191**: 1058–65.

24 Pasipanodya JG, McIlleron H, Burger A *et al*. Serum drug concentrations predictive of pulmonary tuberculosis outcomes. *J Infect Dis* 2013; **208**: 1464–73.

25 Moher D, Liberati A, Tetzlaff J *et al*. Preferred reporting items for systematic reviews and meta-analyses: the PRISMA statement. *PLoS Med* 2009; **151**: 264–9, w64.

26 Roberts JA, Taccone FS, Lipman J. Understanding PK/PD. *Intensive Care Med* 2016; **42**: 1797–800.

27 Choudhri SH, Hawken M, Gathua S *et al*. Pharmacokinetics of antimycobacterial drugs in patients with tuberculosis, AIDS, and diarrhea. *Clin Infect Dis* 1997; **25**: 104–11.

28 Agrawal S, Singh I, Kaur KJ *et al*. Bioequivalence assessment of rifampicin, isoniazid and pyrazinamide in a fixed dose combination of rifampicin, isoniazid, pyrazinamide and ethambutol vs. separate formulations. *Int J Clin Pharmacol Ther* 2002; **40**: 474–81.

29 Wan X, Wang W, Liu J *et al*. Estimating the sample mean and standard deviation from the sample size, median, range and/or interquartile range. *BMC Med Res Methodol* 2014; **14**: 135.

30 Acocella G. Clinical pharmacokinetics of rifampicin. *Clin Pharmacokinet* 1978; **3**: 108–27.

31 Viechtbauer W. Conducting meta-analyses in R with the metafor package. *J Stat Softw* 2010; **36**: 1–48.

32 DerSimonian R, Laird N. Meta-analysis in clinical trials. *Control Clin Trials* 1986; **7**: 177–88.

33 Garg SK, Chakrabarti A, Panigrahi D *et al*. Comparative bioavailability and in-vitro antimicrobial activity of two different brands of rifampicin. *Eur J Drug Metab Pharmacokinet* 1991; **16**: 223–9.

34 Orisakwe OE, Ofoefule SI. Plasma and saliva concentrations of rifampicin in man after oral administration. *Tokai J Exp Clin Med* 1996; **21**: 45–9.

35 Orisakwe OE, Agbasi PU, Afonne OJ *et al*. Rifampicin pharmacokinetics with and without ciprofloxacin. *Am J Ther* 2001; **8**: 151–3.

36 Potkar C, Gogtay N, Gokhale P *et al*. Phase I pharmacokinetic study of a new 3-azinomethyl-rifamycin (rifametane) as compared to rifampicin. *Chemotherapy* 1999; **45**: 147–53.

37 Schon T, Jureen P, Giske CG *et al*. Evaluation of wild-type MIC distributions as a tool for determination of clinical breakpoints for *Mycobacterium tuberculosis*. *J Antimicrob Chemother* 2009; **64**: 786–93.

38 Roberts JA, Abdul-Aziz MH, Lipman J *et al*. Individualised antibiotic dosing for patients who are critically ill: challenges and potential solutions. *Lancet Infect Dis* 2014; **14**: 498–509.

39 Alobaid AS, Wallis SC, Jarrett P *et al*. Effect of obesity on the population pharmacokinetics of fluconazole in critically ill patients. *Antimicrob Agents Chemother* 2016; **60**: 6550–7.

40 Chen J, Raymond K. Roles of rifampicin in drug-drug interactions: underlying molecular mechanisms involving the nuclear pregnane X receptor. *Ann Clin Microbiol Antimicrob* 2006; **5**: 3.

41 Loos U, Musch E, Jensen JC *et al*. Pharmacokinetics of oral and intravenous rifampicin during chronic administration. *Klin Wochenschr* 1985; **63**: 1205–11.

42 Schaaf HS, Willemse M, Cilliers K *et al*. Rifampin pharmacokinetics in children, with and without human immunodeficiency virus infection, hospitalized for the management of severe forms of tuberculosis. *BMC Med* 2009; **7**: 19.

43 Ahmed R, Cooper R, Foisy M *et al*. Factors associated with reduced antituberculous serum drug concentrations in patients with HIV-TB coinfection. *J Int Assoc Physicians AIDS Care (Chic)* 2012; **11**: 273–6.

44 Gurumurthy P, Ramachandran G, Hemanth Kumar AK *et al*. Decreased bioavailability of rifampin and other antituberculosis drugs in patients with advanced human immunodeficiency virus disease. *Antimicrob Agents Chemother* 2004; **48**: 4473–5.

45 McIlleron H, Wash P, Burger A *et al*. Widespread distribution of a single drug rifampicin formulation of inferior bioavailability in South Africa. *Int J Tuberc Lung Dis* 2002; **6**: 356–61.

46 Nyazema NZ, Rabvukwa P, Gumbo J *et al*. Bioavailability of rifampicin in a separate formulation and fixed dose combination with isoniazid NIH: a case for a fixed dose combination (FDC) for the treatment of tuberculosis. *Cent Afr J Med* 1999; **45**: 141–4.

47 Schipani A, Pertinez H, Mlota R *et al*. A simultaneous population pharmacokinetic analysis of rifampicin in Malawian adults and children. *Br J Clin Pharmacol* 2016; **81**: 679–87.

48 Verbeeck RK, Günther G, Kibuule D *et al*. Optimizing treatment outcome of first-line anti-tuberculosis drugs: the role of therapeutic drug monitoring. *Eur J Clin Pharmacol* 2016; **72**: 905–16.

49 Peloquin CA, Velásquez GE, Lecca L *et al*. Pharmacokinetic evidence from the HIRIF trial to support increased doses of rifampin for tuberculosis. *Antimicrob Agents Chemother* 2017; **61**: e00038–17.

50 Yunivita V, Dian S, Ganiem AR *et al*. Pharmacokinetics and safety/tolerability of higher oral and intravenous doses of rifampicin in adult tuberculous meningitis patients. *Int J Antimicrob Agents* 2016; **48**: 415–21.

51 Boeree MJ, Heinrich N, Aarnoutse R *et al*. High-dose rifampicin, moxifloxacin, and SQ109 for treating tuberculosis: a multi-arm, multi-stage randomised controlled trial. *Lancet Infect Dis* 2017; **17**: 39–49.

Expert Opinion on Drug Metabolism & Toxicology

ISSN: 1742-5255 (Print) 1744-7607 (Online) Journal homepage: http://www.tandfonline.com/loi/iemt20

Pharmacokinetics–pharmacodynamics of antifungal agents in the central nervous system

Katharine E Stott & William Hope

To cite this article: Katharine E Stott & William Hope (2018): Pharmacokinetics–pharmacodynamics of antifungal agents in the central nervous system, Expert Opinion on Drug Metabolism & Toxicology, DOI: 10.1080/17425255.2018.1492551

To link to this article: https://doi.org/10.1080/17425255.2018.1492551

Accepted author version posted online: 26 Jun 2018.
Published online: 09 Jul 2018.

EXPERT OPINION ON DRUG METABOLISM & TOXICOLOGY
https://doi.org/10.1080/17425255.2018.1492551

Taylor & Francis
Taylor & Francis Group

REVIEW

Pharmacokinetics–pharmacodynamics of antifungal agents in the central nervous system

Katharine E Stott[a,b] and William Hope[a]

[a]Antimicrobial Pharmacodynamics and Therapeutics Laboratory, Department of Molecular and Clinical Pharmacology, University of Liverpool, Liverpool, UK; [b]Malawi-Liverpool-Wellcome Trust Clinical Research Programme, Blantyre, Malawi

ABSTRACT

Introduction: Mortality from invasive fungal disease involving the central nervous system (CNS) is excessive. Achieving therapeutic drug concentrations at the site of infection within the CNS is always difficult and its evaluation is complex due to anatomical barriers and variable pathophysiological lesions.

Areas covered: This review provides an updated summary of the CNS PK of antifungal therapies. It considers factors that influence the success of antifungal regimens for CNS infection as well as preclinical and clinical data that quantify antifungal pharmacokinetics (PK) in the CNS. Furthermore, it presents state-of-the-art technologies to enhance the clinical use of existing antifungal drugs, and introduces novel antifungal drugs in development.

Expert opinion: The antifungal drugs currently available are either suboptimal, or are being used suboptimally, for CNS disease. Therapeutic drug monitoring is mandatory to enhance their effectiveness. Novel drugs in development may offer more efficacious options. In all cases, contemporary technologies to assess CNS PK offer the opportunity to enhance our understanding and use of antifungal drugs for CNS fungal disease.

ARTICLE HISTORY
Received 26 January 2018
Accepted 20 June 2018

KEYWORDS
Antifungal; central nervous system; cerebrospinal fluid; brain; pharmacokinetics; distribution

1. Introduction

Mortality from invasive fungal diseases involving the central nervous system (CNS) frequently exceeds 50% [1]. There are unique challenges for drug penetration within the CNS. The blood–brain barrier (BBB) and blood–cerebrospinal fluid barrier (BCSFB) create an obstacle for free diffusion of compounds into the CNS. Hence, plasma drug concentrations are not reliable surrogates for concentrations within diseased areas of the brain [2]. Complex pathophysiology and nonspecific clinical presentations often lead to a late diagnosis of CNS mycoses and this further compromises pharmacological treatment. This review provides a summary of current knowledge of the CNS pharmacokinetics (PK) of antifungal therapies.

2. CNS PK of antifungal drugs

The CNS is comprised of multiple sub-compartments that include the cerebrospinal fluid (CSF), cerebral parenchyma, ventricles, and meninges [3]. These areas are pharmacologically distinct. A number of issues are pertinent for a complete understanding of the potential utility of an antifungal agent for the treatment of CNS mycoses: first, pathological changes within the CNS resulting from fungal invasion; second, physicochemical drug properties that influence the extent of partitioning into the CNS and areas of diseased tissue; and finally, PK variability.

2.1. Pathophysiology of CNS fungal infections

Fungi vary considerably in the extent to which they are neurotropic. For some pathogens, such as *Cryptococcus neoformans* and *Cladophiolophra*, involvement of the CNS is so characteristic that it must be actively excluded if a diagnosis is established from a non-CNS site. For others, such as *Aspergillus* spp., CNS involvement is well characterized but is not invariably present. In addition, involvement of the CNS may depend on the host. For example, hematogenous *Candida* meningoencephalitis (HCME) is a disease that is characteristic of premature neonates, but highly unusual in adults. Table 1 summarizes the considerable pathophysiological differences between CNS mycoses.

The nature and extent of underlying immunological deficits also has an important impact on patterns of infection and the cadence of clinical disease. For example, profoundly immunosuppressed patients with invasive CNS aspergillosis often present with a stroke-like illness resulting from cerebral infarction. This results from invasion and thrombosis of cerebral arteries by *Aspergillus* spp. In contrast, patients with chronic sinus aspergillosis may develop CNS disease via direct hyphal invasion through the lamina papyracea. These patients often only have mild immunological deficits (e.g. diabetes, low-dose corticosteroid treatment) with clinical signs and symptoms that develop over many months. The histopathology of these two diseases is distinct. Cerebrovascular aspergillosis is associated with a paucity of inflammation, infarction and cerebral

CONTACT William Hope william.hope@liverpool.ac.uk Antimicrobial Pharmacodynamics and Therapeutics Laboratory, Department of Molecular and Clinical Pharmacology, University of Liverpool, UK

Article highlights

- The pathophysiology of fungal infections of the CNS is varied and impacts the pharmacokinetic-pharmacodynamic targets of antifungal drugs for these infections.
- Physicochemical properties of drugs influence their propensity to reach therapeutic CNS concentrations.
- Antifungal pharmacokinetic variability is significant, and heightened in the context of CNS penetration.
- Several new antifungal agents are in development and may be of clinical utility for CNS infections.
- Advancing technologies enhance our ability to quantify and evaluate CNS pharmacokinetics.

This box summarizes key points contained in the article

Box 1. Desirable information for the accurate setting of PK–PD targets for fungal CNS infection

1. Principal PK parameter of interest, depending on whether drug activity is determined bymaximum concentration (Cmax), area under the curve (AUC), or time above a given therapeutic threshold.
2. Drug susceptibility/ MIC of the infecting fungus.
3. Magnitude of the PK–PD index required in terms of the unbound concentration of drug that issufficient to exert PD effect on the target organism.
4. Histopathological site(s) of disease within the CNS.
5. Rate constant describing the movement of drug into the CNS from the circulation.
6. Rate constant(s) describing the movement of drug within CNS compartments of interest.
7. Rate constant(s) describing the clearance of drug from the target site.
8. Rate constant(s) describing the clearance of drug from the body.
9. Time-dependent differences in plasma and tissue drug concentrations (hysteresis).
10. PK parameters associated with toxicity in measurable physiological compartments (usually thesystemic circulation).
11. Clinical and physiological covariates that influence the PK of the drug in question.

hemorrhage. In contrast, chronic *Aspergillus* sinusitis is associated with florid pyogranulomatous inflammation.

Systemic physiological changes associated with CNS mycoses may also have an impact on the PK of antifungal drugs. Systemic infection alters cerebral blood flow, blood and tissue pH and intra- and extra-cellular fluid volumes, all of which exert profound influence on systemic PK and drug penetration into the CNS [52–54]. Meningeal inflammation may increase the concentration of antimicrobial agents in the CSF by over 10-fold [55]. In some cases, the BBB is completely disrupted, allowing unfettered access of the drug to the pathogen.

2.2. Physicochemical properties of the drug

The CNS is protected from many circulating xenobiotics by the presence of blood tissue barriers that limit diffusion from the endovascular compartment into the CSF and brain parenchyma. A summary of antifungal drug characteristics that influence the degree to which drugs partition across the BBB and the BCSFB is presented in Table 2. Tight cellular connections in the BBB and BCSFB (approximately 2 nm) prevent the passive diffusion of large compounds into the CNS [3]. Efficient diffusion is possible only to an upper molecular weight limit of 300–400 g/mol [56].

The lipophilicity of compounds influences the extent of CNS partitioning [52,67]. Drug lipophilicity is quantified as the partition coefficient (LogP) between aqueous and lipophilic phases (usually determined with water and octanol). A more physiologically relevant expression of lipophilicity is LogD, which accounts for the fact that many drugs are ionized at physiological pH. Compounds that are not ionized at physiological pH have the greatest lipophilicity and better penetrate the BBB and BCSFB [52,68]. LogP and LogD values of approximately 2–4 are associated with optimal BBB penetration [68,69]. Protein binding also influences the degree of partitioning into the CNS. Passive diffusion of molecules into the CNS depends on a concentration gradient between unbound drug in the plasma and that in the brain [70]. Protein binding is often inversely correlated with LogP.

Finally, efflux pumps in the BBB and BCSFB may remove compounds from the CNS via an energy-dependent process [3,52]. P-glycoprotein is a membrane-bound efflux pump with an affinity for lipophilic molecules. Some triazole agents (itraconazole, posaconazole and isavuconazole [71]) are substrates for P-glycoprotein, while other triazoles (fluconazole and voriconazole) are not. There is conflicting evidence regarding the role of P-glycoprotein in the efflux of amphotericin B from the CNS [72,73].

2.3. PK variability

Several antifungal drugs exhibit nonlinear and/or highly variable PK. The PK of itraconazole, voriconazole, posaconazole, and flucytosine are sufficiently variable to warrant routine therapeutic drug monitoring (TDM) in the context of invasive fungal disease, regardless of whether there is CNS involvement [74]. This variability is inevitably more extreme when penetration into the CNS is considered, since it is amplified by barriers such as the BBB and BCSFB as well as pathological changes within the CNS itself. Thus, while plasma drug concentrations are highly variable, CNS drug concentrationslikely more so, and the former are an unreliable surrogate for the latter.

The prediction and evaluation of the CNS PK of antifungals is thereby complex. Inter- and intra-individual variability in each contributing factor extends this complexity [52,74]. Ideally, the information required to establish robust pharmacokinetic–pharmacodynamic (PK–PD) targets at the site of infection in the CNS includes all of the points listed in Box 1. Using this information, data can be modeled using a variety of approaches to predict human CNS PK. These approaches can broadly be categorized into classical population PK modeling (the 'top–down' approach) and physiologically based PK (PBPK) modeling (the 'bottom–up' approach) [75]. For example, population PK models have been constructed from preclinical investigations of micafungin [76] and anidulafungin [77], with Monte Carlo simulation used to bridge the results to neonatal populations at risk of *Candida* meningoencephalitis. While PBPK models describing the CNS PK of antifungals are scarce,

Table 1. Overview of CNS mycoses

Fungal species	Clinical setting	Predilection for CNS involvement in invasive disease [a] [§]	Pathophysiological manifestations	Mortality with treatment (%)	Antifungal drug options	References
Cryptococcus spp. *C. neoformans*	Advanced HIV infection, defective cellular immunity, corticosteroid therapy	++++	Subacute – chronic meningitis Cerebral abscesses/ cryptococcomas Cerebral infarction Raised intracranial pressure	24–58	Amphotericin B Flucytosine High-dose fluconazole	[4–9,89,90,152]
C. gattii	Normal hosts mainly in restricted geographical locations (Australia, Southern California, British Columbia, Washington State), solid organ transplant recipients	++++	Meningitis Cryptococcomas Raised intracranial pressure	0–13		[10–12]
Coccidioides *C. immitis* *C. posadasii*	HIV infection, steroid therapy, travel to southwest USA, Central and South America	+++	Subacute – chronic meningitis Cerebral abscesses Cerebral vasculitis Encephalitis	~ 30	Fluconazole Itraconazole Voriconazole Intrathecal amphotericin B	[13–17,94]
Cladosporium spp.	Immunodeficiency, immunosuppression, normal host, trauma	+++	Intracerebral abscesses Meningitis Encephalitis	29–50	Amphotericin B in combination with vori-, itra- or posaconazole	[18–21]
Aspergillus spp.	Neutropenia, advanced HIV infection, haematopoetic stem-cell transplantation, corticosteroid therapy, chronic granulomatous disease	++	Cerebrovascular aspergillosis with cortical and subcortical infarction and hemorrhage Abscesses Rarely: chronic meningitis	62–90	Voriconazole Amphotericin B Isavuconazole Consider: High-dose adjunctive echinocandins	[22–25]
Scedosporium/ Pseudallescheria spp.	Neutropenia Near-drowning	++	Chronic meningitis Cerebral abscess	79–100*	*S. apiospermum*: voriconazole monotherapy *S. prolificans*: voriconazole + terbinafine ± echinocandin	[26–30]
Candida spp.	Prematurity,	+	Subacute meningitis Multiple micro-abscesses Macroabscesses	10–53	Amphotericin B Flucytosine Fluconazole Voriconazole in fluconazole-resistant disease	[31–35]
Histoplasma capsulatum	Advanced HIV infection Primary or iatrogenic immunosuppression Steroid therapy Solid organ transplant recipients	+	Meningitis Cerebral mass lesions Diffuse encephalitis Raised intracranial pressure Cerebral vasculitis	20–40	Amphotericin B Itraconazole Fluconazole Salvage therapy (limited data): Posaconazole Isavuconazole Voriconazole	[36–41,139]
Blastomycosis dermatitidis	Normal host mainly in restricted geographical locations (southeastern, south central and midwestern USA, St Lawrence river)	+	Chronic meningitis Cerebral abscesses/ blastomycomas	~ 18	Amphotericin B Step down to azole: Voriconazole Fluconazole Itraconazole	[26,42,43,153]
Mucormycosis/ Zygomycetes	Diabetic ketoacidosis Hematological malignancy	+	Rhino-orbital-cerebral infection Cerebral abscesses	25–62	Amphotericin B Step down to azole: Posaconazole Isavuconazole	[44,45,154]
Sporothrix schenckii	HIV infection Alcoholism Environmental exposure	+	Chronic meningitis Encephalitis Hydrocephalus	30–90	Amphotericin B Step down: Itraconazole	[26,155]

(*Continued*)

Table 1. (Continued).

Fungal species	Clinical setting	Predilection for CNS involvement in invasive disease [a] [§]	Pathophysiological manifestations	Mortality with treatment (%)	Antifungal drug options	References
Paracoccidioides brasiliensis	Environmental exposure, Latin America Male predominance (~ 23:1)	+/-	Intracerebral abscesses Spinal cord involvement Hydrocephalus	~ 17	Trimethoprim-sulfamethoxazole Voriconazole Itraconazole	[26,46–48]
Trichosporon spp.	Hematological malignancy, HIV infection, extensive burns, intravenous catheters, heart valve surgery	No data	Intracerebral abscesses Meningitis	70–80	Amphotericin B Voriconazole Itraconazole Posaconazole Isavuconazole	[49,50]

* Disseminated infection.
[a] From [51].
[§] Key: ++++, very common, through +/–, very rare.

examples of the application of PK modeling to the prediction of CNS PK exist in the general pharmacology literature. A multi-compartmental PBPK model has been shown to adequately describe the PK profiles of nine structurally diverse drugs in the plasma, brain extracellular fluid and CSF of rats [78]. The model was additionally able to predict human concentration-time profiles in brain compartments [78,79]. PBPK models can also predict the influence of genetic polymorphisms on CNS PK and PD [80].

3. Evaluation of data relating to the CNS PK of antifungal drugs

Studies of the CNS penetration of antifungal drugs in humans are often limited. Firstly, drug concentrations in CSF, which is the only readily available biological matrix in clinical studies, may not be representative of concentrations in other CNS sub-compartments. Secondly, studies tend to report point estimates of CNS drug partitioning rather than integral measures-drug concentrations over time (i.e. area under the concentration-time curve; AUC) in the plasma and the CNS.

For ethical and technical reasons, quantification of drug in the CNS using conventional methods such as collecting samples of tissue for liquid chromatography–mass spectrometry (LC–MS) or bioassay in clinical studies is challenging (see e.g. [81,82]). Information of this type is usually derived from preclinical models. Using more contemporary technologies, clinically relevant estimation of CNS drug partitioning is becoming easier. Examples of these technologies are intracerebral microdialysis [70] and non-invasive imaging techniques such as positron emission tomography (PET) [83] and magnetic resonance (MR) imaging [84]. Key findings that preclinical and clinical studies have provided are presented in the following section of this review, alongside a review of their clinical application.

4. The triazoles

4.1. Fluconazole

Fluconazole has physicochemical properties that enable it to traverse the BBB and BCSFB (Table 2). The equilibration of fluconazole between plasma and cerebral extracellular fluid occurs rapidly and is independent of dose [85]. Relatively high concentrations are found in the CSF. PK studies in rabbits and adult Rhesus monkeys demonstrated mean CSF:plasma AUC ratios of 0.84 and 0.86, respectively, with a long half-life in the CSF of approximately 27 h [86,87].

Early human CNS PK studies using bioassay or LC–MS reported a range of partition ratios from 0.52 to 0.89 [81,88]. Subsequently, a combined approach using PET scanning and plasma PK sampling demonstrated an approximately uniform distribution of fluconazole in the healthy human brain, with a brain:plasma penetration ratio of 1.31 [83]. This was corroborated by an analysis of four patients undergoing brain tumor excision in whom healthy brain parenchyma was also removed. In these patients, HPLC demonstrated a mean healthy brain:plasma fluconazole ratio of 1.33 [82].

A fluconazole regimen of 1200 mg/day for the 2-week induction phase of treatment for cryptococcal meningoencephalitis is often used in settings where polyenes are unavailable. This dosage is more rapidly fungicidal than 800 mg/day [89]. The addition of flucytosine to fluconazole is recommended because it reduces mortality [90]. These oral regimens for cryptococcal meningitis are pragmatic recommendations given the unavailability of polyenes in many regions with a high burden of cryptococcal meningitis, despite broad agreement that amphotericin B deoxycholate is currently the agent of choice [91,92]. Fluconazole is also used at dosages of 400–1200 mg/day to treat CNS infection with *Coccidioides* [93,94].

4.2. Itraconazole

Itraconazole concentrations in CSF are negligible, with CSF:plasma concentration ratios of < 0.002 to 0.12 in preclinical models [2,95–97]. Even in the setting of infection and inflammation, itraconazole is undetectable in rabbit CSF [97]. Low CSF concentrations have been attributed to rapid binding to red blood cells and circulating plasma proteins, inhibiting BCSFB penetration [98]. However, murine experiments have demonstrated rapid, dose-dependent penetration and linear accumulation of itraconazole in brain tissue up to 8 min post-dose, implying that it does cross the BBB [99]. In a murine model of CNS histoplasmosis, itraconazole levels were almost universally undetectable in brain tissue 3 h post-dose [100]. Itraconazole has a strong affinity for P-glycoprotein, which

results in rapid efflux from the CNS such that half-life in cerebral tissue may be considerably shorter than that in plasma (0.4 h versus 5 h, respectively) [99,101].

The efficacy of itraconazole for the treatment of cryptococcal meningoencephalitis [97], CNS aspergillosis [102], and *Coccidioides* meningitis [95] is well established in laboratory animal models. The apparent discrepancy between CNS drug concentrations and therapeutic efficacy of itraconazole in CNS fungal infections may be due to a combination of higher drug concentrations in the brain tissue than in CSF, and the relatively low minimum inhibitory concentration (MIC) of itraconazole against target fungi such as *Candida* [103] and *Histoplasma* [100]. In addition, the pharmacologically active metabolite of itraconazole, hydroxyl-itraconazole, has been detected in brain parenchyma with greater consistency than has the parent drug [100]. In humans, itraconazole is effective for primary prophylaxis of cryptococcal meningitis, with a relative risk of incident cryptococcal meningitis of 0.12 (95% confidence interval, 0.03, 0.51) versus placebo [104]. Inconsistent success rates have been reported for the treatment of cryptococcal meningitis with itraconazole. The treatment of six patients with 200 mg/day resulted in therapeutic failure (deterioration or death) in three patients (50%) [105]. Of 20 evaluable patients with culture- or antigen-diagnosed cryptococcal meningitis treated with itraconazole 400 mg/day, 13 (65%) achieved clinical and microbiological cure [106]. Cryptococcal meningitis progressed in two patients receiving itraconazole 600 mg/day [107]. After recovery from cryptococcal meningitis, maintenance therapy with itraconazole is associated with significantly more relapses of cryptococcal meningitis compared with fluconazole [108].

Itraconazole is not included in current cryptococcal meningitis treatment guidelines from the World Health Organization [109], though it may be used as prophylaxis against cryptococcal meningitis, particularly in patients with CD4 counts < 100 cells/μL [110]. Despite the availability of newer antifungal agents, the oral bioavailability and broad spectrum of antifungal activity of itraconazole mean that it remains a useful drug for the management of invasive mycoses worldwide [111]. It is recommended as second-line therapy for CNS infection with *Candida, Aspergillus, Histoplasma*, and *Coccidioides* spp [93].

4.3. Voriconazole

Voriconazole has a relatively low molecular weight (349 g/mol), is moderately lipophilic and is a weak substrate for P-gp (Table 1). It exhibits good CNS penetration. In guinea pigs, 10-mg/kg voriconazole penetrates the BBB into brain parenchyma rapidly, reaching peak concentrations of 6.8 μg/g and 2.7 μg/g 15 min and 1 h post dose, respectively [112]. The CSF:plasma ratio in healthy animals is 0.68 [112].

Studies in humans have demonstrated that voriconazole penetrates the BBB and BCSFB, including into brain parenchyma [113] and cerebral abscesses [114]. A wide range of concentrations in human CSF range have been reported, from 0.08 to 3.93 μg/mL in the initial 10 h post voriconazole administration. CSF:plasma ratios are 0.22–1.0 [112]. This wide range is likely due to the extensive PK variability of voriconazole [74,115–119]. In contrast to CSF, concentrations in the brain are ≥ 2-fold plasma levels [84]. A study that used fluorine-19 MR spectroscopy reported steady-state brain:plasma voriconazole concentration ratios of 3.0 (90% CI 1.9–4.7) pre-dose and 1.9 (90% CI 1.2–3.0) post-dose in healthy adult men [84].

Voriconazole exhibits potent activity against *Aspergillus* spp. (Table 2) and is a standard-of-care for CNS aspergillosis [120]. It is also indicated for CNS infection with *Scedosporium apiospermum* complex and fluconazole-resistant *Candida* spp. (Table 2), the latter being primarily confined to the neonatal setting.

4.4. Posaconazole

Posaconazole is structurally similar to itraconazole, but less lipophilic [2]. It is both a substrate and an inhibitor of P-gp *in vitro* [121], although polymorphisms of P-gp do not affect posaconazole AUC *in vivo* [122]. The oral suspension of posaconazole exhibits variable bioavailability and inconsistent PK [123,124]. Alternative tablet, capsule and intravenous formulations have been partly successful in addressing these issues [125–129]. Based on the physicochemical properties of posaconazole, poor CNS penetration is expected (Table 2). In murine models of infection with *C. gattii* and *Fonseca monophora*, mean posaconazole brain:serum concentration ratios are < 0.54 with dosages of

Table 2. Physicochemical properties of antifungal drugs

Drug	Molecular weight (g/mol)[a]	Particle size (μm)[b]	LogP [a]	LogD at pH 7.4 (indicative of lipophilicity)[b]	Plasma protein binding (%)[c]	Efflux pump affinity (P-gp substrate)	Correlation of measurable CNS concentration with biological activity	References
Fluconazole	309		2.17	0.5	10	No	Good	[57–59]
Itraconazole	705		6.99	4.9	98	Yes	Poor	[58,59]
Voriconazole	349		2.56	2.1	58	No	Good/variable	[59]
Posaconazole	700		6.1	4.4	99	Yes	Poor	[59]
Isavuconazole	718		−3.33	3.6	99	No	Good	[60,61]
DAmB	924	< 0.4	0.95	−2.8	> 95	No	Poor	[62,63]
LAmB	924	0.05–0.08	0.95	−2.8	> 95	Contentious	Poor	[63,72,73]
ABLC	924	1.6–11	0.95	−2.8	> 95	No	Poor	[3,63]
ABCD	924	0.12–0.14	0.95	−2.8	> 95	No	Poor	[3,63]
5FC	120		−0.89	−2.34	5	No	Good	[3,58]
Caspofungin	1093		−2.8	−3.88	98	No	Good	[64,65]
Micafungin	1140		−3.8	−1.62	98	No	Good	[64,65]
Anidulafungin	1291		0.21	−3.32	98	No	Good	[65,175]

[a] From Ref. [3].
[b] From Refs. [2,66].
[c] From Refs. [3,59]

10–20 mg/kg. These increase to 0.69–0.84 following dosages of 40 mg/kg [130,131].

Human CNS PK data for posaconazole are sparse and limited to case reports. The CSF:plasma concentration ratios range from 0 (single CSF sample analyzed in each case) [132,133] to < 0.009 (in six serial CSF samples) [134] in patients without significant meningeal inflammation. In patients with bacterial meningitis and cerebral fungal infection, CSF:plasma posaconazole concentration ratios as high as 0.44 and 2.37 are reported, suggesting that meningeal inflammation may improve CNS penetration [133]. Posaconazole penetrates into fungal brain abscesses [133].

Posaconazole is not recommended as a first-line agent for any fungal infection of the CNS. Posaconazole is indicated as second line therapy for coccidioidomycosis [135], and mucormycosis [136] and as salvage therapy for invasive aspergillosis [137,138] and histoplasmosis [139] (Table 2 [93],).

4.5. Isavuconazole

Isavuconazole is structurally similar to fluconazole and voriconazole, although it has a higher molecular weight and LogD value (Table 2). Studies in healthy rats suggest that the mean brain:plasma isavuconazole concentration ratio is 1.8 [140]. Following administration of ^{14}C-labeled isavuconazonium sulfate, radioactivity in brain tissue increases in proportion with radioactivity in blood, and reaches a maximum at 2h post-dose before declining to undetectable levels 24 h post-dose [140]. Similar CNS penetration is evident in a murine model of cryptococcal meningitis with brain:plasma AUC ratios of approximately 1.35 [141].

Data describing the PK of isavuconazole in the human CNS are scant. However, isavuconazole is non-inferior to voriconazole for the treatment of suspected invasive aspergillosis [142] and has been used effectively for the treatment of invasive mucormycosis with brain involvement [143].

5. Polyenes

There are several formulations of amphotericin B (AmB) available for clinical use: amphotericin B deoxycholate (DAmB), liposomal amphotericin B (LAmB), amphotericin B lipid complex (ABLC) and amphotericin B colloidal dispersion (ABCD) [93,144]. ABCD is no longer marketed in many countries. All approved formulations are administered intravenously. The large molecular weight of AmB is likely to be the primary reason for its relatively poor CNS penetration [145,146] (Table 2). An *in vitro* model of the BBB demonstrated that permeability to both LAmB and DAmB was significantly increased in response to enlargement of endothelial cell junctions via exposure to either tumor necrosis factor alpha or lipopolysaccharide [147]. In addition, AmB may be a substrate for efflux pumps at the BBB [72,73].

In a rabbit model of CNS *C. albicans* infection, CSF:plasma ratios ≤ 0.02 and brain:plasma ratios ≤ 0.27 were reported for all four AmB formulations [145]. The CNS penetration ratios of all formulations are higher in the setting of CNS infection compared with healthy brain tissue (maximum AmB CSF:plasma ratio 0.03 with ABCD and ABLC; maximum brain:plasma ratio 0.11 with ABCD) [145].

LAmB has the lowest CNS penetration ratio of all formulations despite its smaller particle size (Table 2). However, the PK of LAmB is characterized by serum concentrations 30-fold greater than other AmB formulations. Thus, the absolute concentration of AmB in brain tissue following LAmB administration is ultimately several times higher than following administration of the other formulations [3,145]. An immunohistochemistry study of LAmB in brain sections of mice with cryptococcal meningitis revealed that amphotericin B was present in both intravascular and perivascular spaces [148]. The proportion of liposome-associated AmB versus free drug in brain tissue after administration of LAmB is unknown.

After as few as three dosages of DAmB, there is prolonged mean residence time of AmB in rabbit brain tissue despite negligible concentrations in CSF [149]. In human studies of LAmB PK, CSF:plasma concentration ratios of 0.001 have been reported [150]. Autopsy studies have found concentrations of AmB in human cerebral cortex to be lower than those in liver, spleen, kidney and lung, with no significant difference between the concentrations detected after administration of LAmB and ABCD [151].

Despite consistent reports of low or undetectable CNS concentrations of AmB, its efficacy against many CNS mycoses in humans, including cryptococcal meningitis, is well established [152–155]. A likely explanation for this is that amphotericin B concentrations are high in the meninges where the yeast predominantly resides.

The clinical utility of polyenes in regions of the world with high burden of fungal CNS infection, in particular cryptococcal meningitis but also CNS histoplasmosis, murcomycosis, sporotrichosis and trichosporonosis, is limited by the requirement for intravenous administration, prolonged inpatient admission and close monitoring for toxicity.

6. Flucytosine

Flucytosine has several attributes that are conducive to high CNS penetration including low molecular weight, low-protein binding and polarity (Table 2). High-dose-proportional concentrations are consistently recorded in both brain parenchyma [156] and CSF, with CSF:plasma ratios 0.74–0.84 in humans from 1–2 h after dosing [157,158]. The activity of flucytosine appears to be time- rather than concentration-dependent [157,159,160].

Flucytosine is active against *Cryptococcus* spp., most *Candida* species and has some activity against *Aspergillus* species [74,109]. Its use in monotherapy is widely thought to be precluded by the development of resistance, which has been consistently documented *in vitro* [161–163]. While reports on the clinical use of flucytosine monotherapy are sparse, a case series of 23 patients with cryptococcal meningitis treated with flucytosine monotherapy reported that of 12 patients who failed therapy, the development of resistance was implicated in 50% [164].

In practice, flucytosine is used in combination therapy. In this setting, flucytosine is vital to secure optimal outcomes in cryptococcal meningitis: Trials comparing DAmB alone with DAmB in combination with either flucytosine or fluconazole have

demonstrated superior outcomes in the flucytosine combination arms, in terms of CSF sterilization [165,166] and mortality [165]. Its addition to AmB facilitates reduced treatment durations for cryptococcal meningitis [167]. 5FC may also have a role in HCME, where its addition to AmB is at least additive and may be synergistic in preclinical models [168,169]. A retrospective study of humans with *Candida* meningitis reported survival in 15 of 17 patients treated with the combination of flucytosine and AmB [170]. This combination is recommended for *Candida* meningitis in children [171] though caution is advised because of the risk of toxicity, particularly in premature neonates [172].

7. Echinocandins

Caspofungin, micafungin, and anidulafungin do not extensively partition into the CNS due to their large molecular weight and high level of protein binding (Table 2 [173],). Micafungin achieves brain:plasma concentration ratios < 0.01 at doses of 0.5–2 mg/kg in healthy rabbits [174]. In rabbits with HCME, micafungin penetrates all CNS compartments (cerebrum, cerebellum, spinal cord, meninges and CSF) in a dose-dependent fashion, but only with dosages > 2 mg/kg [76]. The presence of CNS infection and inflammation does not increase the CNS penetration of micafungin [76]. Brain tissue concentrations of anidulafungin also increase in a dose-dependent manner, achieving brain:plasma ratios of 0.10–0.12 at doses of 0.5–10 mg/kg in neutropenic rabbits with disseminated *C. albicans* infection [175]. Studies of radiolabelled caspofungin at dosages of 1–2 mg/kg demonstrate brain:plasma penetration ratios of < 0.09 in rodents [176]. For all three echinocandins, penetration into each of lung, liver, spleen and kidney exceeds that into brain tissue [174–176].

Human CNS PK data for echinocandins is limited to case reports. A patient with a cerebral mass treated with micafungin at a dosage of 100mg q24h achieved a brain:plasma concentration ratio of 0.18, 23 h after dosing [177]. A patient dosed with micafungin 300 mg/day for CNS aspergillosis achieved a CSF: plasma ratio of 0.0005 [178]. A case report of a patient treated for *Candida* endocarditis describes the development of new cerebral abscesses during caspofungin treatment [179].

There is experimental evidence from well characterized rabbit models of HCME that anidulafungin and micafungin are potentially effective agents [76,77]. The weight-based dosages predicted for efficacy from PK–PD bridging studies are in excess of those recommended in adults for invasive candidiasis. This finding promoted further clinical studies of micafungin that included dosages up to 15 mg/kg. The European Society of Clinical Microbiology and Infectious Diseases recommends that a dosage of 10 mg/kg is considered for neonatal HCME [76]. Echinocandins may also be considered as an adjunct to other first-line antifungal agents for the treatment of CNS infection caused by *Aspergillus* spp., *S. apiospermum* complex, and *Lemontospora prolificans* (Table 1).

8. Expert opinion

The antifungal drugs currently available are either suboptimal or are being used suboptimally, for CNS disease. However, the technological and scientific capacity to improve this situation exists.

Reformulation of drugs may improve their distribution through the BBB and BCSFB. In particular, nanoparticulate drug formulations offer promise in terms of CNS distribution. These submicrometer units may improve drug transport across the BBB by transiently increasing BBB permeability or by internalizing into brain capillary endothelial cells and thus traversing the intact BBB transvascularly [180,181]. These concepts and a description of specific carriers are presented elsewhere [182,183]. A number of examples of the exploration of nanostructured antifungal drug preparations exist. A nanosuspension formulation of amphotericin B increased AmB concentrations in mouse brains by a factor of 2.5–4.25 relative to LAmB [184]. Amphotericin B-containing micelles, modified using a ligand of low-density lipoprotein receptor-related protein present on the BBB, have shown better BBB penetration than unmodified micelles or amphotericin B deoxycholate both *in vitro* and *in vivo* [185]. Nanostructured liposomes can increase itraconazole concentrations by 2-fold in mouse brains [186]. These chemical modifications represent potential avenues to maximize the utility of currently available antifungal drugs for CNS infections.

TDM is a standard of care for the triazoles and 5FC regardless of the site of infection [187,188]. For CNS mycoses, antifungal TDM is even more critical to ensure adequate concentration at the effect site. Targets for TDM for efficacy are generally based on non-CNS disease. Hence, clinicians must use their judgment as to which target to aim for in TDM. From a pragmatic perspective, aiming for higher concentrations within the therapeutic range is a reasonable strategy (rather than being reassured by concentrations that are just within the therapeutic range).

8.1. Novel antifungal drugs with potential for use as CNS agents

Several promising new antifungal compounds are under investigation and may hold promise as treatments for CNS disease. Viamet Pharmaceuticals (Durham, NC, USA) have developed VT-1129, a quaternary azole that is efficacious in murine models of cryptococcal meningitis [189] and systemic candidiasis [190]. Cidara Therapeutics (San Diego, CA, USA) is developing a novel semisynthetic echinocandin, CD101. CD101 is active against *Candida* and *Aspergillus* spp [191]., but in preclinical models displays tissue distribution patterns in keeping with currently available echinocandins, penetrating poorly into brain parenchyma [192].

F901318 (F2G limited, Eccles, UK) is the leading compound in a novel class of antifungals, the orotomides, which block fungal pyrimidine synthesis [193]. F901318 is active against *Aspergillus* spp., including resistant strains [194], as well as *Penicillium* spp., *Coccidiodes immitis, H. capsulatum, Blastomyces dermatitidis, Fusarium* spp., and *Scedosporium* spp [193]. F901318 is detectable in brain tissue after administration to mice [193]. Amplyx Pharmaceuticals (San Diego, CA, USA) have developed a novel antifungal agent, APX001, which inhibits a glycosylphosphatidylinositol-anchored fungal wall transfer protein [195]. APX001 exhibits highly selective *in vitro* antifungal activity against *Candida* spp., including strains resistant to fluconazole, *Aspergillus fumigatus, A. niger, A. flavus, A. terreus, Fusarium, Pseudallescheria boydii*, and *S.*

prolificans [196,197]. In a murine model of disseminated *C. auris* infection, APX001 improves survival by up to 2-fold relative to anidulafungin, with demonstrable PD effect in brain tissue [195]. APX001 was granted orphan drug status by the US Food and Drug Administration in 2016 [198]. Another novel first-in-class antifungal agent is SCY-078 (SCYNEXIS, Jersey City, NJ, USA). SCY-078 is a semisynthetic derivative of enfumafungin and the only compound in the triterpene class of antifungals [199]. It is a potent inhibitor of β-[1,3]-D-glucan synthesis in fungal cell walls and demonstrates broad spectrum activity against *Candida* spp [200]., including *C. auris* [201] and *Aspergillus* spp [202] *in vitro*. Preclinical *in vivo* models using SCY-078 for treatment of disseminated candidiasis have demonstrated promising potency and PK [199].

8.2. New technologies for the assessment of CNS PK of antifungals

Historically, studies assessing the CNS PK of antifungals *in vivo* have taken brain tissue homogenates and measured drug using LC–MS, as demonstrated in this review. Modern techniques enable more refined CNS PK models including information about the spatial distribution of drug within tissues. We have seen that PK differences in various brain compartments can be assessed using microdialysis. This technique measures drug penetration into fluid compartments of the CNS using a dialysis probe to detect free drug in the cerebral interstitial fluid. The use of microdialysis in humans is limited to intraoperative settings and the technique may be unsuitable for the quantification of highly protein-bound or lipophilic drugs [203]. PET scanning and MR spectroscopy are non-invasive techniques that can estimate drug distribution into the human brain by detecting radiolabelled molecules. PET can provide longitudinal trends in drug distribution but its use is limited by cost, the inability to distinguish parent compounds from metabolites, and the requirement for radioactive labeling [75,204,205].

Matrix-Assisted Laser Desorption and Ionization – Mass Spectroscopy Imaging (MALDI-MSI) does not require radiolabelling and can provide rapid, highly resolved spatial drug distribution data. In murine brains, MALDI-MSI has been employed to quantify a number of antibiotics including gatifloxacin [206], doxycycline [207], pretomanid [208], and rifampicin [209] to the subcompartmental level. Serial tissue sections taken over time can yield longitudinal data. The technique has not yet been applied to assess the CNS distribution of antifungal drugs. To do so could elucidate information regarding mechanisms of drug action, distribution, and inter-subject variability in CNS drug penetration. This would enable precision spatial PK modeling with vastly enhanced translational utility from laboratory animals to humans and from plasma drug levels to those in the CNS.

Funding

K Stott receives funding from the Wellcome Trust [grant number 203919/Z/16/Z].

Declaration of interest

W Hope holds or has recently held research grants with F2G, AiCuris, Astellas Pharma, Spero Therapeutics, Matinas Biosciences, Antabio, Amplyx, Allecra and Pfizer. W Hope holds awards from the National Institutes of Health, Medical Research Council, National Institute of Health Research, and the European Commission (FP7 and IMI). W Hope has received personal fees in his capacity as a consultant for F2G, Amplyx, Ausperix, Spero Therapeutics, Medicines Company, Gilead and Basilea. W Hope is Medical Guideline Director for the European Society of Clinical Microbiology and Infectious Diseases, and an Ordinary Council Member for the British Society of Antimicrobial Chemotherapy. The authors have no other relevant affiliations or financial involvement with any organization or entity with a financial interest in or financial conflict with the subject matter or materials discussed in the manuscript apart from those disclosed.

Reviewer disclosures

Peer reviewers on this manuscript have no relevant financial or other relationships to disclose.

References

Papers of special note have been highlighted as either of interest (•) or of considerable interest (••) to readers.

1. Brown GD, Denning DW, Gow NAR, et al. Hidden Killers: human Fungal Infections. Sci Transl Med. 2012;4(165):165rv13–rv13.
2. Felton T, Troke PF, Hope WW. Tissue penetration of antifungal agents. Clin Microbiol Rev. 2014;27(1):68–88.
3. Kethireddy S, Andes D. CNS pharmacokinetics of antifungal agents. Expert Opin Drug Metab Toxicol. 2007;3(4):573–581.
4. Lee SC, Dickson DW, Casadevall A. Pathology of cryptococcal meningoencephalitis: analysis of 27 patients with pathogenetic implications. Hum Pathol. 1996;27(8):839–847.
5. Charlier C, Dromer F, Leveque C, et al. Cryptococcal neuroradiological lesions correlate with severity during cryptococcal meningoencephalitis in HIV-positive patients in the HAART era. PLoS ONE. 2008;3(4):e1950.
6. Lan SH, Chang WN, Lu CH, et al. Cerebral infarction in chronic meningitis: a comparison of tuberculous meningitis and cryptococcal meningitis. Qjm. 2001;94(5):247–253.
7. Chen SF, Lu CH, Lui CC, et al. Acute/subacute cerebral infarction (ASCI) in HIV-negative adults with cryptococcal meningoencephalitis (CM): a MRI-based follow-up study and a clinical comparison to HIV-negative CM adults without ASCI. BMC Neurology. 2011;11:12.
8. Jarvis JN, Meintjes G, Rebe K, et al. Adjunctive interferon-gamma immunotherapy for the treatment of HIV-associated cryptococcal meningitis: a randomized controlled trial. Aids. 2012;26(9):1105–1113.
9. Jarvis JN, Bicanic T, Loyse A, et al. Determinants of mortality in a combined cohort of 501 patients with HIV-associated Cryptococcal meningitis: implications for improving outcomes. Clin Infect Dis. 2014;58(5):736–745.
10. Speed B, Dunt D. Clinical and host differences between infections with the two varieties of Cryptococcus neoformans. Clin Infect Dis. 1995;21(1):28–34. discussion 5-6.
11. CDC. Emergence of Cryptococcus gattii– pacific Northwest, 2004-2010. MMWR Morb Mortal Wkly Rep. 2010;59(28):865–868.
12. Chen SC, Slavin MA, Heath CH, et al. Clinical manifestations of Cryptococcus gattii infection: determinants of neurological sequelae and death. Clin Infect Dis. 2012;55(6):789–798.
13. Stockamp NW, Thompson GR. Coccidioidomycosis. Infect Dis Clin North Am. 2016;30(1):229–246.
14. de Carvalho CA, Allen JN, Zafranis A, et al. Coccidioidal meningitis complicated by cerebral arteritis and infarction. Hum Pathol. 1980;11(3):293–296.
15. Stevens DA, Shatsky SA. Intrathecal amphotericin in the management of coccidioidal meningitis. Semin Respir Infect. 2001;16(4):263–269.

16. Berry CD, Happs EL, Sahrakar K, et al. Method for the Treatment of Chronic Fungal Meningitis: continuous Infusion into the Cerebrospinal Fluid for Coccidioidal Meningitis. Am J Med Sci. 2009;338(1):79–82.
17. Goldstein EJC, Johnson RH, Einstein HE. Coccidioidal Meningitis. Clin Infect Dis. 2006;42(1):103–107.
18. Garg N, Devi IB, Vajramani GV, et al. Central nervous system cladosporiosis: an account of ten culture-proven cases. Neurol India. 2007;55(3):282–288.
19. Dixon DM, Walsh TJ, Merz WG, et al. Infections due to Xylohypha bantiana (Cladosporium trichoides). Rev Infect Dis. 1989;11(4):515–525.
20. Filizzola MJ, Martinez F, Rauf SJ. Phaeohyphomycosis of the central nervous system in immunocompetent hosts: report of a case and review of the literature. Int J Infect Dis. 2003;7(4):282–286.
21. Revankar SG, Sutton DA, Rinaldi MG. Primary central nervous system phaeohyphomycosis: a review of 101 cases. Clin Infect Dis. 2004;38(2):206–216.
22. Ashdown BC, Tien RD, Felsberg GJ. Aspergillosis of the brain and paranasal sinuses in immunocompromised patients: CT and MR imaging findings. AJR Am J Roentgenol. 1994;162(1):155–159.
23. Wang RX, Zhang JT, Chen Y, et al. Cerebral aspergillosis: a retrospective analysis of eight cases. Int J Neurosci. 2017;127(4):339–343.
24. Pongbhaesaj P, Dejthevaporn C, Tunlayadechanont S, et al. Aspergillosis of the central nervous system: a catastrophic opportunistic infection. Southeast Asian J Trop Med Public Health. 2004;35(1):119–125.
25. Spapen H, Spapen J, Taccone FS, et al. Cerebral aspergillosis in adult critically ill patients: a descriptive report of 10 patients from the AsplCU cohort. Int J Antimicrob Agents. 2014;43(2):165–169.
26. Hamill RJ. Fungal infections of the central nervous system. In: Anaissie EJ, McGinnis MR, Phaller MA, editors. Clinical Mycology. 2nd ed. London: Churchill Livingstone (Elselvier); 2009. p. 591–608.
27. Rodriguez-Tudela JL, Berenguer J, Guarro J, et al. Epidemiology and outcome of Scedosporium prolificans infection, a review of 162 cases. Med Mycol. 2009;47(4):359–370.
28. Lamaris GA, Chamilos G, Lewis RE, et al. Scedosporium Infection in a Tertiary Care Cancer Center: A Review of 25 Cases from 1989–2006. Clin Infect Dis. 2006;43(12):1580–1584.
29. Troke P, Aguirrebengoa K, Arteaga C, et al. Treatment of scedosporiosis with voriconazole: clinical experience with 107 patients. Antimicrob Agents Chemother. 2008;52(5):1743–1750.
30. Husain S, Munoz P, Forrest G, et al. Infections due to Scedosporium apiospermum and Scedosporium prolificans in transplant recipients: clinical characteristics and impact of antifungal agent therapy on outcome. Clin Infect Dis. 2005;40(1):89–99.
31. Sanchez-Portocarrero J, Perez-Cecilia E, Corral O, et al. The central nervous system and infection by Candida species. Diagn Microbiol Infect Dis. 2000;37(3):169–179.
32. Voice RA, Bradley SF, Sangeorzan JA, et al. Chronic candidal meningitis: an uncommon manifestation of candidiasis. Clin Infect Dis. 1994;19(1):60–66.
33. Casado JL, Quereda C, Oliva J, et al. Candidal meningitis in HIV-infected patients: analysis of 14 cases. Clin Infect Dis. 1997;25 (3):673–676.
34. Benjamin DK Jr., Stoll BJ, Fanaroff AA, et al. Neonatal candidiasis among extremely low birth weight infants: risk factors, mortality rates, and neurodevelopmental outcomes at 18 to 22 months. Pediatrics. 2006;117(1):84–92.
35. Nguyen MH, Yu VL. Meningitis caused by Candida species: an emerging problem in neurosurgical patients. Clin Infect Dis. 1995;21(2):323–327.
36. Schestatsky P, Chedid MF, Amaral OB, et al. Isolated central nervous system histoplasmosis in immunocompetent hosts: a series of 11 cases. Scand J Infect Dis. 2006;38(1):43–48.
37. Saccente M, McDonnell RW, Baddour LM, et al. Cerebral histoplasmosis in the azole era: report of four cases and review. South Med J. 2003;96(4):410–416.
38. Wheat LJ, Musial CE, Jenny-Avital E. Diagnosis and management of central nervous system histoplasmosis. Clin Infect Dis. 2005;40(6):844–852.
39. Freifeld A, Proia L, Andes D, et al. Voriconazole use for endemic fungal infections. Antimicrob Agents Chemother. 2009;53(4):1648–1651.
40. Thompson GR 3rd, Wiederhold NP. Isavuconazole: a comprehensive review of spectrum of activity of a new triazole. Mycopathologia. 2010;170(5):291–313.
41. Black KE, Baden LR. Fungal infections of the CNS: treatment strategies for the immunocompromised patient. CNS Drugs. 2007;21 (4):293–318.
42. Gonyea EF. The spectrum of primary blastomycotic meningitis: a review of central nervous system blastomycosis. Ann Neurol. 1978;3(1):26–39.
43. Chapman SW, Dismukes WE, Proia LA, et al. Clinical practice guidelines for the management of blastomycosis: 2008 update by the Infectious Diseases Society of America. Clin Infect Dis. 2008;46 (12):1801–1812.
44. Trifilio SM, Bennett CL, Yarnold PR, et al. Breakthrough zygomycosis after voriconazole administration among patients with hematologic malignancies who receive hematopoietic stem-cell transplants or intensive chemotherapy. Bone Marrow Transplant. 2007;39 (7):425–429.
45. Bitar D, Van Cauteren D, Lanternier F, et al. Increasing incidence of zygomycosis (mucormycosis), France, 1997-2006. Emerg Infect Dis. 2009;15(9):1395–1401.
46. Aristizabal BH, Clemons KV, Cock AM, et al. Experimental paracoccidioides brasiliensis infection in mice: influence of the hormonal status of the host on tissue responses. Med Mycol. 2002;40(2):169–178.
47. Elias J Jr., Colli BO, Canheu A, et al. Central nervous system paracoccidioidomycosis: diagnosis and treatment. Surg Neurol. 2005;63 (Suppl 1):S13–S21. discussion S.
48. Queiroz-Telles F, Goldani LZ, Schlamm HT, et al. An open-label comparative pilot study of oral voriconazole and itraconazole for long-term treatment of paracoccidioidomycosis. Clin Infect Dis. 2007;45(11):1462–1469.
49. Surmont I, Vergauwen B, Marcelis L, et al. First report of chronic meningitis caused byTrichosporon beigelii. Eur J Clin Microbiol Infect Dis. 1990;9(3):226–229.
50. Watson KC, Kallichurum S. Brain abscess due to Trichosporon cutaneum. J Med Microbiol. 1970;3(1):191–193.
51. Gottfredsson M, Perfect JR. Fungal meningitis. Semin Neurol. 2000;20(3):307–322.
•• **Excellent review of fungal meningitis.**
52. de Lange ECM. The mastermind approach to CNS drug therapy: translational prediction of human brain distribution, target site kinetics, and therapeutic effects. Fluids Barriers CNS. 2013;10(1):12.
53. Nau R, Sorgel F, Eiffert H. Penetration of drugs through the blood-cerebrospinal fluid/blood-brain barrier for treatment of central nervous system infections. Clin Microbiol Rev. 2010;23(4):858–883.
54. Di Paolo A, Gori G, Tascini C, et al. Clinical pharmacokinetics of antibacterials in cerebrospinal fluid. Clin Pharmacokinet. 2013;52 (7):511–542.
55. Fong IW, Tomkins KB. Penetration of ceftazidime into the cerebrospinal fluid of patients with and without evidence of meningeal inflammation. Antimicrob Agents Chemother. 1984;26(1):115–116.
56. Pardridge WM. Blood-brain barrier drug targeting: the future of brain drug development. Mol Interv. 2003;3(2):90–105. 51.
57. Pasko MT, Piscitelli SC, Van Slooten AD. Fluconazole: a new triazole antifungal agent. Dicp. 1990;24(9):860–867.
58. Troke PF, Andrews RJ, Pye GW, et al. Fluconazole and Other Azoles: translation of in Vitro Activity to in Vivo and Clinical Efficacy. Rev Infect Dis. 1990;12(Supplement_3):S276–S80.
59. Gubbins PA, E J. Antifungal therapy. In: Anaissie EJ, McGinnis MR, Phaller MA, editors. Clinical Mycology. 2nd ed. London: Churchill Livingstone, Elsevier; 2009. p. 161–196.
60. Girmenia C. New generation azole antifungals in clinical investigation. Expert Opin Investig Drugs. 2009;18(9):1279–1295.
61. NationalCenterforBiotechnologyInformation. Isavuconazonium. PubChem Compound Database; CID=6918606: national Center for Biotechnology Information. [cited 2017 Nov 8]. Available from: https://pubchem.ncbi.nlm.nih.gov/compound/6918606

62. Bekersky I, Fielding RM, Dressler DE, et al. Plasma protein binding of amphotericin B and pharmacokinetics of bound versus unbound amphotericin B after administration of intravenous liposomal amphotericin B (AmBisome) and amphotericin B deoxycholate. Antimicrob Agents Chemother. 2002;46(3):834–840.
63. Hartsel S, Bolard J. Amphotericin B: new life for an old drug. Trends Pharmacol Sci. 1996;17(12):445–449.
64. Clemons KV, Espiritu M, Parmar R, et al. Comparative efficacies of conventional amphotericin b, liposomal amphotericin B (AmBisome), caspofungin, micafungin, and voriconazole alone and in combination against experimental murine central nervous system aspergillosis. Antimicrob Agents Chemother. 2005;49(12):4867–4875.
65. Hospenthal DR. Approach to patients with Suspected Fungal Infections. In: Hospenthal DR, Rinaldi MG, editors. Diagnosis and Treatment of Fungal Infections. 2nd ed. New York City: Springer International Publishing; 2015. p. 3-7
66. Larger P, Wenzler U, Schmitt-Hoffmann A. Isavuconazole and Other Azoles with Respect to Physicochemical and Pharmacokinetic Properties Affecting Tissue Penetration. Vienna: ECCMID; 2017.
67. de Lange, EC, Danhof M. Considerations in the use of cerebrospinal fluid pharmacokinetic to predict brain target concentrations in the clinical setting. Implications of the barriers between blood and brain. Clin Pharmacokinet. 2002;41(10):691–703.
68. Andes DR, Craig WA. Pharmacokinetics and pharmacodynamics of antibiotics in meningitis. Infect Dis Clin North Am. 1999;13(3):595–618.
69. Atkinson F, Cole S, Green C, et al. Lipophilicity and other parameters affecting brain penetration. Curr Med Chemistry-Central Nerv Syst Agents. 2002;2(3):229–240.
70. Yamamoto Y, Danhof M, de Lange ECM. Microdialysis: the Key to Physiologically Based Model Prediction of Human CNS Target Site Concentrations. AAPS J. 2017;19(4):891–909.
•• **Excellent introduction to the concept of microdialysis.**
71. Lempers VJC, van den Heuvel JJMW, Russel FGM, et al. Inhibitory Potential of Antifungal Drugs on ATP-Binding Cassette Transporters P-Glycoprotein, MRP1 to MRP5, BCRP, and BSEP. Antimicrob Agents Chemother. 2016;60(6):3372–3379.
72. Wu JQ, Shao K, Wang X, et al. In vitro and in vivo evidence for amphotericin B as a P-glycoprotein substrate on the blood-brain barrier. Antimicrob Agents Chemother. 2014;58(8):4464–4469.
73. Stevens DA, Clemons KV, Martinez M, et al. The Brain, Amphotericin B, and P-Glycoprotein. Antimicrob Agents Chemother. 2015;59 (2):1386.
74. Stott KE, Hope WW. Therapeutic drug monitoring for invasive mould infections and disease: pharmacokinetic and pharmacodynamic considerations. J Antimicrob Chemother. 2017;72(suppl_1): i12–i8.
75. Srinivas N, Maffuid K, Kashuba ADM. Clinical Pharmacokinetics and Pharmacodynamics of Drugs in the Central Nervous System. Clin Pharmacokinet. 2018.
76. Hope WW, Mickiene D, Petraitis V, et al. The Pharmacokinetics and Pharmacodynamics of Micafungin in Experimental Hematogenous Candida Meningoencephalitis: implications for Echinocandin Therapy in Neonates. J Infect Dis. 2008;197(1):163–171.
• **Clear demonstration of the potential for PK–PD models based on preclinical data to predict clinical efficacy.**
77. Warn PA, Livermore J, Howard S, et al. Anidulafungin for neonatal hematogenous Candida meningoencephalitis: identification of candidate regimens for humans using a translational pharmacological approach. Antimicrob Agents Chemother. 2012;56(2):708–714.
78. Yamamoto Y, Välitalo PA, van den Berg DJ, et al. A Generic Multi-Compartmental CNS Distribution Model Structure for 9 Drugs Allows Prediction of Human Brain Target Site Concentrations. Pharm Res. 2017;34(2):333–351.
79. Yamamoto Y, Valitalo PA, Wong YC, et al. Prediction of human CNS pharmacokinetics using a physiologically-based pharmacokinetic modeling approach. Eur J Pharm Sci. 2018;112:168–179.
80. Alqahtani S, Kaddoumi A. Development of a Physiologically Based Pharmacokinetic/Pharmacodynamic Model to Predict the Impact of Genetic Polymorphisms on the Pharmacokinetics and Pharmacodynamics Represented by Receptor/Transporter Occupancy of Central Nervous System Drugs. Clin Pharmacokinet. 2016;55(8):957–969.
81. Tucker RM, Williams PL, Arathoon EG, et al. Pharmacokinetics of fluconazole in cerebrospinal fluid and serum in human coccidioidal meningitis. Antimicrob Agents Chemother. 1988;32(3):369–373.
82. Thaler F, Bernard B, Tod M, et al. Fluconazole penetration in cerebral parenchyma in humans at steady state. Antimicrob Agents Chemother. 1995;39(5):1154–1156.
83. Fischman AJ, Alpert NM, Livni E, et al. Pharmacokinetics of 18F-labeled fluconazole in healthy human subjects by positron emission tomography. Antimicrob Agents Chemother. 1993;37(6):1270–1277.
84. Henry ME, Bolo NR, Zuo CS, et al. Quantification of brain voriconazole levels in healthy adults using fluorine magnetic resonance spectroscopy. Antimicrob Agents Chemother. 2013;57(11):5271–5276.
85. Yang H, Wang Q, Elmquist WF. Fluconazole distribution to the brain: a crossover study in freely-moving rats using in vivo microdialysis. Pharm Res. 1996;13(10):1570–1575.
86. Arndt CA, Walsh TJ, McCully CL, et al. Fluconazole penetration into cerebrospinal fluid: implications for treating fungal infections of the central nervous system. J Infect Dis. 1988;157(1):178–180.
87. Madu A, Cioffe C, Mian U, et al. Pharmacokinetics of fluconazole in cerebrospinal fluid and serum of rabbits: validation of an animal model used to measure drug concentrations in cerebrospinal fluid. Antimicrob Agents Chemother. 1994;38(9):2111–2115.
88. Brammer KW, Farrow PR, Faulkner JK. Pharmacokinetics and tissue penetration of fluconazole in humans. Rev Infect Dis. 1990;12(Suppl 3):S318–S26.
89. Longley N, Muzoora C, Taseera K, et al. Dose response effect of high-dose fluconazole for HIV-associated cryptococcal meningitis in southwestern Uganda. Clin Infect Dis. 2008;47(12):1556–1561.
90. Nussbaum JC, Jackson A, Namarika D, et al. Combination flucytosine and high-dose fluconazole compared with fluconazole monotherapy for the treatment of cryptococcal meningitis: a randomized trial in Malawi. Clin Infect Dis. 2010;50(3):338–344.
91. Bicanic T, Meintjes G, Wood R, et al. Fungal Burden, Early Fungicidal Activity, and Outcome in Cryptococcal Meningitis in Antiretroviral-Naive or Antiretroviral-Experienced Patients Treated with Amphotericin B or Fluconazole. Clin Infect Dis. 2007;45(1):76–80.
92. Brouwer AE, Rajanuwong A, Chierakul W, et al. Combination antifungal therapies for HIV-associated cryptococcal meningitis: a randomised trial. Lancet. 2004;363(9423):1764–1767.
93. Joint_Formulary_Committee. British National Formulary (online) London: BMJ Group and Pharmaceutical Press. 2016
94. Galgiani JN, Ampel NM, Blair JE, et al. Infectious Diseases Society of America (IDSA) Clinical Practice Guideline for the Treatment of Coccidioidomycosis. Clin Infect Dis. 2016;63(6):e112–e46. 2016.
95. Sorensen KN, Sobel RA, Clemons KV, et al. Comparison of Fluconazole and Itraconazole in a Rabbit Model of Coccidioidal Meningitis. Antimicrob Agents Chemother. 2000;44(6):1512–1517.
96. Heykants J, Michiels M, Meuldermans W, et al. The pharmacokinetics of itraconazole in animals and man: an overview. In: Ra F, editor. Recent trends in the discovery, development and evaluation of antifungal agents. Barcelona, Spain: J R Prous; 1987. p. 223–259.
97. Perfect JR, Savani DV, Durack DT. Comparison of itraconazole and fluconazole in treatment of cryptococcal meningitis and candida pyelonephritis in rabbits. Antimicrob Agents Chemother. 1986;29 (4):579–583.
• **Important study comparing efficacy of these two azoles in well-established animal models of fungal meningitis.**
98. Poirier JM, Cheymol G. Optimisation of itraconazole therapy using target drug concentrations. Clin Pharmacokinet. 1998;35(6):461–473.
99. Miyama T, Takanaga H, Matsuo H, et al. P-Glycoprotein-Mediated Transport of Itraconazole across the Blood-Brain Barrier. Antimicrob Agents Chemother. 1998;42(7):1738–1744.
100. Haynes RR, Connolly PA, Durkin MM, et al. Antifungal therapy for central nervous system histoplasmosis, using a newly developed intracranial model of infection. J Infect Dis. 2002;185(12):1830–1832.

101. Imbert F, Jardin M, Fernandez C, et al. Effect of efflux inhibition on brain uptake of itraconazole in mice infected with Cryptococcus neoformans. Drug Metab Dispos. 2003;31(3):319–325.
102. Chiller TM, Sobel RA, Luque JC, et al. Efficacy of amphotericin B or itraconazole in a murine model of central nervous system Aspergillus infection. Antimicrob Agents Chemother. 2003;47 (2):813–815.
103. Pfaller MA, Espinel-Ingroff A, Canton E, et al. Wild-type MIC distributions and epidemiological cutoff values for amphotericin B, flucytosine, and itraconazole and Candida spp. as determined by CLSI broth microdilution. J Clin Microbiol. 2012;50(6):2040–2046.
104. Chang LW, Phipps WT, Kennedy GE, et al. Antifungal interventions for the primary prevention of cryptococcal disease in adults with HIV. Cochrane Database Syst Rev. 2005 Jul 20;(3):CD004773.
105. Nelson MR, Bower M, Smith D, et al. The value of serum cryptococcal antigen in the diagnosis of cryptococcal infection in patients infected with the human immunodeficiency virus. J Infect. 1990;21(2):175–181.
106. Denning DW, Tucker RM, Hanson LH, et al. Itraconazole therapy for cryptococcal meningitis and cryptococcosis. Arch Intern Med. 1989;149(10):2301–2308.
107. Sharkey PK, Rinaldi MG, Dunn JF, et al. High-dose itraconazole in the treatment of severe mycoses. Antimicrob Agents Chemother. 1991;35(4):707–713.
108. Saag MS, Cloud GA, Graybill JR, et al. A comparison of itraconazole versus fluconazole as maintenance therapy for AIDS-associated cryptococcal meningitis. National Institute of Allergy and Infectious Diseases Mycoses Study Group. Clin Infect Dis. 1999;28 (2):291–296.
109. WHO. Rapid advice: Diagnosis, prevention and management of cryptococcal disease in HIV-infected adults, adolescents and children. 2011.
110. McKinsey DS, Wheat LJ, Cloud GA, et al. Itraconazole prophylaxis for fungal infections in patients with advanced human immunodeficiency virus infection: randomized, placebo-controlled, double-blind study. National Institute of Allergy and Infectious Diseases Mycoses Study Group. Clin Infect Dis. 1999;28(5):1049–1056.
111. Lestner J, Hope WW. Itraconazole: an update on pharmacology and clinical use for treatment of invasive and allergic fungal infections. Expert Opin Drug Metab Toxicol. 2013;9(7):911–926.
112. Lutsar I, Roffey S, Troke P. Voriconazole concentrations in the cerebrospinal fluid and brain tissue of guinea pigs and immunocompromised patients. Clin Infect Dis. 2003;37(5):728–732.
113. Elter T, Sieniawski M, Gossmann A, et al. Voriconazole brain tissue levels in rhinocerebral aspergillosis in a successfully treated young woman. Int J Antimicrob Agents. 2006;28(3):262–265.
114. Denes E, Pichon N, Debette-Gratien M, et al. Pharmacokinetics of voriconazole in the cerebrospinal fluid of an immunocompromised patient with a brain abscess due to Aspergillus fumigatus. Clin Infect Dis. 2004;39(4):603–604.
115. Walsh TJ, Karlsson MO, Driscoll T, et al. Pharmacokinetics and safety of intravenous voriconazole in children after single- or multiple-dose administration. Antimicrob Agents Chemother. 2004;48 (6):2166–2172.
116. Hope WW. Population pharmacokinetics of voriconazole in adults. Antimicrob Agents Chemother. 2012;56(1):526–531.
117. Friberg LE, Ravva P, Karlsson MO, et al. Integrated population pharmacokinetic analysis of voriconazole in children, adolescents, and adults. Antimicrob Agents Chemother. 2012;56(6):3032–3042.
    - **Excellent example of the potential for population PK modeling to quantify PK variability in different populations.**
118. Kadam RS, van den Anker JN. Pediatric Clinical Pharmacology of Voriconazole: role of Pharmacokinetic/Pharmacodynamic Modeling in Pharmacotherapy. Clin Pharmacokinet. 2016;Sep;55(9):1031–1043. doi: 10.1007/s40262-016-0379-2.
119. Luong M-L, Al-Dabbagh M, Groll AH, et al. Utility of voriconazole therapeutic drug monitoring: a meta-analysis. J Antimicrob Chemother. 2016;71(7):1786–1799.
120. Patterson TF, Thompson GR III, Denning DW, et al. Practice Guidelines for the Diagnosis and Management of Aspergillosis: 2016 Update by the Infectious Diseases Society of America. Clin Infect Dis. 2016;63(4):e1–e60.
121. Nagappan V, Deresinski S. Posaconazole: a Broad-Spectrum Triazole Antifungal Agent. Clin Infect Dis. 2007;45(12):1610–1617.
122. Sansone-Parsons A, Krishna G, Simon J, et al. Effects of age, gender, and race/ethnicity on the pharmacokinetics of posaconazole in healthy volunteers. Antimicrob Agents Chemother. 2007;51 (2):495–502.
123. Ullmann AJ, Cornely OA, Burchardt A, et al. Pharmacokinetics, safety, and efficacy of posaconazole in patients with persistent febrile neutropenia or refractory invasive fungal infection. Antimicrob Agents Chemother. 2006;50(2):658–666.
124. Gubbins PO, Krishna G, Sansone-Parsons A, et al. Pharmacokinetics and safety of oral posaconazole in neutropenic stem cell transplant recipients. Antimicrob Agents Chemother. 2006;50(6):1993–1999.
125. Petitcollin A, Boglione-Kerrien C, Tron C, et al. Population Pharmacokinetics of Posaconazole Tablets and Monte Carlo Simulations To Determine whether All Patients Should Receive the Same Dose. Antimicrob Agents Chemother. 2017;61:11.
126. Durani U, Tosh PK, Barreto JN, et al. Retrospective Comparison of Posaconazole Levels in Patients Taking the Delayed-Release Tablet versus the Oral Suspension. Antimicrob Agents Chemother. 2015;59(8):4914–4918.
127. Cumpston A, Caddell R, Shillingburg A, et al. Superior Serum Concentrations with Posaconazole Delayed-Release Tablets Compared to Suspension Formulation in Hematological Malignancies. Antimicrob Agents Chemother. 2015;59(8):4424–4428.
128. Krishna G, Ma L, Martinho M, et al. Single-Dose Phase I Study To Evaluate the Pharmacokinetics of Posaconazole in New Tablet and Capsule Formulations Relative to Oral Suspension. Antimicrob Agents Chemother. 2012;56(8):4196–4201.
129. Kersemaekers WM, van Iersel T, Nassander U, et al. Pharmacokinetics and Safety Study of Posaconazole Intravenous Solution Administered Peripherally to Healthy Subjects. Antimicrob Agents Chemother. 2015;59(2):1246–1251.
130. Calvo E, Pastor FJ, Rodríguez MM, et al. Antifungal Therapy in a Murine Model of Disseminated Infection by Cryptococcus gattii. Antimicrob Agents Chemother. 2010;54(10):4074–4077.
131. Calvo E, Pastor FJ, Rodríguez MM, et al. Murine Model of a Disseminated Infection by the Novel Fungus Fonsecaea monophora and Successful Treatment with Posaconazole. Antimicrob Agents Chemother. 2010;54(2):919–923.
132. Calcagno A, Baietto L, De Rosa FG, et al. Posaconazole cerebrospinal concentrations in an HIV-infected patient with brain mucormycosis. J Antimicrob Chemother. 2011;66(1):224–225.
133. Ruping MJ, Albermann N, Ebinger F, et al. Posaconazole concentrations in the central nervous system. J Antimicrob Chemother. 2008;62(6):1468–1470.
134. Reinwald M, Uharek L, Lampe D, et al. Limited penetration of posaconazole into cerebrospinal fluid in an allogeneic stem cell recipient with invasive pulmonary aspergillosis. Bone Marrow Transplant. 2009;44(4):269–270.
135. Anstead GM, Corcoran G, Lewis J, et al. Refractory coccidioidomycosis treated with posaconazole. Clin Infect Dis. 2005;40(12):1770–1776.
136. Vehreschild JJ, Birtel A, Vehreschild MJGT, et al. Mucormycosis treated with posaconazole: review of 96 case reports. Crit Rev Microbiol. 2013;39(3):310–324.
137. Simmonds L, Mitchell S, White B, et al. Aspergillus niger infection in an immunosuppressed patient confined solely to the brain. BMJ Case Rep. 2017;2017. doi:10.1136/bcr-2016-218658.
138. Walsh TJ, Raad I, Patterson TF, et al. Treatment of invasive aspergillosis with posaconazole in patients who are refractory to or intolerant of conventional therapy: an externally controlled trial. Clin Infect Dis. 2007;44(1):2–12.
139. Restrepo A, Tobon A, Clark B, et al. Salvage treatment of histoplasmosis with posaconazole. J Infect. 2007;54(4):319–327.
140. Schmitt-Hoffmann AH, Kato K, Townsend R, et al. Tissue Distribution and Elimination of Isavuconazole Following Single and Repeat Oral-Dose Administration of Isavuconazonium Sulfate to Rats. Antimicrob Agents Chemother. 61(12). doi: 10.1128/aac.01292-17.

141. Wiederhold NP, Kovanda L, Najvar LK, et al. Isavuconazole Is Effective for the Treatment of Experimental Cryptococcal Meningitis. Antimicrob Agents Chemother. 2016;60(9):5600–5603.
142. Maertens JA, Raad II, Marr KA, et al. Isavuconazole versus voriconazole for primary treatment of invasive mould disease caused by Aspergillus and other filamentous fungi (SECURE): a phase 3, randomised-controlled, non-inferiority trial. Lancet. 2016;387 (10020):760–769.
143. Peixoto D, Gagne LS, Hammond SP, et al. Isavuconazole treatment of a patient with disseminated mucormycosis. J Clin Microbiol. 2014;52(3):1016–1019.
144. Hamill RJ. Amphotericin B Formulations: a Comparative Review of Efficacy and Toxicity. Drugs. 2013;73(9):919–934.
145. Groll AH, Giri N, Petraitis V, et al. Comparative efficacy and distribution of lipid formulations of amphotericin B in experimental Candida albicans infection of the central nervous system. J Infect Dis. 2000;182(1):274–282.
146. Lee JW, Amantea MA, Francis PA, et al. Pharmacokinetics and safety of a unilamellar liposomal formulation of amphotericin B (AmBisome) in rabbits. Antimicrob Agents Chemother. 1994;38(4):713–718.
147. Pyrgos V, Mickiene D, Sein T, et al. Effects of immunomodulatory and organism-associated molecules on the permeability of an in vitro blood-brain barrier model to amphotericin B and fluconazole. Antimicrob Agents Chemother. 2010;54(3):1305–1310.
148. Lestner J, McEntee L, Johnson A, et al. Experimental Models of Short Courses of Liposomal Amphotericin B for Induction Therapy for Cryptococcal Meningitis. Antimicrob Agents Chemother. 2017;61: e00090-17.
- **Important preclinical study demonstrating the efficacy of abbreviated liposomal amphotericin B regimens.**
149. Livermore J, Howard SJ, Sharp AD, et al. Efficacy of an abbreviated induction regimen of amphotericin B deoxycholate for cryptococcal meningoencephalitis: 3 days of therapy is equivalent to 14 days. MBio. 2014;5(1):e00725–13.
- **Important preclinical study demonstrating the efficacy of abbreviated liposomal amphotericin B regimens.**
150. Strenger V, Meinitzer A, Donnerer J, et al. Amphotericin B transfer to CSF following intravenous administration of liposomal amphotericin B. J Antimicrob Chemother. 2014;69(9):2522–2526.
151. Vogelsinger H, Weiler S, Djanani A, et al. Amphotericin B tissue distribution in autopsy material after treatment with liposomal amphotericin B and amphotericin B colloidal dispersion. J Antimicrob Chemother. 2006;57(6):1153–1160.
152. Bicanic T, Wood R, Meintjes G, et al. High-dose amphotericin B with flucytosine for the treatment of cryptococcal meningitis in HIV-infected patients: a randomized trial. Clin Infect Dis. 2008;47(1):123–130.
153. Bariola JR, Perry P, Pappas PG, et al. Blastomycosis of the Central Nervous System: a Multicenter Review of Diagnosis and Treatment in the Modern Era. Clin Infect Dis. 2010;50(6):797–804.
154. Roden MM, Zaoutis TE, Buchanan WL, et al. Epidemiology and outcome of zygomycosis: a review of 929 reported cases. Clin Infect Dis. 2005;41(5):634–653.
155. Moreira JAS, Freitas DFS, Lamas CC. The impact of sporotrichosis in HIV-infected patients: a systematic review. Infection. 2015;43(3):267–276.
156. O'Connor L, Livermore J, Sharp AD, et al. Pharmacodynamics of liposomal amphotericin B and flucytosine for cryptococcal meningoencephalitis: safe and effective regimens for immunocompromised patients. J Infect Dis. 2013;208(2):351–361.
157. Brouwer AE, van Kan HJM, Johnson E, et al. Oral versus Intravenous Flucytosine in Patients with Human Immunodeficiency Virus-Associated Cryptococcal Meningitis. Antimicrob Agents Chemother. 2007;51(3):1038–1042.
158. Block ER, Bennett JE. Pharmacological studies with 5-fluorocytosine. Antimicrob Agents Chemother. 1972;1(6):476–482.
159. Andes D, van Ogtrop M. In vivo characterization of the pharmacodynamics of flucytosine in a neutropenic murine disseminated candidiasis model. Antimicrob Agents Chemother. 2000;44(4):938–942.
160. Lewis RE, Klepser ME, Pfaller MA. In vitro pharmacodynamic characteristics of flucytosine determined by time-kill methods. Diagn Microbiol Infect Dis. 2000;36(2):101–105.
161. Polak A, Scholer HJ. Mode of action of 5-fluorocytosine and mechanisms of resistance. Chemotherapy. 1975;21(3–4):113–130.
162. Normark S, Schonebeck J. In vitro studies of 5-fluorocytosine resistance in Candida albicans and Torulopsis glabrata. Antimicrob Agents Chemother. 1972;2(3):114–121.
163. Tassel D, Madoff MA. Treatment of Candida sepsis and Cryptococcus meningitis with 5-fluorocytosine: a new antifungal agent. Jama. 1968;206(4):830–832.
164. Hospenthal DR, Bennett JE. Flucytosine monotherapy for cryptococcosis. Clin Infect Dis. 1998;27(2):260–264.
165. Day JN, Chau TT, Wolbers M, et al. Combination antifungal therapy for cryptococcal meningitis. N Engl J Med. 2013;368(14):1291–1302.
166. van der Horst CM, Saag MS, Cloud GA, et al. Treatment of Cryptococcal Meningitis Associated with the Acquired Immunodeficiency Syndrome. New England J Med. 1997;337(1):15–21.
167. Bennett JE, Dismukes WE, Duma RJ, et al. A Comparison of Amphotericin B Alone and Combined with Flucytosine in the Treatment of Cryptoccal Meningitis. New England J Med. 1979;301 (3):126–131.
168. Medoff G, Comfort M, Kobayashi GS. Synergistic action of amphotericin B and 5-fluorocytosine against yeast-like organisms. Proc Soc Exp Biol Med. 1971;138(2):571–574.
169. Montgomerie JZ, Edwards JE Jr., Guze LB. Synergism of amphotericin B and 5-fluorocytosine for candida species. J Infect Dis. 1975;132(1):82–86.
170. Smego RA Jr., Perfect JR, Durack DT. Combined therapy with amphotericin B and 5-fluorocytosine for Candida meningitis. Rev Infect Dis. 1984;6 (6):791–801.
171. Joint_Formulary_Committee. British National Formulary for Children (online) London: BMJ Group, Royal Pharmaceutical Society of Great Britain. RCPCH Publications; 2018.
172. Brian Smith P, Steinbach WJ, Benjamin DK. Invasive Candida infections in the neonate. Drug Resistance Updates. 2005;8(3):147–162.
173. Schwartz S, Thiel E. Cerebral aspergillosis: tissue penetration is the key. Med Mycol. 2009;47(Suppl 1):S387–S93.
- **Review outlining complexity and importance of antifungal penetration into the CNS.**
174. Groll AH, Mickiene D, Petraitis V, et al. Compartmental pharmacokinetics and tissue distribution of the antifungal echinocandin lipopeptide micafungin (FK463) in rabbits. Antimicrob Agents Chemother. 2001;45(12):3322–3327.
175. Groll AH, Mickiene D, Petraitiene R, et al. Pharmacokinetic and pharmacodynamic modeling of anidulafungin (LY303366): reappraisal of its efficacy in neutropenic animal models of opportunistic mycoses using optimal plasma sampling. Antimicrob Agents Chemother. 2001;45(10):2845–2855.
176. Hajdu R, Thompson R, Sundelof JG, et al. Preliminary animal pharmacokinetics of the parenteral antifungal agent MK-0991 (L-743,872). Antimicrob Agents Chemother. 1997;41(11):2339–2344.
177. Lat A, Thompson GR, Rinaldi MG, et al. Micafungin Concentrations from Brain Tissue and Pancreatic Pseudocyst Fluid. Antimicrob Agents Chemother. 2010;54(2):943–944.
178. Okugawa S, Ota Y, Tatsuno K, et al. A case of invasive central nervous system aspergillosis treated with micafungin with monitoring of micafungin concentrations in the cerebrospinal fluid. Scand J Infect Dis. 2007;39(4):344–346.
179. Prabhu RM, Orenstein R. Failure of caspofungin to treat brain abscesses secondary to Candida albicans prosthetic valve endocarditis. Clin Infect Dis. 2004;39(8):1253–1254.
180. Garcia-Garcia E, Andrieux K, Gil S, et al. Colloidal carriers and blood-brain barrier (BBB) translocation: a way to deliver drugs to the brain? Int J Pharm. 2005;298(2):274–292.
181. Alyautdin R, Khalin I, Nafeeza MI, et al. Nanoscale drug delivery systems and the blood–brain barrier. Int J Nanomedicine. 2014;9:795–811.
182. Li X, Tsibouklis J, Weng T, et al. Nano carriers for drug transport across the blood–brain barrier. J Drug Target. 2017;25 (1):17–28.
183. He Q, Liu J, Liang J, et al. Towards Improvements for Penetrating the Blood–brain Barrier—recent Progress from a Material and Pharmaceutical Perspective. Cells. 2018;7(4):24.

•• **Excellent review of state-of-the-art technologies to improve CNS drug distribution.**

184. Lemke A, Kiderlen AF, Petri B, et al. Delivery of amphotericin B nanosuspensions to the brain and determination of activity against Balamuthia mandrillaris amebas. Nanomedicine. 2010;6(4):597–603.
185. Shao K, Huang R, Li J, et al. Angiopep-2 modified PE-PEG based polymeric micelles for amphotericin B delivery targeted to the brain. J Control Release. 2010;147(1):118–126.
186. Lim WM, Rajinikanth PS, Mallikarjun C, et al. Formulation and delivery of itraconazole to the brain using a nanolipid carrier system. Int J Nanomedicine. 2014;9:2117–2126.
187. Pascual A, Calandra T, Bolay S, et al. Voriconazole therapeutic drug monitoring in patients with invasive mycoses improves efficacy and safety outcomes. Clin Infect Dis. 2008;46(2):201–211.
188. Lestner JM, Roberts SA, Moore CB, et al. Toxicodynamics of Itraconazole: implications for Therapeutic Drug Monitoring. Clin Infect Dis. 2009;49(6):928–930.
189. Wiederhold N.P., Najvar L.K., Alimardanov A, et al. The novel fungal Cyp51 inhibitor VT-1129 demonstrates potent in vivo activity in mice against cryptococcal meningitis with a loading/maintenance dose strategy. Copenhagen: ECCMID; 2015.
190. Hoekstra WJ, Garvey EP, Moore WR, et al. Design and optimization of highly-selective fungal CYP51 inhibitors. Bioorg Med Chem Lett. 2014;24(15):3455–3458.
191. Pfaller MA, Messer SA, Rhomberg PR, et al. Activity of a long-acting echinocandin, CD101, determined using CLSI and EUCAST reference methods, against Candida and Aspergillus spp., including echinocandin- and azole-resistant isolates. J Antimicrob Chemother. 2016;71(10):2868–2873.
192. Ong V, James KD, Smith S, et al. Pharmacokinetics of the Novel Echinocandin CD101 in Multiple Animal Species. Antimicrob Agents Chemother. 2017;61:4.
193. Oliver JD, Sibley GEM, Beckmann N, et al. F901318 represents a novel class of antifungal drug that inhibits dihydroorotate dehydrogenase. Proc Natl Acad Sci. 2016;113(45):12809–12814.
194. Buil JB, Rijs A, Meis JF, et al. In vitro activity of the novel antifungal compound F901318 against difficult-to-treat Aspergillus isolates. J Antimicrob Chemother. 2017;72(9):2548–2552.
195. Hager CL, Larkin EL, Long L, et al. In Vitro and In Vivo Evaluation of the Antifungal Activity of APX001A/APX001 against Candida auris. Antimicrob Agents Chemother. 2018;62:e02319-17.
196. Miyazaki M, Horii T, Hata K, et al. In vitro activity of E1210, a novel antifungal, against clinically important yeasts and molds. Antimicrob Agents Chemother. 2011;55(10):4652–4658.
197. Watanabe NA, Miyazaki M, Horii T, et al. E1210, a new broad-spectrum antifungal, suppresses Candida albicans hyphal growth through inhibition of glycosylphosphatidylinositol biosynthesis. Antimicrob Agents Chemother. 2012;56(2):960–971.
198. AmplyxPharmaceuticals. Amplyx Pharmaceuticals Announces Qualified Infectious Disease Product Designation for APX001 in Three Life-threatening Fungal Infections 2016 [cited 2017 Dec 8]. Available from: http://amplyx.com/amplyx-pharmaceuticals-announces-qualified-infectious-disease-product-designation-for-apx001-in-three-life-threatening-fungal-infections/.
199. Wring SA, Randolph R, Park S, et al. Preclinical Pharmacokinetics and Pharmacodynamic Target of SCY-078, a First-in-Class Orally Active Antifungal Glucan Synthesis Inhibitor, in Murine Models of Disseminated Candidiasis. Antimicrob Agents Chemother. 2017;61:4.
200. Pfaller MA, Messer SA, Motyl MR, et al. Activity of MK-3118, a new oral glucan synthase inhibitor, tested against Candida spp. by two international methods (CLSI and EUCAST). J Antimicrob Chemother. 2013;68(4):858–863.
201. Berkow EL, Angulo D, Lockhart SR. In Vitro Activity of a Novel Glucan Synthase Inhibitor, SCY-078, against Clinical Isolates of Candida auris. Antimicrob Agents Chemother. 2017;61:7.
202. Pfaller MA, Messer SA, Motyl MR, et al. In vitro activity of a new oral glucan synthase inhibitor (MK-3118) tested against Aspergillus spp. by CLSI and EUCAST broth microdilution methods. Antimicrob Agents Chemother. 2013;57(2):1065–1068.
203. Shannon RJ, Carpenter KLH, Guilfoyle MR, et al. Cerebral microdialysis in clinical studies of drugs: pharmacokinetic applications. J Pharmacokinet Pharmacodyn. 2013;40(3):343–358.
204. Varnas K, Varrone A, Farde L. Modeling of PET data in CNS drug discovery and development. J Pharmacokinet Pharmacodyn. 2013;40(3):267–279.
205. Neuwelt EA, Abbott NJ, Abrey L, et al. Strategies to advance translational research into brain barriers. Lancet Neurol. 2008;7(1):84–96.
206. Shobo A, Baijnath S, Bratkowska D, et al. MALDI MSI and LC-MS/MS: towards preclinical determination of the neurotoxic potential of fluoroquinolones. Drug Test Anal. 2016;8(8):832–838.
207. Munyeza CF, Shobo A, Baijnath S, et al. Rapid and widespread distribution of doxycycline in rat brain: a mass spectrometric imaging study. Xenobiotica. 2016;46(5):385–392.
208. Shobo A, Bratkowska D, Baijnath S, et al. Tissue distribution of pretomanid in rat brain via mass spectrometry imaging. Xenobiotica. 2016;46(3):247–252.
209. Shobo A, Bratkowska D, Baijnath S, et al. Visualization of Time-Dependent Distribution of Rifampicin in Rat Brain Using MALDI MSI and Quantitative LCMS/MS. Assay Drug Dev Technol. 2015;13(5):277–284.

AMERICAN SOCIETY FOR MICROBIOLOGY | Antimicrobial Agents and Chemotherapy®

PHARMACOLOGY

Population Pharmacokinetics and Cerebrospinal Fluid Penetration of Fluconazole in Adults with Cryptococcal Meningitis

Katharine E. Stott,[a,b] Justin Beardsley,[c] Ruwanthi Kolamunnage-Dona,[d] Anahi Santoyo Castelazo,[a] Freddie Mukasa Kibengo,[e] Nguyen Thi Hoang Mai,[f] Nguyễn Lê Nhu' Tùng,[f] Ngo Thi Kim Cuc,[f] Jeremy Day,[c,g] William Hope[a]

[a]Antimicrobial Pharmacodynamics and Therapeutics Laboratory, Department of Molecular and Clinical Pharmacology, Institute of Translational Medicine, University of Liverpool, Liverpool, United Kingdom

[b]Malawi-Liverpool-Wellcome Trust Clinical Research Programme, Blantyre, Malawi

[c]Oxford University Clinical Research Unit, Ho Chi Minh City, Vietnam

[d]Department of Biostatistics, Institute of Translational Medicine, University of Liverpool, Liverpool, United Kingdom

[e]MRC/UVRI Uganda Research Unit on AIDS, Entebbe, Uganda

[f]Hospital for Tropical Diseases, Ho Chi Minh City, Vietnam

[g]Centre for Tropical Medicine and Global Health, Nuffield Department of Medicine, University of Oxford, Oxford, United Kingdom

ABSTRACT Robust population pharmacokinetic (PK) data for fluconazole are scarce. The variability of fluconazole penetration into the central nervous system (CNS) is not known. A fluconazole PK study was conducted in 43 patients receiving oral fluconazole (usually 800 mg every 24 h [q24h]) in combination with amphotericin B deoxycholate (1 mg/kg q24h) for cryptococcal meningitis (CM). A four-compartment PK model was developed, and Monte Carlo simulations were performed for a range of fluconazole dosages. A meta-analysis of trials reporting outcomes of CM patients treated with fluconazole monotherapy was performed. Adjusted for bioavailability, the PK parameter means (standard deviation) were the following: clearance, 0.72 (0.24) liters/h; volume of the central compartment, 18.07 (6.31) liters; volume of the CNS compartment, 32.07 (17.60) liters; first-order rate constant from the central to peripheral compartment, 12.20 (11.17) h^{-1}, from the peripheral to central compartment, 18.10 (8.25) h^{-1}, from the central to CNS compartment, 35.43 (13.74) h^{-1}, and from the CNS to central the compartment, 28.63 (10.03) h^{-1}. Simulations of the area under concentration-time curve resulted in median (interquartile range) values of 1,143.2 (range, 988.4 to 1,378.0) mg · h/liter in plasma (AUC_{plasma}) and 982.9 (range, 781.0 to 1,185.9) mg · h/liter in cerebrospinal fluid (AUC_{CSF}) after a dosage of 1,200 mg q24h. The mean simulated ratio of AUC_{CSF}/AUC_{plasma} was 0.89 (standard deviation [SD], 0.44). The recommended dosage of fluconazole for CM induction therapy fails to attain the pharmacodynamic (PD) target in respect to the wild-type MIC distribution for *C. neoformans*. The meta-analysis suggested modest improvements in both CSF sterility and mortality outcomes with escalating dosage. This study provides the pharmacodynamic rationale for the long-recognized fact that fluconazole monotherapy is an inadequate induction regimen for CM.

KEYWORDS cryptococcal meningitis, pharmacokinetics, pharmacodynamics, fluconazole, central nervous system pharmacokinetics, central nervous system infections, meta-analysis

Received 30 April 2018 **Returned for modification** 29 May 2018 **Accepted** 8 June 2018

Accepted manuscript posted online 18 June 2018

Citation Stott KE, Beardsley J, Kolamunnage-Dona R, Castelazo AS, Kibengo FM, Mai NTH, Tùng NLN, Cuc NTK, Day J, Hope W. 2018. Population pharmacokinetics and cerebrospinal fluid penetration of fluconazole in adults with cryptococcal meningitis. Antimicrob Agents Chemother 62:e00885-18. https://doi.org/10.1128/AAC.00885-18.

Address correspondence to William Hope, hopew@liverpool.ac.uk.

K.E.S. and J.B. contributed equally to this article.

[This article was published on 27 August 2018 without Nguyễn Lê Nhu' Tùng and Ngo Thi Kim Cuc in the author list. The byline was updated in the current version, posted on 5 November 2018.]

Mortality from cryptococcal meningitis remains unacceptably high. More than 90% of the estimated 223,100 annual incident cases of cryptococcal meningitis occur in Sub-Saharan Africa and Asia-Pacific regions (1). The most effective regimen for induction is amphotericin B deoxycholate and flucytosine (2, 3). However, access to these drugs is limited in many regions where the burden of cryptococcal meningitis is greatest (4, 5). In these settings, high-dose fluconazole is used for induction monotherapy, despite consistent evidence of reduced survival in comparison to that with other agents and combinations (6–8).

Fluconazole was discovered by Pfizer, Inc. (Sandwich, United Kingdom) in 1978 (9). The objective was to discover an orally bioavailable agent for the treatment of invasive mycoses with a lower propensity to develop resistance than flucytosine (9). Fluconazole inhibits cytochrome P450-dependent demethylation of lanosterol in the ergosterol biosynthetic pathway (10). The ratio of the area under the concentration-time curve (AUC) to the MIC is the pharmacodynamic (PD) index that best links drug exposure of fluconazole with the observed antifungal effect (11, 12).

Successful antimicrobial therapy within the central nervous system depends on the achievement of effective drug concentrations within relevant subcompartments that include the cerebrum, meninges, and cerebrospinal fluid (CSF) (13). Fluconazole has a low molecular weight (approximately 300 g/mol), is weakly protein bound, and is not known to be a substrate for central nervous system (CNS) efflux pumps (14, 15). Its ability to partition from the endovascular compartment into the CNS has been established in laboratory animal models (16, 17) and clinical studies (18, 19). Brain/plasma penetration ratios of up to 1.33 have been reported in humans (19). However, there is a surprising paucity of population pharmacokinetic (PK) data for fluconazole in all clinical contexts. Furthermore, the extent and variability of penetration into the CNS are not known.

The primary aim of this study was to quantify the extent and variability of CNS penetration of fluconazole in adults with cryptococcal meningitis. We developed a population PK model that quantified the interindividual variability in drug exposure in plasma and cerebrospinal fluid (CSF). We investigated the impact of a range of clinically relevant covariates on fluconazole PK. Monte Carlo simulation was used to assess the implications of PK variability in terms of achieving fluconazole PD targets. Finally, we conducted a meta-analysis of clinical trials of fluconazole monotherapy to estimate the contribution of dosage to clinical outcome.

RESULTS

Patients. A total of 43 patients (23 from Vietnam and 20 from Uganda) were recruited over an 11-month period between January and November 2016. Twenty-two patients (52%) were female. Patient characteristics (overall median [range]) were the following: age, 33 years (20 to 73 years); weight, 48 kg (32 to 68 kg); body mass index (BMI), 18 kg/m^2 (12 to 25 kg/m^2); creatinine at enrollment, 70 μmol/liter (37 to 167 μmol/liter); and estimated glomerular filtration rate (eGFR) using the Cockcroft-Gault equation, 84.8 ml/min/1.73 m^2 (35.4 to 146.7 ml/min/1.73 m^2). The baseline creatinine concentration was significantly lower in Vietnamese patients than in Ugandan patients (median, 56 versus 79 μmol/liter; *P* value, 0.02). However, this did not manifest as a significant difference in eGFR due to different age, sex, and weight profiles between the two patient populations. There were no statistically significant differences between ethnic groups for other demographic variables. The demographic data are shown by ethnicity and for the study population as a whole in Table 1.

Pharmacokinetic data. The final data set included 312 plasma observations and 52 CSF observations from the Vietnamese cohort. From the Ugandan cohort, the data set included 196 plasma observations and 115 CSF observations. A single CSF observation from one Ugandan patient was excluded because no fluconazole was detectable in an isolated sample after 13 days of therapy. This was inconsistent with results from other patients and could not be verified. The mean numbers of plasma samples and CSF samples per patient were 11.8 and 3.9, respectively. Figure 1 shows the raw plasma and CSF concentration-time profiles from study participants.

TABLE 1 Patient demographics

Demographic or clinical characteristic[a]	Value for the group			*P* value[g]
	Vietnam	Uganda	Combined	
Sex[b]				
No. of males	13	8	23	
No. of females	10	12	20	
Age (yr)[c]				0.75
Mean	38	33	35	
Median	33	33	33	
Range	20–73	24–50	20–73	
Weight (kg)[d]				0.23
Mean	46	49	48	
Median	45	49	48	
Range	32–68	35–60	32–68	
BMI (kg/m^2)[e]				0.73
Mean	18	18	18	
Median	18	18	18	
Range	12–25	15–22	12–25	
Creatinine (μmol/liter)[b]				0.02
Mean	67	81	74	
Median	56	79	70	
Range	37–167	43–145	37–167	
eGFR (ml/min/1.73 m^2)[f]				0.10
Mean	88.3	80.7	84.7	
Median	84.8	81.4	84.8	
Range	35.4–136.1	49.8–146.7	35.4–146.7	

[a]BMI, body mass index; eGFR, estimated glomerular filtration rate, by Cockcroft-Gault equation.
[b]$n = 43$.
[c]$n = 31$.
[d]$n = 41$.
[e]$n = 35$.
[f]$n = 33$.
[g]*P* value for difference between Vietnam and Uganda groups by Mann-Whitney test of significance.

Population pharmacokinetic analysis. The final mathematical model was a linear model comprised of an absorption compartment, central compartment, peripheral compartment, and CSF compartment. The fit of the final model to the clinical data was acceptable. The mean parameter estimates better fitted the data than medians and were used to calculate Bayesian estimates of drug exposure for each individual patient. A linear regression of the observed-versus-predicted fluconazole concentrations in plasma after the Bayesian step was given by the following calculation: observed fluconazole concentration = 1.03 × predicted fluconazole concentration + 0.27 (r^2 = 0.80). For the observed-versus-predicted fluconazole concentrations in CSF, the linear regression was given by the following: observed fluconazole concentration = 1.03 × predicted fluconazole concentration − 0.07 (r^2 = 0.81) (Fig. 2 and Table 2). The mean weighted population bias values for fluconazole concentrations in plasma and CSF were 0.20 and −0.30, respectively. The bias-adjusted population imprecision values in plasma and CSF were 2.21 and 1.55, respectively. The population PK parameter estimates for the final model are shown in Table 3.

Covariate investigation. Multivariate linear regression of each subject's covariates versus the Bayesian posterior parameter values revealed a weak relationship between patient weight and estimated volume of distribution (slope, 0.22; 95% confidence interval (CI) for the slope, −0.06 to 0.51; *P* value, 0.05). Incorporation of weight into the PK model was therefore explored. However, values for log likelihood, Akaike information criterion (AIC), and population bias and imprecision were comparable between the two models. The simple base model was therefore used to describe the data and for the

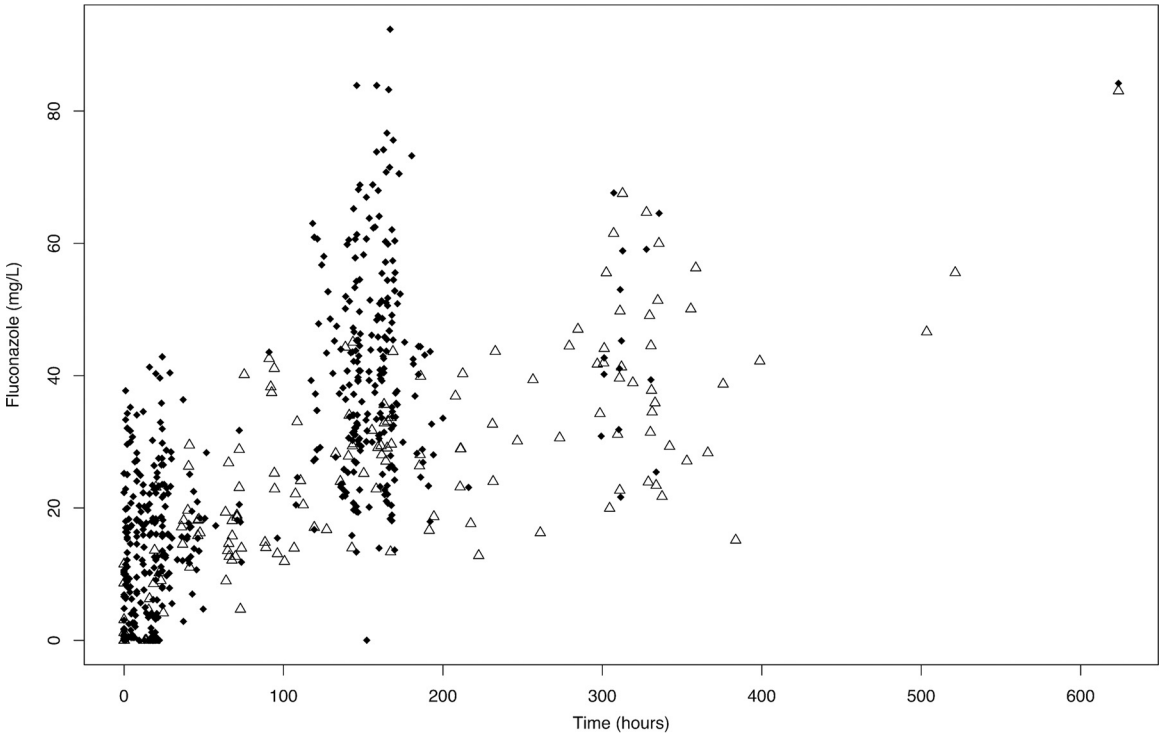

FIG 1 Fluconazole concentrations in 43 patients. Black diamonds represent plasma concentrations. White triangles represent CSF concentrations.

subsequent simulations. The model comparisons and the fit to data are summarized in Table 2.

There was no relationship between the Bayesian estimates of clearance and volume and the covariate of either ethnicity or sex in the base model. The mean (95% CI) clearance was 0.74 liters/h (0.64 to 0.83 liters/h) and 0.71 liters/h (0.59 to 0.82 liters/h) for Vietnamese and Ugandan patients, respectively ($P = 0.51$). The mean (95% CI) volume was 16.88 liters (14.33 to 19.44 liters) and 19.44 liters (16.88 to 22.0 liters) for Vietnamese and Ugandan patients, respectively ($P = 0.16$). In males, the mean (95% CI) clearance was 0.79 liters/h (0.67 to 0.90 liters/h). In females, clearance was 0.66 liters/h (0.57 to 0.75 liters/h) ($P = 0.09$). In males, the mean (95% CI) volume was 18.07 liters (15.47 to 20.67 liters). In females, the mean volume was 18.07 liters (15.41 to 20.73 liters) ($P = 0.97$).

Fluconazole penetration into the CSF. There was large variability in the AUCs generated from each patient's posterior estimates. The 38 patients who received 800 mg of fluconazole q24h had a median (interquartile range [IQR]) AUC from 144 to 168 h after treatment initiation ($AUC_{144-168}$) of 945.4 (799.2 to 1,139.8) mg · h/liter in plasma (AUC_{plasma}) and 784.2 mg · h/liter (615.9 to 879.4) in CSF (AUC_{CSF}). From these posterior estimates, the mean ratio of AUC_{CSF}/AUC_{plasma} was 0.82 (standard deviation, 0.22).

Monte Carlo simulation was used to estimate the distribution of drug exposure for dosages of 400 mg, 800 mg, 1,200 mg, and 2,000 mg q24h of fluconazole (Fig. 3). PK variability was marked, both in plasma and CSF. After administration of a dosage of 1,200 mg of fluconazole q24h, the median (IQR) simulated plasma $AUC_{144-168}$ was 1,143.2 (988.4 to 1,378.0) mg · h/liter and the CSF $AUC_{144-168}$ was 982.9 (781.0 to 1,185.9) mg · h/liter. The mean simulated ratio of AUC_{CSF}/AUC_{plasma} was 0.89 (SD, 0.44).

Probability of target attainment analysis. Monte Carlo simulation was used to predict the probability of achieving a total drug AUC/MIC ratio of ≥389.3 in plasma. This PD target was shown in a murine model of cryptococcal meningitis to be associated with a stasis endpoint (i.e., no net change in fungal density at the end of the experiment compared with that at treatment initiation) (11). Only 61% of simulated

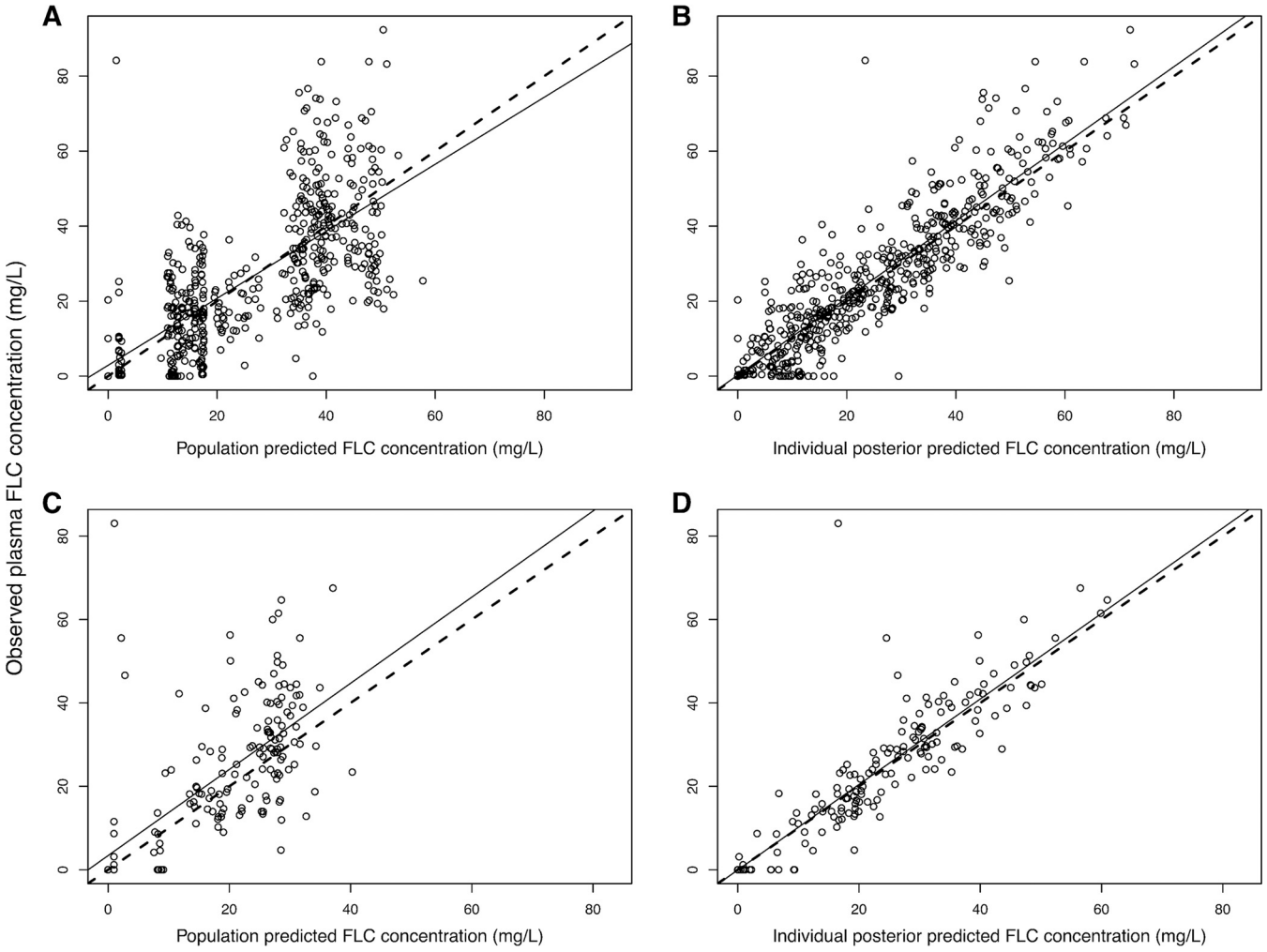

FIG 2 Scatter plots showing observed-versus-predicted values for the chosen population pharmacokinetic model after the Bayesian step. (A) Population predicted concentration of fluconazole in plasma. $R^2 = 0.49$; intercept, 2.89 (95% CI, 0.51 to 5.27); slope, 0.89 (95% CI, 0.82 to 0.97). (B) Individual posterior predicted concentration of fluconazole in plasma. $R^2 = 0.80$; intercept, 0.27 (95% CI, −1.08 to 1.62); slope, 1.03 (95% CI, 0.98 to 1.07). (C) Population predicted concentration of fluconazole in CSF. $R^2 = 0.46$; intercept, 3.39 (95% CI, −0.09 to 6.87); slope, 1.03 (95% CI, 0.87 to 1.2). (D) Individual posterior predicted concentration of fluconazole in CSF. $R^2 = 0.81$; intercept, −0.07 (95% CI, −1.97 to 1.84); slope, 1.03 (95% CI, 0.95 to 1.10). Circles, dashed lines, and solid lines represent individual observed-predicted data points, line of identity, and the linear regression of observed-predicted values, respectively. FLC, fluconazole; CI, confidence interval.

patients receiving 1,200 mg of fluconazole q24h achieved this PD target when the MIC for the infecting strain was 2.0 mg/liter. For MICs of ≥4.0 mg/liter, <1% of simulated patients administered 1,200 mg q24h achieved the PD target (Fig. 4).

Meta-analysis of clinical outcome data. A systematic review identified 163 relevant manuscripts, of which 11 were duplicates. After reviewing titles and abstracts, 28 studies were deemed potentially relevant for inclusion in the meta-analysis. Detailed examination of these studies resulted in the ultimate inclusion of 12 papers describing clinical outcomes from cryptococcal meningitis treated with fluconazole monotherapy. In total, 28 patients in 1 study received 200 mg of fluconazole q24h (20), 19 patients in 2 studies received 400 mg of fluconazole q24h (7, 21), 97 patients in 3 studies received 800 mg q24h (22–24), 113 patients in 4 studies received 1,200 mg q24h (8, 23–25), and 1 study described outcomes of 16 patients on 1,600 mg (24) and 8 patients on 2 g of fluconazole q24h (24). All included patients were HIV positive. Baseline characteristics and reported clinical outcomes are presented in Table 4.

The final model suggests that the combination of dose and baseline fungal burden explains the total heterogeneity in the estimated proportion of patients with sterile CSF after 10 weeks of treatment (*P* value for residual heterogeneity, 0.64). However, there

TABLE 2 Evaluation of the predictive performance of the considered and final models

Model and measured compartment[a]	Log likelihood	AIC[b]	Population bias	Population imprecision	Linear regression of observed-predicted values for each patient			*P* value[d]
					R^{2c}	Intercept	Slope	
Model 1								
Plasma	−2,451	4,928	0.20	2.21	0.80	0.27	1.03	0.56
CSF			−0.30	1.55	0.81	−0.07	1.03	
Model 2								
Plasma	−2,413	4,854	0.36	2.38	0.80	0.01	1.03	
CSF			−0.41	1.81	0.80	0.89	1.01	

[a]Model 1 did not include any covariates. Model 2 incorporated a function to scale the volume of distribution in central compartment to patient weight.
[b]AIC, Akaike information criterion.
[c]Relative to the regression line fitted for the observed-versus-predicted values after the Bayesian step.
[d]Comparison of the joint distribution of population parameter values for each model.

was not a significant relationship between dose and CSF sterility at 8 to 10 weeks (*P* value, 0.45). After adjustment for dose, the test for residual heterogeneity in both 2- and 10-week mortality was not significant (*P* values, 0.70 and 0.22, respectively), indicating that dose alone adequately explained total heterogeneity in mortality outcomes at both time points. For both 2- and 10-week mortality outcomes, there was a nonsignificant trend toward reduced mortality with escalating dosage (Fig. 5).

DISCUSSION

Fluconazole is the only drug available for induction therapy for cryptococcal meningitis in many regions of the world where the incidence of disease is highest. An accumulating body of evidence suggests that fluconazole is a suboptimal agent for this indication (26). While this has long been recognized, an explanation for the relatively poor efficacy of fluconazole is absent. This study presents a uniquely comprehensive clinical data set describing the PK of fluconazole. It provides robust estimates of CNS penetration and the variability of those estimates. A high degree of CNS partitioning has been observed in previous clinical studies with fluconazole (19, 27). Distribution into the CNS is facilitated by low molecular weight, low protein binding, and moderate lipophilicity (15, 28). Fluconazole has proven activity against *Cryptococcus neoformans* (29, 30). This study provides a further understanding as to why, despite these attributes, fluconazole is inferior to amphotericin B deoxycholate as an agent for induction monotherapy for cryptococcal meningitis (6–8).

In contrast to previous studies of fluconazole PK (31–33), our data do not suggest a

TABLE 3 Population parameter estimates from the final 4-compartment pharmacokinetic model

Parameter[a]	Mean	Median	SD
K_a (h^{-1})	8.78	1.73	11.98
SCL/*F* (liters/h)	0.72	0.65	0.24
V_c/F (liters)	18.07	17.41	6.31
K_{cp} (h^{-1})	12.20	8.36	11.17
K_{pc} (h^{-1})	18.10	18.34	8.25
IC_{gut} (mg)	34.67	49.99	22.74
$IC_{central}$ (mg)	35.86	49.98	19.67
IC_{CNS} (mg)	31.06	49.96	23.47
$IC_{peripheral}$ (mg)	34.29	49.96	13.21
K_{cs} (h^{-1})	35.43	42.55	13.74
K_{sc} (h^{-1})	28.63	29.04	10.03
V_{cns}/F (liters)	32.07	30.49	17.60

[a]SCL, clearance; V_c, volume of distribution in central compartment; *F*, bioavailability; K_{cp}, first-order rate constant from the central to peripheral compartment; K_{pc}, first-order rate constant from the peripheral to central compartment; IC, initial condition in the respective compartment; K_{cs}, first-order rate constant from the central to CNS compartment; K_{sc}, first-order rate constant from CNS to central compartment; V_{cns}, volume of distribution in CNS compartment.

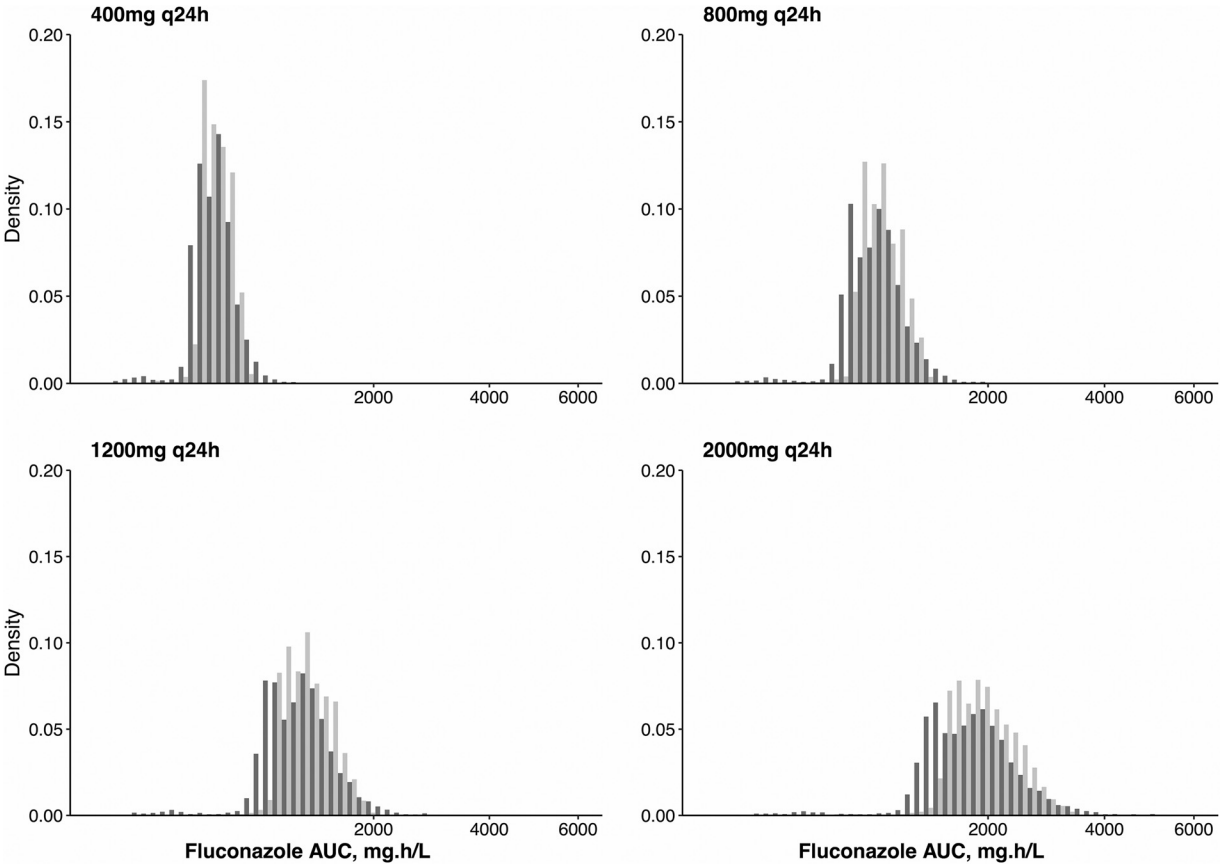

FIG 3 AUC distributions in 5,000 simulated patients at escalating fluconazole dosages. Light gray bars indicate simulated plasma $AUC_{144-168}$. Dark gray bars indicate simulated CSF $AUC_{144-168}$.

significant relationship between fluconazole clearance and creatinine clearance nor between patient weight and volume of distribution. The reason for this is not immediately clear but may relate to the relatively narrow range of creatinine clearance in our population and the fact that the vast majority of patients in our cohort had low body weight, with the range of this covariate also being relatively narrow.

The PK model suggests that current regimens of fluconazole are inadequate for induction therapy for cryptococcal meningitis. This has routinely been ascribed to the

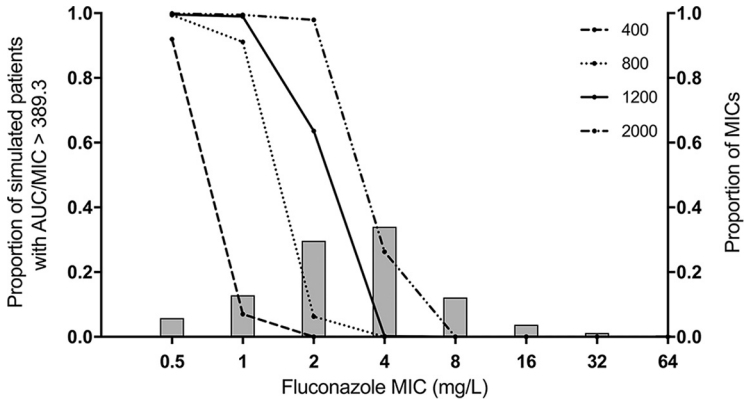

FIG 4 Probability of pharmacodynamic target attainment in plasma as a function of isolate MIC and fluconazole dosage. Each line represents the proportion of 5,000 simulated patients that achieve the PD target at the respective dosage (in milligrams) of fluconazole. The PD target was a plasma AUC/MIC ratio of ≥389.3. Bars show the proportion of WT strains of *C. neoformans* at the indicated MIC.

TABLE 4 Baseline characteristics and clinical outcomes from trial data of fluconazole monotherapy by dosing regimen

Fluconazole dosage (mg)	Country	No. of patients	Age (yr)[a]	GCS <15 (%)	No. of CD4 cells/mm^3[a]	CSF burden (log_{10} CFU/ml)	CSF sterility[e]	CSF sterility time point (wk)	2-wk mortality (%)[e]	10-wk mortality (%)[e]	Reference
200	Uganda	28	33 (23–50)[b]	43	73[c]		4/8 (50)	8	10/25 (40)	16/25 (64)	Mayanja-Kizza et al. (20)
400	USA	14	38 (2)[c]	0	44 (13)[c]	4[d]	6/14 (43)	10	NR	4/14 (29)	Larsen et al. (21)
	South Africa	5	39 (37–51)	60	41	5.53	NR[f]	NR	NR	3/4 (75)	Bicanic et al. (7)
800	Malawi	58	32 (29–39)	24	37 (11–58)		NR	NR	17/58 (29)	33/58 (57)	Rothe et al. (22)
	Uganda	30	35 (30–38)	33	7 (3–17)	5.7	NR	NR	11/30 (37)	18/30 (60)	Longley et al. (23)
	USA	9	35	100	8	4.8[d]	1/9 (11)	10	NR	8/9 (89)	Milefchik (24)
1,200	Malawi	47	35 (32–40)	24	36 (17–62)		NR	NR	16/47 (34)	26/47 (55)	Gaskell et al. (25)
	Uganda	30	33 (28–42)	60	14 (4–33)	5.9	NR	NR	6/27 (22)	13/27 (48)	Longley et al. (23)
	USA	16	40	100	36	3.5[d]	6/16 (37.5)	10	NR	10/16 (62.5)	Milefchik et al. (24)
	Malawi	20	36.5 (27–71)[b]	40	25 (1–66)[b]	5.30	1/20 (5)	2	7/19 (37)	11/19 (58)	Nussbaum et al. (8)
1,600	USA	16	35	100	33	3[d]	10/16 (62.5)	10	NR	6/16 (37.5)	Milefchik et al. (24)
2,000	USA	8	36	100	35	2.4[d]	5/8 (62.5)	10	NR	3/8 (37.5)	Milefchik et al. (24)

[a]Median (interquartile rage) unless otherwise specified.
[b]Values in parentheses are range.
[c]Value is mean (standard error).
[d]Extrapolated from cryptococcal antigen titer.
[e]Fraction (%) of patients.
[f]NR, not reported.

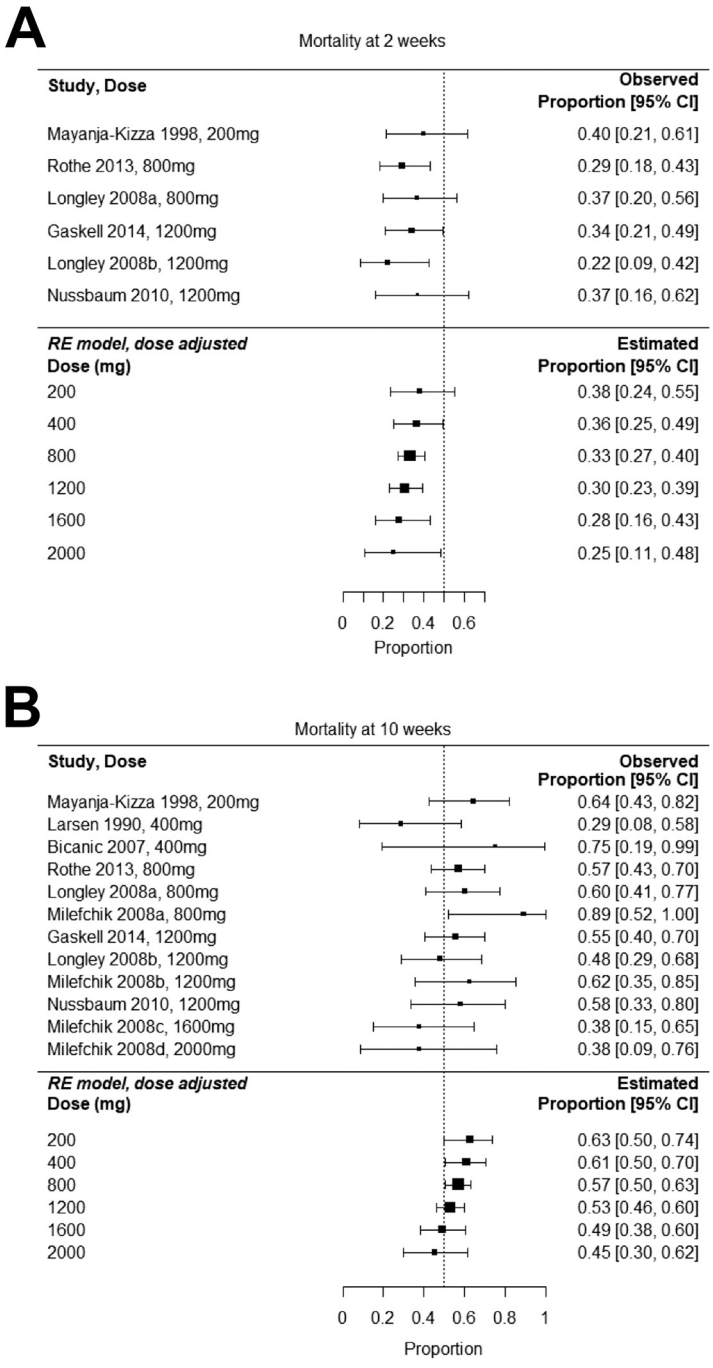

FIG 5 Meta-analysis of clinical trials of fluconazole monotherapy showing dose-adjusted effects on 2-week mortality (A) and 10-week mortality (B). Right-hand columns provide observed and estimated proportions of patients dead at the indicated time.

overly simplistic notion that fluconazole is a fungistatic agent. Our analyses provide further insight into the limitations of this drug. Previous estimates of fluconazole CNS/plasma partition ratios have ranged from 0.52 to 1.33 (18, 19, 27, 34). We have extended these estimates by rigorously quantifying the marked variability in the CSF PK. This variability has consequences at both microbiological and clinical levels. Suboptimal exposure of fluconazole promotes the expansion of intrinsically resistant cryptococcal subpopulations present at the initiation of therapy (35). In addition, the evolution of *C. neoformans* during therapy to become increasingly triazole resistant has

been demonstrated in clinical studies (36, 37). To be clinically effective, adequate concentrations of drug must be present at the site of infection for long enough to exert an antimicrobial effect on both susceptible and resistant subpopulations. The present analysis demonstrates the challenges in achieving that aim.

At the recommended fluconazole dosage of 1,200 mg q24h, the probability of PD target attainment (PTA) bisects the MIC distribution for wild-type (WT) *C. neoformans* isolates. This is consistent with the findings of Sudan et al. (11). Approximately half of patients will fail therapy because they are not able to generate the drug exposure required to prevent progressive fungal growth. Since clinical PK-PD targets are not available for fluconazole in cryptococcal meningitis, we have used a target derived from a murine study (11). This assumes that CNS partitioning is the same in mice and humans. The cerebrum/plasma AUC ratio in the murine study was 46.9% (11). It is conceivable that this is in keeping with our CSF/plasma AUC ratio of 82% though clearly it would be preferable to have clinical PK-PD targets defined. Nevertheless, our PTA analysis is supported by the 53% 10-week mortality outcomes for patients receiving 1,200 mg of fluconazole q24h, estimated in the meta-analysis. Importantly, such PTA analyses are based on an AUC/MIC of 389.3, which is more than an order of magnitude greater than the AUC/MIC ratio required for *Candida albicans* (12).

Progressive escalation of the dosage of fluconazole is not likely to be an effective strategy for improving cryptococcal meningitis induction therapy. The drug exposure required to reliably treat isolates with MICs of ≥4.0 mg/liter is difficult to achieve and potentially toxic. Our meta-analysis suggests that escalating dosages of fluconazole do not increase the proportion of patients with sterile CSF at 10 weeks. Dosages of 2,000 mg q24h do not appear to significantly improve 10-week mortality outcomes in comparison to a dose of 1,200 mg q24h. The AIDS Clinical Trials Group (ACTG) study (https://clinicaltrials.gov/show/NCT00885703) is investigating the use of higher dosages of fluconazole (1,600 mg and 2,000 mg q24h) for the treatment of cryptococcal meningitis in HIV-infected individuals, and results are pending. The addition of flucytosine to high-dose fluconazole (≥1,200 mg q24h) for cryptococcal meningitis increases antifungal activity and improves mortality outcomes (8, 24), suggesting that combination therapy is required to optimize antifungal activity in fluconazole-containing regimens.

In summary, this study provides part of the pharmacodynamic rationale for the long-recognized fact that fluconazole monotherapy is an ineffective induction regimen for cryptococcal meningitis. We have developed a fluconazole population PK model that suggests that approximately half of patients with cryptococcal meningitis caused by WT strains of *C. neoformans* will be undertreated by currently recommended dosages of fluconazole for induction therapy. In doing so, we have addressed a knowledge gap regarding the reason for the inferiority of this drug for cryptococcal meningitis. There is a pressing need for improved provision of affordable combination treatments and development of more effective drugs.

MATERIALS AND METHODS

Clinical pharmacokinetic studies. Patients from whom plasma and CSF samples were obtained for this PK study have been described previously (38). Briefly, adult patients ($n = 3$) were initially recruited from a multicenter randomized controlled trial of adjuvant dexamethasone in HIV-associated cryptococcal meningitis. The trial is reported elsewhere (International Standard Registered Clinical Number 59144167) (38). Following the early cessation of this trial, patients were recruited from a prospective descriptive study at the same sites ($n = 40$). Study sites were The Hospital for Tropical Diseases in Ho Chi Minh City, Vietnam, and Masaka General Hospital, Uganda. The study protocols were approved by the relevant institutional review boards and regulatory authorities at each trial site and by the Oxford University Tropical Research Ethics Committee.

Fluconazole was administered orally. In cases where the conscious level of the patient did not enable oral administration, fluconazole was administered via nasogastric tube. The majority of patients received 800 mg of fluconazole q24h. Two patients received one-off doses of 400 mg q24h. Two received one-off doses of 600 mg q24h. One patient's regimen of 800 mg of fluconazole q24h was escalated to 1,200 mg q24h for 6 days from day 8 of treatment. All patients received combination therapy with amphotericin B deoxycholate at 1 mg per kg infused over 5 to 6 h.

Measurement of fluconazole concentrations. Fluconazole concentrations were measured using a validated liquid chromatography-tandem mass spectrometry (LC-MS/MS) methodology (1260 Agilent UPLC [ultra-performance liquid chromatograph] coupled to an Agilent 6420 Triple Quad mass spectrometer; Agilent Technologies UK, Ltd., Cheshire, United Kingdom). Briefly, fluconazole was extracted by protein precipitation; 300 μl of cold methanol containing the internal standard fluconazole-D4 at 0.625 mg/liter (TRC, Canada) was added to 10 μl of sample (plasma or CSF). The solution was vortex mixed for 5 s and filtered through a Sirocco precipitation plate (Waters, Ltd., Cheshire, United Kingdom). Supernatant (150 μl) was transferred to a 96-well auto sampler plate, and 3 μl was injected on an Agilent Zorbax C_{18} Rapid Resolution High Definition (RRHD) column (2.1 by 50 mm; particle size, 1.8 μm) (Agilent Technologies UK, Ltd., Cheshire, United Kingdom).

Chromatographic separation was achieved using a gradient consisting of 70% A/30% B (0.1% formic acid in water as mobile phase A and 0.1% formic acid in methanol as mobile phase B). The organic phase was increased to 100% over 90 s, with an additional 90 s of equilibration.

The mass spectrometer was operated in multiple-reaction-monitoring scan mode in positive polarity. The precursor ions were 307.11 *m/z* and 311.1 *m/z* for fluconazole and the internal standard, respectively. The product ions for fluconazole were 220.1 *m/z* and 238.1 *m/z*; for the internal standard the product ions were 223.2 *m/z* and 242.1 *m/z*. The source parameters were set as follows: capillary voltage, 4,000 V; gas temperature, 300°C; and nebulizer gas, 15 lb/in^2.

The standard curve for fluconazole encompassed the concentration range of 1 to 120 mg/liter and was constructed using blank matrix. The limit of quantitation was 1 mg/liter. In plasma, the intraday coefficient of variation (CV) was <3.4%, and the interday CV was <6.7% over the concentration range of 1 to 90 mg/liter. In CSF, the intraday CV was <5.2%, and the interday CV was <5.3% over the same concentration range.

Population pharmacokinetic modeling. The concentration-time data for fluconazole in plasma and CSF were analyzed using the nonparametric adaptive grid (NPAG) algorithm of the program Pmetrics (39), version 1.5.0, for the R statistical package, version 3.1.1. The initial PK mathematical model fitted to the data contained four compartments and took the following form:

$$\frac{dX(1)}{dt} = -K_a \times X(1) \tag{1}$$

$$\frac{dX(2)}{dt} = K_a \times X(1) - \left(K_{cp} + K_{cs} + \frac{SCL}{V}\right) \times X(2) + K_{sc} \times X(3) + K_{pc} \times X(4) \tag{2}$$

$$\frac{dX(3)}{dt} = K_{cs} \times X(2) - K_{sc} \times X(3) \tag{3}$$

$$\frac{dX(4)}{dt} = K_{cp} \times X(2) - K_{pc} \times X(4) \tag{4}$$

$$Y(1) = X(2)/V \tag{5}$$

$$Y(2) = X(3)/V_{cns} \tag{6}$$

where equations 1, 2, 3, and 4 describe the rate of change in amount of drug in milligrams in the gut, central, CSF, and peripheral compartments, respectively. K_a is the absorption rate constant from the gut to the central compartment. *X*(*1*), *X*(*2*), *X*(*3*), and *X*(*4*) are the amounts of fluconazole (in milligrams) in the gut, central (c), CSF (s) and peripheral compartments (p), respectively. K_{cp}, K_{pc}, K_{cs}, and K_{sc} represent first-order transfer constants connecting the various compartments. SCL is the first-order clearance of drug (liters/hour) from the central compartment. *V* is the volume of the central compartment. The CSF compartment [*X*(*3*)] has an apparent CSF volume (V_{cns}), given in liters. Equations 5 and 6 are the output equations describing fluconazole levels in the central and CSF compartments, respectively. The output in each compartment is denoted *Y*.

Model error was attributed separately to process noise (including errors in sampling times or dosing) and assay variance. Process noise was modeled using lambda, an additive error term. The data were weighted by the inverse of the estimated assay variance.

The data for some patients indicated that they had taken fluconazole at an undocumented time prior to study enrollment since there was detectable drug in the first PK sample. To accommodate this, nonzero initial conditions of all four compartments were estimated in the structural model. A switch was coded whereby the parameterized estimate of each initial condition was multiplied by a binary covariate equal to 1 when fluconazole was detected in the first PK sample or by 0 when no fluconazole was detected in the first PK sample.

Population pharmacokinetic covariate screening. The impacts of patient weight, BMI, sex, ethnicity, and baseline eGFR on the PK of fluconazole were investigated. Bidirectional stepwise multivariate linear regression was employed to assess the relationship between each covariate and the Bayesian estimates for volume of distribution and clearance from the central compartment from the standard population PK model. Covariates that were retained with significant multivariate *P* values ($\leq$0.05) in the regression model were explored individually. The relationship between retained continuous covariates and Bayesian estimates of PK parameters was explored using univariate linear regression. The difference between Bayesian estimates of volume and clearance according to categorical covariates (sex and ethnicity) was compared using a Mann-Whitney test.

Population pharmacokinetic model diagnostics. The fit of the model to the data was assessed by visual inspection of diagnostic scatterplots displaying observed-versus-predicted values before and after

the Bayesian step. Linear regression was performed, and the coefficient of determination, intercept, and regression slope were noted for each model. In addition, the log-likelihood value, Akaike information criterion (AIC), mean weighted error (a measure of bias), and bias-adjusted, mean weighted squared error (a measure of precision) were calculated and compared for each model.

Monte Carlo simulation and calculation of probability of target attainment. Monte Carlo simulation ($n = 5{,}000$) was performed in Pmetrics (39). The support points from the final joint density were used. For the simulations, the initial conditions of all compartments were defaulted to zero. Fluconazole was administered at a range of dosages: 400 mg q24h, 800 mg q24h, 1,200 mg q24h, and 2,000 mg q24h. The plasma and CSF AUC values for fluconazole were calculated using trapezoidal approximation after the sixth dose, from 144 to 168 h after treatment initiation.

Wild-type fluconazole MIC data were obtained from a previously published collection of 5,733 *C. neoformans* isolates estimated using Clinical and Laboratory Standards Institute (CLSI) methodology (40). The modal MIC was 4 mg/liter (1,629 of 5,733 strains; 28%). Almost half of strains had MICs of ≥4 mg/liter (2,834 of 5,733 strains; 49%). The epidemiological cutoff value for *C. neoformans* versus fluconazole was 8 mg/liter. This collection of strains included molecular types VNI to VNIV, and the patterns of MIC distribution were comparable across all molecular types (40). The proportion of simulated patients that would achieve a previously published plasma AUC/MIC target of 389.3 was determined. This target was defined as the magnitude of drug exposure required for fungal stasis (defined as prevention of progressive fungal growth) in a murine study that employed CLSI methodology (11). To our knowledge, no CSF PK/PD target has been defined in preclinical or clinical studies of fluconazole for cryptococcal meningitis. In the present study, the probability of attaining this plasma PK/PD target was examined at each simulated fluconazole dose.

Meta-analysis of clinical outcome data. The AUC/MIC target used in the probability of target attainment analysis was derived from murine studies. To enhance clinical relevance, we sought PD data from humans. The PD data from patients in the present PK study are confounded by the coadministration of amphotericin B deoxycholate. For this reason, a search for clinical trials of fluconazole monotherapy for cryptococcal meningitis was performed. The electronic databases Pubmed and Medline were searched on 31 January 2018 using the terms "fluconazole" and "cryptococcal meningitis." Preclinical studies and case reports were excluded. To reduce potential heterogeneity, only studies of HIV-positive participants were included in the meta-analysis. Baseline variables were chosen *a priori* for extraction from the studies if they had previously been determined to have a significant impact on clinical outcome. These were mental status, CSF fungal burden, and patient age (6, 41). Where it was not reported, baseline CSF fungal burden was extrapolated from CSF cryptococcal antigen titer according to a correlation published by Jarvis et al. (6).

For consistency with the literature, we collected data on clinical outcomes commonly presented in cryptococcal meningitis trials: CSF sterility at 8 to 10 weeks, 2-week mortality, and 10-week mortality. Mixed-effects meta-analysis adjusted for fluconazole dosage was performed. Fungal burden in CSF, CD4 count, and proportion of patients with reduced Glasgow coma score (GCS) at baseline were explored to assess the degree to which these modifiers accounted for interstudy heterogeneity in clinical outcome. The mixed-effects model took the form: $\theta_i = \beta_0 + \beta_1 Z_{i1} + \ldots + \beta_1 Z_{ij} + u_i$, where θ_i is the corresponding (unknown) true effect of the ith study, Z_{ij} is the value of the jth moderator variable for the ith study with corresponding model coefficients β, and u_i are study-specific random effects such that $u_i \sim N(0,\tau^2)$. Here, N indicates that the random effects are normally distributed, 0 is the mean of the random effects, and τ^2 denotes the amount of residual heterogeneity, estimated using the DerSimonian-Laird estimator (42). Additional model parameters were estimated via weighted least squares with weights relative to the estimated τ^2. The null hypothesis $H_0{:}\tau^2 = 0$ was tested using Cochran's Q-test, and model parameters were tested with the Wald-type test statistic.

ACKNOWLEDGMENTS

W.H. holds or has recently held research grants with F2G, AiCuris, Astellas Pharma, Spero Therapeutics, Matinas Biosciences, Antabio, Amplyx, Allecra, and Pfizer. W.H. holds awards from the National Institutes of Health, Medical Research Council, National Institute of Health Research, and the European Commission (FP7 and IMI). W.H. has received personal fees in his capacity as a consultant for F2G, Amplyx, Ausperix, Spero Therapeutics, Medicines Company, Gilead, and Basilea. W.H. is Medical Guideline Director for the European Society of Clinical Microbiology and Infectious Diseases and an Ordinary Council Member for the British Society of Antimicrobial Chemotherapy. J.D. holds or has recently held research awards from The Wellcome Trust, The Medical Research Council UK, The UK Department for International Development, The National Institutes for Health, The Li Ka Shing Foundation, The British Infection Society and The British Medical Association. J.D. has received personal fees in his capacity as a consultant to Viamet Pharmaceuticals.

This work was supported by the United Kingdom Department for International Development, the Wellcome Trust, and the Medical Research Council through a grant (G1100684/1) from the Joint Global Health Trials program, part of the European and Developing Countries Clinical Trials Partnership, supported by the European Union.

K.E.S. is a Wellcome Trust Clinical PhD Fellow (203919/Z/16/Z). J.D. is a Wellcome Trust Intermediate Fellow (WT097147MA).

REFERENCES

1. Rajasingham R, Smith RM, Park BJ, Jarvis JN, Govender NP, Chiller TM, Denning DW, Loyse A, Boulware DR. 2017. Global burden of disease of HIV-associated cryptococcal meningitis: an updated analysis. Lancet Infect Dis 17:873–881. https://doi.org/10.1016/S1473-3099(17)30243-8.
2. Day JN, Chau TT, Wolbers M, Mai PP, Dung NT, Mai NH, Phu NH, Nghia HD, Phong ND, Thai CQ, Thai le H, Chuong LV, Sinh DX, Duong VA, Hoang TN, Diep PT, Campbell JI, Sieu TP, Baker SG, Chau NV, Hien TT, Lalloo DG, Farrar JJ. 2013. Combination antifungal therapy for cryptococcal meningitis. N Engl J Med 368:1291–1302. https://doi.org/10.1056/NEJMoa1110404.
3. Molloy SF, Kanyama C, Heyderman RS, Loyse A, Kouanfack C, Chanda D, Mfinanga S, Temfack E, Lakhi S, Lesikari S, Chan AK, Stone N, Kalata N, Karunaharan N, Gaskell K, Peirse M, Ellis J, Chawinga C, Lontsi S, Ndong JG, Bright P, Lupiya D, Chen T, Bradley J, Adams J, van der Horst C, van Oosterhout JJ, Sini V, Mapoure YN, Mwaba P, Bicanic T, Lalloo DG, Wang D, Hosseinipour MC, Lortholary O, Jaffar S, Harrison TS, ACTA Trial Study Team. 2018. Antifungal combinations for treatment of cryptococcal meningitis in Africa. N Engl J Med 378:1004–1017. https://doi.org/10.1056/NEJMoa1710922.
4. Bicanic T, Wood R, Bekker LG, Darder M, Meintjes G, Harrison TS. 2005. Antiretroviral roll-out, antifungal roll-back: access to treatment for cryptococcal meningitis. Lancet Infect Dis 5:530–531. https://doi.org/10.1016/S1473-3099(05)70197-3.
5. Loyse A, Thangaraj H, Easterbrook P, Ford N, Roy M, Chiller T, Govender N, Harrison TS, Bicanic T. 2013. Cryptococcal meningitis: improving access to essential antifungal medicines in resource-poor countries. Lancet Infect Dis 13:629–637. https://doi.org/10.1016/S1473-3099(13)70078-1.
6. Jarvis JN, Bicanic T, Loyse A, Namarika D, Jackson A, Nussbaum JC, Longley N, Muzoora C, Phulusa J, Taseera K, Kanyembe C, Wilson D, Hosseinipour MC, Brouwer AE, Limmathurotsakul D, White N, van der Horst C, Wood R, Meintjes G, Bradley J, Jaffar S, Harrison T. 2014. Determinants of mortality in a combined cohort of 501 patients with HIV-associated cryptococcal meningitis: implications for improving outcomes. Clin Infect Dis 58:736–745. https://doi.org/10.1093/cid/cit794.
7. Bicanic T, Meintjes G, Wood R, Hayes M, Rebe K, Bekker L-G, Harrison T. 2007. Fungal burden, early fungicidal activity, and outcome in cryptococcal meningitis in antiretroviral-naive or antiretroviral-experienced patients treated with amphotericin B or fluconazole. Clin Infect Dis 45:76–80. https://doi.org/10.1086/518607.
8. Nussbaum JC, Jackson A, Namarika D, Phulusa J, Kenala J, Kanyemba C, Jarvis JN, Jaffar S, Hosseinipour MC, Kamwendo D, van der Horst CM, Harrison TS. 2010. Combination flucytosine and high-dose fluconazole compared with fluconazole monotherapy for the treatment of cryptococcal meningitis: a randomized trial in Malawi. Clin Infect Dis 50:338–344. https://doi.org/10.1086/649861.
9. Richardson K, Cooper K, Marriott MS, Tarbit MH, Troke PF, Whittle PJ. 1990. Discovery of fluconazole, a novel antifungal agent. Rev Infect Dis 12:S267–S271. https://doi.org/10.1093/clinids/12.Supplement_3.S267.
10. Vanden Bossche H, Koymans L, Moereels H. 1995. P450 inhibitors of use in medical treatment: focus on mechanisms of action. Pharmacol Ther 67:79–100. https://doi.org/10.1016/0163-7258(95)00011-5.
11. Sudan A, Livermore J, Howard SJ, Al-Nakeeb Z, Sharp A, Goodwin J, Gregson L, Warn PA, Felton TW, Perfect JR, Harrison TS, Hope WW. 2013. Pharmacokinetics and pharmacodynamics of fluconazole for cryptococcal meningoencephalitis: implications for antifungal therapy and in vitro susceptibility breakpoints. Antimicrob Agents Chemother 57:2793–2800. https://doi.org/10.1128/AAC.00216-13.
12. Andes D, van Ogtrop M. 1999. Characterization and quantitation of the pharmacodynamics of fluconazole in a neutropenic murine disseminated candidiasis infection model. Antimicrob Agents Chemother 43:2116–2120.
13. Felton TW, McCalman K, Malagon I, Isalska B, Whalley S, Goodwin J, Bentley AM, Hope WW. 2014. Pulmonary penetration of piperacillin and tazobactam in critically ill patients. Clin Pharmacol Ther 96:438–448. https://doi.org/10.1038/clpt.2014.131.
14. Kethireddy S, Andes D. 2007. CNS pharmacokinetics of antifungal agents. Expert Opin Drug Metab Toxicol 3:573–581. https://doi.org/10.1517/17425255.3.4.573.
15. Gubbins PO, Anaissie EJ. 2009. Antifungal therapy, p 161–195. *In* Anaissie EJ, McGinnis MR, Pfaller MA (ed), Clinical mycology, 2nd ed. Churchill Livingstone, London, United Kingdom.
16. Arndt CA, Walsh TJ, McCully CL, Balis FM, Pizzo PA, Poplack DG. 1988. Fluconazole penetration into cerebrospinal fluid: implications for treating fungal infections of the central nervous system. J Infect Dis 157:178–180. https://doi.org/10.1093/infdis/157.1.178.
17. Madu A, Cioffe C, Mian U, Burroughs M, Tuomanen E, Mayers M, Schwartz E, Miller M. 1994. Pharmacokinetics of fluconazole in cerebrospinal fluid and serum of rabbits: validation of an animal model used to measure drug concentrations in cerebrospinal fluid. Antimicrob Agents Chemother 38:2111–2115. https://doi.org/10.1128/AAC.38.9.2111.
18. Tucker RM, Williams PL, Arathoon EG, Levine BE, Hartstein AI, Hanson LH, Stevens DA. 1988. Pharmacokinetics of fluconazole in cerebrospinal fluid and serum in human coccidioidal meningitis. Antimicrob Agents Chemother 32:369–373. https://doi.org/10.1128/AAC.32.3.369.
19. Thaler F, Bernard B, Tod M, Jedynak CP, Petitjean O, Derome P, Loirat P. 1995. Fluconazole penetration in cerebral parenchyma in humans at steady state. Antimicrob Agents Chemother 39:1154–1156. https://doi.org/10.1128/AAC.39.5.1154.
20. Mayanja-Kizza H, Oishi K, Mitarai S, Yamashita H, Nalongo K, Watanabe K, Izumi T, Ococi J, Augustine K, Mugerwa R, Nagatake T, Matsumoto K. 1998. Combination therapy with fluconazole and flucytosine for cryptococcal meningitis in Ugandan patients with AIDS. Clin Infect Dis 26:1362–1366. https://doi.org/10.1086/516372.
21. Larsen RA, Leal MA, Chan LS. 1990. Fluconazole compared with amphotericin B plus flucytosine for cryptococcal meningitis in AIDS. A randomized trial. Ann Intern Med 113:183–187. https://doi.org/10.7326/0003-4819-113-3-183.
22. Rothe C, Sloan DJ, Goodson P, Chikafa J, Mukaka M, Denis B, Harrison T, van Oosterhout JJ, Heyderman RS, Lalloo DG, Allain T, Feasey NA. 2013. A prospective longitudinal study of the clinical outcomes from cryptococcal meningitis following treatment induction with 800 mg oral fluconazole in Blantyre, Malawi. PLoS One 8:e67311. https://doi.org/10.1371/journal.pone.0067311.
23. Longley N, Muzoora C, Taseera K, Mwesigye J, Rwebembera J, Chakera A, Wall E, Andia I, Jaffar S, Harrison TS. 2008. Dose response effect of high-dose fluconazole for HIV-associated cryptococcal meningitis in southwestern Uganda. Clin Infect Dis 47:1556–1561. https://doi.org/10.1086/593194.
24. Milefchik E, Leal MA, Haubrich R, Bozzette SA, Tilles JG, Leedom JM, McCutchan JA, Larsen RA. 2008. Fluconazole alone or combined with flucytosine for the treatment of AIDS-associated cryptococcal meningitis. Med Mycol 46:393–395. https://doi.org/10.1080/13693780701851695.
25. Gaskell KM, Rothe C, Gnanadurai R, Goodson P, Jassi C, Heyderman RS, Allain TJ, Harrison TS, Lalloo DG, Sloan DJ, Feasey NA. 2014. A prospective study of mortality from cryptococcal meningitis following treatment induction with 1200 mg oral fluconazole in Blantyre, Malawi. PLoS One 9:e110285. https://doi.org/10.1371/journal.pone.0110285.
26. Beyene T, Zewde AG, Balcha A, Hirpo B, Yitbarik T, Gebissa T, Rajasingham R, Boulware DR. 2017. Inadequacy of high-dose fluconazole monotherapy among cerebrospinal fluid cryptococcal antigen (CrAg)-positive human immunodeficiency virus-infected persons in an Ethiopian CrAg screening program. Clin Infect Dis 65:2126–2129. https://doi.org/10.1093/cid/cix613.
27. Fischman AJ, Alpert NM, Livni E, Ray S, Sinclair I, Callahan RJ, Correia JA, Webb D, Strauss HW, Rubin RH. 1993. Pharmacokinetics of 18F-labeled fluconazole in healthy human subjects by positron emission tomography. Antimicrob Agents Chemother 37:1270–1277. https://doi.org/10.1128/AAC.37.6.1270.
28. Pasko MT, Piscitelli SC, Van Slooten AD. 1990. Fluconazole: a new triazole antifungal agent. DICP 24:860–867. https://doi.org/10.1177/106002809002400914.
29. Palou de Fernandez E, Patino MM, Graybill JR, Tarbit MH. 1986. Treat-

ment of cryptococcal meningitis in mice with fluconazole. J Antimicrob Chemother 18:261–270. https://doi.org/10.1093/jac/18.2.261.
30. Kartalija M, Kaye K, Tureen JH, Liu Q, Tauber MG, Elliott BR, Sande MA. 1996. Treatment of experimental cryptococcal meningitis with fluconazole: impact of dose and addition of flucytosine on mycologic and pathophysiologic outcome. J Infect Dis 173:1216–1221. https://doi.org/10.1093/infdis/173.5.1216.
31. Aoyama T, Hirata K, Hirata R, Yamazaki H, Yamamoto Y, Hayashi H, Matsumoto Y. 2012. Population pharmacokinetics of fluconazole after administration of fosfluconazole and fluconazole in critically ill patients. J Clin Pharm Ther 37:356–363. https://doi.org/10.1111/j.1365-2710.2011.01297.x.
32. Alobaid AS, Wallis SC, Jarrett P, Starr T, Stuart J, Lassig-Smith M, Mejia JL, Roberts MS, Sinnollareddy MG, Roger C, Lipman J, Roberts JA. 2016. Effect of obesity on the population pharmacokinetics of fluconazole in critically ill patients. Antimicrob Agents Chemother 60:6550–6557. https://doi.org/10.1128/AAC.01088-16.
33. McLachlan AJ, Tett SE. 1996. Pharmacokinetics of fluconazole in people with HIV infection: a population analysis. Br J Clin Pharmacol 41:291–298. https://doi.org/10.1046/j.1365-2125.1996.03085.x.
34. Brammer KW, Farrow PR, Faulkner JK. 1990. Pharmacokinetics and tissue penetration of fluconazole in humans. Rev Infect Dis 12(Suppl 3):S318–S326. https://doi.org/10.1093/clinids/12.Supplement_3.S318.
35. Sanglard D. 2002. Resistance of human fungal pathogens to antifungal drugs. Curr Opin Microbiol 5:379–385. https://doi.org/10.1016/S1369-5274(02)00344-2.
36. Chen Y, Farrer RA, Giamberardino C, Sakthikumar S, Jones A, Yang T, Tenor JL, Wagih O, Van Wyk M, Govender NP, Mitchell TG, Litvintseva AP, Cuomo CA, Perfect JR. 2017. Microevolution of serial clinical isolates of *Cryptococcus neoformans* var. *grubii* and *C. gattii*. mBio 8:e00166–17. https://doi.org/10.1128/mBio.00166-17.
37. Bicanic T, Harrison T, Niepieklo A, Dyakopu N, Meintjes G. 2006. Symptomatic relapse of HIV-associated cryptococcal meningitis after initial fluconazole monotherapy: the role of fluconazole resistance and immune reconstitution. Clin Infect Dis 43:1069–1073. https://doi.org/10.1086/507895.
38. Beardsley J, Wolbers M, Kibengo FM, Ggayi AB, Kamali A, Cuc NT, Binh TQ, Chau NV, Farrar J, Merson L, Phuong L, Thwaites G, Van Kinh N, Thuy PT, Chierakul W, Siriboon S, Thiansukhon E, Onsanit S, Supphamongkholchaikul W, Chan AK, Heyderman R, Mwinjiwa E, van Oosterhout JJ, Imran D, Basri H, Mayxay M, Dance D, Phimmasone P, Rattanavong S, Lalloo DG, Day JN, CryptoDex Investigators. 2016. Adjunctive dexamethasone in HIV-associated cryptococcal meningitis. N Engl J Med 374:542–554. https://doi.org/10.1056/NEJMoa1509024.
39. Neely M, van Guilder MG, Yamada WM, Schumitzky A, Jelliffe RW. 2012. Accurate detection of outliers and subpopulations with Pmetrics, a nonparametric and parametric pharmacokinetic modeling and simulation package for R. Ther Drug Monit 34:467–476. https://doi.org/10.1097/FTD.0b013e31825c4ba6.
40. Espinel-Ingroff A, Aller AI, Canton E, Castañón-Olivares LR, Chowdhary A, Cordoba S, Cuenca-Estrella M, Fothergill A, Fuller J, Govender N, Hagen F, Illnait-Zaragozi MT, Johnson E, Kidd S, Lass-Flörl C, Lockhart SR, Martins MA, Meis JF, Melhem MSC, Ostrosky-Zeichner L, Pelaez T, Pfaller MA, Schell WA, St-Germain G, Trilles L, Turnidge J. 2012. Cryptococcus neoformans-Cryptococcus gattii species complex: an international study of wild-type susceptibility endpoint distributions and epidemiological cutoff values for fluconazole, itraconazole, posaconazole, and voriconazole. Antimicrob Agents Chemother 56:5898–5906. https://doi.org/10.1128/AAC.01115-12.
41. Montezuma-Rusca JM, Powers JH, Follmann D, Wang J, Sullivan B, Williamson PR. 2016. Early fungicidal activity as a candidate surrogate endpoint for all-cause mortality in cryptococcal meningitis: a systematic review of the evidence. PLoS One 11:e0159727. https://doi.org/10.1371/journal.pone.0159727.
42. DerSimonian R, Laird N. 1986. Meta-analysis in clinical trials. Control Clin Trials 7:177–188. https://doi.org/10.1016/0197-2456(86)90046-2.

AMERICAN SOCIETY FOR MICROBIOLOGY | Antimicrobial Agents and Chemotherapy®

PHARMACOLOGY

Population Pharmacokinetic Model and Meta-analysis of Outcomes of Amphotericin B Deoxycholate Use in Adults with Cryptococcal Meningitis

Katharine E. Stott,[a,b] Justin Beardsley,[c] Sarah Whalley,[a] Freddie Mukasa Kibengo,[d] Nguyen Thi Hoang Mai,[f] Ruwanthi Kolamunnage-Dona,[e] William Hope,[a] Jeremy Day[c,g]

[a]Antimicrobial Pharmacodynamics and Therapeutics Laboratory, Department of Molecular and Clinical Pharmacology, Institute of Translational Medicine, University of Liverpool, Liverpool, United Kingdom

[b]Malawi-Liverpool-Wellcome Trust Clinical Research Programme, Blantyre, Malawi

[c]Oxford University Clinical Research Unit, Ho Chi Minh City, Vietnam

[d]MRC/UVRI Uganda Research Unit on AIDS, Entebbe, Uganda

[e]Department of Biostatistics, Institute of Translational Medicine, University of Liverpool, Liverpool, United Kingdom

[f]Hospital for Tropical Diseases, Ho Chi Minh City, Vietnam

[g]Centre for Tropical Medicine and Global Health, Nuffield Department of Medicine, University of Oxford, Oxford, United Kingdom

ABSTRACT There is a limited understanding of the population pharmacokinetics (PK) and pharmacodynamics (PD) of amphotericin B deoxycholate (DAmB) for cryptococcal meningitis. A PK study was conducted in $n = 42$ patients receiving DAmB (1 mg/kg of body weight every 24 h [q24h]). A 2-compartment PK model was developed. Patient weight influenced clearance and volume in the final structural model. Monte Carlo simulations estimated drug exposure associated with various DAmB dosages. A search was conducted for trials reporting outcomes of treatment of cryptococcal meningitis patients with DAmB monotherapy, and a meta-analysis was performed. The PK parameter means (standard deviations) were as follows: clearance, 0.03 (0.01) × weight + 0.67 (0.01) liters/h; volume, 0.82 (0.80) × weight + 1.76 (1.29) liters; first-order rate constant from central compartment to peripheral compartment, 5.36 (6.67) h^{-1}; first-order rate constant from peripheral compartment to central compartment, 9.92 (12.27) h^{-1}. The meta-analysis suggested that the DAmB dosage explained most of the heterogeneity in cerebrospinal fluid (CSF) sterility outcomes but not in mortality outcomes. Simulations of values corresponding to the area under concentration-time curve from h 144 to h 168 ($AUC_{144-168}$) resulted in median (interquartile range) values of 5.83 mg · h/liter (4.66 to 8.55), 10.16 mg · h/liter (8.07 to 14.55), and 14.51 mg · h/liter (11.48 to 20.42) with dosages of 0.4, 0.7, and 1.0 mg/kg q24h, respectively. DAmB PK is described adequately by a linear model that incorporates weight with clearance and volume. Interpatient PK variability is modest and unlikely to be responsible for variability in clinical outcomes. There is discordance between the impact that drug exposure has on CSF sterility and its impact on mortality outcomes, which may be due to cerebral pathology not reflected in CSF fungal burden, in addition to clinical variables.

KEYWORDS cryptococcal meningitis, pharmacokinetics, pharmacodynamics, amphotericin B deoxycholate, meta-analysis, population pharmacokinetics

Cryptococcal meningitis is a leading infectious cause of morbidity and mortality worldwide, with approximately 223,100 incident cases and 181,100 deaths annually (1). The 10-week mortality rate for patients receiving the current standard of care is 24%

Received 13 December 2017 **Returned for modification** 7 March 2018 **Accepted** 27 April 2018

Accepted manuscript posted online 7 May 2018

Citation Stott KE, Beardsley J, Whalley S, Kibengo FM, Mai NTH, Kolamunnage-Dona R, Hope W, Day J. 2018. Population pharmacokinetic model and meta-analysis of outcomes of amphotericin B deoxycholate use in adults with cryptococcal meningitis. Antimicrob Agents Chemother 62:e02526-17. https://doi.org/10.1128/AAC.02526-17.

Address correspondence to William Hope, hopew@liverpool.ac.uk.

to 31% (2–5). There have been no new antifungal agents developed for use in low-to-middle-income countries in the last 3 decades. Given the paucity of new agents, one important strategy for improving clinical outcomes is a better understanding and use of currently available compounds.

Amphotericin B (AmB) is a polyene antifungal agent with broad-spectrum activity against yeasts and molds, as well as against some parasites. AmB was initially isolated from a streptomycete and was originally described in 1955 (6). AmB was the first therapeutic option for treatment of lethal invasive fungal diseases such as cryptococcal meningitis (7, 8). Amphotericin B deoxycholate (DAmB) is the most potent formulation of AmB on a milligram-to-milligram basis (9, 10) and is a mainstay for the treatment of cryptococcal meningitis.

Clinical studies have progressively examined escalating dosages of 0.4 mg/kg of body weight every 24 h (q24h) (11, 12), 0.7 mg/kg q24h (13–15), and 1.0 mg/kg q24h (5) of DAmB for cryptococcal meningitis. The primary motivation of these studies was identification of the dosage that induces maximal antifungal activity. A regimen of 1.0 mg/kg q24h in combination with 5FC (flucytosine) for 1 week is currently recommended for induction therapy (16). High DAmB dosages are associated with increased rates of cerebrospinal fluid (CSF) sterilization (2) and improved mortality (4, 5, 17). However, the broad clinical utility of DAmB is compromised by dose-limiting toxicities that include infusional reactions, phlebitis, nephrotoxicity, and anemia (18, 19). A detailed understanding of the therapeutic index for each DAmB dosage level is lacking.

Here, we describe the development of a population pharmacokinetic model of DAmB. In addition, a meta-analysis of clinical trials of DAmB monotherapy was performed to estimate the contribution of various DAmB dosages to the observed heterogeneity in study outcomes. Finally, Monte Carlo simulations were performed to estimate the mean, median, and dispersion values corresponding to drug exposures that are associated with microbiological and clinical outcomes of DAmB monotherapy.

RESULTS

Demographics. A total of 42 patients (22 from Vietnam and 20 from Uganda) were recruited over an 11-month period between January and November 2016. A total of 22 (52%) of the patients were female. The overall median (range) age was 33 years (20 to 73 years), the overall median weight was 48 kg (32 to 68 kg), the overall median body mass index was 18 kg/m^2 (12 to 25 kg/m^2), the overall median level of creatinine at enrollment was 69 μmol/liter (37 to 167 μmol/liter), and the overall median estimated glomerular filtration rate (determined using the Cockcroft-Gault equation) was 76.7 ml/min/1.73 m^2 (35.4 to 146.7 ml/min/1.73 m^2). The demographic data are shown by ethnicity and overall in Table 1. There were no statistically significant differences between ethnic groups in any demographic variable.

Pharmacokinetic data. The final data set included 282 of 312 total observations from the Vietnamese cohort and 197 of 241 total observations from the Ugandan cohort (mean, 11.4 samples per patient; range, 6 to 18). In total, 74 plasma samples were excluded because of absent information regarding the time that the pharmacokinetic (PK) samples were drawn. Figure 1 shows the raw plasma concentration-time profiles from study participants.

Population pharmacokinetic models. Initial exploration of structural models revealed that a two-compartment model fitted the data better than a three-compartment model. Specifically, the three-compartment structural model resulted in a more negative log likelihood value (−55.5 versus −42.8) and a higher Akaike information criterion (AIC) value (127.3 versus 101.9). Accordingly, subsequent model development was based on a two-compartment base model.

Model 1 was a standard two-compartment model without inclusion of covariates. Linear regressions of the Bayesian estimates of clearance and volume (derived from the mean population PK parameter values from model 1) with weight and estimated glomerular filtration rate (eGFR) as covariates are presented in Fig. 2a and b, respec-

TABLE 1 Patient demographics

Demographic or clinical characteristic[a]	Value(s)			*P* value for difference between Vietnam and Uganda data
	Vietnam	Uganda	Combined	
Sex[b] (no. of males:no. of females)	12:10	8:12	20:22	
Age (yrs)[c]				
Mean	38	33	36	0.75[g]
Median	33	33	33	
Range	20–73	24–50	20–73	
Weight (kg)[d]				
Mean	47	49	48	0.21[g]
Median	46	49	48	
Range	32–68	35–60	32–68	
BMI (kg/m^2)[e]				
Mean	18	18	18	0.73[h]
Median	18	19	18	
Range	12–25	15–22	12–25	
Creatinine (μmol/liter)[b]				
Mean	71	81	75	0.06[g]
Median	62	79	69	
Range	37–167	43–145	37–167	
eGFR (ml/min/1.73 m^2)[f]				
Mean	90.6	79.3	84.7	0.19[g]
Median	89.8	73.5	76.7	
Range	35.4–136.1	49.8–146.7	35.4–146.7	

[a]BMI, body mass index; eGFR, estimated glomerular filtration rate (by Cockcroft-Gault equation).
[b]$n = 42$.
[c]$n = 28$.
[d]$n = 39$.
[e]$n = 33$.
[f]$n = 26$.
[g]Mann-Whitney test of significance.
[h]Unpaired *t* test of significance.

tively. A relationship was apparent between patient weight and both estimated clearance (slope, 0.05; 95% confidence interval [CI] for estimate of slope, 0.02 to 0.08; $P = 0.002$) and estimated volume of the central compartment (slope, 1.08; 95% CI, 0.05 to 2.11; $P < 0.001$). Similarly, linear regression data showed a positive relationship

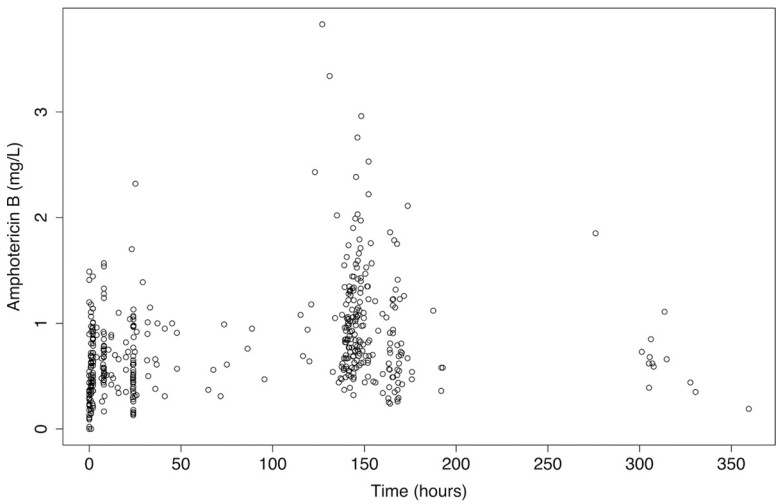

FIG 1 Amphotericin B serum concentrations in 42 patients. Patients received 1.0 mg/kg of amphotericin B deoxycholate (DAmB), infused over 5 to 6 h.

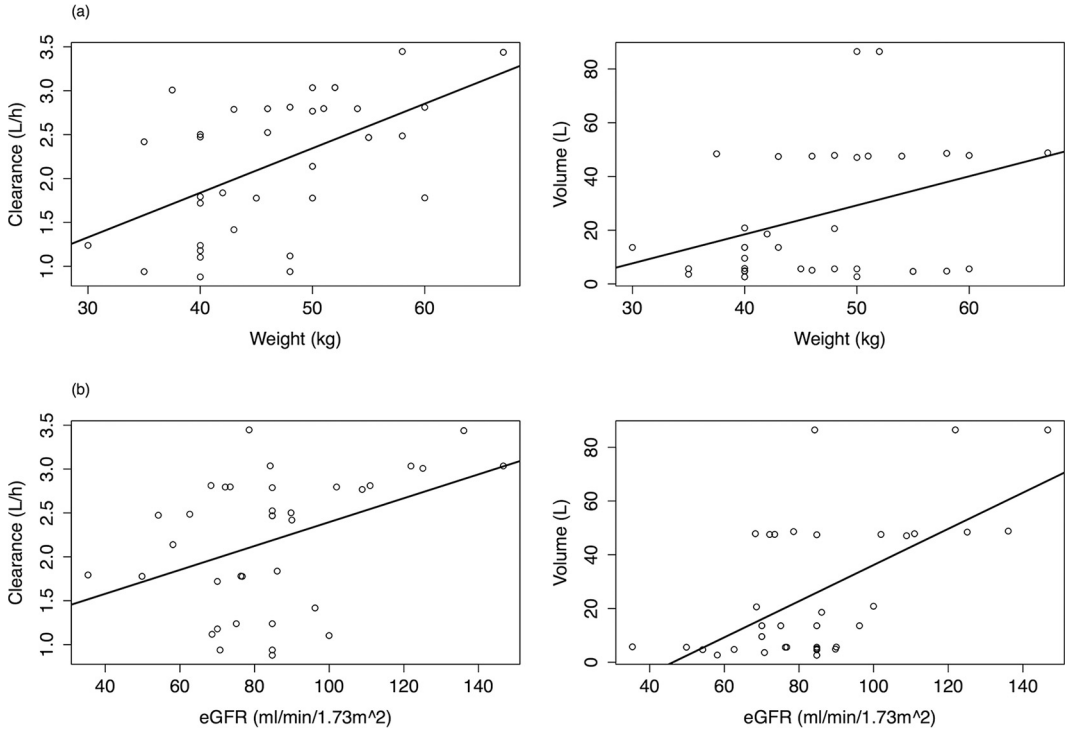

FIG 2 Linear regression of the relationship between (a) patient weight and (b) estimated glomerular filtration rate and Bayesian posterior estimates for clearance and volume of distribution. Circles are Bayesian estimates from each patient. Solid line: linear regression. (a) (Left panel) $R^2 = 0.32$. Clearance = 0.05 · weight − 0.2. (Right panel) $R^2 = 0.12$. Volume = 1.08 · weight − 24.8. (b) (Left panel) $R^2 = 0.17$. Clearance = 0.01 · eGFR + 1.03. (Right panel) $R^2 = 0.36$. Volume = 0.67 · eGFR − 31.13.

between eGFR and estimated clearance (slope of linear regression, 0.01; 95% CI for the slope, 0 to 0.02; $P < 0.05$) and volume (slope, 0.67; 95% CI, 0.36 to 0.98; $P < 0.001$). These covariates were incorporated into the structural model as follows: model 2 incorporated weight as a covariate with a linear term for clearance; model 3 incorporated weight as a covariate with a nonlinear term for clearance; and model 4 incorporated both weight and baseline renal function as covariates in the structural model, with linear clearance. Population PK parameter estimates for all 4 models are shown in Table 2. There were no statistically significant differences in the estimated clearance and volume data from the standard model (model 1) according to ethnicity. The mean (95% CI) values for clearance were 2.03 liters/h (1.69 to 2.38) and 2.24 liters/h (1.91 to 2.56) for Vietnamese and Ugandan patients, respectively (*P* value, 0.37). The mean (95% CI) volumes were 33.55 liters (17.96 to 49.13) and 63.93 liters (40.98 to 86.88) for Vietnamese and Ugandan patients, respectively (*P* value, 0.09).

The fit of the model to the data was acceptable for all 4 two-compartment models. The model diagnostics are presented in Table 3. The values corresponding to the coefficient of determination of a linear regression of observed-versus-predicted plots after the Bayesian step were 0.72, 0.74, 0.69, and 0.73 for models 1, 2, 3, and 4, respectively. The values for intercept and slope approximated 0 and 1, respectively, for each regression (Table 3). The mean parameter values predicted the observed values better than the medians. The measures of population bias and imprecision were comparable between the models, with bias values of −0.85, −0.34, −0.23, and −0.43 and imprecision values of 3.13, 2.97, 2.16, and 3.29 for models 1, 2, 3, and 4, respectively. The more positive log likelihood value and lower Akaike information criterion (AIC) value for model 2 suggested that the inclusion of weight as a covariate explained a portion of the observed variance.

The model that incorporated an exponential term for clearance (model 3) decreased the log likelihood value and increased the AIC value (Table 3). The inclusion of eGFR in

TABLE 2 Parameter estimates for the initial and modified two-compartment pharmacokinetic models

Parameter[a]	Value		
	Mean	Median	SD
Model 1			
SCL (liters/h)	2.19	2.46	0.77
Vc (liters)	27.77	13.88	28.06
K12 (h^{-1})	3.84	2.16	6.57
K21 (h^{-1})	1.14	0.32	3.06
Model 2			
SCL_{slope} (liters/h/kg)	0.03	0.03	0.01
$SCL_{intercept}$ (liters/h)	0.67	0.57	0.01
Vc_{slope} (liters/kg)	0.82	0.36	0.80
$Vc_{intercept}$ (liters)	1.76	1.99	1.29
K12 (h^{-1})	5.36	3.83	6.76
K21 (h^{-1})	9.92	0.46	12.27
Model 3			
SCL (liters/h/kg)	0.12	0.12	0.04
Vc (liters/kg)	1.40	0.51	1.75
K12 (h^{-1})	1.69	0.50	4.09
K21 (h^{-1})	8.31	0.27	12.32
Model 4			
SCL_{slope} (liters/h/kg)	0.01	0.01	0.01
$SCL_{intercept}$ (liters/h)	1.50	1.31	0.74
Vc_{slope} (liters/kg)	1.26	0.52	1.39
$Vc_{intercept}$ (liters)	1.64	0.01	2.96
K12 (h^{-1})	3.86	0.73	7.74
K21 (h^{-1})	11.24	0.40	13.44

[a]SCL, first-order clearance of drug (in liters per hour) from the central compartment; Vc, volume of distribution in the central compartment; K12, first-order rate constant from the central compartment to the peripheral compartment; K21, first-order rate constant from the peripheral compartment to the central compartment.

model 4 failed to increase the log likelihood value or reduce the AIC value further. In addition, there was no statistically significant difference between model 1 and either model 3 or model 4; the latter models were therefore rejected. Model 2 was chosen as the final model. Observed-versus-predicted plots for the population and Bayesian posterior values in the final model are shown in Fig. 3. Figure 4 shows a visual predictive check (VPC) of the final model.

Meta-analysis of clinical outcome data. Five clinical trials that included a DAmB monotherapy arm were identified. There was one trial in which 63 patients received 0.4 mg/kg of body weight q24h (11), 3 trials in which a combined total of 208 patients received 0.7 mg/kg q24h (13–15), and 1 trial in which 99 patients received 1.0 mg/kg

TABLE 3 Evaluation of the predictive performance of the initial model and final model[a]

Model	Log likelihood	No. of cycles to convergence	AIC	Population bias	Population imprecision	Linear regression of observed-predicted values for each patient		
						R^{2b}	Intercept	Slope
Model 1	−56.3	1,137	124.8	−0.85	3.13	0.72	0.08	0.97
Model 2	−42.8	1,251	101.9	−0.34	2.97	0.74	0.01	1.01
Model 3	−102.7	577	221.7	−0.23	2.16	0.69	0.00	1.04
Model 4	−43.1	1,704	102.7	−0.43	3.29	0.73	0.01	1.02

[a]Model 2 included a linear function to scale DAmB clearance to patient weight. Model 3 included a nonlinear function to scale DAmB clearance to patient weight. Model 4 included a function to scale DAmB clearance to patient weight and eGFR.

[b]R^2 values are expressed relative to the regression line fitted for the observed versus predicted values after the Bayesian step.

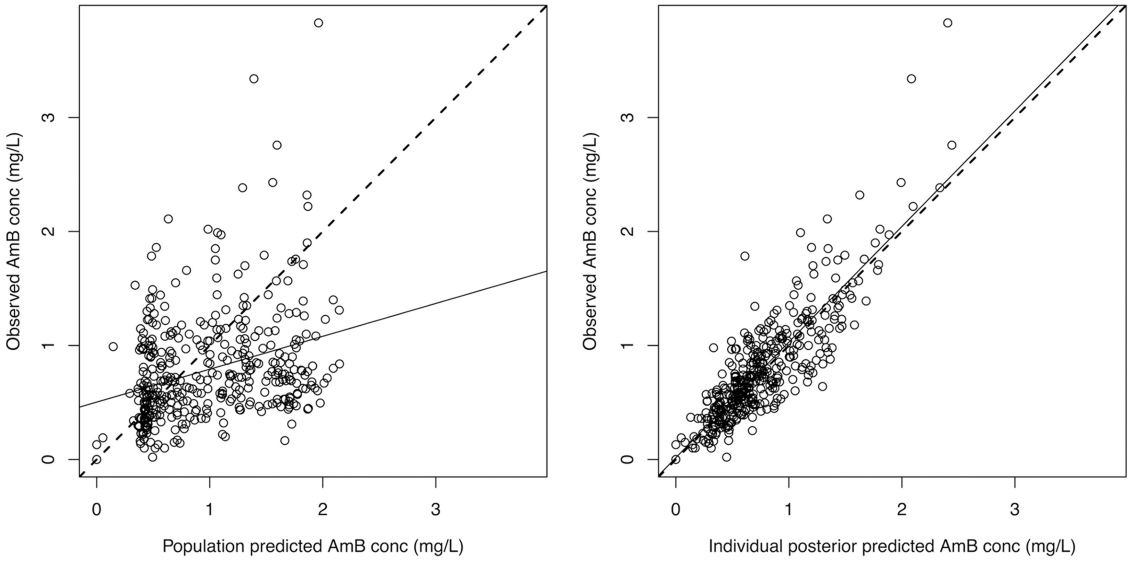

FIG 3 Scatter plots showing observed versus predicted values for the chosen population pharmacokinetic model after the Bayesian step (model 2). (Left panel) $R^2 = 0.17$. Intercept = 0.18 (95% CI, 0.03 to 0.32). Slope = 0.89 (95% CI, 0.70 to 1.09). (Right panel) $R^2 = 0.74$. Intercept = 0.01 (95% CI, −0.04 to 0.07). Slope = 1.01 (95% CI, 0.95 to 1.07). Circles, dashed lines, and solid lines represent individual observed-predicted data points, the line of identity, and the linear regression of observed and predicted values, respectively. All observed and predicted amphotericin B concentrations (conc) are indicated in milligrams per liter. AmB, amphotericin B; CI, confidence interval.

q24h (5). An additional study that reported clinical outcomes in untreated cryptococcal meningitis patients was also included. The baseline variables and clinical outcomes of these study arms are summarized in Table 4. Due to the small number of studies, we were unable to adjust for baseline variables that may have had an impact on outcome

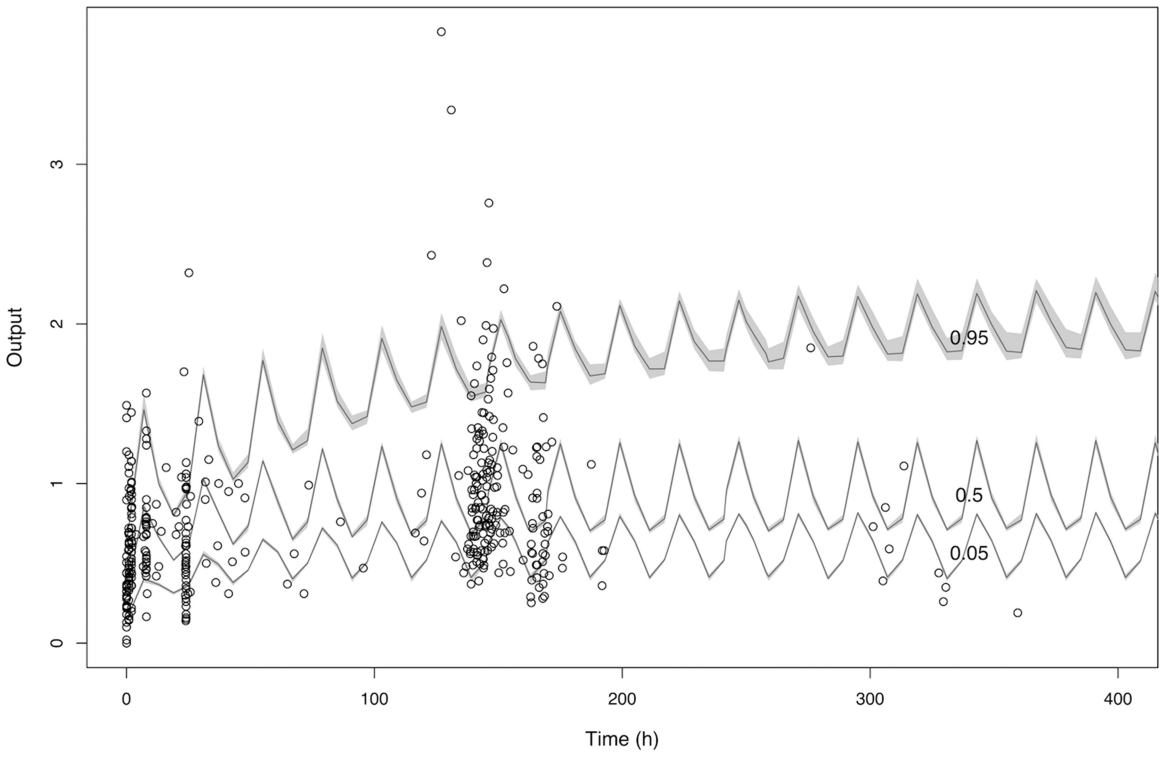

FIG 4 Visual predictive check of the final model. The black circles indicate observed DAmB concentrations. The continuous lines represent the 5th, 50th, and 95th percentiles of DAmB concentrations for 1,000 simulated patients. In total, 83.4% of observed DAmB concentrations fall within the 5th and 95th percentiles estimated by the final model, indicating adequate model fit.

TABLE 4 Clinical outcomes from trial data of DAmB monotherapy, by dosing regimen[a]

DAmB regimen (mg/kg q24h)	Location(s)	No. of patients	Median age (yrs)	Median CD4 cell count per mm^3	No. of patients with reduced LOC at baseline/total no. of patients (%)	Median baseline fungal burden, $\log_{10}$ CFU/ml (range)	Baseline CSF CrAg titer, median	Documented CSF sterility/total no. of patients (%)	No. of patients with mortality at 2 wks/total no. of patients (%)	No. of patients with mortality at 10 wks/total no. of patients (%)	No. of patients with indicated grade of anemia/total no. of patients (%)	No. of patients with hypokalemia/total no. of patients (%)	Reference
No treatment	Zambia	100	32	NR	NR	NR	NR	*0/100* (presumed)	65/100 (65)	100/100 (100)	NR	NR	20
0.4	United States	63	37	NR	16/63 (25)	NR; *~4.2*	1:512[c]	25/63 (40)	5/63 (8)	NR; 9/63 at 12 wks (14)	NR	NR	11
0.7	Thailand	16	34	9	1/16 (6)	5.63 (5.19–5.97)	1:512	NR	2/16 (13)	3/16 (19)	NR	NR	15
0.7	Australia/The Netherlands	13	41	35	2/13 (15)	NR; *~3.9*	1:256	3/8 (37)	0/13 (0)	2/13 (15)	−20 (−45 to 5)[b] at 10 wks; fall in Hb > 2 g/dl, 2/13 (15)	4/13 (31); <3 mEq/liter	13
0.7	United States	179	37	18	18/179 (10)	NR; *~4.8*	1:1,024	91/179 (51)	11/202 (5)	NR	NR in comparable manner	NR in comparable manner	14
1.0	Vietnam	99	28	18	31/97 (32)	5.91 (5.49–6.48)	NR; *~1:4,096*	52/99 (53)	25/99 (25)	44/99 (44)	All anemia, 62/99 (63); grade 3–4 anemia (<8 g/dl), 46/99 (46)	All, 54/99 (55); grade 3–4 (<2.5 mmol/liter), 20/99 (20)	5

[a]LOC, level of consciousness; NR, not reported; CSF, cerebrospinal fluid; CrAg, cryptococcal antigen; Hb, hemoglobin; mEq, milliequivalents. Italic text indicates values that were extrapolated from available data.
[b]% decrease in hemoglobin, median (range).
[c]Reported in reference 14.

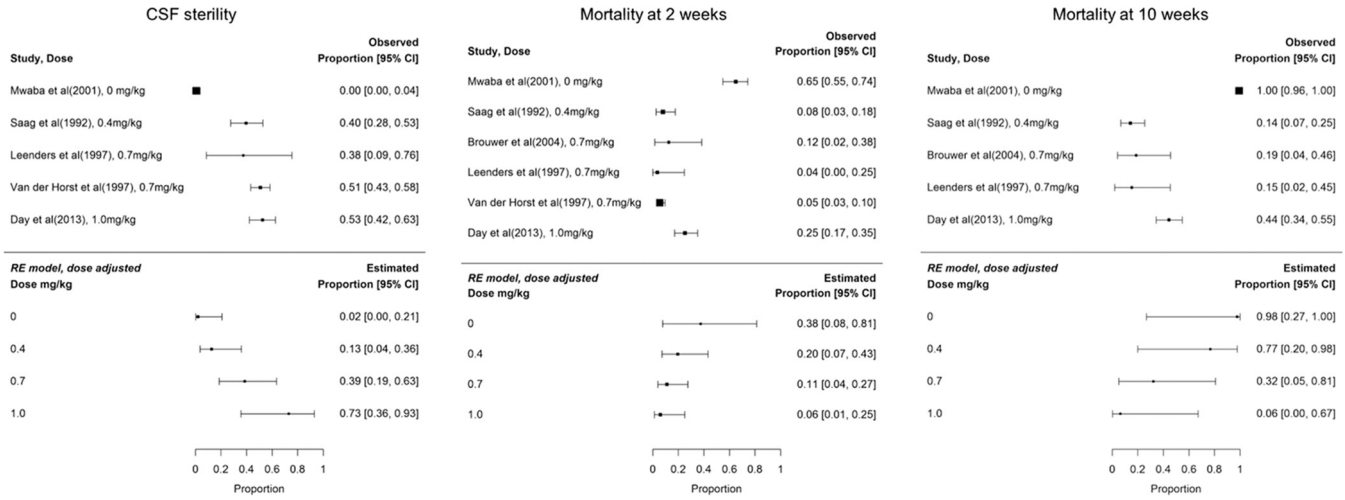

FIG 5 Meta-analysis of clinical trials of DAmB monotherapy, showing dose-adjusted effects on CSF sterility (left panel), mortality at 2 weeks (middle panel), and mortality at 10 weeks (right panel). (Left panel) Tau value for unadjusted model: 4.22. Tau value for dose-adjusted model: 0.98. Dose adjustment accounts for (4.22 − 0.98)/4.22 = 77% of the heterogeneity in clinical outcomes. *P* value for dose adjustment, 0.007. (Middle panel) Tau value for unadjusted model: 1.90. Tau value for dose-adjusted model: 1.28. Dose adjustment accounts for (1.90 − 1.28)/1.90 = 33% of the heterogeneity in clinical outcomes. *P* value for dose adjustment, 0.14. (Right panel) Tau value for unadjusted model: 9.0. Tau value for dose-adjusted model: 4.93. Dose adjustment accounts for (9.00 − 4.93)/9.00 = 45% of heterogeneity in clinical outcomes. *P* value for dose adjustment, 0.07. RE, random effects. Day et al., reference 5; Saag et al., reference 11; Leenders et al., reference 13; van der Horst et al., reference 14; Brouwer et al., reference 15; Mwaba et al., reference 20.

measures (e.g., age, CD4 cell count, baseline level of consciousness, baseline fungal burden, and baseline cryptococcal antigenemia). The forest plots of the dose-adjusted random-effects model are shown in Fig. 5. The model suggests that dose adjustment accounted for 77% of the heterogeneity in CSF sterility ($P = 0.007$) but that it did not have a significant impact on the heterogeneity in either the 2-week mortality outcomes (33%, $P = 0.14$) or the 10-week mortality outcomes (45%, $P = 0.07$).

Monte Carlo simulations. Monte Carlo simulations ($n = 5{,}000$) were performed using the final population PK model. This enabled exploration of the consequences of the population PK variability, quantified in the final model, on plasma DAmB concentrations in a simulated population receiving the dosage regimens for which clinical trial outcome data were available. The median (interquartile range) area under the concentration-time curve from h 144 to h 168 ($AUC_{144-168}$) was 5.83 mg/liter · h (4.66 to 8.55 mg/liter · h) for patients receiving DAmB 0.4 mg/kg q24h, 10.16 mg/liter · h (8.07 to 14.55 mg/liter · h) for 0.7 mg/kg q24h, and 14.51 mg/liter · h (11.48 to 20.42 mg/liter · h) for 1.0 mg/kg q24h. The $AUC_{144-168}$ distributions from the simulations are shown in Fig. 6.

DISCUSSION

We conducted a PK study in HIV-positive adults with cryptococcal meningitis in regions of high disease burden and developed a population PK model that enabled the extent of interpatient variability to be quantified. We described the PK of DAmB using a 2-compartment PK model with intravenous (i.v.) infusion and first-order clearance of drug from the central compartment. Simulated AUC values revealed relatively modest PK variability, suggesting that the frequently poor clinical outcomes are not the result of significant PK variability. The relationship between weight and drug clearance suggests that weight accounts for a portion of the observed variance. Dosage adjustment on the basis of weight is necessary to ensure that lighter patients are not overdosed and heavier patients are not underdosed. However, the lack of impact of either eGFR or ethnicity on the PK data suggests that dosage adjustment for these variables is not necessary to achieve comparable levels of drug exposure across patient populations.

The model-simulated median AUC value of 10.17 mg · h/liter following a regimen of 0.7 mg/kg of body weight q24h is consistent with AUC values estimated using

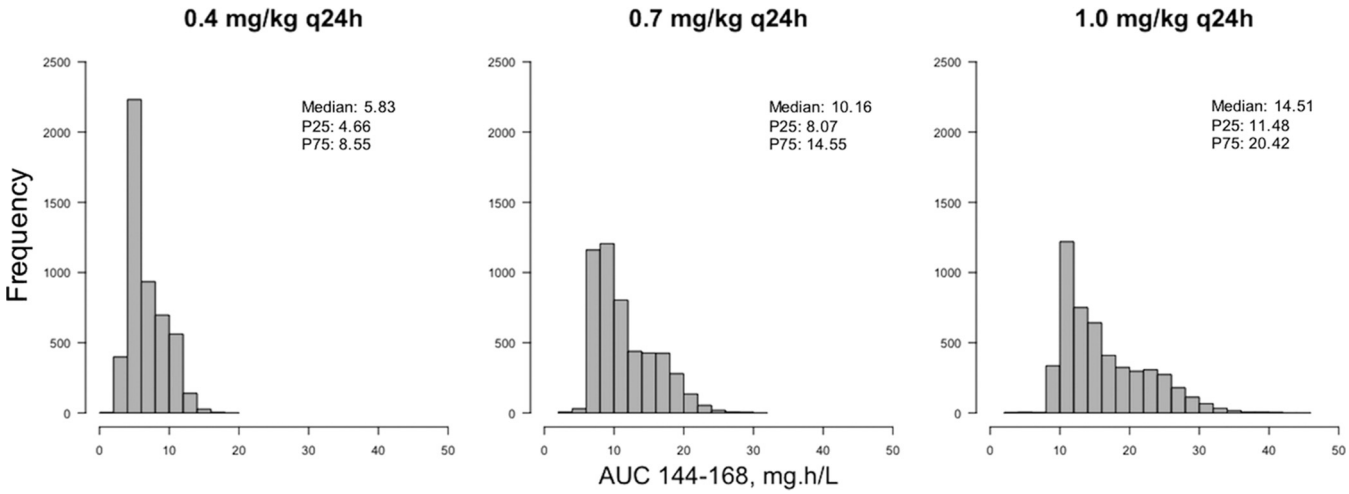

FIG 6 AUC distributions based on Monte Carlo simulations. Simulated dosing regimens are 0.4, 0.7, and 1.0 mg/kg q24h. Medians, 25th percentiles (P25), and 75th percentiles (P75) are displayed on each histogram.

noncompartmental techniques. For example, Bekersky et al. calculated an AUC_{0-24} value of 13.9 ± 2 mg · h/liter after administration of 0.6 mg/kg i.v. in healthy volunteers (21). However, the simulations performed following administration of 1 mg/kg resulted in a median AUC value of 14.51 mg · h/liter, which is considerably lower than that derived from a noncompartmental analysis (NCA) conducted by Ayestarán et al. for the same dose administered to neutropenic patients (28.98 ± 15.46 mg · h/liter) (22). The reason for this is not immediately clear but may relate to physiological differences between these two critically unwell patient cohorts (23).

Our meta-analysis of clinical outcomes of studies of DAmB monotherapy is limited by the fact that the included studies recorded CSF sterility at diverse time points ranging from 2 weeks (14) to 10 weeks (11). Nevertheless, the meta-analysis suggests that the dosage of DAmB has a significant impact on the proportion of patients with sterile CSF and that achieving CSF sterility is dose dependent up to 1 mg/kg q24h. However, the DAmB data did not have a dose-dependent relationship with mortality rates at either 2 or 10 weeks.

The potential reasons that DAmB dosage had a positive impact on CSF sterilization but not on mortality are as follows. First, AmB toxicity may contribute to mortality (18, 19). Nephrotoxicity is dose dependent and likely multifactorial. It is associated with a 4.5× increase in the odds of mortality from cryptococcal meningitis at 10 weeks (18). Free drug interacts with the distal tubules of the nephron causing increased monovalent ion delivery, with consequent afferent arteriolar constriction (24). Direct tubular toxicity results in hypokalemia and hypomagnesemia, leading to cardiotoxicity (24, 25). Conversely, rapid infusion of AmB can result in an extracellular shift of potassium, causing hyperkalemia and cardiac dysrhythmias (26). Anemia occurs in up to 75% of patients treated with DAmB as a result of direct suppression of erythropoiesis (24). Severe anemia more than doubles the odds of 10-week mortality from cryptococcal meningitis (18). Second, mortality may be driven by factors not directly resulting from either disease or treatment. For example, nosocomial bacteremia may occur in up to 15% to 18% of patients hospitalized for cryptococcal meningitis (27). Third, fungal burden—and therefore, conceivably, time to CSF sterility—is just one of multiple clinical variables associated with mortality in cryptococcal meningitis. Older age, altered mental status, low body weight, high peripheral white blood cell count, and anemia are independently associated with mortality at either 2 or 10 weeks (4). Immune reconstitution inflammatory syndrome (IRIS) remains a significant cause of mortality, occurring in 3% to 49% of cryptococcal meningitis patients who survive to initiation of antiretroviral treatment and carrying a mortality rate of up to 36% (17, 28). Raised intracranial

pressure is an additional factor associated with mortality, and treatment incorporating at least 1 therapeutic lumbar puncture imparts a relative survival advantage of 69% in the first 10 days of treatment (29). Finally, the trial cohorts included in the meta-analysis were from diverse sites in Africa, Asia, Europe, and the United States. Factors such as health-seeking behavior and nutritional status may have influenced the mortality outcomes. Our meta-analysis did not include any baseline factors other than DAmB dosage, and we are therefore unable to determine whether they account for the heterogeneity in mortality that is not explained by DAmB dosage.

The discordance between the influence that drug dosage has on CSF sterilization and mortality is reflective of a growing consensus that CSF sterility is just one of many determinants of mortality in cryptococcal meningitis. A systematic review of 27 clinical trials determined that there was no correlation between CSF sterility at 2 weeks and all-cause mortality at either 2 or 10 weeks (30). The most biologically plausible explanation for this is that fungal burden in the CSF may not reflect the extensive encephalitis that is characteristic of cryptococcal meningitis (which is more accurately termed "meningoencephalitis"). Histopathological defects are more marked in patients coinfected with HIV; fungi accumulate in perivascular spaces, are deposited [predominantly extracellularly] in brain parenchyma, and form granulomatous cryptococcomas in brain tissue (31, 32). It is conceivable that brain parenchymal damage is a dominant determinant of mortality and that clearance of fungi in CSF is not mirrored by clearance in the cerebrum and other CNS subcompartments. CSF sterility is an imperfect surrogate for the extent to which drug has penetrated into and sterilized the central nervous system.

The meta-analysis suggests a strong dose exposure-response relationship. Higher dosages are likely to be required to achieve efficacious drug exposure at the site of infection. DAmB has high molecular mass (924 g/mol) and complex binding properties (33). It does not readily penetrate the intact blood-brain barrier. Its concentration in meninges and cryptococcomas has been technically difficult to quantify in any finer detail than in brain homogenates in preclinical models (34, 35). This challenge is compounded by a lack of clarity regarding the DAmB concentration required for therapeutic efficacy at the site of infection. Animal studies have produced estimates indicating that the cerebral concentrations of DAmB at which the suppression of growth is half-maximal are 0.02 mg/liter in mice and 0.154 mg/liter in rabbits (34). AmB exposure above the level required to optimize antifungal activity appears to contribute only to toxicity (34, 36). Our simulations suggested that the optimal plasma AUC value in humans lies somewhere between 10 and 15 mg · h/liter, though the information required to extrapolate this to cerebral DAmB concentrations is not currently available. The application of noninvasive, high-resolution technologies, including matrix-assisted laser desorption ionization–mass spectroscopy imaging (MALDI-MSI), is now possible and offers the exciting potential to elucidate the pharmacokinetic/pharmacodynamic (PK/PD) index associated with efficacy at the site of infection by enabling quantification of drug in specific cerebral sites, as has been demonstrated in murine models that used gatifloxacin (37), doxycycline (38), pretomanid (39), and rifampin (40).

It may be the case that the maximal antifungal effect of DAmB is achieved with a dose of approximately 0.7 mg/kg, or slightly higher, and that gains made above this dose in terms of CSF sterility are offset by losses in terms of excessive toxicity. This may explain why significant increases in the proportions of patients achieving CSF sterility are not mirrored by reductions in mortality. The present analysis is not sufficient to more precisely define the optimal dosage of DAmB. This is partly due to the lack of consensus regarding DAmB exposure targets. We are unable to propose exposure targets based on our data set, which does not include site-specific PK or detailed toxicodynamic data. In addition, the pharmacodynamic and clinical outcome data presented here were derived from patient cohorts that were distinct from the patients that provided samples for the PK analysis. Outcomes from DAmB monotherapy at dosages of 0.7 mg/kg q24h and 1.0 mg/kg q24h have not been directly

compared in a randomized controlled trial. However, comparison of these dosages in combination with 5FC has been performed. Bicanic et al. demonstrated increased early fungicidal activity with DAmB at 1 mg/kg q24h versus 0.7 mg/kg q24h, both in combination with 5FC at 100 mg/kg/day in four divided dosages, but this was not reflected in reductions in mortality. A higher percentage of deaths was seen in the higher-dose DAmB arm at both 2 weeks (9% versus 3%) and 10 weeks (26% versus 21%), but the data were not statistically significant ($P = 0.62$ and 0.77 at 2 and 10 weeks, respectively) (2).

In summary, these analyses suggest that the optimal dosage of DAmB for the treatment of cryptococcal meningitis lies between 0.7 and 1.0 mg/kg q24h. The precise drug exposure target that optimizes clinical outcomes without producing significant toxicity remains to be defined. The extent of interindividual PK variability in DAmB is modest and unlikely to account for the consistently poor clinical outcomes from treatment of cryptococcal meningitis.

MATERIALS AND METHODS

Clinical pharmacokinetic studies. Plasma samples were obtained from adults with HIV-associated cryptococcal meningitis. Patients were initially recruited from a multicenter randomized controlled trial of adjuvant treatment with dexamethasone in HIV-associated cryptococcal meningitis, reported elsewhere ($n = 3$; International Standard Registered Clinical Number 59144167) (17). Following the early cessation of that trial, they were recruited from a prospective descriptive study at the same sites ($n = 39$). Patients were recruited at 2 sites: The Hospital for Tropical Diseases in Ho Chi Minh City, Vietnam, and Masaka General Hospital, Uganda. The study protocols were approved by the relevant institutional review boards and regulatory authorities at each trial site and by the Oxford University Tropical Research Ethics Committee.

The protocol for the randomized controlled trial has been described previously (41). Briefly, patients had HIV infection, a syndrome consistent with cryptococcal meningitis, and laboratory evidence of cryptococcal infection. Patients who were pregnant, had renal failure, had gastrointestinal bleeding, had received more than 7 days of anticryptococcal antifungal therapy, were already taking corticosteroids, or required corticosteroid therapy for coexisting conditions were excluded. The inclusion and exclusion criteria for the prospective descriptive study were identical to those of the clinical trial. Patients received DAmB at 1 mg/kg of body weight once daily by intravenous infusion over 5 to 6 h, as well as 800 mg fluconazole per day. Two patients recruited during the clinical trial received dexamethasone according to the following regimen: 0.3 mg/kg/day intravenously (i.v.) for week 1 and 0.2 mg/kg/day i.v. for week 2 and then orally at 0.1 mg/kg/day for week 3, 3 mg/day for week 4, 2 mg/day for week 5, and 1 mg/day for week 6, followed by cessation of treatment. For the first five patients enrolled, blood samples were obtained immediately prior to intravenous DAmB infusion and then at h 1, 2, 4, 8, 12, 16, 20, and 24. The results for these patients informed a subsequent sampling strategy defined using optimal design theory such that patients were sampled predose and then at 1, 2, 4, 8, 12, and 24 h after initiation of the infusion. PK sampling occurred on treatment days 1 or 2 and 7. Whenever patients had lumbar punctures performed for other clinical indications such as raised intracranial pressure, paired plasma samples were collected for subsequent PK analysis. Therefore, additional sparse samples were taken for up to 17 days after initial dosing. Quantitative fungal counts were determined for each lumbar puncture, as described previously (15).

Measurement of amphotericin B concentrations. Amphotericin B concentrations in plasma were measured using high-performance liquid chromatography (HPLC) with a Shimadzu Prominence HPLC system (Shimadzu, Milton Keynes, United Kingdom). Amphotericin B was extracted by protein precipitation. A total of 300 μl of methanol that contained piroxicam (Sigma-Aldrich, Dorset, United Kingdom) at 2 mg/liter was added as an internal standard to 100 μl of matrix. Samples were vortex mixed for 5 s and then centrifuged at 13,000 $\times$ *g* for 3 min.

A 150-μl volume of supernatant was removed and placed in a 96-well plate, to which 50 μl of water was added. A 50-μl aliquot was injected into a Kinetex 5μ XB-C18 liquid chromatography column (Phenomenex, Macclesfield, United Kingdom). Chromatographic separation was achieved using a gradient under starting conditions of 75% mobile phase A/25% mobile phase B (with 0.1% formic acid–water as mobile phase A and 0.1% formic acid–acetonitrile as mobile phase B). Mobile phase B was increased to 80% over 5 min and then reduced to the starting conditions for 2 min of equilibration. Amphotericin B and the internal standard were detected using UV detection at wavelengths of 406 nm and 385 nm; they eluted after 4.1 and 4.6 min, respectively.

The standard curve for amphotericin B encompassed the concentration range of 0.05 to 8.0 mg/liter and was constructed using blank matrix. The limit of quantitation was 0.05 mg/liter. The coefficient of variation was <9.3% over the concentration range of 0.05 to 8 mg/liter. The intraday variation and interday variation were <7.9%.

Population pharmacokinetic modeling. A PK model was fitted to the data using the nonparametric adaptive grid (NPAG) algorithm of the program Pmetrics (42) version 1.5.0 for R statistical package 3.1.1. The data were weighted using the inverse of the estimated assay variance. Both two- and three-compartment models were tested, with zero-order intravenous input and first-order elimination from the central compartment. The two-compartment model took the following form:

$$\frac{dX(1)}{dt} = R(1) - \left[\frac{\mathrm{SCL}}{V} + K12\right] \times X(1) + K21 \times X(2) \quad \text{(a)}$$

$$\frac{dX(2)}{dt} = K12 \times X(1) - K21 \times X(2) \quad \text{(b)}$$

$$Y(1) = \frac{X(1)}{V} \quad \text{(c)}$$

where equations a and b describe the rates of change of the amount of drug (in milligrams) in the central and peripheral compartments, respectively. *X*(1) and *X*(2) represent the amounts of amphotericin B (in milligrams) in the central (c) and peripheral (p) compartments, respectively. *R*(1) represents the intravenous infusion of DAmB into the central compartment. SCL represents the first-order clearance of drug (in liters per hour) from the central compartment. *V* represents the volume of the central compartment. *K*12 and *K*21 represent the first-order intercompartmental rate constants. Equation c represents the model output. The three-compartment model contained the following additional equation to connect the third compartment to the second compartment in series:

$$\frac{dX(3)}{dt} = K23 \times X(2) - K32 \times X(3) \quad \text{(d)}$$

An initial condition was estimated to accommodate detectable drug in the first PK sample from those patients who had received a dose of DAmB at an undocumented time before study enrollment. The nonzero initial condition was estimated by assigning the respective parameters in the structural model (not shown in the equations above). A switch was coded whereby a parameterized estimate of the initial condition was multiplied by a binary covariate equal to 1 (where the first PK sample was drawn after a dose of DAmB) or 0 (where this represented a predose sample).

Once the standard model (model 1) was fitted, the effects of patient weight, baseline eGFR, and patient ethnicity on the PK of DAmB were investigated. Bidirectional stepwise multivariate linear regression of each subject's covariates versus the Bayesian posterior parameter values revealed a significant ($P < 0.05$) relationship between both weight and eGFR and estimated PK parameters. Univariate linear regression was employed first to assess the relationship between patient weight and the Bayesian estimates for both clearance and volume. Since a positive relationship was observed between weight and both PK parameters, the population PK model was refitted to the data (model 2) with incorporation of the following equations to describe clearance (SCL) (equation e) and volume (*V*) (equation f) as functions of patient weight (Wt):

$$\mathrm{SCL} = \mathrm{Int}\_c + (\mathrm{Wt} \times \mathrm{Sl}\_c) \quad \text{(e)}$$

$$V = \mathrm{Int}\_v + (\mathrm{Wt} \times \mathrm{Sl}\_v) \quad \text{(f)}$$

where Int is the intercept and Sl the slope of the linear regression describing the relationship between weight and clearance or volume; the intercept and slope for each of these PK parameters are parameterized separately. Thus, equation a of the structural model was replaced with the following equation:

$$\frac{dX(1)}{dt} = R(1) - \left[\frac{\mathrm{Int}_c + (\mathrm{Wt} \times \mathrm{Sl}_c)}{\mathrm{Int}_v + (\mathrm{Wt} \times \mathrm{Sl}_v)} + K12\right] \times X(1) + K21 \times X(2) \quad \text{(a.2)}$$

In addition, a power function was explored to describe the relationship between weight and clearance. In this model (model 3), clearance was parameterized and scaled with weight to the exponent 0.75. This exponent has previously been demonstrated to usefully scale for size (43, 44). A linear relationship was maintained between volume and weight. Thus, in model 3, equation a was replaced with the following equation:

$$\frac{dX(1)}{dt} = R(1) - \left[\frac{\mathrm{SCL} \times \mathrm{Wt}^{0.75}}{V \times \mathrm{Wt}} + K12\right] \times X(1) + K21 \times X(2) \quad \text{(a.3)}$$

Univariate linear regression was similarly employed to assess the relationship between eGFR and the Bayesian estimates for clearance and volume from model 1. A weaker but nevertheless positive association was demonstrated. Consequently, a further structural model (model 4) was fitted to the data, with the following equation (equation g) employed to describe clearance (SCL):

$$\mathrm{SCL} = \mathrm{Int}\_c + (\mathrm{Wt} \times \mathrm{Sl}\_c) \times \left(\frac{\mathrm{eGFR}}{\mathrm{med}_{\mathrm{eGFR}}}\right) \quad \text{(g)}$$

where eGFR represents the estimated glomerular filtration rate calculated for each patient by the use of the Cockcroft-Gault equation and med_eGFR represents the population median estimated glomerular filtration rate. In model 4, equation a was replaced with the following equation:

$$\frac{dX(1)}{dt} = R(1) - \left[\frac{\mathrm{Int}_c + (\mathrm{Wt} \times \mathrm{Sl}_c) \times \left(\frac{\mathrm{eGFR}}{\mathrm{med}_{\mathrm{eGFR}}}\right)}{\mathrm{Int}_v + (\mathrm{Wt} \times \mathrm{Sl}_v)} + K12\right] \times X(1) + K21 \times X(2) \quad \text{(a.4)}$$

To explore whether there were significant differences between the model-predicted PK parameters in Vietnamese and Ugandan patients, Bayesian estimates of volume of distribution and clearance from the central compartment were compared using a Mann-Whitney test and Student's *t* test, respectively. Since no significant relationship between ethnicity and DAmB PK was apparent, this variable was not incorporated in the final model.

The fit of the model to the data was assessed using a linear regression of observed-versus-predicted values before and after the Bayesian step. The coefficient of determination of the linear regression was noted in combination with the intercept and slope of the regression for each model. Model comparison was achieved through calculation of the log likelihood value, the Akaike information criterion (AIC), the mean weighted error (a measure of bias), and the bias-adjusted, mean weighted squared error (a measure of precision). To verify the ability of the final model to predict observed concentrations with acceptable accuracy, a visual predictive check (VPC) of the data was performed. For the VPC, the covariance matrix in Pmetrics was utilized to simulate 1,000 patients administered DAmB on a milligram-per-kilogram basis. Simulated weight values were limited to the range observed in our clinical cohort.

Meta-analysis of clinical outcome data. The pharmacodynamic data from patients enrolled in the present clinical study are confounded by the coadministration of fluconazole (17). Therefore, a search was performed for clinical trials of treatment for cryptococcal meningitis with at least one arm comprised of adult patients receiving DAmB monotherapy. For consistency, the included trials were limited to those that recruited HIV-positive patients. Baseline clinical variables with a demonstrated ability to predict patient mortality—namely, altered mental status, patient age, and baseline CSF fungal burden—were selected *a priori* and extracted from the studies (4, 30). To aid meaningful trial comparison, baseline fungal burden and baseline CSF cryptococcal antigen titer values were extrapolated from one another where they were not explicitly reported in the study, applying a correlation presented by Jarvis et al. (4).

We collated a variety of clinical trial outcomes based on those that were commonly reported across trials of DAmB monotherapy: documented CSF sterility during trial follow-up, mortality at 2 weeks, and, where possible, mortality at 10 weeks. Meta-analysis was performed on each outcome using a dose-adjusted random-effects model to account for the baseline heterogeneity in the included studies. We included dose as a moderator variable in the model to assess the degree to which it explained heterogeneity in clinical outcomes (45). The resulting mixed-effects model took the form $\theta_i = \beta_0 + \beta_1 \text{dose}_i + u_i$, where β_0 and β_1 are the model parameters intercept and dose, respectively; dose_i is the dose given in the ith study, assuming study-specific random effects; and $u_i = \sim N(0, \tau^2)$, where τ^2 is the amount of residual heterogeneity among the true effects θ_i that is not accounted for by dose. We calculated to what extent dose as a moderator influenced the true average effect and estimated the corresponding proportions of each outcome measure.

Monte Carlo simulation. Monte Carlo simulations were performed in Pmetrics (42). Model 2 was used. Amphotericin B was administered on a milligram-per-kilogram basis and infused over 5.5 h. The initial conditions of the central and peripheral compartments were set at a default value of zero. The weight-based dosage of DAmB was converted to an absolute dosage by multiplying by the simulated patient's weight. This process served to mimic the bedside drug administration in the original clinical trial, in which dosing was planned on a milligram-per-kilogram basis but the absolute dose that was ultimately administered was determined by the patient's weight.

Drug exposure was quantified using the DAmB AUC (9, 10, 46). The simulated AUC for each patient was estimated 144 to 168 h post-therapy initiation. Simulations were performed to estimate the AUC that resulted from dosages administered in clinical trials of DAmB monotherapy for which PD measures were available—specifically, 0.4, 0.7, and 1.0 mg/kg q24h (5, 11, 13–15).

ACKNOWLEDGMENTS

W.H. holds or has recently held research grants with F2G, AiCuris, Astellas Pharma, Spero Therapeutics, Matinas Biosciences, Antabio, Amplyx, Allecra, Auspherix and Pfizer. He holds awards from the National Institutes of Health, the Medical Research Council, the National Institute of Health Research of the United Kingdom, and the European Commission (FP7 and IMI). W.H. has received personal fees in his capacity as a consultant for F2G, Amplyx, Ausperix, Spero Therapeutics, Medicines Company, Gilead, and Basilea. W.H. is Medical Guideline Director for the European Society of Clinical Microbiology and Infectious Diseases and is an Ordinary Council Member for the British Society of Antimicrobial Chemotherapy. The work described here was supported by the United Kingdom Department for International Development, the Wellcome Trust, and the Medical Research Council through a grant (G1100684/1) from the Joint Global Health Trials program, part of the European and Developing Countries Clinical Trials Partnership, supported by the European Union. K.E.S. is a Wellcome Trust Clinical Ph.D. Fellow (203919/Z/16/Z). J.D. is a Wellcome Trust Intermediate Fellow (WT097147MA).

REFERENCES

1. Rajasingham R, Smith RM, Park BJ, Jarvis JN, Govender NP, Chiller TM, Denning DW, Loyse A, Boulware DR. 2017. Global burden of disease of HIV-associated cryptococcal meningitis: an updated analysis. Lancet Infect Dis https://doi.org/10.1016/S1473-3099(17)30243-8.
2. Bicanic T, Wood R, Meintjes G, Rebe K, Brouwer A, Loyse A, Bekker LG, Jaffar S, Harrison T. 2008. High-dose amphotericin B with flucytosine for the treatment of cryptococcal meningitis in HIV-infected patients: a randomized trial. Clin Infect Dis 47:123–130. https://doi.org/10.1086/588792.
3. Jarvis JN, Meintjes G, Rebe K, Williams GN, Bicanic T, Williams A, Schutz C, Bekker LG, Wood R, Harrison TS. 2012. Adjunctive interferon-gamma immunotherapy for the treatment of HIV-associated cryptococcal meningitis: a randomized controlled trial. AIDS 26:1105–1113. https://doi.org/10.1097/QAD.0b013e3283536a93.

4. Jarvis JN, Bicanic T, Loyse A, Namarika D, Jackson A, Nussbaum JC, Longley N, Muzoora C, Phulusa J, Taseera K, Kanyembe C, Wilson D, Hosseinipour MC, Brouwer AE, Limmathurotsakul D, White N, van der Horst C, Wood R, Meintjes G, Bradley J, Jaffar S, Harrison T. 2014. Determinants of mortality in a combined cohort of 501 patients with HIV-associated cryptococcal meningitis: implications for improving outcomes. Clin Infect Dis 58:736–745. https://doi.org/10.1093/cid/cit794.
5. Day JN, Chau TT, Wolbers M, Mai PP, Dung NT, Mai NH, Phu NH, Nghia HD, Phong ND, Thai CQ, Thai le H, Chuong LV, Sinh DX, Duong VA, Hoang TN, Diep PT, Campbell JI, Sieu TP, Baker SG, Chau NV, Hien TT, Lalloo DG, Farrar JJ. 2013. Combination antifungal therapy for cryptococcal meningitis. N Engl J Med 368:1291–1302. https://doi.org/10.1056/NEJMoa1110404.
6. Donovick R, Gold W, Pagano JF, Stout HA. 1955–1956. Amphotericins A and B, antifungal antibiotics produced by a streptomycete. I. In vitro studies. Antibiot Annu 3:579–586.
7. Carton CA. 1952. Treatment of central nervous system cryptococcosis: a review and report of four cases treated with actidione. Ann Intern Med 37:123–154. https://doi.org/10.7326/0003-4819-37-1-123.
8. Mosberg WH, Jr, Arnold JG, Jr. 1950. Torulosis of the central nervous system; review of literature and report of 5 cases. Ann Intern Med 32:1153–1183. https://doi.org/10.7326/0003-4819-32-6-1153.
9. Andes D, Safdar N, Marchillo K, Conklin R. 2006. Pharmacokinetic-pharmacodynamic comparison of amphotericin B (AMB) and two lipid-associated AMB preparations, liposomal AMB and AMB lipid complex, in murine candidiasis models. Antimicrob Agents Chemother 50:674–684. https://doi.org/10.1128/AAC.50.2.674-684.2006.
10. Lestner JM, Howard SJ, Goodwin J, Gregson L, Majithiya J, Walsh TJ, Jensen GM, Hope WW. 2010. Pharmacokinetics and pharmacodynamics of amphotericin B deoxycholate, liposomal amphotericin B, and amphotericin B lipid complex in an in vitro model of invasive pulmonary aspergillosis. Antimicrob Agents Chemother 54:3432–3441. https://doi.org/10.1128/AAC.01586-09.
11. Saag MS, Powderly WG, Cloud GA, Robinson P, Grieco MH, Sharkey PK, Thompson SE, Sugar AM, Tuazon CU, Fisher JF, Hyslop N, Jacobson JM, Hafner R, Dismukes WE; the NIAID Mycoses Study Group and the AIDS Clinical Trials Group. 1992. Comparison of amphotericin B with fluconazole in the treatment of acute AIDS-associated cryptococcal meningitis. The NIAID Mycoses Study Group and the AIDS Clinical Trials Group. N Engl J Med 326:83–89. https://doi.org/10.1056/NEJM199201093260202.
12. Bennett JE, Dismukes WE, Duma RJ, Medoff G, Sande MA, Gallis H, Leonard J, Fields BT, Bradshaw M, Haywood H, McGee ZA, Cate TR, Cobbs CG, Warner JF, Alling DW. 1979. A comparison of amphotericin B alone and combined with flucytosine in the treatment of cryptococcal meningitis. N Engl J Med 301:126–131. https://doi.org/10.1056/NEJM197907193010303.
13. Leenders AC, Reiss P, Portegies P, Clezy K, Hop WC, Hoy J, Borleffs JC, Allworth T, Kauffmann RH, Jones P, Kroon FP, Verbrugh HA, de Marie S. 1997. Liposomal amphotericin B (AmBisome) compared with amphotericin B both followed by oral fluconazole in the treatment of AIDS-associated cryptococcal meningitis. AIDS 11:1463–1471. https://doi.org/10.1097/00002030-199712000-00010.
14. van der Horst CM, Saag MS, Cloud GA, Hamill RJ, Graybill JR, Sobel JD, Johnson PC, Tuazon CU, Kerkering T, Moskovitz BL, Powderly WG, Dismukes WE. 1997. Treatment of cryptococcal meningitis associated with the acquired immunodeficiency syndrome. N Engl J Med 337:15–21. https://doi.org/10.1056/NEJM199707033370103.
15. Brouwer AE, Rajanuwong A, Chierakul W, Griffin GE, Larsen RA, White NJ, Harrison TS. 2004. Combination antifungal therapies for HIV-associated cryptococcal meningitis: a randomised trial. Lancet 363:1764–1767. https://doi.org/10.1016/S0140-6736(04)16301-0.
16. WHO. 2018. Guidelines for the diagnosis, prevention and management of cryptococcal disease in HIV-infected adults, adolescents and children. WHO, Geneva, Switzerland.
17. Beardsley J, Wolbers M, Kibengo FM, Ggayi AB, Kamali A, Cuc NT, Binh TQ, Chau NV, Farrar J, Merson L, Phuong L, Thwaites G, Van Kinh N, Thuy PT, Chierakul W, Siriboon S, Thiansukhon E, Onsanit S, Supphamongkholchaikul W, Chan AK, Heyderman R, Mwinjiwa E, van Oosterhout JJ, Imran D, Basri H, Mayxay M, Dance D, Phimmasone P, Rattanavong S, Lalloo DG, Day JN; CryptoDex Investigators. 2016. Adjunctive dexamethasone in HIV-associated cryptococcal meningitis. N Engl J Med 374:542–554. https://doi.org/10.1056/NEJMoa1509024.
18. Bicanic T, Bottomley C, Loyse A, Brouwer AE, Muzoora C, Taseera K, Jackson A, Phulusa J, Hosseinipour MC, Van Der Horst C, Limmathurotsakul D, White NJ, Wilson D, Wood R, Meintjes G, Harrison TS, Jarvis JN. 2015. Toxicity of amphotericin B deoxycholate-based induction therapy in patients with HIV-associated cryptococcal meningitis. Antimicrob Agents Chemother 59:7224–7231. https://doi.org/10.1128/AAC.01698-15.
19. Wingard JR, Kubilis P, Lee L, Yee G, White M, Walshe L, Bowden R, Anaissie E, Hiemenz J, Lister J. 1999. Clinical significance of nephrotoxicity in patients treated with amphotericin B for suspected or proven aspergillosis. Clin Infect Dis 29:1402–1407. https://doi.org/10.1086/313498.
20. Mwaba P, Mwansa J, Chintu C, Pobee J, Scarborough M, Portsmouth S, Zumla A. 2001. Clinical presentation, natural history, and cumulative death rates of 230 adults with primary cryptococcal meningitis in Zambian AIDS patients treated under local conditions. Postgrad Med J 77:769–773. https://doi.org/10.1136/pgmj.77.914.769.
21. Bekersky I, Fielding RM, Dressler DE, Lee JW, Buell DN, Walsh TJ. 2002. Pharmacokinetics, excretion, and mass balance of liposomal amphotericin B (AmBisome) and amphotericin B deoxycholate in humans. Antimicrob Agents Chemother 46:828–833. https://doi.org/10.1128/AAC.46.3.828-833.2002.
22. Ayestarán A, López RM, Montoro JB, Estíbalez A, Pou L, Julià A, López A, Pascual B. 1996. Pharmacokinetics of conventional formulation versus fat emulsion formulation of amphotericin B in a group of patients with neutropenia. Antimicrob Agents Chemother 40:609–612.
23. Roberts JA, Abdul-Aziz MH, Lipman J, Mouton JW, Vinks AA, Felton TW, Hope WW, Farkas A, Neely MN, Schentag JJ. 2014. Individualised antibiotic dosing for patients who are critically ill: challenges and potential solutions. Lancet Infect Dis 14:498–509. https://doi.org/10.1016/S1473-3099(14)70036-2.
24. Laniado-Laborín R, Cabrales-Vargas MN. 2009. Amphotericin B: side effects and toxicity. Rev Iberoam Micol 26:223–227. https://doi.org/10.1016/j.riam.2009.06.003.
25. Deray G. 2002. Amphotericin B nephrotoxicity. J Antimicrob Chemother 49(Suppl 1):37–41. https://doi.org/10.1093/jac/49.suppl_1.37.
26. Barcia JP. 1998. Hyperkalemia associated with rapid infusion of conventional and lipid complex formulations of amphotericin B. Pharmacotherapy 18:874–876.
27. Rajasingham R, Williams D, Meya DB, Meintjes G, Boulware DR, Scriven J. 2014. Nosocomial drug-resistant bacteremia in 2 cohorts with cryptococcal meningitis, Africa. Emerg Infect Dis 20:722–724. https://doi.org/10.3201/eid2004.131277.
28. Longley N, Harrison TS, Jarvis JN. 2013. Cryptococcal immune reconstitution inflammatory syndrome. Curr Opin Infect Dis 26:26–34. https://doi.org/10.1097/QCO.0b013e32835c21d1.
29. Rolfes MA, Hullsiek KH, Rhein J, Nabeta HW, Taseera K, Schutz C, Musubire A, Rajasingham R, Williams DA, Thienemann F, Muzoora C, Meintjes G, Meya DB, Boulware DR. 2014. The effect of therapeutic lumbar punctures on acute mortality from cryptococcal meningitis. Clin Infect Dis 59:1607–1614. https://doi.org/10.1093/cid/ciu596.
30. Montezuma-Rusca JM, Powers JH, Follmann D, Wang J, Sullivan B, Williamson PR. 2016. Early fungicidal activity as a candidate surrogate endpoint for all-cause mortality in cryptococcal meningitis: a systematic review of the evidence. PLoS One 11:e0159727. https://doi.org/10.1371/journal.pone.0159727.
31. Lee SC, Dickson DW, Casadevall A. 1996. Pathology of cryptococcal meningoencephalitis: analysis of 27 patients with pathogenetic implications. Hum Pathol 27:839–847. https://doi.org/10.1016/S0046-8177(96)90459-1.
32. Klock C, Cerski M, Goldani LZ. 2009. Histopathological aspects of neurocryptococcosis in HIV-infected patients: autopsy report of 45 patients. Int J Surg Pathol 17:444–448. https://doi.org/10.1177/1066896908320550.
33. Kethireddy S, Andes D. 2007. CNS pharmacokinetics of antifungal agents. Expert Opin Drug Metab Toxicol 3:573–581. https://doi.org/10.1517/17425255.3.4.573.
34. Livermore J, Howard SJ, Sharp AD, Goodwin J, Gregson L, Felton T, Schwartz JA, Walker C, Moser B, Muller W, Harrison TS, Perfect JR, Hope WW. 2014. Efficacy of an abbreviated induction regimen of amphotericin B deoxycholate for cryptococcal meningoencephalitis: 3 days of therapy is equivalent to 14 days. mBio 5:e00725-13. https://doi.org/10.1128/mBio.00725-13.
35. Groll AH, Giri N, Petraitis V, Petraitiene R, Candelario M, Bacher JS, Piscitelli SC, Walsh TJ. 2000. Comparative efficacy and distribution of lipid formulations of amphotericin B in experimental Candida albicans

infection of the central nervous system. J Infect Dis 182:274–282. https://doi.org/10.1086/315643.
36. Lestner J, McEntee L, Johnson A, Livermore J, Whalley S, Schwartz J, Perfect JR, Harrison T, Hope W. 24 May 2017. Experimental models of short courses of liposomal amphotericin B for induction therapy for cryptococcal meningitis. Antimicrob Agents Chemother https://doi.org/10.1128/AAC.00090-17.
37. Shobo A, Baijnath S, Bratkowska D, Naiker S, Somboro AM, Bester LA, Singh SD, Naicker T, Kruger HG, Govender T. 2016. MALDI MSI and LC-MS/MS: towards preclinical determination of the neurotoxic potential of fluoroquinolones. Drug Test Anal 8:832–838. https://doi.org/10.1002/dta.1862.
38. Munyeza CF, Shobo A, Baijnath S, Bratkowska D, Naiker S, Bester LA, Singh SD, Maguire GE, Kruger HG, Naicker T, Govender T. 2016. Rapid and widespread distribution of doxycycline in rat brain: a mass spectrometric imaging study. Xenobiotica 46:385–392. https://doi.org/10.3109/00498254.2015.1081307.
39. Shobo A, Bratkowska D, Baijnath S, Naiker S, Somboro AM, Bester LA, Singh SD, Naicker T, Kruger HG, Govender T. 2016. Tissue distribution of pretomanid in rat brain via mass spectrometry imaging. Xenobiotica 46:247–252. https://doi.org/10.3109/00498254.2015.1067935.
40. Shobo A, Bratkowska D, Baijnath S, Naiker S, Bester LA, Singh SD, Maguire GE, Kruger HG, Govender T. 2015. Visualization of time-dependent distribution of rifampicin in rat brain using MALDI MSI and quantitative LCMS/MS. Assay Drug Dev Technol 13:277–284. https://doi.org/10.1089/adt.2015.634.
41. Day J, Imran D, Ganiem AR, Tjahjani N, Wahyuningsih R, Adawiyah R, Dance D, Mayxay M, Newton P, Phetsouvanh R, Rattanavong S, Chan AK, Heyderman R, van Oosterhout JJ, Chierakul W, Day N, Kamali A, Kibengo F, Ruzagira E, Gray A, Lalloo DG, Beardsley J, Binh TQ, Chau TT, Chau NV, Cuc NT, Farrar J, Hien TT, Van Kinh N, Merson L, Phuong L, Tho LT, Thuy PT, Thwaites G, Wertheim H, Wolbers M. 2014. CryptoDex: a randomised, double-blind, placebo-controlled phase III trial of adjunctive dexamethasone in HIV-infected adults with cryptococcal meningitis: study protocol for a randomised control trial. Trials 15:441. https://doi.org/10.1186/1745-6215-15-441.
42. Neely M, van Guilder MG, Yamada WM, Schumitzky A, Jelliffe RW. 2012. Accurate detection of outliers and subpopulations with Pmetrics, a nonparametric and parametric pharmacokinetic modeling and simulation package for R. Ther Drug Monit 34:467–476. https://doi.org/10.1097/FTD.0b013e31825c4ba6.
43. Hope WW, Seibel NL, Schwartz CL, Arrieta A, Flynn P, Shad A, Albano E, Keirns JJ, Buell DN, Gumbo T, Drusano GL, Walsh TJ. 2007. Population pharmacokinetics of micafungin in pediatric patients and implications for antifungal dosing. Antimicrob Agents Chemother 51:3714–3719. https://doi.org/10.1128/AAC.00398-07.
44. Brown JH, West GB (ed). 2000. Scaling in biology. Oxford University Press, New York, NY.
45. Viechtbauer W. 2010. Conducting meta-analyses in R with the metafor package. J Stat Softw 36:1–48. https://doi.org/10.18637/jss.v036.i03.
46. Andes D, Stamsted T, Conklin R. 2001. Pharmacodynamics of amphotericin B in a neutropenic-mouse disseminated-candidiasis model. Antimicrob Agents Chemother 45:922–926. https://doi.org/10.1128/AAC.45.3.922-926.2001.

J Antimicrob Chemother 2017; **72** Suppl 1: i12–i18
doi:10.1093/jac/dkx029

Journal of Antimicrobial Chemotherapy

Therapeutic drug monitoring for invasive mould infections and disease: pharmacokinetic and pharmacodynamic considerations

Katharine E. Stott and William W. Hope*

Antimicrobial Pharmacodynamics and Therapeutics, Department of Molecular and Clinical Pharmacology, University of Liverpool, Liverpool L69 3GE, UK

*Corresponding author. Tel: +44-151-794-5941; E-mail: william.hope@liverpool.ac.uk

Therapeutic drug monitoring (TDM) may be required to achieve optimal clinical outcomes in the setting of significant pharmacokinetic variability, a situation that applies to a number of anti-mould therapies. The majority of patients receiving itraconazole should routinely be managed with TDM. Voriconazole exhibits highly variable inter-individual pharmacokinetics, and a trough concentration of 1.0–5.5 mg/L is widely accepted although it is derived from relatively low-quality evidence. The case for TDM of posaconazole is currently in a state of flux following the introduction of a newer tablet formulation with improved oral bioavailability, but it may be indicated when used for either prophylaxis or treatment of established disease. The novel broad-spectrum azole drug isavuconazole does not currently appear to require TDM but 'real-world' data are awaited and TDM could be considered in selected clinical cases. For both polyene and echinocandin agents, there are insufficient data regarding the relationship between serum concentrations and therapeutic outcomes to support the routine use of TDM. A number of practical challenges to the implementation of TDM in the treatment of invasive mould infections remain unsolved. The delivery of TDM as a future standard of care will require real-time measurement of drug concentrations at the bedside and algorithms for dosage adjustment. Finally, measures of pharmacodynamic effect are required to deliver therapy that is truly individualized.

Introduction

Dose is a notoriously poor measure of drug exposure, both in individual patients and in larger patient populations. The use of a standard fixed regimen often results in considerable pharmacokinetic variability. While it is possible to estimate pharmacokinetic variability using population pharmacokinetic modelling approaches, the sources of observed variance cannot generally be fully explained by fixed effects (covariates) such as weight, height, ethnicity, pharmacogenetics and organ dysfunction. This limitation is further compounded by the physiological changes that are associated with various stages of illness. Thus, a fixed dosing strategy or a 'one-size-fits-all' approach will always result in some patients experiencing low drug exposure, with an increased probability of concentration-dependent therapeutic failure, while others have higher exposures than intended, placing them at increased risk of toxicity. In the management of infections, the clinical consequences of this variability vary according to the drug–pathogen combination.

The rationale for therapeutic drug monitoring (TDM) of antifungal therapies is the same as for any other therapeutic agent. First, for TDM to be of potential benefit, the drug should have largely unpredictable pharmacokinetic behaviour so that dose alone, or in conjunction with covariates such as renal function or weight, is inadequate to predict safe and effective drug exposure. Second, the drug should have a narrow therapeutic index so that under- or over-exposure could render the treatment ineffective or toxic, respectively. Third, the drug should have a defined concentration range that is associated with a satisfactorily high probability of both safety and efficacy.[1] In general, the anti-*Aspergillus* triazoles (i.e. itraconazole, voriconazole, posaconazole) and flucytosine fulfil these criteria. In contrast, the echinocandins and amphotericin B generally do not.[2] An understanding of antifungal TDM has been relatively mature for some time. Nevertheless, the arrival of new therapeutic options (i.e. isavuconazole) will extend the debate until further clinical evidence is gained.

Here, we review current knowledge regarding TDM of antifungal agents.

Application of TDM to commonly used antifungal agents

Itraconazole

Itraconazole was the first orally bioavailable antifungal agent with activity against moulds such as *Aspergillus* species. It is indicated for the treatment of oral and oesophageal candidiasis, prophylaxis against fungal infections in the setting of prolonged neutropenia, and for treatment of invasive aspergillosis and cryptococcosis infections that are refractory to first-line therapy.[3] The safety profile of itraconazole is less favourable than fluconazole and it has been associated with cardiotoxicity, gastrointestinal intolerance, neurological deficits and hepatitis.[3,4] Itraconazole is available as oral

capsules, oral solution and an intravenous (iv) preparation, although the latter is not available in the USA.

Itraconazole exhibits highly variable and non-linear pharmacokinetics, the basis for which is multifactorial. Itraconazole solution has an oral bioavailability that is ~30% higher than capsules. The absorption of itraconazole from capsules is largely dependent on gastric acidity and as such, capsules should always be administered with food or even an acidic beverage (e.g. cola).[4–6] Itraconazole is extensively protein bound in plasma, highly lipophilic and only moderately water soluble.[7] It undergoes oxidative metabolism, primarily by the CYP3A4 isoenzyme, which the drug also inhibits, and as a result drug–drug interactions are important.[8–10] Alterations in hepatic metabolism may also contribute to pharmacokinetic variability.[2]

Itraconazole was developed before the advent of modern pharmacodynamic approaches. The pharmacodynamic drug exposure target is quantified in terms of C_{min} (i.e. trough concentration) rather than AUC (or AUC/MIC ratio). The C_{min} is a relatively pragmatic measure of drug exposure. The pharmacokinetic profile of itraconazole is relatively flat, meaning that deviations from true C_{min} values are unlikely to be clinically significant. A C_{min} range of 0.5–1 mg/L, when measured using HPLC/mass spectrometry,[11] is generally used although this target is somewhat arbitrary. Pharmacodynamic targets are based on studies performed in a variety of clinical settings. In neutropenic patients receiving itraconazole for the prevention of invasive fungal infections, C_{min} <0.5 mg/L is associated with an increased likelihood of breakthrough infections[12–14] as well as a significantly higher mortality.[14] When used for the treatment of oropharyngeal candidiasis, serum itraconazole concentrations <1 mg/L are predictive of therapeutic failure.[15] Clinical outcomes for patients with cryptococcal meningitis and respiratory coccidioidomycosis are improved with higher steady-state itraconazole concentrations.[16] Finally, when itraconazole is administered in patients with invasive aspergillosis[17] or histoplasmosis,[18] higher C_{min} values tend to lead to better clinical outcomes. Importantly, therapeutic targets for TDM of itraconazole were derived in an era before triazole resistance emerged in *Aspergillus*. Such practice is illustrative of the limitations that result from setting pharmacodynamic targets without accounting for the susceptibility of the target organism. The appropriate C_{min} target for the treatment of *Aspergillus* with non-wild-type MICs is unknown,[11] although the majority of isolates with common resistance mechanisms tend to have very high MIC values and are unlikely to be treatable with dosage escalation and a well-demonstrated upper toxicity boundary.[4]

The majority of patients receiving itraconazole should routinely be managed with TDM. The rationale for this is 5-fold: (i) high inherent pharmacokinetic variability of all itraconazole formulations; (ii) evidence of clinically relevant drug exposure–response relationships (as summarized above); (iii) evidence of drug exposure–toxicity relationships;[19] (iv) potential for drug–drug interactions;[8–10] and (v) potential issues with compliance given the unpalatability of itraconazole suspension.[4,11] The accumulation of itraconazole occurs slowly and target trough concentrations are only reached after 7–15 days of dosing.[20] These estimates are further complicated by overt non-linear pharmacokinetics in at least some patients, who experience early toxicity due to high C_{min} values. Therapeutic C_{min} values can only be confidently achieved with the use of an oral loading dose or use of an iv formulation, although this is a relatively uncommon scenario with the advent of new antifungal agents.[21] A suggested strategy for TDM of itraconazole is to measure the trough concentration after the first week of therapy and then at regular intervals (e.g. every 1–2 weeks) according to the clinical context (e.g. when interacting drugs are started or discontinued, or if there are concerns about gastrointestinal absorption or compliance). C_{min} should be re-estimated 5–7 days following dose adjustment to ensure that target concentrations have been achieved.[11]

Voriconazole

Voriconazole is a structural congener of fluconazole that has a broader spectrum of antifungal activity but maintains the high oral bioavailability of fluconazole.[22] It is indicated for the treatment of invasive aspergillosis, invasive candidiasis exhibiting fluconazole resistance and infections caused by *Scedosporium* spp. and *Fusarium* spp.[3] Voriconazole can be used for the prevention of invasive fungal diseases in HSCT recipients.[23,24] Voriconazole is available as a tablet, an oral suspension, and a powder for infusion.[3]

Voriconazole exhibits highly variable inter-individual pharmacokinetics.[25] This variability can be attributed to many factors, including pharmacogenetic polymorphisms, drug–drug interactions, altered gastrointestinal absorption, inflammation and body weight.[26] Voriconazole undergoes extensive hepatic metabolism via CYP3A4, CYP2C9 and CYP2C19. Important pharmacogenetic determinants of clearance in CYP2C19 are responsible for ethnic differences in pharmacokinetics.[27] Voriconazole exhibits classical non-linear (Michaelis–Menten) pharmacokinetics in adults as a result of saturable clearance.[26] In contrast, young children display linear pharmacokinetics and have higher weight-corrected clearance[28] and higher weight-based dosages (9 mg/kg twice daily) are required to achieve pharmacodynamic targets that are associated with therapeutic success.[29] There are scant data from neonates and considerable uncertainty about the appropriate regimen in this setting.[30] Voriconazole is not widely used in this population because *Aspergillus* is such an uncommon pathogen.

The British Society for Medical Mycology (BSMM) recommends a voriconazole C_{min} target for TDM of between 1.0 and 5.5 mg/L when the drug is used to treat established invasive infection.[11] This target is widely accepted although it is derived from relatively low-quality evidence, based on studies that were limited by the difficulty of estimating voriconazole exposure in individual patients and in controlling for confounding factors that may have an impact upon clinical outcome.[11] The majority of studies assessing the utility of voriconazole TDM have been relatively small, were generally conducted at a single centre and are retrospective, and the methodological approaches were somewhat variable.[26,31] Two meta-analyses suggest that a target voriconazole concentration of ≥1.0 mg/L is predictive of clinical success,[26,32] although the more recent of these reported some uncertainty about this estimate.[26] For prophylactic use, the target concentration for TDM is less clear. The achievement of serum voriconazole concentrations within the therapeutic range does not appear to predict successful prophylaxis when using absence of breakthrough invasive fungal infection and/or fungal colonization as the outcome measure.[26] If the MIC of the invading pathogen is known, the recommended target for TDM is a C_{min}/MIC ratio of 2.0–5.0 (when the MIC is measured according to CLSI methodology). This has been demonstrated

using an experimental pharmacodynamic model[33] and in a retrospective study.[34]

Changes in voriconazole concentration occur more quickly than those of itraconazole and posaconazole. Initial serum sampling for TDM is recommended within the first 2–5 days of therapy. If clearance mechanisms are saturated in a particular patient, the initial level may not predict future concentrations, so subsequent sampling should be performed.[11,22] This strategy also applies to dose adjustments, initiation or discontinuation of interacting drugs, and changes in clinical circumstances. The timing of repeat sampling to determine voriconazole concentrations is difficult to define rigorously. If a patient is unstable or critically unwell and there is some uncertainty about voriconazole concentrations, then repeat sampling may be warranted every 3–5 days. In other circumstances, less intensive monitoring may be appropriate.

Posaconazole

Posaconazole has broad antifungal activity against medically important fungal pathogens including *Candida* spp., *Aspergillus* spp., *Cryptococcus neoformans* and the Mucorales.[35] It is licensed for use in fusariosis as salvage therapy; in invasive aspergillosis that is refractory or intolerant to first-line agents; for chromoblastomycosis and mycetoma when there is resistance and/or intolerance of itraconazole; and for coccidioidomycosis where there is resistance to, or intolerance of amphotericin, itraconazole or fluconazole.[3] Posaconazole is available as a solid tablet, an oral suspension and an iv formulation.

Posaconazole is structurally similar to itraconazole. It is highly protein bound and widely distributed in tissues.[36] Posaconazole suspension exhibits linear pharmacokinetics with daily doses up to 800 mg, beyond which further dose increases do not result in proportional increases in drug exposure.[37] It has a T_{max} of 5 h. The oral bioavailability of posaconazole suspension is increased in an acidic environment and in the presence of food.[37,38] The long terminal half-life of posaconazole (∼34 h) means that steady-state serum concentrations are only achieved after 1 week.[11] Metabolism is primarily by glucuronidation rather than oxidation. Posaconazole inhibits CYP3A4 activity, and as such has a number of clinically relevant drug–drug interactions.[39]

The case for TDM of posaconazole is currently in a state of flux following introduction of a newer tablet formulation, which has improved oral bioavailability. TDM of posaconazole may be indicated when used for either prophylaxis or treatment of established disease. C_{min} should be measured 7 days after initiation of therapy or a dosage adjustment. When posaconazole suspension is used, TDM is particularly indicated if there are concerns about gastrointestinal absorption and if there is uncertainty about compliance. The oral bioavailability of posaconazole tablets and capsules is better than the suspension although considerable variability is still seen,[40] suggesting that TDM should be considered. The tablet and oral suspension formulations of posaconazole are not considered interchangeable due to different dosing and pharmacokinetics.[41] For patients with established disease, the probability of a clinical response increases with increasing drug exposure.[42–44] For salvage therapy, target trough concentrations should be >1.0 mg/L, though this does not incorporate an estimate of MIC.[11]

Isavuconazole

Isavuconazole is a novel broad-spectrum azole drug with activity against yeasts, moulds and dimorphic fungi including *Aspergillus* spp., Mucorales, *Candida* spp. and *Cryptococcus* spp.[45–47] It has been approved by the EMA and the FDA for treatment of invasive aspergillosis, and by the EMA for invasive mucormycosis in cases where amphotericin B is inappropriate.[45] Isavuconazole is administered as a prodrug (isavuconazonium sulphate) and is available in both oral and iv formulations.[48]

Isuvaconazole has been shown to be non-inferior to voriconazole for the treatment of invasive disease caused by *Aspergillus* spp. and other filamentous fungi in a Phase III, randomized controlled trial.[49] A multicentre, double-blind Phase II trial has demonstrated non-inferiority of isavuconazole versus fluconazole for the treatment of uncomplicated oesophageal candidiasis.[50] In the treatment of mucormycosis, the efficacy of isavuconazole is similar to that of amphotericin B and the former is well tolerated.[51] Isavuconazole displays high oral bioavailability (nearly 100%), is relatively rapidly absorbed with a C_{max} of 2–3 h after oral administration, and is highly protein bound (∼98%).[52] It undergoes hepatic metabolism and has a long half-life (∼130 h). Accordingly, a loading dose of 200 mg isavuconazole is given three times a day for 2 days, followed by a maintenance dose of 200 mg once daily, with the aim of reaching steady-state concentrations at day 3.[53] Dose adjustment is not required in renal impairment.[52] Relative to other azole antifungals, the pharmacokinetics of isavuconazole are predictable[46,54] and is linear up to dosages of 600 mg/day. Isavuconazole is better tolerated than voriconazole with statistically fewer visual, skin or subcutaneous tissue and hepatobiliary disorders.[49]

The case for TDM of isavuconazole is uncertain at the present time. Analysis of clinical trial data does not reveal any relationship between various measures of drug exposure (e.g. AUC, C_{min}) and efficacy endpoints (all-cause mortality, clinical response) or safety endpoints, although this information is only available in abstract form at present.[55] It is important to recognize that these analyses were performed on the Phase III clinical trial using an optimized regimen. Consequently, there is little opportunity to observe concentration-dependent clinical failures and therefore identify a threshold for TDM. Whether the same conclusion holds with more 'real world' data remains to be seen. TDM could be considered in selected clinical cases where drug exposure needs to be confirmed (e.g. severe gut disease from graft-versus-host disease where oral absorption may be problematic, treatment of central nervous system disease, or treatment of a non-wild-type fungal pathogen). TDM may also be indicated in circumstances where there is currently little information (e.g. dosing in children or adolescents).

Concentrations of isavuconazole can be currently determined in a small number of reference laboratories in Europe but materials are available for units that are interested in developing an assay. There are no algorithms that have been developed to adjust dosage and we are not aware of any clinical experience. One consideration that is particularly pertinent to dosage adjustment of isavuconazole is that although concentrations will begin to change immediately after the dose or dosing interval is amended, the impact of changes will not be fully apparent for 4 weeks (the time to a new steady state), after which many clinically relevant issues will have either progressed or resolved.

Flucytosine

Flucytosine therapy is a standard-of-care for cryptococcal meningitis. Flucytosine is a pyrimidine analogue that has no intrinsic antifungal activity, but which is taken up by susceptible fungal cells and deaminated to the active metabolite, 5-fluorouracil (5-FU), by the fungal enzyme cytosine deaminase.[56] 5-FU is further converted to metabolites that inhibit fungal RNA and DNA synthesis.[57] 5-FU is active against most *Candida* spp. and *C. neoformans* and has some activity against *Aspergillus* spp. Administration of flucytosine should always be combined with other antifungal agents because of the significant risk of resistance acquisition when used as monotherapy.[56] It is indicated as an adjunct to amphotericin for the treatment of some cases of severe systemic candidiasis and is a routine component of induction therapy for cryptococcal meningitis.[3]

Flucytosine displays excellent bioavailability (~90%) following oral administration. Protein binding is negligible (2%–4%).[58] Flucytosine readily penetrates the blood–brain barrier and achieves effective concentrations in the vitreous, peritoneal and synovial fluid, making it valuable for the treatment of deep *Candida* infections that are otherwise refractory to first-line agents.[11,57,59] Since hepatic metabolism is minimal and >90% of the drug is excreted unchanged in urine, dose reduction is required in renal impairment.[11,60] In patients with normal renal function, C_{max} is reached within 1–2 h at steady state. The half-life is 3–4 h in patients with normal renal function but this can increase to several days in those with renal impairment or anuria.[61]

Flucytosine exhibits significant inter-patient pharmacokinetic variability.[62] A precise target range for serum concentrations of flucytosine for TDM is not universally agreed. Recommendations from the BSMM are based on *in vitro* evidence that yeasts exposed to trough concentrations <20–40 mg/L develop resistance, and that peak concentrations >100 mg/L are associated with myelotoxicity and hepatotoxicity.[63,64] The impact of trough level on clinical outcomes is unknown. Moreover, target concentrations for flucytosine in combination with other antifungal agents are not defined. Published data on TDM of flucytosine has revealed alarmingly infrequent achievement of concentrations in this putative therapeutic range, with two studies from the UK revealing <20% of concentrations within range,[62,65] and a further study achieving only 64.3% of concentrations within range.[66]

TDM is standard of care for the use of flucytosine. Serum concentrations should be determined: at 72 h post-therapy initiation; after dose adjustment; if there is uncertain compliance with oral therapy; and if there are clinical or laboratory signs of toxicity. The BSMM recommends an upwards dose adjustment of 50% if levels are sub-therapeutic.[11]

Polyenes

The polyenes comprise amphotericin B deoxycholate, licensed for systemic fungal infections; liposomal amphotericin B, licensed for severe or deep mycoses where toxicity precludes the use of conventional amphotericin B, for infection in febrile neutropenic patients unresponsive to broad-spectrum antifungals and for aspergillosis; and amphotericin B lipid complex, for severe invasive candidiasis and systemic fungal infections refractory to conventional amphotericin or where toxicity precludes its use.[3]

Despite over 50 years of clinical use of amphotericin B deoxycholate, and 20 years use of liposomal amphotericin B and amphotericin B lipid complex, relatively little is understood about the pharmacology of amphotericin B and the requirement for TDM.[67–69] The C_{max} and AUC/MIC ratio are recognized as the indices that predict clinical response.[70] However, there is currently insufficient evidence to support the routine use of TDM for polyenes.[71]

Echinocandins

The echinocandin class comprises anidulafungin, caspofungin and micafungin. These drugs inhibit synthesis of 1,3-β-D-glucan, an essential component of the fungal cell wall.[72] Anidulafungin is indicated for the treatment of invasive candidiasis. Caspofungin can additionally be used to treat invasive aspergillosis and systemic fungal infections in neutropenic patients. Micafungin is licensed for the treatment of invasive and oesophageal candidiasis, and for prophylaxis in the neutropenic phase of bone marrow transplantation.[3] The echinocandins offer potential for use against azole-resistant fungal pathogens.[72]

All echinocandins have low oral bioavailability and are only available for parenteral use.[3,72] They exhibit linear pharmacokinetics following iv administration, and distribute into tissues. CNS penetration is possible but only with use of higher dosages than are licensed for the treatment of bloodstream infection.[72,73] Drug interactions are less clinically important for the echinocandins than for other agents as they are weak substrates for, and do not inhibit, cytochrome P450 enzymes. Neither are they substrates for the P-glycoprotein transport systems.[72,74] As is the case with the polyenes, there are insufficient data regarding the relationship between echinocandin serum concentrations and therapeutic outcomes to support the routine use of TDM for these agents.[11,72]

Advancing the field: what are the immediate challenges for individualized antifungal therapy?

Much has been written about antifungal TDM, and the current state of knowledge is relatively stable. Several guidelines have been developed. What then are the remaining challenges to ensure TDM becomes a practical and more widely used adjunct to the routine use of antifungal agents?

Challenge 1. Measuring drug concentrations at the bedside

In many institutions, the turnaround time for antifungal drug measurement is too slow to be clinically helpful. Measurement requires relatively expensive equipment and highly trained laboratory personnel. TDM services are often centralized, leading to delays in transportation and reporting. A radical change in approach is required to enable measurement of drug concentrations at the bedside or in the clinic. This, in turn, would allow rapid modifications to the antifungal regimen which would be expected to provide a far more significant clinical benefit than waiting a week or longer, as is currently often the case.

Challenge 2. Development of algorithms for dosage adjustment

There is a distinct lack of published guidance on how to adjust the dosage of antifungal agents in response to a level that is outside a specified therapeutic range. Some authors suggest changing the dose by 50%. Even for agents with relatively simple pharmacology (e.g. fluconazole and flucytosine), such an approach is crude at best. We have for some time been developing software that enables precise calculation of the regimen that is required to shift a patient from their current state to a new, safer and more effective state. Our approach uses a multiple model approach (BestDose), which is a natural extension of the non-parametric adaptive grid algorithms developed by the Laboratory of Applied Pharmacokinetics in Los Angeles. Other approaches are certainly possible, although the complex pharmacology of almost all antifungal agents (e.g. non-linear pharmacokinetics) is an obstacle to the use of simple dosage calculators based on simple covariates. Furthermore, the problem of extreme variability in pharmacokinetics becomes significantly heightened in special populations such as neonates and children.

The development of software (or other dosage selection tools) is not trivial. Safe use will require expansion of the currently limited pool of clinicians who are well trained in clinical pharmacology. In addition, there are significant regulatory hurdles to ensure that software developed in academic settings fulfils the necessary standards for use in patients. Nevertheless, we are clear that this is the only path forward. Taking time and effort to measure drug concentrations in the laboratory with a coefficient of variation <10% and then guessing the dosage seems haphazard at the very least, and in our view is completely unacceptable for clinical practice.

Challenge 3. Real-time pharmacodynamic monitoring in patients with invasive mould disease

Current paradigms of drug concentration measurement and dosage adjustment are somewhat crude and counter to notions of truly individualized therapy. Considerable energy has been expended on developing population pharmacokinetic models that estimate drug exposure in individual patients with a high degree of precision. Interpretation of the result is then made with reference to a concentration target range that is constructed from a population of patients (usually determined using logistic regression models or classification and regression tree analysis). Such an approach is necessarily a violation of any principle of individualized dosing, whereby a patient should receive the right dose for their given disease. Some patients will require more drug, others will require less. Consider the differences in a patient who has been neutropenic for 6 weeks and has disseminated aspergillosis with bulky disease near the mediastinum and a small CNS lesion on CT, compared with a patient who received an allogeneic transplant 120 days ago and is well and currently an outpatient, but has a small nodule on a chest CT. Clearly, these patients are different and require different intensities of therapy. Yet, a TDM laboratory will report the same range for antifungal therapy and dosage adjustment.

Recently, we have been investigating the use of galactomannan (GM) to follow the pharmacodynamic effect of antifungal therapy. This is not necessarily a new concept. While much early work on GM focused on its role as a diagnostic modality, there are many reports that suggest that high unremitting GM levels are associated with poor clinical outcomes, including death.[75–78] Thus, circulating GM is a means by which patients can 'tell' their physician how much drug they need, without recourse to therapeutic ranges that are constructed from populations of patients. Accordingly, a patient with unremittingly high GM levels needs more drug, regardless of the measured plasma drug concentration and whether it is deemed 'therapeutic'. If this is not possible because of toxicity, or if dosage escalation and an increase in serum concentration does not result in normalization of the biomarker, then a second drug needs to be added or the therapy needs to be changed altogether. Such an approach constitutes true individualized therapy. Both a fixed dosing strategy and a therapeutic concentration range is a 'one-size-fits-all' approach, and neither is consistent with any notion of individualized antifungal therapy.

This is also an argument for the development of biomarkers with prognostic value that can be used to follow the disease course. Medical mycology is full of such possibilities, some of which are already established (e.g. use of quantitative cerebrospinal fluid counts of 1,3-β-D-glucan to monitor therapy for cryptococcal meningitis).[79] Most fungi produce a myriad of secondary metabolites that can potentially be used to track the effect of antifungal therapy, and the same could apply to transcriptomic and metabolomic approaches as they are further developed. Volumetric radiological analyses are a further extension of this idea.

Conclusion

Much remains to be done to ensure that patients with rapidly advancing life-threatening fungal infections are treated in an optimal manner. Such challenges include the development of methods to measure plasma concentrations of antifungal agents at the bedside in a timely manner, algorithms to enable rapid and precise dosage adjustment, and mechanisms by which the treatment of infection can be followed and managed in real-time. The last point remains an important challenge to enable true individualized therapy for patients with invasive fungal diseases.

Funding

This Supplement was funded by Basilea Pharmaceutica International Ltd, Basel, Switzerland. Editorial support was provided by a freelance medical writer (C. Dunstall) with funding from Basilea.

Transparency declarations

W. H. has received research funding from Pfizer, Gilead, Astellas, AiCuris, Amplyx, Spero Therapeutics and F2G, and acted as a consultant and/or given talks for Pfizer, Basilea, Astellas, F2G, Nordic Pharma, Medicines Company, Amplyx, Mayne Pharma, Spero Therapeutics, Auspherix, Cardeas and Pulmocide. K. E. S. has no conflicts of interest to declare.

This article forms part of a Supplement sponsored by Basilea Pharmaceutica International Ltd, Basel, Switzerland.

Author contributions

The authors co-wrote the article and approved the final version for publication.

References

1 Schumacher G. Introduction to therapeutic drug monitoring. In: G Schumacher, ed. *Therapeutic Drug Monitoring*. East Norwalk, CT: Appleton and Lange, 1995; 1–17.

2 Lewis RE. Antifungal therapeutic drug monitoring. *Curr Fungal Infect Rep* 2010; **4**: 158–67.

3 Joint Formulary Committee. *British National Formulary* (online). London: BMJ Group and Pharmaceutical Press, 2016. https://www.bnf.org/products/bnf-online/.

4 Lestner J, Hope WW. Itraconazole: an update on pharmacology and clinical use for treatment of invasive and allergic fungal infections. *Expert Opin Drug Metab Toxicol* 2013; **9**: 911–26.

5 Van de Velde VJ, Van Peer AP, Heykants JJ *et al*. Effect of food on the pharmacokinetics of a new hydroxypropyl-β-cyclodextrin formulation of itraconazole. *Pharmacotherapy* 1996; **16**: 424–8.

6 Abuhelwa AY, Mudge S, Hayes D *et al*. Population in vitro-in vivo correlation model linking gastrointestinal transit time, pH, and pharmacokinetics: itraconazole as a model drug. *Pharm Res* 2016; **33**: 1782–94.

7 Lass-Flörl C. Triazole antifungal agents in invasive fungal infections: a comparative review. *Drugs* 2011; **71**: 2405–19.

8 Andes D, Azie N, Yang H *et al*. Drug-drug interaction associated with mold-active triazoles among hospitalized patients. *Antimicrob Agents Chemother* 2016; **60**: 3398–406.

9 Liu L, Bello A, Dresser MJ *et al*. Best practices for the use of itraconazole as a replacement for ketoconazole in drug-drug interaction studies. *J Clin Pharmacol* 2016; **56**: 143–51.

10 Dodds-Ashley E. Management of drug and food interactions with azole antifungal agents in transplant recipients. *Pharmacotherapy* 2010; **30**: 842–54.

11 Ashbee HR, Barnes RA, Johnson EM *et al*. Therapeutic drug monitoring (TDM) of antifungal agents: guidelines from the British Society for Medical Mycology. *J Antimicrob Chemother* 2014; **69**: 1162–76.

12 Boogaerts MA, Verhoef GE, Zachee P *et al*. Antifungal prophylaxis with itraconazole in prolonged neutropenia: correlation with plasma levels. *Mycoses* 1989; **32** Suppl 1: 103–8.

13 Tricot G, Joosten E, Boogaerts MA *et al*. Ketoconazole vs. itraconazole for antifungal prophylaxis in patients with severe granulocytopenia: preliminary results of two nonrandomized studies. *Rev Infect Dis* 1987; **9** Suppl 1: S94–9.

14 Glasmacher A, Hahn C, Leutner C *et al*. Breakthrough invasive fungal infections in neutropenic patients after prophylaxis with itraconazole. *Mycoses* 1999; **42**: 443–51.

15 Cartledge JD, Midgely J, Gazzard BG. Itraconazole solution: higher serum drug concentrations and better clinical response rates than the capsule formulation in acquired immunodeficiency syndrome patients with candidosis. *J Clin Pathol* 1997; **50**: 477–80.

16 Sharkey PK, Rinaldi MG, Dunn JF *et al*. High-dose itraconazole in the treatment of severe mycoses. *Antimicrob Agents Chemother* 1991; **35**: 707–13.

17 Denning DW, Tucker RM, Hanson LH *et al*. Itraconazole in opportunistic mycoses: cryptococcosis and aspergillosis. *J Am Acad Dermatol* 1990; **23**: 602–7.

18 Wheat J, Hafner R, Korzun AH *et al*. Itraconazole treatment of disseminated histoplasmosis in patients with the acquired immunodeficiency syndrome. AIDS Clinical Trial Group. *Am J Med* 1995; **98**: 336–42.

19 Lestner JM, Roberts SA, Moore CB *et al*. Toxicodynamics of itraconazole: implications for therapeutic drug monitoring. *Clin Infect Dis* 2009; **49**: 928–30.

20 Hardin TC, Graybill JR, Fetchick R *et al*. Pharmacokinetics of itraconazole following oral administration to normal volunteers. *Antimicrob Agents Chemother* 1988; **32**: 1310–3.

21 Willems L, van der Geest R, de Beule K. Itraconazole oral solution and intravenous formulations: a review of pharmacokinetics and pharmacodynamics. *J Clin Pharm Ther* 2001; **26**: 159–69.

22 Theuretzbacher U, Ihle F, Derendorf H. Pharmacokinetic/pharmacodynamic profile of voriconazole. *Clin Pharmacokinet* 2006; **45**: 649–63.

23 Wingard JR, Carter SL, Walsh TJ *et al*. Randomized, double-blind trial of fluconazole versus voriconazole for prevention of invasive fungal infection after allogeneic hematopoietic cell transplantation. *Blood* 2010; **116**: 5111–8.

24 Marks DI, Pagliuca A, Kibbler CC *et al*. Voriconazole versus itraconazole for antifungal prophylaxis following allogeneic haematopoietic stem-cell transplantation. *Br J Haematol* 2011; **155**: 318–27.

25 Hope WW. Population pharmacokinetics of voriconazole in adults. *Antimicrob Agents Chemother* 2012; **56**: 526–31.

26 Luong M-L, Al-Dabbagh M, Groll AH *et al*. Utility of voriconazole therapeutic drug monitoring: a meta-analysis. *J Antimicrob Chemother* 2016; **71**: 1786–99.

27 Hyland R, Jones BC, Smith DA. Identification of the cytochrome p450 enzymes involved in the N-oxidation of voriconazole. *Drug Metab Dispos* 2003; **31**: 540–7.

28 Walsh TJ, Karlsson MO, Driscoll T *et al*. Pharmacokinetics and safety of intravenous voriconazole in children after single- or multiple-dose administration. *Antimicrob Agents Chemother* 2004; **48**: 2166–72.

29 Friberg LE, Ravva P, Karlsson MO *et al*. Integrated population pharmacokinetic analysis of voriconazole in children, adolescents, and adults. *Antimicrob Agents Chemother* 2012; **56**: 3032–42.

30 Kadam RS, Van Den Anker JN. Pediatric clinical pharmacology of voriconazole: role of pharmacokinetic/pharmacodynamic modeling in pharmacotherapy. *Clin Pharmacokinet* 2016; **55**: 1031–43.

31 Elewa H, El-Mekaty E, El-Bardissy A *et al*. Therapeutic drug monitoring of voriconazole in the management of invasive fungal infections: a critical review. *Clin Pharmacokinet* 2015; **54**: 1223–35.

32 Hamada Y, Seto Y, Yago K, Kuroyama M. Investigation and threshold of optimum blood concentration of voriconazole: a descriptive statistical meta-analysis. *J Infect Chemother* 2012; **18**: 501–7.

33 Jeans AR, Howard SJ, Al-Nakeeb Z *et al*. Combination of voriconazole and anidulafungin for treatment of triazole-resistant *Aspergillus fumigatus* in an in vitro model of invasive pulmonary aspergillosis. *Antimicrob Agents Chemother* 2012; **56**: 5180–5.

34 Troke PF, Hockey HP, Hope WW. Observational study of the clinical efficacy of voriconazole and its relationship to plasma concentrations in patients. *Antimicrob Agents Chemother* 2011; **55**: 4782–8.

35 Sabatelli F, Patel R, Mann PA *et al*. In vitro activities of posaconazole, fluconazole, itraconazole, voriconazole, and amphotericin B against a large collection of clinically important molds and yeasts. *Antimicrob Agents Chemother* 2006; **50**: 2009–15.

36 Ezzet F, Wexler D, Courtney R *et al*. Oral bioavailability of posaconazole in fasted healthy subjects: comparison between three regimens and basis for clinical dosage recommendations. *Clin Pharmacokinet* 2005; **44**: 211–20.

37 Courtney R, Pai S, Laughlin M *et al*. Pharmacokinetics, safety, and tolerability of oral posaconazole administered in single and multiple doses in healthy adults. *Antimicrob Agents Chemother* 2003; **47**: 2788–95.

38 Courtney R, Wexler D, Radwanski E *et al*. Effect of food on the relative bioavailability of two oral formulations of posaconazole in healthy adults. *Br J Clin Pharmacol* 2004; **57**: 218–22.

39 Niwa T, Imagawa Y, Yamazaki H. Drug interactions between nine antifungal agents and drugs metabolized by human cytochromes P450. *Curr Drug Metab* 2014; **15**: 651–79.

40 Krishna G, Ma L, Martinho M *et al*. Single-dose phase I study to evaluate the pharmacokinetics of posaconazole in new tablet and capsule

formulations relative to oral suspension. *Antimicrob Agents Chemother* 2012; **56**: 4196–201.

41 European Medicines Agency. *EMA Warns That Noxafil Tablets and Oral Suspension Have Different Doses and Are Not Interchangeable*. *EMA/425762/2016*. http://www.ema.europa.eu/docs/en_GB/document_library/Press_release/2016/06/WC500209313.pdf.

42 Cattaneo C, Panzali A, Passi A *et al*. Serum posaconazole levels during acute myeloid leukaemia induction therapy: correlations with breakthrough invasive fungal infections. *Mycoses* 2015; **58**: 362–7.

43 Dolton MJ, Ray JE, Chen SC *et al*. Multicenter study of posaconazole therapeutic drug monitoring: exposure-response relationship and factors affecting concentration. *Antimicrob Agents Chemother* 2012; **56**: 5503–10.

44 Walsh TJ, Raad I, Patterson TF *et al*. Treatment of invasive aspergillosis with posaconazole in patients who are refractory to or intolerant of conventional therapy: an externally controlled trial. *Clin Infect Dis* 2007; **44**: 2–12.

45 Rybak JM, Marx KR, Nishimoto AT *et al*. Isavuconazole: pharmacology, pharmacodynamics, and current clinical experience with a new triazole antifungal agent. *Pharmacotherapy* 2015; **35**: 1037–51.

46 Miceli MH, Kauffman CA. Isavuconazole: a new broad-spectrum triazole antifungal agent. *Clin Infect Dis* 2015; **61**: 1558–65.

47 McCormack PL. Isavuconazonium: first global approval. *Drugs* 2015; **75**: 817–22.

48 Pettit NN, Carver PL. Isavuconazole: a new option for the management of invasive fungal infections. *Ann Pharmacother* 2015; **49**: 825–42.

49 Maertens JA, Raad II, Marr KA *et al*. Isavuconazole versus voriconazole for primary treatment of invasive mould disease caused by *Aspergillus* and other filamentous fungi (SECURE): a phase 3, randomised-controlled, non-inferiority trial. *Lancet* 2016; **387**: 760–9.

50 Viljoen J, Azie N, Schmitt-Hoffmann AH *et al*. A phase 2, randomized, double-blind, multicenter trial to evaluate the safety and efficacy of three dosing regimens of isavuconazole compared with fluconazole in patients with uncomplicated esophageal candidiasis. *Antimicrob Agents Chemother* 2015; **59**: 1671–9.

51 Marty FM, Ostrosky-Zeichner L, Cornely OA *et al*. Isavuconazole treatment for mucormycosis: a single-arm open-label trial and case-control analysis. *Lancet Infect Dis* 2016; **16**: 828–37.

52 Girmenia C. New generation azole antifungals in clinical investigation. *Expert Opin Investig Drugs* 2009; **18**: 1279–95.

53 European Medicines Agency. *Cresemba Assessment Report*. *EMA 596950/2015*. http://www.ema.europa.eu/docs/en_GB/document_library/EPAR_-_Public_assessment_report/human/002734/WC500196130.pdf.

54 Schmitt-Hoffmann A, Roos B, Maares J *et al*. Multiple-dose pharmacokinetics and safety of the new antifungal triazole BAL4815 after intravenous infusion and oral administration of its prodrug, BAL8557, in healthy volunteers. *Antimicrob Agents Chemother* 2006; **50**: 286–93.

55 Kaindl T, Engelhardt M, Townsend R *et al*. Intra-subject variability and exposure-response relationship of isavuconazole in the phase 3 SECURE study in patients with invasive mould disease caused by Aspergillus spp. and other filamentous fungi. Abstract O424. Presented at European Society of Clinical Microbiology and Infectious Diseases (ECCMID) 26th Congress, 9–12 April 2016, Amsterdam, Netherlands.

56 Polak A, Scholer HJ. Mode of action of 5-fluorocytosine and mechanisms of resistance. *Chemotherapy* 1975; **21**: 113–30.

57 Vermes A, Guchelaar HJ, Dankert J. Flucytosine: a review of its pharmacology, clinical indications, pharmacokinetics, toxicity and drug interactions. *J Antimicrob Chemother* 2000; **46**: 171–9.

58 Block ER, Bennett JE, Livoti LG *et al*. Flucytosine and amphotericin B: hemodialysis effects on the plasma concentration and clearance. Studies in man. *Ann Intern Med* 1974; **80**: 613–7.

59 Cutler RE, Blair AD, Kelly MR. Flucytosine kinetics in subjects with normal and impaired renal function. *Clin Pharmacol Ther* 1978; **24**: 333–42.

60 Goodwin ML, Drew RH. Antifungal serum concentration monitoring: an update. *J Antimicrob Chemother* 2008; **61**: 17–25.

61 Block ER, Bennett JE. Pharmacological studies with 5-fluorocytosine. *Antimicrob Agents Chemother* 1972; **1**: 476–82.

62 Pasqualotto AC, Howard SJ, Moore CB *et al*. Flucytosine therapeutic monitoring: 15 years experience from the UK. *J Antimicrob Chemother* 2007; **59**: 791–3.

63 Normark S, Schonebeck J. In vitro studies of 5-fluorocytosine resistance in *Candida albicans* and *Torulopsis glabrata*. *Antimicrob Agents Chemother* 1972; **2**: 114–21.

64 Stamm AM, Diasio RB, Dismukes WE *et al*. Toxicity of amphotericin B plus flucytosine in 194 patients with cryptococcal meningitis. *Am J Med* 1987; **83**: 236–42.

65 Soltani M, Tobin CM, Bowker KE *et al*. Evidence of excessive concentrations of 5-flucytosine in children aged below 12 years: a 12-year review of serum concentrations from a UK clinical assay reference laboratory. *Int J Antimicrob Agents* 2006; **28**: 574–7.

66 Petersen D, Demertzis S, Freund M *et al*. Individualization of 5-fluorocytosine therapy. *Chemotherapy* 1994; **40**: 149–56.

67 Saravolatz LD, Ostrosky-Zeichner L, Marr KA *et al*. Amphotericin B: time for a new 'gold standard'. *Clin Infect Dis* 2003; **37**: 415–25.

68 Stone NR, Bicanic T, Salim R, Hope W. Liposomal amphotericin B (AmBisome®): a review of the pharmacokinetics, pharmacodynamics, clinical experience and future directions. *Drugs* 2016; **76**: 485–500.

69 Rapp RP, Gubbins PO, Evans ME. Amphotericin B lipid complex. *Ann Pharmacother* 1997; **31**: 1174–86.

70 Andes D, Stamsted T, Conklin R. Pharmacodynamics of amphotericin B in a neutropenic-mouse disseminated-candidiasis model. *Antimicrob Agents Chemother* 2001; **45**: 922–6.

71 Andes D, Pascual A, Marchetti O. Antifungal therapeutic drug monitoring: established and emerging indications. *Antimicrob Agents Chemother* 2009; **53**: 24–34.

72 Chen SC, Slavin MA, Sorrell TC. Echinocandin antifungal drugs in fungal infections: a comparison. *Drugs* 2011; **71**: 11–41.

73 Reminiac F, Sonneville R, Massias L *et al*. Very-high-dose caspofungin combined with voriconazole to treat central nervous system aspergillosis: substantial penetration of caspofungin into cerebrospinal fluid. *Antimicrob Agents Chemother* 2014; **58**: 3568–9.

74 Dowell JA, Knebel W, Ludden T *et al*. Population pharmacokinetic analysis of anidulafungin, an echinocandin antifungal. *J Clin Pharmacol* 2004; **44**: 590–8.

75 Miceli MH, Grazziutti ML, Woods G *et al*. Strong correlation between serum aspergillus galactomannan index and outcome of aspergillosis in patients with hematological cancer: clinical and research implications. *Clin Infect Dis* 2008; **46**: 1412–22.

76 Woods G, Miceli MH, Grazziutti ML *et al*. Serum Aspergillus galactomannan antigen values strongly correlate with outcome of invasive aspergillosis: a study of 56 patients with hematologic cancer. *Cancer* 2007; **110**: 830–4.

77 Maertens J, Buve K, Theunissen K *et al*. Galactomannan serves as a surrogate endpoint for outcome of pulmonary invasive aspergillosis in neutropenic hematology patients. *Cancer* 2009; **115**: 355–62.

78 Nouér SA, Nucci M, Kumar NS *et al*. Earlier response assessment in invasive aspergillosis based on the kinetics of serum *Aspergillus* galactomannan: proposal for a new definition. *Clin Infect Dis* 2011; **53**: 671–6.

79 Salvatore CM, Chen TK, Toussi SS *et al*. (1→3)-β-D-glucan in cerebrospinal fluid as a biomarker for *Candida* and *Aspergillus* infections of the central nervous system in pediatric patients. *J Pediatric Infect Dis Soc* 2016; **5**: 277–86.